Biological and Medical Physics, Biomedical Engineering

Mair Zamir

Hemo-Dynamics



Hemo-Dynamics

BIOLOGICAL AND MEDICAL PHYSICS, BIOMEDICAL ENGINEERING

The fields of biological and medical physics and biomedical engineering are broad, multidisciplinary and dynamic. They lie at the crossroads of frontier research in physics, biology, chemistry, and medicine. The Biological and Medical Physics, Biomedical Engineering Series is intended to be comprehensive, covering a broad range of topics important to the study of the physical, chemical and biological sciences. Its goal is to provide scientists and engineers with textbooks, monographs, and reference works to address the growing need for information.

Books in the series emphasize established and emergent areas of science including molecular, membrane, and mathematical biophysics; photosynthetic energy harvesting and conversion; information processing; physical principles of genetics; sensory communications; automata networks, neural networks, and cellular automata. Equally important will be coverage of applied aspects of biological and medical physics and biomedical engineering such as molecular electronic components and devices, biosensors, medicine, imaging, physical principles of renewable energy production, advanced prostheses, and environmental control and engineering.

Editor-in-Chief:

Elias Greenbaum, Oak Ridge National Laboratory, Oak Ridge, Tennessee, USA

Editorial Board:

Masuo Aizawa, Department of Bioengineering, Tokyo Institute of Technology, Yokohama, Japan

Olaf S. Andersen, Department of Physiology, Biophysics and Molecular Medicine, Cornell University, New York, USA

Robert H. Austin, Department of Physics, Princeton University, Princeton, New Jersey, USA

James Barber, Department of Biochemistry, Imperial College of Science, Technology and Medicine, London, England

Howard C. Berg, Department of Molecular and Cellular Biology, Harvard University, Cambridge, Massachusetts, USA

Victor Bloomfield, Department of Biochemistry, University of Minnesota, St. Paul, Minnesota, USA

Robert Callender, Department of Biochemistry, Albert Einstein College of Medicine, Bronx, New York, USA

Steven Chu, Lawrence Berkeley National Laboratory, Berkeley, California, USA

Louis J. DeFelice, Department of Pharmacology, Vanderbilt University, Nashville, Tennessee, USA

Johann Deisenhofer, Howard Hughes Medical Institute, The University of Texas, Dallas, Texas, USA

George Feher, Department of Physics, University of California, San Diego, La Jolla, California, USA

Hans Frauenfelder, Los Alamos National Laboratory, Los Alamos, New Mexico, USA

Ivar Giaever, Rensselaer Polytechnic Institute, Troy, New York, USA

Sol M. Gruner, Cornell University, Ithaca, New York, USA

Judith Herzfeld, Department of Chemistry, Brandeis University, Waltham, Massachusetts, USA Mark S. Humayun, Doheny Eye Institute, Los Angeles, California, USA

Pierre Joliot, Institute de Biologie Physico-Chimique, Fondation Edmond de Rothschild, Paris, France

Lajos Keszthelyi, Institute of Biophysics, Hungarian Academy of Sciences, Szeged, Hungary

Robert S. Knox, Department of Physics and Astronomy, University of Rochester, Rochester, New York, USA

Aaron Lewis, Department of Applied Physics, Hebrew University, Jerusalem, Israel

Stuart M. Lindsay, Department of Physics and Astronomy, Arizona State University, Tempe, Arizona, USA

David Mauzerall, Rockefeller University, New York, New York, USA

Eugenie V. Mielczarek, Department of Physics and Astronomy, George Mason University, Fairfax, Virginia, USA

Markolf Niemz, Medical Faculty Mannheim, University of Heidelberg, Mannheim, Germany

V. Adrian Parsegian, Physical Science Laboratory, National Institutes of Health, Bethesda, Maryland, USA

Linda S. Powers, University of Arizona, Tucson, Arizona, USA

Earl W. Prohofsky, Department of Physics, Purdue University, West Lafayette, Indiana, USA

Andrew Rubin, Department of Biophysics, Moscow State University, Moscow, Russia

Michael Seibert, National Renewable Energy Laboratory, Golden, Colorado, USA

David Thomas, Department of Biochemistry, University of Minnesota Medical School, Minneapolis, Minnesota, USA

More information about this series at http://www.springer.com/series/3740

Mair Zamir

Hemo-Dynamics



Mair Zamir Departments of Applied Mathematics and of Medical Biophysics University of Western Ontario London, Canada

ISSN 1618-7210 ISSN 2197-5647 (electronic)
Biological and Medical Physics, Biomedical Engineering
ISBN 978-3-319-24101-2 ISBN 978-3-319-24103-6 (eBook)
DOI 10.1007/978-3-319-24103-6

Library of Congress Control Number: 2015952630

Springer Cham Heidelberg New York Dordrecht London © Springer International Publishing Switzerland 2016

This work is subject to copyright. All rights are reserved by the Publisher, whether the whole or part of the material is concerned, specifically the rights of translation, reprinting, reuse of illustrations, recitation, broadcasting, reproduction on microfilms or in any other physical way, and transmission or information storage and retrieval, electronic adaptation, computer software, or by similar or dissimilar methodology now known or hereafter developed.

The use of general descriptive names, registered names, trademarks, service marks, etc. in this publication does not imply, even in the absence of a specific statement, that such names are exempt from the relevant protective laws and regulations and therefore free for general use.

The publisher, the authors and the editors are safe to assume that the advice and information in this book are believed to be true and accurate at the date of publication. Neither the publisher nor the authors or the editors give a warranty, express or implied, with respect to the material contained herein or for any errors or omissions that may have been made.

Printed on acid-free paper

Springer International Publishing AG Switzerland is part of Springer Science+Business Media (www.springer.com)

To the memory of Professor R.D. Milne (1930–2014). He taught tenaciously that in science, before all else, we must **understand**. This book is largely about understanding, inspired in no small part by his teaching.



Ronald D. Milne was born on August 3, 1930, in Aberdeen. He attended Aberdeen Grammar School and Aberdeen University, then continued his studies at Cranfield College of Aeronautics and Queen Mary College, London, where he became Lecturer in 1956 and Reader in 1964. In August 1971, he became Chair of Theoretical Mechanics at the University of Bristol which he renamed Engineering Mathematics, and in 1977 he became Dean of Engineering. He developed a mathematical framework for aeroelasticity and made a milestone contribution to the dynamics of the deformable aeroplane. His commitment to mathematics was unequivocal and his understanding of fluid dynamics was absolute. His influence on me was immeasurable.

In Praise of Hemo-Dynamics

"Zamir carries the reader from first principles to the complexity of pulsatile blood flow with an elegance and fluidity not unlike the very subject matter he is describing. The journey from Newton's second law, through the Navier-Stokes equations and finally to the dynamics of pulsatile blood flow and pathology is presented in a clear, accessible manner; perfect for students and researchers new to the field." *Matthew Betti, PhD candidate, Applied Mathematics, The University of Western Ontario.*

"Avoiding the math, even me, a clinician, enjoyed reading this book, I can follow it easily, as it is well written. Chapter 3 was very interesting and made me wonder if pressure recovery is a topic that would be of interest, i.e. in severe aortic stenosis. The section on arterial bifurcations (which cause all sorts of trouble in the coronary system; treatment is difficult and almost never ideal) provoked a chain of thought about whether one could develop mathematical models for most common bifurcations, look retrospectively into coronary PCI cases and bifurcations and predict an outcome. Chapter 9 brought to mind LVAD therapy (left ventricular assist devices for heart failure) and how complex the interplay of machine and blood vessel function is, almost unsolvable; there must be a "mess" of flows created by LVADs." Mario Gössl, MD, Adjunct Assistant Professor of Medicine, University of Wisconsin School of Medicine and Public Health; Director, Heart Valve and Structural Heart Disease Clinic, Dean Clinic, Madison, WI.

"Incredible, the figures alone are to die for... At first glance "Hemo-Dynamics" seems like a deep engineering and modeling dive into the mechanical properties of the cardiovascular system, blood, and how they interact to generate flow and pressure. However, the text is laid out in a stepwise manner and I was especially impressed in the way that the key conceptual figures illustrate the essential concepts. In keeping with the philosophical underpinnings of engineering, Professor Zamir has also constructed his book so that the format, text, equations and the figures are self-reinforcing. This is a book that will be of great use to those who seek to understand the cardiovascular system from a mechanical and modeling perspective." *Michael J. Joyner, MD, Professor of Anesthesiology, Mayo Clinic, Rochester MN*.

"I have read your Magnum Opus! It is excellent ... Prof. Mair Zamir has written extensively concerning pulsatile blood flow in the arterial system. This

book summarizes his research on this important subject... It is a great book and deserves to be read. Diseases of the arterial system are the most common cause of death in our society hence such fundamental knowledge is a requirement for those proposing care and treatment." *Gerald Klassen, MD, Professor of Cardiology (retired), Dalhousie University.*

"I feel uniquely qualified to assess the utility of this book as I have no background in fluid dynamics, physics, or mathematics. The effectiveness of this large body of work to communicate fluid dynamics to readers of all levels is tremendous. I glazed over most of the intimidating mathematical formulas, yet finished with a far greater understanding of fluids and fluid flow properties than when I began. Dr. Zamir's ability to explain these concepts so that they are accessible by all is fantastic. I would highly recommend this book to any learner looking for an understanding of fluid dynamics, especially within the cardiovascular system." *Katelyn Norton, PhD candidate, Faculty of Health Sciences, The University of Western Ontario.*

"I like the Introduction in that it motivates me to understand flow by delving into the mathematics so that I can get insight into some emerging characteristics of the blood flow system. The distinction between the concept of blood flow (driven by blood pressure gradient) and just blood volume (driven by blood pressure) is of particular physiological importance as tissues need the flow to deliver nutrients and remove metabolic products. Moreover blood pressure itself and its pulsatile nature are critically important signals for maintaining arterial wall tension and thereby lumen diameter. Hence the detailed analysis of the role of arterial tree branching geometry and the role of elastic vessels are particularly instructive." Erik L. Ritman MD, PhD, Professor of Physiology and Medicine, Mayo Clinic College of Medicine, Rochester, MN.

"I enjoyed the book (the parts I understood) and it would be a resource for my lab. I think it would make a strong text for an interdisciplinary graduate program. The book is clearly organized to take the reader by the hand and guide them carefully and slowly through the important elements of steady state and pulsatile flow." *Kevin Shoemaker, PhD, Professor of Kinesiology, The University of Western Ontario.*

"As a physiologist reading the introductory chapters of this book, I was inclined to skip ahead to the sections which I felt might be more relevant to my work, but instead I just kept reading as each section was so informative that I didn't want to risk missing anything. I learn concepts in a very "step by step" fashion, and this book caters to that learning style, describing very complex concepts with language that is both easily understood, and also quite enchanting. The enchantment, I think, is the true strength of the book - Dr. Zamir does an enviable job of instilling his love of the mathematics and physics of fluids into the reader. After I'd started reading this book, I traveled to Jasper National Park for a short vacation, and as I sat by a majestic glacier lake, all I could think about was the beauty of fluids." Charlotte W. Usselman, PhD, Postdoctoral Fellow, Faculty of Physical Education and Recreation, University of Alberta.

"This book provides an elegant and intuitive derivation of the fundamental mathematics underlying fluid flow, and then applies these in a straightforward way to pulsatile blood flow in all its complexity. One of the triumphs of the book is that

Zamir succeeds in making essential concepts such as the Navier-Stokes equations completely accessible to any reader with a knowledge of basic calculus. The author succeeds in conveying both the beauty of his subject matter, and his passion for the elegance and intricacies of fluid flow more generally." *Lindi Wahl, PhD, Professor of Applied Mathematics, The University of Western Ontario.*

Preface

In the first editions of *The Physics of Pulsatile Flow*¹ and *The Physics of Coronary Blood Flow*,² which appeared in 2000 and 2005, respectively, I used the word "physics" in the titles to emphasize that while the subject of the two books is of interest in biology and medicine, the basic principles underlying blood flow reside firmly in physics and by implication in mathematics. I was convinced then and am even more convinced today that a good understanding of these principles is a necessary prerequisite for a study of the myriad of biological and medical phenomena involving fluids and fluid flow, particularly those relating to blood flow. This book, like the earlier two, is strongly fashioned by this conviction.

That is not to say that blood flow and related phenomena in health and in disease can be understood entirely within the spheres of mathematics and physics. Rather, it is to say that blood flow and related phenomena *cannot* be understood entirely within the spheres of physiology and medicine either. To students and teachers alike, this reality has always presented a dilemma: Which sphere does the subject belong to?

Electing to place the subject of blood flow in the spheres of mathematics and physics as we do in this book is not in any way a claim that the subject resides exclusively within these spheres, but rather that this is where the subject has its roots. In the spheres of physiology and medicine, by contrast, one is faced with "end-point" or "emergent" phenomena with unknown beginnings. Heart disease and stroke in all their forms, for example, are end-point phenomena, end results. They emerge at the end of a tortuous course of pathogeneses involving the cardiovascular system, the autonomic nervous system, and likely others. In each case there is an end-result but no clear beginning. The obvious temptation is to declare the observed pathology at hand as a beginning: a blocked artery, a ruptured aneurysm, high blood pressure, and then proceed from there to search for answers. The practicing clinician is well justified in yielding to this temptation rather than search for answers in the

¹Springer-Verlag, New York, 2000.

²Springer, New York, 2005.

xii Preface

spheres of mathematics and physics, but, alas, emergent phenomena rarely point the way to their origin because they have no unique origin. They result from a *confluence* of events each of which has its own beginning, not unlike the confluence of water tributaries converging onto a river.

The choice of where to place the subject of blood flow and related phenomena is therefore not a clear one and it is certainly not a matter of advantage of one choice over the other. The two choices, in fact, bear some *asymmetry*. In the spheres of mathematics and physics, one *constructs* scenarios that reach out like tentacles in the hope of finding some of the complex emergent phenomena observed in the living system. In the spheres of biology and medicine, one *deconstructs* the observed complex phenomena at hand in the hope of finding their roots in mathematics and physics. The first is clearly the easier of the two, and the scientist has the luxury of making that choice. The clinician does not have that luxury.

Thus, the choice made in this book of placing the subject of blood flow in the spheres of mathematics and physics is certainly less daunting than that of the practicing clinician, but it is predicated in the hope that the book may serve as an aide to the practicing clinician in his or her search for answers. In the least, it will introduce the clinician to the beautiful grounds in mathematics and physics where blood flow and related phenomena have their roots, not in terms of equations and formulas but in terms of a large amount of explanatory text which has been added specifically for the non-mathematical reader. To the mathematician, the physicist, and the engineer, the book will hopefully provide a useful compilation of those equations and formulas in a single source. To all readers, the book will hopefully provide a glimpse into the extraordinary way in which biology has made use of (or indeed invented?) the unique properties of fluids and fluid flow to serve the function of pulsatile blood flow and the cardiovascular system. One of my highest hopes is that the book will serve the full spectrum of readers who are interested in this subject.

I owe an apology to my clinical colleagues for appropriating the term "Hemodynamics" for the title of this book, as I am fully aware that the term is used somewhat differently in the clinical setting. My defense is that when stripped down to its literal elements, the term "hemo-dynamics" represents precisely what this book is about, namely the "dynamics of blood," with the emphasis being on "dynamics." For this reason, and to avoid confusion, the term has been hyphenated in the title.

I owe an apology also to my non-clinical colleagues for the absence of a comprehensive list of references to the enormous amount of work that has been done and is being done in the area of blood flow. This is not an omission but a deliberate decision that I have made, for three reasons. First, the book is not intended to be a *survey* of advances or recent developments in the subject, but rather a concise synthesis of its roots in mathematics and physics. Second, in an effort to make this synthesis as self-contained as possible, I chose to provide the required details wherever possible, rather than refer the reader elsewhere. The number of references is thus limited mainly to classical work or to the source of data that are being used to illustrate a specific result or phenomenon. Third, an outstanding list of references

Preface xiii

as well as a comprehensive survey of past and recent work in the field is available in the modern editions of McDonald's classical book on *Blood Flow in Arteries*.³ I am in awe of the breadth of that book and strongly recommend it for everything in which my book is lacking.

One of the ironies of modern science is that it has become so heavily aided by computer technology that "understanding" the subject of blood flow is becoming less and less necessary. Today, it is possible to solve many problems in blood flow and in fluid flow in general by using ready-made computer programs, without the need to delve into the details of the underlying mathematics and physics. Indeed, it is possible to bypass most, if not all, of the entire content of this book and yet solve problems in hemo-dynamics using readily available software designed specifically for the purpose. The irony in this development lies in that it is gradually eliminating the *need* to understand the subject. This is a great loss indeed, for there is a substantial amount of benefit and beauty in the process of understanding the intricacies of pulsatile blood flow and of fluid flow in general. I may be excused for lamenting these realities at the preface to a book devoted primarily to this purpose. I feel a sense of duty to inform the reader at the outset that he or she does not actually need this book if understanding the subject is not his or her main objective.

London, ON, Canada July 5, 2015 Mair Zamir

³Nichols WW, O'Rourk MF, Vlachopoulos C. McDonald's Blood Flow in Arteries. Hodder Arnold, UK, 2011.

Acknowledgment

I sincerely hope that this book will demonstrate that only the most elementary laws of physics and a moderate level of mathematics are needed to describe the dynamics of blood flow in all its complexity. This betrays both the beauty and the sad reality of the subject—the beauty of the simple analytical tools with which the subject can be described, and the sad reality that for far too long the subject has been practically inaccessible to those who need it most. My deepest hope is that in this book I have made the subject somewhat more accessible, and this I owe largely to the clinical colleagues I have worked with over the years, and to the wonderful students of all stripes who have asked questions.

The only "new" element that I will lay claim to in this book relates to my own understanding of the subject. I humbly confess that the main impetus for writing the book was a growing sense that I finally understand the subject, or at least that I now understand it better than I ever did before. And this better understanding, again, I owe largely to the people I have worked with and learned from over the past four decades or so.

I owe my training in fluid dynamics to two remarkable professors at the University of London: Alec D. Young and Ronald D. Milne, for instilling in me not only a deep understanding of fluid dynamics but also a sense of how important, indeed sacred, is *understanding* in the pursuit of science. It is due largely to Professor Milne, to whom I dedicate this book, that to this day I can never proceed from point A to point B without first fully understanding point A.

My first introduction to blood flow occurred here at my home university where I was fortunate to have on hand the first department of biophysics in the country, later renamed Medical Biophysics. I owe this introduction in the first place to Professor Margot R. Roach who presented me with the very "simple" question which anyone trained in fluid dynamics would feel a sense of duty to come up with an immediate answer: Why do brain aneurysms occur at vascular junctions? I also had the pleasure of working briefly with Professor Alan C. Burton who founded the department and who had similar "simple" questions which he thought mathematics should be able to answer. Hemodynamics was one of the principal subjects of interest in the early days of that department.

xvi Acknowledgment

For my introduction to the "grit" of blood flow, I am indebted to Professor Malcom D. Silver who made it possible for me to spend a sabbatical leave in his department of pathology at University Hospital here in London. The introduction marked a pivotal moment in my work not only for seeing the vascular system, particularly that of the heart, literally "in the flesh", but also for coming face to face, for the first time, with the wide gap between the mathematics and physics view of blood flow and the corresponding "clinical" view of the subject. I was not only puzzled but somewhat intimidated by this gap between the two views. Malcolm D. Silver, an outstanding pathologist with interest in heart disease and coronary blood flow, was firmly in the clinical camp (fortuitously, with the letters MD on both sides of his name!), while I was firmly in the physics and mathematics camp. He was looking at shades of pink in myocardial tissue to detect different forms of myocardial necrosis, while I was looking at branching angles in coronary vasculature in search of clues on branching architecture. It struck me then that this gap between the two camps should not or indeed cannot exist. How can there be two such disparate views of blood flow? Surely, biology did not assign the subject to one camp or the other. My struggle with this question persists to this day, as is reflected perhaps in much of this book.

My work in the Physiological Imaging Research Laboratory at the Mayo Clinic in Rochester, MN, in collaboration with its Director Professor Erik L. Ritman marked another pivotal moment in my understanding of blood flow. The wonderful facilities in that lab allowed us to probe further and further into the depths of vascular beds to the level of vasa vasora, the micro vessels that supply blood to the wall tissue of larger blood vessels. Having spent many years prior to coming to this lab searching desperately for some quantitative data on vascular branching, and struggling with the most primitive techniques I used for obtaining such data, Dr. Ritman's lab was a panacea for me. It provided me with a window on vasculature which was not available to me before and which opened my eyes to a deeper understanding of vascular architecture.

Some of the happiest years of my (academic) life were spent in the Neurovascular Research Laboratory in the Faculty of Health Sciences at this university in collaboration with its Director, Professor J. Kevin Shoemaker. Dr. Shoemaker provided me with the opportunity of not only working with some of the nicest people on the planet but also working on what I consider to be the next and most exciting frontier in the study of blood flow, namely that of the *control and regulation* of blood flow within the living body. In the world of mathematics and physics, we (myself included) tend to think that blood flow cannot be governed by anything other than the laws of physics. While this thinking is of course correct, it must be qualified when applied to blood flow in the living system where other factors come into play. Briefly, in the living system there are biological laws that control the laws of physics that control the flow of blood, not in the sense of biology *changing* the laws of physics but in the sense of biology *exploiting* the laws of physics to its own end. In hemodynamics, this interplay unfolds in the form of neural control of blood

Acknowledgment xvii

flow which I truly believe is the next most important frontier in the study of blood flow, and which is one of the principal frontiers being pursued in Dr. Shoemaker's lab.

Of course I must not forget my own home department of Applied Mathematics which provided me with an environment in which this interdisciplinary work was not only possible but also encouraged. Indeed I owe the very start of my work on blood flow to the chair and founder of the department of Applied Mathematics, Professor John H. Blackwell, who was responsible for introducing me to the then department of Biophysics. I owe much to all my colleagues in the department of Applied Mathematics for the continuous support and stimulation I received over the years.

Writing a single author book is a lonely undertaking. I am grateful to the "first responders" who kindly answered my call to read an early draft of the book and gave me their comments. For this I owe a debt of gratitude to Matthew Betty, Mario Gössl, Michael Joyner, Gerald Klassen, Katelyn Norton, Erik Ritman, Kevin Shoemaker, Charlotte Usselman, and Lindi Wahl. I owe special thanks to my wife, Lilian Zamir, who diligently proofread every word in the book, a particularly heroic act considering her fairly low level interest in the subject.

I owe very special thanks to Ian Craig for helping me with the nightmare of digitizing the figures that are such an important part of this book.

Finally, I owe gratitude to Elias Greenbaum, Chief Editor of the Biological and Medical Physics series who has been providing me with continuous support since the publication of the Physics of Pulsatile Blood Flow in 2000; to Christopher Coughlin and Ho Ying Fan at Springer New York for taking the book from concept to reality; and to Vijay Shanker for orchestrating the actual production of the book with admirable patience notwithstanding my interference.

Contents

1	Intro	duction	1			
	1.1	The Essence of Life Is <i>Not</i> Blood	1			
	1.2	Fluidity and the Fluid State	1			
	1.3	Life Without Fluids?	2			
	1.4	Mechanics of Fluids and Fluid Flow	4			
	1.5	Physics of Fluids and Fluid Flow	6			
	1.6	Continuum Concept: Sand Is Not a Fluid	7			
	1.7	Mathematical Basis of Fluid Flow	9			
2	Math	Mathematical Description of Fluid Flow				
	2.1	Introduction	13			
	2.2	Equations at a Point	13			
	2.3	Eulerian and Lagrangian Descriptions	15			
	2.4	Conservation of Mass: Equation of Continuity	17			
	2.5	Acceleration of Fluid Elements	21			
	2.6	Forces Acting on a Fluid Element	24			
	2.7	The Stress Tensor	25			
	2.8	Newton's Second Law "At a Point"	30			
	2.9	Mechanical Properties: Viscosity	31			
	2.10	Constitutive Equations	35			
	2.11	Navier-Stokes Equations	38			
3	Stead	ly Flow in a Tube	43			
	3.1	Introduction	43			
	3.2	Condition of "No-Slip"	45			
	3.3	Laminar and Turbulent Flow	47			
	3.4	Entry Length	50			
	3.5	Simplified Equations	53			
	3.6	Balance of Forces	56			
	3.7	Poiseuille Flow	57			
	3.8	Properties of Poiseuille Flow	60			
	3.9	Energy Expenditure and Pumping Power	64			

xx Contents

	3.10	Non Circular Cross Sections	67
	3.11	Cube Law	72
	3.12	Two Tubes or One?	75
4	Basic	Elements of Pulsatile Flow	81
	4.1	Introduction: Why Pulsatile?	81
	4.2	Pulsatile Poiseuille Flow	82
	4.3	Pulsatile = Steady + Oscillatory	84
	4.4	Using Complex Exponential Functions	86
	4.5	Bessel Equation and Solution	88
	4.6	Oscillatory Velocity Profiles	91
	4.7	Oscillatory Flow Rate	93
	4.8	Oscillatory Shear Stress	96
	4.9	Energy Expenditure and Pumping Power	98
	4.10	Oscillatory Flow at Low Frequency	103
	4.11	Oscillatory Flow at High Frequency	111
	4.12	Oscillatory Flow in Tubes of Elliptic Cross Sections	115
5	Pulsa	tile Flow in an Elastic Tube	123
	5.1	Introduction	123
	5.2	Wave Motion	124
	5.3	Equations Governing the Fluid Motion	130
	5.4	Solution of Flow Equations	131
	5.5	Elastic Wall Movement	133
	5.6	Equations Governing the Wall Motion	137
	5.7	Coupling of Fluid and Wall Motions	141
	5.8	Matching at the Fluid-Wall Interface	142
	5.9	Wave Speed ("Pulse Wave Velocity")	144
	5.10	Arbitrary Constants	148
	5.11	Properties of Pulsatile Flow in an Elastic Tube	150
6	Wave	Reflections	159
	6.1	Introduction	159
	6.2	One Dimensional Wave Equations	161
	6.3	Solution of Wave Equation	165
	6.4	Primary Wave Reflections	169
	6.5	Pressure-Flow Relations	173
	6.6	Effective Admittance/Impedance	180
	6.7	Reflection Coefficients	182
	6.8	Secondary Wave Reflections	185
7		in Branching Tubes	191
	7.1	Introduction	191
	7.2	Arterial Bifurcation	192
	7.3	Steady Flow Along Tubes in Series	198
	7.4	Steady Flow Through a Bifurcation	205
	7.5	Branching Tubes: <i>j</i> , <i>k</i> Notation	211

Contents xxi

	7.6	Steady Flow in Branching Tubes	215
	7.7	What Is an "Artery"?	224
	7.8	Pulsatile Flow in Branching Rigid Tubes	231
	7.9	Wave Speed in Branching Elastic Tubes	237
	7.10	Effective Impedance, Admittance	241
8	Dyna	mics of Pulsatile Blood Flow I	247
	8.1	Introduction	247
	8.2	The Lumped Parameter Concept	249
	8.3	Flow in a Tube Revisited	250
	8.4	Transient and Steady States	253
	8.5	Fluid Inertia: Inductance	255
	8.6	Elasticity of the Tube Wall: Compliance	266
	8.7	Mechanical Analogy	271
	8.8	Electrical Analogy	276
	8.9	Summary	279
9	Dyna	mics of Pulsatile Blood Flow II	283
	9.1	Introduction	283
	9.2	Pulsatile Blood Flow Revisited	284
	9.3	Resistive-Capacitive Interplay I	285
	9.4	The Capacitive Chamber	289
	9.5	Transient States	292
	9.6	Steady State Oscillations	296
	9.7	Full Dynamics of the Capacitive Chamber	297
	9.8	The Concept of Reactance	299
	9.9	Impedance, Complex Impedance	307
	9.10	Pressure-Flow Relations	311
10	Anal	ysis of Composite Waveforms	317
	10.1	Introduction	317
	10.2	Basic Theory	320
	10.3	Example: Single-Step Waveform	324
	10.4	Example: Piecewise Waveform	329
	10.5	Numerical Formulation	337
	10.6	Example: "Cardiac" Waveform	342
11	Dyna	mics of Pulsatile Blood Flow III	349
	11.1	Introduction	349
	11.2	Composite Pressure-Flow Relations	350
	11.3	Baseline Example: Pure Resistance	352
	11.4	Resistive-Capacitive Interplay II	357
	11.5	Resistive-Capacitive Interplay III	360
	11.6	Resistive-Capacitive Interplay IV	363
	11.7	Resistive-Capacitive Interplay V	366

xxii Contents

12	Dyna	mic Pathologies	375
	12.1	Introduction	375
	12.2	Swing in the Park	377
	12.3	Dynamic Markers I	378
	12.4	Dynamic Markers II	384
		Coronary Blood Flow	
Apj	pendix	A Viscosity: A Story	397
Apj	pendix	B Poiseuille Flow: A Story	399
Ind	ex		401

Chapter 1 Introduction

1.1 The Essence of Life Is *Not* Blood

It is remarkable how readily we accept the proposition that blood is the essence of life, our life. Yet we miss the point. The essence of life is not blood, it is blood *flow*. When the heart stops beating, the body dies not because of lack of blood but because of lack of *blood flow*. In most cases the dead body is still awash in blood, the same amount of blood as before, but this blood is of little use because it is not flowing.

The essence of life is not blood, it is blood flow.

Blood flow is the life-line to every living cell within our body. The driving force that maintains this life-line is of course the heart, by its pumping action, but what makes blood *able* to flow is its *fluidity*. The fluidity of blood is as essential to life as are the nutrients which blood carries. The scheme which biology has concocted for keeping our body alive is predicated entirely on the fluidity of blood, on the ability of blood to flow.

To be more accurate, therefore, the essence of our life is ultimately not blood but the fluidity of blood.

It is remarkable how readily we miss this point.

1.2 Fluidity and the Fluid State

It is so often said that life is not possible without air and water, without oxygen, hydrogen, nitrogen and carbon which air and water carry, but here again we miss the point, this time in a big way. It is somewhat like standing in awe in front of a painter and his masterpiece and declaring, correctly, that the essence of this masterpiece is the canvas and the paint. But would the canvas and the paint alone have produced

1

© Springer International Publishing Switzerland 2016 M. Zamir, *Hemo-Dynamics*, Biological and Medical Physics, Biomedical Engineering, DOI 10.1007/978-3-319-24103-6_1

2 1 Introduction

the painting? And would the chemical ingredients of air and water alone make life possible?

Life is not possible without air and water not only because of their chemical ingredients but also, in fact more so, because of the fluidity of air and water.

Fluidity is one of the most remarkable phenomena in nature, surpassed perhaps only by life itself. It is the closest-to-life phenomenon in the non-living world, and is more animated than some forms of life. The fluidity of air and water allows them to bend without the slightest effort, so much so in fact that it is inappropriate to use the term "bend" in this context. They squeeze through the most tortuous passages with ease and emerge fully collected. They are so compliant as to yield to the slightest force, and so acquiescent as to always fit the mold of their surroundings. No other (non-fluid) objects we know, animate or inanimate, are capable of such feats.

Air and water behave in this way not because of their chemical substance but because they are in the *fluid state*. Matter as we know it is commonly found in three distinct states which we call the solid, liquid, and gaseous states.¹

The word "fluid" as a noun or adjective is used in a generic manner to mean any substance in the fluid state. Any liquid or gas is referred to as a fluid. Though there are some differences between liquids and gases, they both posses the basic characteristics of the fluid state. When a substance is in the fluid state it exhibits a mode of behavior which is governed almost totally by the state, not the substance.

Some confusion between state and substance arises in everyday language. "Water" is strictly the name of a substance, not a state, but we use the word rather loosely to mean one or the other. There is solid water which we call ice, gaseous water which we call steam, and liquid water which we call simply "water" but actually mean "water in the liquid state". In the same way, while "rock" is strictly the name of a substance, we use the word rather loosely to mean "rock in the solid state". Indeed, on that basis we commonly use the expression "solid as a rock". But rock is not always in the solid state- in fact in the earth's interior it is permanently liquid. With equal justification, therefore, we could sometime use the expression "fluid as a rock".

1.3 Life Without Fluids?

Life as we know it is not possible without the fluid state. Not even in the realm of science fiction can we imagine a form of life of any degree of complexity without the fluid state. From amoebae to elephant, from fish to tree, and from the most primitive

¹Plasma is sometimes listed as a fourth state. It differs from the other states only in its *electrical* property. This property of the plasma component of blood is important in some processes but not in the *dynamics* of blood flow which is the main subject of this book. More important in blood flow is the *corpuscular composition of blood* as will be discussed in Sect. 2.9.

1.3 Life Without Fluids?

virus to man, none can exist without the fluid state. The more sophisticated forms of life depend even more on it. Humans are doomed to do nothing without it. It is remarkable how readily we miss the point that fluidity is as essential to life as is oxygen or DNA. Indeed, the evolution of life is so closely intertwined with fluids and fluid flow that it is not unreasonable to think of fluidity as an integral part of biology, and even wonder:

Did biology discover the fluid state or did it invent it?

Humans cannot breath, eat, move, reproduce or even think without the fluid state. When a man takes a breath, a large volume of air from all around him rushes towards his face and promptly threads itself through any opening that leads it towards the narrow passages of his lungs' airways. Through a maze of ever branching tree of smaller and smaller vessels, the fresh body of air meticulously divides itself into millions of thin separate streams which, like tentacles, reach for the inner compartments of the lungs. There, a little packet of air that fills each compartment makes a generous donation of oxygen,² then turns back immediately for its return journey. Millions of individual air packets now travel through the same tree of airways, but in reverse, moving from smaller to larger airways, and eventually out into the open. All of this is being accomplished in a most orderly manner, at every breath of every breathing man and woman, many thousand times every day. Imagine, if you will, how this could be accomplished without the fluid state.

Similar scenarios go on in almost every facet of life: blood flow, marine life and locomotion, food transport in plants, and the internal operation of the living cell, are but a few example. In the inanimate world of stars, planets, and non-living substances, the fluid state is equally pervasive. Our planet is composed of a fluid core. The sun and many other stars are entirely gaseous. The evolution of the universe involves key events which, if current theories on the subject are correct, would not have been possible without the fluid state. Interstellar gases and gaseous stars are as essential elements in the evolution of the universe as air and water were in the evolution of life.

Even the world of physics and chemistry would be somewhat incomplete without the fluid state. The laws of physics would be deprived of a fascinating field of application, and the laws of chemistry would have to wait much longer for the results of any chemical reaction in the absence of a fluid medium to facilitate mixing. The laws of mechanics find some of their most beautiful expressions in the behavior of fluids. Fluid motion, alas, is as different from the motion of a rigid object as the graceful movements of a ballet dancer are different from the chugging motion of a tank.

In the world of engineering and technology not much would seem possible without fluids. A steam engine, internal combustion engine, jet engine or any other form of engine without fluids? A rocket without fluids? A machine of any kind without a fluid lubricant? A nuclear reactor without fluids? And what form of

²Weibel ER. The Pathway For Oxygen. Harvard University Press, 1984.

4 1 Introduction

transport would be possible without engines on land, without water in the seas and without air in the skies? The feat of an aircraft in flight is only one of many examples of our technological use of the fluid state. The massive weight of an airliner in flight, with hundreds of passengers and their luggage on board, is carried entirely by air. The wings of the airliner are slightly bulged at the top and fairly flat at the bottom. As the wings move through the air, air particles on their upper surface are forced to move faster because of that bulge, and in so doing they create suction in the same way that blowing gently through our lips over a strip of paper causes it to lift up. The two phenomena are not only similar, they are precisely the same. In both cases the lifting force is suction created by speeding air over the top surface. This suction supports the enormous weight of the airliner during the entire flight. Tiny packets of air speeding relentlessly around the top surface of the wings to keep the airliner up: How would this be possible without the fluid state?

1.4 Mechanics of Fluids and Fluid Flow

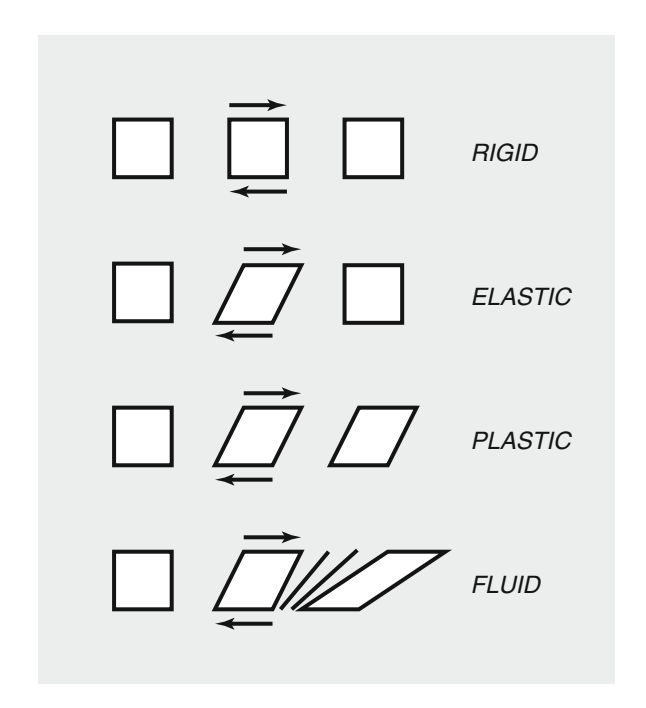
Fluidity is a mechanical wonder bordering on magic. We tend to overlook the phenomenon because our contact with fluids is so commonplace that we have become accustomed to the way they behave. But if we intentionally focus on a body of water as it wobbles or as it swirls, or a filament of smoke as it rises with exquisite grace, we will be struck by the question: How exactly does this happen? We do not normally ask this question, not because we know the answer but because we have become so accustomed to this behavior that we have come to expect it.

Fluidity is more than flexibility. A spring is flexible, the branch of a tree is flexible, putty and dough are very flexible, but none can flow. None can squeeze through the minute airways of the lungs or the maze of blood vessels of the cardiovascular system with the same grace and efficiency as do air, water and blood. Fluids are all of flexible, limber, pliable and supple, yet none of these terms adequately describes fluidity. The elements of a fluid body appear to be not at all constrained by each other, yet they are somehow held together. They move far apart, yet do not tear apart. What is the quality of fluids that allows them to do all that? What is fluidity?

To address the second question first, fluidity has to do with the "mechanical behavior" of material objects, that is the manner in which they respond to the application of a deforming force, a force attempting to change their shape. Rigidity, flexibility, pliability and fluidity are all to do with the way different objects respond when an attempt is made to change their shape. A simple test of mechanical behavior consists of subjecting a material body to a deforming force, the force is applied momentarily and then removed as illustrated in Fig. 1.1. When this test is applied to deformable bodies of different materials it is found that there are three main types of behavior after the deforming force has been removed: the body may (i) return to its original shape, (ii) remain in its deformed shape, or (iii) continue to deform.

• An elastic band, a spring, rubber, jelly, the branch of a tree or the wing of an aircraft will all bend or deform under the action of a deforming force, then regain

Fig. 1.1 Mechanical classification of material bodies. An initially rectangular body (left column) is subjected to a shearing force (middle column), then the force is removed (right column). A rigid body does not deform at all under the action of the force. An elastic body deforms under the action of the force but regains its shape when the force is removed. A plastic body deforms under the action of the force and remains in the deformed state when the force is removed. A fluid body deforms under the action of the force and continues to deform even after the force is removed.



their original shape when the force has been removed. This mechanical behavior is known as "elasticity".

- Putty, dough, plasticine and some soft metals will deform under the action of a deforming force and remain in their deformed shape after the force has been removed. This mechanical behavior is known as "plasticity".
- Water, air, blood or milk, will deform under the action of a deforming force and continue to deform even after the force has been removed. This mechanical behavior is known as "fluidity".

How do we know when a body of air or water is deforming? By observing the waves on the surface of water as we disturb it; the distortions of visible bodies of smoke, steam and the like, or clouds as they move; and the spinning pattern on the surface of coffee in a cup or water above the drain in a bath tub. In each case a force has been applied to deform the fluid, and the fluid continues to deform even after the force has been removed. Walking through air, or heating it as in the case of rising smoke, causes it to deform. Swimming or stirring a cup of coffee causes the liquid to deform. In each case the force of our action produces the initial deformation, but the fluid continues to deform, continues to move, even after our action has ceased.

It may seem odd to describe jelly or a rubber band as an elastic "solid", but this is only because we often confuse solidity with rigidity. In mechanics the term "solid" is an antonym of the term "fluid". "Solid" means "not fluid". Rigidity, on the other hand, has to do with the *degree* of elasticity, namely the amount of force required to produce a given amount of deformation. Rubber and steel are both elastic solids

6 1 Introduction

since they both deform under the action of a force and then regain their shape after the force has been removed. The difference between the two is only in the amount of force required to produce a given amount of deformation. In common language the term "rigidity" is used loosely to describe this difference, thus we say steel is more rigid than rubber. However, in the more accurate language of mechanics the term "rigid" is reserved for the ultimate extreme in which a body cannot be deformed at all, no matter how high the applied force. Diamond comes close to this extreme.

In the yet more accurate and somewhat strange language of mathematics, to say that an object cannot be deformed is the same as saying that the object requires an infinite amount of force to deform it or, equivalently, that it offers an infinite amount of resistance to deformation. This play of words is in fact useful because it brings out another extraordinary mechanical feature of fluids and fluidity. If rigidity is thought of as a scale on which objects are placed according to the amount of force which they require to be deformed or, equivalently, according to the amount of resistance to deformation which they offer, then fluids fit at the very bottom of that scale.

One of the most remarkable properties of fluids is that they offer barely any resistance to deformation, practically zero, and therefore the force which they require to be deformed is also practically zero.

Fluids are at the bottom of the rigidity scale also because the amount of deformation which a fluid body can undergo is unlimited. No other material objects behave in this way. Elastic or plastic solids have a limit beyond which they cease to behave as elastic or plastic solids, and may break or yield to another form of behavior thereafter. An elastic band will eventually snap if stretched beyond this limit and a bridge will collapse if its structure is deformed beyond its limit. Interestingly, an elastic object may yield to plastic behavior first and then break. A spring stretched beyond the limit of its "springiness" is a good example. A fluid object has no such limits. It can be deformed indefinitely.

Indeed, "flow" is nothing but a state of continuous deformation.

Thus, zero rigidity, zero resistance to deformation and no limit to the amount of possible deformation are the hallmarks of the fluid state. Fluidity is the embodiment of these remarkable properties.

1.5 Physics of Fluids and Fluid Flow

Now to address the first question posed earlier: What is the quality of fluids that allows them to do all that? What makes fluids fluid and solids solid? How can fluids behave in the remarkable way that they do?

The answers to these questions lie in the molecular structure of matter, solid or fluid alike. The molecules comprising a material body are not cemented together like bricks, nor physically connected to each other in any way. They are in fact separated from each other by vast amounts of space, not unlike the objects we see in the sky. While they are completely detached, however, they are not entirely free

from each other. There is a force of attraction between them, which makes them want to move towards each other, and a force of repulsion, which makes them want to move away from each other. Both forces are in effect simultaneously and at all times. A molecule surrounded by a few others is thus trapped by these two opposing forces as they relate to each one of its neighbors. Forces are constantly pulling and pushing it as it makes a move in any direction. It and its neighbors are in constant wobble as a result, like a group of exotic dancers packed together in a dance hall.

How then does a material body, being as exceedingly sparse as this, hold itself together? How does this strange world lead the the mechanical behavior of material objects and in particular to the difference between solid and fluid objects described earlier? What is fluidity on the molecular scale?

The answers to these questions lie in the precarious balance between the attractive and repulsive forces that hold molecules together within a material body.³ Briefly, the degree to which the molecules are confined to their positions within the body, under this balance of forces, determines the degree to which a material body holds itself together. It is this that determines the mechanical behavior of the body as we encounter it on our larger scale. It is this that makes fluids fluid and solids solid.

When a material body is in the solid state it is believed that the balance between repulsive and attractive forces among its molecules is such that each molecule is completely imprisoned by its neighbors, unable to break away from them or from the position to which it is confined.

In the fluid state it is believed that the repulsive and attractive forces between molecules are so precariously balanced that either single molecules or groups of molecules are able to break away from each other and wander freely from one position to another within their host body.

Thus, a material body in the solid state is rigid and hard to break or manipulate because its molecules, particularly groups of molecules, cannot break away from each other or move from one part of the body to another. A material body in the fluid state is supple and easy to manipulate because its molecules are fairly free from each other and free to move about within the body.

1.6 Continuum Concept: Sand Is Not a Fluid

The loose molecular structure of fluids is what gives them their fluidity and enables them to flow. It enables them to be in a state of continuous deformation. Yet, flow is a contradiction. While fluidity points to how loosely a fluid body is held together, flow points to how well a fluid body in fact stays together as it moves. When a fluid body is at rest, we are struck by the ease with which it can be disturbed, the ease with which it can be deformed and manipulated. This suggests that the body might

³Goldstein DL. States of Matter. Dover Publications, 2014.

8 1 Introduction

easily disintegrate or fall apart. Yet when the body flows, it is together at all times. It does not fall apart.

A body of sand falls apart as it "flows". When sand is poured and it appears to be flowing, it is not actually flowing. The body of sand is not together as it moves. The grains of sand are completely detached from each other and their motion consists of sliding and toppling over each other. What actually occurs when sand is poured is a landslide, or an avalanche. It is not flow.

When a fluid body flows, by contrast, its elements are not detached from each other. They do not slide or topple over each other. The body is whole and integral at all times and its elements are in complete contact with each other as the body moves. To make sand behave this way, every grain of sand must be made infinitely flexible, stretchable and deformable. Then the grains must be somehow attached to each other so that they would be in complete contact with each other as they move, with no empty gaps between them.

The ability of a fluid body to stay together as it moves, even though its molecules are so far apart and so loosely held together, is at the core of fluidity and fluid flow. While on the molecular or "microscopic" scale there are large gaps between molecules, on the larger "macroscopic" scale there are no such gaps between small chunks or "elements" of the fluid as there are between grains of sand.

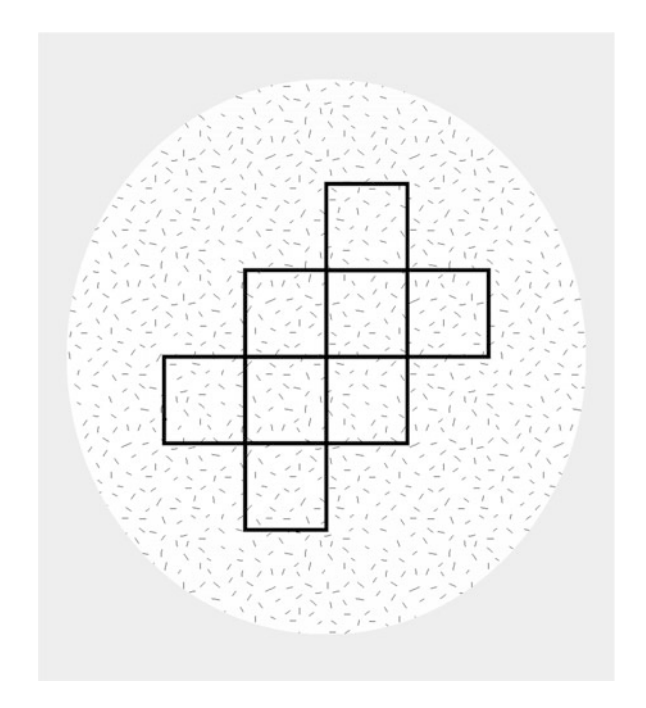
We may think of the microscopic scale as the scale on which molecules are visible and the macroscopic scale as the scale on which grains of sand are visible. The difference between these two scales is enormous because one cubic millimeter of air under standard temperature and pressure, for example, contains approximately 10^{16} molecules. Thus, if a grain of sand is considered to be one thousandths or even one millionth of a cubic millimeter, a volume of air of this size would still contain 10^{10} molecules. Thus a volume of fluid of this minute size contains a sufficient number of molecules to retain its fluidity and behave as a fluid.

On this basis the molecular structure of fluids can be abandoned in favor of a view on the macroscopic scale where a fluid body can be thought of as consisting of small "elements" which are completely continuous with each other (Fig. 1.2).

This view of a fluid body as a "continuum" has been pivotal in the study of fluids and fluid flow because it enabled a mathematical description and analysis of fluidity and fluid flow which would not be possible on the microscopic scale. Fluids not only conform perfectly with this continuum model but they maintain it at all times as they move. Sand is not a continuum since its elements are not continuous with each other. Sand does not flow since its elements lose touch with each other as the body of sand moves. A fluid body on the macroscopic scale is viewed as consisting of minute elements that are continuous with each other in favor of a view on the microscopic scale where it has a vastly discontinuous molecular structure.

The validity of the continuum view of fluids rests on the fact that a fluid element is exceedingly large on the microscopic scale and exceedingly small on the macroscopic scale.

Fig. 1.2 The concept of fluid as a continuum. On the microscopic scale a fluid body consists of a discontinuous collection of molecules. On the macroscopic scale we view it as a continuous collection of elements. The figure depicts the relation between the two scales only in concept, not in proportion, because the difference between the two scales is much too large to be shown in the same figure.



1.7 Mathematical Basis of Fluid Flow

Newton's laws of motion provide the basis for a mathematical description of the motion of material objects, but in their most basic form the laws can be applied only if the object is moving as a whole, "en masse", as a stone or a rock. More precisely, the laws are actually concerned with only the mass of the object, as in

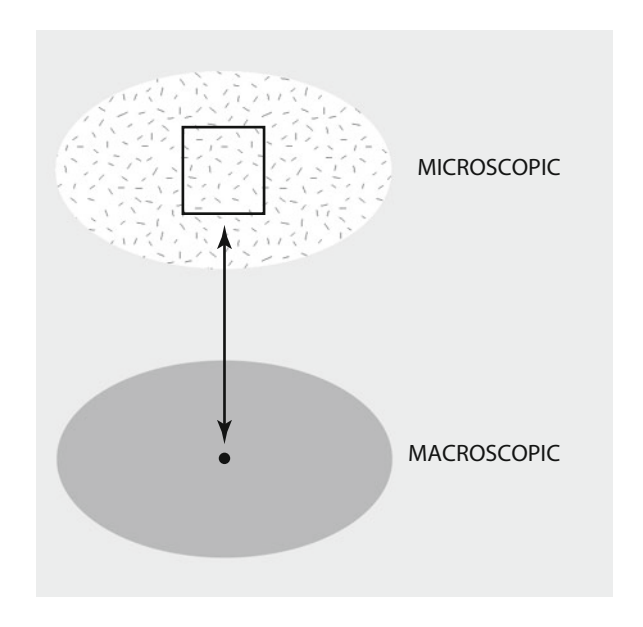
$$force = mass \times acceleration$$
 (1.1)

with no reference to or acknowledgment of different parts of the object.

The laws of motion as they stand, therefore, cannot be applied directly to a body of fluid in motion because a body of fluid rarely moves *en masse*. A bucket full of water, lifted ever so slowly so as not to disturb the water within, is an example of a body of fluid moving *en masse*, but this scenario is hardly typical of a body of fluid in motion. Typically, indeed almost invariably, a body of fluid is in a state of flow, a state in which different parts of the body are moving at different speeds or in different directions or both. Very rarely do we find a body of air, water, or indeed blood, moving *en masse*. This is because, as we noted earlier, a body of fluid offers zero resistance to deformation, thus any small external force will cause it to deform and continue to deform even after the force has been removed. When a spoon stirring the coffee in a cup is removed, the coffee does not stop turning. How and why does it *ever* stop? We find out later.

10 1 Introduction

Fig. 1.3 A fluid element on the microscopic scale becomes a "point" on the macroscopic scale. Equations governing the mechanics of fluid elements therefore become "point equations" on the macroscopic scale. They govern conditions at every point in a flow field, on the macroscopic scale.



For a mathematical description of a fluid body in motion, therefore, the laws of motion must be applied not globally to the body as a whole but individually to every small part of the body.

How small should the part of the body be? This question has in fact already been answered in our earlier discussion of a fluid body as a continuum. The laws of motion must be applied to what we have referred to as fluid "elements" which, as we recall, are very small on the macroscopic scale but very large on the microscopic (molecular) scale.

In fact, a fluid element is so small on the macrosopic scale that it can be treated as a "point" within the fluid body, as illustrated in Fig. 1.3. And since the fluid body is being treated as a continuum where fluid elements are contiguous with each other, then the "points" representing these elements within the fluid body are contiguous with each other.

The continuum view of fluids therefore enables the use of continuous mathematical functions to navigate through different parts of a fluid body because every point of a given mathematical function describing some property within the body of fluid can now be identified with a geometrical position within that body as well as a fluid element occupying that position that has mass which the laws of motion can be applied to.

The notion that a "point" has mass may seem at odds with the mathematical concept of a point, but the difficulty is only one of semantics. We shall avoid this difficulty by defining a point within a fluid body as either

- (a) a geometrical position within the space occupied by the fluid body, or
- (b) a fluid element occupying that position.

To avoid confusion between the two we may use the explicit terms "geometrical point" and "material point" respectively, but in most cases the intended meaning will be sufficiently clear so that we dispense with the adjectives. In the way of notation, in rectangular Cartesian coordinates for example, we shall keep the distinction between the two by using (x, y, z) to denote the geometrical point at these coordinates and (X, Y, Z) to denote the corresponding material point at the same coordinates. As before, the two coordinate systems shall be referred to as "position coordinates" and "material coordinates", respectively.

These conventions lay the grounds for applying the laws of motion to every material point within a body of fluid, but the laws require further that the mass of these material points be specified. One of the most remarkable triumphs of the continuum view of fluids and its cornerstone concept of a fluid element is that, as we shall see later, it enables the application of the laws of motion to every element of the body, in other words at every point within the body, without having to specify explicitly the mass or volume present at that point. This is accomplished by defining the *density* $\rho(x, y, z)$ at a point, which in turn is done by considering a volume V surrounding the point (x, y, z) and containing a mass M of fluid (Fig. 1.3), then writing

$$\rho(x, y, z) = \lim_{V \to v} \left(\frac{M}{V}\right) = \frac{m}{v}$$
 (1.2)

where m and v are respectively the mass and volume of the fluid element at (x, y, z). The limit does not go to zero because the smallest volume of fluid which we recognize on the continuum scale is that of a fluid element. But since the density $\rho(x, y, z)$ is to be represented mathematically by a continuous function on the continuum scale where a fluid element is represented by a (material) point, then the limit in Eq. 1.2 can be written appropriately as

$$\rho(x, y, z) = \lim_{V \to 0} \left(\frac{M}{V}\right) \tag{1.3}$$

We shall find in the next chapter that the limit in Eq. 1.3, which contains neither the mass nor volume of the fluid element at (x, y, z), can be applied in the same way to the forces acting on that element. Thus the laws governing the motion of individual fluid elements within a body of fluid can be applied without having to specify explicitly either the mass or volume of these elements.

Chapter 2 Mathematical Description of Fluid Flow

2.1 Introduction

With the grounds laid in Sect. 1.7, we are now in a position to apply the laws of motion at every point within a body of fluid. The equations of motion obtained in this way can be thought of as *point equations* in the sense that they do not govern the motion of the fluid body as a whole but the motion of individual material points (fluid elements) within that body.

2.2 Equations at a Point

Since within a body of fluid material points are continuous with each other, both the governing equations and their solutions can be expressed mathematically in terms of continuous functions whose range of values covers the entire fluid body to describe the motion of every material point within it. The result is a description of a *motion field*. Compared with the motion of the single object governed by Eq. 1.1, a motion field is somewhat like a map of the motion of many objects governed by a simple extension of Eq. 1.1, namely

force
$$(x, y, z) = mass(x, y, z) \times acceleration(x, y, z)$$
 (2.1)

The law is being applied at every position (x, y, z) within the fluid body, and the solution of the equation will yield the motion of the fluid elements identified with these positions.

Equation 2.1 is actually not quite workable yet because when the fluid body is in motion the fluid elements identified with the positions (x, y, z) are at these positions only at a particular point in time. At a later point in time their positions will have changed. What is required is to lock in the identity of fluid elements

so that they can be followed as they move. We can do that by using the concept and notation of "position coordinates x, y, z" and "material coordinates X, Y, Z" introduced in Sect. 1.7, whereby (X, Y, Z) is used to identify the fluid element in coordinate position (x, y, z) within the fluid body. For example, (III, I, IV) shall denote the identity or label of the fluid element in coordinate position (3, 1, 4), etc.

However, the above scheme is workable only when the body of fluid is not moving and all fluid elements identified with their coordinate positions remain in these positions. When the body of fluid is in motion, the coordinate positions of fluid elements are continuously changing. What we must do in this case is recognize that (X, Y, Z) is now simply a label of an object in motion whose coordinate position at time t is given by

$$\begin{cases} X = X(x, y, z, t) \\ Y = Y(x, y, z, t) \\ Z = Z(x, y, z, t) \end{cases}$$
(2.2)

This equation reads:

(X, Y, Z) is the fluid element whose coordinate position at time t is (x, y, z).

In particular, if we consider the motion to have started at time t = 0, then the *initial* position of that fluid element is given by

$$\begin{cases} X_0 = X(x, y, z, 0) = x \\ Y_0 = Y(x, y, z, 0) = y \\ Z_0 = Z(x, y, z, 0) = z \end{cases}$$
 (2.3)

as in the above example where we had x = 3, y = 1, z = 4 and X = III, Y = I, Z = IV.

It is now clear that the laws of motion within a body of fluid must be applied not at *coordinate positions* (x, y, z) within the body but to *fluid elements* (X, Y, Z). Accordingly, Eq. 2.1 must finally be written more appropriately as

force
$$(X, Y, Z) = mass(X, Y, Z) \times acceleration(X, Y, Z)$$
 (2.4)

Equation 2.4 highlights the difference between an application of the laws of motion to a single isolated object and to a fluid element within a body of fluid. In the case of a single isolated object in motion as, for example, the motion of a stone thrown up against gravity, there is no issue regarding the identity of the object, and the motion is governed by Eq. 1.1. In the case of a fluid element in motion, the identity of the element is required because the ultimate aim is to construct a *motion field* which involves all the elements within a fluid body.

Furthermore, in the case of a single isolated object in motion the mass of the object and the force acting on it will generally be given, thus the acceleration can be readily calculated. In the case of a fluid element in motion the following difficulties arise:

- (i) The force acting on a fluid element within a fluid body is not known because the element is continuous with other fluid elements which exert forces on each other apart from any external force that is driving the motion.
- (ii) As discussed in Sect. 1.7, the mass of a fluid element within a body of fluid is not known explicitly and, in any case, it would not be practical or useful to specify the mass or volume of all the elements within the fluid body.
- (iii) The acceleration of a fluid element in motion is not easily determined because, as we see later, the motion of the element is not being tracked individually as in the case of a single isolated object in motion. Instead, the motions of all elements within the fluid body are tracked collectively in terms of instantaneous "snapshots" of the motion field as a whole.

These difficulties are addressed in the remaining sections of the present chapter. It is remarkable that an entire chapter is actually needed to do no more than apply the most basic law of motion to the elements of a fluid body in motion. The equations governing that collective motion, or motion field, indeed represent nothing more than an application of Eq. 1.1 to different elements of the fluid body. The difficulties listed above are not with the physical principles involved but with the mathematical expression of these principles within the confines of a fluid body.

2.3 Eulerian and Lagrangian Descriptions

It would seem overwhelming to track the motion of every (material) point within a body of fluid to get a complete picture of the motion field within that body. There are two different ways of doing so, generally referred to as the Lagrangian and the Eulerian methods.

In the Lagrangian method the initial position of each fluid element is recorded and then the motion of each element is followed individually as in the case of a single isolated object in motion. In particular, the velocity of each element under this scheme will be a function of time only, again as in the case of a single isolated object in motion. However, the aggregate of all such velocities within the body of fluid will be a function of time and of the *identity* of each element because, unlike the case of an isolated object in motion, we are now dealing with a *motion field*, that is the simultaneous motion of all the fluid elements within the body of fluid.

The initial positions of fluid elements, namely their position coordinates before the motion started, are used as their identities. Thus, in rectangular Coordinates x, y, z these will be denoted by X_0, Y_0, Z_0 as in Eq. 2.3. The velocities of these individual fluid elements are then referred to as "Lagrangian velocities" because they track the motion of each fluid element individually. If the components of these

velocities in the x, y, z directions are denoted by U, V, W, respectively, then these will clearly be functions of the identities of the fluid elements which they represent and of time t, i.e.

$$\begin{cases} U = U(X_0, Y_0, Z_0, t) \\ V = V(X_0, Y_0, Z_0, t) \\ W = W(X_0, Y_0, Z_0, t) \end{cases}$$
 (2.5)

Each set of values X_0 , Y_0 , Z_0 identifies a particular element (material point) within the fluid body, then the Lagrangian velocity components U, V, W describe the motion of that particular element at different points in time t.

While this method of describing a body of fluid in motion seems logical, it is actually impractical. The requirement that each element (material point) within the fluid body be associated with a unique label is extremely difficult to meet in practice, and this requirement is also inconsistent with the continuum view of a fluid body as being composed of fairly generic "pieces" rather than distinct identifiable objects. Under the continuum concept, a fluid element is imagined to be somewhat like a "bag of molecules" contiguous with other bags of molecules all around it. The shapes of these bags of molecules are not defined and the borders between them are not real borders- they are only imagined for the purpose of defining a fluid element.

These difficulties are demonstrated clearly in practice when an attempt is made to actually follow the motion of an individual element within a body of fluid, which can be done, for example, by attaching color to a small "blob" of fluid and then tracking its motion. The result will come close to tracking the motion of a fluid element, although the size of the blob will likely be such that it will encompass not one but many thousands of fluid elements. Furthermore, because the borders of the blob as well as the borders between individual fluid elements do not actually exist, the color will ultimately diffuse to other parts of the fluid body.

In summary, the Lagrangian method of describing a body of fluid in motion may seem to be a fairly logical extension of the method of describing the motion of a single isolated object, but in practice it challenges the concept of a fluid element by taking that concept beyond its intended limits. The method is also almost intractable because of the large number of (ill-defined) fluid elements that must be identified and tracked individually. While this can be done mathematically, and is indeed done in some applications, the utility of the method is highly limited.

The second way in which the motion field within a fluid body can be mapped, which is known as the "Eulerian method", is based not on the motion of identifiable fluid elements but on the motion recorded at fixed *coordinate positions* (x, y, z) within the space occupied by the fluid body. In rectangular Cartesian coordinates, if the motion is recorded in terms of velocity components u, v, w in the x, y, z directions, respectively, then these so called Eulerian velocities will be functions of x, y, z and t, i.e.

$$\begin{cases} u = u(x, y, z, t) \\ v = v(x, y, z, t) \\ w = w(x, y, z, t) \end{cases}$$
 (2.6)

The most important difference here is that the identities of fluid elements and hence their initial positions are not involved. Thus, u(2, 1, 4, t) is the velocity measured at (fixed) position x = 2, y = 1, z = 4 at time t within the motion field. Since at different times this coordinate position is occupied by different fluid elements, the Eulerian velocities at a point in a flow field do not represent the velocities of the *same* fluid element. They represent the velocities of different elements which occupy that position at different times.

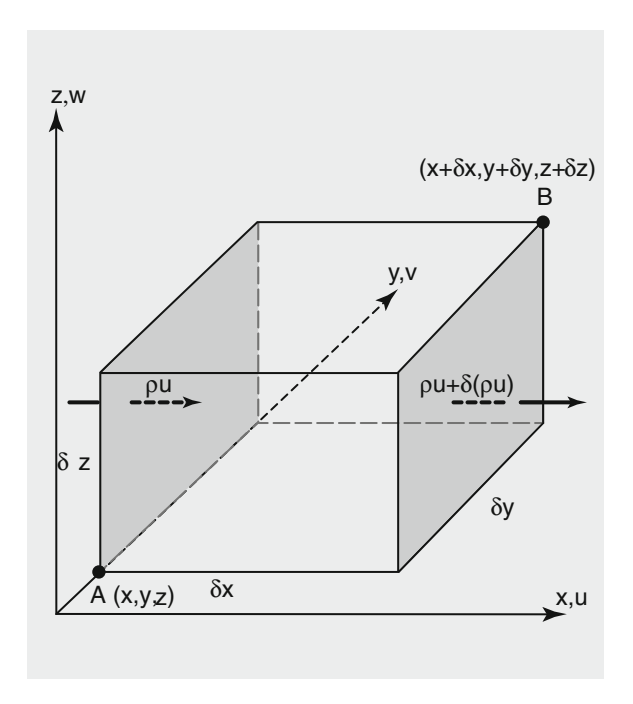
How then does one apply the laws of motion in terms of Eulerian velocity, because the laws in their basic form apply only to a single identifiable object in motion? Eulerian velocities represent the motion of different unidentifiable objects. We shall find that the difficulties involved in answering this question are both mathematical and conceptual but they are surmountable.

In summary, while Eulerian velocities seem less logical and less easy to interpret, they are the velocities of choice in most fluid flow problems because their practicality far outweighs the conceptual and analytical difficulties which they entail. The practicality results from the ease with which the velocities can be measured at specific coordinate positions within a flow field, by simply placing instruments at the required positions. And the analysis of fluid flow problems is more meaningful in terms of Eulerian velocities because in practice it is these velocities that we would normally be interested in: the velocities at this or that point in a flow field, rather than the velocities of this or that identifiable fluid element.

2.4 Conservation of Mass: Equation of Continuity

The continuum view of fluids introduced in Sect. 1.6 requires that a fluid body remains continuous as it moves, at all times and at every point within the body. Another way of looking at this requirement is in terms of the mass of the fluid body. For the fluid body to remain continuous, its mass must be conserved not only as a whole but at every "point" within the body. Conservation of mass, of course, is a "sacred" law of physics but the notion of *conservation of mass at a point* may seem odd. However, if we recall that every point within a fluid body is a *material point*, a fluid element, then the requirement that mass must be conserved at every point within a body of fluid should not seem odd. It is simply the requirement that the mass of fluid elements be conserved. For a body of fluid to remain continuous at all times, this requirement must be satisfied particularly when the body of fluid is in motion.

Fig. 2.1 Conservation of mass. Rates of mass flow entering three sides of a box formed by coordinate surfaces are shown. If the same flow rates leave the box through the opposite three sides, the net mass change within the box is zero. In general the rates will be different, however, because of changes in velocities or density. Conservation of mass requires that the difference between rates of mass flow into and out of the box be equal to the rate of change of mass of fluid within the box. As the box is shrunk to a point, this requirement becomes an equation of conservation of mass at a "point".



To apply this requirement at a point, meaning to a fluid element, within a body of fluid in motion, we consider a fixed volume of the fluid body in the form of a closed rectangular box surrounding that point, then require that the mass contained within the box be conserved. Of course, because the body of fluid as a whole is in motion, some fluid will flow into and out of the box at different times. Thus, to satisfy conservation of mass within the box, the mass flow into and out of the box must add up to zero. Then, to satisfy conservation of mass *at a point*, we simply allow the volume of the box to shrink to the volume of a fluid element.

In a rectangular Cartesian coordinate system x, y, z, we consider a rectangular box defined by $\delta x, \delta y, \delta z$ as shown in Fig. 2.1. The volume V of the box is given by

$$V = \delta x \delta y \delta z \tag{2.7}$$

and the mass M contained within this volume is

$$M \approx \rho V$$
 (2.8)

where ρ is the fluid density, which may vary within the box, hence the equality is only approximate.

Mass within the box will change as flow enters and leaves the different sides of the box. Because of the way these sides are oriented with respect to the coordinate axes, each side of the box will be affected by only one of the velocity components u, v, w as shown in Fig. 2.1, the other two being tangential to it and hence do not contribute to mass flow through it. Thus, in the x direction, mass will enter the box

at a rate $\rho u \delta y \delta z$ and leave at a rate $\rho(u + \delta u) \delta y \delta z$. The only difference between the two is in the incremental velocity change δu due to a possible change in the velocity component u from point x to point $x + \delta x$, recalling that the velocity u is a function of position x, y, z and time t (Eq. 2.6). A change of u in time t is of no concern here since we are comparing the two values of the velocity at the same moment in time.

Thus the balance of mass flow into and out of the box in the *x* direction can be expressed as

$$\underbrace{\rho u \delta y \delta z}_{\text{in}} - \underbrace{(\rho u + \delta(\rho u)) \delta y \delta z}_{\text{out}} \approx -\underbrace{\delta(\rho u) \delta y \delta z}_{\text{net}}$$
(2.9)

The equality is approximate because the values of ρ and u may vary over the $\delta y \delta z$ sides of the box and are here taken only as average values. The equality becomes exact when the volume of the box is allowed to shrink to the volume of a fluid element, which on the continuum scale is a point, and the values of ρ and u become their exact values at that point.

The incremental change $\delta(\rho u)$ represents a possible change in the product ρu in the *x* direction only, which can be written as

$$\delta(\rho u) = \frac{\partial(\rho u)}{\partial x} \delta x \tag{2.10}$$

and the net rate of mass flow into the box in the x direction thus becomes

$$-\frac{\partial(\rho u)}{\partial x}\delta x\delta y\delta z\tag{2.11}$$

If ρ and u are constant, the gradient of ρu will be zero and there will be no net rate of change of mass within the box resulting from flow in the x direction. The minus sign indicates that if the gradient of ρu is positive, mass is leaving the box at a higher rate than that entering the box and hence the net result is negative. Conversely, the result will be positive if the gradient of ρu is negative.

Repeating this entire process in the y and z directions, we find similarly that the net rates of mass flow into the box in these two directions are respectively given by

$$-\frac{\partial(\rho v)}{\partial y}\delta x\delta y\delta z\tag{2.12}$$

and

$$-\frac{\partial(\rho w)}{\partial z}\delta x\delta y\delta z\tag{2.13}$$

Conservation of mass requires that the total of these net rates of mass flow be equal to the rate of change of mass within the box.

$$-\left(\frac{\partial(\rho u)}{\partial x} + \frac{\partial(\rho v)}{\partial y} + \frac{\partial(\rho w)}{\partial z}\right) \delta x \delta y \delta z \approx \frac{\partial M}{\partial t}$$
 (2.14)

Now, mass contained within the box is equal to the product of density ρ and volume δV of the box (Eq. 2.8), where

$$\delta V = \delta x \delta y \delta z \tag{2.15}$$

Since the volume of the box is fixed, the rate of change of mass within the box is simply the rate of change of density times the volume of the box, i.e.

$$\frac{\partial M}{\partial t} = \frac{\partial \rho}{\partial t} \delta x \delta y \delta z \tag{2.16}$$

Thus, finally, conservation of mass requires

$$-\left(\frac{\partial(\rho u)}{\partial x} + \frac{\partial(\rho v)}{\partial y} + \frac{\partial(\rho w)}{\partial z}\right)\delta x \delta y \delta z \approx \frac{\partial \rho}{\partial t}\delta x \delta y \delta z \tag{2.17}$$

Since the volume of the box, $\delta x \delta y \delta z$, is a factor on both sides, it can be divided out. Furthermore, if at the same time the volume of the box is now allowed to shrink to the volume of a fluid element, in other words to shrink to a point, the density and velocities become the density ρ and velocities u, v, w at that point. The equality thus becomes exact, and we obtain

$$\frac{\partial \rho}{\partial t} + \frac{\partial (\rho u)}{\partial x} + \frac{\partial (\rho v)}{\partial y} + \frac{\partial (\rho w)}{\partial z} = 0$$
 (2.18)

Since the velocity components u, v, w and the density ρ are functions of position x, y, z, this equation represents the law of conservation of mass $at\ a\ point$ within a body of fluid in motion. However, since a "point" on the continuum scale is a material point which represents a fluid element, Eq. 2.18 represents the law of conservation of mass applied to a fluid element within a body of fluid in motion.

What is remarkable about Eq. 2.18 is that it represents conservation of mass of a fluid element, yet it does not contain either the mass or volume of that element. Instead, the equation contains only the density at a point which, as we recall (Eq. 1.3), represents the average density of the fluid element at that point. Furthermore, if the density is constant in time, the equation becomes

$$\frac{\partial(\rho u)}{\partial x} + \frac{\partial(\rho v)}{\partial y} + \frac{\partial(\rho w)}{\partial z} = 0 \tag{2.19}$$

and if, finally, the density is constant throughout the fluid body, the equation reduces further to

$$\frac{\partial u}{\partial x} + \frac{\partial v}{\partial y} + \frac{\partial w}{\partial z} = 0 {(2.20)}$$

Equations 2.18, 2.19, 2.20 represent unique expressions of the law of conservation of mass for a fluid body in motion. The expressions are unique because they apply the law not to the fluid body as a whole but *at every point* within that

body, which means to every fluid element within the body. The equations are also remarkable in that they ensure the conservation of mass of a fluid element, yet they do not contain the mass, volume, or shape of that element. The last form of the equation, Eq. 2.20, is particularly remarkable because it expresses the law of conservation of mass at every point within the fluid body in terms of only the Eulerian velocities at each point.

These mathematical feats represent a triumph of the continuum concept and of the concept of a fluid element. Equations 2.18, 2.19, 2.20 are only possible if the fluid body can be treated as a continuum, and the fluid body can be treated as a continuum only by using the concept of a fluid element. For these reasons, Eqs. 2.18, 2.19, 2.20 are often referred to as "equations of continuity" rather than equations of conservation of mass. By either name, however, they represent the most important law governing fluids in motion since conservation of mass is a fundamental law of physics that must be satisfied in all circumstances.

2.5 Acceleration of Fluid Elements

Acceleration is a simple concept. The acceleration of an object in motion is the rate of change of its velocity with time. If the object is a fluid element within a flow field, its acceleration is then simply the rate of change of its Lagrangian velocity components with time. This is because, as we have seen in Sect. 2.3, the Lagrangian velocities describe the motion of each fluid element as a single isolated object in motion. If the acceleration components in the x, y, z directions are denoted by a_x , a_y , a_z , respectively, we then have

$$\begin{cases} a_x = \frac{\partial U(X_0, Y_0, Z_0, t)}{\partial t} \\ a_y = \frac{\partial V(X_0, Y_0, Z_0, t)}{\partial t} \\ a_z = \frac{\partial W(X_0, Y_0, Z_0, t)}{\partial t} \end{cases}$$
(2.21)

The time derivatives are *partial* derivatives because the other independent variables, namely X_0 , Y_0 , Z_0 , are being held constant. This is required if a_x , a_y , a_z are to be the acceleration components of the particular fluid element identified by the material coordinates X_0 , Y_0 , Z_0 .

The subject of acceleration would end here if the fluid element in question was indeed being identified as a single isolated object and its motion is being described by its Lagrangian velocities. This is not the case, however. As discussed in Sect. 2.3, the use of Lagrangian velocities is rather impractical and the velocities of choice when describing a fluid body in motion, indeed the velocities which we shall use in the remainder of this book, are the Eulerian velocities.

But how can the acceleration components of a *particular* fluid element be expressed in terms of Eulerian velocity components which represent the velocities recorded at a particular coordinate position, not the velocities of particular fluid elements? As discussed earlier, a particular coordinate position within a body of fluid in motion will be occupied by different fluid elements at different times. The partial derivatives of the Eulerian velocity with time, namely

$$\begin{cases}
\frac{\partial u(x, y, z, t)}{\partial t} \\
\frac{\partial v(x, y, z, t)}{\partial t} \\
\frac{\partial w(x, y, z, t)}{\partial t}
\end{cases}$$
(2.22)

therefore do not represent the acceleration of a particular fluid element because they imply that the coordinate positions x, y, z are being held constant. They represent the rate of change of velocities at particular *locations* within the body of fluid, not the velocities of particular elements of that body. And, as stated before, these locations are occupied by different fluid elements at different times.

Yet, the laws of motion can only be applied to particular fluid elements, individually.

These difficulties can be resolved if we now treat x, y, z not as a fixed coordinate position within the fluid body but as the *instantaneous position at time t of a fluid element in motion*. This makes x, y, z functions of time t, and we now write Eq. 2.6 as

$$\begin{cases} u = u\{x(t), y(t), z(t), t\} \\ v = v\{x(t), y(t), z(t), t\} \\ w = w\{x(t), y(t), z(t), t\} \end{cases}$$
 (2.23)

Thus the Eulerian velocity components u, v, w are now seen not as the velocities recorded at a fixed location x, y, z within the fluid body, but as the velocity components of the fluid element which happens to occupy that location at time t.

With this interpretation, and in view of Eq. 2.23, the acceleration of that fluid element is now given appropriately by the *total derivatives* of these velocities with time, that is

$$\begin{cases} a_x = \frac{Du}{Dt} = \frac{\partial u}{\partial t} + \frac{\partial u}{\partial x} \frac{dx}{dt} + \frac{\partial u}{\partial y} \frac{dy}{dt} + \frac{\partial u}{\partial z} \frac{dz}{dt} \\ a_y = \frac{Dv}{Dt} = \frac{\partial v}{\partial t} + \frac{\partial v}{\partial x} \frac{dx}{dt} + \frac{\partial v}{\partial y} \frac{dy}{dt} + \frac{\partial v}{\partial z} \frac{dz}{dt} \end{cases}$$

$$(2.24)$$

$$a_z = \frac{Dw}{Dt} = \frac{\partial w}{\partial t} + \frac{\partial w}{\partial x} \frac{dx}{dt} + \frac{\partial w}{\partial y} \frac{dy}{dt} + \frac{\partial w}{\partial z} \frac{dz}{dt}$$

Furthermore, since x, y, z are the instantaneous coordinates of the fluid element in motion, then the time derivatives of these coordinates represent the Eulerian velocity components at that location and that instant in time, that is

$$\begin{cases} \frac{dx}{dt} = u \\ \frac{dy}{dt} = v \\ \frac{dz}{dt} = w \end{cases}$$
 (2.25)

and the expressions for the acceleration components finally become

$$\begin{cases} a_x = \frac{\partial u}{\partial t} + u \frac{\partial u}{\partial x} + v \frac{\partial u}{\partial y} + w \frac{\partial u}{\partial z} \\ a_y = \frac{\partial v}{\partial t} + u \frac{\partial v}{\partial x} + v \frac{\partial v}{\partial y} + w \frac{\partial v}{\partial z} \\ a_z = \frac{\partial w}{\partial t} + u \frac{\partial w}{\partial x} + v \frac{\partial w}{\partial y} + w \frac{\partial w}{\partial z} \end{cases}$$
(2.26)

If the acceleration is denoted by a vector \mathbf{a} , then

$$\mathbf{a} = (a_{\mathbf{x}}, a_{\mathbf{y}}, a_{\mathbf{z}}) \tag{2.27}$$

It is important to note that the partial derivatives

$$\frac{\partial u}{\partial t}, \frac{\partial v}{\partial t}, \frac{\partial w}{\partial t}$$
 (2.28)

are rates of change of u, v, w with time, *keeping* x, y, z *constant*, and that these derivatives do not represent the acceleration of the fluid element at x, y, z. They represent only part of that acceleration. The total acceleration of the element in terms of Eulerian velocities depend not only on the partial derivatives of these velocities with time but also on the *velocity gradients* at that point within the fluid body. Velocity gradients within a fluid body in motion, mathematically speaking, are represented by the partial derivatives of the Eulerian velocities with position coordinates x, y, z, as in the extra terms beyond the time derivative terms in Eq. 2.26.

Mathematically, the combination of time and space derivatives of the Eulerian velocities are known as *total* derivatives. From the perspective of physics, the space derivative terms within the total derivative are known as the *convective* terms. The name is important in that it highlights the difference between the acceleration of an isolated object in motion and that of a fluid element within a fluid body in motion. The latter is driven not only by the direct forces that are causing its acceleration or deceleration but also by the velocity field within which it is moving.

The situation is analogous to that of a runner sprinting uphill or downhill. The runner's acceleration or deceleration consists of two parts. One part is the acceleration which the runner's effort would produce on level ground, the other is the acceleration or deceleration caused by the slope of the hill. The first of these would be represented by the time rate of change of the runner's velocity on level ground. The second would be represented by the rate at which his or her velocity is being changed by the terrain.

A fluid element within a body of fluid in motion, such as flow in a tube, would face the analogue of a "downhill" situation if the tube had a narrowing where fluid is forced to move faster because of the constricted space. As the fluid element approaches the narrowing, it would be accelerated forward in the same way that the runner is accelerated downhill.

2.6 Forces Acting on a Fluid Element

Having dealt with the acceleration of a fluid element, the second important term in the equation of motion (Eq. 2.4) is the force acting on the fluid element to cause that acceleration.

In the case of an isolated object in motion, the force acting to accelerate or decelerate it is typically an external force which can be easily identified, such as the gravitational force acting downward on an aircraft in flight, the aerodynamic lift force acting to keep it up, the thrust of the engines pulling it forward, or the force of air friction acting against that pull. Whether the aircraft accelerates or decelerates and in which direction is determined by the *net* of these forces. In the end, the net force will precisely equal the mass of the aircraft times any acceleration or deceleration it is undergoing, precisely as dictated by Newton's law of motion in Eq. 1.1.

And so it is for a fluid element within a body of fluid in motion. We have already seen that the law of motion cannot be applied to the fluid body as a whole. It must be applied to individual elements of that body, which on the continuum scale means it must be applied at every (material) point within the body as in Eq. 2.4. But, unlike an aircraft in flight, a fluid element within a fluid body in motion is typically surrounded by other elements which are in contact with it on all sides and at all times. It is actually *part of the fluid body as a whole* and, as such, it is unlike an isolated object in motion. What then are the forces acting on a fluid element and how are they to be determined?

To answer these questions it is helpful to think of the forces acting on a fluid element in general as being of two types: internal "boundary forces" exerted by the push and pull of neighboring elements that are in contact with it and acting directly on its boundary, and external "body forces" acting directly on the mass of the fluid element, independently of its neighbors.

2.7 The Stress Tensor 25

Examples of body forces are those resulting from gravitational or magnetic fields affecting a body of fluid. Since these act directly on the mass of fluid elements, their effect on the acceleration or deceleration of these elements is similar to that in the case of an isolated object in motion under the same forces. The only, though very important, difference between the two is that in the case of a fluid element these body forces must be combined with the boundary forces acting on the same element to determine the net force that would cause it to accelerate or decelerate. Flow in a river is the quintessential example of a body force (gravity) acting on the elements of water, causing it to flow down the river.

Boundary forces, by contrast, are transmitted internally within a body of fluid from one fluid element to the next. The most important example of a boundary force is pressure. Pressure at one end of a fluid filled tube causes the fluid to "flow" along the tube simply by one fluid element *pushing* another, from the high pressure end of the tube to the other end, in a process not unlike that of a domino effect. We shall find out later that in the resulting flow along the tube not all fluid elements are able to move forward at the same speed. The reason for this is another important boundary force that acts on fluid elements, namely the shear force resulting from one fluid element *rubbing* against another or against a solid boundary such as the tube wall in this case. The same is true of the flow in a river mentioned above. Here again the flow is not uniform, in the sense that not all elements of the water are moving with the same speed down the river, because of boundary forces.

What we see in these two examples is that flow in a tube would typically be determined largely by boundary forces, specifically pressure. Certainly, flow in a horizontal tube would be so driven and would not be affected by the body force of gravity. In the case of an inclined tube, flow may be driven by a combination of both. However, if the tube is stationary in its inclined position, the effect of gravity would be equally stationary and the only variability in the flow would result from the variability in pressure. This is precisely the situation in blood flow and hence the focus in this book will be on boundary forces only, specifically pressure and shear forces. The force of gravity plays a role in some blood flow problems, as in the effects of going from a lying to standing position or vice versa, or in the effects of the absence of gravity on astronauts in outer space, but, like flow in a tube going from a horizontal to an inclined position, after an initial transition period, the effect of gravity will become stationary and any variability in the flow will be dominated by variability in pressure. This is the case in blood flow.

2.7 The Stress Tensor

Following the previous section, it is clear that in order to apply the laws of motion to a fluid element the internal forces acting on its boundary must be somehow accounted for. At a first glance this may seem to be an impossible task because a fluid element is not well defined as a material entity- neither the mass nor shape or volume of the element are known. Only the "density at a point" has so far been used,

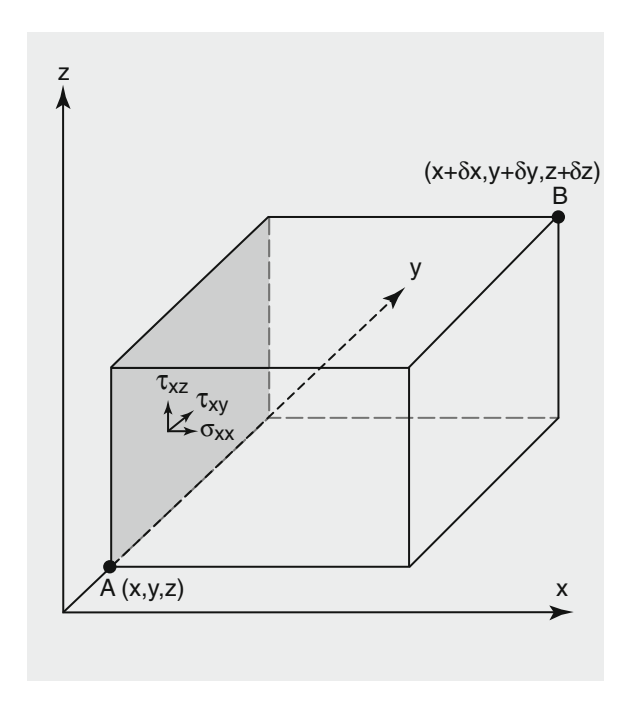


Fig. 2.2 Stress tensor. Boundary stresses acting on three sides of a closed box formed by coordinate surfaces, a stress being force per area. On each side there is one stress acting normal to that side and two acting tangential to it. Normal stresses are denoted by σ 's and tangential stresses by τ 's, with the first subscript identifying the normal to the face on which the stress is acting and the second identifying the direction in which the stress itself is acting. Stresses acting on the opposite three sides may in general be different, thus producing a net force acting on the volume of fluid contained within the box. As the box is shrunk to a point, this force becomes the net boundary force acting at a "point", that is, acting on the fluid element at that point.

as in Eq. 1.3, to "acknowledge" the presence of a fluid element at that point within a larger body of fluid. In fact, the concept of a fluid element does not go any further than this in the way of detail. How then does one determine the internal forces that act on a fluid element in order to determine its motion?

Surprisingly, the task is not as daunting as it seems. Essentially, we follow the same procedure as that followed in Sect. 2.4 to determine conservation of mass. As in that section, we begin by considering a rectangular box with edges δx , δy , δz that are aligned with the three coordinate axes. The box is positioned such that one of its corners, to be referred to as 'A', is at the point x, y, z and the diagonally-opposite corner, to be referred to as 'B', is at $x + \delta x$, $y + \delta y$, $z + \delta z$. Three of the six faces of the box intersect at A, the other three intersect at B, as illustrated in Fig. 2.2.

Our plan is to determine the forces acting on each of the six faces of the volume of fluid contained in this box, and then, as was done in Sect. 2.4, allow the volume of the box to shrink to the corner A by letting δx , δy , $\delta z \rightarrow 0$. In that process, the

2.7 The Stress Tensor 27

forces acting on the six faces of the box become the forces acting at a point, hence the forces acting on a *fluid element* at that point, namely the point (x, y, z). In fact, as we shall see, the forces acting on each face are divided by the area of that face, thus converting the forces into *stresses* acting on a fluid element—"stress", by definition, being force divided by the area on which that force is acting.

In rectangular Cartesian coordinates, a stress τ , being a vector (as is a force), can be specified in terms of its three components in the x,y,z directions. Thus, in general, there will be three stress components acting on each face of the rectangular box. We use a two-subscript notation for this purpose, one to identify the face on which the stress component is acting and another to identify the direction in which that component is acting. Thus τ_{xy} , for example, shall denote a stress component acting in the y-direction on the face normal to the x-axis, while τ_{yx} shall denote a stress component acting in the x-direction acting on the face normal to the y-axis. In this way, the stress components acting on the first three faces of the box, namely the three faces that intersect at the point A(x, y, z), form a 3 × 3 matrix known as the "stress tensor"

$$T = \begin{bmatrix} \sigma_{xx} & \tau_{xy} & \tau_{xz} \\ \tau_{yx} & \sigma_{yy} & \tau_{yz} \\ \tau_{zx} & \tau_{zy} & \sigma_{zz} \end{bmatrix}$$
 (2.29)

The diagonal components of the stress tensor are denoted by a different symbol (σ) because they are different in that the direction in which they act is *normal* to the face on which they are acting, while the off-diagonal components, denoted by τ , represent stress components that act *tangential* to the face on which they are acting. For example, of the three stress components acting on the face normal to the *x*-axis, which are in the top row of the stress tensor (Eq. 2.29), τ_{xy} and τ_{xz} act tangential to that face while σ_{xx} acts normal to it. Similarly, we note that the stress components acting on the faces normal to the *y*-axis and the *z*-axis are in the second and third rows of the stress tensor, respectively.

As noted above, the nine components of the stress tensor in Eq. 2.29 represent stress components acting on only three faces of the box, namely those that intersect at the point A(x, y, z). Stress components acting on the other (opposite) three faces, namely those that intersect at the point $B(x+\delta x, y+\delta y, z+\delta z)$, are generally different because the forces acting within the body of fluid may in general be different from point to point. Thus, the stress components on the two faces normal to the *x*-axis are

$$\begin{cases} \sigma_{xx} \\ \tau_{xy} \\ \tau_{xz} \end{cases} \tag{2.30}$$

on the face intersecting the x-axis at A(x, y, z), and

$$\begin{cases} \sigma_{xx} + \frac{\partial \sigma_{xx}}{\partial x} \delta x \\ \tau_{xy} + \frac{\partial \tau_{xy}}{\partial x} \delta x \\ \tau_{xz} + \frac{\partial \tau_{xz}}{\partial x} \delta x \end{cases}$$
(2.31)

on the face intersecting the *x*-axis at $B(x+\delta x, y+\delta y, z+\delta z)$. The difference between the two is

$$\left(\frac{\partial \sigma_{xx}}{\partial x}, \frac{\partial \tau_{xy}}{\partial x}, \frac{\partial \tau_{xz}}{\partial x}\right) \delta x \tag{2.32}$$

and if this difference between the *stresses* acting on the two opposite faces is multiplied by the area of these faces, namely $\delta y \delta z$, we obtain, finally, the *net force* resulting from the difference between the forces acting on the two faces of the box that are normal to the *x*-axis

$$\left(\frac{\partial \sigma_{xx}}{\partial x}, \frac{\partial \tau_{xy}}{\partial x}, \frac{\partial \tau_{xz}}{\partial x}\right) \delta x \delta y \delta z \tag{2.33}$$

In a similar way we find the net force resulting from the difference between the forces acting on the two faces of the box that are normal to the *y*-axis

$$\left(\frac{\partial \tau_{yx}}{\partial y}, \frac{\partial \sigma_{yy}}{\partial y}, \frac{\partial \tau_{yz}}{\partial y}\right) \delta y \delta x \delta z \tag{2.34}$$

and the net force resulting from the difference between the forces acting on the two faces of the box that are normal to the *z*-axis

$$\left(\frac{\partial \tau_{zx}}{\partial z}, \frac{\partial \tau_{zy}}{\partial z}, \frac{\partial \sigma_{zz}}{\partial z}\right) \delta z \delta y \delta x \tag{2.35}$$

In each of Eqs. 2.33, 2.34, 2.35, the force is a vector with three components acting in the x, y, z directions. The sum of all these forces can therefore be denoted by a single vector $\mathbf{F}(F_x, F_y, F_z)$ representing the total force acting on the volume of fluid contained within the box defined by $\delta x, \delta y, \delta z$. The components of \mathbf{F} in the x, y, z directions are given by

2.7 The Stress Tensor 29

$$\begin{cases} F_{x} \approx \left(\frac{\partial \sigma_{xx}}{\partial x} + \frac{\partial \tau_{yx}}{\partial y} + \frac{\partial \tau_{zx}}{\partial z}\right) \delta x \delta y \delta z \\ F_{y} \approx \left(\frac{\partial \tau_{xy}}{\partial x} + \frac{\partial \sigma_{yy}}{\partial y} + \frac{\partial \tau_{zy}}{\partial z}\right) \delta x \delta y \delta z \end{cases}$$

$$F_{z} \approx \left(\frac{\partial \tau_{xz}}{\partial x} + \frac{\partial \tau_{yz}}{\partial y} + \frac{\partial \sigma_{zz}}{\partial z}\right) \delta x \delta y \delta z$$

$$(2.36)$$

The equalities are approximate because the forces acting on each face of the box defined by $\delta x \delta y \delta z$ are only *average* forces. To make the equalities exact requires that the forces be exactly those acting at the point x, y, z, which is achieved by letting $\delta x, \delta y, \delta z \to 0$. Another way of putting it, the volume of fluid within the box defined by $\delta x \delta y \delta z$ contains many fluid elements and, in general, the forces acting on these elements will not be the same. The forces in Eq. 2.36 represent only the *average* of the forces acting on all fluid elements within the box. To turn this average into the *actual* forces acting on the fluid element at the point x, y, z is achieved, again, by letting $\delta x, \delta y, \delta z \to 0$.

To implement this limiting process, we use a technique similar to that used in Sect. 2.4 where the mass of fluid within the box was divided by the volume $\delta V = \delta x \delta y \delta z$ while at the same time letting $\delta V \to 0$. This process led to the use of the density at a point, which is the density of the fluid element at that point, instead of the actual mass of that element. Here too, we divide the forces $\mathbf{F}(F_x, F_y, F_z)$ acting on the volume of fluid within the box by the volume of the box while at the same time letting $\delta V \to 0$, thereby defining the "force per volume"

$$\mathbf{f}(f_x, f_y, f_z) = \lim_{\delta V \to 0} \left(\frac{\mathbf{F}(F_x, F_y, F_z)}{\delta V} \right)$$
 (2.37)

Applying this limit to Eq. 2.36 leads to

$$\begin{cases}
f_x = \left(\frac{\partial \sigma_{xx}}{\partial x} + \frac{\partial \tau_{yx}}{\partial y} + \frac{\partial \tau_{zx}}{\partial z}\right) \\
f_y = \left(\frac{\partial \tau_{xy}}{\partial x} + \frac{\partial \sigma_{yy}}{\partial y} + \frac{\partial \tau_{zy}}{\partial z}\right) \\
f_z = \left(\frac{\partial \tau_{xz}}{\partial x} + \frac{\partial \tau_{yz}}{\partial y} + \frac{\partial \sigma_{zz}}{\partial z}\right)
\end{cases} (2.38)$$

The force *vector* is given by

$$\mathbf{f} = (f_x, f_y, f_z) \tag{2.39}$$

Again we see that the difficulty of specifying the actual mass, volume, or shape of a fluid element has been avoided. Only the exact *location* of the element is specified, namely the point (x, y, z). This is a fundamental technique in the study of fluid flow.

It represents a triumph of the concept of a "fluid element" whereby, despite the vagueness of that concept, the laws of conservation of mass and, as we shall see, the laws of motion can be applied at every "point" within a body of fluid in motion.

2.8 Newton's Second Law "At a Point"

As fundamental as it is in its scope, Newton's second law of motion cannot be applied to a body of fluid in motion. This problem has already been introduced and the reasons for it briefly discussed in Sect. 2.2. Essentially, the law does not apply to a fluid body as a whole because different elements of a fluid body in motion are in general under different forces and are moving individually, not *en masse*. While they are continuous with each other and to some extent constrained by each other, elements of fluid are typically able to move faster or slower than each other. Indeed, as we shall gradually come to understand, "flow" is nothing but the ability of different elements of a fluid body to move at different velocities while at the same time remaining continuous with each other.

In essence, fluid elements negotiate Newton's second law individually and, under these conditions, the law must be applied separately to each element of a fluid body in motion. And since on the continuum scale an element of fluid is a "point", a material point, then Newton's second law must be applied at every point within a fluid body in motion. The task of doing so is not as daunting as it seems, however, because preliminary steps in that direction have already been taken in previous sections.

We begin with the law itself as presented in Eq. 1.1, only now we switch the left and right sides of the equation because, interestingly, as the law migrated from its origin in classical physics to the more modern studies of fluid flow and hemodynamics, the term representing "force" established itself firmly on the right side of the equation, not the left. In that tradition, therefore, we write

$$mass \times acceleration = force$$
 (2.40)

Assuming that the mass of that element is m and its volume is v, we may write this as

$$m \times acceleration = v \times (force/volume)$$
 (2.41)

The key step in the application of Newton's second law to every element of a fluid body in motion, i.e. at every point within a fluid body in motion, is that Eq. 2.41 is now divided by v and the ratio m/v is replaced by the density ρ as was done in Sect. 2.4, which leads to

$$density \times acceleration = (force/volume)$$
 (2.42)

In doing so the actual mass m and volume v of the element are eliminated and the equation becomes applicable to every element of the fluid body in motion, i.e. at every point within the fluid body. Different elements are identified only by their locations x, y, z, and it is in this sense that Eq. 2.42 is now an equation "at a point".

Thus, using the acceleration **a** introduced in Sect. 2.5 and the total force per volume acting on that element **f** introduced in Sect. 2.6, we write, in vector form

$$\rho(x, y, z) \times \mathbf{a}(x, y, z) = \mathbf{f}(x, y, z) \tag{2.43}$$

or in component form

$$\begin{cases} \rho(x, y, z) \times a_x(x, y, z) = f_x(x, y, z) \\ \rho(x, y, z) \times a_y(x, y, z) = f_y(x, y, z) \\ \rho(x, y, z) \times a_z(x, y, z) = f_z(x, y, z) \end{cases}$$
(2.44)

Every term in these equations is a function of coordinate position x, y, z and, again, it is in this sense that the equation is an equation at a point.

Substituting for the acceleration components from Sect. 2.5 and for the force components from Sect. 2.6 we finally have

$$\begin{cases}
\rho \left(\frac{\partial u}{\partial t} + u \frac{\partial u}{\partial x} + v \frac{\partial u}{\partial y} + w \frac{\partial u}{\partial z} \right) = \frac{\partial \sigma_{xx}}{\partial x} + \frac{\partial \tau_{yx}}{\partial y} + \frac{\partial \tau_{zx}}{\partial z} \\
\rho \left(\frac{\partial v}{\partial t} + u \frac{\partial v}{\partial x} + v \frac{\partial v}{\partial y} + w \frac{\partial v}{\partial z} \right) = \frac{\partial \tau_{xy}}{\partial x} + \frac{\partial \sigma_{yy}}{\partial y} + \frac{\partial \tau_{zy}}{\partial z} \\
\rho \left(\frac{\partial w}{\partial t} + u \frac{\partial w}{\partial x} + v \frac{\partial w}{\partial y} + w \frac{\partial w}{\partial z} \right) = \frac{\partial \tau_{xz}}{\partial x} + \frac{\partial \tau_{yz}}{\partial y} + \frac{\partial \sigma_{zz}}{\partial z}
\end{cases} (2.45)$$

The brackets (x, y, z, t) have been omitted from these equations and will be omitted in future, with the understanding that the position coordinates x, y, z and the time t are implicit in all subsequent equations. All subsequent equations are *point* equations, representing Newton's second law of motion as applied to the fluid element at (x, y, z, t).

2.9 Mechanical Properties: Viscosity

The mechanical properties of material objects have to do with the way they respond to a deforming force. Briefly, as discussed in Sect. 1.4, the more "rigid" an object the higher the resistance it offers to deformation. Fluids are at the bottom of this scale; they offer zero resistance to deformation. Within a flow field, fluid elements are in a state of "continuous deformation".

Indeed, fluid "flow" can be appropriately defined as a state of continuous deformation.

But if flow is a state of continuous deformation and fluids offer zero resistance to deformation, how and why does flow ever stop? Every day experience indicates clearly that it does. Tea or coffee stirred in a cup ultimately stops spinning. Water disturbed by a swimmer in a pool ultimately becomes still again. Air disturbed by a flying object will become calm again. Or more to the subject at hand, blood, driven by the heart through our labyrinth of arteries and, as we shall see later, is in a state of continuous deformation, a state of flow, stops flowing when the heart stops pumping. In all cases, the action triggers the start of a state of continuous deformation, a state of flow, but when the action ceases the flow ultimately stops. Why?

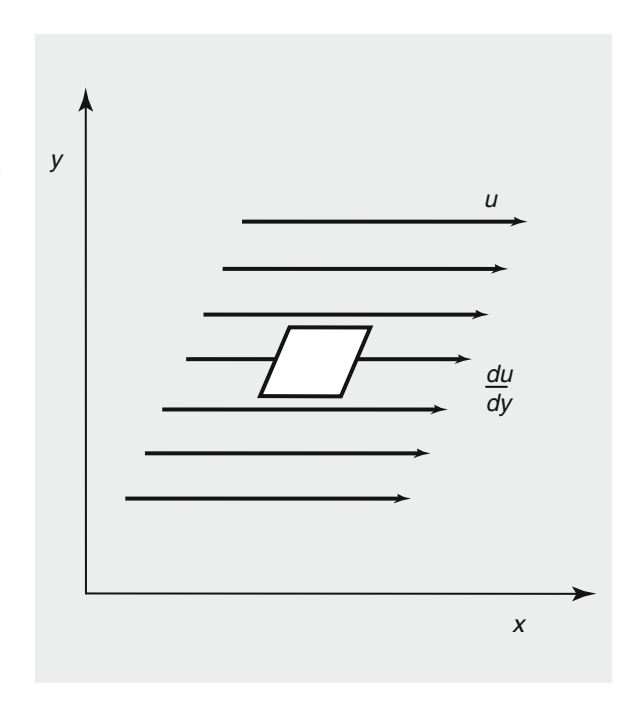
Furthermore, since an aircraft in flight is merely deforming the elements of air around it, and since air, being a fluid, offers no resistance to deformation, why does the aircraft require an engine to continue its motion through the air once it started? Similarly, since a swimmer in a pool of water is merely deforming the elements of water around his or her body as it moves and again, since water, being a fluid, offers no resistance to deformation, why does the act of swimming require a continuous supply of energy? Or again, more to the subject at hand, why does blood flow require a pump?

Remarkably, we encounter the answers to these questions in every day life, yet, as with other aspects of fluids and fluid flow, we simply accept the experience without pursuing it any further. If we do pursue the issue we soon find that moving our arms at low speed through the water while swimming meets less resistance and requires less energy than doing so at higher speed. In both cases the water is being continuously deformed, but the *rate* at which it is being deformed is different. Another, somewhat mundane but no less instructive example, is that of unscrewing the cap of a jar of honey in which the thread on the cap has been smeared with the stuff. An attempt to do so with excessive force, thus causing a high rate of shear (deformation) of the honey caught between the cap and the jar, will meet high resistance. The cap will open more easily if it is unscrewed very slowly.

Thus, while fluids offer zero resistance to deformation, they resist the rate at which they are being deformed, the higher the rate of deformation the higher the resistance. This fundamental property of fluids is known as their "viscosity".

In its simplest form, a state of continuous deformation can be represented by a "velocity gradient", that is a state in which adjacent layers of fluid are moving at gradually higher and higher velocities, as illustrated in Fig. 2.3. It is somewhat like the traffic on a multi-lane highway. A fluid element within a velocity gradient is in a state of continuous deformation, the *rate of deformation* being proportional to the velocity gradient. The viscous force τ with which fluids resist the rate of deformation is therefore related to the velocity gradients within the flow field. The relation most commonly used is a linear one, with a constant of proportionality μ

Fig. 2.3 Flow is a state of velocity gradients. Only one gradient is illustrated here, resulting from variation of the x-component of velocity u in the y-direction. An element of fluid within this gradient is in a state of continuous deformation, a state of flow.



known as the "coefficient of viscosity" and whose value is a characteristic property of the fluid, that is

$$\tau = \mu \frac{du}{dy} \tag{2.46}$$

This relation was first derived by Newton, and fluids whose behavior is consistent with it are referred to as *Newtonian fluids*.¹

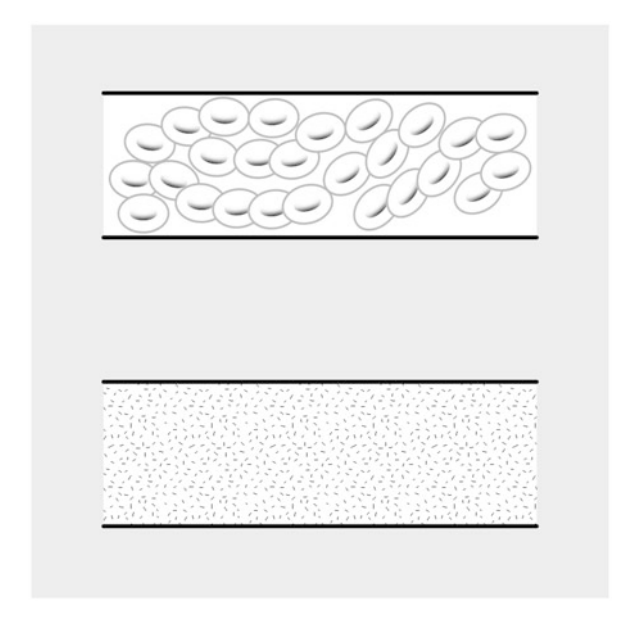
Many common fluids are found to behave as Newtonian fluids, among them air, water, and oil. Others may behave as Newtonian fluids when the rates of deformation and hence velocity gradients within a flow field are small, and as non-Newtonian fluids when the gradients are large. Theoretical studies have concluded, in fact, that the linear relation in Eq. 2.46 is only an approximation for small rates of deformation, but one that has a wide range of validity. Other relations have been explored in both theoretical and experimental studies.²

The question of whether blood is a Newtonian fluid is a long standing one. Indeed, the corpuscular nature of whole blood raises the question of whether it can be treated as a continuum, and the peculiar makeup of plasma makes it *seem*

¹Tokaty GA. A History & Philosophy of Fluidmechanics. Foulis & Co, 1971.

²Larsen RG. The Structure and Rheology of Complex Fluids. Oxford University Press, New York, 1999.

Fig. 2.4 Is blood a Newtonian fluid? The question is tied much to the diameter of the tube in which blood is flowing. When the diameter is comparable with the scale of the corpuscular structure of blood (top), the assumption of a Newtonian fluid, indeed the assumption of blood as a fluid continuum, is clearly untenable. The reason for the latter is that the blood cells are not fluid. However, when the tube diameter is large on the corpuscular scale (bottom), both assumptions are found to be fairly adequate.



different from more common fluids. There is no doubt that blood cannot be treated as a Newtonian fluid in general and under all circumstances, but there is equally no doubt that under many of the normal physiological circumstances of blood circulation it can. A great deal of understanding, indeed the overwhelming majority of what we know to date about the dynamics of blood flow, has been achieved by treating blood as a Newtonian fluid, or more accurately by using Newtonian relations between shear stresses and velocity gradients. This is not to say that blood is a Newtonian fluid, but only that the Newtonian relations have proved adequate for much of what has been studied so far. Near the capillary level of the vascular tree where vessel diameters become comparable with the size of the discrete corpuscles of blood, the continuum model of blood and its assumed Newtonian behavior become clearly inadequate, but in the core of more common blood flow problems the Newtonian model has proved adequate so far (Fig. 2.4). The effects of viscosity are an inseparable part of fluid flow because of the ever presence of velocity gradients in fluid flow. Indeed, as has been mentioned previously, velocity gradients are absent only when a fluid body is moving en masse, that is when all its elements are moving at the same speed and in the same directions, as the body of fluid in a cup when the cup is being moved gently without disturbing the fluid within. In this case the body of fluid is moving as a solid object and there are no velocity gradients and no flow. Outside this rather artificial example, however, flow and velocity gradients go hand in hand- where there is flow there are velocity gradients and vice versa. We shall see later how these gradients arise as we consider specific flow fields, most notable that of flow in a tube.

Thick liquid honey provides a vivid demonstration of a viscous fluid, but all fluids are viscous to some extent, including water, milk, blood and, surprisingly, even air

and other gases. The difference is only in the degree of viscosity: some fluids are more viscous than others. The force and energy which a swimmer requires to move through the water is almost entirely spent on overcoming the effects of viscosity, and the same is true of the force and energy which the engine of an aircraft must provide. While the viscosity of air is very low, the rate at which layers of air are sheared by the passage of a high speed aircraft is very high, and hence the viscous resistance is correspondingly high.

The effects of fluid viscosity are as ubiquitous in our life as are the effects of gravity. A world without fluid viscosity would be as magical as a world without gravity. Without viscosity it would be possible to fly through air without any resistance. An aircraft would need only to be taken up to a certain height and given a push to then continue flying in that direction without engine or fuel. A swimmer would be able to kick the wall at one end of a swimming pool and reach the other end without any further effort. The force of gravity would no longer be needed to maintain the flow in a river, that is, the flow in a river would no longer need to be downhill. Once started, it would be possible for the flow to continue indefinitely on level ground without the need to overcome viscous resistance. Above all, in the absence of viscosity blood would circulate through our arteries without the need for a pump. The circulation of blood would be "primed" only once at birth and it would then go on indefinitely. Oddly, or perhaps sadly, a world without viscosity would be a world without the human heart!

How does the viscous property of fluids come about? See Appendix A.

2.10 Constitutive Equations

The purpose of applying Newton's second law at every point within a fluid body in motion, as was done in the previous section, is to provide a map of the variable motion within the body, a map of the *flow field* within that body. For the map of a flow field to be useful, it must describe that field in terms of variables that are both accessible (can be measured) and meaningful (can be interpreted). In Sect. 2.3 it was concluded that the Eulerian velocities u, v, w meet these criteria because they represent the velocity components at every point within a fluid body in motion. In Sect. 2.5 it was seen how the acceleration of fluid elements can be expressed in terms of these velocity components, thus providing one part of Newton's law, as in Eq. 2.45. However, the other part of these equations which represents the "force" side of Newton's law is expressed in terms of components of the stress tensor which certainly do not meet the criteria of being accessible or meaningful. We recall that components of the stress tensor represent internal forces which fluid elements exert on each other and, so far, in Sects. 2.6 and 2.7, these forces have only been "named" in terms of their components in the three coordinate directions. It is not clear as yet how these forces come about and how they relate to what can actually be measured in a flow field. Ideally, if components of the stress tensor can be expressed in terms of the Eulerian velocities, as was done with the acceleration components, then this would not only give meaning to these components but also complete the expression of Newton's law in Eq. 2.45 in terms of the same variables. This can indeed be done and it is the subject of the present section. Equations relating the stresses acting on a fluid element to the Eulerian velocities and pressure within a flow field are known as "constitutive equations" because the form of that relation, as we shall see, depends on the constitution of the particular fluid, on its mechanical properties.

The Newtonian relation discussed in the previous section (Eq. 2.46) was based on only one velocity gradient and one shear stress τ . More generally each of the three velocity components in a flow field may have a gradient in each of the three coordinate directions, and there are as many possible shear stress components on the boundary of a fluid element as we saw in the previous section. The constitutive equations of a given fluid are usually based on the relations between these velocity gradients and corresponding shear stresses. In the case of Newtonian fluids the relations are more complicated than that in Eq. 2.46 but they remain linear. Linearity of the relations between shear stresses and velocity gradients is a defining characteristic of Newtonian fluids.

Constitutive equations are generally based on a combination of theory and empirical data.³ For many common fluids the following equations are found to hold when velocity gradients are not large.

$$\begin{cases}
\sigma_{xx} = -p + 2\mu \frac{\partial u}{\partial x} \\
\sigma_{yy} = -p + 2\mu \frac{\partial v}{\partial y} \\
\sigma_{zz} = -p + 2\mu \frac{\partial w}{\partial z}
\end{cases} (2.47)$$

$$\begin{cases}
\tau_{xy} = \tau_{yx} = \mu \left(\frac{\partial u}{\partial y} + \frac{\partial v}{\partial x} \right) \\
\tau_{xz} = \tau_{zx} = \mu \left(\frac{\partial w}{\partial x} + \frac{\partial u}{\partial z} \right) \\
\tau_{yz} = \tau_{zy} = \mu \left(\frac{\partial w}{\partial y} + \frac{\partial v}{\partial z} \right)
\end{cases} (2.48)$$

where μ is the coefficient of viscosity introduced in the previous section and p is "pressure" at that point within the fluid body and whose interpretation is discussed below.

Direct verification of constitutive equations is rarely possible. More commonly they are tested indirectly by using them as the basis of equations of motion, as

³Schlichting H. Boundary-Layer Theory. McGraw-Hill 1979.

we do in the next section. The equations are subsequently solved for a given flow situation, and it is the *solutions* that are then compared directly with experiment or observation. Such indirect verification of course does not test the assumptions on which the constitutive equations are based, and it is important to identify these at this point.

The central assumption is that of *linearity* of the relation between shear stress and velocity gradient. It is well recognized that this is only an approximation for small gradients but its range of validity seems to be fairly wide. Solutions of equations of motion based on the constitutive equations of Newtonian fluids have been applied to most common fluids and have been tested successfully against experiment for many years. Many problems in blood flow have been modelled successfully by these equations, even though the Newtonian character of blood can be questioned. In particular, the classical solutions for pulsatile flow which we use in this book have been based on the constitutive equations of Newtonian fluids.

The second important issue concerns the pressure p appearing in the constitutive equations. Pressure is strictly a thermodynamic property which is subject to the laws of thermodynamics applied to a body of fluid *at rest*. In that state the pressure represents a force which acts in the direction of the normal to the boundary of fluid elements and which is independent of the orientation of that boundary. The constitutive equations above are consistent with this state, as when the fluid is at rest $(u \equiv v \equiv w \equiv 0)$ they reduce to

$$\sigma_{xx} = \sigma_{rr} = \sigma_{\theta\theta} = -p \tag{2.49}$$

Thus in this state the thermodynamic pressure is identified with the normal components of the stress tensor. The negative sign arises because normal stresses are defined to be positive in the direction of outward normal while pressure in thermodynamics is defined to be positive in the direction of inward normal.

When fluid is in motion, however, the normal stresses are no longer equal to each other and the thermodynamic concept of pressure in fact no longer applies. What has been done to overcome this difficulty is to assume that the pressure in a moving fluid is equal to the *average* of the normal stresses, namely (see Footnote 3)

$$p = -\frac{1}{3}(\sigma_{xx} + \sigma_{rr} + \sigma_{\theta\theta})$$
 (2.50)

The constitutive equations are based on this assumption as can be readily verified by adding Eqs. 2.47 and then using the equation of continuity (Eq. 2.20). The assumption inherent in this is sometimes referred to as the "mechanical definition of pressure", and it is on the basis of this assumption that the thermodynamic pressure p appears in the constitutive equations and subsequently in the equations of motion.

Finally, the constitutive equations assume that the stress tensor is symmetrical, namely

$$\begin{cases} \tau_{xy} = \tau_{yx} \\ \tau_{yz} = \tau_{zy} \\ \tau_{xz} = \tau_{zx} \end{cases}$$
 (2.51)

and this again is recognized to be an approximation, but one which is found to work well under normal circumstances. Asymmetry of the stress tensor would give rise to forces which have spinning effects on fluid elements. The assumption of symmetry is based on the fact that such forces are found to be absent under normal flow conditions. An external field of force is required to produce them such as an electrostatic field, and in the absence of such field the fluid does not support such asymmetry in the components of the stress tensor.

2.11 Navier-Stokes Equations

Having dealt with the internal forces acting on a fluid element within a body of fluid in motion, it is now possible to complete the application of Newtons's law of motion at every point within that body by substituting for the components of the stress tensor from Eqs. 2.47 and 2.48 into the equations of motion (Eq. 2.45) to get, after some algebra

$$\begin{cases} \rho \left(\frac{\partial u}{\partial t} + u \frac{\partial u}{\partial x} + v \frac{\partial u}{\partial y} + w \frac{\partial u}{\partial z} \right) + \frac{\partial p}{\partial x} = \mu \left(\frac{\partial^2 u}{\partial x^2} + \frac{\partial^2 u}{\partial y^2} + \frac{\partial^2 u}{\partial z^2} \right) \\ \rho \left(\frac{\partial v}{\partial t} + u \frac{\partial v}{\partial x} + v \frac{\partial v}{\partial y} + w \frac{\partial v}{\partial z} \right) + \frac{\partial p}{\partial y} = \mu \left(\frac{\partial^2 v}{\partial x^2} + \frac{\partial^2 v}{\partial y^2} + \frac{\partial^2 v}{\partial z^2} \right) \\ \rho \left(\frac{\partial w}{\partial t} + u \frac{\partial w}{\partial x} + v \frac{\partial w}{\partial y} + w \frac{\partial w}{\partial z} \right) + \frac{\partial p}{\partial z} = \mu \left(\frac{\partial^2 w}{\partial x^2} + \frac{\partial^2 w}{\partial y^2} + \frac{\partial^2 w}{\partial z^2} \right) \\ \frac{\partial u}{\partial x} + \frac{\partial v}{\partial y} + \frac{\partial w}{\partial z} = 0 \end{cases}$$

$$(2.52)$$

The last equation will be recognized as the equation of continuity (Eq. 2.20) which was derived previously as a condition of conservation of mass when the density ρ is assumed constant. It arises here again when differentiating the components of the stress tensor on the right hand side of Eq. 2.45, but again only if it is assumed that the density ρ is constant. To illustrate this, substituting for components of the stress tensor in the first line of Eq. 2.45 we have

$$\begin{cases}
\rho \left(\frac{\partial u}{\partial t} + u \frac{\partial u}{\partial x} + v \frac{\partial u}{\partial y} + w \frac{\partial u}{\partial z} \right) = \frac{\partial \sigma_{xx}}{\partial x} + \frac{\partial \tau_{yx}}{\partial y} + \frac{\partial \tau_{zx}}{\partial z} = \\
\frac{\partial}{\partial x} \left(-p + 2\mu \frac{\partial u}{\partial x} \right) + \frac{\partial}{\partial y} \left(\mu \left(\frac{\partial u}{\partial y} + \frac{\partial v}{\partial x} \right) \right) + \frac{\partial}{\partial z} \left(\mu \left(\frac{\partial w}{\partial x} + \frac{\partial u}{\partial z} \right) \right)
\end{cases} (2.53)$$

and after the differentiation is carried out this reduces to

$$\begin{cases}
\rho \left(\frac{\partial u}{\partial t} + u \frac{\partial u}{\partial x} + v \frac{\partial u}{\partial y} + w \frac{\partial u}{\partial z} \right) + \frac{\partial p}{\partial x} = \\
\mu \left(\frac{\partial^2 u}{\partial x^2} + \frac{\partial^2 u}{\partial y^2} + \frac{\partial^2 u}{\partial z^2} \right) + \frac{\partial}{\partial x} \left(\frac{\partial u}{\partial x} + \frac{\partial v}{\partial y} + \frac{\partial w}{\partial z} \right)
\end{cases} (2.54)$$

The last term in this equation is zero if it is assumed that Eq. 2.20 is valid, which is the case only when the density ρ is constant as shown in Sect. 2.4. Thus, based on the assumption of constant density, Eq. 2.54 reduces to the first and last lines in Eq. 2.52, namely

$$\begin{cases} \rho \left(\frac{\partial u}{\partial t} + u \frac{\partial u}{\partial x} + v \frac{\partial u}{\partial y} + w \frac{\partial u}{\partial z} \right) + \frac{\partial p}{\partial x} = \mu \left(\frac{\partial^2 u}{\partial x^2} + \frac{\partial^2 u}{\partial y^2} + \frac{\partial^2 u}{\partial z^2} \right) \\ \frac{\partial u}{\partial x} + \frac{\partial v}{\partial y} + \frac{\partial w}{\partial z} = 0 \end{cases}$$

The other two lines in Eq. 2.52 are obtained in the same way, with the equation of continuity arising again in each case. It is therefore both important and appropriate that the equations of motion in the form of Eq. 2.52 always contain the equation of continuity even though that equation is not part of Newton's second law. It must be included because the validity of the first three lines of Eq. 2.52 is contingent on the validity of the last line.

Equation 2.52 is widely known as the Navier-Stokes equations^{4,5,6} in recognition of its first authors. They are also referred to as the "momentum equations" because the terms on the left side of the equations, which represent " $mass \times acceleration$ ", can also be seen as representing rate of change of momentum.

$$mass \times acceleration = mass \times (velocity/time)$$

= $(mass \times velocity)/time$
= $momentum/time$

⁴Tokaty GA. A History & Philosophy of Fluidmechanics. Foulis & Co., Henley-On-Thames, 1971.

⁵Rouse H, Ince S. History of Hydraulics. Dover, New York, 1957.

⁶Schlichting H. Boundary-Layer Theory. McGraw-Hill, New York, 1979.

Equation 2.52 is remarkable in that they represent no more than Newton's exquisitely simple second law of motion, yet an entire chapter was required for their derivation. The law is applied at every "point" within a flow field, that is to every fluid element within that flow field, individually, yet the equations contain neither the identity nor mass of these elements. Finally, the range of application and validity of these equations to fluid flow problems in general and blood flow in particular has been extraordinary.

Detailed derivation of the Navier-Stokes equations in this book was carried out in rectangular Cartesian coordinates x, y, z in order to keep focus on the main physical issues involved, particularly those relating to the application of Newton's second law of motion to a fluid body. When the equations are derived in cylindrical polar coordinates x, r, θ , as was done in an earlier edition of this book, further complications arise because of added curvature terms in the equations and, while these raise some important points relating to the characteristics of curvilinear coordinates, they tend to obscure the main issues at hand.

Paradoxically, however, the Navier-Stokes equations in cylindrical polar coordinates is best suited for the study of flow in tubes and therefore for the study of hemodynamics, which is the main subject of this book. Therefore we present the equations below for use in the remainder of this book.

$$\rho \left(\frac{\partial u}{\partial t} + u \frac{\partial u}{\partial x} + v \frac{\partial u}{\partial r} + \frac{w}{r} \frac{\partial u}{\partial \theta} \right) + \frac{\partial p}{\partial x}$$

$$= \mu \left(\frac{\partial^2 u}{\partial x^2} + \frac{\partial^2 u}{\partial r^2} + \frac{1}{r} \frac{\partial u}{\partial r} + \frac{1}{r^2} \frac{\partial^2 u}{\partial \theta^2} \right)$$
(2.55)

$$\rho \left(\frac{\partial v}{\partial t} + u \frac{\partial v}{\partial x} + v \frac{\partial v}{\partial r} + \frac{w}{r} \frac{\partial v}{\partial \theta} - \frac{w^2}{r} \right) + \frac{\partial p}{\partial r}$$

$$= \mu \left(\frac{\partial^2 v}{\partial x^2} + \frac{\partial^2 v}{\partial r^2} + \frac{1}{r} \frac{\partial v}{\partial r} - \frac{v}{r^2} + \frac{1}{r^2} \frac{\partial^2 v}{\partial \theta^2} - \frac{2}{r^2} \frac{\partial w}{\partial \theta} \right)$$
(2.56)

$$\rho \left(\frac{\partial w}{\partial t} + u \frac{\partial w}{\partial x} + v \frac{\partial w}{\partial r} + \frac{w}{r} \frac{\partial w}{\partial \theta} + \frac{vw}{r} \right) + \frac{1}{r} \frac{\partial p}{\partial \theta}$$

$$= \mu \left(\frac{\partial^2 w}{\partial x^2} + \frac{\partial^2 w}{\partial r^2} + \frac{1}{r} \frac{\partial w}{\partial r} - \frac{w}{r^2} + \frac{1}{r^2} \frac{\partial^2 w}{\partial \theta^2} + \frac{2}{r^2} \frac{\partial v}{\partial \theta} \right)$$
(2.57)

$$\frac{\partial u}{\partial x} + \frac{\partial v}{\partial r} + \frac{v}{r} + \frac{1}{r} \frac{\partial w}{\partial \theta} = 0$$
 (2.58)

⁷Zamir M. The Physics of Pulsatile Flow. Springer-Verlag, New York, 2000.

⁸Moon PH, Spencer DE. Field Theory for Engineers. Van Nostrand Reinhold Inc., New York, 1961.

Velocity components u, v, w in this case are in the directions of x, r, θ , respectively, where x is in the cylindrical axis direction, r is in the radial direction, and θ is in the circumferential direction. The last equation is the equation of continuity.

The components of the stress tensor in cylindrical polar coordinates r, θ, z are given by

$$\begin{cases}
\sigma_{xx} = -p + 2\mu \left(\frac{\partial u}{\partial x}\right) \\
\sigma_{rr} = -p + 2\mu \left(\frac{\partial v}{\partial r}\right) \\
\sigma_{\theta\theta} = -p + 2\mu \left(\frac{1}{r}\frac{\partial w}{\partial \theta} + \frac{v}{r}\right)
\end{cases} (2.59)$$

$$\begin{cases}
\tau_{xr} = \tau_{rx} = \mu \left(\frac{\partial u}{\partial r} + \frac{\partial v}{\partial x} \right) \\
\tau_{x\theta} = \tau_{\theta x} = \mu \left(\frac{\partial w}{\partial x} + \frac{1}{r} \frac{\partial u}{\partial \theta} \right) \\
\tau_{r\theta} = \tau_{\theta r} = \mu \left(\frac{\partial w}{\partial r} - \frac{w}{r} + \frac{1}{r} \frac{\partial v}{\partial \theta} \right)
\end{cases} (2.60)$$

Chapter 3 Steady Flow in a Tube

3.1 Introduction

Flow in tubes is one of the most common physical phenomena, indeed one of the most common physical *tools*, in biology. Its evolution as a form of transport in biology^{1,2,3} is so closely intertwined with the evolution of life that it is difficult to view the two as separate from each other. Not even in the realm of science fiction can we imagine a living organism of any degree of complexity without the facility of flow in tubes.

There are many spectacular phenomena in fluid flow^{4,5}: the whirling of a tornado and the ominous whip-like posture of its axis as it rises to the sky; the massive bulk of ocean waves and the open "jaw" of a breaker wave; the calm and innocent looking flow towards the edge of a fall and the complete breakdown of that innocence as flow reaches the edge.

There are many beautiful fluid flow phenomena: the meticulous forming of a water drop at the mouth of a slowly dripping tap and the drama of its eventual breakaway; the anatomy of a splash and the choreography of the blobs and tentacles of displaced fluid as they rise from the site of the splash in a splendid variety of geometrical forms, particularly when seen in slow motion and when minute details

¹LaBarbera M, 1990. Principles of design of fluid transport systems in zoology. Science 249: 992–1000.

²LaBarbera M, 1991. Inner currents: How fluid dynamics channels natural selection. Sciences Sept/Oct:30–37.

³LaBarbera M, Vogel S, 1982. The design of fluid transport systems in organisms. Am Scientist 70:54–60.

⁴Van Dyke M. An Album of Fluid Motion. Parabolic Press, 1982.

⁵Nakayama Y. Visualized Flow. Pergamon Press, 1988.

are magnified; the pattern of rings that form on the surface of still water when gently disturbed by a small object, by the touch of a stick, or even by the landing of an insect.

And then there are many intriguing fluid flow phenomena: the tireless race of air elements over the bulged top surface of an aircraft wing. The bulge in effect presents a constriction which reduces the space available to the flow and forces it to either move faster or become denser. The second option would seem natural for air because of the ease with which it can compress, but for reasons of its own the flow takes the first option. The situation is not unlike that of the traffic on a multi-lane highway when presented with a constriction which reduces the number of available lanes, but here, interestingly, the second option is chosen. Cars slow down and come closer together (density is increased), though usually not enough to maintain the same flow rate as that of incoming cars. What is intriguing further in the case of air flow is that when the flight speed exceeds the speed of sound, the behavior of air becomes a combination of the first and second options, giving rise to the well known phenomena of shock waves and sonic booms.

There is truly no end to the variety and range of fluid flow phenomena, and it is no more possible to illustrate this variety with a few examples than it is possible to illustrate the variety of life forms by describing the elephant and the fly. Yet, astonishingly, the heart and soul of fluid flow is neither spectacular nor intriguing or beautiful. It is perhaps the most innocuous of all fluid flow phenomena. It is the flow in a tube.

The distinctive features of the flow in a tube are its simplicity, its flexibility, its remarkable reliability and, above all, its unfailing delivery. It is by far the most important mode of transport on this planet, a most efficient way of moving mass, heat energy, or chemical ingredients, a way perhaps unmatched by any other, natural or man-made.

If a vast amount of heat energy is to be removed in a hurry and is to be carried away from its source to another destination, as is the case at a nuclear reactor, flow in a tube is the only way in which the task has been achieved so far. A scheme based on heat removal by solids would be doomed from the start. While solids usually have the capacity to contain more heat energy than do fluids, the elements of a solid are limited by the slow speed of *diffusion* in moving that heat from one location to another. By contrast, the elements of fluid in a tube are able to "take the heat and run" using the much faster process of *convection*. Without the facility of flow in tubes the enormous heat generated in a nuclear power plant simply cannot be removed fast enough, thus turning the power plant into a nuclear bomb. Indeed, the plant *is* a nuclear bomb but for the flow of fluid in the tubes of its cooling system.

The control of temperature in our own body is less spectacular but no less critical, and the consequences of not moving sufficient heat energy from one part of the body to another is no less dire, and here too, flow in tubes is the method of choice. Blood flow, having access to every corner of the body, achieves this task with relative ease. It is hard to imagine how else it could be done.

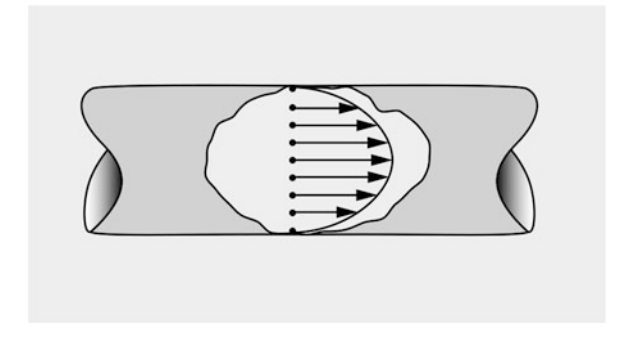
Of course, the more familiar function of blood flow is not the transport of heat but the transport of nutrients and waste products, and the hauling of a multitude of chemical messages to and from every corner of our body. Again, any scheme for doing so without the use of flow in tubes would seem inconceivable. Indeed, flow in tubes is an indispensable facility in the inner workings of all living things. Only the most primitive life forms can do without it. To us, sapiens, flow in tubes is how we take in most of our food, much of how we deal with it once it is in, how we bring the nutrients from it to where they are needed, how we eliminate what is left, how we breath to bring in the gases we need from the atmosphere and to expel those we do not need, how we reproduce, and even how we think. Not even the most daring science fiction can produce a design of our body without the facility of flow in tubes.

3.2 Condition of "No-Slip"

When moving through a tube, fluid does not slide in bulk through the tube, as a pellet. Fluid elements in contact with the tube wall actually grab on to the wall, or more accurately "smear" onto the wall and become stuck to it in a condition known as "no-slip". The next layer of fluid then uses the first layer, somewhat as a lubricant, to move slowly forward. The third layer does the same over the second layer, moving a little faster than the second, and so on, the fastest moving fluid being along the axis of the tube. The result, in a cross section of the tube, is a "velocity profile" with zero velocity at the tube wall, gradually increasing from there to a maximum at the center, as illustrated schematically in Fig. 3.1. The situation is somewhat like the bulge of a sail, two edges of the sail being firmly held by the posts, then the bulge of the sail gradually increasing from there to a maximum at the center.

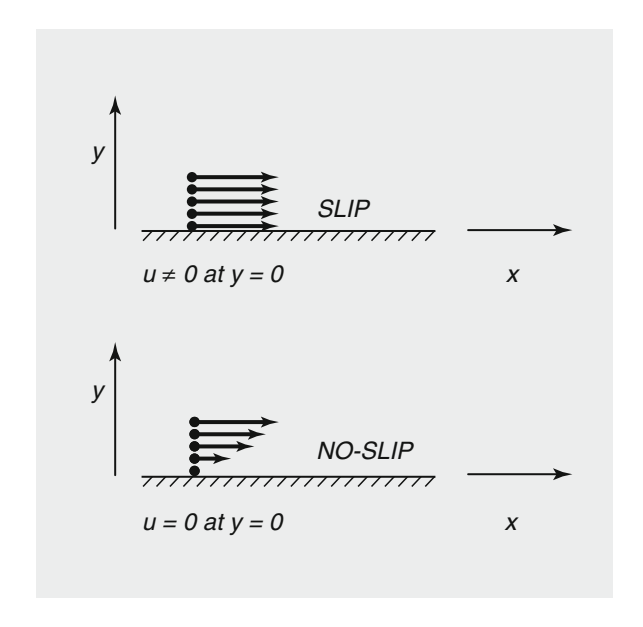
A picture of the flow in a tube thus emerges in which cylindrical layers of the fluid move forward, one inside the other in a concentric fashion. The layers do not slide over each other as they move but rather shear each other as the inner ones move

Fig. 3.1 Velocity "profile" of the flow in a tube. Flow velocity at the tube wall is zero, rising gradually and smoothly to a maximum at the tube center.



⁶Schlichting H. Boundary-Layer Theory. McGraw-Hill, 1979.

Fig. 3.2 Condition of no-slip at a solid-fluid interface. Viscosity does not allow a fluid to slip past a solid boundary. Fluid in contact with the boundary must have zero velocity, and the velocities of neighboring elements must change smoothly to meet that value at the wall.



faster than the outer ones and as they remain forever stuck to each other. Shearing, but not sliding or slipping, is the hallmark of fluid flow.

This remarkable picture of the flow in a tube is a result of two factors: the condition of no-slip and the viscous property of fluids. For a somewhat more animated picture see "Poiseuille Flow: A Story" in Appendix B.

The condition of no-slip is one of the most fundamental condition at the interface between a fluid body in motion and a solid boundary. It requires that there be no velocity difference between the solid boundary and fluid elements in contact with it as illustrated schematically in Fig. 3.2. In fact this is only a special case of a more general condition, imposed by the viscous property of fluids, that there be no finite velocity difference between any two adjacent layers of fluid, no step change in velocity anywhere within a flow field. This, as we recall, is because an external force is required to produce a rate of deformation within the fluid. The force is required to overcome the viscous resistance of the fluid and is (Eq. 2.46) proportional to the velocity gradient. Since a step change in velocity would imply an infinite velocity gradient, it would require an infinite force to maintain. Thus, only a smooth velocity gradient is possible, whereby the velocity difference between adjacent layers of fluid is infinitely small. In particular, a smooth velocity gradient, not a step change, is established within the flow field in a tube, starting at the wall of the tube where the velocity increases gradually from zero at the wall to a maximum at the center of the tube. This velocity gradient at the wall represents the viscous resistance between the tube and the moving fluid. It is the resistance which needs to be overcome in order to drive the flow through the tube. Only a fluid without viscosity would be able to slide through the tube without the need for a force to drive it.

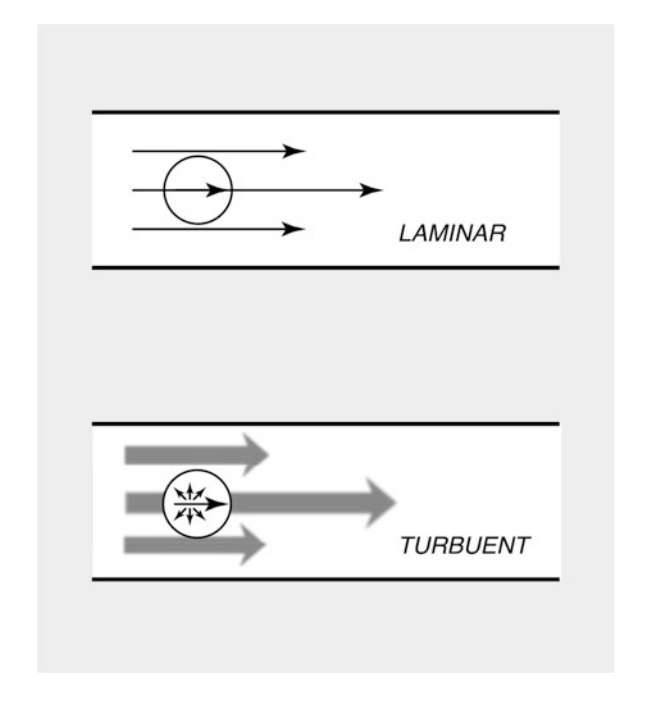
3.3 Laminar and Turbulent Flow

In late nineteenth century, Osborne Reynolds made one of the most important discoveries about the flow in a tube.^{7,8} In a series of experiments designed to study the basic characteristics of the flow, Reynolds rendered the flow visible by injecting dye at the tube's entrance, then changed the flow rate to see how this affected what he observed. The injection of dye had the effect of "marking" elements of fluid so that their subsequent course could be observed.

Reynolds found that at low flow rates the marked elements produced streaklines which were fairly distinct and ran parallel to the axis of the tube. At higher flow rates, however, the streaklines became increasingly unstable, eventually breaking down and causing the dye to diffuse over the whole cross section of the tube, streaklines being no longer distinct or visible. Reynolds identified what he observed as two different types of flow. Today they are known widely as "laminar" and "turbulent" flow.

Later, more advanced technology which was not available to Reynolds showed that in laminar flow fluid elements move only in the direction of the flow, in the direction of the Eulerian velocity vector at each point (Fig. 3.3).

Fig. 3.3 Laminar and turbulent flow. In laminar flow, fluid elements move only in the main flow direction. In turbulent flow, fluid elements vibrate randomly in all directions as they move in the main flow direction.



⁷Tokaty GA. A History & Philosophy of Fluidmechanics. Foulis & Co., Henley-On-Thames, 1971.

⁸Rouse H, Ince S. History of Hydraulics. Dover, New York, 1957.

In turbulent flow, by contrast, fluid elements vibrate randomly in all directions, at high frequency and with small amplitude, as they move in the main flow direction. Thus in turbulent flow a fluid element typically has a "mean" velocity component in the main flow direction, plus small amplitude oscillatory velocity components in all directions.

The phenomenon of turbulence is a remarkable revisiting of the random motion of molecules on the microscopic scale, which is dealt with by treating a fluid body as a continuum of fluid elements on the much larger macroscopic scale. The difficulty with turbulence is that the scale on which it occurs is already the larger macroscopic scale, and it is the fluid elements themselves that are now engaged in unnecessary random motion.

As a consequence, more energy is expended in turbulent flow in order to produce this motion. Some of this energy is wasted in the form of heat energy produced by viscous friction and some is wasted in the form of sound energy. Indeed, turbulent motion is actually *audible*.

Reynolds found that the onset of turbulence depends not only on the average flow velocity through the tube, \overline{u} , but also on the density ρ and viscosity μ of the fluid, and diameter d of the tube. His most important contribution was to then recognize that the onset of turbulence actually depends not on \overline{u} , ρ , μ , d individually but on the nondimensional combination

$$R = \frac{\rho \overline{u}d}{\mu} \tag{3.1}$$

which today is known universally and appropriately as the Reynolds number. Reynolds' experiments suggested that transition from laminar to turbulent flow occurred at $R \approx 2000$, but since then it has been found that transition can be delayed to much higher values of R if flow disturbances at entrance to the tube and surface roughness at the tube wall are kept to a minimum. Present understanding is that the value R = 2000 is a "lower bound" below which flow will remain in the laminar state even if disturbed. At higher values of R the flow becomes increasingly unstable and may become turbulent depending on prevailing destabilizing conditions.

In blood flow, the highest flow velocities occur in the aorta as it leaves the heart for distribution to the rest of the body. Assuming *steady* flow at first, in a human aorta of approximately 2.5 cm in diameter and an average cardiac output of 5 L/min, the average velocity is given by

$$\overline{u} = \frac{5000/60}{\pi \times 2.5^2/4} \approx 17 \,\text{cm/s}$$
 (3.2)

⁹Schlichting H. Boundary-Layer Theory. McGraw-Hill, 1979.

Taking the density $\rho \approx 1 \,\mathrm{g/cm^3}$ and viscosity $\mu \approx 0.04 \,\mathrm{g/cm}$ s, we obtain

$$R = \frac{\rho \overline{u}d}{\mu} = \frac{1 \times 17 \times 2.5}{0.04} \approx 1063$$
 (3.3)

indicating that under these assumptions the Reynolds number is well below 2000.

In *pulsatile* flow, at the peak of the oscillatory cycle (systole), and under conditions of high cardiac output, this value of *R* can be exceeded considerably, thus the possibility exists for turbulent flow to occur at this level of the arterial tree and in part of the oscillatory cycle. At higher levels of the vascular tree, however, the Reynolds number diminishes rapidly because average flow velocities, vessel diameters and oscillatory flow peaks, all diminish rapidly, leaving conditions under which laminar flow is stable and the possibility of turbulent flow is considerably reduced. For this reason much of the work on pulsatile flow deals with laminar flow, and we follow this practice in this book. The mathematical description of fluid flow in Chap. 2 and the equations derived in that chapter relate strictly to laminar flow.

Turbulence as described above may be referred to as "high-Reynolds-number-turbulence" to be distinguished from eddies or vortices which occur on a larger scale and the details of which can in many cases be visualized and mathematically described. By contrast, high-Reynolds-number-turbulence is totally random and occurs on the much finer scale of fluid elements and cannot be easily visualized. Vortices and eddies are in effect only disturbed or unstable forms of laminar flow.

In blood flow it is important to distinguish between these two physically distinct phenomena because the situations in which they arise are very different. At the peak of each oscillatory cycle in pulsatile flow, for example, the Reynolds number may become momentarily high enough for high-Reynolds-number-turbulence to occur in the aorta. By contrast, flow emerging from a constriction within a blood vessel or from a malfunctioning heart valve as it closes often leads to vortices and eddies. The underlying cause in one case is high velocity while in the other it is disturbed or disorderly flow. It is important both clinically and phenomenologically that the two phenomena not be described by the same word. For this reason, in this book the word "turbulence" shall be used exclusively in reference to high-Reynolds-number turbulence, while disturbed or disorderly flow, eddies and vortices shall be referred to simply as such.

Another element of confusion may arise in the clinical setting because both turbulence and disturbed or disorderly flow produce sound which can be heard with the aid of a stethoscope. The word "murmur" is generally used to describe sounds originating from the heart, caused by a defective heart valve. It is important that the same word not be used to describe every sound originating from the heart or from other locations within the cardiovascular system as the clinical interpretation of these may be very different from that generally associated with the word "murmur".

3.4 Entry Length

The velocity profile of flow in a tube discussed qualitatively in Sect. 3.2, with zero velocity at the tube wall and increasing gradually to a maximum at the tube center, prevails only far downstream from the tube entrance. As will be described below, the velocity profile at the entrance is actually different and it only gradually evolves into that form as the flow progresses downstream as shown schematically in Fig. 3.4. The length of tube required for the velocity profile to reach its final form is known as the "entry length", and the final form of the flow and of the velocity profile is said to be "fully developed". The form of flow in a tube discussed in Sect. 3.2 is that of fully developed flow. In this section we describe briefly how that form is reached and how far downstream from the entrance it does so.

When flow enters a tube, the no-slip boundary condition on the tube wall arrests fluid elements in contact with the wall while elements along the axis of the tube charge ahead, less influenced by that condition. Since viscosity of the fluid does not allow a step change in velocity to occur anywhere in the flow field, a smooth velocity profile must develop to join the faster moving fluid along the axis of the tube with the stationary fluid at the tube wall. At the tube entrance this velocity profile consists of a straight line representing the bulk of the fluid moving uniformly down the tube, then dropping rapidly but smoothly to zero near the wall. Further downstream, however, because of viscosity, the arrested layer of fluid at the tube wall begins to slow down the layer of fluid in contact with it on the other side, and this effect propagates further and further away from the wall as the flow progresses further and further downstream from the entrance. Thus the region of influence of the no-slip boundary condition grows further and further away from the wall, with the result that the velocity profile becomes more and more rounded. When the wall effect engulfs the entire cross section of the tube, the velocity profile reaches its fully developed form.

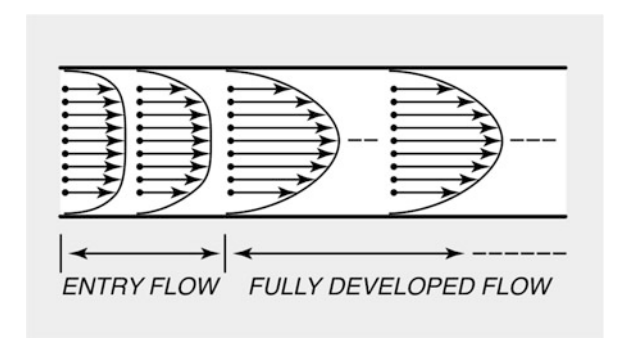


Fig. 3.4 Entry flow in a tube. When flow enters a tube, only fluid near the tube wall or in contact with it is influenced by the no-slip boundary condition there. As flow moves further downstream, however, this region of influence grows, leading ultimately to a more rounded velocity profile. Flow in this region is called "fully developed" in the sense that it has reached its ultimate form, while developing flow in the preceding region is called "entry flow".

3.4 Entry Length 51

An inherent difficulty with the computation or measurement of the entry length is that the flow reaches its fully developed state only *asymptotically*. Thus, mathematically, the entry length is infinite. For practical purposes, however, flow in a tube becomes *very nearly fully developed* at a finite distance from the tube entrance which can be determined both theoretically and experimentally once a criterion is prescribed for how close the flow must be to its ultimate form.

A criterion which has been commonly used is that the flow is deemed fully developed when the centerline velocity has reached 99 % of its ultimate value. Other criteria, based on integral properties of the velocity profile, have also been used. In either case, the actual value of the entry length depends on the form in which flow enters the tube and the assumption usually made here is that the flow enters the tube with uniform velocity U. The entry length, of course, also depends on the viscosity μ and density ρ of the fluid.

With these considerations in mind, if the entry length is denoted by l_e and the tube diameter is denoted by d, the generally accepted value of the entry length, expressed in non-dimensional form, is given by

$$\frac{l_e}{d} = 0.04R_d \tag{3.4}$$

where R_d is the Reynolds number based on the diameter of the tube, namely

$$R_d = \frac{\rho U d}{\mu} \tag{3.5}$$

Thus at $R_d = 1000$, for example, the entry length is equal to 40 tube diameters. At $R_d = 100$ it is only four tube diameters.

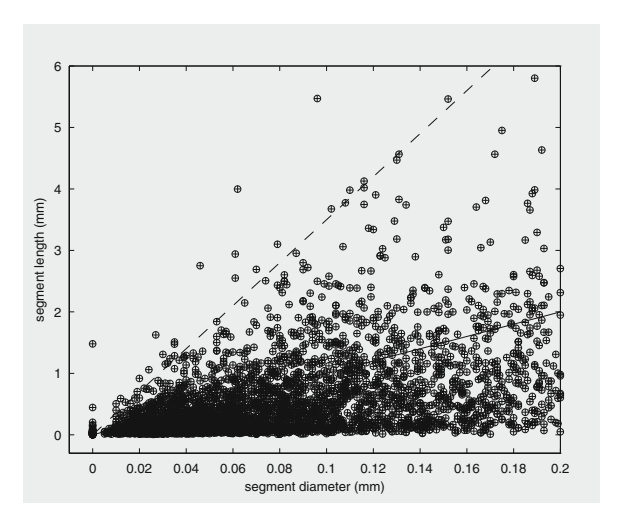
In the cardiovascular system flow is rarely in a very long tube segment as it progresses from one vascular junction to the next. The vascular tree is made up of many millions of vascular segments which typically have a length to diameter ratio of about 10 and ranging anywhere from a minimum near zero to a maximum of 35–40 (Fig. 3.5¹¹). Flow in each vascular segment therefore typically does not have the entry length required for that segment. However, the flow is entering and re-entering these segments not as uniform flow but as *partially developed flow*.

When flow entering a tube is partially developed, or in any case not uniform, its entry length is usually shorter than the corresponding entry length for uniform entry flow. Thus, while flow in the arterial tree may not have sufficient run to become fully developed in each tube segment, it may become increasingly developed as it hops from one segment to the next. Furthermore, as flow progresses from the central segments of the arterial tree towards the periphery, both the diameter of vessel segments and the average velocity within them rapidly decrease. The Reynolds number, from a high of about 1000 in the aorta, decreases rapidly in subsequent

¹⁰Schlichting H. Boundary-Layer Theory. McGraw-Hill, 1979.

¹¹Zamir M. On fractal properties of arterial trees. Journal of Theoretical Biology 197:517–526.

Fig. 3.5 Length of tube segments in a vascular tree. Measurements, here taken from the vascular tree of the human heart (see Footnote 11), indicate that while there is no apparent correlation between the length and diameter of vessel segments, the ratio of length to diameter seems to have a maximum value of about 35 (dashed line) and an average of about 10 (solid line).



segments. The flow in these segments therefore requires smaller and smaller length to diameter ratios to become fully developed.

These considerations suggest that while flow may not be fully developed everywhere in the vascular tree, it may be very close to that state in many parts of the tree. The assumption of a fully developed state when considering *steady* flow in the arterial tree, whether locally or in the tree as a whole, may therefore be somewhat justified on this basis. From a practical view point the assumption is in any case a necessary approximation to make the analysis tractable. Analysis based on individual flow development in each of many millions of tube segments is clearly impractical.

If fluid enters a tube uniformly with velocity U, then U must equal the average velocity \overline{u}_s of the fully developed flow profile which it ultimately reaches. Velocity along the centerline of the tube, however, must change from U to the *maximum* velocity in that profile, which will be shown later to be twice the average velocity. Thus in the entry region of flow in a tube, fluid near the centerline of the tube must be accelerated, and this acceleration requires extra pumping power to maintain. Analysis based on fully developed flow is therefore likely to underestimate the power required to drive the flow in the vascular tree.

In pulsatile blood flow the entry flow problem is further complicated by the combination of flow development in space and time. When the frequency of pulsation is low, the flow reaches the fully developed flow profile at the peak of each cycle in the fully developed region, thus the results of fully developed steady flow bear some relevance to pulsatile flow in that region. In the entry region the situation is more complicated. In its simplest form, the flow at a given distance from the tube's entrance attempts to reach the velocity profile which prevails in steady flow at that location, but the problem is not actually as simple because equations governing the flow in the entrance region are nonlinear.

It is important that "fully developed flow" not be confused with "steady flow". The first relates to a region of the tube where the velocity profile has reached its ultimate form and is no longer changing in space (x). The second relates to the flow anywhere within the tube being fixed in time. Thus, flow in the entry region of a tube is not fully developed in the sense that it is changing in space but it may be steady in the sense that it is not changing in time. Similarly, flow in the fully developed region of the tube is not changing in space but it may be non-steady or steady depending on whether it is or is not changing in time.

3.5 Simplified Equations

The Navier-Stokes equations derived in Sect. 2.11 provide the governing equations for a very wide range of fluid flow problems. Flow in a tube in its most general form requires the full equations, but if it can be assumed that the cross section of the tube is circular and the tube is straight and sufficiently long, and if attention is focused on only the fully developed region of the flow, these equations can be simplified considerably. The classical solutions for steady or pulsatile blood flow are based on a highly simplified form of the Navier-Stokes equations. In this section we present the assumptions on which the simplified equations are based and show how these equations are obtained from the general form of the Navier-Stokes equations (Eqs. 2.55–2.58).

If the tube is straight and has a circular cross section, and in the absence of any external forces which would cause flow rotation, the flow field will be symmetrical about the longitudinal axis of the tube to the effect that the angular component of velocity and all derivatives in the angular direction are then zero, that is

$$w \equiv \frac{\partial w}{\partial \theta} \equiv \frac{\partial v}{\partial \theta} \equiv \frac{\partial u}{\partial \theta} \equiv \frac{\partial p}{\partial \theta} \equiv 0 \tag{3.6}$$

All terms in Eq. 2.57 are then identically zero and the other two equations (Eqs. 2.55 and 2.56), together with the equation of continuity (Eq. 2.58) simplify to

$$\begin{cases}
\rho \left(\frac{\partial u}{\partial t} + u \frac{\partial u}{\partial x} + v \frac{\partial u}{\partial r} \right) + \frac{\partial p}{\partial x} = \mu \left(\frac{\partial^2 u}{\partial x^2} + \frac{\partial^2 u}{\partial r^2} + \frac{1}{r} \frac{\partial u}{\partial r} \right) \\
\rho \left(\frac{\partial v}{\partial t} + u \frac{\partial v}{\partial x} + v \frac{\partial v}{\partial r} \right) + \frac{\partial p}{\partial r} = \mu \left(\frac{\partial^2 v}{\partial x^2} + \frac{\partial^2 v}{\partial r^2} + \frac{1}{r} \frac{\partial v}{\partial r} - \frac{v}{r^2} \right) \\
\frac{\partial u}{\partial x} + \frac{\partial v}{\partial r} + \frac{v}{r} = 0
\end{cases}$$
(3.7)

If these equations are now further restricted to only the fully developed region of the flow, where by definition

$$\frac{\partial u}{\partial x} \equiv \frac{\partial v}{\partial x} \equiv 0 \tag{3.8}$$

then the equation of continuity reduces to

$$\frac{\partial v}{\partial r} + \frac{v}{r} = \frac{1}{r} \frac{\partial (rv)}{\partial r} = 0 \tag{3.9}$$

which can be integrated to give

$$rv = constant$$
 (3.10)

Since v must be zero at the tube wall (r = a), this result implies that the radial component of velocity must be identically zero, that is

$$v \equiv 0 \tag{3.11}$$

As a result of this and Eq. 3.8, the equation of continuity (Eq. 3.9) is now satisfied identically, and all the velocity terms in the second Navier-Stokes equation (Eq. 2.56) are now zero, therefore

$$\frac{\partial p}{\partial r} \equiv 0 \tag{3.12}$$

which implies that p is a function of only x and t. In the remaining Navier-Stokes equation (Eq. 2.55), terms containing velocity gradients in x are zero because of Eq. 3.8 and the term containing v is zero because of Eq. 3.11, thus the entire Navier-Stokes equations together with the equation of continuity reduce to

$$\rho \frac{\partial u}{\partial t} + \frac{\partial p}{\partial x} = \mu \left(\frac{\partial^2 u}{\partial r^2} + \frac{1}{r} \frac{\partial u}{\partial r} \right)$$
 (3.13)

This is the highly simplified form of the governing equations on which the classical solutions for fully developed steady and pulsatile flow in a tube are based. As a result of the simplifying assumptions and their consequences in Eqs. 3.8 and 3.12, the velocity u in Eq. 3.13 is now a function of r and t only, while the pressure p is a function of x and t only, that is

$$\begin{cases} u = u(r, t) \\ p = p(x, t) \end{cases}$$
 (3.14)

This means that as the flow progresses along the tube, only the pressure p is changing, not the velocity u. This can only happen if the tube is rigid. If the tube is not rigid, the change in pressure will cause a corresponding change in the diameter of the tube which in turn will lead to x-changes in not only the magnitude but direction of velocity. As a consequence, not only will u become a function of x but the radial component of velocity (v) will become nonzero. These circumstances will be dealt with later when considering flow in elastic tubes. The purpose of the present discussion is to emphasize that Eq. 3.13 is valid only for flow within a rigid tube.

Finally, if the flow in a tube is *steady*, the velocity and pressure are independent of time and the equation for flow in a tube (Eq. 3.13) reduces further to

$$\frac{dp_s}{dx} = \mu \left(\frac{d^2 u_s}{dr^2} + \frac{1}{r} \frac{du_s}{dr} \right) \tag{3.15}$$

The subscript s has now been introduced to emphasize that we are now dealing with steady flow where the velocity and pressure are not functions of time. It should not be surprising that the equation no longer involves the fluid density ρ . There are no longer any acceleration terms in the equation. In fact, the equation is no longer an expression of Newton's law of "mass×acceleration = force" but rather a degenerate form of this law, namely "force = force"

$$\underbrace{\frac{dp_s}{dx}}_{\text{driving pressure force}} = \underbrace{\mu\left(\frac{d^2u_s}{dr^2} + \frac{1}{r}\frac{du_s}{dr}\right)}_{\text{resisting viscous force}}$$
(3.16)

The progression from Eq. 2.55 to Eq. 3.13 and then to Eq. 3.16 further clarifies the discussion concerning the important difference between "steady" flow and "fully developed" flow at the end of the previous section. In Eq. 2.55 the velocity field is changing in space (x) as well as in time (t), thus the flow is neither fully developed nor steady. In Eq. 3.13 the flow field is no longer changing in x, the velocity as a function of r (velocity profile) is the same at all positions x along the tube but at each position it may be changing in time t. In Eq. 3.16, finally, the velocity field is fixed in both time and space, the flow is both steady and fully developed.

At the core of this discussion is the fact that the acceleration of a fluid element at position x, y, z and time t in a flow field (Eq. 2.26) depends on (a) the rate of change of the Eulerian velocities *in time* at that position and (b) the rate of change of the Eulerian velocities *in space* at that position and that point in time. In steady flow the changes in (a) are zero while in fully developed flow the changes in (b) are zero. Thus, again, "steady flow" and "fully developed flow" are not to be confused with each other.

3.6 Balance of Forces

As noted in Sect. 3.2, the mechanics of steady flow in a tube are remarkably simple. Only two forces are involved: a pressure force driving the flow and a viscous force resisting the flow. The equation governing the flow (Eq. 3.16) can be derived from the Navier-Stokes equations as shown in the previous section. However, to highlight the simple mechanics characterizing the flow, it is instructive to see that the governing equation can actually be derived directly by considering the balance of the two forces which elements of the fluid within the tube are subject to.

Consider a cylindrical volume of fluid within the tube, of length δx , inner radius r and outer radius $r + \delta r$ (Fig. 3.6). This volume of fluid is under a pressure force attempting to move it forward and a viscous force resisting that motion. In steady flow (no acceleration) these two forces are in equilibrium. The pressure force arises because the pressure at the downstream end of that volume is p_s while at the upstream end it is higher, say $p_s + \delta p_s$. The viscous resistance arises because the shear stress acting on its inner surface is τ_s while on the outer surface it is higher, say $\tau_s + \delta \tau_s$. The subscript s is used here again, as in the previous section, to note that the flow is steady and that both p and τ are not functions of time.

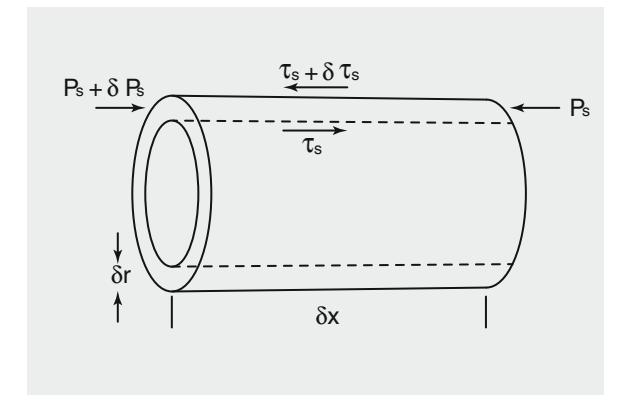
Recalling that both p_s and τ_s are *stresses*, meaning that the *forces* which they give rise to are given by the stresses multiplied by the surface areas on which they are acting, and equating the pressure and viscous forces acting on the cylindrical volume of fluid, we then have

$$\begin{cases} (p_s + \delta p_s) \times 2\pi r \delta r - p_s \times 2\pi r \delta r = \\ (\tau_s + \delta \tau_s) \times 2\pi (r + \delta r) \delta x - \tau_s \times 2\pi r \delta x \end{cases}$$
(3.17)

Simplifying gives

$$\delta p_s \times r \delta r = \tau_s \times \delta r \delta x + \delta \tau_s \times r \delta x + \delta \tau_s \times \delta r \delta x \tag{3.18}$$

Fig. 3.6 Pressure and shear forces acting on a cylindrical volume of fluid within the flow in a tube.



3.7 Poiseuille Flow 57

and on division by $r\delta r\delta x$

$$\frac{\delta p_s}{\delta x} = \frac{\tau_s}{r} + \frac{\delta \tau_s}{\delta r} + \frac{\delta \tau_s}{r} \tag{3.19}$$

Now, as $\delta \tau_s$, δr , $\delta x \rightarrow 0$, the last term vanishes because it is an order of magnitude smaller than the other terms, and the quotient increment terms become derivatives, giving

$$\frac{dp_s}{dx} = \frac{\tau_s}{r} + \frac{d\tau_s}{dr} \tag{3.20}$$

The shear stress τ in this case is simply related to the velocity gradient

$$\tau_s = \mu \frac{du_s}{dr} \tag{3.21}$$

thus, Eq. 3.20 finally becomes

$$\frac{dp_s}{dx} = \mu \left(\frac{d^2 u_s}{dr^2} + \frac{1}{r} \frac{du_s}{dr} \right)$$

which is the same as Eq. 3.16. It is instructive to note that both sides of this equation are negative because the pressure p is decreasing in x (in order to drive the flow in the positive x direction) and the velocity u is decreasing in r (from a maximum at r=0 to zero at r=a). We see this explicitly and more clearly in the next section as we obtain the actual velocity profile in a cross section of the tube, as well as find that the second derivative of the velocity is also negative.

3.7 Poiseuille Flow

Fully-developed, steady flow in a tube is governed by Eq. 3.16 as derived in Sects. 3.5 and 3.6. As discussed in those sections, under steady flow conditions the pressure is a function of x only while the velocity is a function of r only. Both functions are independent of time t and Eq. 3.14 reduces to

$$u = u_s(r), \quad p = p_s(x)$$
 (3.22)

Thus, in the equation governing the flow, namely (Eq. 3.16)

$$\frac{dp_s}{dx} = \mu \left(\frac{d^2 u_s}{dr^2} + \frac{1}{r} \frac{du_s}{dr} \right)$$

the left hand side is a function of x only while the right hand side is a function of r only. The only way that the equation can be satisfied in general, therefore, is by having both sides equal a constant, the same constant, say k_s . Thus the governing equation in effect splits into two separate equations, one for the pressure

$$\frac{dp_s}{dx} = k_s \tag{3.23}$$

and one for the velocity

$$\mu\left(\frac{d^2u_s}{dr^2} + \frac{1}{r}\frac{du_s}{dr}\right) = k_s \tag{3.24}$$

Solving the pressure equation first, gives

$$p_s(x) = k_s x + p_s(0) (3.25)$$

where $p_s(0)$ is the pressure at x = 0, and if $p_s(l)$ is the pressure at a point x = l downstream, then

$$p_s(l) = k_s l + p_s(0) (3.26)$$

The constant k_s is thus given by

$$k_s = \frac{p_s(l) - p_s(0)}{l} \tag{3.27}$$

which is the *pressure gradient* along the tube. For flow in the positive x direction the pressure upstream $(p_s(0))$ must be higher than the pressure downstream $(p_s(l))$, thus the pressure gradient is negative. The pressure difference

$$\Delta p_s = p_s(0) - p_s(l) \tag{3.28}$$

is usually referred to as the corresponding "pressure drop". This leads to some confusion because the pressure difference $\Delta p_s = p_s(0) - p_s(l)$ is *positive* but by using the term "drop" it is implied that one is referring to the *negative* of that pressure difference. It is therefore important to use the concept of "pressure drop" by *definition*, as in Eq. 3.28 (or any other), rather than by *implication*. If Δp_s is defined as above, we then have

$$\Delta p_s = -k_s \times l \tag{3.29}$$

It is clear that the above result is valid only in the *fully developed* region of the flow because the Eq. 3.13 on which the results are based is valid only for fully developed flow. Thus the points x = 0 and x = l are not to be considered as points

3.7 Poiseuille Flow 59

of entry into and exit from *the tube* but rather points of entry into and exit from a *tube segment* of length *l* within the fully developed region of the flow. The relevance of this to flow in the vascular tree was discussed in Sect. 3.4.

To solve the velocity equation, we write Eq. 3.24 in the form

$$\frac{d^2u_s}{dr^2} + \frac{1}{r}\frac{du_s}{dr} = \frac{k_s}{u} \tag{3.30}$$

or

$$\frac{d}{dr}\left(r\frac{du_s}{dr}\right) = \frac{k_s}{\mu}r\tag{3.31}$$

Integrating once gives

$$\frac{du_s}{dr} = \frac{1}{2} \frac{k_s}{\mu} r + \frac{A}{r} \tag{3.32}$$

where A is a constant, and integrating again gives

$$u_s(r) = \frac{k_s}{4\mu}r^2 + A\ln r + B \tag{3.33}$$

where B is a constant.

The constants A, B are evaluated by imposing first that the velocity at the center of the tube be finite, that is

$$|u_s(0)| \neq \infty \tag{3.34}$$

which give

$$A = 0 \tag{3.35}$$

and then impose the no-slip boundary condition at the tube wall (r = a) where a is the tube radius, that is

$$u_s(a) = 0 (3.36)$$

which give

$$B = -\frac{k_s}{4\mu}a^2\tag{3.37}$$

With these values of A and B, Eq. 3.33 becomes

$$u_s = \frac{k_s}{4\mu} (r^2 - a^2) \tag{3.38}$$

This is the classical "velocity profile" in fully developed steady flow in a tube, usually referred to as *Poiseuille flow* after its first author. 12,13,14 The velocity profile is often referred to as a "parabolic" velocity profile because, as a function of r it is in the form of a parabola.

3.8 Properties of Poiseuille Flow

Poiseuille flow has distinctive properties which are unique to fully developed flow in tubes. In this section we examine these properties specifically when the flow is *steady*. However, these basic properties remain relevant when the flow is not steady, particularly in pulsatile flow which will be examined in subsequent chapters. The key assumption in both cases is that the flow be *fully developed*.

Starting with the solution obtained in the previous section and writing

$$u_s(r) = \frac{k_s}{4\mu}(r^2 - a^2) \tag{3.39}$$

we note first that the no-slip boundary condition is satisfied at the tube wall (r = a), that is

$$u_s(a) = 0 (3.40)$$

Maximum (or "peak") velocity, to be denoted by \hat{u}_s , occurs on the axis of the tube (r = 0), that is

$$\hat{u}_s = u_s(0) = \frac{-k_s a^2}{4\mu} \tag{3.41}$$

The minus sign indicates that the direction of velocity is opposite to that of the pressure gradient k_s . The velocity is positive in the direction of negative pressure gradient.

As anticipated, maximum velocity on the axis of the tube and zero velocity at the tube wall are joined by a *smooth* profile, with no step change at any point in between. As noted in the previous section, the shape of that profile is a parabola, which is seen more clearly if Eq. 3.39 is divided by Eq. 3.41 to get the velocity profile in non-dimensional form

$$\frac{u_s(r)}{\hat{u}_s} = 1 - \left(\frac{r}{a}\right)^2 \tag{3.42}$$

¹²Tokaty GA. A History & Philosophy of Fluidmechanics. Foulis & Co., Henley-On-Thames, 1971.

¹³Rouse H, Ince S. History of Hydraulics. Dover, New York, 1957.

¹⁴Schlichting H. Boundary-Layer Theory. McGraw-Hill, New York, 1979.

Flow rate through the tube is usually expressed in terms of volume flow rather than mass flow because the equation of Poiseuille flow (Eq. 3.39) does not contain the density, which in turn is because the flow is steady and fully developed, hence the acceleration of fluid elements is zero. The volumetric flow rate q_s through the tube is obtained by integrating over a cross section of the tube

$$q_s = \int_0^a u_s \times 2\pi r dr$$

$$= \frac{-k_s \pi a^4}{8\mu}$$
(3.43)

Again, the minus sign indicates that flow rate and pressure gradient have opposite signs. That is, negative pressure gradient produces flow in the positive x-direction. The average velocity \overline{u}_s is then given by

$$\bar{u}_s = \frac{q_s}{\pi a^2}$$

$$= \frac{-k_s a^2}{8\mu}$$
(3.44)

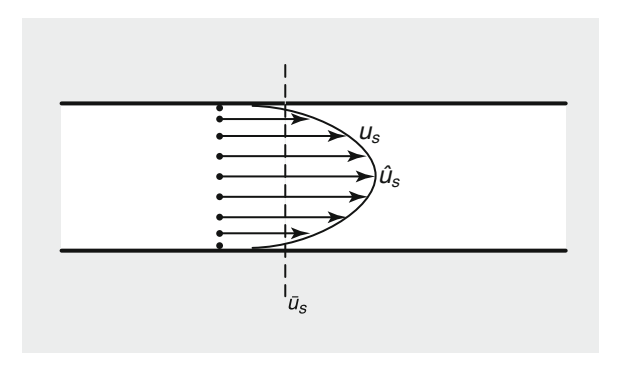
which is seen from Eq. 3.41 to be one half the maximum velocity (Fig. 3.7).

$$\frac{\overline{u}_s}{\hat{u}_s} = \frac{1}{2} \tag{3.45}$$

Of interest is the shear stress prevailing within the flow field and particularly at the tube wall. Of the different components of the stress tensor, τ_{rx} represents shear stress acting in the *x*-direction on surfaces perpendicular to *r* (cylindrical surfaces) and is thus the required component of the stress tensor. From Eq. 2.60 we have

$$\tau_{rx} = \mu \left(\frac{\partial u}{\partial r} + \frac{\partial v}{\partial x} \right) \tag{3.46}$$

Fig. 3.7 Velocity profile in steady fully developed Poiseuille flow (u_s) . The profile has a parabolic form and the average velocity (\overline{u}_s) is one half the maximum velocity (\hat{u}_s) .



and since v is zero in Poiseuille flow, this reduces to

$$\tau_{rx} = \mu \left(\frac{\partial u}{\partial r} \right) \tag{3.47}$$

Now, it will be recalled from Sects. 2.6 and 2.7 that components of the stress tensor represent forces acting on the outer boundary of a fluid element by its surrounding elements. At the wall-fluid interface in Poiseuille flow, therefore, τ_{rx} represents the drag force exerted by the wall on the moving fluid. In blood flow, of interest is the counterpart of this force, namely the force exerted by the fluid on the tube wall because it represents the direct mechanical effect of the moving fluid on endothelial tissue. We shall denote this by τ_s (the subscript "s", as before, referring to steady flow) and write

$$\tau_s = -(\tau_{rx})_{r=a} = -\mu \left(\frac{\partial u}{\partial r}\right)_{r=a}$$
 (3.48)

and using Eq. 3.39 we find

$$\tau_s = \frac{-k_s a}{2} \tag{3.49}$$

or in terms of the flow rate, using Eq. 3.43,

$$\tau_s = \frac{4\mu q_s}{\pi a^3} \tag{3.50}$$

It will be noted that τ_s and q have the same sign, which means that the force which τ_s represents is *in the direction of the flow*, and since it was evaluated at the tube wall (r = a), the force it represents is that exerted by the fluid on the tube wall as intended.

The rate of energy expenditure (power) required to maintain this drag force by the fluid on the tube wall is the pumping power H_s required to maintain the flow. It is given by the product of the total drag force and the average flow velocity. The total drag force in turn is the given by the product of the shear stress and the surface area on which it is acting. Again, to comply with the assumptions on which Poiseuille flow is based, we consider a segment of length l of the tube in which the flow is fully developed to get

$$H_s = \tau_s \times 2\pi al \times \overline{u}_s \tag{3.51}$$

Since the flow under consideration is steady, the two opposing *forces* at play must be equal (the net force must be zero). Specifically, the pressure force driving the flow must equal the shear force at the tube wall resisting the flow, that is

$$\Delta p_s \times \pi a^2 = \tau_s \times 2\pi a l \tag{3.52}$$

which is consistent with Eq. 3.49, recalling from Eq. 3.29 that

$$\Delta p_s = p_s(0) - p_s(l) = -k_s l \tag{3.53}$$

Thus the pumping power may be expressed alternatively as the product of the driving pressure force and the average flow velocity, that is

$$H_s = \Delta p_s \times \pi a^2 \times \overline{u}_s$$

$$= \Delta p_s \times q_s$$

$$= -lk_s q_s$$
(3.54)

$$=\frac{\pi l k_s^2 a^4}{8\mu} \tag{3.55}$$

In other words, the pumping power is equal to the product of the flow rate and the pressure drop.

The simplicity of Poiseuille flow in a tube admits the following analogy with the flow of electric current along a perfect conductor

electric current ⇔ volumetric flow rate

potential difference ⇔ pressure drop

resistance to current flow \Leftrightarrow resistance to fluid flow

To see the analogy more clearly, the pressure drop can be expressed in terms of the flow rate by using Eqs. 3.28 and 3.43, to get

$$\Delta p_s = \left(\frac{8\mu l}{\pi a^4}\right) q_s \tag{3.56}$$

which is analogous to the corresponding relation in the flow of electric current, namely

voltage = resistance
$$\times$$
 current (3.57)

Thus, the bracketed term in Eq. 3.56 is seen to be the resistance R to Poiseuille flow where

$$R = \frac{8\mu l}{\pi a^4} \tag{3.58}$$

Within a given tube, therefore, Eq. 3.56 shows that the pressure drop in Poiseuille flow in a tube is equal to the product of resistance and volumetric flow rate

pressure drop = resistance
$$\times$$
 flow rate (3.59)

in strict analogy with the corresponding electrical relation in Eq. 3.57. Within different tubes, however, Eq. 3.58 indicates that the resistance to flow is inversely proportional to the fourth power of the tube radius.

Finally, the expression for the pumping power in Eq. 3.54 can be put in the following form by substituting for the pressure drop from Eq. 3.56

$$H_s = \left(\frac{8\mu l}{\pi a^4}\right) q_s^2 \tag{3.60}$$

$$= R \times q^2 \tag{3.61}$$

thus

pumping power = resistance
$$\times$$
 (flow rate)² (3.62)

in analogy with

electric power = resistance
$$\times$$
 (current)² (3.63)

Conclusions for blood flow from these results are found in Eq. 3.60 which indicates that the pumping power associated with Poiseuille flow in a tube can be reduced by reducing the viscosity of the fluid, reducing the flow rate, and above all, by increasing the tube radius by even a small amount. It is remarkable that despite the drastic simplifying assumptions on which these results are based, the above three measures are highly relevant and are actually used in clinical practice to reduce the pumping load of an ailing heart. The viscosity of blood is reduced by what is referred to as "blood thinning", flow rate is reduced by reducing physical activity to reduce the demand for blood flow, and tube radii are increased by using pharmaceutical agents to dilate the blood vessels.

3.9 Energy Expenditure and Pumping Power

How much energy does it take to drive fluid through a tube? More accurately, how much power does it require to maintain fully developed Poiseuille flow in a tube? We are now in a position to justify the claim that flow in a tube is one of the most efficient forms of transport on the planet!

The equation governing steady flow in a tube (Eq. 3.24)

$$\underbrace{k_s}_{\text{driving pressure force}} = \underbrace{\mu\left(\frac{d^2u_s}{dr^2} + \frac{1}{r}\frac{du_s}{dr}\right)}_{\text{resisting viscous force}}$$
(3.64)

expresses a balance between the forces affecting the flow, specifically the driving pressure force on the left and the retarding viscous force on the right. At any point in *time* during flow in a tube, these two forces are associated with rates of energy expenditure. The pressure force is associated with the rate of energy expenditure required to drive the flow, or the "pumping power", while the viscous force is associated with the rate of energy dissipation by viscosity. In this section we examine these two rates of energy expenditure and the way in which their balance is based on the equation governing the flow. While in the present case both rates are constant and the balance between them is one of simple equality, this simple case serves as a useful foundation for the same exercise in pulsatile flow which we consider in the next chapter.

As it stands, the equation of motion above actually represents not forces but *forces per unit volume*. This, we recall, is a basic characteristic of the more general Navier-Stokes equations from which the above equation is obtained. In order to consider energy expenditures, therefore, the equation must first be multiplied by some volume of fluid so that its terms will actually represent forces, then determine the rate at which these forces are doing work. It should be recalled that work or energy is produced by force times distance, while power or rate of energy expenditure is produced by force times distance per time, or force times velocity.

It is therefore necessary to consider a small volume of fluid which is moving with the same velocity. A convenient choice is that of a thin cylindrical shell of radius r, thickness δr , and length l (Fig. 3.6). The volume of fluid comprising the shell is then $2\pi r l \delta r$ and the velocity with which its elements are moving is simply the Poiseuille flow velocity at radial position r, namely $u_s(r)$. If the equation of motion above is multiplied by the volume of this shell and by the velocity with which it is moving, the result is an equation representing the balance of energy expenditure associated with this volume of fluid, namely

$$k_s \times 2\pi r l u_s \delta r = \mu \left(\frac{d^2 u_s}{dr^2} + \frac{1}{r} \frac{d u_s}{dr} \right) \times 2\pi r l u_s \delta r$$
 (3.65)

Furthermore, if each side of this equation is now integrated over a cross section of the tube, that is from r = 0 to r = a, the same balance will be established for fluid filling the entire volume of a tube of radius a and length l, that is

$$\int_0^a k_s \times 2\pi r l u_s dr = \int_0^a \mu \left(\frac{d^2 u_s}{dr^2} + \frac{1}{r} \frac{du_s}{dr} \right) \times 2\pi r l u_s dr$$
 (3.66)

The integral on the left hand side of Eq. 3.66 yields

$$\int_0^a k_s \times 2\pi r l u_s dr = k_s l \int_0^a 2\pi r u_s dr$$

$$= k_s l q_s$$

$$= (\Delta p_s \times \pi a^2) \times \overline{u}_s$$
(3.67)

where in the last step the flow rate q_s was replaced by the average velocity times the cross sectional area $(q_s = \pi a^2 \overline{u}_s)$ and the pressure gradient was replaced by the pressure difference between the two ends of the tube over its length $(k_s = \Delta p/l)$. The final result is seen to be the product of the pressure force and the average flow velocity, which is then the rate of energy expenditure or "pumping power" required to maintain the flow within the tube.

The integral on the right hand side of Eq. 3.66 yields

$$\int_{0}^{a} \mu \left(\frac{d^{2}u_{s}}{dr^{2}} + \frac{1}{r} \frac{du_{s}}{dr} \right) \times 2\pi r l u_{s} dr$$

$$= 2\pi \mu l \int_{0}^{a} \frac{d}{dr} \left(r \frac{du_{s}}{dr} \right) dr$$

$$= 2\pi \mu l \int_{r=0}^{r=a} u_{s} d \left(r \frac{du_{s}}{dr} \right)$$

$$= 2\pi \mu l \left\{ \left| u_{s} r \frac{du_{s}}{dr} \right|_{r=0}^{r=a} - \int_{r=0}^{r=a} r \frac{du_{s}}{dr} du_{s} \right\}$$

$$= -2\pi \mu l \int_{0}^{a} r \left(\frac{du_{s}}{dr} \right)^{2} dr$$

$$= 2\pi \mu l \left(\frac{k_{s}}{2\mu} \right)^{2} \int_{0}^{a} r^{3} dr$$

$$= 2\pi \mu l \left(\frac{k_{s}}{2\mu} \right)^{2} \left(\frac{a^{4}}{4} \right)$$

$$= 2\pi a l \left(\frac{k_{s}a^{2}}{8\mu} \right) \left(\frac{k_{s}a}{2} \right)$$

$$= (\tau_{s} \times 2\pi a l) \times (\overline{u}_{s})$$
(3.68)

where earlier expressions for \overline{u}_s and τ_s were used in the last step. The final result is seen to be the product of the viscous force and the average flow velocity, which is then the rate of energy dissipation by viscous resistance at the tube wall.

Equations 3.67 and 3.68, being derived from the two sides of the equality in Eq. 3.65, establish the balance of the rate of energy expenditure in Poiseuille flow, namely

$$(\Delta p_s \times \pi a^2) \times \overline{u}_s = (\tau_s \times 2\pi a l) \times (\overline{u}_s)$$
(3.69)

Each side represents a force multiplied by the average velocity, thus amounting to a rate of energy expenditure, or power. On the left is the pumping power required to drive the flow, while on the right is the rate of energy dissipated by viscous resistance at the tube wall. In each case the force is in the flow direction, τ_s being the drag force being exerted by the fluid on the tube wall (Eq. 3.50), and Δp_s being the difference between the pressure at the tube entrance minus that at x = l (Eq. 3.28).

3.10 Non Circular Cross Sections

The unique geometrical properties of the circle are a matter of legend in science, in mathematics, and in the technological revolution because of its contribution to the invention of the wheel and the basis for rotary components in machinery. Far less known or celebrated are the unique properties of flow in tubes of *circular cross sections*. In the same way that the circle provides the most efficient way of enclosing a given area, a tube of circular cross section provides the most efficient conduit for fluid flow. In the same way that any other than circular perimeter encloses a smaller area than that enclosed by a circle of the same perimeter length, the flow rate in a tube of any other than circular cross section is lower than that in a tube of circular cross section under the same driving pressure. Considering the indispensable role of flow in tubes in the evolution of life, it is again not unreasonable to wonder:

Did biology discover the tube of circular cross section, or did it invent it?

The above remarks apply in the first place to steady, fully developed flow. In the entry region of a tube, where the flow is not fully developed, the effects of noncircular cross sections cannot be generalized because they depend on the particular geometry in each case, especially on whether the cross section involves any sharp kinks as in rectangular or triangular cross sections. The key question here is whether the entry length in a tube of noncircular cross section is higher or lower than that in a tube of circular cross section. We have seen in Sect. 3.4 that in the case of circular cross section the entry length depends on the Reynolds number (Eq. 3.4). In the case of a noncircular cross section, again, the entry length depends on the particular geometry of that cross section. In any case, however, since the flow in the entry region of a tube is always less efficient than that in the fully developed region of that tube, and since fully developed flow in a tube of noncircular cross section is less efficient than that in a tube of circular cross section, these two effects will generally be compounded in a tube of noncircular cross section.

In pulsatile flow, where the flow is not steady, we shall see later that the flow comes close to reaching the fully developed steady flow profile at the peak of each oscillatory cycle, and the extent to which it does so depends on the pulsation frequency. If the fully developed steady state flow is not Poiseuille flow because of any deviation from the ideal conditions of a cylindrical tube with circular cross section, the efficiency of pulsatile flow will be reduced in the same way and for the same reasons for which it is reduced in steady flow, and this reduction will be compounded by the effect of frequency.

In this section we consider briefly steady flow in a tube of elliptic cross section as an example of deviation from the singular case of a tube of circular cross section. An elliptic cross section is particularly relevant in blood flow because it provides an approximation of the cross section of a compressed blood vessel. This situation occurs most prominently in the heart where coronary vasculature is deeply embedded in myocardial tissue. An elliptic cross section also has the advantage of representing a whole family of cross sections, ranging from perfectly circular to highly flattened, and the elliptic geometry makes the problem mathematically tractable.

An important feature of flow in a tube that carries over from the case of circular cross section to that of noncircular cross section is that if the tube is straight, the flow remains one-directional and the transverse velocity components are identically zero as they are in the case of circular cross section. Under these conditions the governing equations for the flow in a tube of any cross section is the same as that for a tube of circular cross section (Eq. 3.15), which in rectangular Cartesian coordinates x, y, z, with x along the axis of the tube and y, z in the plane of a cross section, takes the form

$$\frac{dp_{se}}{dx} = \mu \left(\frac{d^2 u_{se}}{dy^2} + \frac{d^2 u_{se}}{dz^2} \right) \tag{3.70}$$

where u_{se} , p_{se} , μ are as defined previously for the case of a tube of circular cross section, with subscript 'e' being added here as a reference to the case of elliptic cross section to be considered. This equation is also a simplified form of the Navier Stokes equations in rectangular Cartesian coordinates (Eq. 2.52), based on the same simplifying assumptions as those on which Eq. 3.15 is based. In fact, Eqs. 3.15 and 3.70 can be transformed directly from one to the other in a straightforward manner using the relationship between the rectangular and polar coordinates

$$r^2 = x^2 + y^2 (3.71)$$

With the governing equation being the same, the difference between the solution of this equation for a tube of circular cross section and a tube of noncircular cross section appears only in the *boundary conditions*.

Consider an elliptic cross section in the yz-plane, defined by the ellipse

$$\frac{y^2}{b^2} + \frac{z^2}{c^2} = 1\tag{3.72}$$

compared with a circular cross section defined by the circle

$$y^2 + z^2 = a^2 (3.73)$$

¹⁵Maslen SH, 1958. Transverse velocities in fully developed flows. Quarterly Journal of Applied Mathematics 16:173–175.

Taking b > c, the major and minor axes of the ellipse are respectively defined by

$$\begin{cases} z = 0, & y = \pm b \\ y = 0, & z = \pm c \end{cases}$$
 (3.74)

thus the major and minor axes of the ellipse are 2b and 2c while the diameter of the circle is 2a.

To facilitate comparison of the flow in the two cases, the driving pressure gradient is taken to be the same in both cases, that is

$$\frac{dp_{se}}{dx} = \frac{dp_s}{dx} = k \tag{3.75}$$

The condition of no-slip on the boundary of the elliptic cross section is

$$u_{se} = 0$$
 on $\frac{y^2}{h^2} + \frac{z^2}{c^2} = 1$ (3.76)

A solution of Eq. 3.70 satisfying these conditions is given by

$$u_{se}(y,z) = \frac{kb^2c^2}{2\mu(b^2+c^2)} \left(\frac{y^2}{b^2} + \frac{z^2}{c^2} - 1\right)$$
(3.77)

The flow rate in a tube of elliptic cross section is then obtained by integrating over that cross section, which gives

$$q_{se} = 4 \int_0^c \int_0^{b \times \sqrt{1 - z^2/c^2}} u dy dz = \frac{-k\pi}{8\mu} \delta^4$$
 (3.78)

where

$$\delta = \left(\frac{2b^3c^3}{b^2 + c^2}\right)^{1/4} \tag{3.79}$$

and the corresponding pumping power is given by

$$H_{se} = klq_{se} = \frac{8\mu l}{\pi} \frac{q_{se}^2}{\delta^4} \tag{3.80}$$

It will be noted that when b = c = a, $\delta = a$, the ellipse becomes a circle of radius a, and the expressions for flow rate and pumping power reduce to those for a tube of circular cross section of radius a (Eqs. 3.43 and 3.60).

Flow inefficiency in a tube of noncircular cross section manifests itself in terms of lower flow rate for a given pumping power, or higher pumping power for a given flow rate. For a meaningful comparison between the two cases, either the *areas* or the *perimeters* of the circular and the noncircular cross sections must be made equal. In the case of elliptic cross section this establishes a relation between the radius of the circular cross section and the axes of the elliptic cross section.

Comparison of two cross sections of equal perimeter is particularly relevant to the case of compressed blood vessels, and we use it here for illustration. The perimeter of an ellipse of semi minor and major axes b, c is equal to that of a circle of radius a if

$$a^2 \approx \frac{1}{2}(b^2 + c^2).$$
 (3.81)

Two particular scenarios are of interest in which a tube of circular cross section is compressed such that its cross section becomes elliptic while its perimeter remains unchanged.

In the first scenario the pumping power driving the flow is kept unchanged,

$$H_{se} = H_s = H \tag{3.82}$$

therefore the flow rate through the compressed tube will be reduced. For direct comparison we consider the ratio \bar{q} of flow in the elliptic tube (Eq. 3.78) divided by the corresponding flow in the circular tube

$$\bar{q} = q_{se}/q_s$$

$$= \left(\frac{-k_s \pi}{8\mu} \delta^4\right) / \left(\frac{-k_s \pi}{8\mu} a^4\right)$$

$$= (\delta/a)^4 \tag{3.83}$$

and using Eqs. 3.79 and 3.81, and simplifying, this becomes

$$\bar{q} = \left(\frac{2bc}{b^2 + c^2}\right)^3 \tag{3.84}$$

or

$$\bar{q} = \left(\frac{2\lambda}{1+\lambda^2}\right)^3 \tag{3.85}$$

where

$$\lambda = c/b \tag{3.86}$$

In the second scenario the flow rate is kept unchanged as the tube is compressed, writing

$$q_{se} = q_s = q \tag{3.87}$$

therefore the pumping power to maintain the flow will be higher. For direct comparison we consider the ratio \bar{H} of the power required to drive flow in a tube

of elliptic cross section (Eq. 3.80) divided by the corresponding driving power in a tube of circular cross section

$$\bar{H} = H_{se}/H_s$$

$$= \left(\frac{8\mu lq^2}{\pi \delta^4}\right) / \left(\frac{8\mu lq^2}{\pi a^4}\right)$$

$$= (a/\delta)^4 \tag{3.88}$$

and using Eqs. 3.79 and 3.81, and simplifying, this becomes

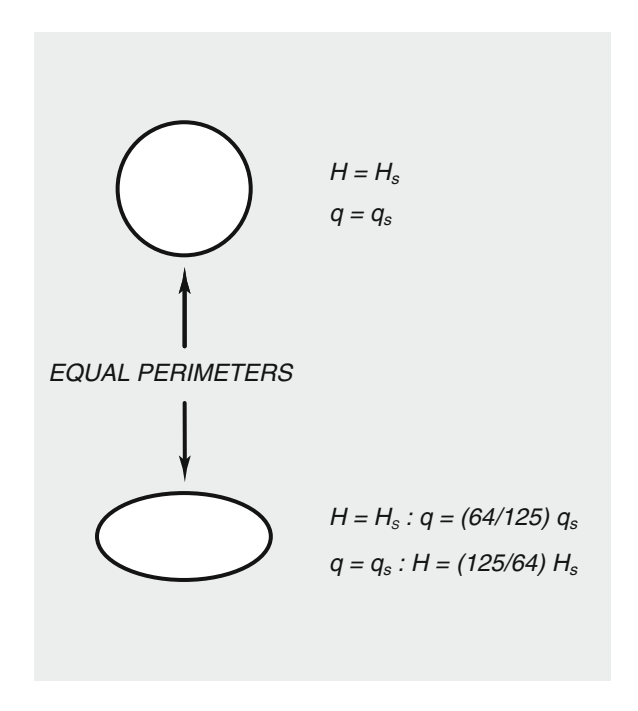
$$\bar{H} = \left(\frac{b^2 + c^2}{2bc}\right)^3 \tag{3.89}$$

or

$$\bar{q} = \left(\frac{1+\lambda^2}{2\lambda}\right)^3 \tag{3.90}$$

Some specific results are shown in (Fig. 3.8).

Fig. 3.8 Flow in a tube of elliptic cross section compared with that in a tube of circular cross section of equal perimeter. For the same flow rate in both tubes, the pumping power required to drive the flow in the elliptic tube is higher by a factor of 125/64. For the same pumping power in both tubes, the flow rate in the elliptic tube is lower by a factor of 64/125. The ratio of major to minor axis of the ellipse is 2:1.



It is clear from these results that as a tube of circular cross section is compressed such that its cross section becomes elliptic with minor-to-major axis ratio $\lambda = c/b$ and with the length of its cross sectional perimeter being unchanged in the process, the flow rate will be reduced unless the driving pumping power is increased to compensate for the increased resistance. This effect intensifies as λ decreases. As an example, with $\lambda = 1/2$, if the driving power is unchanged, the flow rate will drop by approximately 50 %, and if the flow rate is to be kept unchanged, the power required would increase by close to 100 %. With $\lambda = 1/4$, the corresponding drop in flow rate would be close to 90 % and corresponding increase in pumping power would be close to 900 %.

These dramatic changes in flow rate or pumping power may play a significant role in the dynamics of blood flow in situations where blood vessels are being compressed by surrounding tissue. The most important situation, mentioned earlier, is that of coronary vasculature embedded deeply within the myocardium and providing the heart itself with the blood supply it requires for its own metabolic needs. It is well known that when the heart contracts to drive blood flow to the rest of the body, blood flow to the heart itself is drastically reduced or comes to a halt because flow within the coronary vasculature is drastically reduced. However, the way in which this effect is integrated into the overall dynamics of blood supply to the heart has yet to be fully understood, in health and in disease, and particularly in heart failure.

3.11 Cube Law

Properties of Poiseuille flow derived in Sect. 3.8 indicate that the power required to drive flow through a tube is highly sensitive to the diameter (or radius) of the tube, more specifically it varies inversely with the fourth power of the radius 'a' (Eq. 3.60). Thus, to drive the same flow rate through a tube of half the diameter requires 16 times more power. To drive the same flow rate through a tube of double the diameter requires only 1/16 of the power. These dramatic properties of flow in a tube lead inescapably to the question of how did our blood vessels come to have the diameters that they do. For if the diameters of the aorta and all its subsequent branches were to double, the heart would need only 1/16th or approximately 6% of the power to drive the flow through the arterial tree! How and why then did the aorta come to have the diameter that it does?

This question was considered by Cecil D. Murray in 1926 who proposed that alongside the power required to drive the flow through a blood vessel, one must consider the metabolic power required to maintain the volume of blood

3.11 Cube Law 73

within the vessel. When the larger the vessel diameter, the more blood it contains, its volume increasing as a^2 , assuming that its length remains unchanged. Thus if the diameters of all the vessels within the arterial tree were to double, the volume of blood contained within the tree would increase by a factor of four, and so will the metabolic power required to maintain this larger volume of blood. There are therefore two opposing consequences to an increase in the diameter of a blood vessel, the power required to drive the flow decreases as $1/a^4$ while the metabolic power required to maintain the volume of blood increases as a^2 . A simple "optimality" problem is thus established by writing, for a blood vessel of radius 'a'

$$H = \frac{A}{a^4} + Ba^2 \tag{3.91}$$

where H is the *total cost* of driving the flow through the vessel and maintaining the volume of blood within it, and A, B are constants. A minimum value of H occurs when

$$\begin{cases} \frac{dH}{da} = \frac{-4A}{a^5} + 2Ba = 0\\ \frac{d^2H}{da^2} = \frac{20A}{a^6} + 2B > 0 \end{cases}$$
(3.92)

Since both A and B are positive, the inequality is satisfied and the first equation gives

$$a^6 = \frac{2A}{R} \tag{3.93}$$

Now, in Eq. 3.91 the second term represents the metabolic power required to maintain the volume of fluid within the vessel, where B is a constant representing the rate at which this power increases with a^2 , while the first term represents the power required to drive the flow where A represents the rate at which this power increases with $1/a^4$. The first of these constants is unknown and can be estimated from the metabolic rate of blood, but this estimate is not required for the purpose at hand. However, the constant A is known because the first term in Eq. 3.91 represents the power required to drive the flow as was found in Eq. 3.60 and, comparing the two equations we have

$$H_s = \frac{A}{a^4} = \frac{8\mu l q_s^2}{\pi a^4} \tag{3.94}$$

which gives

$$A = \frac{8\mu l q_s^2}{\pi} \tag{3.95}$$

¹⁶Murray CD, 1926. The physiological principle of minimum work. I. The vascular system and the cost of blood volume. Proceedings of the National Academy of Sciences 12:207–214.

Substituting this value of A in Eq. 3.93, we find

$$a^6 = \frac{2A}{B} = \frac{2}{B} \frac{8\mu l q_s^2}{\pi} \tag{3.96}$$

and on the assumption that B, μ , l are constants which do not depend on the flow rate q_s , it follows from Eq. 3.96 that the required condition of minimum power occurs when

$$q_s \propto a^3 \tag{3.97}$$

which is known as the "cube law", or as "Murray's law" after its first author.

The cube law has been tested and used for many years and has shown considerable presence in the cardiovascular system. ¹⁷ It is important to note that the law rests on two important assumptions: (i) that the flow under consideration is steady and fully developed Poiseuille flow, and (ii) that the optimality criterion being used is that of minimizing the total rate of energy expenditure for dynamic and metabolic purposes. More general forms of Murray's law have been considered by a number of authors to address observed departures or scatter away from the cube law (see Footnote 17). It has been found, for example, that in the aorta and its first generation of major branches, a "square law" in which the flow rate is proportional to a^2 may be more appropriate than the cube law. At more peripheral regions of the arterial tree, however, measured data suggest that the cube law eventually prevails, even if with considerable scatter.

One of the most important issues associated with the way in which the flow rate in a blood vessel is related to its diameter is that of the shear stress acting on endothelial tissue because it represents the only mechanism by which the vessel wall is in direct contact with the flow. In particular, the shear stress acting on the endothelium in the very small pre-capillary arterioles is likely to play a key role in the mechanisms and control of local perfusion. To date there has been no definitive measurement or theory to indicate what the level or distribution of shear stress at this level of the vasculature might be, and how these relate to the implementation and control of local perfusion. These issues are paramount in the mechanisms of myocardial perfusion.

Since in Poiseuille flow (Eq. 3.50) the shear stress acting on the tube wall is proportional to q/a^3 , the cube law ($q \propto a^3$) implies that the shear stress no longer depends on the vessel radius, thus the shear stress acting on endothelial tissue in large vessels would be the same as that acting in small vessels. This implication has not been generally accepted on physiological grounds, nor has it been possible to test it because of inherent difficulties associated with direct measurements of shear stress, particularly in small vessels.

¹⁷There is an extensive literature on the subject. For a summary and list of references see "Zamir M. The Physics of Pulsatile Flow. Springer-Verlag 2000."

3.12 Two Tubes or One?

If as an alternative to the cube law it is assumed that the flow rate in a blood vessel varies in accordance with a square law $(q \propto a^2)$ or a quartic law $(q \propto a^4)$, the shear stress acting on the vessel wall would vary as 1/a in the first case and as a in the second. Thus a square law would imply that the shear stress is *larger* in smaller vessels while the quartic law implies that the shear stress is *smaller* in smaller vessels. The second of these options appears more acceptable on physiological grounds. In other words, if the relation between the flow rate and vessel radius is put in the more general form

$$q \propto a^{\gamma}$$
 (3.98)

where γ is an unknown index, then one would suspect on physiological grounds that in the hierarchical structure of the arterial tree the value of γ may be equal to or less than 3.0 within the large distributing vessels and higher than 3.0 within the small pre-capillary vessels. At the present time these issues stand unresolved.

3.12 Two Tubes or One?

A key task of the cardiovascular system is to supply blood from a single source (the heart) to several billion destinations (individual cells within the entire body). It has already been established that the mechanism of choice for meeting this task is flow in tubes. Before discussing the design principles by which this mechanism is implemented within the body, in this section we consider a much simpler question:

Is it more efficient for a given flow rate q_0 to be carried in a single tube of radius a_0 or divided into two flow rates q_1 , q_2 carried in two separate tubes of radii a_1 , a_2 ?

subject, of course, to

$$q_0 = q_1 + q_2 \tag{3.99}$$

To address this question we must define what is meant by "efficient". In the physiological system the amount of power H required to maintain the flow is clearly an important consideration so that lower power expenditure would certainly be considered as higher efficiency. However, other considerations such as the volume V of blood required to fill the two tubes compared with one, the amount of tissue T required to form the two tubes compared with one, and the shear stress τ between the moving fluid and the tube wall in the two cases, are equally important. Below we examine the question of efficiency in terms of each of these.

If the power required to maintain the flow in the single tube is denoted by H_0 and in the two tubes by H_1 , H_2 , then we define a measure of power efficiency as the fractional difference

$$\Delta H = \frac{H_1 + H_2 - H_0}{H_0} \tag{3.100}$$

Using Eq. 3.60 for the power required to drive flow q in a tube of radius a, and assuming for simplicity that the three tubes have the same length and that the fluid properties are the same, Eq. 3.100 reduces to

$$\Delta H = \frac{(q_1^2/a_1^4) + (q_2^2/a_2^4) - (q_0^2/a_0^4)}{(q_0^2/a_0^4)}$$
(3.101)

Assuming further that flow in the two smaller tubes is divided equally such that

$$\begin{cases} q_2 = q_1 \\ a_2 = a_1 \end{cases}$$
 (3.102)

Equation 3.101 reduces to

$$\Delta H = 2\left(\frac{q_1^2/a_1^4}{q_0^2/a_0^4}\right) - 1\tag{3.103}$$

It is seen from the above that the answer to the question at hand, namely that of "two tubes or one?", depends on the relation between the radius of a tube and the flow rate which it carries. If we use the cube law, Eq. 3.97, for that purpose, then Eq. 3.103 becomes

$$\Delta H = 2\left(\frac{a_1}{a_0}\right)^2 - 1\tag{3.104}$$

while from Eq. 3.99 we find

$$a_0^3 = a_1^3 + a_2^3$$

$$= 2a_1^3$$

$$\frac{a_1}{a_0} = 2^{-1/3}$$
(3.105)

Substituting this in Eq. 3.104, we finally get

$$\Delta H = 2 (2^{-1/3})^2 - 1$$

$$= 2^{1/3} - 1$$

$$\approx 0.26$$
(3.106)

3.12 Two Tubes or One?

Thus, based on the cube law relationship between the radius of a tube and the flow which it carries (Eq. 3.97), if the flow in a single tube is divided equally into two separate tubes, the power required to drive the flow will be higher by approximately 26 %.

If instead of the cube law we assume the more general relationship between the radius of a tube and flow which it carries (Eq. 3.98), then instead of Eq. 3.103 we would have

$$\Delta H = 2 \left(\frac{a_1^{2\gamma} / a_1^4}{a_0^{2\gamma} / a_0^4} \right) - 1 \tag{3.107}$$

and instead of Eq. 3.104

$$\Delta H = 2\left(\frac{a_1}{a_0}\right)^{2\gamma - 4} \tag{3.108}$$

The ratio of radii within the bracket is then obtained from

$$q_{0} = q_{1} + q_{2}$$

$$a_{0}^{\gamma} = a_{1}^{\gamma} + a_{2}^{\gamma}$$

$$= 2a_{1}^{\gamma}$$

$$\frac{a_{1}}{a_{0}} = 2^{-1/\gamma}$$
(3.109)

Substituting this into Eq. 3.108, we obtain finally

$$\Delta H = 2^{(4/\gamma)-1} - 1 \tag{3.110}$$

which indicates that

$$\begin{cases} \Delta H = 0 & \text{at} \quad \gamma = 4 \\ > 0 & \text{when} \quad \gamma < 4 \\ < 0 & \text{when} \quad \gamma > 4 \end{cases}$$
 (3.111)

For the volume V_0 of blood in a single tube compared with that in two tubes of volume V_1 each, we define

$$\Delta V = \frac{2V_1 - H_0}{H_0} \tag{3.112}$$

Since the volume V of a tube of length l and radius a is given by $V = l \times \pi a^2$, and since the lengths of all three tubes are assumed to be the same, Eq. 3.112 reduces to

$$\Delta V = 2 \left(\frac{a_1}{a_0}\right)^2 - 1 \tag{3.113}$$

and using Eq. 3.109 we find

$$\Delta V = 2(2^{-2/\gamma}) - 1$$

$$= 2^{1-(2/\gamma)} - 1$$
(3.114)

which indicates that

$$\begin{cases} \Delta V = 0 & \text{at} \quad \gamma = 2 \\ > 0 & \text{when} \quad \gamma > 2 \\ < 0 & \text{when} \quad \gamma < 2 \end{cases}$$
 (3.115)

Similarly, for the surface area of tissue T forming a tube of length l and radius a, where $T = l \times 2\pi a$, we define

$$\Delta T = \frac{2T_1 - T_0}{T_0} \tag{3.116}$$

and again since the lengths of all three tubes are assumed to be the same, this reduces to

$$\Delta T = 2\left(\frac{a_1}{a_0}\right) - 1\tag{3.117}$$

and using Eq. 3.109 we find

$$\Delta T = 2(2^{-1/\gamma}) - 1$$

$$= 2^{1 - (1/\gamma)} - 1$$
(3.118)

which indicates that

$$\begin{cases} \Delta T = 0 & \text{at} \quad \gamma = 1 \\ > 0 & \text{when} \quad \gamma > 1 \\ < 0 & \text{when} \quad \gamma < 1 \end{cases}$$
 (3.119)

Finally, in the case of shear stress τ at the tube wall, there are two issues to consider. First, from a purely physical standpoint τ represents energy dissipation due to viscous friction at the tube wall, thus a relevant comparison in this case would be

3.12 Two Tubes or One?

between the energy dissipated in the single tube compared with that in two separate tubes. Second, in the physiological setting τ is a mechanism of communication between the endothelium and the moving blood and, as such, a relevant comparison would be simply between the value of τ in the single tube compared with that in the two separate tubes. The first of these is in fact already taken care of by ΔH because the rate of energy dissipation within each of the three tubes is equal to the power required to drive the flow. Therefore, below we deal with only the second of the above considerations and accordingly define

$$\Delta \tau = \frac{\tau_1 - \tau_0}{\tau_0} \tag{3.120}$$

and using Eq. 3.50, we have

$$\Delta \tau = \left(\frac{q_1/a_1^3}{q_0/a_0^3}\right) - 1\tag{3.121}$$

and using Eq. 3.98, this becomes

$$\Delta \tau = \left(\frac{a_1}{a_0}\right)^{\gamma - 3} - 1\tag{3.122}$$

and using Eq. 3.109, we get

$$\Delta \tau = (2^{-(\gamma - 3)/\gamma}) - 1$$

$$= 2^{(3/\gamma) - 1} - 1 \tag{3.123}$$

which indicates that

$$\begin{cases} \Delta \tau = 0 & \text{at} \quad \gamma = 3 \\ > 0 & \text{when} \quad \gamma < 3 \\ < 0 & \text{when} \quad \gamma > 3 \end{cases}$$
 (3.124)

The results are shown graphically in Fig. 3.9. In discussing these it is convenient to refer to ΔV and ΔT as "material" costs and to ΔH and $\Delta \tau$ as "energy" costs (although, as discussed earlier, in the comparisons above we considered only the physiological aspect of τ , not its dissipative aspect).

The first important result seen in Fig. 3.9 is that the radius ' a_1 ' of each of the two separate tubes is in all cases smaller than that of the single tube (a_0). The second important result seen in the figure is that *there is no value of the power law exponent* γ *for which flow in two tubes is "better" than one.* More precisely, there is no value of γ for which ΔV , ΔT , ΔH , $\Delta \tau$ are all zero.

Specifically, at $\gamma=1$, the volume cost of having two tubes instead of one is actually favorable ($\Delta V=-0.5$) and the tissue cost is neutral ($\Delta T=0$) but the

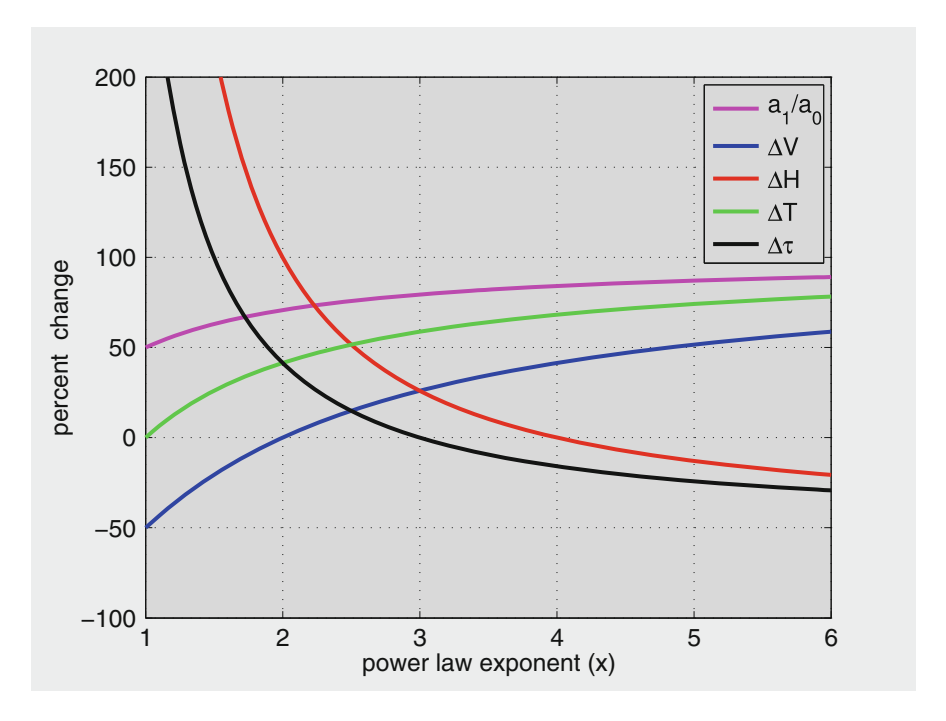


Fig. 3.9 Two tubes or one? The figure shows the percentage cost or gain of replacing the flow rate in one tube of radius ' a_0 ' by the same flow rate divided equally into two tubes of the same length as that of the single tube and of radius ' a_1 ' each. The Δ 's represent percentage difference in lumen volume V, tube wall surface T, power required to drive the flow H, and shear stress at the tube wall τ . The significance of the results is discussed in the text. The power law exponent x in the figure is the same as the power law exponent γ in the text.

energy costs (ΔH and $\Delta \tau$) are so high that this option would not be viable. At $\gamma = 2$, $\Delta V = 0$, $\Delta T > 0$, $\Delta \tau$ is moderately high while ΔH is still considerably high.

At $\gamma=3$ and higher values of γ the material costs continue to increase while the energy costs continue to decrease. Thus, if the flow in a single tube is to be divided into two tubes, only a *compromise* between the energy and material costs is possible. At $\gamma=3$ this compromise is achieved with what seems to be a balance between material and energy costs. At higher values of γ , the compromise is such that higher weight is given to energy costs than to material costs.

Chapter 4 Basic Elements of Pulsatile Flow

4.1 Introduction: Why Pulsatile?

The pressure difference across the two ends of a tube provides only the *force* needed to drive the flow through the tube. In order to maintain the flow it is necessary to maintain this driving force, and to do so requires a source of continuous energy, a power source. The high pressure at one end of a tube is therefore only a momentary source of that power but it is a limited source unless it is constantly replenished.

The situation is much like that of the level of water in a water reservoir. The water level provides the pressure required to drive the flow through the pipe or pipes leaving the reservoir, but unless this water level is maintained, the driving pressure will gradually diminish and so will the flow. It is in this replenishing process that the energy payment for the flow is made. Water must be somehow hauled to the top of the reservoir in order to maintain its level, and the energy spent in this hauling process is in payment for the energy consumed by the flow.

Another way of producing high pressure at one end of a tube is that provided by a reciprocating pump. In this case high pressure is produced only momentarily at each stroke of the pump and then diminishes until the next stroke. In fact, if the pump stroke is aligned with the tube, the process may also be seen as the pump simply pushing fluid directly into the tube and thereby producing forward flow. It is not unlike the process of adding buckets of water into a reservoir at fixed intervals in order to maintain the water level within it. At the delivery of each bucket the level of water rises and so does the pressure available for driving the flow, then they both gradually diminish until the next delivery.

In the cardiovascular system, perhaps not surprisingly, biology has opted for a combination of these two mechanisms. The heart acts as a reciprocating pump that drives blood directly into the aorta, the flow reaching a peak (systol) at each stroke, then diminishing to a low (diastol) until the next stroke. This, as is the case with a reciprocating pump, produces "jerks" of flow at each stroke rather than continuous flow. If the output from the pump is directed to a large reservoir instead,

and the water level from the reservoir is used to drive the flow, these jerks would be moderated. Biology has used precisely this mechanism in order to moderate the jerkiness of blood flow through the vascular system. Of course, there is no room for a large reservoir within the body. Instead, a stretchable container is used for "storing" fluid. The aorta and its major branches are sufficiently compliant that they expand at the peak of each pumping cycle and store some of the blood being pushed forward by the heart, in much the same way that a reservoir stores buckets of water that are being poured into it. The stored fluid is then regurgitated during the low phase of the pumping cycle. Not only is the *fluid* stored between peak cycles in this way, but also, and perhaps more importantly, some of the driving *energy* too. The latter is done by the elasticity of the vessel walls as they stretch at the peak of each cycle. At the low phase of each cycle, the walls recoil and give back most of the energy used in stretching them.

Why pulsatile flow? Biology found no other way of maintaining high pressure at one end of the arterial system in order to drive the flow of blood, continuously and without stop.

Indeed, *there is no other way* of providing a continuous source of high pressure in the physical or engineering world either. What appears to be a continuous supply of water or gas into our homes is in fact also driven by a pulsatile pressure system, but one that has such a large storage capacity that the depletion and replenishing of that capacity is so minute by comparison with the size of that capacity that the jerkiness associated with the pulsatile nature of the driving pressure is practically eliminated. Biology does not have the luxury of such a large capacity reservoir to serve the cardiovascular system.

There are thus two aspects to the study and analysis of pulsatile flow. First, the relationship between pressure and flow in a tube when the driving pressure is not constant. Second, the relationship between the pressure and flow in a tube when the driving pressure is not constant and the tube is stretchable to the extent of providing some storage capacity. While the difference between the two may seem trivial, it is in fact not the case. There is a considerable difference in the mathematical analysis involved in the two cases, as well as in the corresponding physics. For this reason, in the present chapter we deal with only the first of these two aspects of pulsatile flow. The second is dealt with in the next chapter.

4.2 Pulsatile Poiseuille Flow

When the pressure driving the flow in a tube is constant, the resulting flow is steady, as we have seen previously in the form of Poiseuille flow. In that case, the pressure p varies only in the axial direction x as it "drops" from the upstream end to the downstream end of the tube, while the velocity u varies only in the radial direction r, thus p = p(x) and u = u(r) (Sect. 3.8).

When the pressure driving the flow in a tube varies in time, the resulting flow also varies in time, thus in this case p = p(x, t) and u = u(r, t). The equation

governing the flow is then a generalized form of the equation governing Poiseuille flow, namely Eq. 3.13 as derived in Sect. 3.5, which we now write more explicitly as

$$\rho \frac{\partial u(r,t)}{\partial t} + \frac{\partial p(x,t)}{\partial x} = \mu \left(\frac{\partial^2 u(r,t)}{\partial r^2} + \frac{1}{r} \frac{\partial u(r,t)}{\partial r} \right)$$
(4.1)

This equation bears strong relation to the equation governing Poiseuille flow (Eq. 3.15) because it reduces to that equation when the time dependence is absent. Indeed, we shall see that the *physics* of the flow represented by this equation bears a strong relation to the physics of Poiseuille flow.

For the purpose of discussion we consider a specific case in which the driving pressure is oscillatory in time, varying as a trigonometric sine or cosine function. As the pressure rises to its peak, the flow increases gradually in response, and as the pressure falls, the flow follows again. If the change in pressure is very slow, the corresponding change in flow will be almost in phase with it, but if the change in pressure is rapid, the flow will lag behind because of the inertia of the fluid. Because of this lag, the peak which the flow reaches in each cycle will be somewhat short of what it would be in steady Poiseuille flow under a constant driving pressure equal to the peak of the oscillatory pressure.

This loss in peak flow is higher at higher frequency of oscillation of the driving pressure, to the point that at very high frequency the fluid barely moves at all. Only at the other extreme, at very *low* frequency, will the flow rise and fall in phase with the pressure and reach a peak commensurate with the peak pressure at each cycle. In fact at very low frequency the pressure and flow are *instantaneously* what they would be in steady Poiseuille flow. That is, the Poiseuille relation between pressure and flow (Eq. 3.15) is satisfied at every instant in the oscillatory cycle as they both change during the cycle. Not only the flow rate but the velocity profile at each instant will also be the same as it would be in steady Poiseuille flow under a constant driving pressure equal to the value of the oscillatory pressure at that instant in the oscillatory cycle, at *low* frequency. The flow is then somewhat like a *pulsatile Poiseuille flow*. At *high* frequency the velocity profile fails to reach the full form which it would have in Poiseuille flow under the same driving pressure.

The assumptions under which this oscillatory flow takes place are essentially the same as those in steady Poiseuille flow. The cross section of the tube must be circular and axial symmetry must prevail to the effect that velocity and derivatives in the θ -direction are zero. Also, the tube must be sufficiently long for the flow field to be fully developed and independent of x, and we saw in Sect. 3.5 that this requires that the tube be rigid.

The consequences of these restrictions are far more significant in pulsatile flow than in steady Poiseuille flow. In order to satisfy these restrictions in pulsatile flow, fluid at different axial positions along the tube must respond *in unison* to the changing pressure, to the effect that the velocity profile is *instantaneously* the same at all axial positions along the tube. As the pressure changes, the velocity profile changes in response, simultaneously at all axial positions along the tube. It is as if the fluid is moving in bulk.

While this feature of the flow is fairly artificial and somewhat "unphysical", it provides an important foundation for the understanding of more realistic forms of pulsatile flow. In fact the classical solution which we present in this chapter and which has provided the basic understanding of pulsatile flow is based on this model of the flow.

To make the model more realistic the tube must be allowed to be nonrigid. As the pressure changes in a nonrigid tube, the change acts only locally at first because it is able to stretch the tube at that location. Later the stretched section of the tube recoils and pushes the change in pressure further down the tube. This produces a wave which travels down the tube. In the case of a rigid tube, by contrast, there is no wave motion. The flow in a rigid tube, rises and falls simultaneously at all axial positions along the tube.

In the presence of wave motion the axial velocity u is a function of not only r and t but also of x, and the radial velocity v is no longer zero, thus Eq. 4.1 ceases to be valid. More important, the presence of wave motion entails the possibility of wave reflections which introduce further complications in the analysis of the flow. These complications are considered in subsequent chapters. In the current chapter we present the classical solution of Eq. 4.1 which is based on the idealized model of pulsatile flow in a rigid tube.

4.3 Pulsatile = Steady + Oscillatory

The pumping action of the heart produces a pressure difference across the arterial tree which changes rythmically with that action. It is a characteristic of this driving force that it consists of a constant part which does not vary in time and which produces a steady flow forward as in Poiseuille flow, plus an oscillatory part which moves the fluid only back and forth and which produces zero net flow over each cycle. We shall use the terms "steady" and "oscillatory" to refer to these two components of the flow, respectively, and the term "pulsatile" to refer to the combination of the two.

An important feature of Eq. 4.1 is that it is *linear* in both the pressure p(x, t) and velocity u(r, t). As a result of this feature the equation can deal with the steady and oscillatory parts of the flow entirely separately and independently of each other. This is a useful breakdown of the problem because the steady part of the flow has already been dealt with in Sect. 3.7.

The oscillatory part of the problem can be isolated and dealt with separately, which we do in the present chapter. This part of the problem is mathematically more complicated than the steady flow part, and in the midst of the analysis to follow it may seem pointless to consider it since it only moves fluid back and forth with no net flow. It is therefore helpful to remember that the reason for which the oscillatory part is dealt with in such great detail is that it represents an important part of the composite pulsatile flow which we are interested in, and it carries with it most of the seminal features of the composite flow.

If the steady and oscillatory parts of the pressure and velocity are identified by subscripts "s" and " ϕ " respectively, then to isolate the oscillatory flow problem we write

$$\begin{cases}
p(x,t) = p_s(x) + p_{\phi}(x,t) \\
u(r,t) = u_s(r) + u_{\phi}(r,t)
\end{cases}$$
(4.2)

Substituting these in Eq. 4.1, we obtain

$$\left\{ \frac{dp_s}{dx} - \mu \left(\frac{d^2 u_s}{dr^2} + \frac{1}{r} \frac{du_s}{dr} \right) \right\} + \left\{ \frac{\partial p_\phi}{\partial x} - \mu \left(\frac{\partial^2 u_\phi}{\partial r^2} + \frac{1}{r} \frac{\partial u_\phi}{\partial r} \right) + \rho \frac{\partial u_\phi}{\partial t} \right\} = 0$$
(4.3)

where terms have been grouped into those which do not depend on time t (first group) and those which do (second group). Because of that difference between them, each group must equal zero separately.

The first equality then leads to Eq. 3.15 for steady flow which has already been dealt with, and the second leads to a governing equation for the oscillatory part of the flow, namely

$$\frac{\partial p_{\phi}}{\partial x} = \mu \left(\frac{\partial^2 u_{\phi}}{\partial r^2} + \frac{1}{r} \frac{\partial u_{\phi}}{\partial r} \right) - \rho \frac{\partial u_{\phi}}{\partial t}$$
 (4.4)

This equation is entirely independent of the equation governing the steady component of the flow (Poiseuille flow) in the sense that it can be solved separately for u_{ϕ} which we do in what follows.

In Eq. 4.4 the left hand side is a function of x and t only while the right hand side is a function of t and t only, therefore both sides must equal a function of t only, the same function of t, say $k_{\phi}(t)$. Therefore Eq. 4.4 splits into two equations

$$\frac{\partial p_{\phi}}{\partial x} = k_{\phi}(t) \tag{4.5}$$

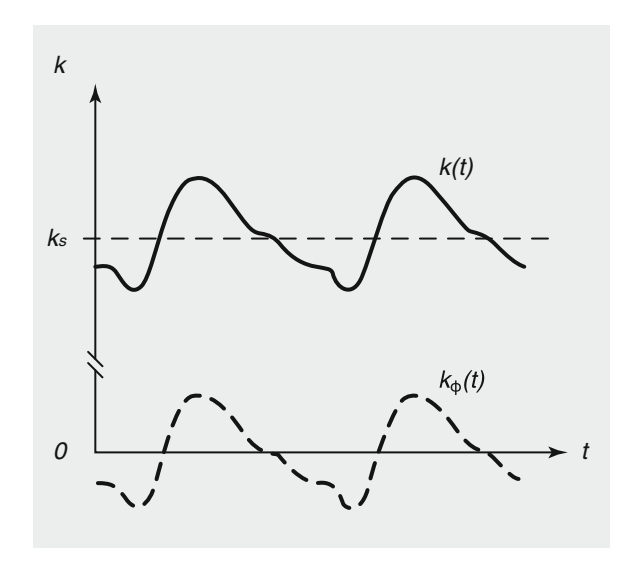
$$\mu \left(\frac{\partial^2 u_{\phi}}{\partial r^2} + \frac{1}{r} \frac{\partial u_{\phi}}{\partial r} \right) - \rho \frac{\partial u_{\phi}}{\partial t} = k_{\phi}(t)$$
 (4.6)

As k_s in steady Poiseuille flow (Eq. 3.23), $k_{\phi}(t)$ here is the pressure gradient driving the oscillatory part of the flow. If the *total* pressure gradient driving the pulsatile flow is denoted by k(t), then from Eq. 4.2 we find

$$k(t) = \frac{\partial p(x, t)}{\partial x}$$

$$= \frac{dp_s(x)}{dx} + \frac{dp_{\phi}(x, t)}{dx}$$
(4.7)

Fig. 4.1 Pulsatile pressure gradient k(t) consists of a constant part k_s plus a purely oscillatory part $k_{\phi}(t)$.



which in view of Eqs. 3.23 and 4.5 gives

$$k(t) = k_s + k_\phi(t) \tag{4.8}$$

Thus k(t) is the "pulsatile" pressure gradient in pulsatile flow, k_s is its steady part, and $k_{\phi}(t)$ is its purely oscillatory part, as illustrated in Fig. 4.1.

Properties of pulsatile flow are obtained by solving Eq. 4.6 for the oscillatory velocity component u_{ϕ} and then adding this to the steady velocity component u_s obtained in Sect. 3.8 to construct the total velocity in pulsatile flow using Eq. 4.2. Thus in what follows our attention is focused only on a solution of Eq. 4.6 for the oscillatory velocity component u_{ϕ} .

4.4 Using Complex Exponential Functions

Solution of Eq. 4.6 for the oscillatory velocity component u_{ϕ} depends clearly on the form of the pressure gradient k_{ϕ} driving the flow as a function of time. We consider first one of the simplest oscillatory functions, namely that of a trigonometric sine or cosine, writing

$$k_{\phi}(t) = k_s \cos \omega t \tag{4.9}$$

or

$$k_{\phi}(t) = k_{s} \sin \omega t \tag{4.10}$$

where ω is the oscillatory frequency and k_s is a constant which we chose to be equal to the constant pressure gradient in Poiseuille flow. This choice makes it easier to compare the oscillatory flow directly with the corresponding Poiseuille flow. In both cases (Eqs. 4.9 and 4.10) k_s serves as the *amplitude* of the oscillatory pressure gradient. Thus the oscillatory pressure gradient varies as a sine or cosine function from a high value of k_s to a low of $-k_s$. In this way the peak value of the oscillatory flow rate and peak form of the oscillatory velocity profile can be compared directly with the corresponding flow rate and velocity profile in steady Poiseuille flow with constant pressure gradient k_s .

Solution of Eq. 4.6 is greatly simplified analytically if instead of taking one of the other of Eqs. 4.10 and 4.9 we take their combination in the form of a complex exponential function

$$k_{\phi}(t) = k_{s}e^{i\omega t}$$

$$= k_{s}(\cos \omega t + i\sin \omega t)$$
(4.11)

where $i = \sqrt{-1}$. Because Eq. 4.6 is linear, a solution with this choice of k_{ϕ} will actually consist of the sum of two solutions, one for which $k_{\phi}(t) = k_s \cos \omega t$ and another for which $k_{\phi}(t) = k_s \sin \omega t$. The first is obtained by taking the real part of the solution and the second by taking the imaginary part. The combined solution is complex because of this choice of $k_{\phi}(t)$.

With this choice of pressure gradient Eq. 4.6 becomes

$$\frac{\partial^2 u_{\phi}}{\partial r^2} + \frac{1}{r} \frac{\partial u_{\phi}}{\partial r} - \frac{\rho}{\mu} \frac{\partial u_{\phi}}{\partial t} = \frac{k_s}{\mu} e^{i\omega t}$$
 (4.12)

This equation admits a solution by separation of variables, that is by a decomposition of $u_{\phi}(r,t)$ into one part which depends on r only and one on t only. Furthermore, the form of the equation and the exponential form of the function of time on the right together dictate that the part of u_{ϕ} which depend on t must have the same exponential form as that on the right. The separation of variables thus arrived at is

$$u_{\phi}(r,t) = U_{\phi}(r)e^{i\omega t} \tag{4.13}$$

Upon substitution into Eq. 4.12, the factor $e^{i\omega t}$ cancels throughout, leaving an ordinary differential equation for $U_{\phi}(r)$ only, namely

$$\frac{d^{2}U_{\phi}}{dr^{2}} + \frac{1}{r}\frac{dU_{\phi}}{dr} - \frac{i\Omega^{2}}{a^{2}}U_{\phi} = \frac{k_{s}}{\mu}$$
 (4.14)

where a is the tube radius and Ω is a nondimensional frequency parameter, given by

$$\Omega = \sqrt{\frac{\rho\omega}{\mu}}a\tag{4.15}$$

We shall see later that the value of Ω has a significant effect on the form of the solution.

It is clear that Eq. 4.14, being an *ordinary* differential equation, is considerably simpler than Eq. 4.12. In fact Eq. 4.14 is a form of Bessel equation which has a standard solution as we see in the next section.

It is important to note that this simplification of the problem has been achieved primarily by the choice of $k_{\phi}(t)$ as a simple trigonometric sine or cosine. However, as we see later, this simplified form of the problem is actually a fundamental prerequisite step towards dealing with more complicated forms of $k_{\phi}(t)$ such as that generated by the heart.

It is also important to note that while the pressure gradient $k_{\phi}(t)$ in Eq. 4.11 and the velocity $u_{\phi}(r,t)$ in Eq. 4.13 appear to have the same oscillatory form in the time variable t, this does not mean that the pressure gradient and velocity are actually in phase with each other. The reason for this is that the other part of the velocity, namely $U_{\phi}(r)$, is complex because of the presence of i in its governing equation (Eq. 4.14). The product of $U_{\phi}(r)$ with $e^{i\omega t}$ in Eq. 4.13 alters the phases of the real and imaginary parts of the velocity $u_{\phi}(r,t)$ so that in general they are not the same as those of the real and imaginary parts of the pressure gradient $k_{\phi}(t)$.

4.5 Bessel Equation and Solution

Equation 4.14 is a form of Bessel equation which has a known general solution, 1,2 namely

$$U_{\phi}(r) = \frac{ik_s a^2}{\mu \Omega^2} + AJ_0(\zeta) + BY_0(\zeta)$$
 (4.16)

where A, B are arbitrary constants and J_0 , Y_0 are Bessel functions of order zero and of the first and second kind, respectively, satisfying the standard Bessel equation

$$\begin{cases} \frac{d^2 J_0}{d\zeta^2} + \frac{1}{\zeta} \frac{dJ_0}{d\zeta} + J_0 = 0\\ \frac{d^2 Y_0}{d\zeta^2} + \frac{1}{\zeta} \frac{dY_0}{d\zeta} + Y_0 = 0 \end{cases}$$
(4.17)

The new variable ζ is related to the radial coordinate r by

$$\zeta(r) = \Lambda \frac{r}{a} \tag{4.18}$$

¹McLachlan NW. Bessel Functions for Engineers. Clarendon Press, 1955.

²Watson GN. Theory of Bessel Functions. Cambridge University Press, 1958.

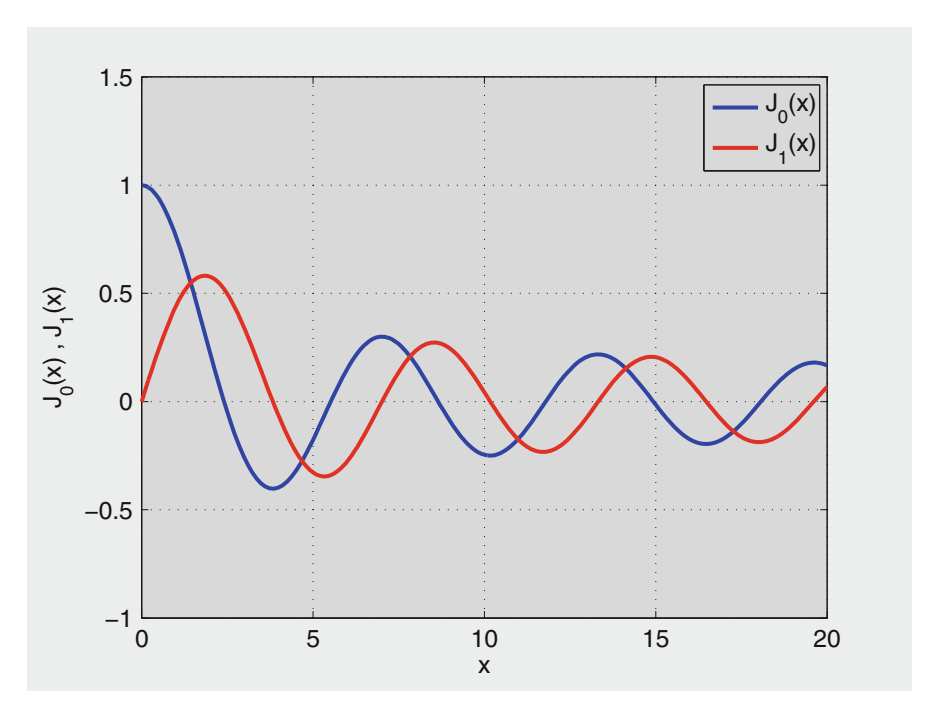


Fig. 4.2 Bessel functions of the first kind of order zero $(J_0(x))$ and of order one $(J_1(x))$ where x is real.

where Λ is a frequency parameter related to the nondimensional frequency Ω by

$$\Lambda = \left(\frac{i-1}{\sqrt{2}}\right)\Omega\tag{4.19}$$

Some of the relevant properties of $J_0(x)$ and $J_1(x)$ are illustrated graphically in Figs. 4.2 and 4.3.

Because of this relation, and because Λ and Ω appear explicitly and implicitly in all elements of the solution, the numerical value of the nondimensional frequency Ω has a key effect on the detailed characteristics of the flow field.

Substituting for $U_{\phi}(r)$ from Eq. 4.16 into the governing equation (Eq. 4.14) readily verifies that the governing equation is satisfied. In particular, it can be readily verified that the first term on the right hand side of Eq. 4.16 represents a *particular* solution of Eq. 4.14 since it satisfies that equation and it does not contain an arbitrary constant. Then it can be verified that each of the second and third terms on the right of Eq. 4.16 satisfies the *homogeneous* form of the governing equation, namely

$$\frac{d^2 U_{\phi}}{dr^2} + \frac{1}{r} \frac{dU_{\phi}}{dr} - \frac{i\Omega^2}{a^2} U_{\phi} = 0 \tag{4.20}$$

Substituting $U_{\phi} = AJ_0$ into this equation produces the first line in Eq. 4.17 which is known to be valid by definition of J_0 . Similarly for Y_0 . Furthermore, it is known

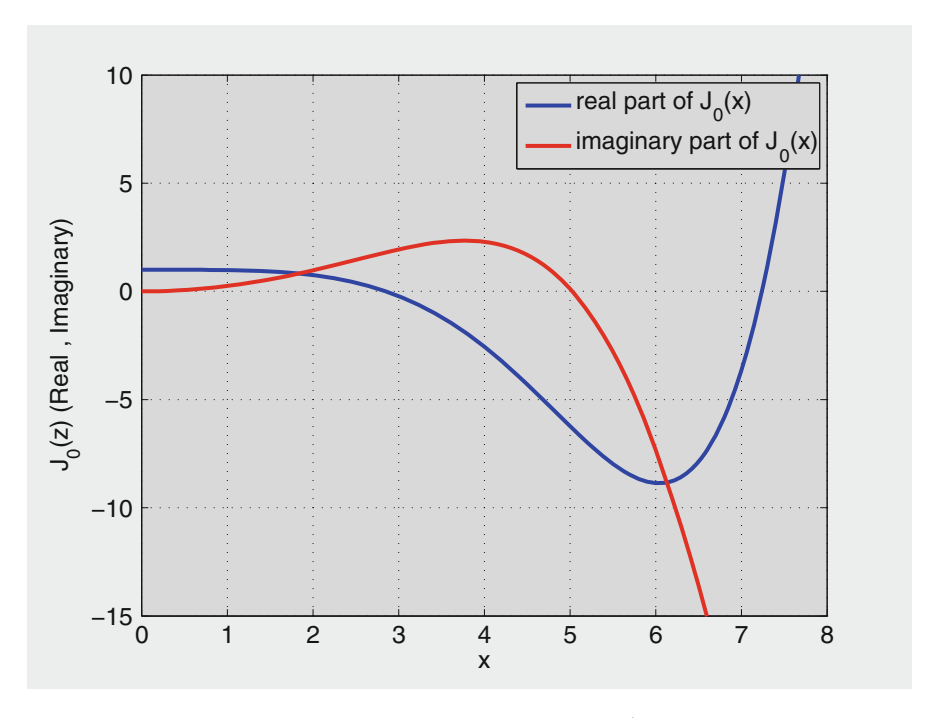


Fig. 4.3 Real and imaginary parts of $J_0(z)$ where $z = (i-1)x/2^{1/2}$.

from the properties of J_0 and Y_0 that they are *independent* of each other, that is one cannot be expressed in terms of the other. Therefore, the three terms on the right hand side of Eq. 4.16 represent the required elements of the general solution of Eq. 4.14, namely two independent solutions of the homogeneous equation (Eq. 4.20) and a particular solution of the full equation (Eq. 4.14).

The boundary conditions which the solution must satisfy for flow in a tube are no-slip at the tube wall and finite velocity along the axis of the tube, that is

$$\begin{cases}
U_{\phi}(a) = 0 \\
|U_{\phi}(0)| < \infty
\end{cases}$$
(4.21)

These provide the two equations required for determining the two arbitrary constants A, B in the general solution.

It is known from the properties of $Y_0(\zeta)$ that it becomes infinite as $\zeta \to 0$,^{3,4} which occurs on the axis of the tube where r = 0, thus the second boundary condition in Eq. 4.21 leads to

$$B = 0 \tag{4.22}$$

³McLachlan NW. Bessel Functions for Engineers. Clarendon Press, 1955.

⁴Watson GN. Theory of Bessel Functions. Cambridge University Press, 1958.

and the first boundary condition then gives

$$A = \frac{-ik_s a^2}{\mu \Omega^2 J_0(\Lambda)} \tag{4.23}$$

noting from Eq. 4.18 that

$$\zeta(a) = \Lambda \tag{4.24}$$

With these values of A, B the solution for U_{ϕ} is finally given by

$$U_{\phi} = \frac{ik_s a^2}{\mu \Omega^2} \left(1 - \frac{J_0(\zeta)}{J_0(\Lambda)} \right) \tag{4.25}$$

4.6 Oscillatory Velocity Profiles

The solution of Eq. 4.12 for the oscillatory flow velocity $u_{\phi}(r,t)$ is now complete. Using the results in Eqs. 4.13 and 4.25, we have

$$u_{\phi}(r,t) = \frac{ik_s a^2}{\mu \Omega^2} \left(1 - \frac{J_0(\zeta)}{J_0(\Lambda)} \right) e^{i\omega t}$$
 (4.26)

This is a classical solution for oscillatory flow in a rigid tube, obtained in different forms and at different times by Sexl,⁵ Womersley,⁶ Uchida,⁷ and discussed at some length by McDonald,⁸ and Milnor.⁹

The first element of the solution is a constant coefficient whose value depends on the amplitude of the pressure gradient k_s , radius of the tube a, viscosity of the fluid μ , and the frequency of oscillation Ω . The second element, inside the large brackets, is a function of r which describes the velocity profile in a cross section of the tube. The third element is a function of time which multiplies and therefore modifies the velocity profile as time changes within the oscillatory cycle, thus producing a sequence of oscillatory velocity profiles.

⁵Sexl T, 1930. Über den von E.G. Richardson entdeckten "Annulareffekt". Zeitschrift für Physik 61:349–362.

⁶Womersley JR, 1955. Oscillatory motion of a viscous liquid in a thin-walled elastic tube, I: The linear approximation for long waves. Philosophical Magazine 46:199–221.

⁷Uchida S, 1956. The pulsating viscous flow superimposed on the steady laminar motion of incompressible fluid in a circular pipe. Zeitschrift für angewandte Mathematik und Physik 7:403–422.

⁸McDonald DA. Blood flow in arteries. Edward Arnold, 1974.

⁹Milnor WR. Hemodynamics. Williams and Wilkins, 1989.

To compare these oscillatory profiles with the constant parabolic profile in Poiseuille flow, we consider steady and oscillatory flows in tubes of the same radius a, and take k_s in Eq. 4.26 to be both the constant pressure gradient in the Poiseuille flow case and the *amplitude* of the oscillatory pressure gradient in the oscillatory flow case. To further facilitate the comparison, the oscillatory flow velocity $u_{\phi}(r,t)$ is divided by the maximum velocity in Poiseuille flow, using Eqs. 3.41 and 4.19, to get

$$\frac{u_{\phi}(r,t)}{\hat{u}_s} = \frac{-4}{\Lambda^2} \left(1 - \frac{J_0(\zeta)}{J_0(\Lambda)} \right) e^{i\omega t} \tag{4.27}$$

This nondimensional form of the oscillatory velocity has the convenient scale in which a value of 1.0 represents a velocity equal to the maximum velocity in the corresponding Poiseuille flow case.

Because of the complex form of the driving pressure gradient (Eq. 4.11) for which the solution was obtained, Eq. 4.27 above represents *two* distinct solutions: one for which the pressure gradient driving the flow varies as the *real* part of k_{ϕ} , namely $\cos \omega t$, and another for which the gradient varies as the imaginary part of k_{ϕ} , namely $\sin \omega t$. It is convenient to introduce the following notation for the real and imaginary parts of the velocity and pressure

$$k_{\phi} = k_{\phi r} + ik_{\phi i}$$

= $k_s(\cos \omega t + i\sin \omega t)$ (4.28)

thus

$$\begin{cases} k_{\phi r} = k_s \cos \omega t \\ k_{\phi i} = k_s \sin \omega t \end{cases}$$
 (4.29)

The corresponding velocities are the real and imaginary parts of u_{ϕ} , that is

$$u_{\phi} = u_{\phi r} + iu_{\phi i}$$

$$= U_{\phi} e^{i\omega t}$$

$$= U_{\phi} (\cos \omega t + i \sin \omega t)$$

$$(4.31)$$

It is important to note that the real and imaginary parts of the velocity *do not* vary as $\cos \omega t$ and $\sin \omega t$ because the parameters Λ , ζ , $J_0(\zeta)$, $J_0(\Lambda)$ in U_ϕ (Eq. 4.25) are all complex. Thus the real and imaginary parts of the velocity in these expressions are generally different from those of the pressure gradient, hence a phase difference exists between the oscillatory pressure gradient and the oscillatory velocity profiles which it produces.

If the real and imaginary parts of U_{ϕ} are denoted by $U_{\phi r}$ and $U_{\phi i}$ respectively, that is

$$U_{\phi} = U_{\phi r} + iU_{\phi i} \tag{4.32}$$

where

$$\frac{U_{\phi r}}{\hat{u}_s} = \Re\left\{\frac{-4}{\Lambda^2} \left(1 - \frac{J_0(\zeta)}{J_0(\Lambda)}\right)\right\} \tag{4.33}$$

$$\frac{U_{\phi i}}{\hat{u}_s} = \Im\left\{\frac{-4}{\Lambda^2} \left(1 - \frac{J_0(\zeta)}{J_0(\Lambda)}\right)\right\} \tag{4.34}$$

then Eq. 4.31 becomes

$$u_{\phi} = (U_{\phi r} + iU_{\phi i})(\cos \omega t + i\sin \omega t) \tag{4.35}$$

and the real and imaginary parts of u_{ϕ} are thus given by

$$\begin{cases} u_{\phi r} = U_{\phi r} \cos \omega t - U_{\phi i} \sin \omega t \\ u_{\phi i} = U_{\phi i} \cos \omega t + U_{\phi r} \sin \omega t \end{cases}$$
(4.36)

It is clear from the expressions in Eq. 4.26 that the shape of the oscillatory velocity profiles will depend critically on the frequency of oscillation ω since it affects the values of the nondimensional frequency Ω , the complex frequency Λ , the complex variable ζ and ultimately the Bessel functions J_0 and oscillatory flow velocity u_{ϕ} . A set of oscillatory velocity profiles corresponding to $\Omega = 3$ and to the real part of the pressure gradient, namely $k_s \cos \omega t$, are shown in Fig. 4.4.

It is observed that velocity profiles oscillate between a peak profile in the forward direction and a peak profile in the backward direction, but neither the phase nor amplitude of these peak profiles correspond with the peaks of the oscillatory pressure. The first because forward and backward peaks of the pressure gradient, being $k_s \cos \omega t$, occur at $\omega t = 0^\circ, 180^\circ$, while the corresponding peak velocity profiles are seen to occur at approximately $\omega t = 90^\circ, 270^\circ$. Thus the oscillatory velocity *lags* the oscillatory pressure, clearly because of the inertia of the fluid. The second because maximum velocity in the peak velocity profile is less than 1.0, which means that it is less than the maximum velocity in the corresponding Poiseuille profile.

4.7 Oscillatory Flow Rate

Volumetric flow rate q_{ϕ} in oscillatory flow through a tube is obtained by integrating the oscillatory velocity profile over a cross section of the tube. Since the oscillatory velocity $u_{\phi}(r,t)$ is a function of r and t, the result is a function of time given by

$$q_{\phi}(t) = \int_{0}^{a} 2\pi r u_{\phi}(r, t) dr$$
 (4.37)

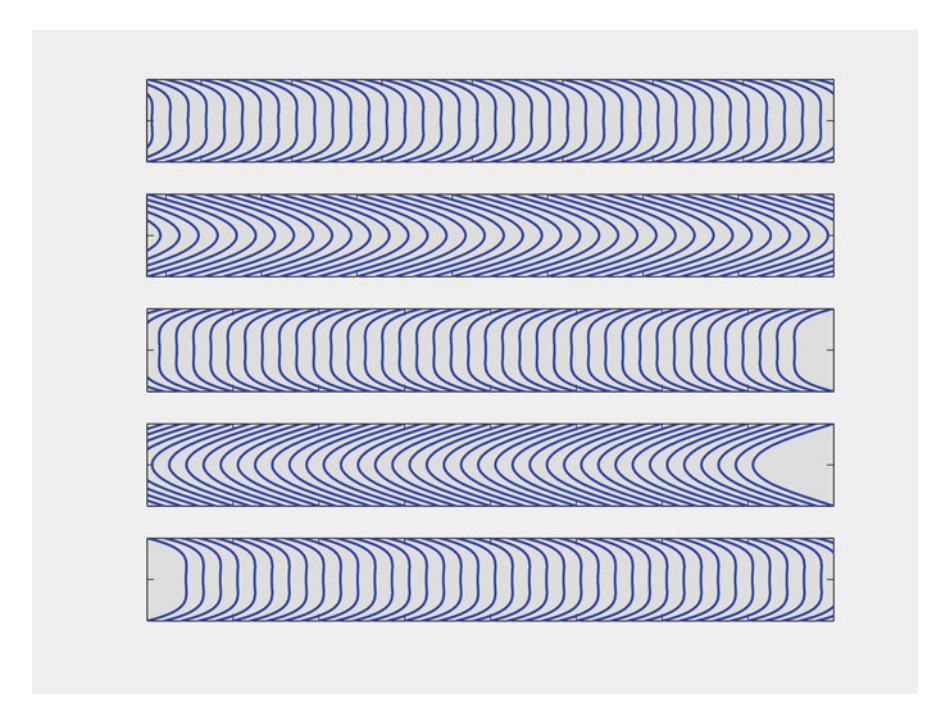


Fig. 4.4 Oscillatory velocity profiles in a rigid tube with frequency parameter $\Omega=3.0$ and corresponding to the *real* part of the pressure gradient, namely $k_{\phi}r=k_{s}\cos\omega t$. The panels represent the profiles at different phase angles (ωt) within the oscillatory cycle, with $\omega t=0$ in the top panel then increasing by 90° for subsequent panels. The impression that the tubes are tapering is only an optical illusion. Oscillatory flow in a *rigid* tube is here seen to be "purposeless" because it produces zero net flow, and entirely wasteful because of the energy being dissipated against the viscous shear stress at the tube wall. While oscillatory flow in a rigid tube is a mathematical simplification of oscillatory blood flow, it becomes increasingly relevant under pathological vascular stiffening, as will be discussed at great length in subsequent chapters.

Using the solution for $u_{\phi}(r,t)$ in Eq. 4.26, this becomes

$$q_{\phi}(t) = \frac{2\pi i k_s a^2}{\mu \Omega^2} e^{i\omega t} \int_0^a r \left(1 - \frac{J_0(\zeta)}{J_0(\Lambda)}\right) dr \tag{4.38}$$

The integral on the right is evaluated as follows

$$\int_0^a r \left(1 - \frac{J_0(\zeta)}{J_0(\Lambda)} \right) dr = \frac{a^2}{\Lambda^2 J_0(\Lambda)} \int_0^{\Lambda} (J_0(\Lambda) - J_0(\zeta)) \zeta d\zeta$$
$$= \frac{a^2}{2} \left(1 - \frac{2J_1(\Lambda)}{\Lambda J_0(\Lambda)} \right) \tag{4.39}$$

where J_1 is a Bessel function of the first order and first kind, related to J_0 by

$$\int \zeta J_0(\zeta) d\zeta = \zeta J_1(\zeta) \tag{4.40}$$

Thus the oscillatory flow rate is finally given by

$$q_{\phi}(t) = \frac{i\pi k_s a^4}{\mu \Omega^2} \left(1 - \frac{2J_1(\Lambda)}{\Lambda J_0(\Lambda)} \right) e^{i\omega t}$$
 (4.41)

The net flow rate Q_{ϕ} over one oscillatory cycle is given by

$$Q_{\phi} = \int_{0}^{T} q_{\phi}(t)dt$$

$$= \frac{i\pi k_{s}a^{4}}{\mu\Omega^{2}} \left(1 - \frac{2J_{1}(\Lambda)}{\Lambda J_{0}(\Lambda)}\right) \int_{0}^{T} (\cos\omega t + i\sin\omega t)dt$$

$$= \frac{i\pi k_{s}a^{4}}{\mu\Omega^{2}} \left(1 - \frac{2J_{1}(\Lambda)}{\Lambda J_{0}(\Lambda)}\right) \int_{0}^{2\pi} (\cos\theta + i\sin\theta)d\theta$$

$$= 0 \tag{4.42}$$

where $T = 2\pi/\omega$ is the period of oscillation. The result confirms that in oscillatory flow the fluid moves only back and forth, with no net flow in either direction.

To examine the variation of flow rate within the oscillatory cycle it is convenient to put Eq. 4.41 in nondimensional form, as was done for the velocity in the previous section. Dividing Eq. 4.41 through by the corresponding flow rate in steady Poiseuille flow, namely q_s in Eq. 3.43, gives

$$\frac{q_{\phi}(t)}{q_s} = \frac{-8}{\Lambda^2} \left(1 - \frac{2J_1(\Lambda)}{\Lambda J_0(\Lambda)} \right) e^{i\omega t} \tag{4.43}$$

The ratio represents the oscillatory flow rate scaled in terms of the corresponding flow rate in Poiseuille flow, thus a value of 1.0 represents a flow rate equal to that in Poiseuille flow in the same tube and under a constant pressure gradient equal to k_s . Numerical computations require values of $J_1(\Lambda)$ in addition to those of $J_0(\Lambda)$. It is clear form the expression on the right of Eq. 4.43 that the oscillatory flow rate depends heavily on the frequency of oscillation. It should also be noted that the expression is *complex*, its real part corresponding to the real part of the pressure gradient, and its imaginary part corresponding to the imaginary part of the pressure gradient.

Variation of $q_{\phi}(t)/q_s$ over one oscillatory cycle, at a moderate frequency, $\Omega = 3.0$, is shown in Fig. 4.5.

It is seen that the flow rate oscillates between a peak in the forward direction and a peak in the backward direction. At this frequency the value of the peak is decidedly less than 1.0, which means that the flow rate falls short of reaching

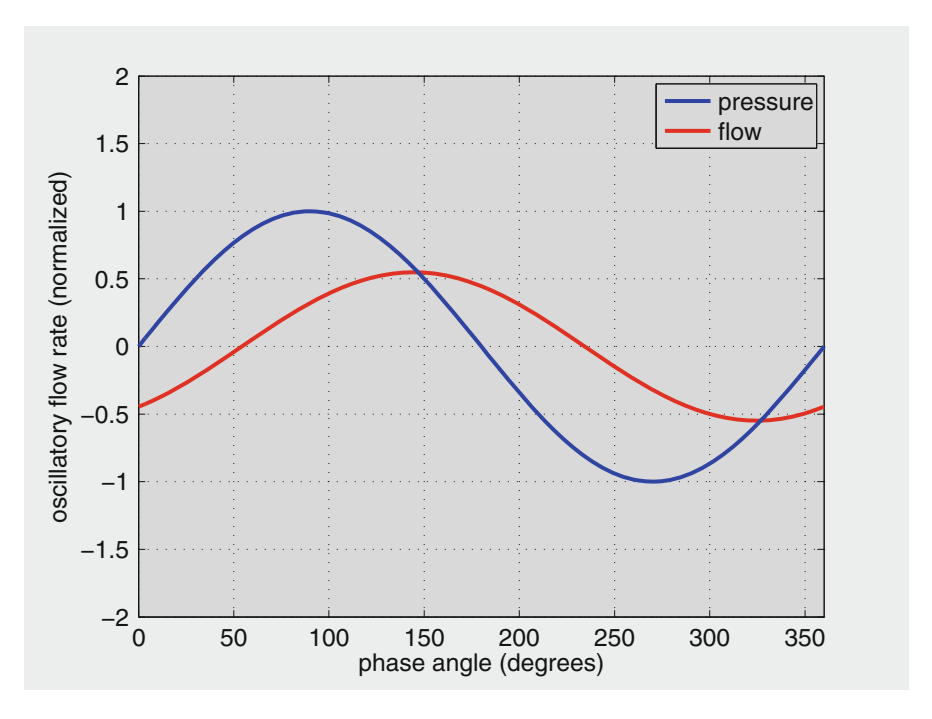


Fig. 4.5 Variation of the oscillatory flow rate q_{ϕ} within an oscillatory cycle, compared with variation of the corresponding pressure gradient, in this case $k_{\phi l} = k_s \sin \omega t$. Peak flow occurs later than peak pressure, that is the flow wave *lags* the pressure wave. Also, normalized peak flow is less than 1.0, which means that peak flow is less than the corresponding Poiseuille flow rate under the same pressure gradient.

the corresponding flow rate in Poiseuille flow under a constant pressure gradient equal to k_s which is the peak value of the oscillatory pressure gradient. The reason for this is clearly the inertia of the fluid which must be accelerated to peak flow in each cycle. We shall see later that this effect intensifies as the frequency of oscillation increases, the fluid having greater and greater difficulty reaching a peak flow commensurate with that in Poiseuille flow.

4.8 Oscillatory Shear Stress

In oscillatory flow, as fluid moves back and forth in response to the oscillatory pressure gradient, the shear stress at the tube wall varies accordingly as a function of time given by

$$\tau_{\phi}(t) = -\mu \left(\frac{\partial u_{\phi}(r, t)}{\partial r}\right)_{r=a} \tag{4.44}$$

It is important to note that since this shear is produced by only the oscillatory velocity u_{ϕ} , it is *in addition* to that produced by the steady velocity u_s when present.

Using the solution for $u_{\phi}(r, t)$ in Eq. 4.26, this becomes

$$\tau_{\phi}(t) = -\frac{ik_{s}a^{2}}{\Omega^{2}} \left\{ \frac{d}{dr} \left(1 - \frac{J_{0}(\zeta)}{J_{0}(\Lambda)} \right) \right\}_{r=a} e^{i\omega t}$$

$$= -\frac{ik_{s}a^{2}}{\Omega^{2}} \left\{ \frac{d}{d\zeta} \left(1 - \frac{J_{0}(\zeta)}{J_{0}(\Lambda)} \right) \right\}_{\zeta=\Lambda} \frac{\Lambda}{a} e^{i\omega t}$$

$$= -\frac{k_{s}a}{\Lambda} \left(\frac{J_{1}(\Lambda)}{J_{0}(\Lambda)} \right) e^{i\omega t}$$
(4.45)

where the relations between ζ , Λ and Ω in Eqs. 4.18 and 4.19, as well as the following relation between Bessel functions of the first and zeroth order ^{10,11}, have been used

$$\frac{dJ_0(\zeta)}{d\zeta} = -J_1(\zeta) \tag{4.46}$$

As before, it is convenient to put Eq. 4.45 in nondimensional form by scaling the oscillatory shear stress by the corresponding shear stress in Poiseuille flow, that is by dividing through by τ_s as given in Eq. 3.49, to get

$$\frac{\tau_{\phi}(t)}{\tau_{s}} = \frac{2}{\Lambda} \left(\frac{J_{1}(\Lambda)}{J_{0}(\Lambda)} \right) e^{i\omega t} \tag{4.47}$$

The expression on the right is complex, its real part representing the shear stress at the tube wall when the driving pressure gradient varies as $\cos \omega t$ and its imaginary part representing that shear when the gradient varies as $\sin \omega t$. In both cases the result is numerically scaled by the corresponding shear stress in Poiseuille flow.

Variation of the imaginary part of $\tau(t)$ within the oscillatory cycle is shown in Fig. 4.6. It is seen that it has a sinosoidal form like that of the imaginary part of the pressure gradient driving the flow, but with a phase difference between the two. The oscillatory shear stress lags the pressure, somewhat like the oscillatory flow rate. The amplitude of the oscillatory shear indicates the highest shear stress reached at the peak of each cycle as the fluid moves back and forth in each direction. This maximum clearly depends heavily on the frequency of oscillation as evident from Eq. 4.47. The results shown in Fig. 4.6 are for $\Omega=3.0$, where it is seen that the oscillatory shear reaches a maximum value at the peak of each cycle of approximately one half the steady Poiseuille flow value.

¹⁰McLachlan NW, 1955. Bessel Functions for Engineers. Clarendon Press, Oxford.

¹¹Watson GN, 1958. A Treatise on the Theory of Bessel Functions. Cambridge University Press. Cambridge.

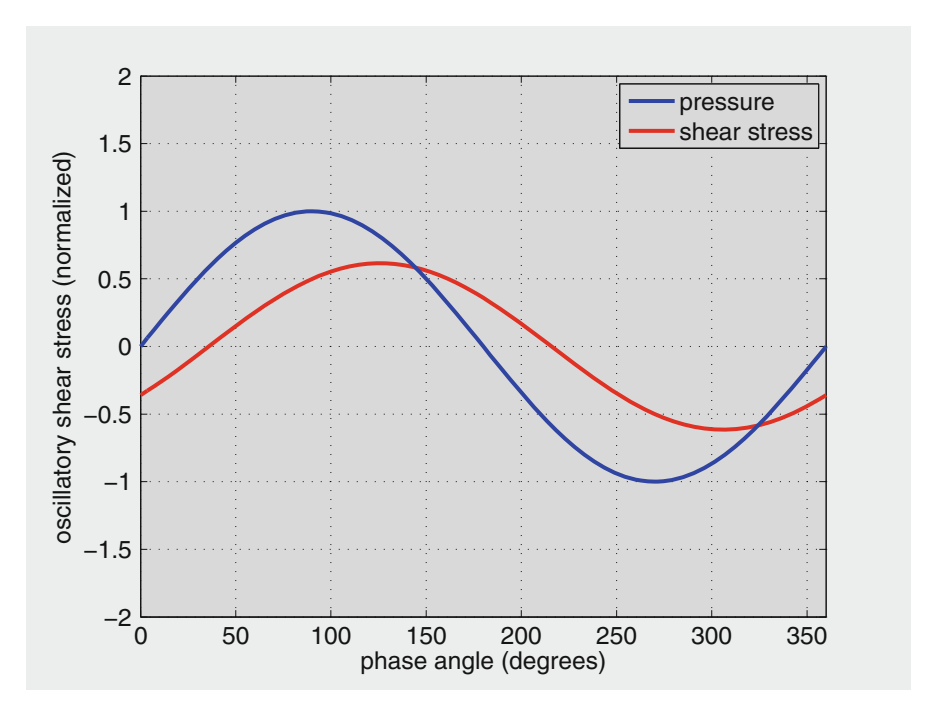


Fig. 4.6 Variation of the imaginary part of oscillatory shear stress $\tau_{\phi I}$ (red) compared with the corresponding part of the pressure gradient $k_{\phi I}$. Shear stress lags the pressure, and its normalized value at its peak is less than 1.0, hence less than the corresponding shear stress in Poiseuille flow. Since the shear stress shown here is produced entirely by the oscillatory flow, it is in addition to the constant shear stress produced by the steady component of pulsatile flow.

In pulsatile flow consisting of steady and oscillatory flow components, the oscillatory shear stress adds to and subtracts from the steady shear stress. The results in Fig. 4.6 show that in pulsatile flow at this particular frequency the shear stress would oscillate between a high of approximately 1.5 to a low of approximately 0.5 times its constant value in steady Poiseuille flow.

4.9 Energy Expenditure and Pumping Power

As in the case of steady Poiseuille flow, in pulsatile flow the equation governing the flow can be used to examine the balance of energy expenditure and in particular, in this case, to determine the pumping power required to drive the flow. Since the oscillatory part of pulsatile flow does not produce any net flow forward, and since the pumping power required to drive the steady part of pulsatile flow is the same as that in steady flow, any power expenditure on the oscillatory part of the oscillatory part of the flow is an "added expense" which reduces the efficiency of the flow. In

this section we examine this added expense by considering the balance of energy expenditures in pulsatile flow, much along the same lines as was done for steady flow in Sect. 3.9.

We begin with the governing equation for oscillatory flow, namely Eq. 4.6, in which we identify the different terms in the equation

$$\underbrace{k_{\phi}(t)}_{\text{driving pressure force}} = \underbrace{\mu\left(\frac{\partial^2 u_{\phi}}{\partial r^2} + \frac{1}{r}\frac{\partial u_{\phi}}{\partial r}\right)}_{\text{resisting viscous force}} \underbrace{-\rho\frac{\partial u_{\phi}}{\partial t}}_{\text{accelerating/decelerating force}}$$
(4.48)

We note that in this equation k_{ϕ} and u_{ϕ} are both complex with real and imaginary components. Therefore, this equation is equally complex and actually embodies two separate equations representing its real and imaginary parts. Using the notation of Sect. 4.6, they are

$$k_{\phi r} = \mu \left(\frac{\partial^2 u_{\phi r}}{\partial r^2} + \frac{1}{r} \frac{\partial u_{\phi r}}{\partial r} \right) - \rho \frac{\partial u_{\phi r}}{\partial t}$$
 (4.49)

$$k_{\phi i} = \mu \left(\frac{\partial^2 u_{\phi i}}{\partial r^2} + \frac{1}{r} \frac{\partial u_{\phi i}}{\partial r} \right) - \rho \frac{\partial u_{\phi i}}{\partial t}$$
 (4.50)

The discussion of energy expenditure is identical in terms of either one of these two equations and for the purpose of the present section we shall use the latter.

As in the case of steady Poiseuille flow, Eq. 4.48 represents a balance of forces. While in the steady flow case this balance is between only the driving pressure term on the left and the viscous resistance term on the right, in the present case there is an added acceleration term. In oscillatory flow, at any point in time, the driving pressure force must equal the *net* sum of viscous and acceleration forces which may add to or subtract from each other at different times within the oscillatory cycle.

As they stand, the terms in Eq. 4.48 represent *forces per unit volume*. The rate of energy expenditure associated with each term is thus obtained by considering a given volume of fluid moving with the same velocity. As in Sect. 3.9, we consider a cylindrical shell of radius r, length l, and thickness δr , moving with velocity $u_{\phi i}(r,t)$, the volume of fluid contained within the shell is then $2\pi r l \delta r$. It is important to recall that axial location x along the tube is not a factor in pulsatile flow through a rigid tube since fluid at all cross sections of the tube is moving with the same velocity profile, hence x does not appear as a variable in the velocity or in the governing equation.

If, as in the case of steady flow, each term in Eq. 4.50 is now multiplied by $2\pi r l \delta r \times u_{\phi i}$ and integrated over the cross section of the tube, we obtain the rate of energy expenditure associated with that particular term for fluid flow within the entire cross section of the tube. However, while in the case of steady flow this rate of energy expenditure is constant, in oscillatory flow it represents only the instantaneous rate of energy expenditure at time t within the oscillatory cycle.

Thus, for the driving pressure term we find

$$\int_0^a k_{\phi i} \times (2\pi r l \delta r) \times u_{\phi i} = lk_{\phi I}(t) \int_0^a 2\pi r u_{\phi i}(r, t) dr$$
$$= lk_{\phi i}(t) q_{\phi i}(t) \tag{4.51}$$

For the viscous dissipation term we find

$$\int_{0}^{a} \mu \left(\frac{\partial^{2} u_{\phi i}}{\partial r^{2}} + \frac{1}{r} \frac{\partial u_{\phi i}}{\partial r} \right) \times (2\pi r l \delta r) \times u_{\phi i} = 2\pi \mu l \int_{0}^{a} u_{\phi i} \frac{\partial}{\partial r} \left(r \frac{\partial u_{\phi i}}{\partial r} \right) dr$$

$$= 2\pi \mu l \left\{ \left| u_{\phi i} \frac{\partial u_{\phi i}}{\partial r} r \right|_{0}^{a} - \int_{0}^{a} \frac{\partial u_{\phi i}}{\partial r} r du_{\phi i} \right\}$$

$$= -2\pi \mu l \int_{0}^{a} \left(\frac{\partial u_{\phi i}}{\partial r} \right)^{2} r dr \qquad (4.52)$$

and for the acceleration term we find

$$\int_{0}^{a} \rho\left(\frac{\partial u_{\phi i}}{\partial t}\right) \times (2\pi r l \delta r) \times u_{\phi i} = 2\pi \rho l \int_{0}^{a} \frac{\partial}{\partial t} \left(\frac{u_{\phi i}^{2}}{2}\right) r dr$$

$$= 2\pi l \frac{d}{dt} \int_{0}^{a} \left(\frac{1}{2}\rho u_{\phi i}^{2}\right) r dr \qquad (4.53)$$

As shown explicitly in Eq. 4.51, since $k_{\phi} = k_{\phi}(t)$ and $u_{\phi} = u_{\phi}(r,t)$, the result of integration is a function of t. The same is implicit in the other two equations, but the functional dependence is omitted to simplify the notation. Thus the balance of energy expenditure in oscillatory flow varies in time within the oscillatory cycle. The *instantaneous* balance at time t is given by

$$-lk_{\phi i}q_{\phi i} = 2\pi\mu l \int_0^a r \left(\frac{\partial u_{\phi i}}{\partial r}\right)^2 dr + 2\pi l \frac{d}{dt} \int_0^a \left(\frac{1}{2}\rho u_{\phi i}^2\right) r dr \tag{4.54}$$

from which it is seen that at any point in time, the pumping power on the left hand side is being expended on the net sum of energy required to accelerate the flow and that required to overcome the viscous resistance. Since as the oscillatory cycle progresses the acceleration term changes sign while the viscous term does not, the net result at any instant may represent the sum or difference of the two terms. Physically, this means that during the acceleration phase of the oscillatory cycle the pumping power pays for both acceleration and viscous dissipation, while during the deceleration phase the flow actually returns some of its kinetic energy.

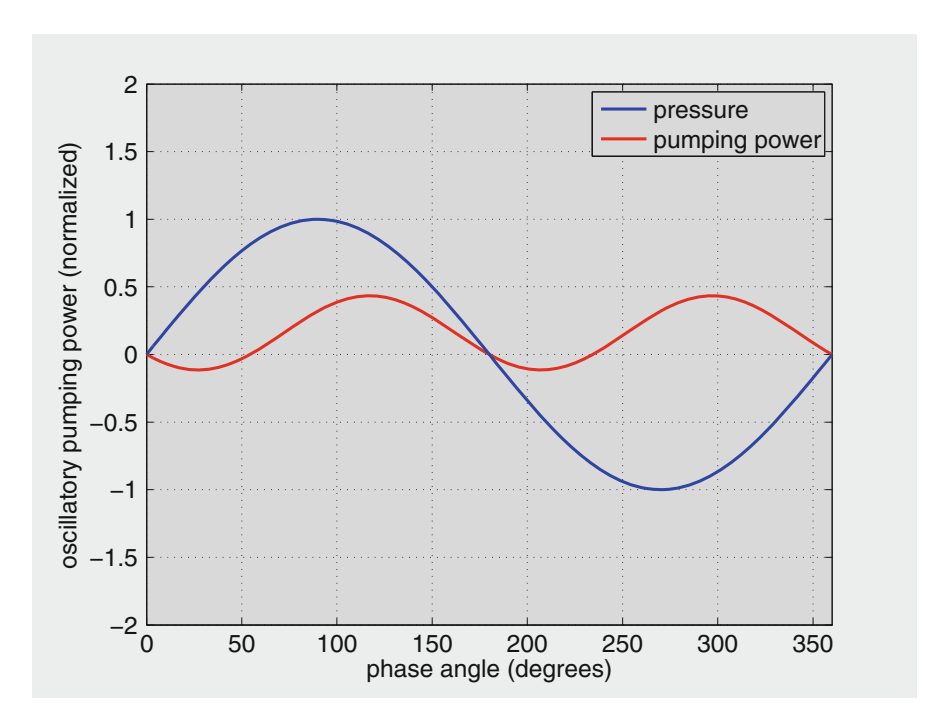


Fig. 4.7 Variation of oscillatory pumping power $H_{\phi I}$ during one cycle compared with the corresponding pressure gradient $k_{\phi I}$. The power has two peaks within each oscillatory cycle because it consists of the product of oscillatory pressure and oscillatory flow. The integral of the power over one cycle is not zero, hence oscillatory flow requires energy to maintain even though the net flow is zero. This energy expenditure is required to maintain the energy dissipation at the tube wall. The net energy expenditure for accelerating and decelerating the flow is zero (see text).

Variation of oscillatory pumping power is shown in Fig. 4.7, where it is seen that the power has two peaks within one oscillatory cycle because it consists of the product of k_{ϕ} and q_{ϕ} . The figure also shows clearly that the integral of the power over one cycle is not zero.

Of ultimate interest is the *average energy expenditure over the oscillatory cycle*. To obtain this the rates of energy expenditures in Eq. 4.54 must be integrated in time over one cycle and divided by the period

$$T = \frac{2\pi}{\omega} \tag{4.55}$$

where ω is the angular frequency in radians/s. The balance of average energy expenditure in pulsatile flow, using Eq. 4.54, is thus given by

$$-\int_{0}^{T} lk_{\phi i} q_{\phi i} dt = 2\pi \mu l \int_{0}^{T} \int_{0}^{a} r \left(\frac{\partial u_{\phi i}}{\partial r}\right)^{2} dr dt$$
$$+ 2\pi l \int_{0}^{T} \frac{d}{dt} \int_{0}^{a} \left(\frac{1}{2}\rho u_{\phi i}^{2}\right) r dr dt \tag{4.56}$$

If the last integral on the right hand side, which represents the average rate of energy expenditure associated with acceleration and deceleration of the flow, is evaluated first, we find

$$2\pi l \int_0^T \frac{d}{dt} \int_0^a \left(\frac{1}{2}\rho u_{\phi i}^2\right) r dr dt = -2\pi \rho l \int_0^a \left\{ \int_0^T d\left(\frac{u_{\phi i}^2}{2}\right) \right\} r dr$$

$$= -2\pi \rho l \int_0^a \left|\frac{u_{\phi l}^2}{2}\right|_{t=0}^{t=T} r dr$$

$$= -2\pi \rho l \int_0^a \left|\frac{(U_{\phi i} \cos \omega t + U_{\phi r} \sin \omega t)^2}{2}\right|_{t=0}^{t=T} r dr$$

$$= 0 \tag{4.57}$$

Thus, while the *instantaneous* energy expenditure required to accelerate the flow is generally nonzero, the net expenditure over one cycle is zero. The energy spent during one half of the cycle is recovered during the other half.

It follows that *over one cycle* the average power expenditure required to drive the oscillatory part of the flow is equal to that being dissipated by viscosity, thus Eq. 4.56 reduces to

$$-\int_{0}^{T} lk_{\phi i} q_{\phi i} dt = 2\pi \mu l \int_{0}^{T} \int_{0}^{a} r \left(\frac{\partial u_{\phi i}}{\partial r}\right)^{2} dr dt \tag{4.58}$$

Only one side of this equation needs to be evaluated to determine the average rate of energy expenditure in oscillatory flow. However, neither side is easy to evaluate in general because of the mix of Bessel and trigonometric functions involved. Approximate results in the limits of low or high frequency are examined in the next two sections.

4.10 Oscillatory Flow at Low Frequency

At low frequency, oscillatory flow in a tube is better able to keep pace with the changing pressure. In fact, at very low frequency, or in the limit of "zero frequency", the relation between flow and pressure becomes *instantaneously* the same as in steady Poiseuille flow. That is, at each point in time within the oscillatory cycle the velocity profile is what it would be in steady Poiseuille flow under a pressure gradient equal to the value of the oscillatory pressure gradient at that instant. The situation suggests the term "oscillatory Poiseuille flow". In this section we demonstrate these features of the flow analytically and derive approximate expressions which are valid at low frequency and which are easier to use than the more general expressions involving Bessel functions.

An appropriate measure of high or low frequency is the non-dimensional frequency parameter Ω as defined in Eq. 4.15 because this parameter appears in the equations governing the flow, either explicitly or implicitly through Λ (Eq. 4.19). At an angular frequency of 1 cycle/s, which is equivalent to an angular frequency of 2π radians/s, density of 1 g/cm^3 , and viscosity of 0.04 Poise (Poise = dyne s/cm²), the value of the nondimensional frequency parameter Ω , using Eq. 4.15, is given by

$$\Omega = \sqrt{\frac{2\pi}{0.04}} a \tag{4.59}$$

where a is the radius of the tube in cm. It is apparent from this that the values of the frequency parameters Ω and Λ , and hence the characteristics of oscillatory flow, will depend not on the value of the angular frequency but on that of Ω . Thus, while the angular frequency of the human heart beat is approximately 1 Hz or 1 cycle/s, the value of Omega and hence the characteristics of pulsatile flow will be different in different parts of the vascular system because of the difference in vessel diameters. Furthermore, the pulse generated by the heart consists of a mix of different frequencies and therefore different components (harmonics) of that pulse will contribute differently to the overall characteristics of the resulting pressure or flow wave. Again, these contributions in each case will depend not on the angular frequency of each harmonic but on the corresponding value of the non-dimensional frequency Omega. Accordingly, in this and the next section we examine the characteristics of oscillatory flow at low and high values of Ω .

Since, as we have seen in Sect. 4.5, the characteristics of oscillatory flow involve Bessel functions, we begin by looking at the behavior of these functions at small values of their argument (independent variable). A series expansion of the Bessel function of the first kind and order zero, $J_0(z)$, for small z is given by 12,13

¹²McLachlan NW. Bessel Functions for Engineers. Clarendon Press, 1955.

¹³Watson GN. Theory of Bessel Functions. Cambridge University Press, 1958.

$$J_0(z) = 1 - \frac{z^2}{2^2} + \frac{z^4}{2^2 \times 4^2} - \frac{z^6}{2^2 \times 4^2 \times 6^2} + \cdots$$
 (4.60)

The expansion is valid for *complex* values of z. Using this, and recalling from Eq. 4.18 that $\zeta = \Lambda r/a$, we find

$$\frac{J_0(\zeta)}{J_0(\Lambda)} = \frac{J_0(\Lambda r/a)}{J_0(\Lambda)}$$

$$\approx \left(1 - \frac{\Lambda^2 r^2}{4a^2} + \frac{\Lambda^4 r^4}{64a^4} - \cdots\right) \times \left(1 - \frac{\Lambda^2}{4} + \frac{\Lambda^4}{64} - \cdots\right)^{-1}$$

$$\approx \left(1 - \frac{\Lambda^2 r^2}{4a^2} + \frac{\Lambda^4 r^4}{64a^4} - \cdots\right) \times \left(1 + \frac{\Lambda^2}{4} + \frac{3\Lambda^4}{64} - \cdots\right)$$

$$\approx 1 + \frac{\Lambda^2}{4} \left\{ \left(1 - \frac{r^2}{a^2} + \cdots\right) + \frac{\Lambda^2}{16} \left(3 - \frac{4r^2}{a^2} + \frac{r^4}{a^4}\right) + \cdots \right\}$$
(4.61)

only terms of order ξ^4 being retained at each step. By substituting this result in Eq. 4.27 for the velocity profile we obtain the following approximate expression

$$\frac{u_\phi(r,t)}{\hat{u}_s} \approx \left\{ \left(1 - \frac{r^2}{a^2}\right) - \frac{i\Omega^2}{16} \left(3 - \frac{4r^2}{a^2} + \frac{r^4}{a^4}\right) \right\} e^{i\omega t} \tag{4.62}$$

The real and imaginary parts of the velocity are then given by

$$\frac{u_{\phi r}(r,t)}{\hat{u}_s} \approx \left(1 - \frac{r^2}{a^2}\right) \cos \omega t + \frac{\Omega^2}{16} \left(3 - \frac{4r^2}{a^2} + \frac{r^4}{a^4}\right) \sin \omega t$$

$$\frac{u_{\phi i}(r,t)}{\hat{u}_s} \approx \left(1 - \frac{r^2}{a^2}\right) \sin \omega t - \frac{\Omega^2}{16} \left(3 - \frac{4r^2}{a^2} + \frac{r^4}{a^4}\right) \cos \omega t \tag{4.63}$$

These expressions are easier to use than Eq. 4.27 since they do not involve Bessel functions and can be used in place of that equation when the frequency is small. Furthermore, substituting for \hat{u}_s from Eq. 3.41, and using Eq. 4.29 for the real and imaginary parts of the pressure gradient, we obtain

$$\begin{cases} u_{\phi r}(r,t) \approx -\frac{k_{\phi r}a^{2}}{4\mu} \left\{ \left(1 - \frac{r^{2}}{a^{2}}\right) + \frac{\Omega^{2}}{16} \left(3 - \frac{4r^{2}}{a^{2}} + \frac{r^{4}}{a^{4}}\right) \tan \omega t \right\} \\ u_{\phi i}(r,t) \approx -\frac{k_{\phi i}a^{2}}{4\mu} \left\{ \left(1 - \frac{r^{2}}{a^{2}}\right) - \frac{\Omega^{2}}{16} \left(3 - \frac{4r^{2}}{a^{2}} + \frac{r^{4}}{a^{4}}\right) \cot \omega t \right\} \end{cases}$$
(4.64)

We see that for small Ω where the second term in each of the two expressions can be neglected, the relation between velocity and pressure becomes

$$\begin{cases} u_{\phi r}(r,t) \approx \frac{k_{\phi R}}{4\mu} (r^2 - a^2) \\ u_{\phi i}(r,t) \approx \frac{k_{\phi I}}{4\mu} (r^2 - a^2) \end{cases}$$
(4.65)

which is the same as that in Eq. 3.38 for steady Poiseuille flow, but with instantaneous values of velocity and pressure, hence justifying the term "oscillatory Poiseuille flow". Velocity profiles with $\Omega = 1.0$ are shown in Fig. 4.8.

For the flow rate we use the series expansion of $J_1(z)$ for small values of $z^{14,15}$

$$J_1(z) = \frac{z}{2} - \frac{z^3}{2^2 \times 4} + \frac{z^5}{2^2 \times 4^2 \times 6} + \frac{z^7}{2^2 \times 4^2 \times 6^2 \times 8} + \dots$$
 (4.66)

Combined with the expansion for J_0 in Eq. 4.60, we find

$$\frac{J_1(\Lambda)}{J_0(\Lambda)} \approx \frac{\Lambda}{2} \left(1 - \frac{\Lambda^2}{8} + \frac{\Lambda^4}{192} \right) \times \left(1 - \frac{\Lambda^2}{4} + \frac{\Lambda^4}{64} \right)^{-1}$$

$$\approx \frac{\Lambda}{2} \left(1 - \frac{\Lambda^2}{8} + \frac{\Lambda^4}{192} \right) \times \left(1 + \frac{\Lambda^2}{4} + \frac{3\Lambda^4}{64} \right)$$

$$\approx \frac{\Lambda}{2} \left(1 + \frac{\Lambda^2}{8} + \frac{\Lambda^4}{48} \right) \tag{4.67}$$

where only terms of order Λ^4 or lower were retained at each step. Substituting this result in Eq. 4.43, we get

$$\frac{q_{\phi}(t)}{q_s} \approx \frac{8i}{\Omega^2} \left(\frac{\Lambda^2}{8} + \frac{\Lambda^4}{48} \right) e^{i\omega t} \tag{4.68}$$

¹⁴McLachlan NW, 1955. Bessel Functions for Engineers. Clarendon Press, Oxford.

¹⁵Watson GN, 1958. A Treatise on the Theory of Bessel Functions. Cambridge University Press. Cambridge.

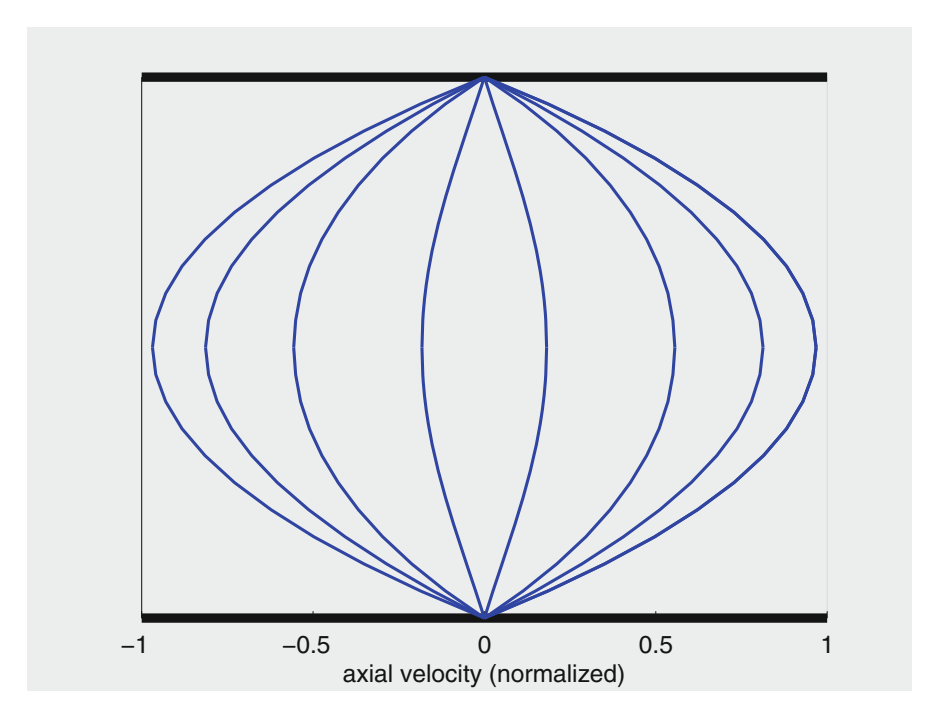


Fig. 4.8 Oscillatory velocity profiles in a rigid tube at low frequency ($\Omega=1.0$) and corresponding to the *real* part of the pressure gradient, namely $k_s \cos \omega t$. The figure shows the profiles at different phase angles (ωt) within the oscillatory cycle. The profiles reach their peak form at the peak of pressure gradient ($\omega t=0^\circ, 180^\circ$), and the maximum velocity at peak has a normalized value near 1.0. Thus flow is almost in phase with pressure gradient, and the relation between the two is as if the flow were Poiseuille flow *at each instant* (see text).

Noting that

$$\begin{cases} \Lambda^2 = -i\Omega^2 \\ \Lambda^4 = -\Omega^4 \end{cases} \tag{4.69}$$

the real and imaginary parts of the flow rate are given by

$$\begin{cases} \frac{q_{\phi r}(t)}{q_s} \approx \cos \omega t + \frac{\Omega^2}{6} \sin \omega t \\ \frac{q_{\phi i}(t)}{q_s} \approx \sin \omega t - \frac{\Omega^2}{6} \cos \omega t \end{cases}$$
(4.70)

Substituting for the steady flow rate from Eq. 3.43 and for the real and imaginary parts of the pressure gradient from Eq. 4.29, we get

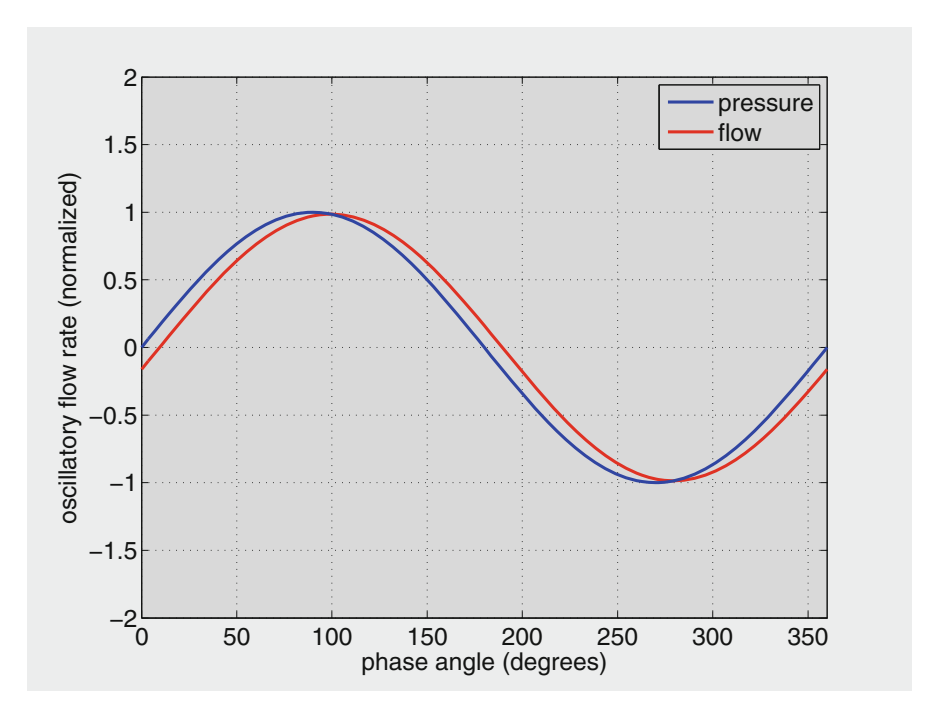


Fig. 4.9 Variation of the oscillatory flow rate q_{ϕ} within an oscillatory cycle, compared with variation of the corresponding pressure gradient, in this case $k_{\phi I} = k_s \sin \omega t$, at low frequency ($\Omega = 1.0$). Flow is almost in phase with pressure gradient, and normalized peak flow is close to 1.0. Flow at each point in time is close to what it would be in steady Poiseuille flow under the instantaneous value of the pressure gradient.

$$\begin{cases} q_{\phi r} \approx \frac{-k_{\phi r} \pi a^4}{8\mu} \left(1 + \frac{\Omega^2}{6} \tan \omega t \right) \\ q_{\phi i} \approx \frac{-k_{\phi i} \pi a^4}{8\mu} \left(1 - \frac{\Omega^2}{6} \cot \omega t \right) \end{cases}$$
(4.71)

At low frequency where the second term in each expression can be neglected, the relation between flow rate and pressure gradient becomes the same as that in steady flow *at each instant*, that is

$$\begin{cases} q_{\phi r} \approx \frac{-k_{\phi r} \pi a^4}{8\mu} \\ q_{\phi i} \approx \frac{-k_{\phi i} \pi a^4}{8\mu} \end{cases}$$

$$(4.72)$$

as in Eq. 3.43 for steady flow. Flow rate with $\Omega = 1.0$ is shown in Fig. 4.9.

Similarly, and omitting the details, we obtain the following expressions for the oscillatory shear stress

$$\begin{cases}
\tau_{\phi r} \approx -\frac{k_{\phi r}a}{2} \left(1 + \frac{\Omega^2}{8} \tan \omega t \right) \\
\tau_{\phi i} \approx -\frac{k_{\phi i}a}{2} \left(1 - \frac{\Omega^2}{8} \cot \omega t \right)
\end{cases}$$
(4.73)

and for the oscillatory maximum velocity

$$\begin{cases}
\hat{u}_{\phi r} \approx \frac{-k_{\phi r}a^2}{4\mu} \left(1 + \frac{3\Omega^2}{16} \tan \omega t \right) \\
\hat{u}_{\phi i} \approx \frac{-k_{\phi i}a^2}{4\mu} \left(1 - \frac{3\Omega^2}{16} \cot \omega t \right)
\end{cases}$$
(4.74)

In each case, if the frequency is low enough for the second term to be neglected, the relation becomes *instantaneously* the same as in steady flow (Eqs. 3.41 and 3.49). If the frequency is small but not negligible, the second term can be used for approximate calculations. Oscillatory shear stress with $\Omega=1.0$ is shown in Fig. 4.10.

For the pumping power, if the real and imaginary parts of the *average oscillatory* power over the oscillatory cycle is denoted by $H_{\phi r}$ and $H_{\phi i}$ then from Eq. 4.51 we have

$$\begin{cases} H_{\phi r} = \frac{-1}{T} \int_0^T lk_{\phi r} q_{\phi r} dt \\ H_{\phi i} = \frac{-1}{T} \int_0^T lk_{\phi i} q_{\phi i} dt \end{cases}$$

$$(4.75)$$

and using Eq. 4.29 for k_{ϕ} and the approximate results for the flow rate in Eq. 4.71 we find

$$\begin{cases} H_{\phi r} \approx \frac{1}{T} \int_0^T \frac{\pi a^4 l}{8\mu} k_s^2 \left(\cos^2 \omega t + \frac{\Omega^2}{6} \cos \omega t \sin \omega t\right) dt \\ H_{\phi i} \approx \frac{1}{T} \int_0^T \frac{\pi a^4 l}{8\mu} k_s^2 \left(\sin^2 \omega t - \frac{\Omega^2}{6} \cos \omega t \sin \omega t\right) dt \end{cases}$$
(4.76)

Comparing this with the rate of energy expenditure (pumping power) in steady Poiseuille flow, namely H_s as given by Eq. 3.55, we find

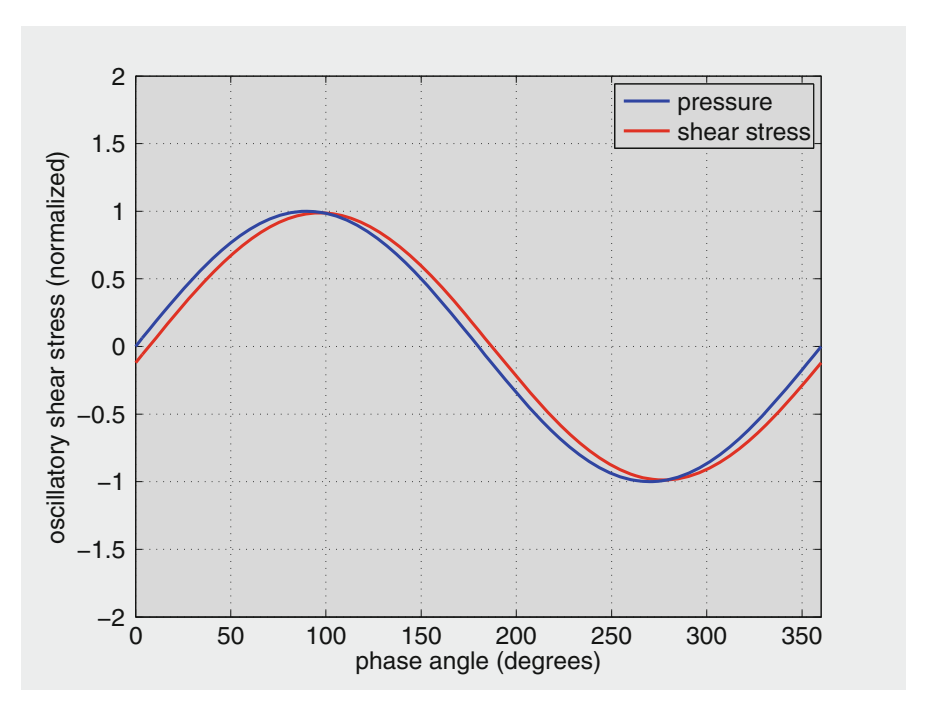


Fig. 4.10 Variation of the imaginary part of oscillatory shear stress $\tau_{\phi I}$ compared with the corresponding part of the pressure gradient $k_{\phi I}$, at low frequency ($\Omega=1.0$). Shear stress is almost in phase with pressure gradient, and normalized peak shear stress is close to 1.0. Shear stress at each point in time is close to what it would be in steady Poiseuille flow under the instantaneous value of the pressure gradient.

$$\begin{cases}
\frac{H_{\phi r}}{H_s} \approx \frac{1}{T} \int_0^T \left(\cos^2 \omega t + \frac{\Omega^2}{6} \cos \omega t \sin \omega t \right) dt \\
\frac{H_{\phi i}}{H_s} \approx \frac{1}{T} \int_0^T \left(\sin^2 \omega t - \frac{\Omega^2}{6} \cos \omega t \sin \omega t \right) dt
\end{cases}$$
(4.77)

With $T = 2\pi/\omega$ and noting that

$$\int_0^{2\pi} \cos^2 \theta d\theta = \int_0^{2\pi} \sin^2 \theta d\theta = \pi \tag{4.78}$$

and

$$\int_0^{2\pi} \cos\theta \sin\theta d\theta = 0 \tag{4.79}$$

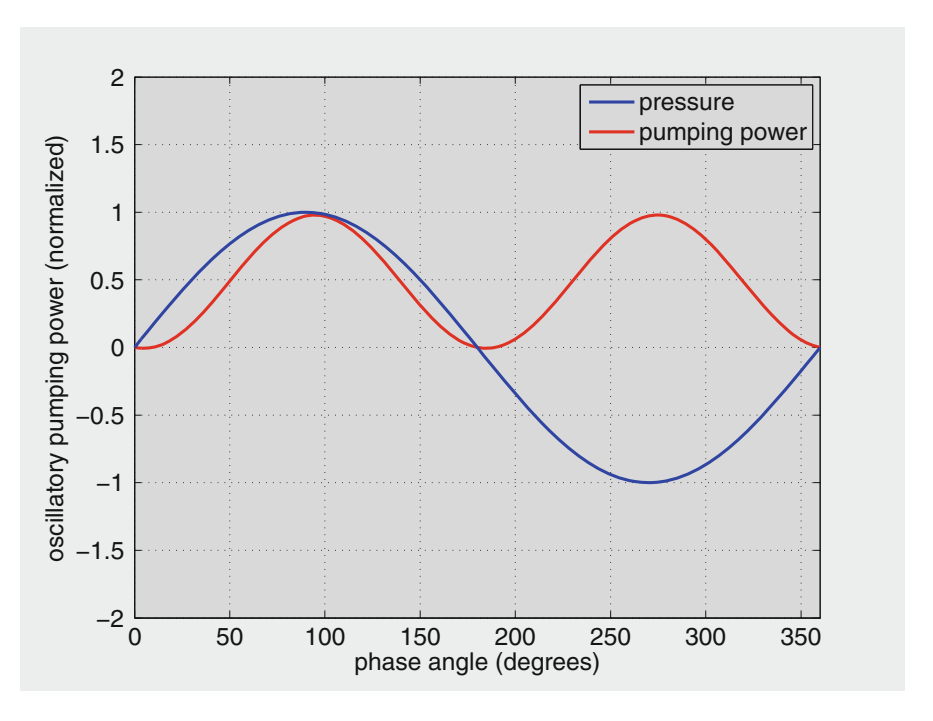


Fig. 4.11 Variation of oscillatory pumping power $H_{\phi I}$ during one cycle compared with the corresponding pressure gradient $k_{\phi I}$, at low frequency ($\Omega=1.0$). The two peaks of the power coincide very closely with the peaks of pressure gradient which at low frequency coincide with the peaks of flow rate (Fig. 4.9). Area under the power curve, which represents the net energy expenditure over one cycle, is not zero. In fact it equals one half the corresponding energy expenditure in steady Poiseuille flow (see text).

we find

$$\frac{H_{\phi r}}{H_s} = \frac{H_{\phi i}}{H_s} = \frac{1}{2} \tag{4.80}$$

Since in oscillatory flow there is no net flow forward, this pumping power is "wasted" in the sense that it is not being utilized to a useful end. Thus in pulsatile flow (steady plus oscillatory), at low frequency, the total power required to drive the flow is equal to the power required to drive the steady part of the flow, as in Poiseuille flow, plus one half of that amount to maintain the oscillatory part of the flow. Pumping power with $\Omega=1.0$ is shown in Fig. 4.11.

4.11 Oscillatory Flow at High Frequency

At high frequency oscillatory flow in a tube is less able to keep pace with the changing pressure, thus reaching less than the fully developed Poiseuille flow profile at the peak of each cycle. The higher the frequency the lower the peak velocity the flow is able to reach. In the limit of infinite frequency the velocity reached at the peak of each cycle is zero, that is the fluid does not move at all. An interesting question is whether the pumping power required to maintain this limiting state of zero flow is zero. In this section we develop approximate expressions describing properties of oscillatory flow at high frequency which are easier to use than the more general expressions involving Bessel functions, and which will be used to answer this question.

An approximate expression for $J_0(z)$ when z is large is given by ^{16,17}

$$J_0(z) \approx \frac{\sin z + \cos z}{\sqrt{\pi z}} \tag{4.81}$$

For the purpose of algebraic manipulation we write $z = iz_1$ so that

$$J_0(z) \approx \frac{\sin(iz_1) + \cos(iz_1)}{\sqrt{\pi i z_1}}$$

$$\approx \frac{i \sinh z_1 + \cosh z_1}{\sqrt{\pi i z_1}}$$

$$\approx \frac{(1+i)}{2} \frac{e^{z_1}}{\sqrt{\pi i z_1}}$$
(4.82)

and similarly, writing $\Lambda = i\Lambda_1$, then

$$J_0(\Lambda) \approx \frac{(1+i)}{2} \frac{e^{\Lambda_1}}{\sqrt{\pi i \Lambda_1}} \tag{4.83}$$

Near the tube wall where $r/a \approx 1$: Inserting the above approximations in Eq. 4.27 for the velocity profile, and recalling from Eq. 4.18 that $\zeta = \Lambda r/a$, hence $\zeta_1 = \Lambda_1 r/a$, we find

$$\frac{u_{\phi}(r,t)}{\hat{u}_s} = \frac{-4}{\Lambda^2} \left(1 - \frac{J_0(\zeta)}{J_0(\Lambda)} \right) e^{i\omega t}$$

$$\approx \frac{-4}{\Lambda^2} \left(1 - \sqrt{\frac{\Lambda_1}{\zeta_1}} e^{(\zeta_1 - \Lambda_1)} \right) e^{i\omega t}$$

¹⁶McLachlan NW. Bessel Functions for Engineers. Clarendon Press, 1955.

¹⁷Watson GN. Theory of Bessel Functions, Cambridge University Press, 1958.

$$\approx \frac{-4}{\Lambda^2} \left(1 - \sqrt{\frac{a}{r}} e^{\Lambda_1(\frac{r}{a} - 1)} \right) e^{i\omega t}$$

$$\approx \frac{4i}{\Lambda} \left(1 - \frac{r}{a} \right) e^{i\omega t} \tag{4.84}$$

The real and imaginary parts of which are given by

$$\begin{cases}
\frac{u_{\phi r}(r,t)}{\hat{u}_s} \approx \frac{2\sqrt{2}}{\Omega} \left(1 - \frac{r}{a}\right) (\cos \omega t + \sin \omega t) \\
\frac{u_{\phi i}(r,t)}{\hat{u}_s} \approx \frac{2\sqrt{2}}{\Omega} \left(1 - \frac{r}{a}\right) (\sin \omega t - \cos \omega t)
\end{cases}$$
(4.85)

Near the center of the tube, where $r/a \approx 0$ but Λ is large because of high frequency: Here the ratio $J_0(\zeta)/J_0(\Lambda)$ in the expression for the velocity (Eq. 4.27) requires an approximation of $J_0(\zeta)$ for small ζ and an expansion of $J_0(\Lambda)$ for large Λ , with the result

$$\frac{u_{\phi}(r,t)}{\hat{u}_{s}} = \frac{-4}{\Lambda^{2}}e^{i\omega t} \tag{4.86}$$

the real and imaginary parts of which are given by

$$\begin{cases} \frac{u_{\phi r}(r,t)}{\hat{u}_s} \approx \frac{4}{\Omega^2} \sin \omega t \\ \frac{u_{\phi i}(r,t)}{\hat{u}_s} \approx \frac{-4}{\Omega^2} \cos \omega t \end{cases}$$
(4.87)

These results indicate that at high frequency fluid near the tube wall (Eq. 4.85) is affected differently from fluid near the center of the tube (Eq. 4.87), thus distorting the parabolic character of the velocity profile. There is also some phase difference between the velocity near the center of the tube and that near the wall. By contrast, at *low* frequency fluid is affected more uniformly by pulsation, and the parabolic character of the velocity profile is fairly well preserved during the oscillatory cycle as we saw in the previous section. Velocity profiles with $\Omega=10$ are shown in Fig. 4.12.

For the flow rate, similarly, we use an approximation of $J_1(z)$ for large z, namely 18,19

$$J_1(z) \approx \frac{\sin z - \cos z}{\sqrt{\pi z}} \tag{4.88}$$

and, as before, writing $z = iz_1$, $\Lambda = i\Lambda_1$, this gives

$$J_1(\Lambda) \approx \frac{(i-1)e^{\Lambda_1}}{2\sqrt{\pi i \Lambda_1}} \tag{4.89}$$

Using this result in combination with the approximation for $J_0(\Lambda)$ in Eq. 4.83 for the flow rate in Eq. 4.43, we get

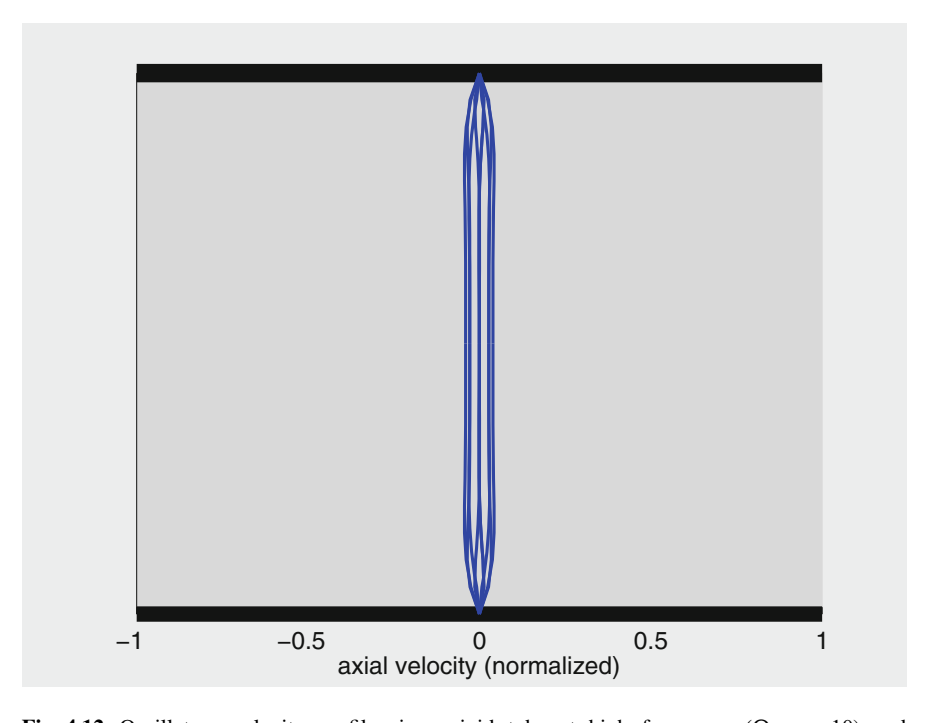


Fig. 4.12 Oscillatory velocity profiles in a rigid tube at high frequency ($\Omega=10$) and corresponding to the *real* part of the pressure gradient, namely $k_s\cos\omega t$. The figure represents the profiles at different phase angles (ωt) within the oscillatory cycle, with $\omega t=0$ in the top panel then increasing by 90° for subsequent panels. While the velocity is everywhere near zero, the profiles reach their peak form in the second panel, which means that they are about 90° out of phase with the pressure gradient (see text).

¹⁸McLachlan NW. Bessel Functions for Engineers. Clarendon Press, 1955.

¹⁹Watson GN. Theory of Bessel Functions. Cambridge University Press, 1958.

$$\frac{q_{\phi}(t)}{q_s} = \frac{-8i}{\Omega^2} \left(1 - \frac{2J_1(\Lambda)}{\Lambda J_0(\Lambda)} \right) e^{i\omega t}$$

$$\approx \frac{-8i}{\Omega^2} \left(1 - \frac{2}{i\Omega^2} \frac{(i-1)}{(i+1)} \right) e^{i\omega t}$$

$$\approx \frac{8}{\Omega^2} \left(\sin \omega t - i \cos \omega t \right) \tag{4.90}$$

where the higher order term in $1/\Omega^2$ is neglected in the last step, and recalling that $\Lambda^2 = -i\Omega^2$. The real and imaginary parts of the flow rate are then given by

$$\begin{cases} \frac{q_{\phi r}(t)}{q_s} \approx \left(\frac{8}{\Omega^2}\right) \sin \omega t \\ \frac{q_{\phi i}(t)}{q_s} \approx \left(\frac{-8}{\Omega^2}\right) \cos \omega t \end{cases}$$
(4.91)

These results have the same form as those for velocity near the center of the tube (Eq. 4.87), thus flow rate at high frequency behaves like velocity near the center of the tube. The results also show how flow rate diminishes at high frequency, as shown in Figs. 4.13 and 4.14.

Corresponding results for shear stress, omitting the details, are given by

$$\begin{cases}
\frac{\tau_{\phi R}(r,t)}{\tau_s} \approx \left(\frac{\sqrt{2}}{\Omega}\right) (\sin \omega t + \cos \omega t) \\
\frac{\tau_{\phi I}(r,t)}{\tau_s} \approx \left(\frac{\sqrt{2}}{\Omega}\right) (\sin \omega t - \cos \omega t)
\end{cases}$$
(4.92)

Variation of shear stress within the oscillatory cycle, and with $\Omega = 10$, is shown in Fig. 4.15.

Finally, for the pumping power, denoting the real and imaginary parts of the oscillatory pumping power by $H_{\phi r}$ and $H_{\phi i}$ respectively, then using Eq. 4.51 and dividing by the corresponding pumping power in steady flow, H_s , we find, omitting the details again

$$\frac{H_{\phi i}}{H_s} = \left(\frac{k_{\phi i}}{k_s}\right) \left(\frac{q_{\phi i}}{q_s}\right)$$

$$\approx \frac{-8}{\Omega^2} \sin \omega t \cos \omega t \tag{4.93}$$

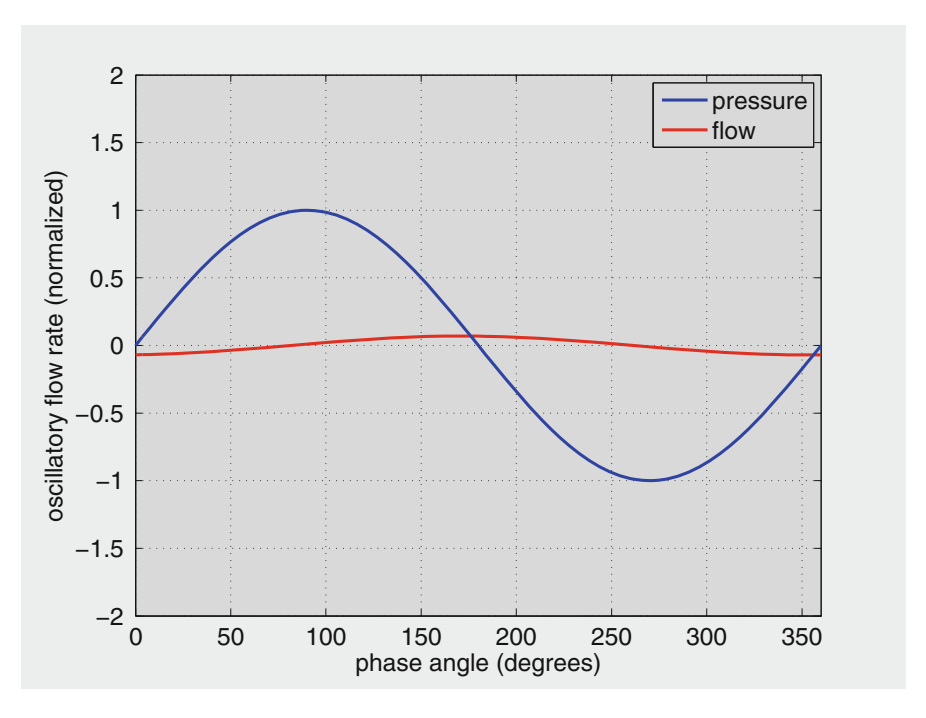


Fig. 4.13 Variation of the oscillatory flow rate q_{ϕ} within an oscillatory cycle compared with variation of the corresponding pressure gradient, in this case $k_{\phi I} = k_s \sin \omega t$, at high frequency ($\Omega = 10$). Flow rate is almost zero throughout the cycle, but there is an approximately 90° phase difference between flow rate and pressure gradient.

and

$$\frac{H_{\phi r}}{H_s} = \left(\frac{k_{\phi r}}{k_s}\right) \left(\frac{q_{\phi r}}{q_s}\right)$$

$$\approx \frac{8}{\Omega^2} \cos \omega t \sin \omega t \tag{4.94}$$

In both cases the pumping power vanishes in the limit of very high frequency. Fluid does not actually move in that limit. Variation of oscillatory pumping power within the oscillatory cycle, and with $\Omega=10$, is shown in Fig. 4.16.

4.12 Oscillatory Flow in Tubes of Elliptic Cross Sections

Pulsatile flow described in this chapter so far relates exclusively to flow in a tube of *circular* cross section. Flow in tubes of noncircular cross sections has not been studied as extensively as that in tubes of circular cross section, and there have been

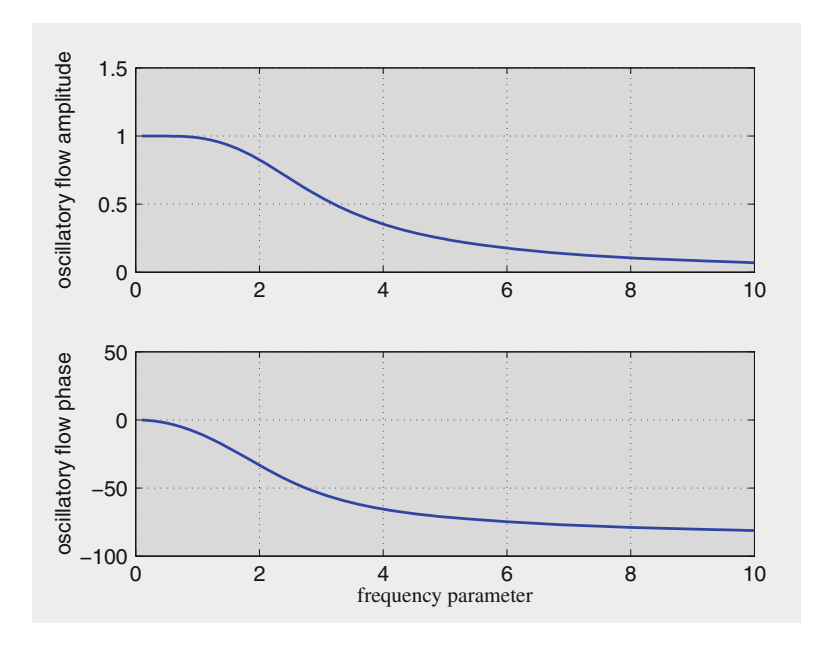


Fig. 4.14 Variation of amplitude and phase of the oscillatory flow rate q_{ϕ} with frequency parameter Ω . The amplitude (normalized in terms of corresponding steady flow rate) is near 1.0 at low frequency but drops rapidly to near zero as the frequency increases. The phase angle (representing the phase difference between flow rate and pressure gradient, in degrees) is near zero at low frequency but drops rapidly to -90° as the frequency increases.

very few studies of *pulsatile* flow in such tubes.²⁰ The problem of pulsatile flow in tubes of *elliptic* cross sections is of particular interest because it offers the possibility of an exact analytical solution. Also, changing the ellipticity of an elliptic cross section produces a wide range of cross sections, including the circular cross section as a special case. Finally, a tube of elliptic cross section provides a good analytical model of a "compressed" blood vessel, which has considerable relevance in hemodynamics.

Solution of the governing equation for pulsatile flow in a tube of elliptic cross section has been obtained in terms of Mathieu functions.²¹ These functions are not as easy to evaluate as Bessel functions, which makes the solution not as readily usable as that for a tube of circular cross section. A brief outline of this solution is presented in this section, with some possible simplifications which make the solution more easy to use, and some results are presented to highlight the effects of ellipticity.

²⁰Haslam M, Zamir M, 1998. Pulsatile flow in tubes of elliptic cross sections. Annals of Biomedical Engineering 26:1–8.

²¹McLachlan NW. Theory and Application of Mathew Functions. Dover Publications, 1964.

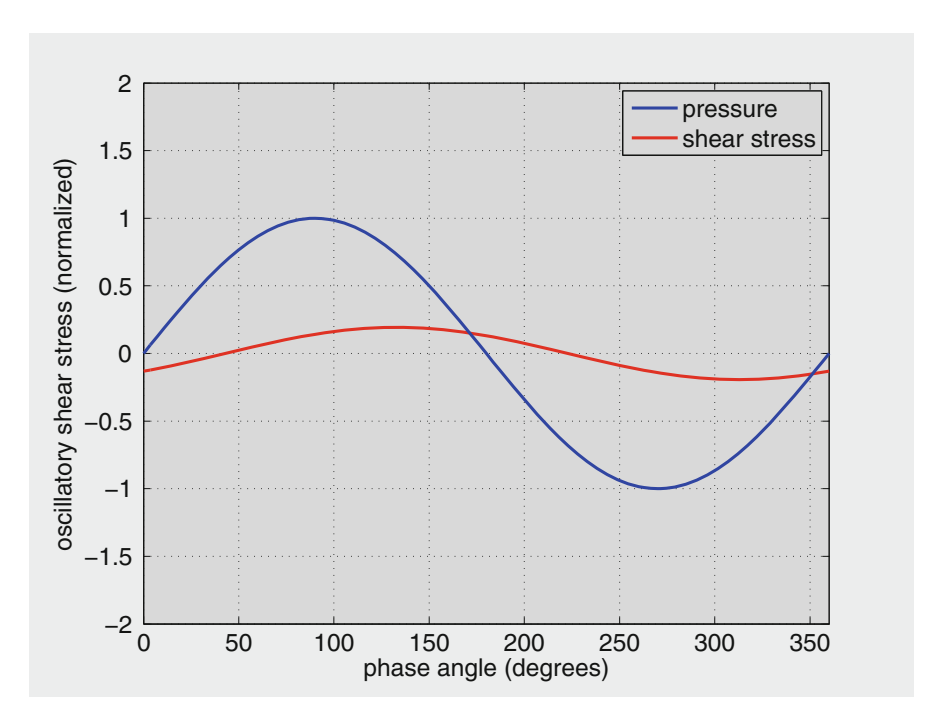


Fig. 4.15 Variation of the imaginary part of oscillatory shear stress $\tau_{\phi I}$ compared with the corresponding part of the pressure gradient $k_{\phi I}$, at high frequency ($\Omega=10$). Shear stress is very low at high frequency, but there is an approximately 90° phase difference between shear stress and pressure gradient.

The equation governing the flow is the same as that for a tube of circular cross section, namely Eq. 4.6. Boundary conditions are the same as those used for steady flow in a tube of elliptic cross section, namely Eq. 3.76. Because this boundary condition is being prescribed on the elliptic boundary of the cross section, it becomes necessary to transform the governing equation to elliptic coordinates²²

$$\begin{cases} y = d \cosh \xi \cos \eta \\ z = d \sinh \xi \sin \eta \end{cases}$$
(4.95)

where y, z are rectangular coordinates in the plane of the elliptic cross section and 2d is the distance between the two foci of the ellipse. In this coordinate system the curves of constant η represent a family of confocal hyperbolas while the curves of constant ξ represent a family of confocal ellipses, as illustrated in Fig. 4.17.

²²Moon PH, Spencer DE. Field Theory for Engineers. Van Nostrand, 1961.

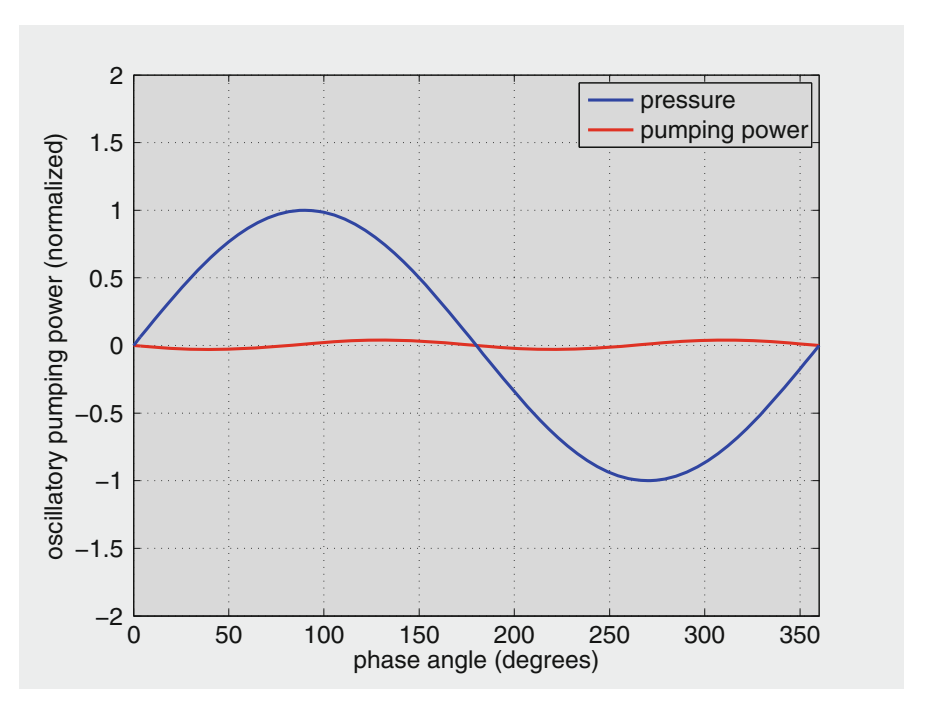


Fig. 4.16 Variation of oscillatory pumping power $H_{\phi l}$ during one cycle compared with the corresponding pressure gradient $k_{\phi l}$, at high frequency ($\Omega=10$). Pumping power is near zero at high frequency, as expected since oscillatory flow rate and shear stress are near zero. By contrast, oscillatory pumping power at *low* frequency is one half the corresponding power in steady flow, even though the *net* flow forward is zero.

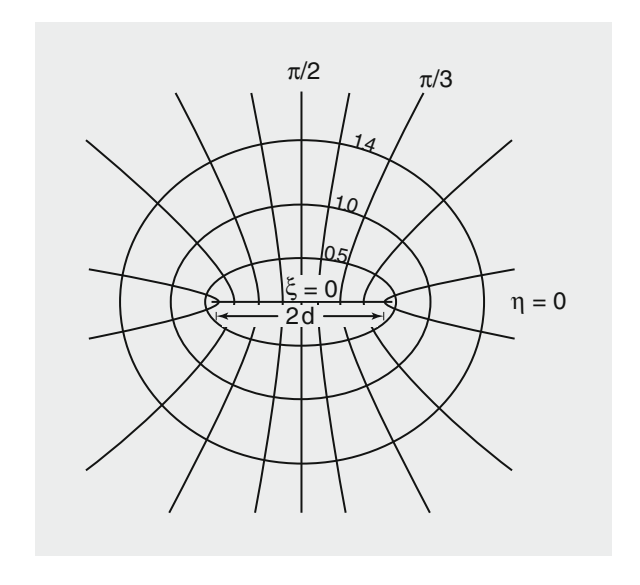
The coordinate ξ varies from 0 on the interfocal line to ξ_o on the tube wall. In terms of the elliptic coordinates ξ , η , the governing equation with no-slip at the tube wall (Eqs. 4.6 and 3.76) become

$$\begin{cases}
\frac{2\mu}{d^2(\cosh 2\xi - \cos 2\eta)} \left(\frac{\partial^2 u_{\phi e}}{\partial \xi^2} + \frac{\partial^2 u_{\phi e}}{\partial \eta^2} \right) - \rho \frac{\partial u_{\phi e}}{\partial t} = k_{\phi e}(t) \\
u_{\phi e}(\xi_o, \eta) = 0
\end{cases} (4.96)$$

where subscript ϕ is being used as in Sect. 4.3 to denote oscillatory flow, subscript e is being added as in Sect. 3.10 to denote elliptic cross section, and $k_{\phi e}$ is the oscillatory pressure gradient in the elliptic tube. Solution is obtained for an oscillatory pressure gradient as in the case of oscillatory flow in a tube of circular cross section, that is

$$k_{\phi e} = k_s e^{i\omega t} \tag{4.97}$$

Fig. 4.17 Elliptic coordinate system used in the solution and description of flow in tubes of elliptic cross sections. Adapted from Haslam and Zamir (1998; see Footnote 20).



the amplitude k_s being taken the same as that in steady flow in tubes of circular and elliptic cross sections, to facilitate comparison.

With this choice of pressure gradient, the oscillatory part of the velocity takes the form

$$u_{\phi e}(\xi, \eta, t) = U_{\phi e}(\xi, \eta)e^{i\omega t} \tag{4.98}$$

and the governing equation finally becomes an equation for $U_{\phi e}$, namely

$$\frac{2}{d^2(\cosh 2\xi - \cos 2\eta)} \left(\frac{\partial^2 U_{\phi e}}{\partial \xi^2} + \frac{\partial^2 U_{\phi e}}{\partial \eta^2} \right) - \frac{i\rho\omega}{\mu} U_{\phi e} = \frac{k_s}{\mu}$$
 (4.99)

A nondimensional frequency parameter is defined by

$$\Omega_e = \sqrt{\frac{\rho\omega}{\mu}}\lambda \tag{4.100}$$

where

$$\lambda = \sqrt{\frac{2b^2c^2}{b^2 + c^2}} \tag{4.101}$$

and b, c are semi-minor and semi-major axes of the ellipse as in the steady flow case.

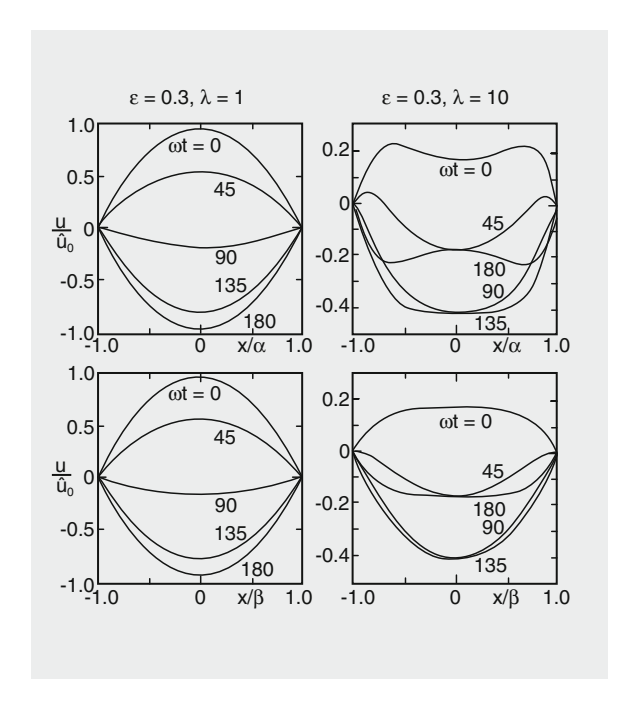


Fig. 4.18 Oscillatory velocity profiles along the major axis (top) and minor axis (bottom) of an elliptic cross section at low frequency ($\lambda=1$, left) and high ($\lambda=10$, right). In each panel, velocity profiles are shown at different phase angles ωt within the oscillatory cycle, ranging from $\omega t=0$ to $\omega t=180^\circ$, the second half of the cycle being omitted because of symmetry. The coordinates x,y and the axes α,β in this figure, from Haslam and Zamir (1998; see Footnote 20), correspond to coordinates y,z and axes b,c used in this book. The effects of ellipticity on the flow are here seen in terms of the difference between velocity profiles along the major axis in the top panels and minor axis in the bottom panels. The difference is seen to be insignificant at low frequency but becomes considerable at high frequency.

Equation 4.102 has a solution of the form (see Footnote 20)

$$U_{\phi e}(\xi, \eta) = \frac{4\hat{u}_{se}}{i\Omega^2} + \sum_{n=0}^{\infty} C_{2n} Ce_{2n}(\xi, -\gamma) ce_{2n}(\eta, -\gamma)$$
(4.102)

where C_{2n} is a constant determined by the boundary condition, ce_{2n} and Ce_{2n} are the ordinary and modified Mathieu functions²³, and

$$\gamma = \frac{i\rho\omega d^2}{4\mu} \tag{4.103}$$

Some velocity profiles are shown in Fig. 4.18 and oscillatory flow rate in Fig. 4.19.

²³McLachlan NW, 1964. Theory and Applications of Mathieu Functions. Dover Publications. New York.

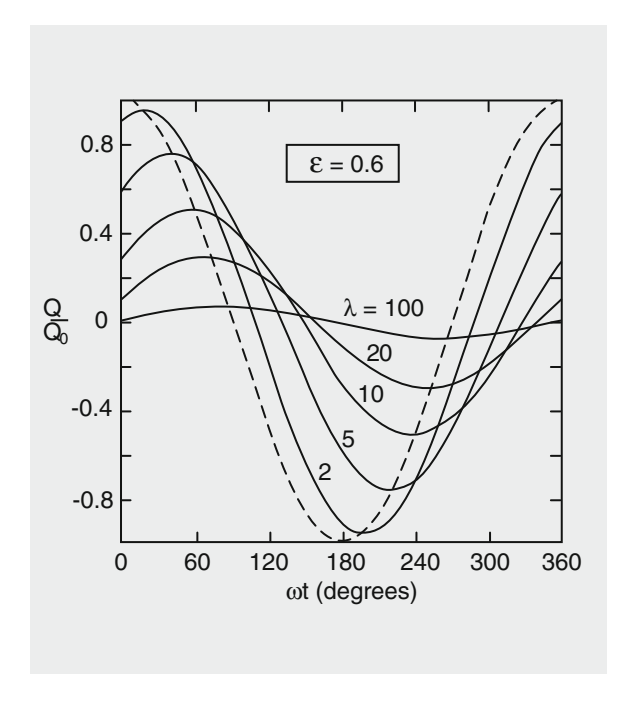


Fig. 4.19 Oscillatory flow rate in a tube of elliptic cross section of ellipticity $\epsilon=0.6$, normalized in terms of the corresponding steady flow rate. The ratio Q/Q_0 and parameter λ in this figure, from Haslam and Zamir (1998; see Footnote 20), correspond to the ratio $q_{\phi e}/q_{se}$ and frequency parameter Ω_e used in this book. Each curve represents variation of the flow rate within one oscillatory cycle for a given value of the frequency parameter. The dotted curve represents the corresponding pressure gradient. As in the case of a tube of circular cross section, flow rate is in phase with pressure gradient at low frequency but becomes increasingly out of phase and diminishes in magnitude as the frequency increases.

Evaluation of this solution is highly cumbersome because of the infinite series in Eq. 4.102 and because of the difficulties involved in the evaluation of Mathieu functions in general. Some simplifications are possible, however, under certain conditions.

At *low frequency* it is found that velocity and flow rate can be put in the form

$$\begin{cases} u_{\phi e}(y, z, t) \approx u_{se}(y, z)e^{i\omega t} \\ q_{\phi e}(t) \approx q_{se}e^{i\omega t} \end{cases}$$
(4.104)

where u_{se} and q_{se} are the corresponding velocity and flow rate in *steady* flow in a tube of elliptic cross section (Eqs. 3.77 and 3.78).

At *low ellipticity* it is found that velocity and flow rate become very close to those in a tube of circular cross section, with the radius of the tube being replaced by λ . In fact for $\epsilon = b/c > 0.9$ it is found that differences from the circular case are negligibly small.

It has also been found that the ratio $q_{\phi e}/q_{se}$ at *all frequencies* is highly insensitive to the value of ellipticity ϵ . In particular, therefore, this ratio for a tube of elliptic cross section is approximately equal to the corresponding ratio for a tube of circular cross section, that is

$$\frac{q_{\phi e}(t)}{q_{se}} \approx \frac{q_{\phi}(t)}{q_{s}} \tag{4.105}$$

the ratio on the right being that for a tube of circular cross section (Eq. 4.43). This permits the following approximation for the flow rate in a tube of elliptic cross section

$$\frac{q_{\phi e}(t)}{q_{se}} \approx \frac{-8}{\Lambda_e^2} \left(1 - \frac{2J_1(\Lambda_e)}{\Lambda_e J_0(\Lambda_e)} \right) e^{i\omega_e t} \tag{4.106}$$

where

$$\Lambda_e = \left(\frac{i-1}{\sqrt{2}}\right)\Omega_e \tag{4.107}$$

and Ω_e , which contains the parameter λ , replacing the radius a of a circular cross section, is defined by Eq. 4.100.

Finally, if the approximate expression in Eq. 4.105 is put in the form

$$\frac{q_{\phi e}(t)}{q_{\phi}(t)} \approx \frac{q_{se}}{q_{s}} \tag{4.108}$$

then the conclusions reached in Sect. 3.10 regarding the effect of ellipticity in steady flow provide a good approximation for the effect of ellipticity in pulsatile flow.

Chapter 5 Pulsatile Flow in an Elastic Tube

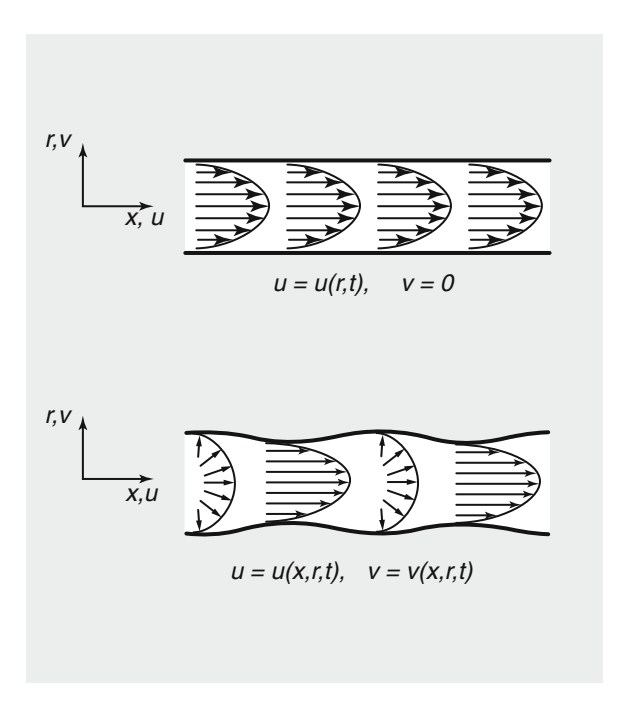
5.1 Introduction

Blood vessels are not rigid. Oscillatory flow in an elastic tube differs in a fundamental way from oscillatory flow in a rigid tube (Fig. 5.1). In a rigid tube, as the driving pressure increases to a peak during the systolic (rising pressure) phase of the oscillatory cycle, the flow can only move faster *along the tube*. In the case of an elastic tube the flow has another option, namely that of *inflating the tube locally* as well as moving faster along the tube, the balance between the two options being dependent on the degree of elasticity of the tube. Biology has chosen pulsatile flow in elastic rather than rigid tubes for a good reason. We saw in the previous chapter that the energy spent on moving the fluid back and forth during the oscillatory cycle is entirely "wasted" because of viscous dissipation at the fluid-wall interface. In the case of an elastic tube, by contrast, the energy spent on inflating the tube during the systolic phase of the cycle is actually recovered during the diastolic (falling pressure) phase of the cycle. It is recovered in full if the tube is purely elastic and largely recovered if the tube is "viscoelastic" as blood vessels are.

In short, the extra energy required for oscillating the flow in a rigid tube is *spent*, while in the case of an elastic tube it is *stored*. It is stored as elastic energy within the walls of the tube in precisely the same way that energy is stored within a spring when the spring is extended or compressed. In both cases the stored energy is recoverable in part or in full.

In the case of oscillatory flow in an elastic tube the energy is recovered as the walls of the tube "recoil" during the diastolic phase of the oscillatory cycle. However, the inflation and recoiling of the tube does not occur uniformly along the tube. Instead, as pressure rises at one end of the tube, the tube inflates only *locally* and then deflates as the pressure subsides. As it deflates it pushes fluid forward along the tube. In fact, it pushes the local inflation of the tube forward, thus forming a wave motion along the tube.

Fig. 5.1 Oscillatory flow in an elastic tube. In the fully developed region of flow in a rigid tube (top) oscillatory pressure changes occur simultaneously at every point along the tube to the effect that the fluid oscillates in bulk. There is no wave motion. In an elastic tube (bottom) pressure changes cause local movements of the fluid and tube wall, which then propagate downstream in the form of a wave. Velocity is no longer independent of x. and the radial velocity v is no longer zero.



From a mathematical standpoint, pulsatile flow in an elastic tube is more complicated because it involves two more dimensions than does pulsatile flow in a rigid tube. In the case of a rigid tube the flow is independent of the axial coordinate x because the flow oscillates *en masse* all along the tube and, as we saw in the previous chapter, the radial velocity component v is zero because the fluid motion is entirely *along* the tube. There is no motion towards the tube wall. In the case of an elastic tube, as described above, both of these simple features of the flow are lost. The flow is now dependent on x, and the radial velocity component v is not zero as illustrated schematically in Fig. 5.1.

We shall find nevertheless that the mathematical treatment of pulsatile flow in rigid tubes presented in the previous chapter provides an important foundation for analysis of the more complicated problem in the present chapter.

5.2 Wave Motion

As stated in the previous section, a fundamental difference between flow in a rigid tube and flow in an elastic tube is that a local change of pressure in a rigid tube is transmitted instantaneously to every part of the tube while in an elastic tube the change is transmitted with a finite speed. The reason for this is that a local increase in pressure in an elastic tube is able to stretch the tube wall outward, forming a local

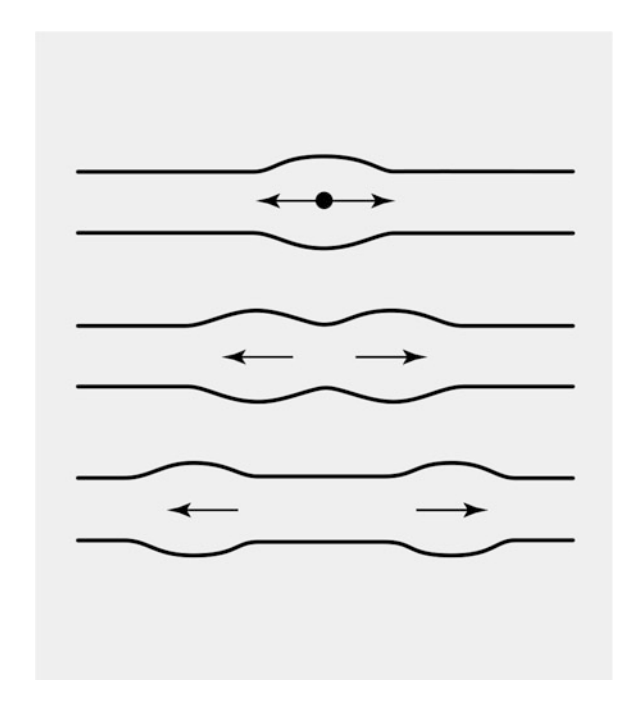
5.2 Wave Motion 125

bulge, and when the change in pressure subsides, the bulge recoils and pushes the excess fluid down the tube. The increase in pressure and the bulge associated with it propagate down the tube like the crest of an advancing wave. This scenario is not possible in a rigid tube because fluid in that case cannot stretch the tube wall, and because, as stated earlier, we assume throughout this discussion that the fluid is incompressible. It is for these two reasons that the local change in pressure in a rigid tube is transmitted instantaneously to every part of the tube. Wave motion is not possible in a rigid tube.

If a change in pressure occurs at some interior position in an elastic tube, the change will propagate equally in both directions, towards both ends of the tube, as illustrated schematically in Fig. 5.2.

A scenario of more practical interest is that in which the change in pressure occurs at one end of the tube and propagates in one direction towards the other end, which happens, for example, when a pump is placed at one end of a tube to drive the flow, or simply when there is a change in the pressure difference driving the flow. In this case wave propagation is in only one direction, namely from entrance to exit, as illustrated in Fig. 5.3, and this is the case we discuss in what follows under the general heading of wave propagation.

Fig. 5.2 A local change in pressure at an interior point in an elastic tube will propagate equally in both directions, towards the two ends of the tube.



¹Lighthill M. Mathematical Biofluiddynamics. Society for Industrial and Applied Mathematics, 1975.

Fig. 5.3 A wave propagation scenario of more practical interest is that in which a change in pressure occurs at one end of a tube and propagates to the other end. This occurs, for example, when flow is driven by the stroke of a pump at the tube entrance, or simply when there is a change in the pressure difference driving the flow.

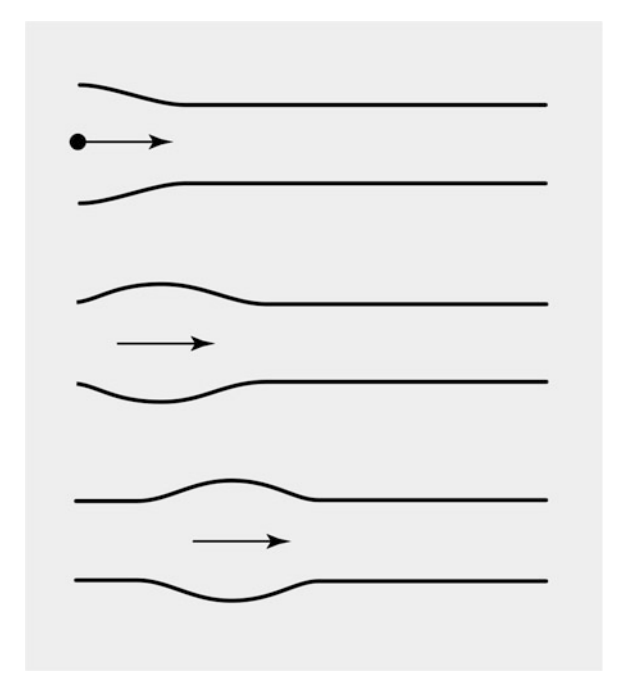
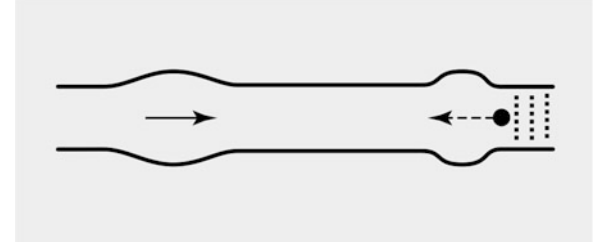


Fig. 5.4 A wave moving in one direction along an elastic tube may be reflected totally or partially by an obstacle, resulting in a secondary wave moving in the opposite direction.



However, the possibility exists that a wave propagating in one direction may be totally or partially reflected by an obstacle, thus leading to a secondary wave moving in the opposite direction as illustrated in Fig. 5.4. This will be discussed later under the heading of wave reflections. Thus, in this section we consider only a primary wave moving from one end of an elastic tube to the other end.

When considering flow in an elastic tube it is important to distinguish between motion of the *wave* and motion of the *fluid*. If the flow is driven by an increase in pressure at the tube entrance, for example, then wave motion refers to the forward motion of the local swelling or bulge in the tube caused by the increase in pressure, as illustrated in Figs. 5.2 and 5.3, much like the motion of the crest of a wave on the surface of a lake. The speed at which the bulge advances along the tube is referred to as the *wave speed*. Fluid motion, on the other hand, refers to the motion of fluid elements within the tube, associated with that wave motion. As the wave crest passes each position along the tube, fluid elements at that location are first swept towards

5.2 Wave Motion 127

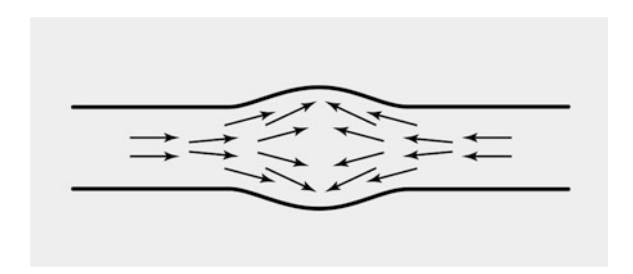


Fig. 5.5 As a wave crest passes each position along an elastic tube, fluid elements at that location are first swept towards the local bulge in the tube and then, as the crest passes and the bulge subsides, they are swept back by the decreasing pressure. This *fluid motion* is to be distinguished from the *wave motion*, illustrated in Figs. 5.2, 5.3, and 5.4, which is concerned with only the motion of the wave itself. Fluid motion is shown above only schematically in order to illustrate the difference between fluid motion and wave motion, the motion of fluid elements is actually considerably more complicated.

the local bulge in the tube, as illustrated schematically in Fig. 5.5, and then as the wave passes and the bulge subsides they are swept back by the decreasing pressure. The situation is again much the same as that experienced by a floating or submerged body swept by the passage of the crest of a wave on the surface of a lake.

The wave speed c in an elastic tube depends on the degree of elasticity of the tube wall, usually referred to as the "modulus of elasticity" or "Young's modulus" and denoted by E. The value of c also depends on the diameter d of the tube and its wall thickness h, and on the density ρ of the fluid. An approximation for the wave speed in terms of these properties, to be denoted by c_0 , is the so called Moens-Korteweg wave speed, 2,3,4 given by

$$c_0 = \sqrt{\frac{Eh}{\rho d}} \tag{5.1}$$

The approximation is based on the assumptions that (a) the fluid density ρ is constant, (b) the effects of fluid viscosity can be neglected, and (c) the wall thickness of the tube is small compared with the tube diameter.

The assumption of constant density ρ is important because if ρ is not constant then changes in pressure will lead to compression and expansion of the *fluid* within the tube, which provides another mechanism for wave propagation which can occur even in a rigid tube. In pulsatile blood flow this scenario is not of interest because under normal circumstances elasticity of the blood vessels far outweighs,

²McDonald DA. Blood Flow in Arteries. Edward Arnold, 1974.

³Caro CG, Pedley TJ, Schroter RC, Seed WA. The Mechanics of the Circulation. Oxford University Press, 1978.

⁴Milnor WR. Hemodynamics. Williams and Wilkins, 1989.

practically precludes, any compression of the blood to provide a mechanism for wave propagation. Indeed, the wave speed as determined by the Moen-Korteweg approximation for the wave speed is used in the clinical setting as a marker of the mechanical health of blood vessels, although in that context it is known as the "pulse wave velocity". In particular, a rise in the wave speed with aging or disease is widely interpreted as a sign of stiffening of the blood vessels or, equivalently, a higher value of E in Eq. 5.1.

Of mathematical interest in particular is the limit of infinite value of E because it represents the case of a rigid tube. In that case Eq. 5.1 indicates that the wave speed becomes infinite, which means that as pressure rises at one end of the tube, the pressure rise reaches the other end of the tube instantaneously. As a result, the flow will accelerate and decelerate in bulk all along the tube, which is precisely what we saw in pulsatile flow in a rigid tube. Thus the bulk motion of fluid in the case of oscillatory flow in a rigid tube can be thought of as resulting from a wave traveling with infinite speed.

The Moens-Korteweg formula for the wave speed (Eq. 5.1) is approximate because it does not take into account some dependence of the wave speed on viscosity of the fluid. Also, the formula is based on the assumption that the wall thickness h is small compared with the tube diameter. Despite these limitations the formula can be used to provide an estimate of the wave speed in the cardiovascular system. This is possible if it is further assumed that an *average* wall-thickness-to-diameter ratio h/d above can be taken for the entire system, which leaves c dependent on E and ρ only. Thus, taking $E = 10^7 \, \mathrm{dyne/cm^2}$, $\rho = 1 \, \mathrm{g/cm^3}$, and h/d = 0.1, we find $c = 1000 \, \mathrm{cm/s}$ or $10 \, \mathrm{m/s}$.

If the pressure at the entrance of an elastic tube does not merely rise once but rises and falls in an oscillatory manner, the result is a *train* of wave crests moving in tandem along the tube, which is commonly referred to as "wave propagation". The distance between two consecutive crests being referred to as the *wave length L*, as illustrated in Fig. 5.6.

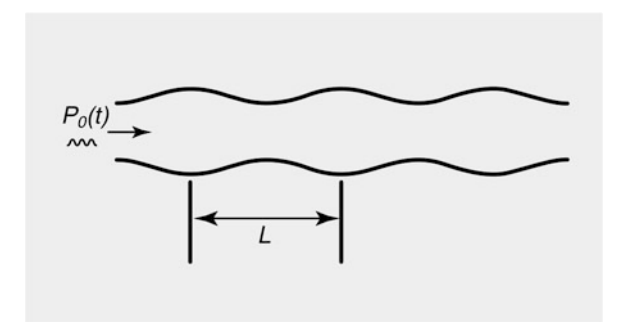


Fig. 5.6 If the pressure at the entrance of a tube does not change only once but continuously, in an oscillatory manner, the result is a train of wave crests moving along the tube, or what is commonly referred to as wave propagation. The distance L between two consecutive crests is referred to as the wave length.

5.2 Wave Motion 129

If the *frequency* of oscillation is f cycles/s or f Hz, then the wave length is related to the wave speed by

$$L = \frac{c}{f}$$

$$= \frac{c}{\omega/2\pi}$$
(5.2)

$$=\frac{c}{\omega/2\pi}\tag{5.3}$$

where ω is the angular frequency in radians/s, related to f by

$$\omega = 2\pi \times f \tag{5.4}$$

The pressure wave generated by the heart is a composite wave with a fundamental frequency of approximately 1 Hz. Thus an estimate of the wave length based on this frequency and a wave speed of 10 m/s is 10 m. The wave length is shorter at higher frequency, being only 5 m at a frequency of 2 Hz, etc. This is relevant when considering higher harmonics of the composite pressure wave generated by the heart. Thus, the fundamental frequency being 1 Hz, the frequency of the second harmonic will be 2 Hz, and that of the third will be 4 Hz, etc. as will be discussed in full detail in Chap. 10.

Finally, the wave speed and the wave length are affected by the degree of elasticity of the vessel wall, via the value of modulus of elasticity E in Eq. 5.1. More rigid walls have higher values of E and therefore lead to higher wave speeds and higher wave lengths, which is relevant to blood vessels as they become more rigid, with age or disease. In the limiting case of a totally rigid tube, E is infinite and hence both the wave speed and wave length become infinite. Wave propagation is therefore not possible in a rigid tube, clearly because a local increase in pressure cannot stretch the tube radially outward and thereby start the propagation process. Nevertheless, it is sometimes convenient to think of wave propagation in a rigid tube as one in which the wave speed is infinite, with a change in pressure at one end reaching all parts of the tube with infinite speed, that is instantaneously. Indeed, if the driving pressure at the entrance of a rigid tube changes in an oscillatory manner, the entire body of fluid within the tube oscillates back and forth in unison, as described in the previous chapter, which is not to be confused with wave propagation⁵.

One of the most important effects of wave propagation in an elastic tube is the possibility of wave reflections. Wave reflections arise when a wave meets a change in one of the conditions under which it is propagating, such as the diameter or elasticity of the tube, or more generally any change in the opposition to wave motion along the tube.

It is important to distinguish between the opposition to flow in a tube and the opposition to wave motion in that tube. The first is caused by the viscous shear at the tube wall, the second is caused by a combination of elasticity of the tube wall and inertia of the fluid. In the context of wave propagation, in order to distinguish

⁵Zamir M, 2000. The Physics of Pulsatile Flow. Springer-Verlag, New York.

between the two, the first is referred to as "pure resistance" but more usually as simply "resistance", the second is referred to as "reactance" and will be defined accurately later in this chapter. Here it is sufficient to note that reactance is higher if the tube wall is less elastic. Reactance is infinite if the tube wall is rigid, hence, as noted earlier, wave propagation is not possible in a rigid tube.

The combined effects of reactance and resistance are commonly referred to as "impedance". We shall see later that wave reflections in a tube arise at a point where there is a change of impedance, which may be caused by a change of diameter or elasticity of the tube. Impedance and wave propagation play a central role in the *dynamics* of blood flow because blood flow is pulsatile.

5.3 Equations Governing the Fluid Motion

Oscillatory flow in an elastic tube does not satisfy the simplifying assumptions on which Eq. 3.13 for oscillatory flow in a rigid tube was based. We must therefore return to the full Navier-Stokes equations, assuming only axial symmetry at first, namely Eq. 3.7 which we reproduce here to derive the required governing equations:

$$\begin{cases}
\rho \left(\frac{\partial u}{\partial t} + u \frac{\partial u}{\partial x} + v \frac{\partial u}{\partial r} \right) + \frac{\partial p}{\partial x} = \mu \left(\frac{\partial^2 u}{\partial x^2} + \frac{\partial^2 u}{\partial r^2} + \frac{1}{r} \frac{\partial u}{\partial r} \right) \\
\rho \left(\frac{\partial v}{\partial t} + u \frac{\partial v}{\partial x} + v \frac{\partial v}{\partial r} \right) + \frac{\partial p}{\partial r} = \mu \left(\frac{\partial^2 v}{\partial x^2} + \frac{\partial^2 v}{\partial r^2} + \frac{1}{r} \frac{\partial v}{\partial r} - \frac{v}{r^2} \right) \\
\frac{\partial u}{\partial x} + \frac{\partial v}{\partial r} + \frac{v}{r} = 0
\end{cases} (5.5)$$

Simplification of these equations is possible if it can be assumed that the length L of the propagating wave is much higher than the tube radius a (so called "long wave" approximation), and wave speed c_0 is much higher than the average flow velocity \overline{u} within the tube, that is if

$$\frac{a}{L}, \frac{\overline{u}}{c_0} << 1 \tag{5.6}$$

Under these conditions some of the terms in Eq. 5.5 will be much larger than others, namely

$$\begin{cases} u \frac{\partial u}{\partial x}, v \frac{\partial u}{\partial r} << \frac{\partial u}{\partial t} \\ u \frac{\partial v}{\partial x}, v \frac{\partial v}{\partial r} << \frac{\partial v}{\partial t} \\ \frac{\partial^{2} u}{\partial x^{2}} << \frac{\partial^{2} u}{\partial r^{2}} \\ \frac{\partial^{2} v}{\partial x^{2}} << \frac{\partial^{2} v}{\partial r^{2}} \end{cases}$$

$$(5.7)$$

and if the smaller terms are neglected, Eq. 5.5 reduce to

$$\begin{cases}
\rho \frac{\partial u}{\partial t} + \frac{\partial p}{\partial x} = \mu \left(\frac{\partial^2 u}{\partial r^2} + \frac{1}{r} \frac{\partial u}{\partial r} \right) \\
\rho \frac{\partial v}{\partial t} + \frac{\partial p}{\partial r} = \mu \left(\frac{\partial^2 v}{\partial r^2} + \frac{1}{r} \frac{\partial v}{\partial r} - \frac{v}{r^2} \right) \\
\frac{\partial u}{\partial x} + \frac{\partial v}{\partial r} + \frac{v}{r} = 0
\end{cases} (5.8)$$

There are three equations for three dependent variables, namely u(x, r, t), v(x, r, t), p(x, r, t), compared with only one equation (Eq. 3.13) for u(r, t) in the case of rigid tube.

5.4 Solution of Flow Equations

As in the case of a rigid tube, a solution of the governing equations is possible when the input pressure at the tube entrance is a simple "sinosoidal" oscillatory function. In this case, however, as discussed earlier, the resulting pressure and flow distributions within the tube are oscillatory both in space and time. At any point in time, the pressure and flow distributions are sinosoidal in x, and at any fixed position they are sinosoidal in t. As in the case of a rigid tube, the analysis is considerably easier if the oscillations are considered as complex exponential functions rather than sine or cosine functions. Mathematically, then, the simplified governing equations are found to have a solution for which the 3 dependent variables are of the form

$$\begin{cases} p(x,r,t) = P(r)e^{i\omega(t-x/c)} \\ u(x,r,t) = U(r)e^{i\omega(t-x/c)} \\ v(x,r,t) = V(r)e^{i\omega(t-x/c)} \end{cases}$$
(5.9)

As in the case of a rigid tube, ω is the frequency of oscillation of the input pressure, and as in that case, the oscillations *within* the tube have the same frequency. The analytical advantage of the complex exponential form is noted upon substitution of these into Eq. 5.8 with the result that the exponential terms cancel throughout, leaving *ordinary* differential equations for P(r), U(r), V(r), namely

$$\begin{cases} \frac{d^2 U}{dr^2} + \frac{1}{r} \frac{dU}{dr} - \frac{i\rho\omega}{\mu} U = -\frac{i\omega}{\mu c} P \\ \frac{d^2 V}{dr^2} + \frac{1}{r} \frac{dV}{dr} - \left(\frac{1}{r^2} + \frac{i\rho\omega}{\mu}\right) V = \frac{1}{\mu} \frac{dP}{dr} \\ \frac{dV}{dr} + \frac{V}{r} - \frac{i\omega}{c} U = 0 \end{cases}$$
(5.10)

The first two of these equations are forms of Bessel equations with known solutions in terms of Bessel functions.^{6,7} To put the equations in standard form we introduce the following non-dimensional parameters, as in the case of a rigid tube

$$\begin{cases} \Omega = \sqrt{\frac{\rho\omega}{\mu}} a \\ \Lambda = \left(\frac{i-1}{\sqrt{2}}\right) \Omega \end{cases}$$

$$\zeta = \Lambda \frac{r}{a}$$
(5.11)

thus, in terms of ζ , the governing equations now become

$$\begin{cases} \frac{d^2 U}{d\xi^2} + \frac{1}{\xi} \frac{dU}{d\xi} + U = \frac{1}{\rho c} P \\ \frac{d^2 V}{d\xi^2} + \frac{1}{\xi} \frac{dV}{d\xi} + \left(1 - \frac{1}{\xi^2}\right) V = \frac{i\Lambda}{\rho a \omega} \frac{dP}{d\xi} \\ \frac{dV}{d\xi} + \frac{V}{\xi} - \frac{i\omega a}{c\Lambda} U = 0 \end{cases}$$
(5.12)

The boundary conditions are zero velocities at the tube wall and finite velocity at the tube center. Since the tube wall is in motion, the first of these makes it difficulty to obtain an analytical solution. As a reasonable approximation, the boundary condition is applied instead at a fixed radius *a* which is taken to be the *neutral* position of the tube wall. Thus the approximate boundary conditions become

$$\begin{cases} U(a), V(a) = 0\\ U(0), V(0) < \infty \end{cases}$$

$$(5.13)$$

Solutions of the first two governing equations (Eq. 5.12) which satisfy the third equation as well as these boundary conditions are given by

$$\begin{cases} U(r) = AJ_0(\zeta) + B \frac{a\gamma}{\mu(i\Omega^2 + \gamma^2)} J_0\left(\frac{\gamma}{\Lambda}\zeta\right) \\ V(r) = A \frac{\gamma}{\Lambda} J_1(\zeta) + B \frac{a\gamma}{\mu(i\Omega^2 + \gamma^2)} J_1\left(\frac{\gamma}{\Lambda}\zeta\right) \\ P(r) = BJ_0\left(\frac{\gamma r}{a}\right) \end{cases}$$
(5.14)

⁶McLachlan NW. Bessel Functions for Engineers. Clarendon Press, 1955.

⁷Watson GN. Theory of Bessel Functions. Cambridge University Press, 1958.

where A, B are arbitrary constants and

$$\gamma = \frac{i\omega a}{c} \tag{5.15}$$

Using the long wave approximation (Eq. 5.6) we note that

$$\begin{cases} \gamma \sim \left(\frac{a}{L}\right) << 1 \\ J_0\left(\frac{\gamma r}{a}\right) \approx J_0(0) \approx 1 \\ J_1\left(\frac{\gamma r}{a}\right) \approx J_1(0) \approx \frac{1}{2} \frac{\gamma r}{a} \end{cases}$$
 (5.16)

Applying these approximations, the solutions reduce to

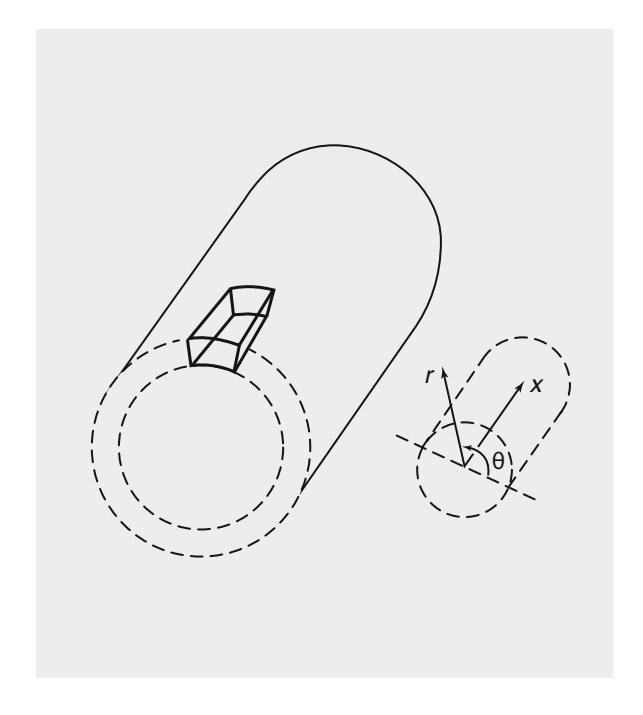
$$\begin{cases} U(r) = AJ_0(\zeta) + B \times \frac{1}{\rho c} \\ V(r) = A \times \frac{i\omega a}{c\Lambda} J_1(\zeta) + B \times \frac{i\omega r}{2\rho c^2} \\ P(r) = B \end{cases}$$
 (5.17)

The constants A, B are determined by matching the velocities of the fluid and the tube wall at the fluid-wall interface (r=a), which requires that the motion of the tube wall be considered. This may seem to contradict the assumption made earlier (Eq. 5.13) that the no-slip boundary conditions for U(r) and V(r) are applied at a fixed radius (r=a). However, it must be remembered that U(r) and V(r) represent only the *amplitudes* of the velocities u(x,r,t) and v(x,r,t) (see Eq. 5.9). What is required further is that the oscillatory velocities of the fluid u(x,r,t) and v(x,r,t) be matched with the oscillatory motion of the tube wall in x and t.

5.5 Elastic Wall Movement

Elastic movement of the tube wall are governed by the equations of elasticity which in their most general form are considerably more complicated than the equations of fluid flow. The reasons for this is that in fluid flow one is usually concerned with three velocity components and pressure, while in the case of elasticity one may be concerned with three displacement components and six internal stresses. To deal with the elasticity problem in its most general form is far more than is required for the present purpose. In what follows, therefore, rather than derive the equations of elasticity in their general form we simply consider the forces acting on an element of the vessel wall, then extract from the theory of elasticity only what is required for the purpose at hand.

Fig. 5.7 An element of the tube wall considered for analysis of movement of the tube wall. Dimensions of the element in the three coordinate directions are δx , δr , and $a\delta\theta$, where a is the tube radius. On the assumption that the wall thickness h is small compared with a, we take $\delta r = h$, which implies that the radial gradients within the tube wall are neglected.



Furthermore, here and in the rest of the book we follow the classical treatment of pulsatile flow in elastic tubes in which the tube wall is assumed to be "thin", specifically h << a where h is the wall thickness and a is the neutral radius of the tube. Events within the wall thickness such as any compression or shearing stresses and strains are neglected, which means that any differential movements within the wall thickness are also neglected. These assumptions form the mathematical basis of the classical theory of pulsatile flow in elastic tubes to be presented in what follows. The theory still stands today as the only comprehensive method of analysis of physiological pulsatile flow phenomenon. A comprehensive theory of pulsatile flow in elastic tubes in which the walls are "thick" to the extent that they do not satisfy the above assumptions is currently lacking.⁸

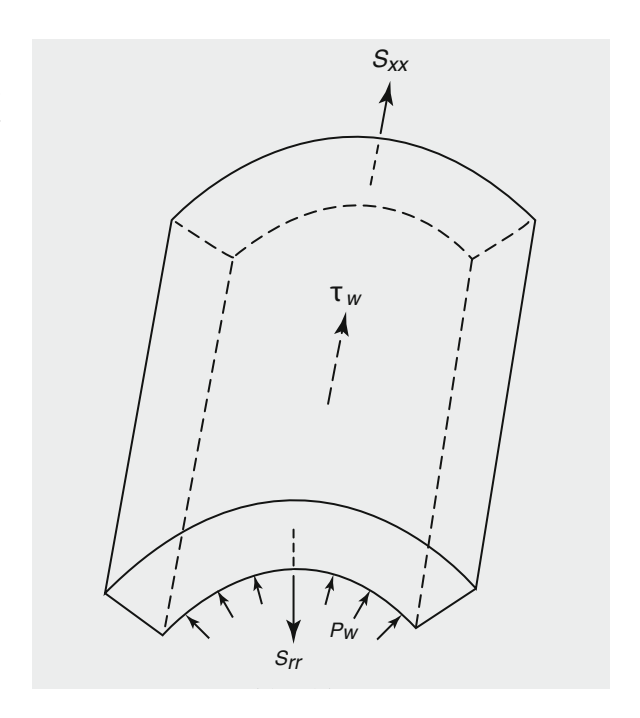
Consider an element of the tube wall defined by an arc length $a\delta\theta$ and axial length δx (Fig. 5.7).

The volume and mass of the element are then respectively given by

$$\begin{cases} \delta V \approx ha\delta\theta\delta x \\ \delta m \approx \rho_w \delta V \end{cases} \tag{5.18}$$

⁸Hodis S, Zamir M, 2011. Mechanical events within the arterial wall under the forces of pulsatile flow: A review. Journal of the Mechanical Behavior of Biomedical Materials 4:1595–1602.

Fig. 5.8 Equations governing motion of the tube wall are based on a balance of forces acting on an element of the tube wall (this figure), shown here enlarged. The forces arise from four stresses (which have the dimensions of force/area): axial tension S_{xx} within the tube wall, radial tension S_{rr} pulling elements of the tube wall towards the tube axis and arising from angular tension $S_{\theta\theta}$ in the tube wall (Fig. 5.9), shear stress τ_w exerted by the fluid on the inner surface of the tube, and pressure p_w exerted radially by the fluid on the inner surface of the tube.



where ρ_w is density of the wall material. Forces acting on this element of the tube wall result from four mechanical stresses, each having the dimensions of *force per unit area* (Fig. 5.8).

1. Axial tension within the vessel wall, to be denoted by S_{xx} . A change δS_{xx} in this tension over the length of the element leads to a force in the *x*-direction, given by

$$\delta S_{xx} \times ha\delta\theta = \frac{\partial S_{xx}}{\partial x} \delta x \times ha\delta\theta \tag{5.19}$$

2. Radial stress, to be denoted by S_{rr} , resulting from *circumferential* tension within the vessel wall, and producing a force pushing the tube wall towards the center of the tube, given by

$$-S_{rr} \times a\delta\theta\delta x$$
 (5.20)

While S_{rr} may in general vary within the thickness of the tube wall, that is it may be a function of r, thus producing another part of the radial force due to a change δS_{rr} over the thickness of the vessel wall, this part is here being neglected on the assumption that the tube wall is thin as described above.

3. Fluid pressure within the vessel wall, being the net difference between pressures acting on the inside and outside of the tube wall, to be denoted by p_w , and leading to a force in the positive r-direction given by

$$p_w \times a\delta\theta\delta x$$
 (5.21)

4. Shear stress τ_w exerted by the moving fluid on the tube wall and leading to a force in the flow direction given by

$$\tau_w \times a\delta\theta \delta x \tag{5.22}$$

The net force in each of the three coordinate directions must equal the acceleration of the element in that direction times its mass, thus providing an equation of motion in each direction. If ξ , η , ϕ represent displacements of this element of the vessel wall in the x, r, θ directions respectively, then in the axial direction we have

$$\rho_{w} \times ha\delta\theta \delta x \times \frac{d^{2}\xi}{dt^{2}} = ha\delta\theta \times \frac{\partial S_{xx}}{\partial x} \delta x + a\delta\theta \delta x \times \tau_{w}$$

which simplifies to

$$\rho_w h \frac{d^2 \xi}{dt^2} = h \frac{\partial S_{xx}}{\partial x} + \tau_w \tag{5.23}$$

Similarly, in the radial direction we have

$$\rho_{w} \times ha\delta\theta\delta x \times \frac{d^{2}\eta}{dt^{2}} = a\delta\theta\delta x \times p_{w} - a\delta\theta\delta x \times S_{rr}$$

which simplifies to

$$\rho_w h \frac{d^2 \eta}{dt^2} = p_w - S_{rr} \tag{5.24}$$

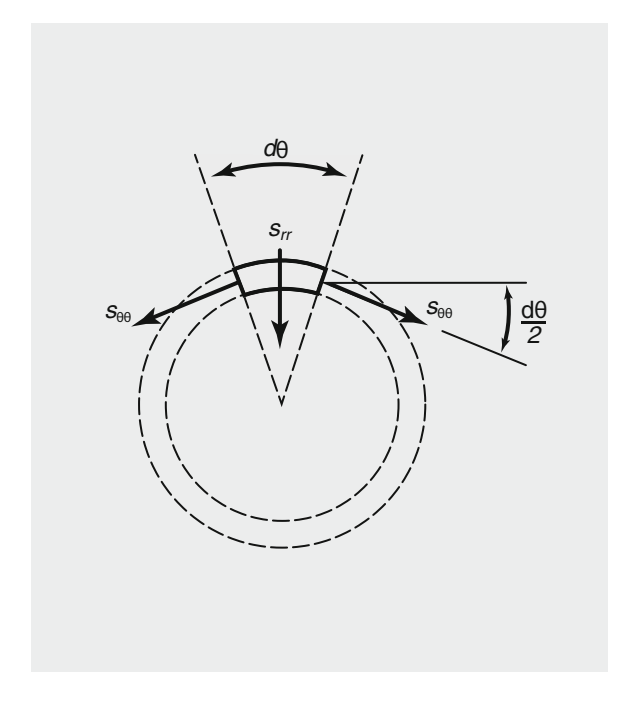
In the angular (circumferential) direction acceleration is zero because of axial symmetry and because of the absence of any external force in that direction. As stated earlier, however, because of curvature of the tube wall the internal angular stress (tension) $S_{\theta\theta}$ produces not only radial strain (change in wall thickness) but also a *movement* of the wall in the radial direction. The latter is caused by change in the tube radius which in turn is caused by change in the circumference of the tube circular cross section, that is by angular strain. In fact a useful relation between the angular and radial stresses can be obtained by equating forces in the radial direction for a small segment of the wall when in a state of equilibrium (Fig. 5.9), namely

$$a\delta\theta \times S_{rr} = 2 \times h \times S_{\theta\theta} \times \sin\left(\frac{\delta\theta}{2}\right)$$
$$\approx hS_{\theta\theta}\delta\theta \tag{5.25}$$

which gives

$$S_{rr} = -\frac{h}{a} S_{\theta\theta} \tag{5.26}$$

Fig. 5.9 Radial stress S_{rr} , which acts to pull the vessel wall towards the axis of the tube, is related to angular tension $S_{\theta\theta}$ within the vessel wall (Eq. 5.26).



5.6 Equations Governing the Wall Motion

In order to complete the equations of wall motion, the stresses $(S_{xx}, S_{rr}, S_{\theta\theta})$ in Eqs. 5.23 and 5.24 must be expressed in terms of the displacements ξ, η . This is achieved by stress-strain relations which are found to exist in an elastic body. The relations are analogous to the relations between stresses and *rates-of-strain* which exist in a fluid body, as considered in the previous chapter. In both cases the relations are empirical in origin.

If the strains in the axial, radial and angular directions are denoted by e_{xx} , e_{rr} , $e_{\theta\theta}$, the stress-strain relations for an elastic body are given by 9,10,11

$$\begin{cases} e_{xx} = \frac{1}{E} \left[S_{xx} - \sigma(S_{rr} + S_{\theta\theta}) \right] \\ e_{rr} = \frac{1}{E} \left[S_{rr} - \sigma(S_{\theta\theta} + S_{xx}) \right] \\ e_{\theta\theta} = \frac{1}{E} \left[S_{\theta\theta} - \sigma(S_{rr} + S_{xx}) \right] \end{cases}$$
(5.27)

⁹Sechler EE. Elasticity in Engineering. Dover Publications, 1968.

¹⁰Wempner G. Mechanics of Solids With Applications to Thin Bodies. McGraw-Hill, 1973.

¹¹Shames IH, Cozzarelli FA, 1992. Elastic and Inelastic Stress Analysis. Prentice Hall, 1992.

where E, σ are two constant properties of the elastic material, known as Young's modulus or modulus of elasticity, and Poisson's ratio, respectively. The relations express a fundamental characteristic of elastic materials whereby the strain in one direction depends not only on stress in that direction but also on stresses in the other two directions.

Using the relation between the radial and angular stresses (Eq. 5.26), only two of the above stress-strain relations are required, namely

$$\begin{cases} e_{xx} = \frac{1}{E} \left[S_{xx} - \sigma S_{rr} \left(1 + \frac{a}{h} \right) \right] \\ e_{\theta\theta} = \frac{1}{E} \left[S_{rr} \left(\frac{a}{h} - \sigma \right) - \sigma S_{xx} \right] \end{cases}$$
 (5.28)

Invoking the thin wall approximation, specifically that a/h is sufficiently large compared with 1.0 or σ , the above relations reduce to

$$\begin{cases} e_{xx} = \frac{1}{E} \left[S_{xx} - \frac{\sigma a}{h} S_{rr} \right] \\ e_{\theta\theta} = \frac{1}{E} \left[\frac{a}{h} S_{rr} - \sigma S_{xx} \right] \end{cases}$$
 (5.29)

and solving for the two stresses, we obtain finally

$$\begin{cases}
S_{xx} = E_{\sigma}(e_{xx} + \sigma e_{\theta\theta}) \\
S_{rr} = \frac{hE_{\sigma}}{a}(e_{\theta\theta} + \sigma e_{xx})
\end{cases}$$
(5.30)

where

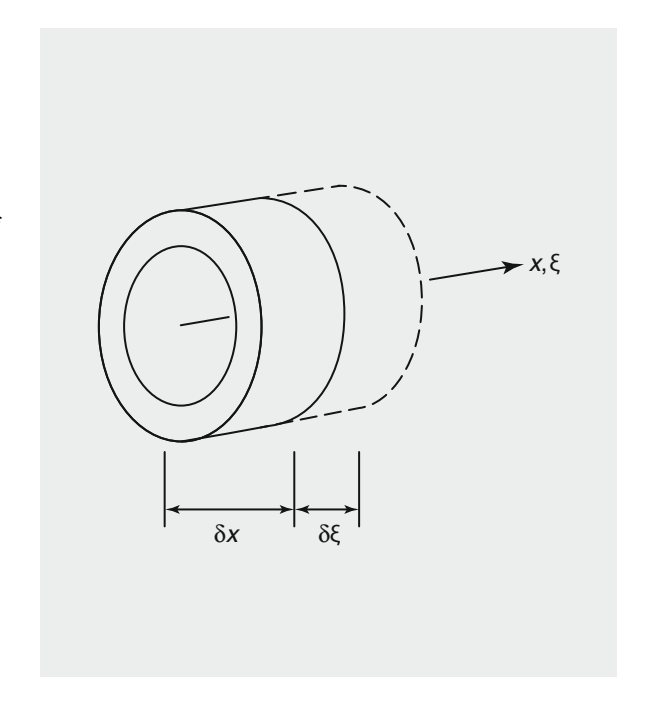
$$E_{\sigma} = \frac{E}{1 - \sigma^2} \tag{5.31}$$

Axial strain is caused by axial elongation of the tube which in turn is caused by variation of the axial displacement ξ along the tube, that is by ξ being a function of x. If all elements of the tube undergo the *same* axial displacement, that is if ξ is constant, the axial strain is zero. More generally ξ is a function of x and a small element of the wall of original length δx will have length

$$\delta x + \delta \xi = \delta x + \frac{\partial \xi}{\partial x} \delta x \tag{5.32}$$

in its strained state (Fig. 5.10).

Fig. 5.10 Axial displacement ξ is in general different at different points along the tube wall. As a result, an element of original length δx may stretch by an amount $\delta \xi$, where $\delta \xi$ is the change in ξ over the length of the element.



Axial strain is defined as the ratio of the change in length over original length, that is

$$e_{xx} = \frac{1}{\delta x} \left[\delta x - \left(\delta x + \frac{\partial \xi}{\partial x} \delta x \right) \right]$$
$$= -\frac{\partial \xi}{\partial x}$$
 (5.33)

Angular strain may arise in two ways. First in analogy with axial strain, a segment of the tube subtended by angle $\delta\theta$ and of original length $a\delta\theta$ may change its length because the angular displacement ϕ is not the same all around the tube, that is because of a gradient $\partial\phi/\partial\theta$ (Fig. 5.11).

Because of axial symmetry, however, this gradient is here assumed to be zero and hence this source of angular strain is zero. Another, more important, source of angular strain is *radial* displacement η which changes the radius of the tube from its neutral radius a to $a + \eta$ and therefore changes the arc length of the segment from $a\delta\theta$ to $(a + \eta)\delta\theta$ (Fig. 5.12).

Angular strain is defined as the ratio of change in length over original length, that is

$$e_{\theta\theta} = \frac{1}{a\delta\theta} [(a+\eta)\delta\theta - a\delta\theta]$$
$$= \frac{\eta}{a}$$
(5.34)

Fig. 5.11 Angular displacement ϕ may in general be different at different points around the tube wall, leading to angular elongation. On the assumption of axial symmetry, however, angular displacement ϕ is uniform around the tube, that is $\delta \phi = 0$, and hence this source of angular elongation is zero. A more important source of angular strain, which does not conflict with axial symmetry, is shown in Fig. 5.12.

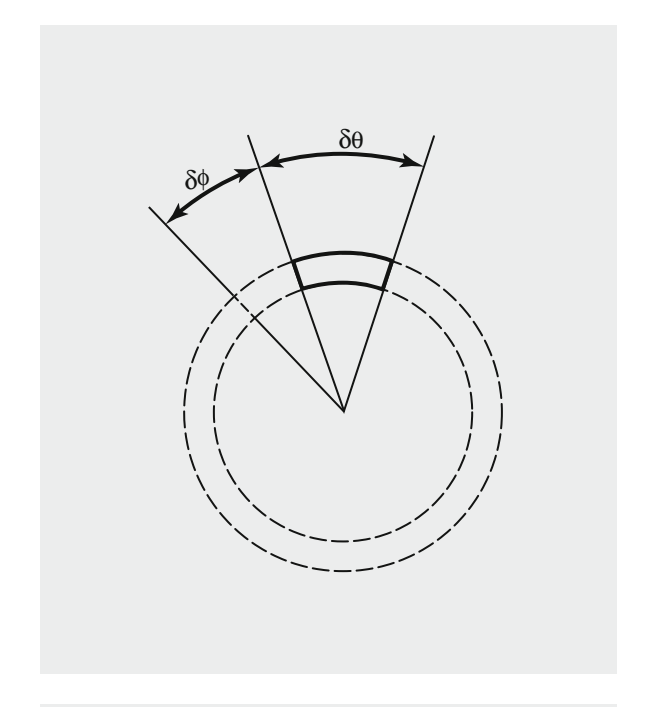
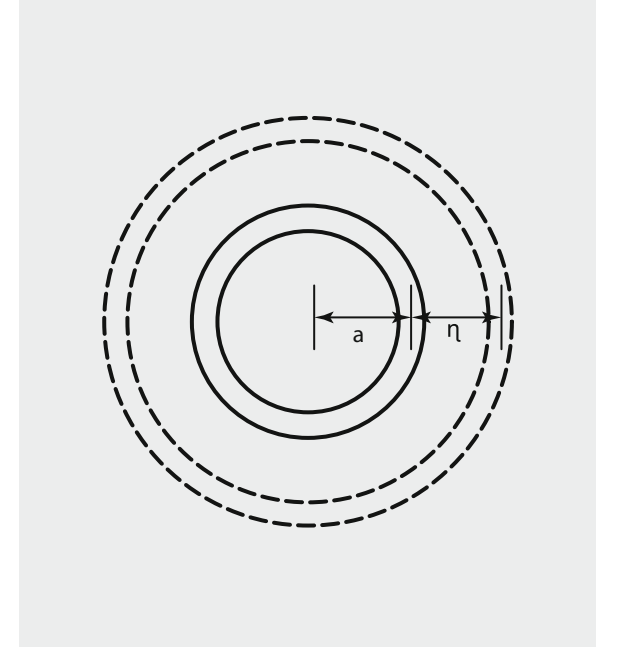


Fig. 5.12 An important source of angular strain is a change in tube radius, as shown, from a to $a + \eta$. The resulting *angular* strain, as discussed in the text, is η/a (Eq. 5.34).



Substituting these results for the strains in Eq. 5.30, the expressions for the axial and radial stresses become

$$\begin{cases} S_{xx} = E_{\sigma} \left(\frac{\partial \xi}{\partial x} + \sigma \frac{\eta}{a} \right) \\ S_{rr} = \frac{hE_{\sigma}}{a} \left(\frac{\eta}{a} + \sigma \frac{\partial \xi}{\partial x} \right) \end{cases}$$
 (5.35)

and substituting these in turn into Eqs. 5.23 and 5.24, the equations of motion of the tube wall become

$$\begin{cases}
\frac{\partial^2 \xi}{\partial t^2} = \frac{E_{\sigma}}{\rho_w} \left(\frac{\partial^2 \xi}{\partial x^2} + \frac{\sigma}{a} \frac{\partial \eta}{\partial x} \right) - \frac{\tau_w}{\rho_w h} \\
\frac{\partial^2 \eta}{\partial t^2} = \frac{p_w}{\rho_w h} - \frac{E_{\sigma}}{\rho_w a} \left(\frac{\eta}{a} + \sigma \frac{\partial \xi}{\partial x} \right)
\end{cases} (5.36)$$

These equations are coupled with those of the flow field through the pressure p_w and shear stress τ_w and this coupling is dealt with in the next section.

5.7 Coupling of Fluid and Wall Motions

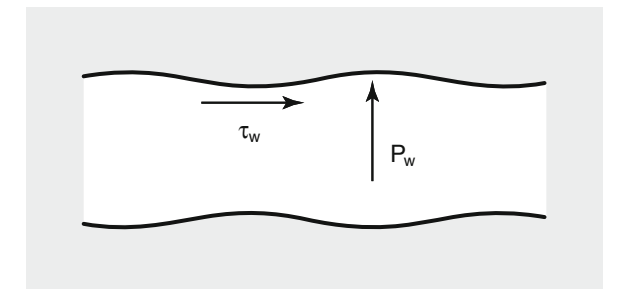
Motion of the tube wall is coupled to the motion of the fluid through the action of fluid pressure and shear stress on the tube wall as illustrated in Fig. 5.13.

Mathematically, the coupling occurs through the presence of p_w and τ_w in the equations of wall motion (Eq. 5.36). To solve the equations these flow parameters must be determined from the flow field solution.

The pressure acting on the tube wall, from Eqs. 5.9 and 5.17, is given by

$$p_w = p(x, a, t) = Be^{i\omega(t - x/c)}$$
(5.37)

Fig. 5.13 Motion of the tube wall is mediated by two stresses exerted by the moving fluid on the inner surface of the tube: pressure p_w and shear stress τ_w .



The shear stress acting on the tube wall is, from Eq. 3.46, given by

$$\tau_w = -(\tau_{xr})_{r=a} = -\mu \left(\frac{\partial u}{\partial r} + \frac{\partial v}{\partial x}\right)_{r=a}$$
 (5.38)

Applying the approximations used before, namely that the length of the traveling wave is much larger than the tube radius, the second gradient above is much smaller than the first and can be neglected, so that we take

$$\tau_w = -\mu \left(\frac{\partial u}{\partial r}\right)_{r=a} \tag{5.39}$$

Substituting for u(r) from Eq. 5.9, we have

$$\tau_w = -\mu \left(\frac{dU(r)}{dr}\right)_{r=a} e^{i\omega(t-x/c)}$$
(5.40)

and substituting for U(r) from Eq. 5.14, this gives, after some algebra

$$\tau_w = \left(-\frac{\mu A \Lambda J_1(\Lambda)}{a} + \frac{\mu B \omega^2 a}{2\rho c^3}\right) e^{i\omega(t-x/c)}$$
 (5.41)

where we have used again the approximations used in the flow field (Eq. 5.16) Substituting for p_w and τ_w from above into the equations of wall motion (Eq. 5.36), the latter finally become

$$\begin{cases}
\frac{\partial^{2} \xi}{\partial t^{2}} = \frac{E_{\sigma}}{\rho_{w}} \left(\frac{\partial^{2} \xi}{\partial x^{2}} + \frac{\sigma}{a} \frac{\partial \eta}{\partial x} \right) - \frac{1}{\rho_{w}h} \left(-\frac{\mu A \Lambda J_{1}(\Lambda)}{a} + \frac{\mu B \omega^{2} a}{2\rho c^{3}} \right) e^{i\omega(t - x/c)} \\
\frac{\partial^{2} \eta}{\partial t^{2}} = -\frac{E_{\sigma}}{\rho_{w}a} \left(\frac{\eta}{a} + \sigma \frac{\partial \xi}{\partial x} \right) + \frac{B}{\rho_{w}h} e^{i\omega(t - x/c)}
\end{cases}$$
(5.42)

5.8 Matching at the Fluid-Wall Interface

The equations of wall motion (Eq. 5.42) contain two arbitrary constants A, B yet to be determined. These constants provide the link between motion of the fluid and motion of the tube wall, and their values are determined by matching the two motions at the wall-fluid interface. The matching is expressed in terms of two boundary conditions at the interface, which require that the radial and axial velocities of the wall be equal to the radial and axial velocities of the fluid in contact with the wall. As before, since the wall is itself in motion, these boundary conditions are applied only approximately at the *neutral position* of the wall, namely r=a. Thus, we take

$$\begin{cases} \frac{\partial \xi}{\partial t} = u(x, a, t) \\ \frac{\partial \eta}{\partial t} = v(x, a, t) \end{cases}$$
 (5.43)

It is reasonable to assume that the axial and radial oscillatory movements of the wall have the same frequency as that prevailing in the flow field, thus we write

$$\begin{cases} \xi(x,t) = Ce^{i\omega(t-x/c)} \\ \eta(x,t) = De^{i\omega(t-x/c)} \end{cases}$$
 (5.44)

where C,D are two new constants to be determined. Note that this form does not imply that the wall motion is *in phase* with the oscillatory motion of the fluid, since these constants, as we shall find out, are generally complex quantities. Substituting from the above expressions for ξ , η and their derivatives into the two equations of wall motion (Eq. 5.42) and two boundary conditions (Eq. 5.44), we obtain a set of four equations for the constants A, B, C, D, namely

$$\begin{cases}
-\omega^{2}C = \frac{E_{\sigma}}{\rho_{w}} \left[-\frac{\omega^{2}}{c^{2}}C + \frac{\sigma}{a} \left(\frac{-i\omega}{c} \right) D \right] - \frac{1}{\rho_{w}h} \left[-\frac{\mu\Lambda J_{1}(\Lambda)}{a} A + \frac{\mu\omega^{2}a}{2\rho c^{3}} B \right] \\
-\omega^{2}D = \frac{B}{\rho_{w}h} - \frac{E_{\sigma}}{\rho_{w}a} \left[\frac{D}{a} + \sigma \left(\frac{-i\omega}{c} \right) C \right] \\
i\omega C = J_{0}(\Lambda)A + \frac{B}{\rho c} \\
i\omega D = \frac{i\omega aJ_{1}(\Lambda)}{c\Lambda} A + \frac{i\omega a}{2\rho c^{2}} B
\end{cases} (5.45)$$

Some simplifications are possible by noting that in the first equation

$$-\frac{1}{\rho_{w}h} \times \left(-\frac{\mu \Lambda J_{1}(\Lambda)}{a}A + \frac{\mu \omega^{2} a}{2\rho c^{3}}B\right) = \frac{\mu}{\rho_{w}hca} \left(\Lambda J_{1}(\Lambda)cA - \frac{\omega^{2} a^{2}}{2c^{2}}B\right)$$

$$\approx \frac{\mu \Lambda J_{1}(\Lambda)}{\rho_{w}ha}A \tag{5.46}$$

and in the second equation

$$-\omega^2 D + \frac{E_{\sigma}}{\rho_w a^2} D = \frac{c^2}{a^2} \left(-\frac{\omega^2 a^2}{c^2} + \frac{E_{\sigma}}{\rho_w c^2} \right) D$$

$$\approx \frac{E_{\sigma}}{\rho_w a^2} D \tag{5.47}$$

In both cases the term $\omega^2 a^2/c^2$ is neglected as it is of order $(a/L)^2$.

With these simplifications the four combined equations for A, B, C, D take the final form

$$\begin{cases}
-\omega^{2}C = \frac{E_{\sigma}}{\rho_{w}} \left[-\frac{\omega^{2}}{c^{2}}C + \frac{\sigma}{a} \left(\frac{-i\omega}{c} \right) D \right] + \left[\frac{\mu \Lambda J_{1}(\Lambda)}{\rho_{w} h a} \right] A \\
0 = \frac{B}{\rho_{w} h} - \frac{E_{\sigma}}{\rho_{w} a} \left[\frac{D}{a} + \sigma \left(\frac{-i\omega}{c} \right) C \right] \\
i\omega C = J_{0}(\Lambda) A + \frac{B}{\rho c} \\
i\omega D = \frac{i\omega a J_{1}(\Lambda)}{c\Lambda} A + \frac{i\omega a}{2\rho c^{2}} B
\end{cases} (5.48)$$

5.9 Wave Speed ("Pulse Wave Velocity")

Equations 5.48 can be put in the form of the following four linear equations in A, B, C, D

$$\begin{cases} a_{11}A + a_{13}C + a_{14}D = 0 \\ a_{22}B + a_{23}C + a_{24}D = 0 \\ a_{31}A + a_{32}B + a_{33}C = 0 \\ a_{41}A + a_{42}B + a_{44}D = 0 \end{cases}$$
(5.49)

where the coefficients a_{ij} are given by

$$\begin{cases} a_{11} = \frac{\mu \Lambda J_{1}(\Lambda)}{\rho_{w} h a}, & a_{13} = \omega^{2} \left(1 - \frac{E_{\sigma}}{\rho_{w} c^{2}}\right), & a_{14} = \frac{-i\omega\sigma E_{\sigma}}{\rho_{w} a c} \\ a_{22} = \frac{1}{h}, & a_{23} = \frac{i\omega\sigma E_{\sigma}}{a c}, & a_{24} = \frac{-E_{\sigma}}{a^{2}} \\ a_{31} = J_{0}(\Lambda), & a_{32} = \frac{1}{\rho c}, & a_{33} = -i\omega \\ a_{41} = \frac{i\omega J_{1}(\Lambda) a}{c\Lambda}, & a_{42} = \frac{i\omega a}{2\rho c^{2}}, & a_{44} = -i\omega \end{cases}$$

$$(5.50)$$

Since this system of four equations is *homogeneous*, a nontrivial solution is obtained by setting the determinant of the coefficients to zero^{12,13,14}, that is

$$\begin{vmatrix} a_{11} & 0 & a_{13} & a_{14} \\ 0 & a_{22} & a_{23} & a_{24} \\ a_{31} & a_{32} & a_{33} & 0 \\ a_{41} & a_{42} & 0 & a_{44} \end{vmatrix} = 0$$
 (5.51)

or

$$\begin{cases}
a_{11}[a_{22}(a_{33}a_{44}) - a_{23}(a_{32}a_{44}) + a_{24}(-a_{42}a_{33})] \\
+a_{13}[-a_{22}(a_{31}a_{44}) + a_{24}(a_{31}a_{42} - a_{41}a_{32})] \\
-a_{14}[-a_{22}(-a_{41}a_{33}) + a_{23}(a_{31}a_{42} - a_{41}a_{32})] = 0
\end{cases} (5.52)$$

Substituting for the coefficients, this gives, after some algebra

$$[(g-1)(\sigma^2-1)]z^2 + \left[\frac{\rho_w h}{\rho a}(g-1) + \left(2\sigma - \frac{1}{2}\right)g - 2\right]z + \frac{2\rho_w h}{\rho a} + g = 0$$
(5.53)

where

$$z = \frac{E_{\sigma}h}{\rho ac^2} \tag{5.54}$$

and

$$g = \frac{2J_1(\Lambda)}{\Lambda J_0(\Lambda)} \tag{5.55}$$

Equation 5.53 is a quadratic equation in z and its solution furnishes a value of the wave speed (or pulse wave velocity) c in terms of parameters of the fluid and tube wall. In particular, recalling that the wave speed in *inviscid* flow is given by (Eq. 5.1)

$$c_0^2 = \frac{Eh}{2\rho a}$$

¹²Bradley GL, 1975. A Primer of Linear Algebra. Prentice Hall, Englewood Cliffs, New Jersey.

¹³Noble B, Daniel JW, 1977. Applied Linear Algebra. Prentice Hall, Englewood Cliffs, New Jersey.

¹⁴Lay DC, 1994. Linear Algebra and its Applications. Addison-Wesley, Reading, Massachusetts.

then, combined with Eq. 5.54, this gives

$$\left(\frac{c_0}{c}\right) = \frac{1}{2} \frac{E}{E_{\sigma}} z \tag{5.56}$$

Substituting for E_{σ} from Eq. 5.31, we finally have

$$c = \sqrt{\frac{2}{(1 - \sigma^2)z}} c_0 \tag{5.57}$$

Thus the solution of Eq. 5.53 for z is in effect a solution for the wave speed c. The equation is indeed referred to as the wave speed equation. It is important at this point to recall the difference between this wave speed c and the Moen-Korteweg wave speed c_0 . Both wave speeds are based on pulsatile flow in an elastic tube but c_0 is based on flow which does not satisfy the no-slip boundary condition at the tube wall, hence it is sometimes referred to as the "inviscid" wave speed. On the other hand, the wave speed c as derived in this chapter, based on the classical solution of pulsatile flow in an elastic tube, take into account the no-slip boundary conditions at the tube wall. Here the equations governing the dynamics of the fluid are fully coupled with the equations governing the dynamics of the tube wall. Thus c is more accurate than c_0 in the sense that it adheres more closely to the physics of the problem.

It is important to note, however, that c is still based on the assumptions inherent in the classical solution of pulsatile flow as described in this chapter and therefore it too is only an approximation. The most important of these is the assumption that the tube wall is "thin" to the extent that events within the wall are neglected. This is clearly not the case when the tube wall is appreciably thick compared with the tube radius. A solution of the governing equations of pulsatile flow in a *thick-walled* elastic tube is considerably more complicated than the classical solution described above and is yet to be achieved (see Footnote 8).

Since z is complex, it follows that the wave speed c is also complex, meaning that it has a real and an imaginary part whereas c_0 is entirely real. What does this mean in physical terms, and what are the consequences of this?

In answer to this question it would seem at first that c is not a true "speed" because it does not simply replace the inviscid wave speed c_0 in the wave propagation expression $e^{i\omega(t-x/c_0)}$. Furthermore, while c_0 depends only on constant properties of the tube wall and of the fluid (Eq. 5.1), c depends also on c (Eq. 5.57) which in turn depends on frequency (Eq. 5.53), therefore c depends on frequency. The latter implies that the speed at which the wave propagates depends on the frequency with which it is propagating.

To examine the consequences (indeed the physical meaning) of this, it is convenient to write

$$\frac{1}{c} = \frac{1}{c_1} + i\frac{1}{c_2} \tag{5.58}$$

or equivalently

$$c = \frac{c_1 c_2^2}{c_1^2 + c_2^2} - i \frac{c_1^2 c_2}{c_1^2 + c_2^2}$$
 (5.59)

Using Eq. 5.58 we find

$$e^{i\omega(t-x/c)} = e^{i\omega(t-x/c_1-ix/c_2)}$$

$$= e^{\omega x/c_2} e^{i\omega(t-x/c_1)}$$
(5.60)

Comparing this expression for wave propagation with the corresponding expression for wave propagation in *inviscid* flow, we have

$$\{e^{\omega x/c_2}\}\ e^{i\omega(t-[x/c_1])}\tag{5.61}$$

in the present viscous flow case, compared with

$$e^{i\omega(t-[x/c_0])} \tag{5.62}$$

in the inviscid flow case. The two expressions differ in two places as indicated by the square brackets. First, it is seen that viscosity has the effect of changing *amplitude* of the wave from a reference value of 1.0 in the inviscid case to $e^{\omega x/c_2}$ in the viscous case, an effect usually referred to as "attenuation". Second, it is seen that viscosity has the effect of changing the *wave speed* from c_0 in the inviscid case to c_1 in the viscous case. Since c_1 depends on frequency, the magnitude of this effect will also depend on frequency and, hence, as stated earlier, the change in wave speed due to viscosity will also depend on frequency. This effect of viscosity on the wave speed is known as "dispersion".

The significance of this in pulsatile blood flow lies in the fact that the pressure waveform generated by the heart, as we shall see in the next chapter, is composed of sinosoidal waves (harmonics) that are propagating at different frequencies. Dispersion causes these harmonic components to propagate at different speeds, thereby altering the shape of the composite wave as it progresses along the vascular tree.

Solution of Eq. 5.53 provides a value of c for each value of the frequency, hence the equation is sometimes also referred to as the "frequency equation". Results in Fig. 5.14 show that in the limit of high frequency the imaginary part of c goes to zero while the real part of c becomes the same as c_0 . In the same limit, the value of c_1 becomes the same as that of c_0 while the value of c_2 becomes infinite as shown in Fig. 5.15. Together, these results indicate that the attenuation and dispersion effects of viscosity vanish at high frequency, rendering pulsatile flow of viscous fluid in an elastic tube the same as that of inviscid fluid in an elastic tube. In particular, the wave speed c becomes the same as the Moen-Korteweg wave speed c_0 at the limit of high frequency. However, as the two figures indicate, at lower frequencies ($\Omega < 3$ or so) the value of c is significantly different from that of c_0 and must be determined

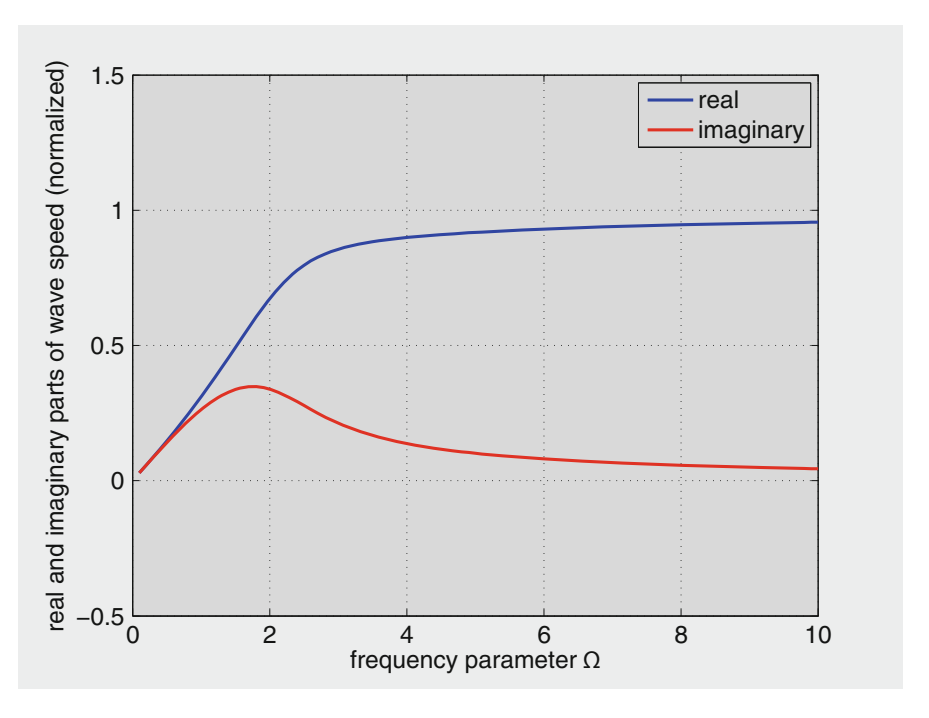


Fig. 5.14 Variation of the real and imaginary parts of the wave speed c, normalized in terms of the wave speed in invisicid flow, c_0 , with frequency parameter Ω . As the frequency increases, the imaginary part of c vanishes while the real part becomes the same as c_0 .

from the full solution of the governing equations as detailed in this chapter. This is particularly so because, as we shall see in the next chapter, the lower frequencies are associated with the more dominant harmonic components of the composite pressure wave generated by the heart.

5.10 Arbitrary Constants

To determine the arbitrary constants A, B, C, D, we note that Eq. 5.49 A, B, C, D are a set of homogeneous linear equations, with a 4×4 coefficient matrix which is of rank 3, therefore one of A, B, C, D must remain arbitrary. That is, the solution determines only 3 of A, B, C, D in terms of the fourth. Results in Eq. 5.17 suggest that the obvious choice to make is that of expressing A, C, D in terms of B, since the latter represents the amplitude of the input oscillatory pressure which would

¹⁵Noble B, Daniel JW. Applied Linear Algebra. Prentice Hall, 1977.

¹⁶Lay DC, 1994. Linear Algebra and its Applications. Addison-Wesley, 1994.

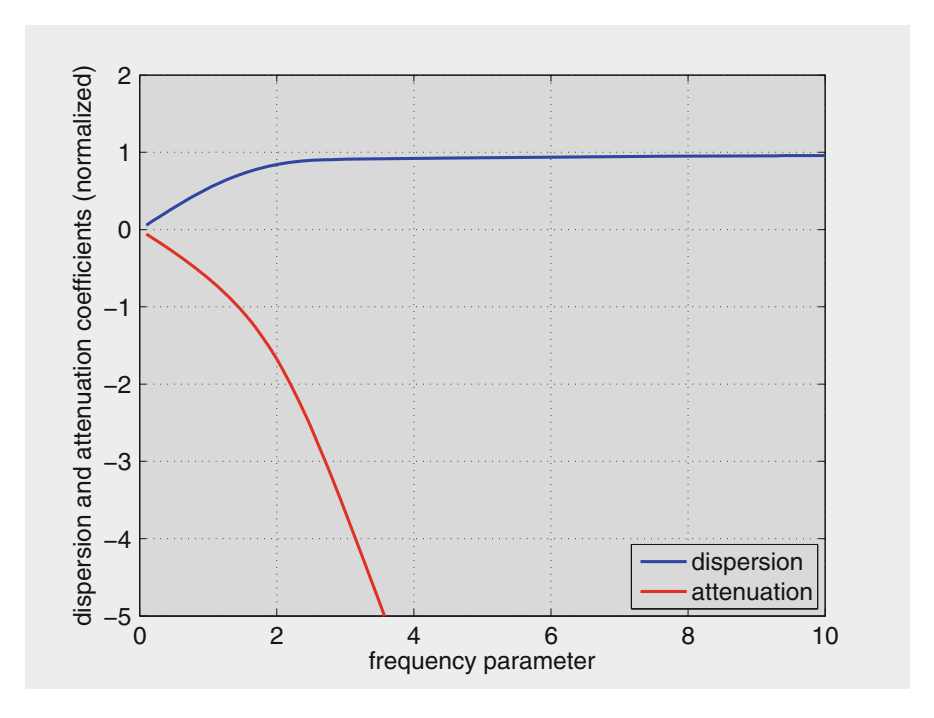


Fig. 5.15 Variation of dispersion and attenuation coefficients, c_1 and c_2 respectively in Eq. 5.61, normalized in terms of the wave speed in inviscid flow, c_0 . As the frequency increases, $c_2 \to -\infty$ and $c_1 \to 1.0$, and both attenuation and dispersion effects vanish from Eq. 5.61.

normally be known or specified. Thus from Eqs. 5.9 and 5.17 we have

$$p(x, r, t) = P(r)e^{i\omega(t - x/c)}$$

$$= Be^{i\omega(t - x/c)}$$
(5.63)

which, as stated above, shows that *B* is the amplitude of the input oscillatory pressure and may therefore be considered known.

Using the second and forth of Eq. 5.48 to eliminate D and combining the result with the third equation we then find

$$A = \frac{a_{33}a_{24}a_{42} - a_{33}a_{44}a_{22} + a_{44}a_{23}a_{32}}{-a_{33}a_{24}a_{41} - a_{44}a_{23}a_{31}}B$$
 (5.64)

Substituting this in the third of Eq. 5.48 we then have

$$C = \frac{a_{31}A + a_{32}B}{-a_{33}} \tag{5.65}$$

and from the forth equation in Eq. 5.48, finally

$$D = \frac{a_{41}A + a_{42}B}{-a_{44}} \tag{5.66}$$

Substituting for the coefficients from Eq. 5.50, we find finally, after some algebra

$$\begin{cases}
A = \frac{1}{\rho c J_0(\Lambda)} \left[\frac{2 + z(2\sigma - 1)}{z(g - 2\sigma)} \right] B \\
C = \frac{i}{\rho c \omega} \left[\frac{2 - z(1 - g)}{z(2\sigma - g)} \right] B \\
D = \frac{a}{\rho c^2} \left[\frac{g + \sigma z(g - 1)}{z(g - 2\sigma)} \right] B
\end{cases} (5.67)$$

5.11 Properties of Pulsatile Flow in an Elastic Tube

All the required elements are now in place to complete the solution of pulsatile flow in elastic tubes, using Eqs. 5.9, 5.17, and 5.67. For the axial velocity component we find

$$u(x, r, t) = \frac{B}{\rho c} \left[1 - G \frac{J_0(\zeta)}{J_0(\Lambda)} \right] e^{i\omega(t - x/c)}$$
(5.68)

where

$$G = \frac{2 + z(2\sigma - 1)}{z(2\sigma - g)}$$
 (5.69)

This is the classical solution of the problem of oscillatory flow in an elastic tube, obtained by Morgan and Kiely¹⁷ and Womersley¹⁸ and enlarged upon by

¹⁷Morgan GW, Kiely JP, 1954. Wave propagation in a viscous liquid contained in a flexible tube. Journal of Acoustical Society of America 26:323–328.

¹⁸Womersley JR, 1955. Oscillatory motion of a viscous liquid in a thin-walled elastic tube-I: The linear approximation for long waves. Philosophical Magazine 46:199–221.

others, ^{19,20,21} though the rudiments of the solution can be traced back to pioneering work by Korteweg, ²² Lamb, ²³ Witzig, ²⁴ and Lambossy. ²⁵

To compare this and other properties of the flow with corresponding properties of *steady* flow in a rigid tube, we recall from Eq. 5.63 that the constant B in the present case represents the amplitude of the input oscillatory pressure which must be specified for the problem to be complete. For comparison we take the amplitude of the oscillatory pressure gradient to be equal to the constant pressure gradient in steady flow, namely k_s as defined in Eq. 3.23, then using Eq. 5.63 we find

$$\begin{cases} p(x, r, t) = Be^{i\omega(t - x/c)} \\ \frac{\partial p}{\partial x} = -\frac{i\omega}{c} Be^{i\omega(t - x/c)} \end{cases}$$
(5.70)

thus we take

$$\begin{cases} \frac{-i\omega}{c}B = k_s \\ B = \frac{ic}{\omega}k_s \end{cases}$$
 (5.71)

It is useful also to normalize the axial velocity in oscillatory flow in terms of the maximum velocity \hat{u} in steady flow, using Eq. 3.41,

$$\hat{u}_s = -\frac{k_s a^2}{4\mu}$$

¹⁹Atabek HB, Lew HS, 1966. Wave propagation through a viscous incompressible fluid contained in an initially elastic tube. Biophysical Journal 6:481–503.

²⁰Cox RH, 1969. Comparison of linearized wave propagation models for arterial blood flow analysis. Journal of Biomechanics 2:251–265.

²¹Ling SC, Atabek HB, 1972. A nonlinear analysis of pulsatile flow in arteries. Journal of Fluid Mechanics 55:493–511.

²² Korteweg DJ, 1878. Über die Fortpflanzungsgeschwindigkeit des Schalles in elastischen Rohren. Annalen der Physik und Chemie 5:525–542.

²³Lamb H, 1897. On the velocity of sound in a tube, as affected by the elasticity of the walls. Memoirs and Proceedings, Manchester Literary and Philosophical Society A42:1–16.

²⁴Witzig K, 1914. Über erzwungene Wellenbewegungen zäher, inkompressibler Flüssigkeiten in elastischen Rohren. Inaugural Dissertation, Universität Bern.

²⁵Lambossy P, 1950. Apercu historique et critique sur le probleme de la propagation des ondes dans un liquide compressible enferme dans un tube elastique. Helvetica Physiologica et Pharmalogica Acta 8:209–227.

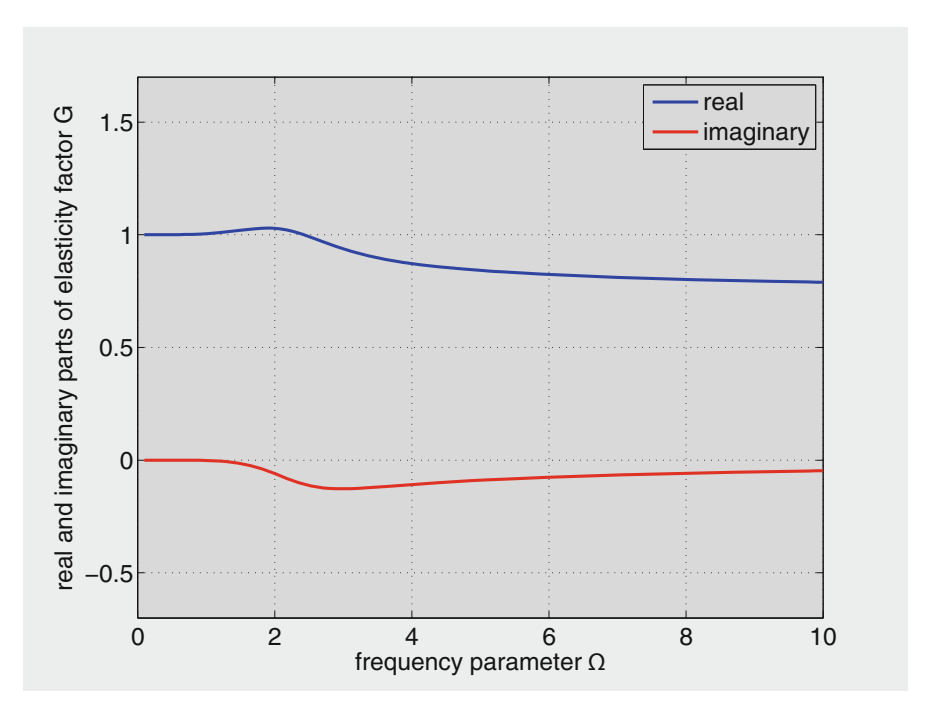


Fig. 5.16 Real and imaginary parts of the elasticity factor G which embodies the difference between oscillatory flow in rigid and elastic tubes (see text).

thus we finally have

$$\frac{u(x, r, t)}{\hat{u}_s} = \frac{-4}{\Lambda^2} \left[1 - G \frac{J_0(\zeta)}{J_0(\Lambda)} \right] e^{i\omega(t - x/c)}$$
 (5.72)

In comparison with the corresponding expression for pulsatile flow in a *rigid* tube (Eq. 4.27), the above result indicates that the difference between the two is contained entirely in the function G as defined in Eq. 5.69. However, since G is complex and both its real and imaginary parts depend on the frequency ω , the effect is not easily apparent. Variation of the real and imaginary parts of G with frequency are shown in Fig. 5.16.

In a similar way for the radial velocity component, using Eqs. 5.17 and 5.67, we find

$$\frac{v(x,r,t)}{\hat{u}_s} = \frac{2a\omega}{i\Lambda^2 c} \left[\frac{r}{a} - G \frac{2J_1(\zeta)}{\Lambda J_0(\Lambda)} \right] e^{i\omega(t-x/c)}$$
 (5.73)

The radial velocity of the fluid at the tube wall is of particular interest because it is equal to the motion of the tube wall in the radial direction. Thus, setting r=a in Eq. 5.73 and, from Eq. 4.18, noting that $\zeta(a)=\Lambda$, we find

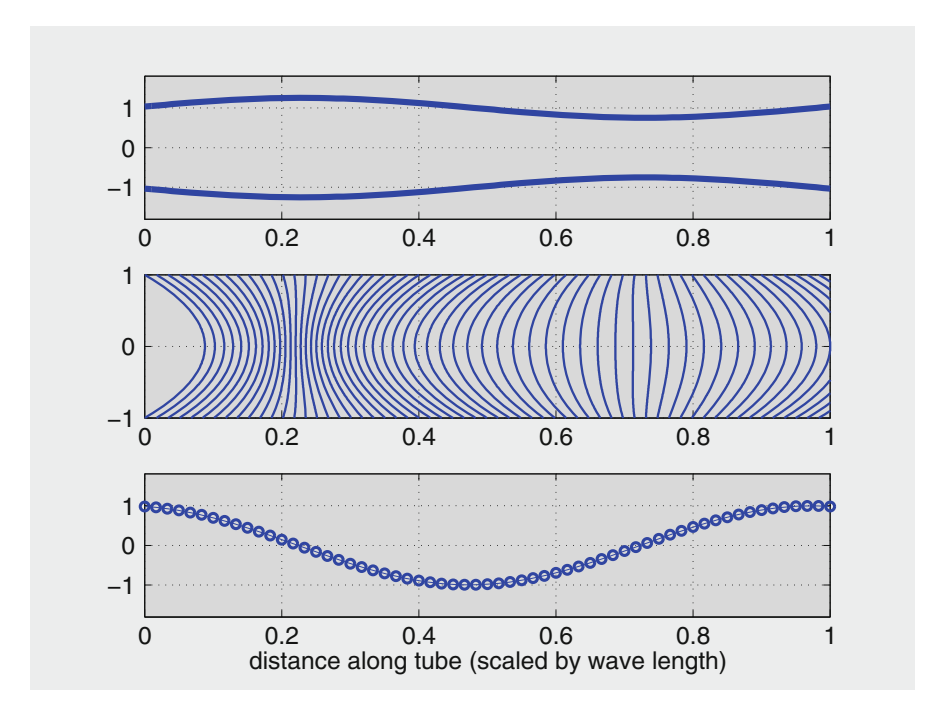


Fig. 5.17 Oscillatory flow in an elastic tube where the tube length l is the same as the wave length L, that is l/L = 1.0. In this case the entire cycle of the wave unfolds within the length of the tube. The *top panel* shows the tube wall movements. Velocity profiles within the tube are shown in the *middle panel*, and the peak velocity reached at each point along the tube is shown in the *bottom panel*. The latter being normalized in terms of the peak velocity in steady Poiseuille flow.

$$\frac{v(x,a,t)}{\hat{u}_s} = \frac{2a\omega}{i\Lambda^2 c} [1 - Gg] e^{i\omega(t-x/c)}$$
(5.74)

It is important to note that oscillatory flow in an elastic tube consists of *two* oscillations, one in time and one in space. This, indeed, is the essence of wave propagation. Both oscillations have the same frequency ω and hence the same period $T=2\pi/\omega$. During this time period, the input oscillatory pressure gradient completes one cycle, in time, while the pressure gradient within the tube completes one cycle, *in space*. The length of tube which this cycle occupies is the wave length $E=cT=2\pi c/\omega$. Thus, if the tube length is denoted by I then when I/L=1 the entire oscillatory cycle unfolds within the length of the tube, as illustrated in Fig. 5.17. However, if I/L<1, only part of the wave will unfold, as illustrated in seen in Figs. 5.18 and 5.19.

In Fig. 5.19, where l/L = 0.1, the velocity profiles are seen to be moving almost in unison as in the case of a rigid tube (Fig. 4.4). The comparison indicates that pulsatile flow in an elastic tube that is much shorter than the oscillatory wave length will be fairly close to the corresponding flow in a rigid tube. In the human

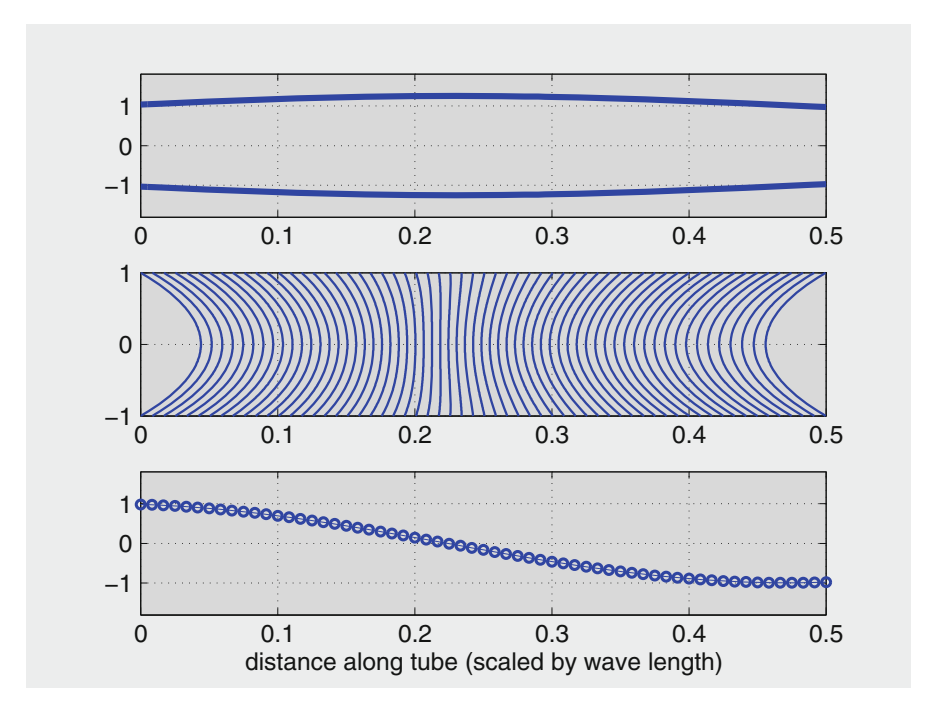


Fig. 5.18 Oscillatory flow in an elastic tube as in Fig. 5.17 but l/L = 0.5, that is, the tube length here is only one half the wave length, therefore only one half of the wave unfolds within the tube length.

cardiovascular system the wave speed is in the range of 26 5–10 m/s which means that at a frequency of 1 Hz the wave length would be between 5 and 10 m.

One might be led to believe, therefore, that the further complexity of the analysis of pulsatile flow in an elastic tube is unnecessary since the overwhelming majority of vessel segments within the cardiovascular system are shorter, indeed much shorter, than 5–10 m. The problem with this conclusion, however, is that the wave speed measured within the cardiovascular system is usually taken "across" almost the entire length of the body and hence across many millions of vessel segments of different sizes, which makes the interpretation of the measured wave speed rather uncertain.

Furthermore, the most important difference between pulsatile flow in a rigid tube and that in an elastic tube is that the latter consists of wave motion while the former does not. This difference is fundamental in physics because wave

²⁶Diaz A, Galli C, Tringler M, Ramìrez A, Fischer EIC. Reference values of pulse wave velocity in healthy people from an urban and rural Argentinean population. International Journal of Hypertension, Volume 2014, Article ID 653239, 7 pages.

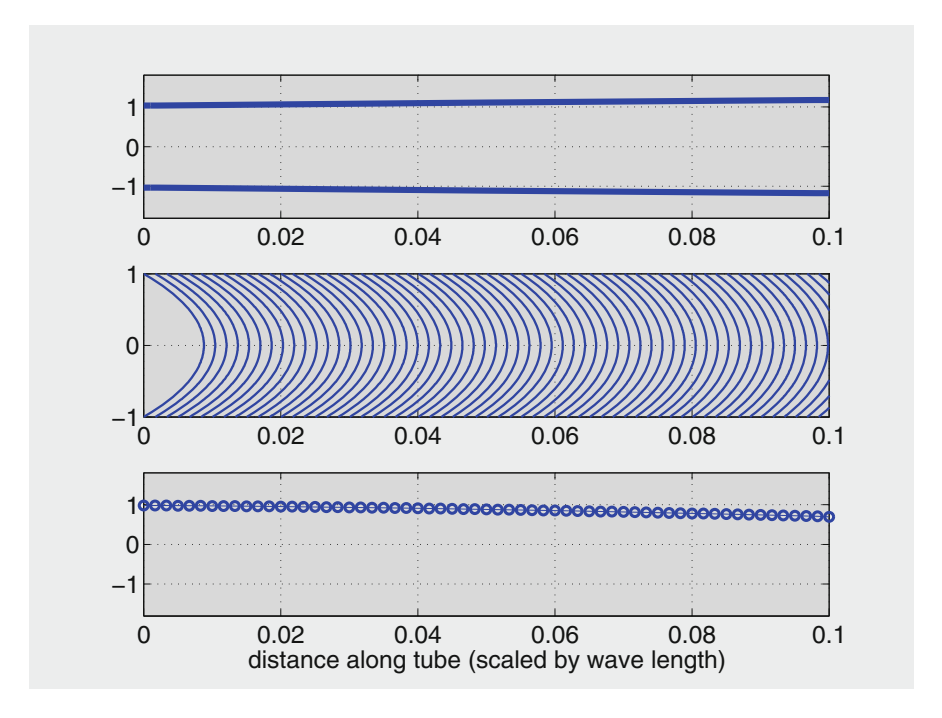


Fig. 5.19 Oscillatory flow in an elastic tube as in Fig. 5.17 but l/L = 0.1, that is, the tube length here is only one tenth of the wave length, therefore only one tenth of the wave unfolds within the tube length.

motion involves wave reflections, as we shall see in the next chapter, and wave reflections alter the relationship between pressure and flow and therefore cannot be ignored. Wave reflections are ubiquitous within the cardiovascular system because they arise at every vascular junction. In a rigid tube wave reflections do not arise because there is no wave motion (again, as long as the fluid density is constant).

The flow rate at each point within the oscillatory cycle, namely

$$q(x,t) = \int_0^a 2\pi r u dr \tag{5.75}$$

depends on the radius 'a' of the tube which here is not constant of course because the tube is not rigid. However, on the assumption that the radial movements of the tube wall are small compared with the tube radius, an approximate value of the flow rate can be obtained by treating a as a constant "neutral" radius. Nondimensionalizing in terms of the flow rate in steady flow, q_s in Eq. 3.43, this gives

$$\frac{q(x,t)}{q_s} = \frac{-8}{\Lambda^2} (1 - Gg)e^{i\omega(t - x/c)}$$
 (5.76)

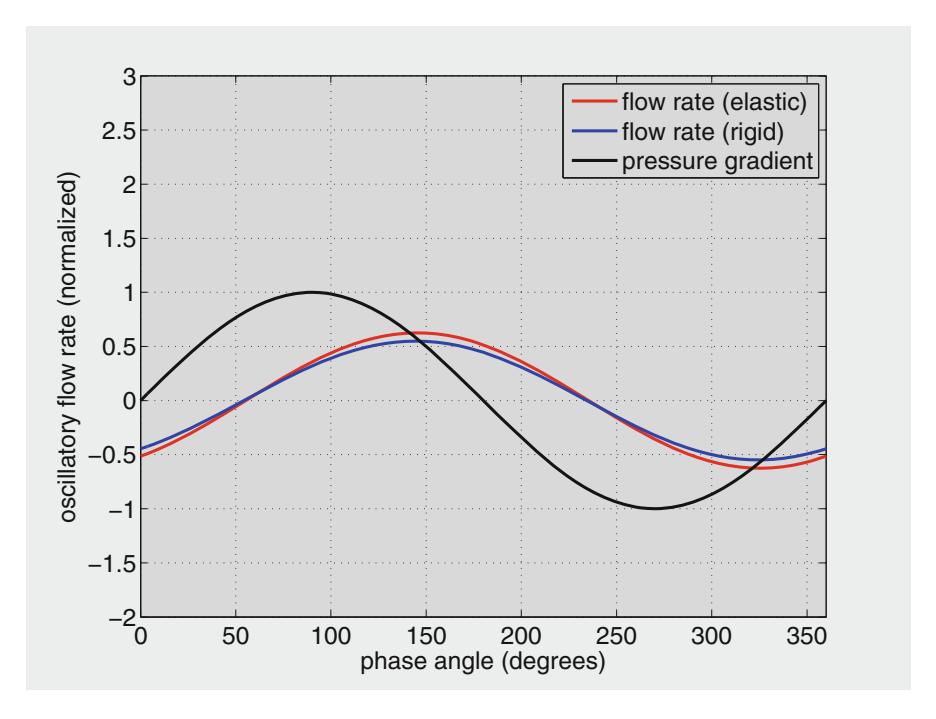


Fig. 5.20 Oscillatory flow rate within the oscillatory cycle in an elastic tube compared with that in a rigid tube at moderate frequency, $\Omega = 3.0$. A small difference exists between the two cases at this frequency, with the flow rate in an elastic tube reaching a somewhat higher peak than that in a rigid tube.

Results for oscillatory flow rate at moderate frequency ($\Omega=3.0$) are shown in Fig. 5.20, compared with the corresponding flow rate in a rigid tube. It is seen that a small difference exists between the two cases at this frequency, with the flow rate in an elastic tube reaching a somewhat higher peak than that in a rigid tube. The percentage difference between the two peaks at different frequencies is shown in Fig. 5.21.

We note, finally, that the classical solution described in this section provides what we might refer to as "field properties" in the sense that these properties describe the velocity field point-by-point. Other, more "integral" or "lumped" properties, such as the flow rate or pumping power are not as easy to determine mathematically, *or indeed interpret physically*, as they are in the case of pulsatile flow in a rigid tube. The reason for this is that in the case of a rigid tube the flow is in only one direction while in an elastic tube it is in two directions. Thus the flow "rate" at any point in time within the oscillatory cycle consists of some forward flow and some radial flow that goes towards inflating the tube. Their proportion of course varies within

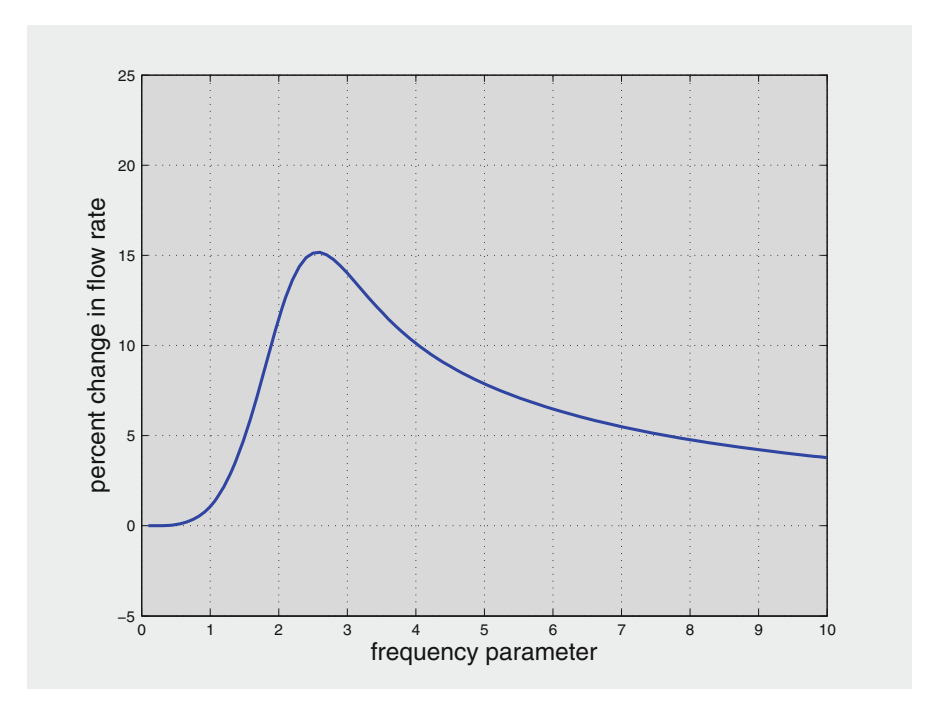


Fig. 5.21 Percentage difference between the peak of flow rate reached within the oscillatory cycle in an elastic tube and that reached in a rigid tube at different frequencies. Peak flow rate is higher in the elastic tube at all frequencies.

the oscillatory cycle as well as at different axial positions along the tube. Similarly, the pumping power required to drive the flow here consists of a certain proportion of power for driving the flow forward and another for driving the radial flow that goes toward inflating the tube.

Thus, the point-by-point description of the flow would be particularly useful in applications where the focus is on a *local* phenomenon, a local disturbance of the flow by vascular pathology such as an obstructive plaque, an aneurysm, or a thrombus. In other applications where the focus is on the *global* properties of an entire vascular bed containing many millions of blood vessels, as in the case of vascular stiffening with aging or in heart failure where the work load of the heart against the entire vascular system is critical, other methods would be required as will be described in subsequent chapters.

Chapter 6 Wave Reflections

6.1 Introduction

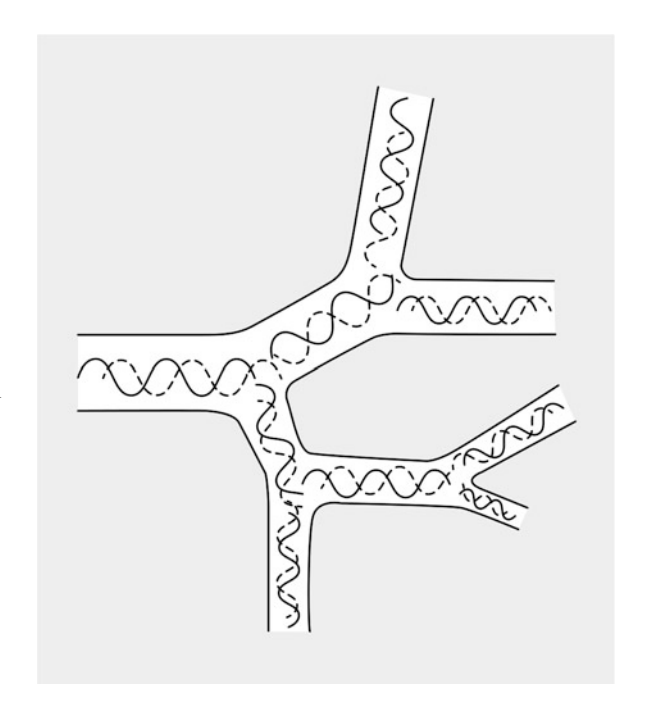
As hinted at the end of the previous chapter, wave reflections are ubiquitous in the cardiovascular system because, as we shall see, they arise at every junction within the vascular system as illustrated schematically in Fig. 6.1. The analysis of wave reflections must be based on the equations of pulsatile flow in an *elastic* tube, of course, because wave reflections do not arise in a rigid tube (so long as the fluid density is constant). The task may seem intractable at first because the vascular system is as much a network of vascular junctions as it is a network of "vessels". In the present chapter we examine how this task can be simplified somewhat, to the point of retaining and highlighting the main features of the phenomenon of wave reflections.

In a rigid tube there is no *wave motion* and therefore the possibility of wave reflections does not exist. A more interesting way of looking at this is to note that the wave speed c_0 as defined by the Moen-Korteweg formula (Eq. 5.1) becomes infinite in a rigid tube because the elastic modulus of the tube wall material E is infinite. There is then wave propagation at infinite speed in a rigid tube, which is equivalent to changes in flow or pressure being transmitted *instantaneously* to every part of the tube. Thus "propagation" in this limit degenerates into "bulk motion" whereby the entire body of fluid is moving in unison as we saw in the previous chapter (Fig. 4.4). In the face of an obstacle such as a vascular branch point, this bulk motion is disturbed in some transient way rather than reflected in the same way that a wave is reflected.

In an elastic tube wave reflections have the effect of modifying the pressure and flow within the tube because the reflected waves combine with the forward waves as illustrated in Fig. 6.2 to produce a new pressure-flow relationship.

160 6 Wave Reflections

Fig. 6.1 Wave reflections are ubiquitous in the cardiovascular system because of the branching structure of the vascular tree where each junction acts as a reflection site. The result is a bewildering array of forward and backward moving waves. Analysis of the pressure distribution along the tree is possible only if the tube segments comprising the tree are treated as one dimensional "transmission lines".



If there are many reflected waves from many different reflection sites this relationship may not be easy to predict or compute. Thus the results of the previous chapter do not depict the most important difference between pulsatile flow in rigid and elastic tubes because the analysis there does not include the effects of wave reflections.

In order to take the effects of wave reflections into account the method of analysis must be simplified. To do so we note that the most important effects of wave reflections in a tube are manifest in terms of changes in pressure and flow *in the axial direction*, thus full details of the flow in a cross section of the tube, as was obtained in the previous chapter, are not required. Instead, flow properties can be *integrated* over cross sections of the tube to become functions of only one space variable x instead of x and x. A method of analysis which follows this avenue successfully is based on the so called Transmission Line Theory. In what follows we show how the equations governing pulsatile flow in an elastic tube can be reduced to one dimensional wave equations, and then use this model for the analysis of wave reflections.

¹Wylie EB, Streeter V. Fluid Transient. McGraw-Hill, 1978.

²Fung YC. Biodynamics: Circulation. Springer-Verlag, 1984.

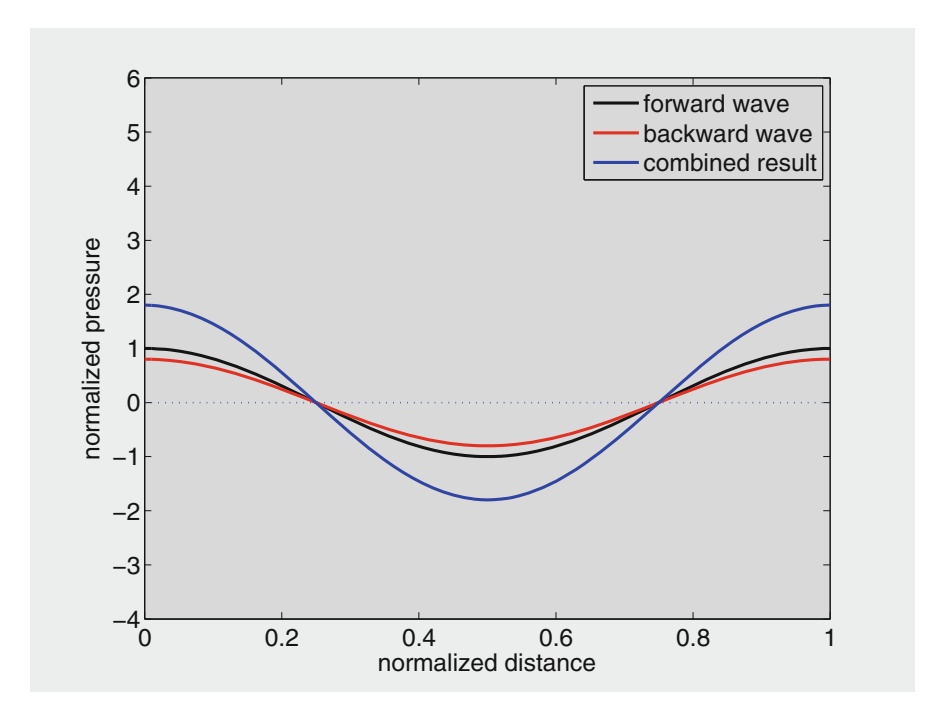


Fig. 6.2 Effect of wave reflection in a tube. Pressure distribution is shown in terms of normalized distance \bar{x} along the tube, where $\bar{x}=0$ at entrance and $\bar{x}=1.0$ at exit. A forward pressure wave is reflected at exit, producing a backward moving wave. The resulting pressure distribution in the tube is the *sum* of the two waves, which is thus greatly affected by the nature and extent of the reflected wave. Here a forward cosine wave is shown reflected at 80 %.

6.2 One Dimensional Wave Equations

One dimensional analysis of pulsatile flow in elastic tubes begins with the *same* equations as those used in the previous chapter where a full (two dimensional) description of the flow was obtained, namely Eq. 5.8. The equations are reproduced below to emphasize the fact that the one dimensional analysis to follow does not introduce any new approximations than those on which the two dimensional analysis was based.

$$\rho \frac{\partial u}{\partial t} + \frac{\partial p}{\partial x} = \mu \left(\frac{\partial^2 u}{\partial r^2} + \frac{1}{r} \frac{\partial u}{\partial r} \right)$$
 (6.1)

$$\rho \frac{\partial v}{\partial t} + \frac{\partial p}{\partial r} = \mu \left(\frac{\partial^2 v}{\partial r^2} + \frac{1}{r} \frac{\partial v}{\partial r} - \frac{v}{r^2} \right) \tag{6.2}$$

$$\frac{\partial u}{\partial x} + \frac{\partial v}{\partial r} + \frac{v}{r} = 0 \tag{6.3}$$

As they stand these equations are two dimensional in space in the sense that the dependent variables are functions of two space variables, namely x and r. In the present analysis the equations are transformed into one dimensional equations by eliminating the dependence on r. This is accomplished by integrating over a cross section of the tube so that the main dependent variable is changed from velocity to $flow\ rate$, and the equation in the radial direction (Eq. 6.2) is then no longer required. It is important to note that this latter step is not the same as taking the radial velocity v to be identically zero as it is in the rigid tube case. In the present analysis v is not zero even though the equation in the radial direction has been eliminated.

Each term in the first and third equations is multiplied by $2\pi r$ and integrated from r = 0 to r = a where a is the tube radius, that is

$$2\pi\rho \int_0^a r \frac{\partial u}{\partial t} dr + 2\pi \int_0^a r \frac{\partial p}{\partial x} dr = 2\pi\mu \int_0^a r \left(\frac{\partial^2 u}{\partial r^2} + \frac{1}{r} \frac{\partial u}{\partial r}\right) dr \tag{6.4}$$

and

$$2\pi \int_0^a r \frac{\partial u}{\partial x} dr + 2\pi \int_0^a r \left(\frac{\partial v}{\partial r} + \frac{v}{r} \right) dr = 0$$
 (6.5)

To these governing equations is added the boundary condition

$$v(a,t) = \frac{\partial a}{\partial t} \tag{6.6}$$

which ensures that the radial velocity of the fluid at the tube wall is equal to the rate of change of the tube radius. This boundary condition is central to the present analysis since it ensures that although the radial direction is being eliminated, the combined effect of radial velocity and elasticity of the tube wall, and hence the essential elements of wave propagation, are preserved. Furthermore, using this boundary condition, the last integral in Eq. 6.5 becomes

$$2\pi \int_0^a r \left(\frac{\partial v}{\partial r} + \frac{v}{r}\right) dr = 2\pi \int_{r=0}^{r=a} d(vr)$$

$$= 2\pi a v(a)$$

$$= \frac{dA}{dt}$$
(6.7)

where

$$A(t) = \pi a^2(t) \tag{6.8}$$

is cross sectional area of the tube. Using this condition, and noting that

$$2\pi \int_0^a r \frac{\partial u}{\partial t} dr = \frac{\partial q}{\partial t} \tag{6.9}$$

$$2\pi \int_0^a r \frac{\partial u}{\partial x} dr = \frac{\partial q}{\partial x} \tag{6.10}$$

$$2\pi \frac{\mu}{\rho} \int_0^a r \left(\frac{\partial^2 u}{\partial r^2} + \frac{1}{r} \frac{\partial u}{\partial r} \right) dr = \frac{2\pi a}{\rho} \tau_w \tag{6.11}$$

$$2\pi \int_0^a r \left(\frac{\partial v}{\partial r} + \frac{v}{r}\right) dr = 2\pi a v(a) \tag{6.12}$$

where q is flow rate through the tube and τ_w is shear stress on the tube wall, given by

$$q = 2\pi \int_0^a rudr \tag{6.13}$$

$$\tau_w = \mu \left(\frac{\partial u}{\partial r}\right)_{r=a} \tag{6.14}$$

Thus Eqs. 6.4 and 6.5 finally become

$$\begin{cases} \frac{\partial q}{\partial t} + \frac{A}{\rho} \frac{\partial p}{\partial x} = \frac{2\pi a}{\rho} \tau_w \\ \frac{\partial q}{\partial x} + \frac{\partial A}{\partial t} = 0 \end{cases}$$
(6.15)

This is the *integral form* of the governing equations (Eqs. 6.1–6.3) on which pulsatile flow in elastic tubes is based. We note again that no further approximations have been introduced in the process, even though the radial direction and radial velocity have been eliminated and axial velocity has been replaced by flow rate. This is the very essence of "one dimensional wave propagation" or "transmission line theory".

The basic form of transmission line theory is usually based on *inviscid* flow where $\tau_w = 0$ and on an *inviscid* wave speed to be denoted by c_{tl} and defined by

$$c_{tl}^2 = \frac{A}{\rho} \frac{\partial p}{\partial A} \tag{6.16}$$

Comparing this with the Moen-Korteweg wave speed (Eq. 5.1) it will be noted that the two wave speeds are essentially the same in the sense that they are both based on inviscid flow. The difference between them is only in the way the elasticity of the tube wall is being represented, as a relationship between pressure and cross sectional area in the case of c_{tl} and as a modulus of elasticity in the case of c_{0} . For this reason,

and in order not to maintain unnecessarily complicated notation, we shall henceforth treat the two wave speeds as being the same, that is

$$c_{tl} \equiv c_0 \tag{6.17}$$

Noting that

$$\frac{\partial A}{\partial t} = \frac{\partial A}{\partial p} \frac{\partial p}{\partial t} = \frac{A}{\rho c_0^2} \frac{\partial p}{\partial t}$$
 (6.18)

Equation 6.15 under inviscid flow conditions reduce to

$$\begin{cases} \frac{\partial q}{\partial t} + \frac{A}{\rho} \frac{\partial p}{\partial x} = 0\\ \frac{\partial q}{\partial x} + \frac{A}{\rho c_0^2} \frac{\partial p}{\partial t} = 0 \end{cases}$$
(6.19)

In many wave propagation studies this basic inviscid form of the wave equations has the advantage of isolating the effects of wave reflections from the effects of viscosity. The main effects of viscosity on wave propagation, as we saw in the previous chapter, is to reduce the speed and amplitude of the traveling wave. These effects are fairly predictable and can in fact be easily reinstated in the one dimensional equations, ^{3,4,5,6} but it is convenient to leave them out while the focus is on wave reflections. With this in mind, cross differentiation of Eq. 6.19 finally leads to

$$\begin{cases} \frac{\partial^2 p}{\partial t^2} = c_0^2 \frac{\partial^2 p}{\partial x^2} \\ \frac{\partial^2 q}{\partial t^2} = c_0^2 \frac{\partial^2 q}{\partial x^2} \end{cases}$$
(6.20)

the coefficients A/ρ and $A/\rho c_0^2$ being treated as constants in the differentiation. Each of these two equations is a standard *one dimensional wave equation*. Pressure and flow are thus governed by the same wave equation and propagate with the same wave speed. This does not mean that they are *in phase*, however, as we see in what follows.

³Wylie EB, Streeter V. Fluid Transient. McGraw-Hill, 1978.

⁴Hardung V. Propagation of pulse waves in viscoelastic tubings. Handbook of Physiology: Circulation. 1:107–135. Williams and Wilkins, 1962.

⁵Lighthill MJ. Mathematical Biofluiddynamics. Society for Industrial and Applied Mathematics, Philadelphia, 1975.

⁶Duan B, Zamir M, 1992. Viscous damping in one-dimensional wave transmission. Journal of Acoustical Society of America 92:3358–3363.

6.3 Solution of Wave Equation

Since the wave equations for pressure and flow are the same, we consider here only the equation for the pressure. Solution of the wave equation for the pressure Eq. 6.20 is obtained by separation of variables, that is by writing

$$p(x,t) = p_x(x)p_t(t) \tag{6.21}$$

The form of the driving pressure applied at entrance to the tube, to be denoted by $p_a(t)$, must be specified to proceed with the solution. We consider a complex exponential form as in the previous chapter, that is we take

$$p_a(t) = p_0 e^{i\omega t} \tag{6.22}$$

where p_0 is amplitude of the applied oscillatory pressure at the tube entrance. This clearly implies that

$$p_x(0) = p_0$$
, and $p_t(t) = e^{i\omega t}$ (6.23)

The second result indicates that the time-dependent part of pressure within the tube must have the same functional form as that applied at the tube entrance. Thus the expression for the pressure is now

$$p(x,t) = p_x(x)e^{i\omega t} (6.24)$$

and it remains to determine only the *x*-dependant part of the pressure. Substituting the above expression for the pressure into the wave equation (Eq. 6.20) leads to an ordinary differential equation for $p_x(x)$, namely

$$\frac{d^2p_x}{dx^2} + \frac{\omega^2}{c_0^2} p_x = 0 ag{6.25}$$

This is a standard second order linear differential equation with the general solution⁷

$$p_x(x) = Be^{-i\omega x/c_0} + Ce^{i\omega x/c_0}$$
 (6.26)

where B, C are arbitrary constants. With this, the complete expression for the pressure (Eq. 6.24) becomes

$$p(x,t) = p_x(x)e^{i\omega t}$$

$$= Be^{i\omega(t-x/c_0)} + Ce^{i\omega(t+x/c_0)}$$
(6.27)

⁷Spiegel MR. Applied Differential Equations. Prentice Hall, Englewood Cliffs, New Jersey, 1967.

The first part of this solution represents a wave traveling in the positive x-direction at a speed c_0 . This interpretation is gained by observing that the pressure is constant when

$$x = c_0 t \tag{6.28}$$

which represents a point moving in the positive x-direction at a speed c_0 . The second part of the solution represents a wave traveling with speed c_0 in the *negative* x-direction. It is not to be confused with waves returning after being reflected, which we shall deal with fully later. Here the reverse wave arises *at the same time* as the forward wave and the two move symmetrically in opposite directions. Reflected waves, by contrast, consist initially of forward waves arising from the first part of the solution, traveling forward to a point where they meet an obstacle and where they give rise to reflected waves traveling back.

Pulsatile flow in a tube is typically driven by a pulsating pressure source at the tube entrance. In the context of this analytical solution, this pressure source gives rise to two waves starting *simultaneously* from the entrance and travelling in opposite directions. Therefore only the forward wave is physically relevant and we take, from Eq. 6.27

$$p(x,t) = Be^{i\omega(t-x/c_0)}$$
(6.29)

The condition at the tube entrance requires that

$$p(0,t) = Be^{i\omega t}$$

$$= p_0 e^{i\omega t}$$
(6.30)

therefore

$$B = p_0 \tag{6.31}$$

and the required solution is finally

$$p(x,t) = p_0 e^{i\omega(t-x/c_0)}$$
(6.32)

It is convenient to normalize pressures in terms of the amplitude of the applied pressure at the tube entrance and introduce the notation

$$\begin{cases}
\overline{p}(x,t) = \frac{p(x,t)}{p_0} \\
\overline{p}_x(x) = \frac{p_x(x)}{p_0} \\
\overline{p}_a(t) = \frac{p_a(t)}{p_0}
\end{cases}$$
(6.33)

The solution (Eq. 6.32) can then be put in the normalized form

$$\bar{p}(x,t) = e^{i\omega(t-x/c_0)} \tag{6.34}$$

$$= \overline{p}_{r}(x)e^{i\omega t} \tag{6.35}$$

thus

$$\overline{p}_{x}(x) = e^{-i\omega x/c_{o}} \tag{6.36}$$

We shall find that this form of the solution of the one dimensional wave equation is more useful. In this form it is seen that the pressure wave within the tube is composed of two periodic functions, one in space and one in time. At any fixed point in time, the pressure distribution within the tube is described by $\bar{p}_x(x)$, and at any fixed position within the tube, the pressure oscillation is described by $e^{i\omega t}$, which is the same oscillatory function in time as the applied pressure at the tube entrance. However, the phase and amplitude of that oscillation depend on $\bar{p}_x(x)$ and therefore this entity plays a central role in the physical characteristics of the propagating wave.

In particular, since the solution $\overline{p}(x,t)$ was obtained in complex form for a complex applied pressure $\overline{p}_a(t)$ at the tube entrance, the real and imaginary parts of $\overline{p}(x,t)$ correspond to the real and imaginary parts of \overline{p}_a . Now the real and imaginary parts and the amplitude of $\overline{p}(x,t)$ are given by

$$\begin{cases}
\Re{\{\overline{p}(x,t)\}} = \Re{\{\overline{p}_x(x)e^{i\omega t}\}} \\
\Im{\{\overline{p}(x,t)\}} = \Im{\{\overline{p}_x(x)e^{i\omega t}\}} \\
|\overline{p}(x,t)| = |\overline{p}_x(x)e^{i\omega t}| = |\overline{p}_x(x)|
\end{cases} (6.37)$$

while the real and imaginary parts and the amplitude of $\bar{p}_a(t)$, from Eq. 6.22, are given by

$$\begin{cases} \Re\{\overline{p}_a\} = \cos \omega t \\ \Im\{\overline{p}_a\} = \sin \omega t \\ |\overline{p}_a| = 1.0 \end{cases}$$
 (6.38)

Equation 6.37 shows the important role which $\bar{p}_x(x)$ plays in determining the characteristics of the propagating pressure wave. The complex form of $\bar{p}_x(x)$ determines the final form of the real and imaginary parts of the pressure within the tube as seen from the first two equations, while the amplitude of $\bar{p}_x(x)$ determines the amplitude of the time oscillations at fixed positions along the tube as is seen from the third equation. Thus the *distribution* of $|\bar{p}_x(x)|$ along the tube is an important

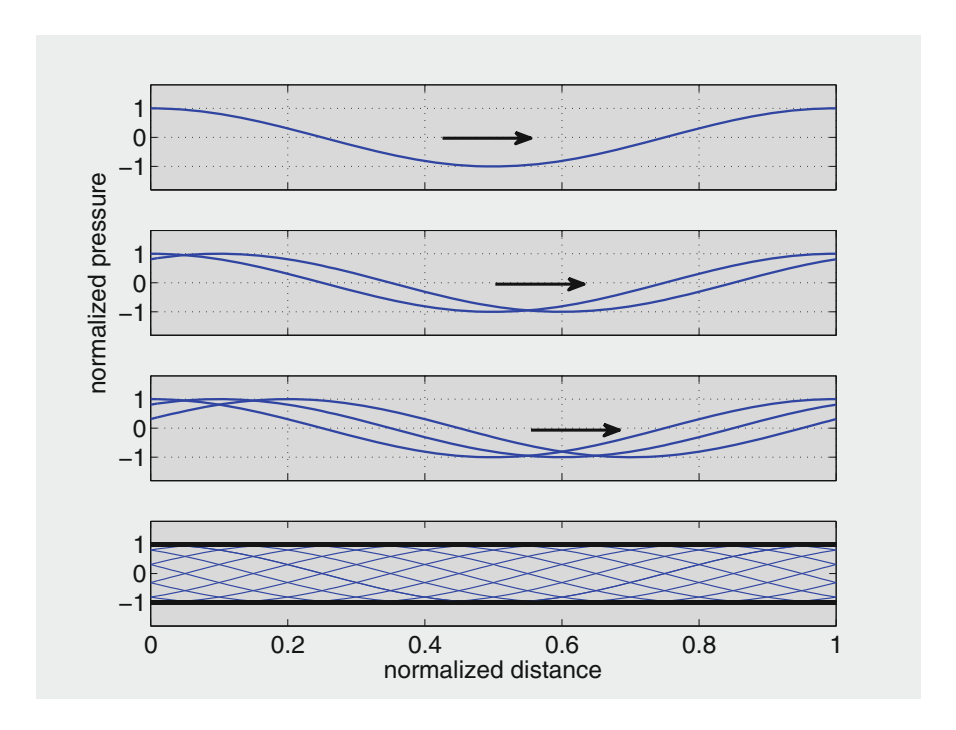


Fig. 6.3 Progression of a cosine pressure wave along an elastic tube in the *absence* of wave reflections. Individual curves in the *top three panels* represent the pressure curve at different times within the oscillatory cycle, plotted in terms of normalized distance \bar{x} along the tube, where $\bar{x}=0$ at entrance and $\bar{x}=1.0$ at exit. The outer envelope in the *bottom panel* represents the peak of the wave at different points along the tube, or the amplitude of *time* oscillations of pressure at different positions along the tube. The ideal pressure amplitude distribution seen in this case, characterized by a straight envelope along the tube, is singular in the sense that it is only possible in the absence of wave reflections.

measure of pressure oscillations within the tube. In particular, in the present case where wave reflections are absent, using Eq. 6.36, this distribution is given by

$$|\bar{p}_x(x)| = |e^{-i\omega x/c_0}| = 1.0$$
 (6.39)

which indicates that the time oscillations of the normalized pressure within the tube have an amplitude of 1.0 at every position along the tube, as illustrated in Fig. 6.3.

It is important not to confuse this distribution of the *amplitude* of the traveling pressure wave, namely $|\bar{p}_x(x)|$ as shown in Fig. 6.3, with the pressure wave itself, namely $\bar{p}_x(x)$. The focus here is only on the former because, as we shall see in what follows, it is the *amplitude* of the traveling pressure wave that is modified by wave reflections. The *uniform* distribution of amplitude of the traveling wave seen in Fig. 6.3 only exists in the absence of wave reflections and it therefore serves as an important reference state as we proceed to consider wave reflections.

6.4 Primary Wave Reflections

When an oscillatory pressure $p_a(t)$, as in Eq. 6.22, is applied at the entrance of an elastic tube of length l, pressure oscillations will travel towards the other end of the tube in the form of a propagating wave as described in the previous section. In the presence of any change in conditions, such as an obstruction or a vascular junction, part of the wave will be reflected back towards the entrance. Depending on conditions at the entrance, part of this backward traveling wave may in turn be reflected back towards the other end of the tube. In principle this may continue indefinitely, although the wave is diminishing in strength (amplitude) in the process. The phenomenon is analogous to that of the surface waves generated by a boat, moving towards the shore and being reflected back towards the boat. Indeed, the underlying physics of the two problems is the same.

In most hemodynamic applications it is rarely necessary to go beyond the first round of wave reflections because subsequent reflections are usually greatly diminished and can be neglected. The former are generally referred to as *primary wave reflections* while the latter are referred to collectively as *secondary wave reflections*. In this section we deal with the analysis of primary wave reflections in full details. Secondary wave reflections are considered briefly at the end of this chapter.

To illustrate the way in which wave reflections affect the pressure distribution in a tube, we focus first on a single tube in which a forward pressure wave $\bar{p}_f(x,t)$ represents the input pressure at one end of the tube (input end) and gives rise to a backward traveling wave $\bar{p}_b(x,t)$ at the other end (reflecting end). We shall see in subsequent sections that the nature of the backward wave depends critically on the type of conditions that exist at the reflecting end of the tube. In the present section, again in order to focus on the way in which forward and backward waves combine to change the pressure distribution in a tube, we shall consider only a basic case in which the backward wave has the *same form* as the forward wave but is moving in the negative *x*-direction. Thus if the forward wave is given by

$$\overline{p}_f(x,t) = e^{i\omega(t-x/c_0)} \tag{6.40}$$

we take

$$\bar{p}_b(x,t) = Be^{i\omega(t+x/c_0)} \tag{6.41}$$

where B is a constant. Since the pressure at the reflecting end of the tube must be single valued, the forward and backward pressure waves must be equal at x = l, where l is the tube length. Thus

$$\bar{p}_b(l,t) = Be^{i\omega(t+l/c_0)}$$
$$= Be^{-2i\omega l}(e^{i\omega(t-l/c_0)})$$

$$= Be^{-2i\omega l}(\bar{p}_f(l,t))$$

$$= R \bar{p}_f(l,t)$$
(6.42)

where R is known as the "reflection coefficient", thus given by

$$R = \frac{\overline{p}_b(l, t)}{\overline{p}_f(l, t)} \tag{6.43}$$

The reflection coefficient is then seen to represent the fraction of the forward wave that is being reflected at the reflecting end of the tube. Specifically, R=1 represents "total" reflection whereby the backward wave is equal to the forward wave in its entirety, while a small value of R represents a small reflection whereby the backward wave is only a small fraction of the forward wave.

We shall see in subsequent sections that this definition of R is only possible when conditions at the reflection site are such that the reflected wave is of the same form as the forward wave. Under more general conditions R may become complex, with real and imaginary parts, thus giving rise to a reflected wave that is not of the same form as the forward wave. Similarly, in the above formulation the wave speed c is assumed to be the inviscid wave speed c_0 . More generally, as seen in Sect. 5.9, c is a complex entity, with real and imaginary parts, thus again causing the reflected wave to be different in form from the input wave.

At any point in time t and position x along the tube the prevailing pressure is the sum of the forward and backward waves evaluated at x, t, that is

$$\bar{p}(x,t) = \bar{p}_f(x,t) + \bar{p}_b(x,t)
= e^{i\omega(t-x/c_0)} + Re^{i\omega(t+x/c_0-2l/c_0)}$$
(6.44)

or, in dimensional form

$$p(x,t) = p_0 \times \left\{ e^{i\omega(t-x/c_0)} + Re^{i\omega(t+x/c_0-2l/c_0)} \right\}$$
 (6.45)

As in the case of no reflections, the oscillations in space can be separated from the oscillations in time by writing

$$\overline{p}(x,t) = \overline{p}_x(x)e^{i\omega t} \tag{6.46}$$

where $\bar{p}_x(x)$ has the same important interpretation as before, namely that of being the amplitude of time oscillations at any position x along the tube, given by

$$\bar{p}_x(x) = e^{-i\omega x/c_0} + Re^{i\omega(x-2l)/c_0}$$
 (6.47)

or, in dimensional form

$$p_x(x) = p_0 \times \left\{ e^{-i\omega x/c_0} + Re^{i\omega(x-2l)/c_0} \right\}$$
 (6.48)

This makes it clear that $|\bar{p}_x(x)|$ is no longer constant along the tube as it is in the absence of wave reflections. In fact it can only become constant if either R=0 or l is infinite. The first scenario corresponds to there being perfect conditions at the end of the tube so that wave reflections are absent, and the second corresponds to the reflecting end of the tube being infinitely far away so that any reflections from that end cannot return in finite time.

The extent to which the pressure distribution in a tube is affected by wave reflections depends also on the frequency ω , as is apparent from Eq. 6.47. Since frequency is related to the wave length L by

$$L = \frac{2\pi c_0}{\omega} \tag{6.49}$$

the pressure distribution in Eq. 6.47 can be put in the form

$$\bar{p}_{x}(x) = e^{-2\pi i x/L} + Re^{2\pi i (x-2l)/L}$$
 (6.50)

It is also convenient to introduce

$$\begin{cases} \overline{x} = x/l \\ \overline{L} = L/l \end{cases}$$
 (6.51)

whereby Eq. 6.50 takes the normalized form

$$\overline{p}_{x}(\overline{x}) = e^{-2\pi i \overline{x}/\overline{L}} + Re^{2\pi i (\overline{x}-2)/\overline{L}}$$
(6.52)

The advantage of this form is that as the ratio of wave length to tube length varies, the full range of positions along the tube is always described by $\bar{x}=0$ to $\bar{x}=1.0$. An important reference case to consider is that for which the wave and tube lengths are equal, thus $\bar{L}=1$, $e^{-4\pi i/\bar{L}}=1$, and Eq. 6.52 reduces to

$$\bar{p}_x(\bar{x}) = e^{-2\pi i \bar{x}} + Re^{2\pi i \bar{x}} \tag{6.53}$$

$$= (R+1)\cos 2\pi \bar{x} + i(R-1)\sin 2\pi \bar{x}$$
 (6.54)

The distribution of $|\overline{p}_x(\overline{x})|$ at different positions along the tube is shown in Fig. 6.4, to be compared with the constant distribution seen in Fig. 6.3 where wave reflections are absent.

Analytically, from Eq. 6.53 we now have

$$|\bar{p}_{r}(\bar{x})| = \sqrt{R^2 + 1 + 2R\cos 4\pi \bar{x}}$$
 (6.55)

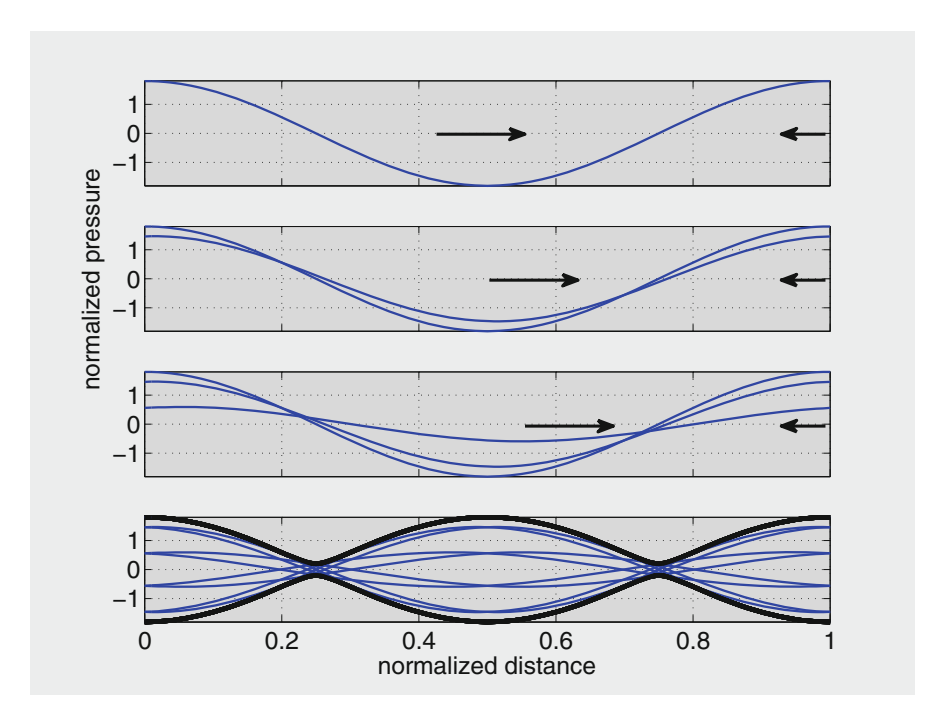


Fig. 6.4 Progression of a sinosoidal pressure wave along an elastic tube in the presence of 80% wave reflections (R=0.8), to be compared with the corresponding results in Fig. 6.3 where wave reflections are absent. Individual curves in the *top three panels* represent the total (forward plus backward) pressure waves at different times within the oscillatory cycle, plotted in terms of normalized distance \bar{x} along the tube, where $\bar{x}=0$ at entrance and $\bar{x}=1.0$ at exit. The outer envelope in the *bottom panel* represents the peaks of these waves at different points along the tube, or the amplitude of *time* oscillations of pressure at different positions along the tube. The shape of the envelope is affected critically by the ratio of wave length over tube length (\bar{L}). In this figure $\bar{L}=1.0$.

compared with the result in Eq. 6.39 for the case in which wave reflections are absent. In particular, the value of $|\bar{p}_x(\bar{x})|$ is maximum at $\bar{x} = 0$, 1/2, 1, and minimum at $\bar{x} = 1/4$, 3/4. At the maximum points the forward and backward waves *add*, while at the minimum points they *subtract*.

Since $|\bar{p}_x(\bar{x})|$ represents the amplitude of time oscillations at normalized position \bar{x} along the tube, it is seen that these oscillations will have different amplitude at different positions whenever $R \neq 0$. The distribution of $|\bar{p}_x(\bar{x})|$ is relatively easy to describe in the special case of $\bar{L} = 1$, but it becomes more complicated for other values of \bar{L} and for specific values of the reflection coefficient R where the forward and backward waves combine in more complicated ways. Results for $\bar{L} = 2, 3, 4, 5, 10$ are shown in Figs. 6.5, 6.6, 6.7, 6.8 and 6.9.

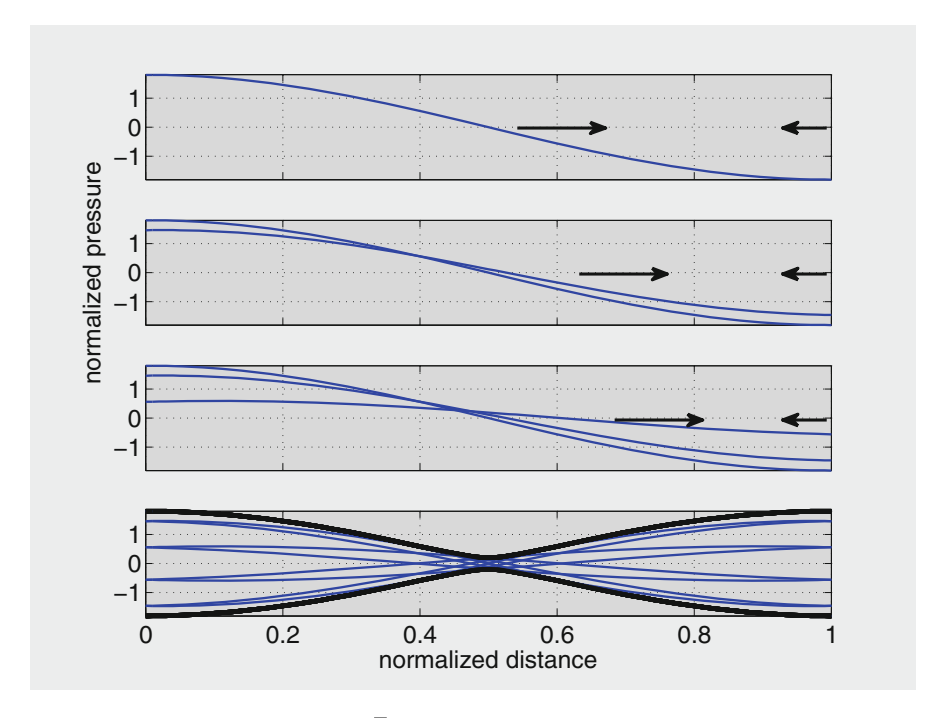


Fig. 6.5 Same as in Fig. 6.4 but with $\overline{L} = 2$.

6.5 Pressure-Flow Relations

The ultimate purpose of determining the pressure distribution in a tube is to obtain a measure of the flow within the tube and determine the relationship between pressure and flow. In *steady* flow, the relation between pressure and flow is dominated and fully determined by the viscous resistance to flow at the tube wall. Equation 3.43 illustrates the simple relation which exists in this case between the flow rate q_s and the constant pressure gradient k_s . In *pulsatile* flow through a *rigid* tube the relation between pressure and flow is again affected by viscous resistance but now also by inertia of the fluid because of repeated acceleration and deceleration of the fluid within the oscillatory cycle. Thus the oscillatory *frequency* becomes an added factor in the relation between pressure and flow, as can be seen in Eq. 4.43 for the oscillatory flow rate $q_{\phi}(t)$ in pulsatile flow through a rigid tube.

In pulsatile flow through an *elastic* tube the elastic properties of the tube become yet another added factor in the relation between pressure and flow. Equation 5.72 for the axial velocity u(x, r, t) in this case involves not only viscosity of the fluid and frequency of oscillation but also elastic properties of the tube wall, embedded in the parameter G and the wave speed c. Furthermore, the pulsating pressure and flow in this case propagate in the form of progressive waves, as is apparent from the presence of x in Eq. 5.72, thus admitting the possibility of wave reflections.

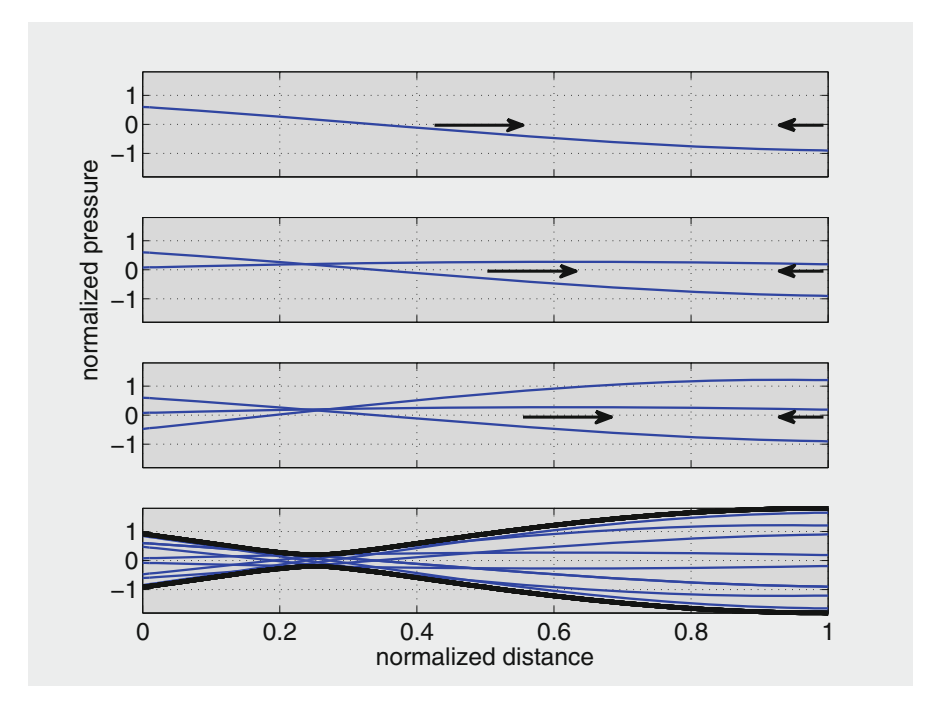


Fig. 6.6 Same as in Fig. 6.4 but with $\overline{L} = 3$.

Results of the previous section demonstrate clearly that wave reflections can affect the pressure distribution in a tube profoundly because of the superposition of forward and backward waves.

This new factor in the relation between pressure and flow is important not only because it can produce major changes in the pressure distribution but also because these changes are not as easily predictable as they are in the case of viscosity or frequency. For this reason, in what follows we focus on this factor in particular and deal with it *in isolation* so as not to mask it by the effects of viscosity and frequency which have already been examined. This approach has the advantage of making the effects of wave reflections more "visible". As seen in the previous section, by appropriate scaling the changes in pressure distribution can be expressed as deviations from a reference state in which the normalized pressure amplitude has the constant value 1.0 all along the tube. This reference state is attained only in the absence of wave reflections, thus any deviation from it can be identified immediately as resulting from wave reflections.

A basic solution for the flow wave follows much the same lines as that for the pressure. Starting with the solution in Eq. 6.32 as an initial forward pressure wave, before any reflections, writing

$$p_f(x,t) = p_0 e^{i\omega(t - x/c_0)}$$
(6.56)

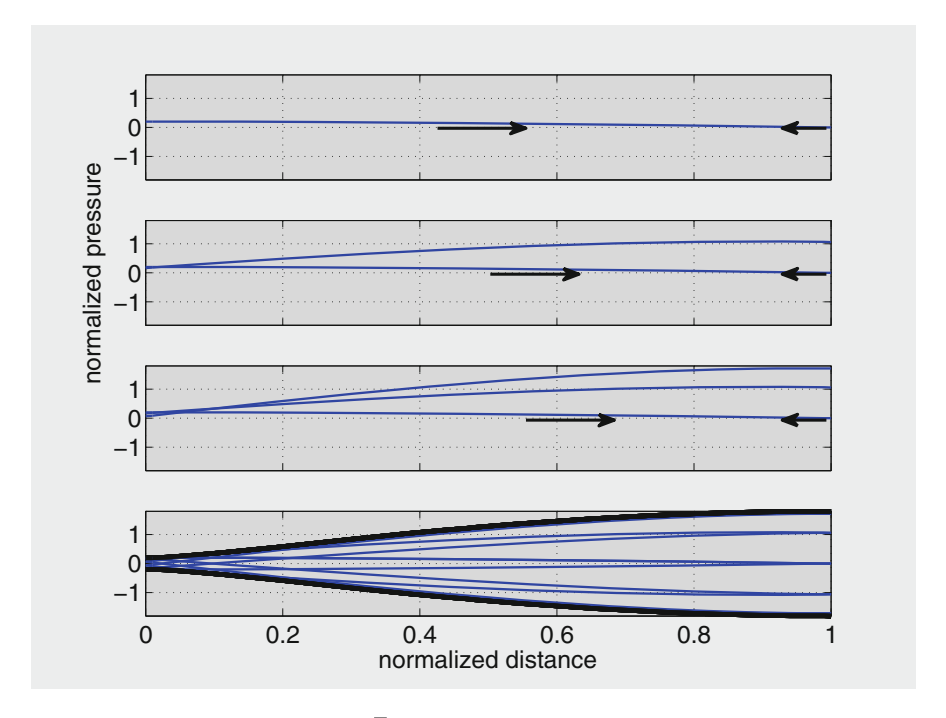


Fig. 6.7 Same as in Fig. 6.4 but with $\overline{L} = 4$.

and since pressure and flow are governed by the same wave equations (Eq. 6.20), we postulate a solution for the corresponding forward flow wave in the form

$$q_f(x,t) = Be^{i\omega(t-x/c_0)}$$
(6.57)

where B is a constant.

The relation between pressure and flow is governed by Eq. 6.19. Applying these to the above pressure and flow waves we obtain

$$\begin{cases} \frac{\partial q_f}{\partial t} + \frac{A}{\rho} \frac{\partial p_f}{\partial x} &= 0\\ \frac{\partial q_f}{\partial x} + \frac{A}{\rho c_0^2} \frac{\partial p_f}{\partial t} &= 0 \end{cases}$$
(6.58)

Substituting for p_f and q_f , both equations yield the same results, namely

$$B = \left(\frac{A}{\rho c_0}\right) p_0 \tag{6.59}$$

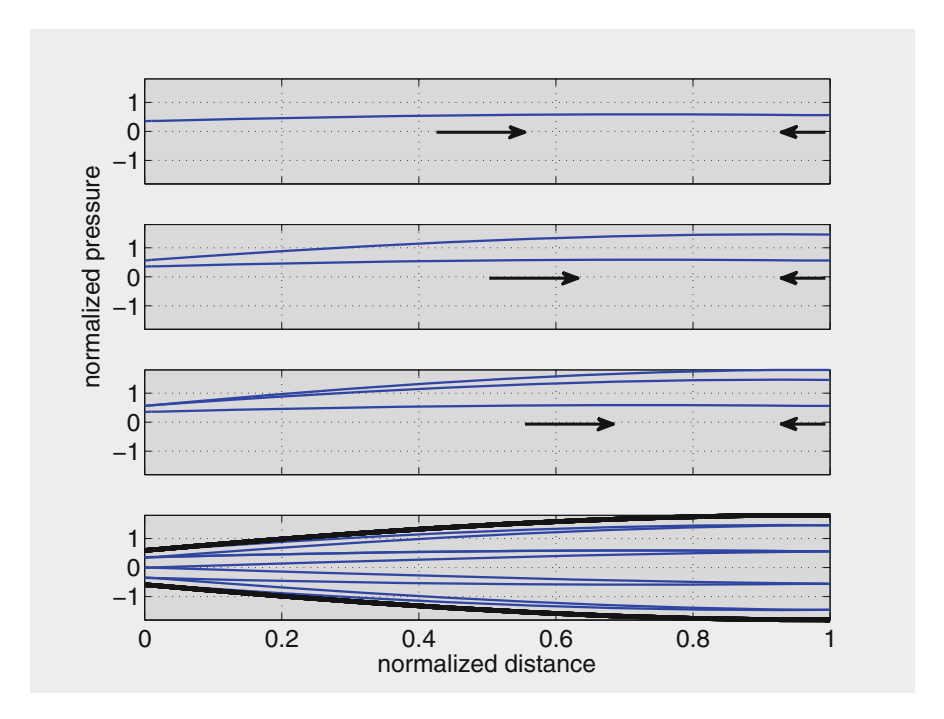


Fig. 6.8 Same as in Fig. 6.4 but with $\overline{L} = 5$.

and

$$q_f(x,t) = \left(\frac{A}{\rho c_0}\right) p_0 e^{i\omega(t-x/c_0)}$$

$$= \left(\frac{A}{\rho c_0}\right) p_f(x,t)$$
(6.60)

Similarly, from the result in Eq. 6.44 we have, for the reflected wave

$$p_b(x,t) = Rp_0 e^{i\omega(t+x/c_0-2l/c_0)}$$
(6.61)

thus, we postulate a corresponding flow wave

$$q_b(x,t) = Ce^{i\omega(t+x/c_0-2l/c_0)}$$
 (6.62)

where C is a constant. Applying the governing equations to these waves we obtain

$$\begin{cases} \frac{\partial q_b}{\partial t} + \frac{A}{\rho} \frac{\partial p_b}{\partial x} &= 0\\ \frac{\partial q_b}{\partial x} + \frac{A}{\rho c_0^2} \frac{\partial p_b}{\partial t} &= 0 \end{cases}$$
(6.63)

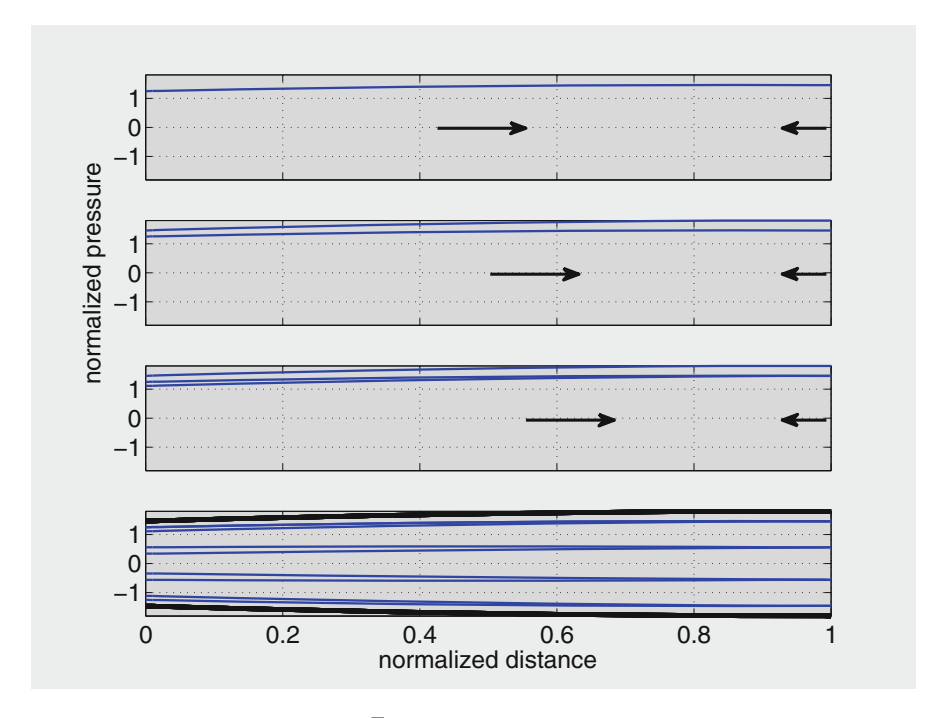


Fig. 6.9 Same as in Fig. 6.4 but with $\overline{L}=10$. Only a small part (10 %) of the wave unfolds within the tube in this case.

Substituting for p_b and q_b , both equations yield the same results, namely

$$C = \left(\frac{-A}{\rho c_0}\right) R p_0 \tag{6.64}$$

and

$$q_b(x,t) = \left(\frac{-A}{\rho c_0}\right) R p_0 e^{i\omega(t+x/c_0-2l/c_0)}$$

$$= \left(\frac{-A}{\rho c_0}\right) p_b(x,t) \tag{6.65}$$

The entity

$$Y_0 = \frac{A}{\rho c_0} \tag{6.66}$$

is known as the "characteristic admittance" ^{8,9,10} of the tube, and it is seen to be a key parameter in the relation between pressure and flow. Its reciprocal

$$Z_0 = \frac{\rho c_0}{A} \tag{6.67}$$

is known as the "characteristic impedance". From Equations 6.60, 6.65, 6.66, 6.67 we then find

$$Y_0 = \frac{q_f(x,t)}{p_f(x,t)} = \frac{-q_b(x,t)}{p_b(x,t)}$$
(6.68)

$$Z_0 = \frac{p_f(x,t)}{q_f(x,t)} = \frac{p_b(x,t)}{-q_b(x,t)}$$
(6.69)

from which we draw the interpretation that Y_0 is indeed a measure of the extent to which the tube "admits" flow, while Z_0 is a measure of the extent to which it "impedes" the flow. The minus sign associated with the backward flow wave indicates that q_b and q_f have opposite signs because of their opposite directions. This issue does not arise in the case of p_b and p_f since pressure is a *scalar* quantity. An important consequence of this is that when the reflected waves are included in the complete expressions for the pressure and flow waves, we obtain, using Eqs. 6.56, 6.60, 6.61, 6.65,

$$p(x,t) = p_f(x,t) + p_b(x,t)$$

$$= p_0 e^{i\omega(t-x/c_0)} + Rp_0 e^{i\omega(t+x/c_0-2l/c_0)}$$

$$q(x,t) = q_f(x,t) + q_b(x,t)$$

$$= Y_0 \left(p_0 e^{i\omega(t-x/c_0)} - Rp_0 e^{i\omega(t+x/c_0-2l/c_0)} \right)$$

$$= q_0 e^{i\omega(t-x/c_0)} - Rq_0 e^{i\omega(t+x/c_0-2l/c_0)}$$
(6.71)

where

$$q_0 = Y_0 p_0 (6.72)$$

From these results we note that the forward and backward pressure waves *add* while the corresponding flow waves *subtract*. Furthermore, from the definition of the reflection coefficient (Eq. 6.43) we have

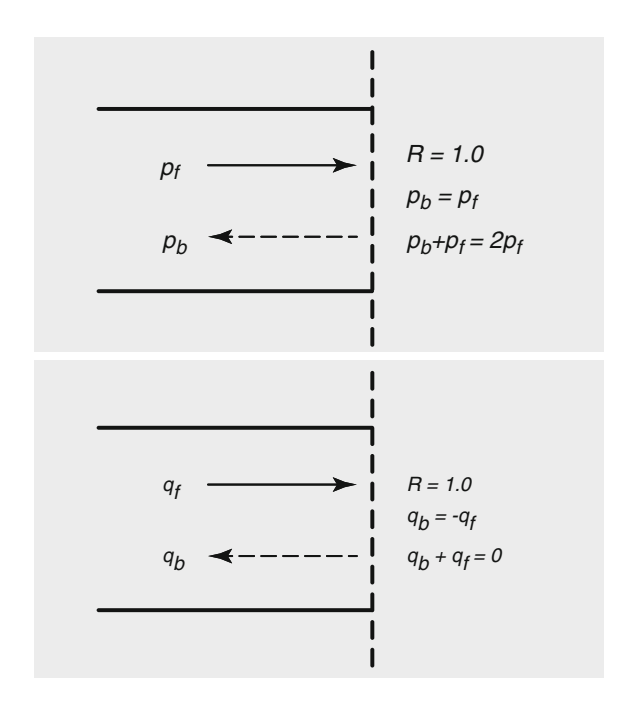
$$R = \frac{p_b(l, t)}{p_f(l, t)} \tag{6.73}$$

⁸McDonald DA. Blood flow in arteries. Edward Arnold, London, 1974.

⁹Fung YC. Biodynamics: Circulation. Springer-Verlag, New York, 1984.

¹⁰Milnor WR. Hemodynamics. Williams and Wilkins, Baltimore, 1989.

Fig. 6.10 At a completely closed end of a tube, the reflection coefficient R = 1.0, the pressure wave is duplicated, and the flow wave is "annihilated".



and in terms of flow waves, using Eq. 6.68

$$R = \frac{-q_b(l, t)}{q_f(l, t)} \tag{6.74}$$

Thus a value of R = 1.0 represents a situation in which the flow wave is *annihilated*, $q_b(l,t) = -q_f(l,t)$, while the pressure wave is *duplicated*, $p_b(l,t) = p_f(l,t)$. This situation would occur when the tube end is completely closed, and the results are therefore consistent with what would be expected on physical grounds (Fig. 6.10).

A value of R=-1.0, similarly, represents a situation in which the flow wave is *duplicated*, $q_b(l,t)=q_f(l,t)$, while the pressure wave is *annihilated*, $p_b(l,t)=p_f(l,t)$. This situation would occur when the tube end is completely open, and the results are again consistent with what would be expected on physical grounds (Fig. 6.11).

A value of R=0, finally, represents a situation in which both the flow and the pressure waves are unchanged, that is $q_b(l,t)=0$, $p_b(l,t)=0$. This situation would occur when the tube end is completely matched with another tube of the same properties. In this case no reflections arise, as would be expected on physical grounds (Fig. 6.12).

Fig. 6.11 At a completely open end of a tube, the reflection coefficient R = -1.0, the pressure wave is "annihilated", and the flow wave is duplicated.

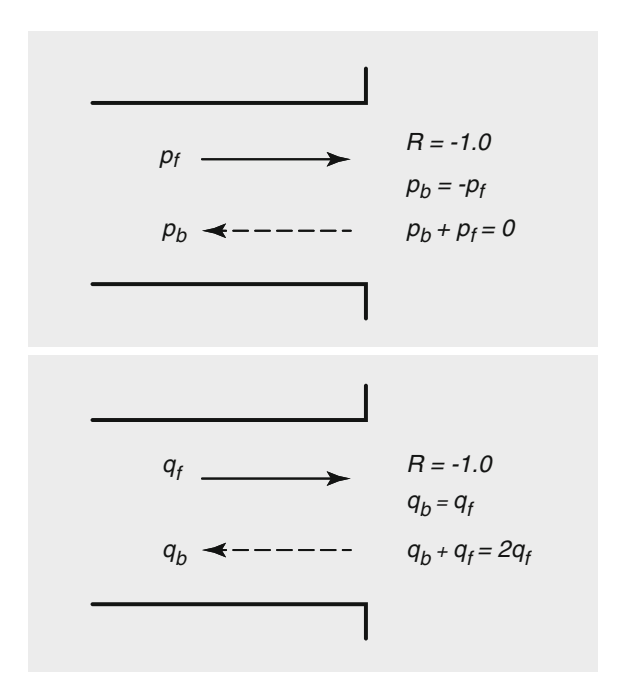
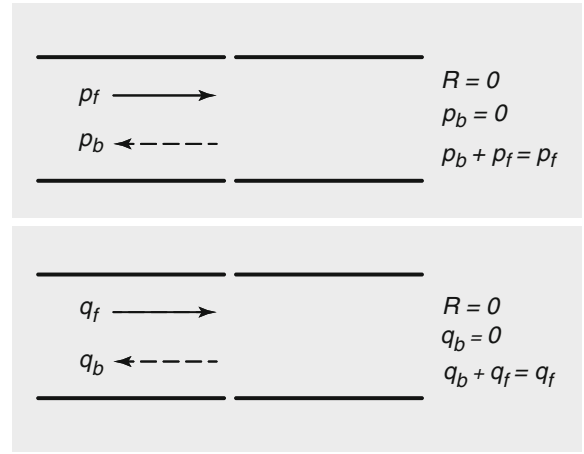


Fig. 6.12 At a completely matched end of a tube, the reflection coefficient R = 0, no reflections arise and the pressure and flow waves are unchanged.



6.6 Effective Admittance/Impedance

Results of the previous section make it clear that in the presence of wave reflections the pressure and flow waves within a tube no longer have the same form (Eqs. 6.70 and 6.71). One of the most important consequences of this is a change in the ratio of flow to pressure and hence a change in the admittance, and by implication impedance, of the tube. The characteristic admittance Y_0 is no longer a measure of the extent to which the tube admits flow, a new "effective admittance" Y_e takes its place.

To determine the effective admittance, consider first a single tube extending from x = 0 to x = l in which the reflection coefficient at x = l is R. By common convention the effective admittance Y_e of the tube is defined as the ratio of flow to pressure at the tube entrance (x = 0), hence it is also known as the "input admittance". By this definition, using Eqs. 6.70 and 6.71 we then have

$$Y_e = \frac{q(l,t)}{p(l,t)}$$
 (6.75)

$$=Y_0\left(\frac{1-Re^{-2i\omega l/c_0}}{1+Re^{-2i\omega l/c_0}}\right)$$
(6.76)

The same comments and discussion apply to *impedance* and to the corresponding concepts of "effective impedance" or "input impedance" Z_e , in which case we have

$$Z_e = \frac{p(l,t)}{q(l,t)} \tag{6.77}$$

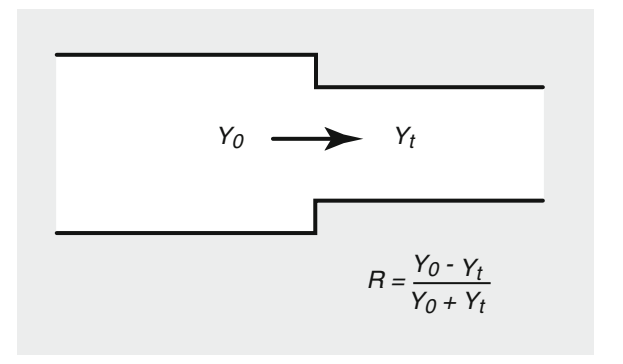
$$= Z_0 \left(\frac{1 + Re^{-2i\omega l/c_0}}{1 - Re^{-2i\omega l/c_0}} \right)$$
 (6.78)

Because of the simple reciprocal relation between admittance and impedance, therefore, in the remainder of this section we shall confine discussion to admittance only.

It is clear from Eq. 6.76 that the effective admittance Y_e will be different from the characteristic admittance Y_0 as long as $R \neq 0$, that is as long as wave reflections are present. In the most basic scenario, the reflection coefficient R at x = l may result from a transition at x = l from one tube in which the characteristic admittance is $Y_{0,1}$ to another in which the admittance is $Y_{0,2}$ (Fig. 6.13).

The reflection coefficient at the junction between the two tubes can be expressed in terms of the difference between the two admittances by applying two conditions at that junction. The first condition requires that the sum of forward and backward

Fig. 6.13 Wave reflections occur when the pressure or flow wave meets a change of admittance from Y_0 in one tube to Y_t in another. The reflection coefficient R is equal to 1.0 when Y_t is zero, -1.0 when Y_t is infinite, and 0 when $Y_t = Y_0$. The three situations are the same as those illustrated in Figs. 6.10, 6.11 and 6.12.



pressure waves evaluated at x = l in the first tube be equal to the forward pressure wave evaluated at x = 0 in the second tube, that is, with obvious notation

$$p_{1,f}(l,t) + p_{1,b}(l,t) = p_{2,f}(0,t)$$
(6.79)

The second condition requires that the *vector* sum of the forward and backward flow at x = l in the first tube be equal to the forward flow at x = 0 in the second tube, that is

$$q_{1,f}(l,t) + q_{1,h}(l,t) = q_{2,f}(0,t)$$
 (6.80)

noting, that $q_{1,f}$ and $q_{1,b}$ have different signs, hence the sum on the left actually represents the *difference* between the two flows.

Substituting from Eq. 6.68 for the flow rates in Eq. 6.80, we then have

$$Y_{0,1} \times p_{1,f}(l,t) - Y_{0,1} \times p_{1,b}(l,t) = Y_{0,2} \times p_{2,f}(0,t)$$
(6.81)

and using Eq. 6.79 this becomes

$$Y_{0,1} \times p_{1,f}(l,t) - Y_{0,1} \times p_{1,b}(l,t) = Y_{0,2} \times \{p_{1,f}(l,t) + p_{1,b}(l,t)\}$$
(6.82)

Since by definition of the reflection coefficient (Eq. 6.73)

$$\frac{p_{1,b}(l,t)}{p_{1,f}(l,t)} = R \tag{6.83}$$

substitution this in Eq. 6.82 yields

$$R = \frac{Y_{0,1} - Y_{0,2}}{Y_{0,1} + Y_{0,2}} \tag{6.84}$$

We see that the reflection coefficient is zero when $Y_{0,1} = Y_{0,2}$, that is when there is no change of admittance at the junction between the two tubes. The coefficient is equal to 1.0 when $Y_{0,2} = 0$, that is when the admittance of the second tube is zero, there is complete blockage and hence total reflection. The reflection coefficient is equal to -1.0, finally, when $Y_{0,2}$ is infinite, that is when the second tube is completely open and offers no impedance to flow (or infinite admittance). These 3 situations are illustrated in Figs. 6.10, 6.11 and 6.12.

6.7 Reflection Coefficients

In the previous section we considered the simple situation of only two tubes in succession, with wave reflections arising at the interface between the two tubes because of a difference in their admittances. As a result of wave reflections,

the admittance of the tube to which the backward waves return changes from its characteristic admittance to an "effective admittance" which depends on the returning waves. This effective admittance, not the characteristic admittance, must then be used in the calculation of pressure or flow within the tube.

The task of extending this scenario into a vascular tree structure consisting of many millions of tubes would seem to be intractable at first. For this reason, we shall begin with only a small generalization from the result of the previous section and consider a succession of *three* tubes instead of two. Following the notation of the previous section, the three tubes shall be identified by subscripts 1, 2, 3 and the reflection coefficients at the end of each tube shall be denoted by R_1 , R_2 , R_3 respectively. The task at hand is how to determine the succession of reflection coefficients R_1 , R_2 , R_3 ?

At our disposal are the two main results from the previous section, namely Eq. 6.76 for the effective admittance Y_e and Eq. 6.84 for the reflection coefficient R. Applying these to the first two tubes, we have

$$Y_{e,1} = Y_{0,1} \left(\frac{1 - R_1 e^{-2i\omega l/c_0}}{1 + R_1 e^{-2i\omega l/c_0}} \right)$$
 (6.85)

and

$$R_1 = \frac{Y_{0,1} - Y_{0,2}}{Y_{0,1} + Y_{0,2}} ? (6.86)$$

or

$$R_1 = \frac{Y_{0,1} - Y_{e,2}}{Y_{0,1} + Y_{e,2}} ? (6.87)$$

where, as in the previous section, subscripts 0, e are being used to denote characteristic and effective admittances, respectively. The questions posed in Eqs. 6.86 and 6.87 illustrate the added complication in extending the results of the previous section to a succession of more than two tubes. It is clear that the reflection coefficient R_1 cannot be based on the *characteristic* admittance of the second tube as in Eq. 6.86 because of wave reflections at the junction of the second and third tubes represented by the reflection coefficient R_2 . In the previous section R_2 was zero, hence this added complication did not arise.

It would seem then that the extension to a succession of more than two tubes must be based on Eqs. 6.85 and 6.87. However, in the way of application, neither of the two equations can proceed *forward* to the third tube (and ultimately larger succession of tubes). This is because in Eq. 6.85 R_1 is not known and in Eq. 6.87 Y_{2e} is not known, which indicates clearly that the analysis must proceed *backward*, starting with the third tube (or higher if any). To do so we note first that in order to simplify the process, Eq. 6.85 can be written as

$$Y_{e,1} = Y_{0,1} \left\{ \frac{e^{i\theta_1} - R_1 e^{-i\theta_1}}{e^{i\theta_1} + e^{-i\theta_1}} \right\}$$

$$= Y_{0,1} \left\{ \frac{(\cos\theta_1 + i\sin\theta_1) - R_1(\cos\theta_1 - i\sin\theta_1)}{(\cos\theta_1 + i\sin\theta_1) + R_1(\cos\theta_1 - i\sin\theta_1)} \right\}$$

$$= Y_{0,1} \left\{ \frac{(1 - R_1)\cos\theta_1 + i(1 + R_1)\sin\theta_1}{(1 + R_1)\cos\theta_1 + i(1 - R_1)\sin\theta_1} \right\}$$
(6.88)

where

$$\theta_1 = \frac{\omega l_1}{c_1} \tag{6.89}$$

and l_1 , c_1 are the length of and the (inviscid) wave speed in the first tube. Then, from Eq. 6.87 we have

$$\begin{cases} 1 + R_1 = \frac{2Y_{0,1}}{Y_{0,1} + Y_{e,2}} \\ 1 - R_1 = \frac{2Y_{e,2}}{Y_{0,1} + Y_{e,2}} \end{cases}$$
(6.90)

which finally yields

$$\begin{cases} Y_{e,1} = Y_{0,1} \left\{ \frac{Y_{e,2} + iY_{0,1} \tan \theta_1}{Y_{0,1} + iY_{e,2} \tan \theta_1} \right\} \\ R_1 = \frac{Y_{0,1} - Y_{e,2}}{Y_{0,1} + Y_{e,2}} \end{cases}$$
(6.91)

Although R_1 has now been eliminated from the equation for $Y_{e,1}$, the expression for R_1 is included here as a reminder that this expression was used in the process. It is therefore important to note that in this process R_1 is defined not in terms of the difference between $Y_{e,1}$ and $Y_{e,2}$ but in terms of the difference between $Y_{0,1}$ and $Y_{e,2}$.

Equations 6.91 thus provide a template for progression from the second tube to the third. Thus, using this template and proceeding to the second and third tubes, with obvious notation, we have

$$\begin{cases} Y_{e,2} = Y_{0,2} \left\{ \frac{Y_{e,3} + iY_{0,2} \tan \theta_2}{Y_{0,2} + iY_{e,3} \tan \theta_2} \right\} \\ R_2 = \frac{Y_{0,2} - Y_{e,3}}{Y_{0,2} + Y_{e,3}} \\ \theta_2 = \frac{\omega l_2}{c_2} \end{cases}$$
(6.92)

and in general, if the number of successive tubes is N, then

$$\begin{cases} Y_{e,j} = Y_{0,j} \left\{ \frac{Y_{e,j+1} + iY_{0,j} \tan \theta_j}{Y_{0,j} + iY_{e,j+1} \tan \theta_j} \right\} \\ R_j = \frac{Y_{0,j} - Y_{e,j+1}}{Y_{0,j} + Y_{e,j+1}}, \quad j = 1 \cdots N - 1 \\ \theta_j = \frac{\omega l_j}{c_j} \end{cases}$$
(6.93)

It will be noted that this formula can only be evaluated *backward* because the effective admittance of each tube requires the effective admittance of the next tube. Also, Eq. 6.93 determines the effective admittances of all the tubes except the last one. The effective admittance of the last tube must be known or specified. Equations 6.93 set the stage for considering the problem of wave propagation and wave reflections in a vascular tree structure, which we deal with in full in the next Chapter.

6.8 Secondary Wave Reflections

So far in this chapter, a wave reflected at one end of a tube and traveling back toward the other end of the tube was assumed not to be reflected again at that end. In this context the first reflection would be referred to as a "primary wave reflection" while subsequent reflections would be referred to as "secondary wave reflections". In this section we consider the latter briefly.

If wave reflections at both ends of a tube are considered, a wave originating at x = 0 in a tube of length l will be partly reflected at x = l and the reflected part will travel back toward x = 0 where it is in turn partly reflected and so on. ¹¹ In principle this process will continue indefinitely, though clearly with diminishing effects since the reflected part of the wave is each time only a fraction of the incident wave as illustrated schematically in Fig. 6.14.

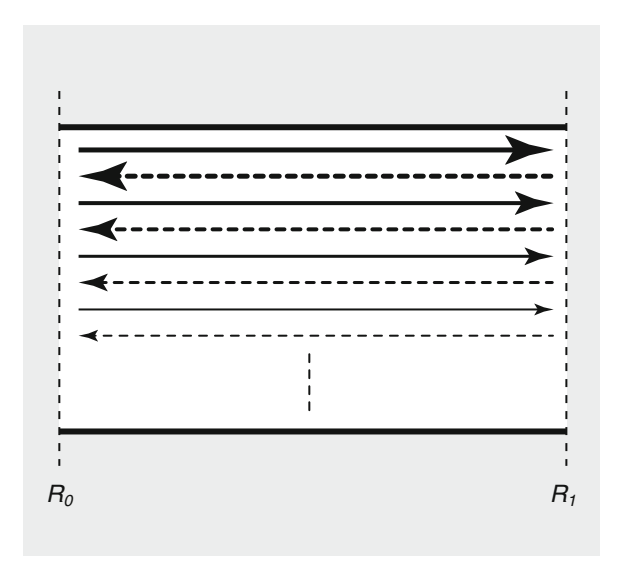
We begin by considering an initial wave propagating in the positive x-direction in a tube of length l, writing, as in Eq. 6.35

$$\bar{p}^{(0,f)}(x,t) = e^{i\omega(t-x/c_0)}$$
 (6.94)

$$= \overline{p}_x^{(0,f)}(x)e^{i\omega t} \tag{6.95}$$

¹¹Kenner T, 1969. The dynamics of pulsatile flow in the coronary arteries. Pflügers Archiv; European Journal of Physiology 310:22–34.

Fig. 6.14 Wave reflections at both ends of a tube. Pressure or flow waves travel back and forth, indefinitely, though each time being reduced in magnitude by the reflection coefficient.



where here the superscript 0 is being used to identify the initial state of the wave, before any reflections, and the superscript f is being used to indicate that this is a forward wave, moving in the positive x-direction. Backward waves, moving in the negative x-direction, shall be identified by a superscript b. As in Eq. 6.35, this wave is being represented here by two oscillatory functions, one in time, represented by $e^{i\omega t}$, and one in space, represented by

$$\bar{p}_x^{(0,f)}(x) = e^{-i\omega x/c_0}$$
 (6.96)

As before, the wave is in normalized form, such that

$$\begin{cases} \overline{p}^{(0f)}(0,0) = 1.0\\ \overline{p}_x^{(0f)}(0) = 1.0\\ \overline{p}_x^{(0f)}(l) = e^{-i\omega l/c_0} \end{cases}$$
(6.97)

As we saw in the previous sections, the effects of wave reflections is to change the form of space oscillations within the tube, leaving the form of time oscillations unchanged. Thus, $\bar{p}_x(x)$ begins as a simple complex exponential function when wave reflections are absent, as in Eq. 6.98, then becomes more composite as the primary reflected wave is added. In this section we pursue this process to its ultimate limit as the primary wave reflections are now followed by secondary wave reflections, that is reflected waves now go back and forth between the two ends of the tube.

To consider this process in detail, it is useful to think of the *x*-oscillatory function as arising from an input pressure amplitude $p0, f_x(0)$ at the tube entrance which is then "operated on" by the complex exponential function representing the translation

of that input into a wave form $p0, f_x(x)$ along the tube. We shall find this concept useful as the wave is reflected back and forth, and to make use of it we write Eq. 6.98 in the form

$$\bar{p}_x^{(0,f)}(x) = \{\bar{p}_x^{(0,f)}(0)\}e^{-i\omega x/c_0}$$
 (6.98)

As this wave reaches the other end of the tube (x = l), its value at that point, multiplied by the reflection coefficient (R_l) there, becomes the "input pressure amplitude" for the reflected wave. This resulting backward wave progresses in the *negative x*-direction, and its distance as it moves away from the reflection site is (l-x) in place of x for the forward wave. The net result is

$$\overline{p}^{(0,b)}(x) = \{R_l e^{-i\omega l/c_0}\} e^{-i\omega(l-x)/c_0}
= R_l e^{-i\omega(2l-x)/c_0}$$
(6.99)

It will be noted that the sum of $\bar{p}^{(0,f)}(x)$ from Eq. 6.98 and $\bar{p}^{(0,b)}(x)$ from Eq. 6.99 is identical with the result obtained in the previous section (Eq. 6.47) for the pressure wave after only one primary reflection. In this section we continue this process beyond the primary stage.

As the backward wave reaches the entrance of the tube and is allowed to be reflected there, the value of $\bar{p}^{(0,b)}(x)$ at that point (x=0), multiplied by the reflection coefficient (R_0) there, becomes the input pressure amplitude for the next forward wave, that is

$$\overline{p}_{x}^{(1f)}(x) = \{R_{0}R_{l}e^{-i\omega 2l/c_{0}}\}e^{-i\omega x/c_{0}}$$

$$= R_{0}R_{l}e^{-i\omega(2l+x)/c_{0}} \tag{6.100}$$

The pattern is now established for subsequent reflections, as waves move back and forth between the two ends of the tube, we have

$$\bar{p}_x^{(1,b)}(x) = \{R_0 R_l^2 e^{-i\omega 3l/c_0}\} e^{-i\omega(l-x/c_0)}$$

$$= R_0 R_l^2 e^{-i\omega(4l-x)/c_0}$$
(6.101)

$$\overline{p}_{x}^{(2f)}(x) = \{R_{0}^{2}R_{l}^{2}e^{-i\omega 4l/c_{0}}\}e^{-i\omega x/c_{0}}$$

$$= R_{0}^{2}R_{l}^{2}e^{-i\omega(4l+x)/c_{0}}$$
(6.102)

$$\overline{p}_{x}^{(2,b)}(x) = \{R_{0}^{2}R_{l}^{3}e^{-i\omega 5l/c_{0}}\}e^{-i\omega(l-x/c_{0})}$$

$$= R_{0}^{2}R_{l}^{3}e^{-i\omega(6l-x)/c_{0}}$$
(6.103)

The net pressure distribution within the tube consists of the sum of all the forward and backward waves, that is

$$\bar{p}_{x}(x) = \bar{p}_{x}^{(0,f)}(x) + \bar{p}_{x}^{(1,f)}(x) + \bar{p}_{x}^{(2,f)}(x) + \cdots
+ \bar{p}_{x}^{(0,b)}(x) + \bar{p}_{x}^{(1,b)}(x) + \bar{p}_{x}^{(2,b)}(x) + \cdots
= e^{-i\omega x/c_{0}} + R_{0}R_{l}e^{-i\omega(2l+x)/c_{0}}
+ R_{0}^{2}R_{l}^{2}e^{-i\omega(4l+x)/c_{0}} + \cdots
+ R_{l}e^{-i\omega(2l-x)/c_{0}} + R_{0}R_{l}^{2}e^{-i\omega(4l-x)/c_{0}}
+ R_{0}^{2}R_{l}^{3}e^{-i\omega(6l-x)/c_{0}} + \cdots
= e^{-i\omega x/c_{0}}\{1 + (R_{0}R_{l}e^{-i\omega 2l/c_{0}})
+ (R_{0}R_{l}e^{-i\omega 2l/c_{0}})^{2} + (R_{0}R_{l}e^{-i\omega 2l/c_{0}})^{3} + \cdots\}
+ R_{l}e^{-i\omega(2l-x)/c_{0}}\{1 + (R_{0}R_{l}e^{-i\omega 2l/c_{0}})
+ (R_{0}R_{l}e^{-i\omega 2l/c_{0}})^{2} + (R_{0}R_{l}e^{-i\omega 2l/c_{0}})
+ (R_{0}R_{l}e^{-i\omega 2l/c_{0}})^{2} + (R_{0}R_{l}e^{-i\omega 2l/c_{0}})^{3} + \cdots\}$$
(6.106)

The series inside the curly brackets is an infinite geometric series in ϵ , where

$$\epsilon = R_0 R_l e^{-i\omega 2l/c_0} < 1 \tag{6.107}$$

and therefore 12

$$1 + \epsilon + \epsilon^2 + \epsilon^3 + \dots = \frac{1}{1 - \epsilon}$$
 (6.108)

Thus Eq. 6.106 for the pressure distribution along the tube reduces to the much simpler form

$$\bar{p}_x(x) = \frac{e^{-i\omega x/c_0} + R_l e^{-i\omega(2l-x)/c_0}}{1 - R_0 R_l e^{-i\omega 2l/c_0}}$$
(6.109)

Comparing this with the result obtained in the previous section (Eq. 6.47), it is seen that the two become identical when $R_0 = 0$, that is when there are no reflections from the tube entrance as was assumed in the previous section. Despite this difference, in many studies of wave reflections it is found adequate to use the

¹²Spiegel MR, 1968. Mathematical handbook of Formulas and Tables. McGraw-Hill, New York.

results of primary reflections only ^{13,14,15,16}. One justification for this is that the term in the denominator of Eq. 6.109 contains the product of two reflection coefficients which usually have values, in magnitude, less than 1.0.

¹³Duan B, Zamir M, 1993. Reflection coefficients in pulsatile flow through converging junctions and the pressure distribution in a simple loop. Journal of Biomechanics 26:1439–1447.

¹⁴Duan B, Zamir M, 1995. Mechanics of wave reflections in a coronary bypass loop model: The possibility of partial flow cut-off. Journal of Biomechanics 28:567–574.

¹⁵McDonald DA, 1974. Blood flow in arteries. Edward Arnold, London.

¹⁶Milnor WR, 1989. Hemodynamics. Williams and Wilkins, Baltimore.

Chapter 7 Flow in Branching Tubes

7.1 Introduction

It seems reasonable to think of blood vessels as "tubes" because the physical principles of flow in tubes is at the core of how blood is conveyed within the body. Indeed, the study of these principles has been the declared theme of this book, and "flow in tubes" has been the language we used so far and the language we will continue to use. Yet, paradoxically, it would be a gross error to think of the arterial tree as only a system of branching tubes, a system of passive conduits.

In the design of the arterial tree biology has taken the use of fluids and fluid flow to a higher level of sophistication than that of flow in a single tube. Here, biology has used the complex pressure-flow relationships made possible by the hierarchical branching structure of the arterial tree as tools by which a seemingly passive system of tubes becomes a *living organ!*.

The notion that the arterial tree is a living organ may seem odd from the perspective of hemodynamics where, as we have seen, the governing principles of pressure and flow reside decidedly in the domains of mathematics and physics. But if the hemodynamic system is viewed more widely, and perhaps more accurately, as part of a living organism, then it should not be odd to view the arterial tree in turn as part of that biological scheme.

There is no contradiction in saying that the physical principles of flow in tubes are at the very core of hemodynamics but that these principles alone do not constitute the entire sphere of hemodynamics. They constitute only the *mechanisms* by which the principles of flow in tubes are used in the cardiovascular system to construct a living hemodynamic system. In this chapter we examine first the structure and then the dynamics of flow in arterial trees to unveil the mechanisms they provide to endow a system of branching "tubes" with the characteristics of a living organ.

7.2 Arterial Bifurcation

When we look at the way biology has dealt with the seemingly impossible task of taking blood from a single source (the heart) and delivering it *individually* to billions of blood cells within the body, what we see is not a mass of long tubes but a meticulous system of *branching* tubes. Repeatedly, we see a blood vessel dividing into two branches, then the branches in turn dividing into branches and so on, thus forming a hierarchical tree structure. Nowhere do we see two tubes running side by side toward two destinations. What we see instead is a single tube running part of the way and then bifurcating to reach the two destinations. The vascular system is indeed better described as a plethora of bifurcations rather than a plethora of tubes or vessels. Indeed, the vast number and close succession of bifurcations within the vascular tree calls into question the wide use of the terms "vessel" or "artery" because, as we shall see, the objects which these terms refer to cannot be easily defined or measured. In what follows and in the rest of this book, therefore, we shall use the terms "vessel segment" or "arterial segment" instead, to mean simply and more accurately the vascular segment between two successive bifurcations.

The branching structure of the arterial tree allows the "sharing" of vessel segments so that blood flow to each tissue cell within the body does not have to be carried individually from source to destination. *The branching tree structure eliminates the need to run tubes in parallel*. In doing so, saving occurs at each bifurcation and is multiplied many times over by the large number (billions) of bifurcations that make up the arterial tree.

Arterial "bifurcation" is thus the *kernel* or the structural unit of the arterial tree whereby typically a parent vessel segment divides into two branch segments. Data from the cardiovascular system have shown that division into more than two branches is very rare. More common are two divisions in very close succession. The three vessel segments forming a bifurcation are usually found to lie in the same plane, but a change in the orientation of this plane from one bifurcation to the next produces highly three dimensional tree structures. Also, wide variation is found in the degree of asymmetry of arterial bifurcations, that is the degree to which the two branch vessel segments are of unequal caliber, thus resulting in highly nonuniform tree structures.

There has been a great deal of work and wide ranging literature on the subject of arterial bifurcations and arterial branching dating back to the classical work of Murray in 1926. The purpose of this section is not to provide a survey of this literature but to provide a basic understanding of the subject for use in subsequent chapters. A comprehensive review of the literature is not available. For partial reviews and some references see below.^{2,3}

¹Murray CD, 1926. The physiological principle of minimum work applied to the angle of branching of arteries. Journal of General Physiology 9:835–841.

²Zamir M. The Physics of Pulsatile Flow. Springer-Verlag, New York, 2000.

³Zamir M. Vascular system of the human heart: Some branching and scaling issues. In: Brown JH, West GB (eds.). Scaling in Biology. Oxford University Press, 2000.

7.2 Arterial Bifurcation 193

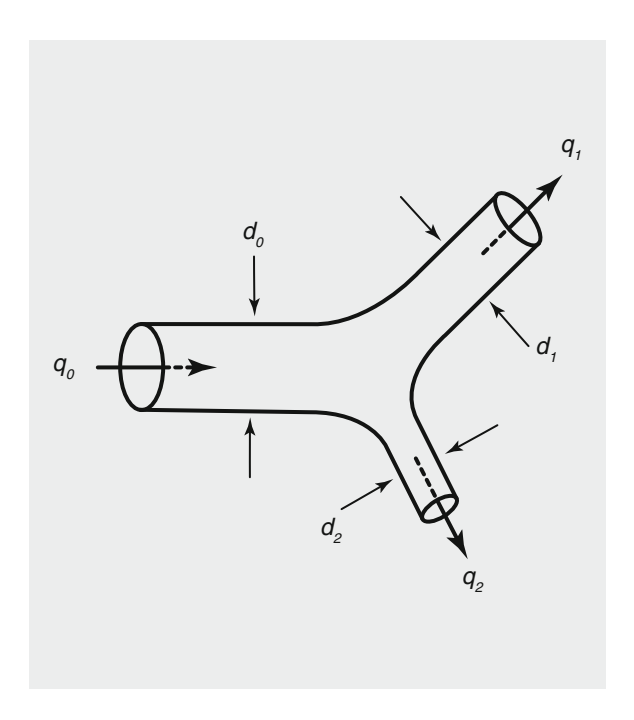


Fig. 7.1 Arterial bifurcation, the basic structural unit of an arterial tree. A parent vessel of diameter d_0 divides into two branch vessel segments of diameters d_1, d_2 . Conservation of mass requires that flow rate q_0 in the parent vessel must equal the sum of flow rates in the daughter vessels, $q_1 + q_2$. Combined with the cube law, this provides an important "optimum" relation between the 3 diameters involved, namely $d_0^3 = d_1^3 + d_2^3$.

The geometrical structure of arterial bifurcations has been found to obey physical principles which can be described mathematically and which are strongly tied to the power law relationship between the radius of a vessel segment and the flow rate which it carries as introduced by Murray in the form of the cube law (Eq. 3.11). In particular, if the radii of the parent and branch vessel segments at an arterial bifurcation are denoted by a_0, a_1, a_2 (Fig. 7.1), and if we use the convention of always taking $a_1 \ge a_2$, then a useful *bifurcation index* can be defined by

$$\alpha = \frac{a_2}{a_1} \tag{7.1}$$

The value of α then ranges conveniently between 0 and 1.0. A highly nonsymmetrical bifurcation is one for which the value of α is near zero, while a "symmetrical" bifurcation is one for which $\alpha = 1.0$.

Another important measure at an arterial bifurcation is the area ratio

$$\beta = \frac{a_1^2 + a_2^2}{a_0^2} \tag{7.2}$$

which is the ratio of the combined cross sectional area of the two daughter segments over that of the parent segment. Values of β greater than 1.0 produce expansion in the total cross sectional area available to flow as it progresses from parents to daughters and thus from one level of the vascular tree to the next.

Conservation of mass at an arterial bifurcation requires that flow rate in the parent vessel segment must equal the sum of flows in the two branch segments, thus if these rates are denoted by q_0 , q_1 , q_2 respectively, then

$$q_0 = q_1 + q_2 \tag{7.3}$$

The geometrical structure of an arterial bifurcation is then determined from an assumed power law relation between the radii of the three vessels involved and the flow rate which they carry, $(q \propto a^{\gamma})$ as in Eq. 3.98. The process is much the same as that discussed in Sect. 3.12. At first we illustrate this process by using the cube law $(\gamma = 3)$. The analysis can be extended to other values of γ in a straightforward manner as in that section. Thus, based on the cube law, Eq. 7.3 provides a relation between the radii of the three vessel segments at an arterial bifurcation, namely

$$a_0^3 = a_1^3 + a_2^3 (7.4)$$

In terms of the bifurcation index α (Eq. 7.1), this relation can be written as

$$\begin{cases} \frac{a_1}{a_0} = \frac{1}{(1+\alpha^3)^{1/3}} \\ \frac{a_2}{a_0} = \frac{\alpha}{(1+\alpha^3)^{1/3}} \end{cases}$$
 (7.5)

and substituting these into Eq. 7.2 yields a relationship between the bifurcation index and the area ratio β

$$\beta = \frac{1 + \alpha^2}{(1 + \alpha^3)^{2/3}} \tag{7.6}$$

For a symmetrical bifurcation ($\alpha = 1.0$) we find

$$\frac{a_1}{a_0} = \frac{a_2}{a_0} = 2^{-1/3} \approx 0.7937 \tag{7.7}$$

$$\beta = 2^{1/3} \approx 1.2599 \tag{7.8}$$

thus, characteristically, and based on the cube law, in the division from parent to daughters at an arterial bifurcation the vessel radii are reduced by approximately 21 % while the cross sectional area is increased by approximately 26 %.

Arterial trees are made up of a large number of repeated bifurcations to produce a large number of small vessels (arterioles, capillaries) at the delivering end of the 7.2 Arterial Bifurcation 195

tree. If the tree structure begins with a single tube segment which bifurcates again and again, each time doubling the number of segments involved, the number of such "generations" required to reach a large number of end vessels is fairly small. Only 30 generations produce over 10^9 end segments.

The total cross sectional area available to the flow generally increases at each generation, the increase being mediated by values of the area ratio β greater than 1.0 at individual bifurcations. An accepted estimate in the systemic arterial tree is that the increase in cross sectional area from the aorta to the capillaries is by a factor of about 1000.⁴ Since flow rate is equal to the average flow velocity times the cross sectional area available to the flow, the increase in cross sectional area available to the flow from the aorta to the capillaries is matched by a corresponding *decrease* in the average velocity from that in the aorta to what is needed in the capillaries in order to allow diffusion to occur across the capillary walls. If the increase in cross sectional area is assumed to occur over 30 generations in a uniform tree structure in which the value of β is the same at every bifurcation, then an estimate of that value is given by

$$\beta^{30} = 1000 \tag{7.9}$$

which yields

$$\beta = 10^{1/10} \approx 1.2589 \tag{7.10}$$

Comparing this value with that obtained from the cube law (Eq. 7.8), the closeness of the two values is quite remarkable because of the widely different considerations on which they are based.

While these results are based on the cube law and are therefore limited by the simplifying assumption on which that law is based (Sect. 3.11), they have found considerable support from biological data. If instead of the cube law a more general power law relationship between flow rate and tube radius is used (Eq. 3.98), the following results are obtained in terms of the power law index γ

$$a_0^{\gamma} = a_1^{\gamma} + a_2^{\gamma} \tag{7.11}$$

$$\begin{cases} \frac{a_1}{a_0} = \frac{1}{(1 + \alpha^{\gamma})^{1/\gamma}} \\ \frac{a_2}{a_0} = \frac{\alpha}{(1 + \alpha^{\gamma})^{1/\gamma}} \end{cases}$$
(7.12)

$$\beta = \frac{1 + \alpha^2}{(1 + \alpha^\gamma)^{2/\gamma}} \tag{7.13}$$

⁴Burton AC. Physiology and Biophysics of the Circulation. Year Book Medical Publishers, Chicago, 1965.

and for a symmetrical bifurcation ($\alpha = 1.0$)

$$\frac{a_1}{a_0} = \frac{a_2}{a_0} = 2^{-1/\gamma} \tag{7.14}$$

$$\beta = 2^{1-2/\gamma} \tag{7.15}$$

The "efficiency" or "optimality" of an arterial bifurcation lies not only in the optimality of the relationship between vessel radius and flow rate but in the optimality of *branching angles* which the two branch vessel segments make as they branch off the parent vessel segment. Specifically, at an arterial bifurcation, blood flow from point A at the upstream end of the parent vessel segment is destined to reach points B and C at the downstream ends of the two branch vessel segments (Fig. 7.2).

Instead of running two separate tubes from A to B and from A to C, the bifurcation makes it possible to share the flow from A to some junction point D and only then dividing into two separate tubes. The saving is approximately that of running only one tube from D instead of two.

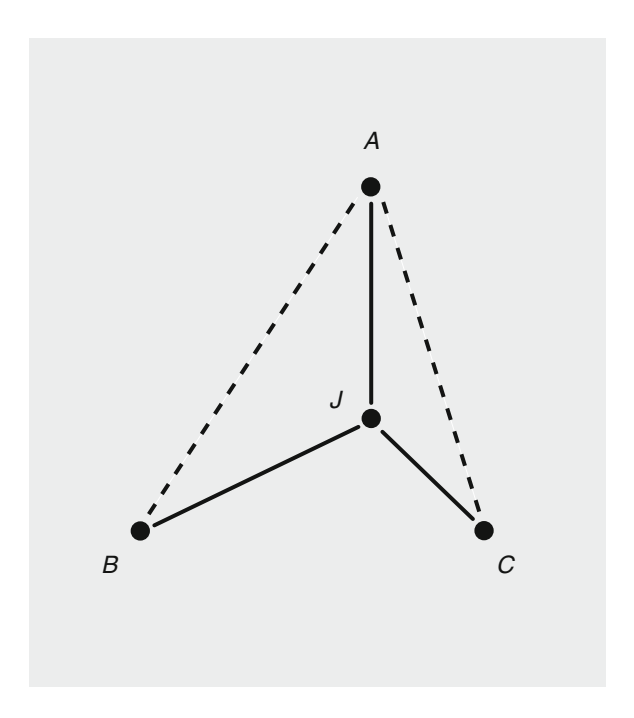


Fig. 7.2 Bifurcation principle: an arterial bifurcation makes it possible for flow from point A to reach points B and C without running two separate tubes from A to B and B. Instead, flow is "shared" from A to some junction point B before dividing into two separate tubes.

7.2 Arterial Bifurcation 197

In Poiseuille flow the power H required to drive a flow rate q through a tube of radius a is proportional to q^2a^{-4} (Eq. 3.60), and if the cube law is assumed to hold (Eq. 3.97), this gives $H \propto a^2$. Thus if the powers required to drive the flow in tubes of radii a_0, a_1, a_2 are denoted by H_0, H_1, H_2 , then the fractional difference between running two tubes of radii a_1, a_2 from A to J or only one tube of radius a_0 , is given by, in nondimensional form,

$$\frac{H_1 + H_2 - H_0}{H_0} = \frac{a_1^2 + a_2^2 - a_0^2}{a_0^2} = \beta - 1 \tag{7.16}$$

Since the value of β is generally higher than 1.0, the result is positive. If the bifurcation is symmetrical and we take $\beta \approx 1.26$ as determined by the cube law (Eq. 7.8), a saving of 26% is realized by running a single tube instead of two.

This calculation is only approximate, however, since a straight line from A to B would be shorter than one from A to D plus one from D to D, and similarly for a line from D to D. In fact to account for these differences an optimality problem must be solved for the position of the junction point D, which determines the branching angles D0, D1, which the two branch vessel segments should optimally make with the direction of the parent vessel (Fig. 7.3). It is found that in order to minimize the pumping power required to drive the flow through the junction, and based on the assumption of Poiseuille flow again, optimum branching angles are given by

$$\begin{cases}
\cos \theta_1 = \frac{(1+\alpha^3)^{4/3} + 1 - \alpha^4}{2(1+\alpha^3)^{2/3}} \\
\cos \theta_2 = \frac{(1+\alpha^3)^{4/3} + \alpha^4 - 1}{2\alpha^2(1+\alpha^3)^{2/3}}
\end{cases} (7.17)$$

These results indicate that the branch with the smaller diameter should optimally make a larger branching angle (Fig. 7.3), which is fairly well supported by observations from the cardiovascular system. In the limit of a very small branch with $\alpha \approx 0$, the results indicate that the branching angle of the larger branch is near zero while that of the smaller branch is near 90°. This again is supported by observations from the cardiovascular system and is in fact the basis of the common term "small side branch". Other optimality principles for branching angles have been used and have produced qualitatively similar results.

⁵Murray CD, 1926. The physiological principle of minimum work applied to the angle of branching of arteries. Journal of General Physiology 9:835–841.

⁶Zamir M, 1978. Nonsymmetrical bifurcations in arterial branching. Journal of General Physiology 72:837–845.

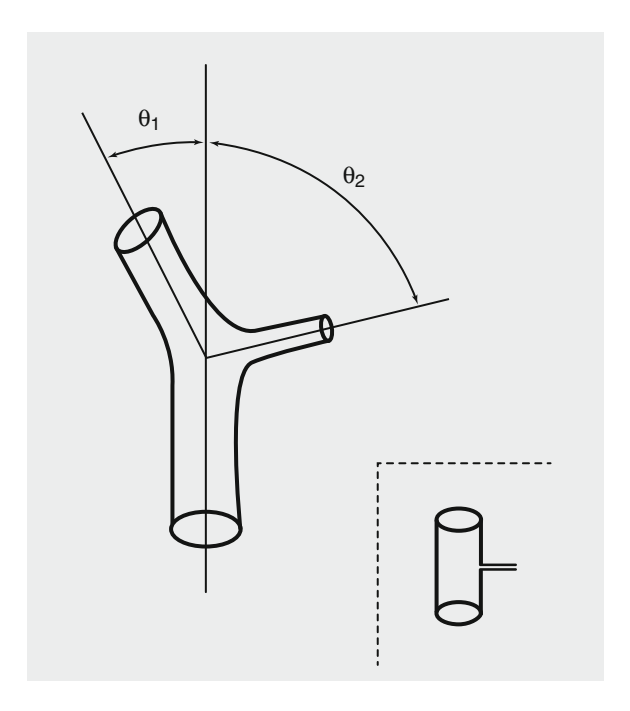


Fig. 7.3 Optimum branching angles. The fluid dynamic efficiency of an arterial bifurcation is affected by the angles at which the two daughter vessels "branch off". Optimally the larger branch makes a smaller branching angle than the smaller branch. In the limit, a small "side branch" comes off at almost 90° while the branching angle of the larger branch is close to zero (*inset*).

7.3 Steady Flow Along Tubes in Series

As a prelude to flow in a sequence of tubes in series, consider flow in a single tube at first, in which we set a coordinate x along the axis of the tube, being zero at the entrance and positive in the direction of the flow. In contrast with the analysis in Sect. 3.8 where flow q is expressed in terms of a pressure difference Δp between the two ends of the tube, the aim here is to consider both the flow and pressure as being functions of position x along the tube, as shown in Fig. 7.4.

To do this we use Eqs. 3.23 and 3.43 to write

$$\frac{dp}{dx} = -\left(\frac{8\mu}{\pi a^4}\right)q\tag{7.18}$$

which, upon integration, gives

$$p(x) = p(0) - \left(\frac{8\mu}{\pi a^4}\right) qx \tag{7.19}$$

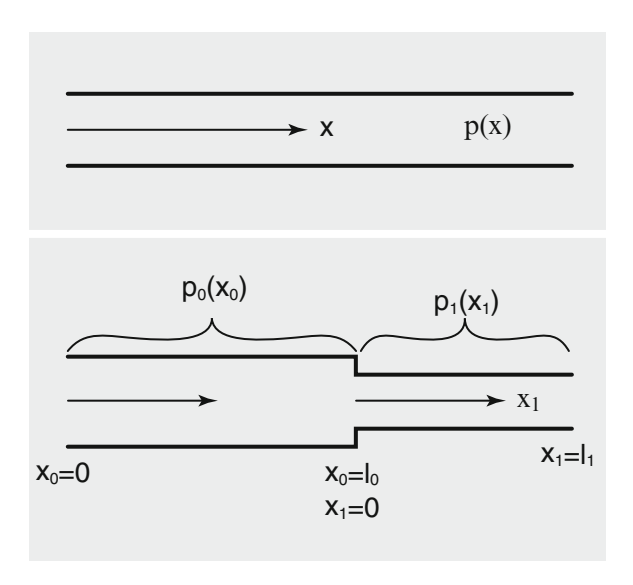


Fig. 7.4 In unlumped-model analysis the pressure p in a tube is considered as a function of streamwise position coordinate x measured from the tube entrance. In a sequence of tube segments in series, the pressure and the position coordinate are re-defined in each tube segment and are confined to that tube only.

where p(0) is the pressure at the tube entrance (x = 0), a is the tube radius and μ is the viscosity of the fluid. If the tube length is l, then the pressure at the other end of the tube is

$$p(l) = p(0) - \left(\frac{8\mu}{\pi a^4}\right) q l \tag{7.20}$$

which is the same as the result obtained in Sect. 3.8, noting that in that section (Eqs. 3.28 and 3.29) a constant pressure gradient was used, defined by

$$k = -\frac{\Delta p}{l} = \frac{p(l) - p(0)}{l} \tag{7.21}$$

The main focus in this section is on Eq. 7.19 in which the pressure is seen as a function of position x, and on using this equation to track the pressure distribution in a system of tubes. For this purpose, consider only two tube segments in series at first, to be identified by subscripts 0 and 1. Allowing the lengths and radii of the two segments to be different but using the same flow rate, then Eq. 7.19 gives

$$\begin{cases} p_0(x_0) = p_0(0) - \left(\frac{8\mu}{\pi a_0^4}\right) q x_0 \\ p_1(x_1) = p_1(0) - \left(\frac{8\mu}{\pi a_1^4}\right) q x_1 \\ \vdots \\ p_n(x_n) = p_n(0) - \left(\frac{8\mu}{\pi a_n^4}\right) q x_n \end{cases}$$
(7.22)

where x_0 and $p_0(x_0)$ are the streamwise coordinate and corresponding pressure in the first tube only, and similarly for the second tube identified by subscript 1, and subsequent tubes identified by subscripts $2, 3 \cdots n$, as illustrated in Fig. 7.4. In these expressions we are clearly assuming that the idealized conditions of Poiseuille flow prevail along the full length of each tube segment, neglecting deviations from these conditions at entry and exit regions and at the junction between two tube segments. Thus, the results to follow will be inaccurate *locally* in these regions, but our interest here and in subsequent sections is primarily in the global pressure distribution along a large number of tube segments connected in series or in a branching pattern.

It is important to note that the domain of p_0 is restricted to the first tube segment only, and the domain of p_1 is restricted to the second tube segment only. Thus, p_1 is a function of x_1 only, and $p_1(0)$ is therefore the value of p_1 at $x_1 = 0$ with no ambiguity. Similarly, p_0 is a function of x_0 only, and $p_0(0)$ and $p_0(l_0)$ are values of p_0 at $x_0 = 0$ and at $x_0 = l_0$, respectively, again without ambiguity.

Accordingly, the junction between the first two tube segments occurs at $x_0 = l_0$ or $x_1 = 0$, and the junction between the second and third tubes occurs at $x_1 = l_0$ or $x_2 = 0$, etc., and on the assumption of pressure continuity at each junction, we have

$$\begin{cases} p_1(0) = p_0(l_0) \\ p_2(0) = p_1(l_1) \\ \vdots \\ p_n(0) = p_{n-1}(l_{n-1}) \end{cases}$$
(7.23)

It is convenient to put these expressions in normalized form, using properties of the first tube segment as reference properties. Thus the pressures everywhere are referred to the initial input pressure $p_0(0)$, and the pressure drop in the first tube segment from Eq. 7.22

$$\Delta p_0 = p_0(0) - p_0(l_0)$$

$$= \left(\frac{8\mu}{\pi a_0^4}\right) q l_0$$
(7.24)

is used to define a normalized form of the pressure in each tube segment, namely

$$P(x) = \frac{p(x) - p_0(0)}{\Delta p_0} \tag{7.25}$$

In addition, the position coordinates in each tube segment are normalized by writing

$$\begin{cases}
X_0 = x_0/l_0 \\
X_1 = x_1/l_1 \\
\vdots \\
X_n = x_n/l_n
\end{cases}$$
(7.26)

so that, in terms of the new position coordinate X, the normalized length of each tube segment is now 1.0.

Thus, the pressure distributions in Eq. 7.22 can now be put in normalized form

$$P_0(X_0) = \frac{p_0(x_0) - p_0(0)}{\Delta p_0}$$

$$= -\left(\frac{a_0}{a_0}\right)^4 \left(\frac{x_0}{l_0}\right)$$

$$= -X_0 \tag{7.27}$$

with

$$P_0(1) = \frac{p_0(l_0) - p_0(0)}{\Delta p_0}$$

$$= -1 \tag{7.28}$$

Similarly, for the pressure distribution in the second tube in normalized form, using Eq. 7.22 and the result in Eq. 7.28, we have

$$P_{1}(X_{1}) = \frac{p_{1}(x_{1}) - p_{0}(0)}{\Delta p_{0}}$$

$$= \frac{p_{1}(x_{1}) - p_{1}(0)}{\Delta p_{0}} + \frac{p_{1}(0) - p_{0}(0)}{\Delta p_{0}}$$

$$= \frac{p_{0}(l_{0}) - p_{0}(0)}{|\Delta p_{0}|} - \left(\frac{a_{0}}{a_{1}}\right)^{4} \left(\frac{x_{1}}{l_{0}}\right)$$

$$= -1 - \left(\frac{a_{0}}{a_{1}}\right)^{4} \left(\frac{l_{1}}{l_{0}}\right) X_{1}$$
(7.29)

with

$$P_{1}(l_{1}) = \frac{p_{1}(l_{1}) - p_{0}(0)}{\Delta p_{0}}$$

$$= -1 - \left(\frac{a_{0}}{a_{1}}\right)^{4} \left(\frac{l_{1}}{l_{0}}\right)$$
(7.30)

An iterative pattern is thus established:

$$P_{2}(X_{2}) = -1 - \left(\frac{a_{0}}{a_{1}}\right)^{4} \left(\frac{l_{1}}{l_{0}}\right) - \left(\frac{a_{0}}{a_{2}}\right)^{4} \left(\frac{l_{2}}{l_{0}}\right) X_{2}$$

$$P_{3}(X_{3}) = -1 - \left(\frac{a_{0}}{a_{1}}\right)^{4} \left(\frac{l_{1}}{l_{0}}\right) - \left(\frac{a_{0}}{a_{2}}\right)^{4} \left(\frac{l_{2}}{l_{0}}\right)$$

$$- \left(\frac{a_{0}}{a_{3}}\right)^{4} \left(\frac{l_{3}}{l_{0}}\right) X_{3}$$

$$(7.32)$$

and in general

$$P_{n}(X_{n}) = -1 - \left(\frac{a_{0}}{a_{1}}\right)^{4} \left(\frac{l_{1}}{l_{0}}\right) - \left(\frac{a_{0}}{a_{2}}\right)^{4} \left(\frac{l_{2}}{l_{0}}\right) - \dots$$

$$- \left(\frac{a_{0}}{a_{n}}\right)^{4} \left(\frac{l_{n}}{l_{0}}\right) X_{n}$$
(7.33)

The results indicate that in this convenient normalized form, the pressure distribution along a sequence of tube segments in series consists of a series of linear pressure drops, with the pressure starting from a normalized value of 0 at entry and dropping linearly to -1 at the end of the first tube. Subsequent values of the pressure depend on the lengths and diameters of subsequent tubes.

If, for the purpose of illustration, it is assumed that the tube lengths are proportional to their diameters, the pressure distribution in each tube segment becomes dependent on the ratios of radii only, namely

$$\begin{cases} P_0(X_0) = -X_0 \\ P_1(X_1) = -1 - \left(\frac{a_0}{a_1}\right)^3 X_1 \\ P_2(X_2) = -1 - \left(\frac{a_0}{a_1}\right)^3 - \left(\frac{a_0}{a_2}\right)^3 X_2 \\ \vdots \\ P_n(X_n) = -1 - \left(\frac{a_0}{a_1}\right)^3 - \left(\frac{a_0}{a_2}\right)^3 - \dots - \left(\frac{a_0}{a_n}\right)^3 X_n \end{cases}$$
(7.34)

If it is assumed further, for the purpose of illustration again, and for reasons to become apparent in the next section, that the radii of successive tube segments are *diminishing* such that

$$\frac{a_0}{a_1} = \frac{a_1}{a_2} = \frac{a_2}{a_3} \dots = 2^{1/3} \tag{7.35}$$

then these results become

$$\begin{cases} P_0(X_0) = -X_0 \\ P_1(X_1) = -1 - 2^1 X_1 \\ P_2(X_2) = -1 - 2^1 - 2^2 X_2 \\ \vdots \\ P_n(X_n) = -1 - 2^1 - 2^2 - \dots - 2^n X_n \end{cases}$$
 (7.36)

and if, for the purpose of comparison, the radii of successive tube segments are *increasing*, such that

$$\frac{a_0}{a_1} = \frac{a_1}{a_2} = \frac{a_2}{a_3} \dots = \left(\frac{1}{2}\right)^{1/3} \tag{7.37}$$

we find

$$\begin{cases} P_0(X_0) = -X_0 \\ P_1(X_1) = -1 - \left(\frac{1}{2}\right)^1 X_1 \\ P_2(X_2) = -1 - \left(\frac{1}{2}\right)^1 - \left(\frac{1}{2}\right)^2 X_2 \\ \vdots \\ P_n(X_n) = -1 - \left(\frac{1}{2}\right)^1 - \left(\frac{1}{2}\right)^2 - \dots - \left(\frac{1}{2}\right)^n X_n \end{cases}$$
(7.38)

Finally, in the trivial case where successive tube segments have the same diameters, the results are

$$\begin{cases} P_0(X_0) = -X_0 \\ P_1(X_1) = -1 - X_1 \\ P_2(X_2) = -1 - 1 - X_2 \\ \vdots \\ P_n(X_n) = -1 - 1 - 1 - \dots - X_n \end{cases}$$
(7.39)

These results are illustrated graphically in Fig. 7.5, where it is seen that the above trivial case serves as a good reference in which the pressure distribution in each tube segment is linear and dropping by the same (normalized) amount of -1.

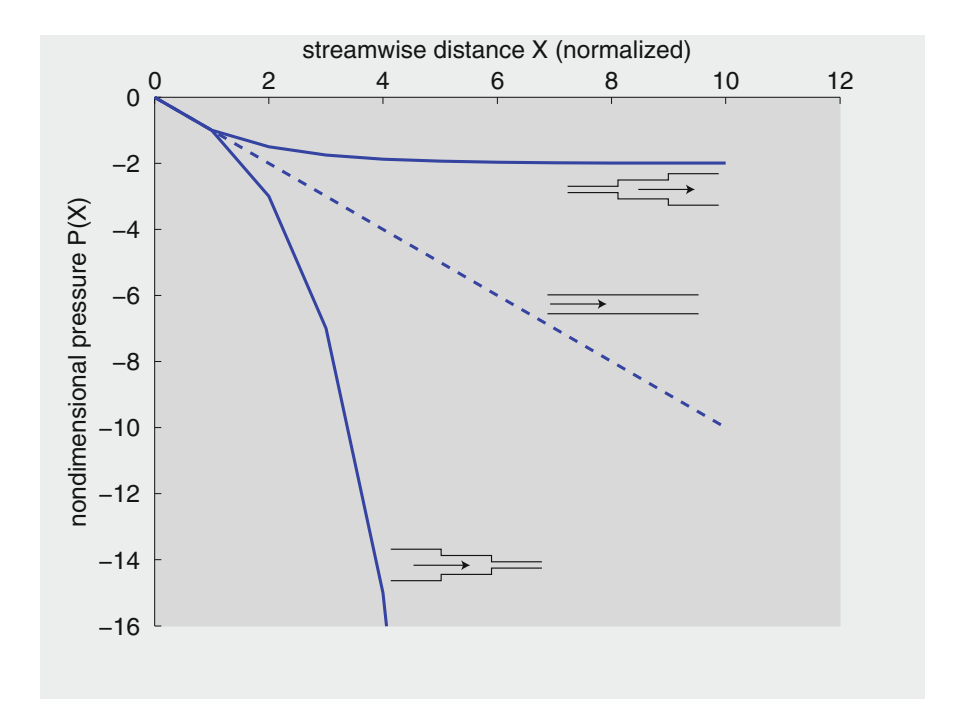


Fig. 7.5 Pressure distribution in steady flow along a sequence of tube segments in series. The streamwise distance X here is a *cumulative* coordinate along the sequence of tube segments whereby the normalized length of each tube segment is 1.0. Thus, the first tube segment extends from X = 0 to X = 1.0, the second extends from X = 1.0 to X = 2.0, etc. If the radii of successive tube segments are increasing, the pressure drops very rapidly, while if the radii are decreasing the pressure drops very slowly. In the trivial case where the radii of successive tube segments remain unchanged, the pressure drops by the same amount (-1.0) in each tube segment, with this case serving as a useful reference for comparison.

In the case where the radii of successive tube segments are diminishing, the drops in pressure in successive segments increase very rapidly, and the reverse happens when the radii of successive tube segments are increasing. While these examples are fairly artificial, they serve as useful guides when considering branching tubes.

7.4 Steady Flow Through a Bifurcation

The concept of "arterial bifurcation" as the main building block of the arterial tree was introduced in Sect. 7.2. In this section we consider the properties of steady flow through a bifurcation, being modeled, as in that section, by three tube segments as shown schematically in Fig. 7.6. Subscripts 0, 1, 2 are used to identify the parent and the two branch segments, respectively, as shown in the figure, with the convention that subscript 1 shall always be used to identify the branch with the larger diameter.

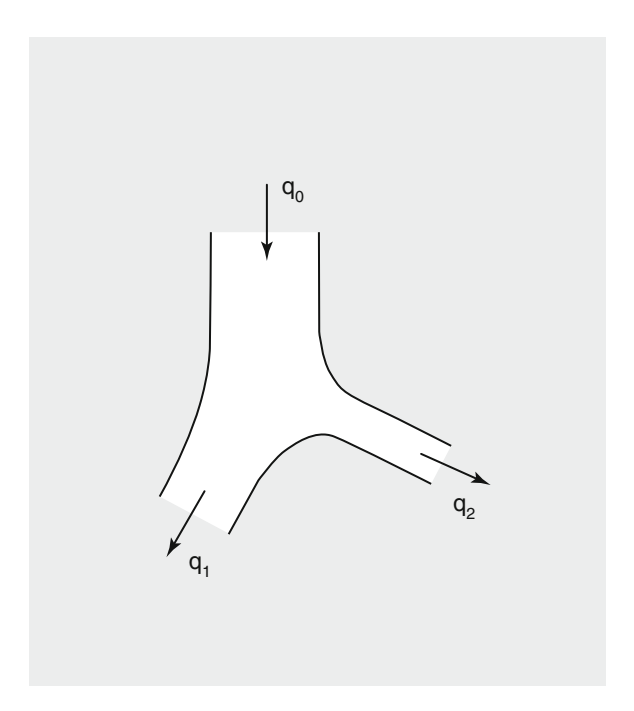


Fig. 7.6 Arterial trees in the cardiovascular system are formed largely by repeated bifurcations whereby a vessel segment divides into two branches and then each of the branches in turn divides into two branches, etc. An arterial bifurcation is shown here schematically, with the parent vessel identified by subscript 0 and the two branches by subscripts 1, 2, with the convention that subscript 1 is always reserved for the branch with the larger radius. Flow rate q_0 in the parent vessel is divided into q_1, q_2 in the branches.

With the flow being from parent to branches, conservation of mass requires that flow rate q_0 in the parent vessel be equal to the sum of the flow rates in the two branches, that is $q_0 = q_1 + q_2$, as in Eq. 7.3.

The pressure distribution under conditions of steady flow through the bifurcation can be considered by following two separate streamwise paths: one from parent to branch-1 and another from parent to branch-2. Along each path the situation is the same as that of two tubes in series, as considered in the previous section. It is important to emphasize again that here too we assume that the idealized conditions of fully developed Poiseuille flow prevail along the full length of each tube segment, ignoring local deviations at the two ends of each segment. The justification for this is that we are interested primarily in the pressure distribution along the tubes forming the bifurcation rather than in the local details of the flow field within the bifurcation. The only difference here is that, because of flow division, the flow rates in consecutive tube segments are not the same.

The pressure distribution along the path from the root segment to the first branch, and the path from the root segment to the second branch, we may then return to Eq. 7.22 in the previous section and, using the same notation as in that section, write

$$\begin{cases} p_0(x_0) = p_0(0) - \left(\frac{8\mu}{\pi a_0^4}\right) q_0 x_0 \\ p_1(x_1) = p_1(0) - \left(\frac{8\mu}{\pi a_1^4}\right) q_1 x_1 \\ p_2(x_2) = p_2(0) - \left(\frac{8\mu}{\pi a_2^4}\right) q_2 x_2 \end{cases}$$
 (7.40)

and for pressure continuity at the junction of the three tubes

$$p_0(l_0) = p_1(0) = p_2(0)$$
 (7.41)

thus the pressure distributions in the three tubes forming the bifurcation (Eq. 7.40) become

$$\begin{cases} p_0(x_0) = p_0(0) - \left(\frac{8\mu}{\pi a_0^4}\right) q_0 x_0 \\ p_1(x_1) = p_0(l_0) - \left(\frac{8\mu}{\pi a_1^4}\right) q_1 x_1 \\ p_2(x_2) = p_0(l_0) - \left(\frac{8\mu}{\pi a_2^4}\right) q_2 x_2 \end{cases}$$
(7.42)

The lengths of the three vessel segments can be normalized by writing

$$\begin{cases}
X_0 = x_0/l_0 \\
X_1 = x_1/l_1 \\
X_2 = x_2/l_2
\end{cases}$$
(7.43)

In terms of these coordinates, the normalized length of each of the three vessel segments is now 1.0, which, as we see shortly, is useful for plotting the pressure distributions along the paths to the two branches using the same scale regardless of their different lengths. Furthermore, these pressure distributions can now be put in normalized form by using the properties of the parent tube segment as reference properties. In particular, the pressure drop in the parent tube segment, namely

$$\Delta p_0 = p_0(0) - p_0(l_0)$$

$$= \frac{8\mu}{\pi a_0^4} q_0 l_0 \tag{7.44}$$

is used to put the pressure distributions in Eq. 7.42 in nondimensional form. Following the same steps as in the previous section and omitting the details, we find

$$\begin{cases} P_0(X_0) = -X_0 \\ P_1(X_1) = -1 - \left(\frac{a_0}{a_1}\right)^4 \left(\frac{q_1}{q_0}\right) \left(\frac{l_1}{l_0}\right) X_1 \\ P_2(X_2) = -1 - \left(\frac{a_0}{a_2}\right)^4 \left(\frac{q_2}{q_0}\right) \left(\frac{l_2}{l_0}\right) X_2 \end{cases}$$
(7.45)

If for the purpose of illustration it is assumed that the vessel lengths are proportional to their radii, the pressure distributions in the three tube segments become

$$\begin{cases} P_0(X_0) = -X_0 \\ P_1(X_1) = -1 - \left(\frac{a_0}{a_1}\right)^3 \left(\frac{q_1}{q_0}\right) X_1 \\ P_2(X_2) = -1 - \left(\frac{a_0}{a_2}\right)^3 \left(\frac{q_2}{q_0}\right) X_2 \end{cases}$$
 (7.46)

Furthermore, as discussed in Sect. 3.11, it is generally suspected on theoretical grounds that a power law relation exists between the radius of a blood vessel and the flow rate which the vessel normally carries, that is, as in Eq. 3.98,

$$a \sim a^{\gamma}$$

If this relation is used, the pressure distributions in Eq. 7.46 become

$$\begin{cases} P_0(X_0) = -X_0 \\ P_1(X_1) = -1 - \left(\frac{a_0}{a_1}\right)^{3-\gamma} X_1 \\ P_2(X_2) = -1 - \left(\frac{a_0}{a_2}\right)^{3-\gamma} X_2 \end{cases}$$
 (7.47)

As discussed in Sect. 3.11, the power law relation in Eq. 3.98 also provides a relation between the radii of the three tubes at a bifurcation, namely

$$a_0^{\gamma} = a_1^{\gamma} + a_2^{\gamma} \tag{7.48}$$

Essentially, this relation dictates that if one branch at a bifurcation has a comparatively large radius then the other must have a comparatively small one. This is clearly a reflection of the conservation of mass requirement namely that if one branch carries a relatively larger proportion of the flow rate then the other must carry a correspondingly small proportion. As in Sect. 3.11 we introduce a "bifurcation index"

$$\alpha = \frac{a_2}{a_1} \tag{7.49}$$

Recalling that by convention branch-1 is taken as the branch with the larger radius, except when the two radii are equal, this index is a measure of the asymmetry of a bifurcation in terms of the relative radii of its two branches. Its value is 1.0 when the bifurcation is perfectly symmetrical, meaning that its two branches have the same radii, and close to zero when the bifurcation is highly asymmetrical, meaning that one of the two branches has a much larger radius than the other. Thus α has the convenient range of values of 0–1.0 for the entire spectrum of possible bifurcations.

The relation between the three radii in Eq. 7.48, upon division by a_1 or a_2 , can be put in terms of the bifurcation index α , that is

$$\begin{cases} \frac{a_0}{a_1} = (1 + \alpha^{\gamma})^{1/\gamma} \\ \frac{a_0}{a_2} = \left(\frac{1 + \alpha^{\gamma}}{\alpha^{\gamma}}\right)^{1/\gamma} \end{cases}$$
(7.50)

Using these in diameter ratios in Eq. 7.47, finally, the pressure distributions become

$$\begin{cases}
P_0(X_0) = -X_0 \\
P_1(X_1) = -1 - \left\{ (1 + \alpha^{\gamma})^{-1 + 3/\gamma} \right\} X_1 \\
P_2(X_2) = -1 - \left\{ \left(\frac{1 + \alpha^{\gamma}}{\alpha^{\gamma}} \right)^{-1 + 3/\gamma} \right\} X_2
\end{cases} (7.51)$$

A considerable volume of work on arterial branching has gone into analysis of the optimal design of arterial bifurcations which, as we see here, depends primarily on the value of the power law index γ in the relation between the radius of a vessel and the flow rate which that vessel normally carries (Eq. 3.98). Three values in particular were considered on theoretical grounds, namely $\gamma=2,3,4$, while vessel diameters actually measured in the cardiovascular system have produced values of γ highly scattered within and beyond this theoretical range.^{7,8}

A key consideration in determining the "optimum" value of γ is the shear stress τ_w which blood flow exerts on endothelial tissue and which under the idealized conditions of Poiseuille flow (Eq. 3.50) is given by

$$\tau_w = \frac{4\mu}{\pi} \left(\frac{q}{a^3} \right) \tag{7.52}$$

or in terms of the pressure drop (Eq. 3.49), to give

$$\tau_w = \frac{\Delta p}{2} \left(\frac{a}{I} \right) \tag{7.53}$$

where Δp is the pressure drop along the tube length l, as defined in Eq. 3.28.

The first of these results indicates that if a power law relation exists between the radius of a vessel and the flow rate which the vessel carries, then the shear stress in vessels of different radii would vary as

$$\tau_w \sim a^{\gamma - 3} \tag{7.54}$$

If the value of γ is less than 3, the shear stress will be *higher* in vessels of smaller radii, which clearly cannot be supported on physiological grounds. If the value of γ is more than 3, the shear stress will be lower in vessels of smaller radii, which is more plausible on physiological grounds. But if the value of γ is equal to 3 (cube law), the shear stress in Eq. 7.52 will be altogether independent of the radius α , which means that the shear stress will be the same in vessels of different radii.

⁷Zamir M, 1999. On fractal properties of arterial trees. J Theor Biol 197:517–526.

⁸Zamir M. Vascular system of the human heart: Some branching and scaling issues. In: Brown JH, West GB (eds.). Scaling in Biology. Oxford University Press, 2000.

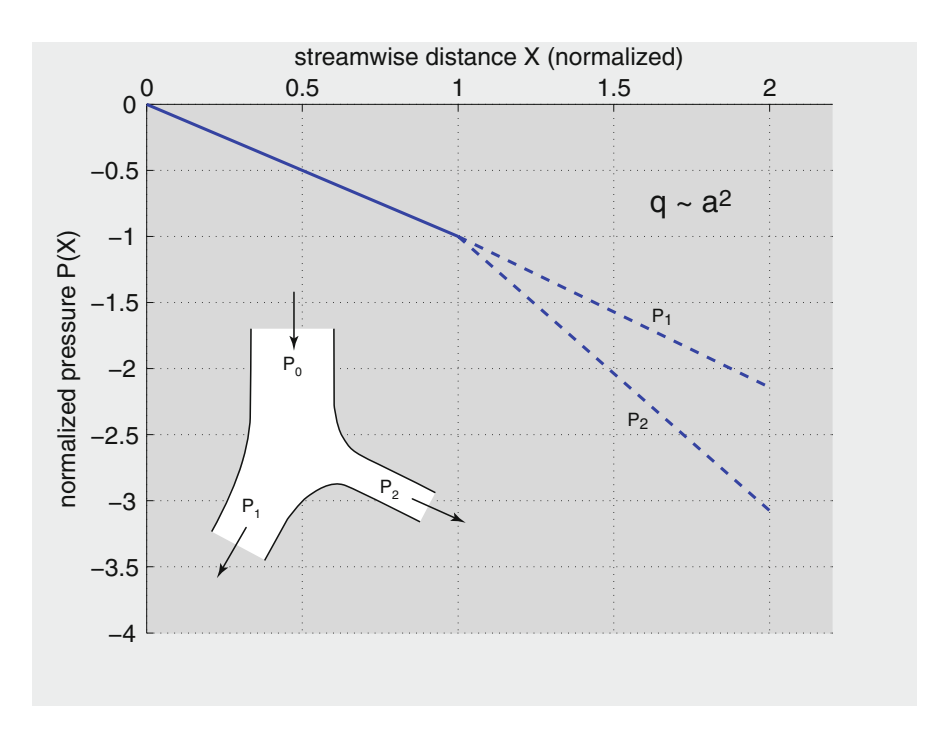


Fig. 7.7 Pressure distributions within the three vessel segments forming an arterial bifurcation, under the idealized conditions of steady Poiseuille flow and on the assumption of a power law relation between the radius of each vessel and the flow rate through it. If the power law index is less than 3, as it is here, the pressure drop in the branch with the smaller radius (branch-2) is higher than that in the other branch.

Of interest in the present context is the second of the above results, namely that in Eq. 7.53, which indicates that if the length of a vessel is assumed to be proportional to its radius then the pressure drop becomes proportional to the shear stress, and hence everything that has been said above about the shear stress now applies equally to the pressure drop. In particular, for the two branches at a bifurcation, if the value of γ is more than 3, the pressure drop along the branch with the smaller radius is lower than that along the branch with the larger radius. This is somewhat unlikely on physiological or fluid dynamic grounds. On the other hand, if the value of γ is less than 3, the reverse is true, which is more plausible on both grounds. If the value of γ is equal to 3, the pressure drop is the same along both branches. These results are illustrated in Figs. 7.7, 7.8 and 7.9.

The foregoing discussion leads to an interesting conundrum. From the point of view of the shear stress acting on endothelial tissue, the more likely values of γ are 3 or higher, but from the point of view of pressure drop the more likely values are 3 or lower. The only possible compromise between these two requirements is clearly $\gamma=3$, which lends further theoretical support to the cube law. As stated earlier, values of γ based on actual measurements from the cardiovascular system have

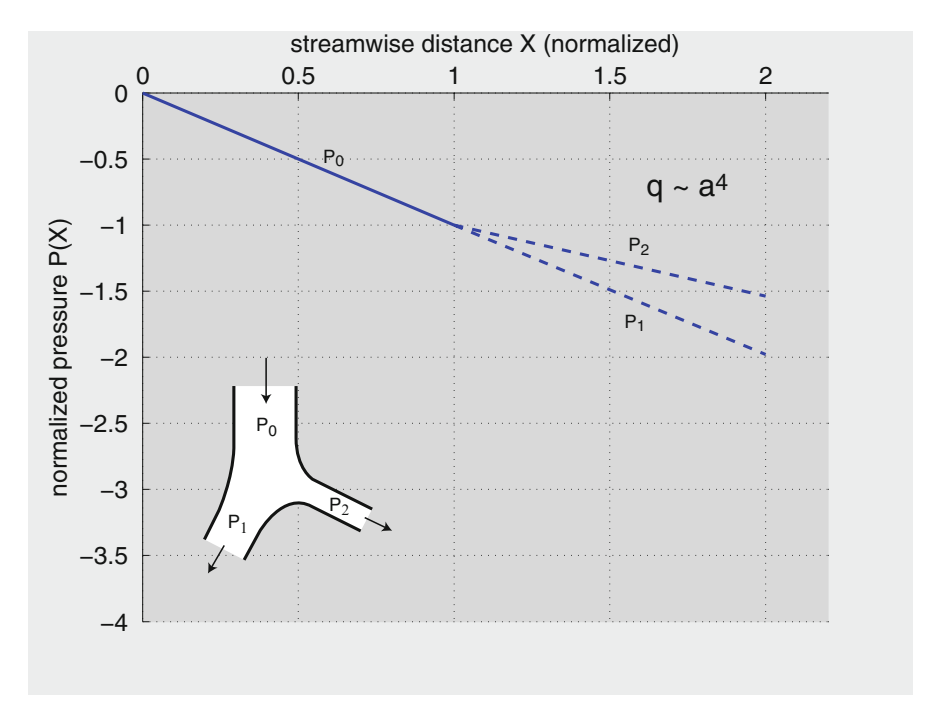


Fig. 7.8 Pressure distributions within the three vessel segments forming an arterial bifurcation, under the idealized conditions of steady Poiseuille flow and on the assumption of a power law relation between the radius of each vessel and the flow rate through it. If the power law index is more than 3, as it is here, the pressure drop in the branch with the smaller radius (branch-2) is lower than that in the other branch.

shown much scatter not only within the range of 2–4 but also outside this range. The scatter, however, is generally found to center around the value $\gamma = 3$.

7.5 Branching Tubes: j, k Notation

Considerations underlying the concept of branching tubes were discussed in Sects. 3.12 and 7.2. Briefly, a system in which the flow to multiple destinations starts out in a single tube and then divides repeatedly as it approaches these destinations is the only practical (and efficient) way for blood flow to reach billions of cells within the body.

Indeed, arterial trees are generally found to consist of a succession of bifurcations whereby a root vessel segment divides into two branches, then each of the branches

⁹Zamir M. Vascular system of the human heart: Some branching and scaling issues. In: Brown JH, West GB (eds.). Scaling in Biology. Oxford University Press, 2000.

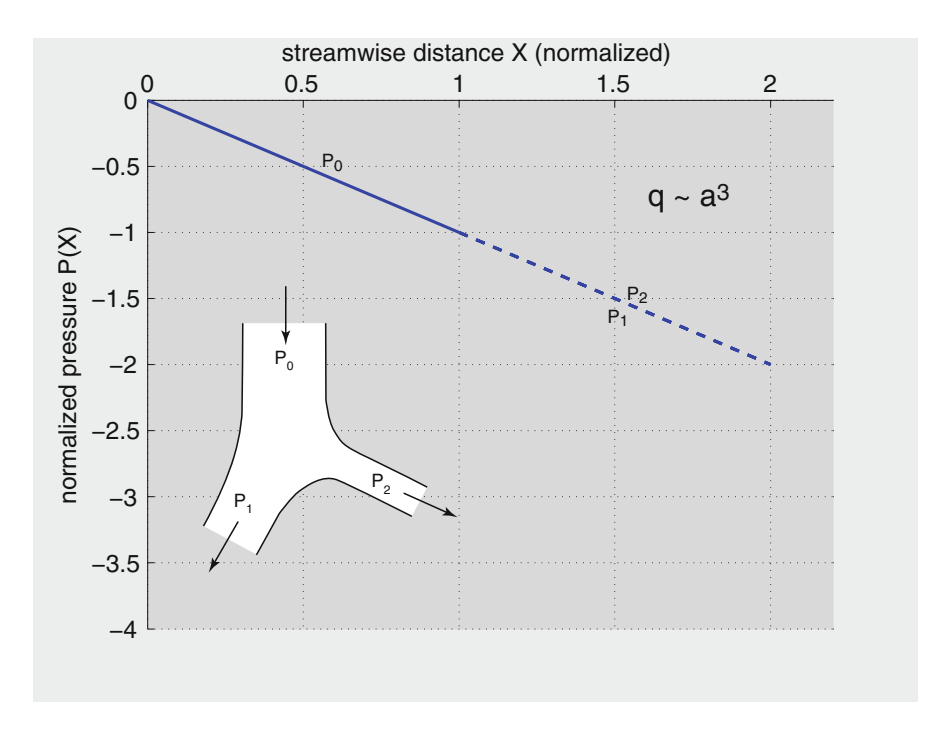


Fig. 7.9 Pressure distributions within the three vessel segments forming an arterial bifurcation, under the idealized conditions of steady Poiseuille flow and on the assumption of a power law relation between the radius of each vessel and the flow rate through it. If the power law index is equal to 3, as it is here, the pressure drop is the same along both branches.

in turn divides into two branches, etc. The "symmetry" of each bifurcation, that is the relative radii of the two branches, is measured by the bifurcation index $\alpha = a_2/a_1$ introduced in the previous section, where a_1, a_2 are radii of the two branches, subscript 1 being reserved by convention to the branch with the larger radius. The branching process is illustrated schematically in Fig. 7.10 where $\alpha = 1.0$ and in Fig. 7.11 where $\alpha = 0.7$. An 11-level tree with $\alpha = 0.7$ is shown in Fig. 7.12

In each case, the value of the bifurcation index α is the same at every bifurcation within the tree structure, thus producing a degree of uniformity which is *not* characteristic of arterial trees in the cardiovascular system. Instead, it is found that the value of α varies widely throughout the tree.^{10,11}

In order to deal with a general branching tree structure, the notation of a single bifurcation used in the previous section must clearly be generalized to cater for a

¹⁰Kassab GS, Rider CA, Tang NJ, Fung YC, Bloor CM, 1993. Morphometry of pig coronary arterial trees. American Journal of Physiology 265:H350–H365.

¹¹Zamir M, 1999. On fractal properties of arterial trees. Journal of Theoretical Biology 197:517–526.

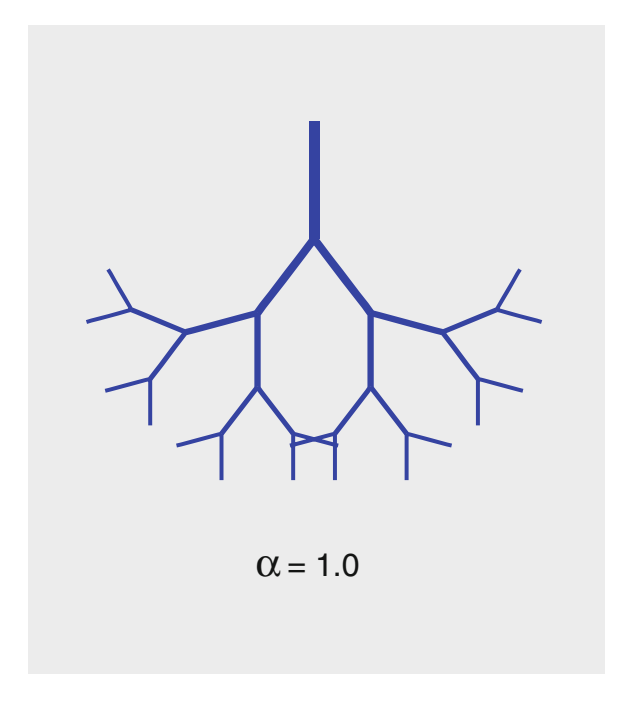


Fig. 7.10 A 5-level branching tree structure in which the value of the bifurcation index α is 1.0, which means that the two branches at each bifurcation along the tree structure have the same radius.

sequence of consecutive bifurcations and a much larger number of branches. In fact, the term "branches" used in the previous section to identify the two branch tube segments at a bifurcation is no longer adequate here because most vessel segments within a tree structure are both parents and branches. The only tube segments that can be identified by name here are the root segment and the terminal branch segments, and we shall continue to use that terminology for these segments.

For general notation throughout the tree structure, however, this descriptive scheme is rather inadequate and a more analytic scheme is required. For this purpose we note that each tube segment within a hierarchical tree structure has a unique position within that structure in terms of the generation or "level" of the tree in which it is located and in terms of its sequential position among other tube segments at that level. The terms "level" and "generation" are used interchangeably in this context and we shall follow this practice.

If the generation at which a vessel segment is situated within a tree structure is denoted by 'j', and its sequential position within that generation is denoted by 'k', then it is appropriate to treat (j, k) as *position coordinates* of a vessel segment within the tree structure. Only two numbers are then required to identify the position of any vessel segment within the tree structure, as illustrated in Fig. 7.13

The convention used in previous sections to designate branch-1 as the branch with the larger radius at a bifurcation can also be extended. Here we note that a tube

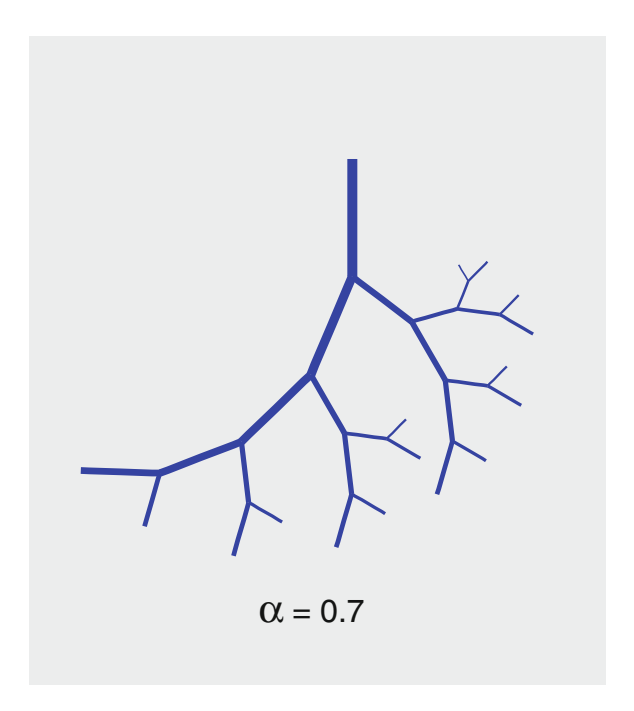


Fig. 7.11 A 5-level branching tree as in Fig. 7.10 but with $\alpha = 0.7$.

segment with position coordinates j, k in general has two branches with position coordinates (j+1, 2k-1) and j+1, 2k. The k-coordinate of the first of these (2k-1) is an *odd* number while that of the second (2k) is an *even* number. Thus, to generalize the convention of the previous sections we reserve the odd k-coordinate at each bifurcation for the branch segment with the larger radius and the even k-coordinate for the branch with the smaller radius. An application of this scheme to the 5-level tree structure is illustrated in Fig. 7.14.

It is important to emphasize that vascular trees within the cardiovascular system are neither as uniform nor as complete as the tree shown in Fig. 7.14. That is, vascular trees within the cardiovascular system rarely have the same value of the bifurcation index at each bifurcation, and they rarely have every coordinate position (j,k) occupied. The latter occurs because some paths reach the capillary level in a smaller number of generations than others as will be discussed in Sect. 7.7. An advantage of the j,k notation system is that the coordinates of occupied positions within a tree structure are not altered by any unoccupied positions within that tree. This has an important practical example when trees from the cardiovascular system are studied by casting or imaging where, invariably, some branches are lost in the process. The j,k coordinates of the remaining vessel segments within the vascular tree are unaltered by the missing branches because the coordinates of each vessel segment are determined only by its parent as shown in Figs. 7.13 and 7.14.

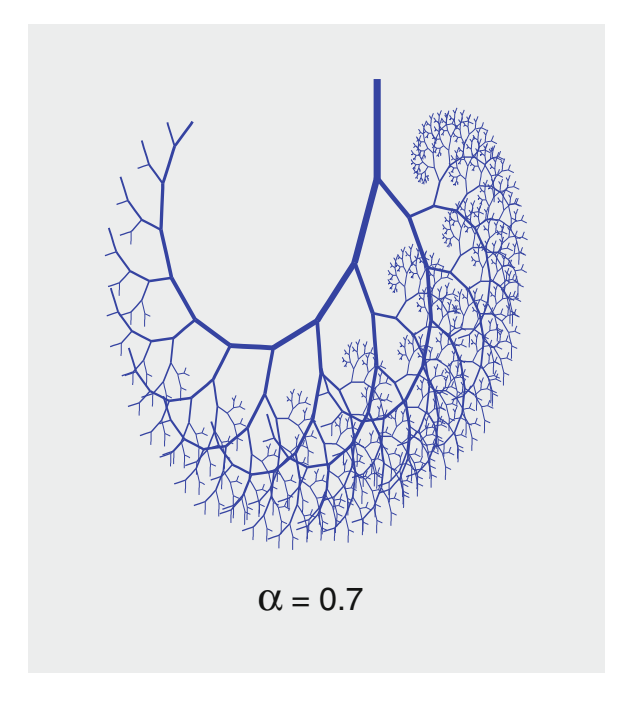


Fig. 7.12 An 11-level branching tree as in with $\alpha = 0.7$.

Finally, the j, k notation provides a simple way of navigating through the hierarchical structure of a branching tree. Thus, as illustrated in Fig. 7.13, to move from a parent tube segment (j, k) to its two branches, we have

$$parent(j, k) \rightarrow branch1(j + 1, 2k - 1), branch2(j + 1, 2k)$$
 (7.55)

and to move from a branch segment (j, k) to its parent, we have

$$\mathbf{branch}(j,k) \to \mathbf{parent}(j-1,\frac{k+1}{2}) \quad if \ k \ is \ odd \tag{7.56}$$

$$or \rightarrow \mathbf{parent}(j-1, \frac{k}{2})$$
 if k is even (7.57)

7.6 Steady Flow in Branching Tubes

Pulsatile flow in the arterial tree consists of a steady flow component and an oscillatory component. Each of these two components relates to different design features of the arterial tree and to different flow phenomena and governing equations. Both components are important for an understanding of the arterial tree as a living organ.

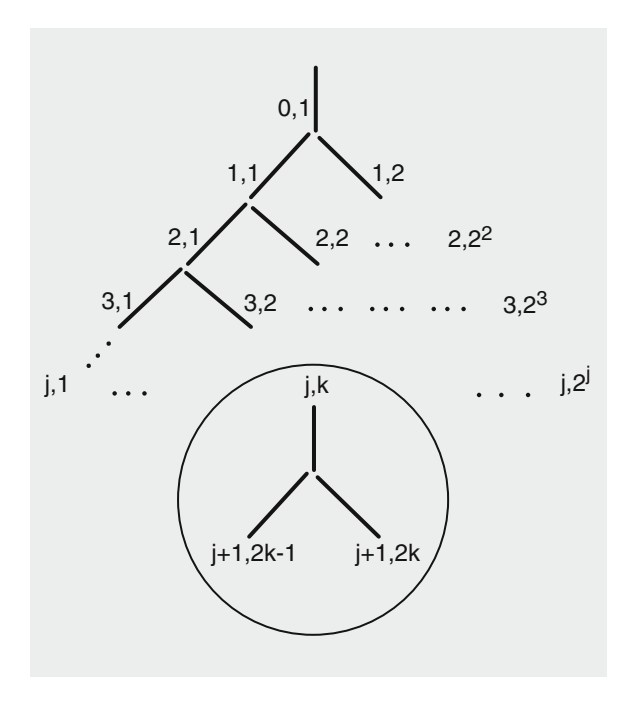


Fig. 7.13 A notation scheme for identifying the positions of vessel segments within a branching tree structure. A coordinate pair j, k is used such that the first identify the level or generation in which a vessel segment is situated and the second identifies its sequential position within that generation. The *inset* shows that in general at each bifurcation one of the two branch segments has an odd sequential number and the other has an even sequential number. We use the convention of reserving the odd sequential number for the branch with the larger radius at each bifurcation.

In this section we examine the steady flow component, using the grounds laid in the previous three sections.

For this purpose we consider a tree consisting of a system of branching tubes in which a root tube segment divides into two branches and each of the branches in turn divides into two branches etc. The pressure distribution within the tree structure is determined simply by following all possible paths from the root segment of the tree to the terminal branch segments. Since each of these paths is unique and consists of a simple succession of tube segments in series, the results of Sect. 7.3 for tubes in series can then be used, noting only that the flow rate in this succession of tube segments is not the same but varies according to the bifurcation rules discussed in Sect. 7.4.

The pressure distribution along any tube segment within the tree structure is determined by simply following the unique path from the root tube segment of the tree to that particular segment, using the j, k notation introduced in the previous section, and following the analysis used in Sect. 7.3. Thus, for the root segment of the tree (j = 0, k = 1) we write, as in Eq. 7.22

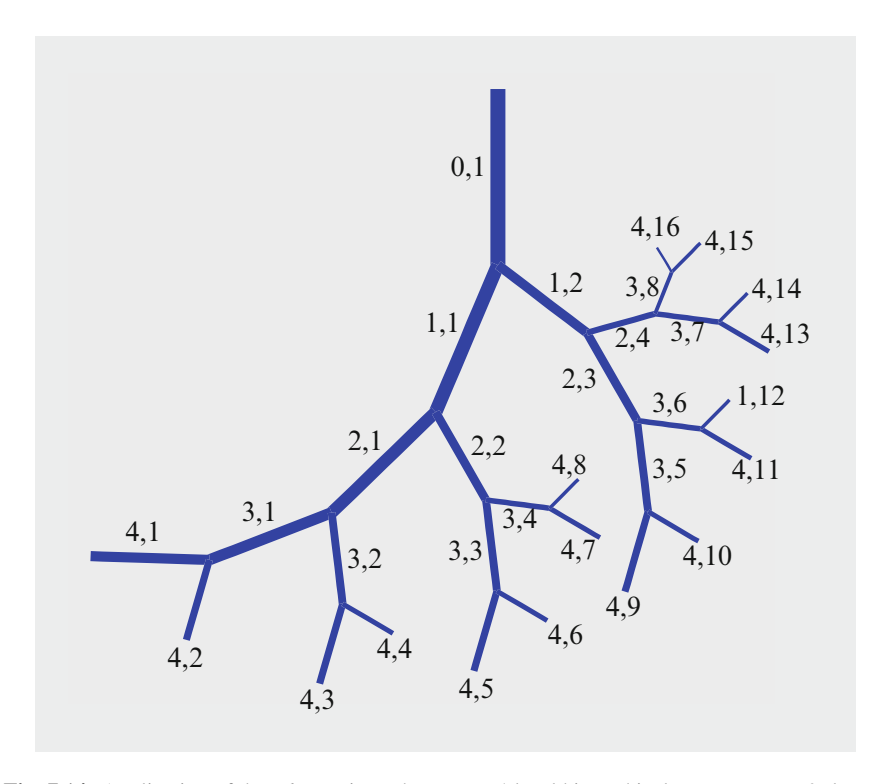


Fig. 7.14 Application of the j, k notation scheme to a 5-level hierarchical tree structure. Only two numbers are required to identify the position of a vessel within the tree structure. The bifurcation index used here is 0.7, which means that at each bifurcation one of the two branches has a larger diameter than the other. By convention, the *odd* k-value at each bifurcation represents the branch with the larger diameter. The path from the root segment to any other segment within the tree structure is unique. One path of particular significance is that of following the branch with the larger radius at each bifurcation, another is that of following the branch with the smaller diameter. We refer to these as "bounding paths", the first being the "major" path and the second the "minor" path.

$$p_{0,1}(x_{0,1}) = p_{0,1}(0) - \left(\frac{8\mu}{\pi}\right) \left(\frac{1}{a_{0,1}}\right)^4 q_{0,1} x_{0,1}$$
 (7.58)

where, as in Sect. 7.3, p(x) is pressure at position x along the tube segment, a is radius and q is flow rate, all being specific to that particular tube segment as indicated by the subscripts. μ is fluid viscosity.

If we now proceed from the root segment to the branch tube with the larger radius, hence with coordinates j = 1, k = 1, then the pressure distribution in that segment is

$$p_{1,1}(x_{1,1}) = p_{1,1}(0) - \left(\frac{8\mu}{\pi}\right) \left(\frac{1}{a_{1,1}}\right)^4 q_{0,1} x_{1,1} \tag{7.59}$$

and if we continue along the hierarchy of the tree, at each bifurcation choosing the branch with the larger diameter, then

$$p_{2,1}(x_{2,1}) = p_{2,1}(0) - \left(\frac{8\mu}{\pi}\right) \left(\frac{1}{a_{2,1}}\right)^4 q_{2,1} x_{2,1}$$
 (7.60)

and in general

$$p_{n,1}(x_{n,1}) = p_{n,1}(0) - \left(\frac{8\mu}{\pi}\right) \left(\frac{1}{a_{n,1}}\right)^4 q_{n,1} x_{n,1}$$
 (7.61)

It is important to note that, as in Sect. 7.3, the domain of $p_{0,1}$ is confined to the root tube segment only, and the domain of $p_{1,1}$ is confined to the branch tube segment with the larger diameter only, etc. Thus, $p_{0,1}$ is a function of $x_{0,1}$ only, and $p_{0,1}(0)$ is therefore the value of $p_{0,1}$ at $x_{0,1} = 0$ with no ambiguity and, similarly, $p_{1,1}$ is a function of $x_{1,1}$ only. The value of $p_{0,1}$ at the downstream end of the root tube segment is $p_{0,1}(l_{0,1})$.

Because of pressure continuity, the pressure at the downstream end of the parent tube segment at each junction point must equal the pressure at the upstream ends of the two branch segments. Accordingly, the following equalities apply at the junction points

$$\begin{cases} p_{1,1}(0) = p_{0,1}(l_{0,1}) \\ p_{2,1}(0) = p_{1,1}(l_{1,1}) \\ \vdots \\ p_{n,1}(0) = p_{n-1,1}(l_{n-1,1}) \end{cases}$$
(7.62)

As in Sect. 7.3, the pressure distribution in successive tube segments can be normalized by using properties of the root tube segment as reference properties. Thus the pressures everywhere are referred to the initial input pressure $p_{0,1}(0)$, and the pressure drop in the first tube segment from Eq. 7.58

$$\Delta p_{0,1} = p_{0,1}(0) - p_{0,1}(l_{0,1}) \tag{7.63}$$

$$= \left(\frac{8\mu}{\pi}\right) \left(\frac{1}{a_{0,1}}\right)^4 q_{0,1} l_{0,1} \tag{7.64}$$

is used to define a nondimensional form of the pressure in each tube segment, writing

$$P(x) = \frac{p(x) - p_{0,1}(0)}{\Delta p_{0,1}} \tag{7.65}$$

In addition, the position coordinates in each tube segment are normalized by writing

$$\begin{cases}
X_{0,1} = x_{0,1}/l_{0,1} \\
X_{1,1} = x_{1,1}/l_{1,1} \\
\vdots \\
X_{n,1} = x_{n,1}/l_{n,1}
\end{cases} (7.66)$$

so that, in terms of the new position coordinate X, the normalized length of each tube segment is now 1.0.

Thus, the pressure distribution in the root tube segment in Eq. 7.58 can now be put in nondimensional normalized form

$$P_{0,1}(X_{0,1}) = \frac{p_{0,1}(x_{0,1}) - p_{0,1}(0)}{\Delta p_{0,1}}$$

$$= -\left(\frac{a_{0,1}}{a_{0,1}}\right)^4 \left(\frac{q_{0,1}}{q_{0,1}}\right) \left(\frac{x_{0,1}}{l_{0,1}}\right)$$

$$= -X_{0,1} \tag{7.67}$$

with

$$P_{0,1}(1) = \frac{p_{0,1}(l_{0,1}) - p_{0,1}(0)}{\Delta p_{0,1}}$$

$$= -1 \tag{7.68}$$

For the pressure distribution in the branch tube with the larger radius, we have

$$P_{1,1}(X_{1,1}) = \frac{p_{1,1}(x_{1,1}) - p_{1,1}(0)}{\Delta p_{0,1}}$$

$$= \frac{p_{1,1}(x_{1,1}) - p_{0,1}(0)}{\Delta p_{0,1}} + \frac{p_{0,1}(0) - p_{1,1}(0)}{\Delta p_{0,1}}$$

$$= \frac{p_{1,1}(x_{1,1}) - p_{0,1}(0)}{\Delta p_{0,1}} + \frac{p_{0,1}(0) - p_{0,1}(l_{0,1})}{\Delta p_{0,1}}$$

$$= -\left(\frac{a_{0,1}}{a_{1,1}}\right)^4 \left(\frac{q_{1,1}}{q_{0,1}}\right) \left(\frac{x_{1,1}}{l_{0,1}}\right) - 1$$

$$= -1 - \left(\frac{a_{0,1}}{a_{1,1}}\right)^4 \left(\frac{q_{1,1}}{q_{0,1}}\right) \left(\frac{l_{1,1}}{l_{0,1}}\right) X_{1,1}$$

$$(7.69)$$

Similarly, and omitting the details, we find

$$P_{2,1}(X_{2,1}) = -1 - \left(\frac{a_{0,1}}{a_{1,1}}\right)^4 \left(\frac{q_{1,1}}{q_{0,1}}\right) \left(\frac{l_{1,1}}{l_{0,1}}\right) - \left(\frac{a_{0,1}}{a_{2,1}}\right)^4 \left(\frac{q_{2,1}}{q_{0,1}}\right) \left(\frac{l_{2,1}}{l_{0,1}}\right) X_{2,1}$$
(7.70)

and in general

$$P_{n,1}(X_{n,1}) = -1 - \left(\frac{a_{0,1}}{a_{1,1}}\right)^4 \left(\frac{q_{1,1}}{q_{0,1}}\right) \left(\frac{l_{1,1}}{l_{0,1}}\right)$$

$$- \left(\frac{a_{0,1}}{a_{2,1}}\right)^4 \left(\frac{q_{2,1}}{q_{0,1}}\right) \left(\frac{l_{2,1}}{l_{0,1}}\right)$$

$$- \cdots$$

$$- \left(\frac{a_{0,1}}{a_{n,1}}\right)^4 \left(\frac{q_{n,1}}{q_{0,1}}\right) \left(\frac{l_{n,1}}{l_{0,1}}\right) X_{n,1}$$

$$(7.71)$$

As in Sect. 7.3, the results indicate that in this convenient nondimensional form, the pressure distribution along the designated sequence of tube segments within the tree structure consists of a series of linear pressure drops, with the pressure starting from a normalized value of 0 at entry to the root segment and dropping linearly from there to -1.0 at the end of that segment. Subsequent values of the pressure depend on the lengths and diameters of subsequent branch segments.

If it is assumed that the tube lengths are proportional to their diameters, the pressure distributions in subsequent segments become

$$\begin{cases} P_{0,1}(X_{0,1}) = -X_{0,1} \\ P_{1,1}(X_{1,1}) = -1 - \left(\frac{a_{0,1}}{a_{1,1}}\right)^3 \left(\frac{q_{1,1}}{q_{0,1}}\right) X_{1,1} \\ P_{2,1}(X_{2,1}) = -1 - \left(\frac{a_{0,1}}{a_{1,1}}\right)^3 \left(\frac{q_{1,1}}{q_{0,1}}\right) - \left(\frac{a_{0,1}}{a_{2,1}}\right)^3 \left(\frac{q_{2,1}}{q_{0,1}}\right) X_{2,1} \\ \vdots \\ P_{n,1}(X_{n,1}) = -1 - \left(\frac{a_{0,1}}{a_{1,1}}\right)^3 \left(\frac{q_{1,1}}{q_{0,1}}\right) - \left(\frac{a_{0,1}}{a_{2,1}}\right)^3 \left(\frac{q_{2,1}}{q_{0,1}}\right) \\ - \cdots - \left(\frac{a_{0,1}}{a_{n,1}}\right)^3 \left(\frac{q_{n,1}}{q_{0,1}}\right) X_{n,1} \end{cases}$$

$$(7.72)$$

If a power law relationship between tube radius and flow rate $(q \sim a^{\gamma})$ is assumed, as in Eq. 3.98, then the pressure distributions in Eq. 7.72 become

$$\begin{cases} P_{0,1}(X_{0,1}) = -X_{0,1} \\ P_{1,1}(X_{1,1}) = -1 - \left(\frac{a_{0,1}}{a_{1,1}}\right)^{3-\gamma} X_{1,1} \\ P_{2,1}(X_{2,1}) = -1 - \left(\frac{a_{0,1}}{a_{1,1}}\right)^{3-\gamma} - \left(\frac{a_{0,1}}{a_{2,1}}\right)^{3-\gamma} X_{2,1} \\ \vdots \\ P_{n,1}(X_{n,1}) = -1 - \left(\frac{a_{0,1}}{a_{1,1}}\right)^{3-\gamma} - \left(\frac{a_{0,1}}{a_{2,1}}\right)^{3-\gamma} \\ - \dots - \left(\frac{a_{0,1}}{a_{n,1}}\right)^{3-\gamma} X_{n,1} \end{cases}$$

$$(7.73)$$

Each of the above equations determines the pressure distribution *along one tube segment* as indicated by the coordinate subscripts. By choice, the selected segments in Eq. 7.73 represent a very specific path from the root segment to the *n*th generation of the tree which we shall refer to as the "major path" because it *follows the branch with the larger radius at each junction*. A counterpart to this path, which is what we shall referred to as the "minor path". The pressure distributions in tube segments along this path are obtained in much the same way as was done along the major path. Omitting the details, we find

$$\begin{cases} P_{0,1}(X_{0,1}) = -X_{0,1} \\ P_{1,2}(X_{1,2}) = -1 - \left(\frac{a_{0,1}}{a_{1,2}}\right)^{3-\gamma} X_{1,2} \\ P_{2,4}(X_{2,4}) = -1 - \left(\frac{a_{0,1}}{a_{1,2}}\right)^{3-\gamma} - \left(\frac{a_{0,1}}{a_{2,4}}\right)^{3-\gamma} X_{2,4} \\ \vdots \\ P_{n,2^n}(X_{n,2^n}) = -1 - \left(\frac{a_{0,1}}{a_{1,2}}\right)^{3-\gamma} - \left(\frac{a_{0,1}}{a_{2,4}}\right)^{3-\gamma} \\ - \dots - \left(\frac{a_{0,1}}{a_{n,2^n}}\right)^{3-\gamma} X_{n,2^n} \end{cases}$$

$$(7.74)$$

As seen in Sect. 7.4, the power law relation between tube radius and flow rate also implies a relation between parent and branch tube radii at a bifurcation (Eq. 7.50). Thus the ratios of radii in Eqs. 7.73 and 7.74 can be determined from Eq. 7.50 by noting that

$$\begin{cases} \frac{a_{0,1}}{a_{1,1}} = (1 + \alpha_{0,1}^{\gamma})^{1/\gamma} \\ \frac{a_{0,1}}{a_{1,2}} = \left(\frac{1 + \alpha_{0,1}^{\gamma}}{\alpha_{0,1}^{\gamma}}\right)^{1/\gamma} \end{cases}$$
(7.75)

where $\alpha_{0,1}$ is the ratio of small to large radius of the two branches of parent (0,1)

$$\alpha_{0,1} = \frac{a_{1,2}}{a_{1,1}} \tag{7.76}$$

For simplicity, we shall assume that this ratio is the same at all junctions throughout the tree, thus dispensing with the subscript and denoting it simply as α . This means that the ratio of the two branch diameters at every bifurcation is assumed to be the same throughout the tree. It then follows that the ratios of radii of parent-to-small and parent-to-large branches in Eq. 7.75 will also be the same throughout the tree

$$\begin{cases} \lambda_1 = \frac{a_{j,k}}{a_{j+1,2k-1}} = (1 + \alpha^{\gamma})^{1/\gamma} \\ \lambda_2 = \frac{a_{j,k}}{a_{j+1,2k}} = \left(\frac{1 + \alpha^{\gamma}}{\alpha^{\gamma}}\right)^{1/\gamma} \end{cases}$$
(7.77)

The ratios of radii in Eqs. 7.73 and 7.74 can now be expressed in terms of λ_1 and λ_2 by noting that

$$\begin{cases} \frac{a_{0,1}}{a_{1,1}} = \lambda_1 \\ \frac{a_{0,1}}{a_{2,1}} = \frac{a_{0,1}}{a_{1,1}} \times \frac{a_{1,1}}{a_{2,1}} = \lambda_1^2 \\ \frac{a_{0,1}}{a_{3,1}} = \frac{a_{0,1}}{a_{1,1}} \times \frac{a_{1,1}}{a_{2,1}} \times \frac{a_{2,1}}{a_{3,1}} = \lambda_1^3 \\ \vdots \\ \frac{a_{0,1}}{a_{n,1}} = \frac{a_{0,1}}{a_{1,1}} \times \frac{a_{1,1}}{a_{2,1}} \times \dots \times \frac{a_{n-1,1}}{a_{n,1}} = \lambda_1^n \end{cases}$$

$$(7.78)$$

$$\begin{cases}
\frac{a_{0,1}}{a_{1,2}} = \lambda_2 \\
\frac{a_{0,1}}{a_{2,4}} = \frac{a_{0,1}}{a_{1,2}} \times \frac{a_{1,2}}{a_{2,4}} = \lambda_2^2 \\
\frac{a_{0,1}}{a_{3,8}} = \frac{a_{0,1}}{a_{1,2}} \times \frac{a_{1,2}}{a_{2,4}} \times \frac{a_{2,4}}{a_{3,8}} = \lambda_2^3 \\
\vdots \\
\frac{a_{0,1}}{a_{n,2^n}} = \frac{a_{0,1}}{a_{1,2}} \times \frac{a_{1,2}}{a_{2,4}} \times \dots \times \frac{a_{n-1,2^{n-1}}}{a_{n,2^n}} = \lambda_2^n
\end{cases}$$
(7.79)

Using these expressions for the radii ratios in Eqs. 7.73 and 7.74, we find

$$\begin{cases}
P_{n,1}(X_{n,1}) = -1 - (\lambda_1)^{3-\gamma} - (\lambda_1^2)^{3-\gamma} - \dots - (\lambda_1^n)^{3-\gamma} X_{n,1} \\
P_{n,2^n}(X_{n,2^n}) = -1 - (\lambda_2)^{3-\gamma} - (\lambda_2^2)^{3-\gamma} - \dots - (\lambda_2^n)^{3-\gamma} X_{n,2^n}
\end{cases} (7.80)$$

Again we note that each of these two equations represents the pressure distribution in one particular tube segment within the hierarchical tree structure. The two segments chosen are somewhat special in that each lies on one of the two singular paths through the tree structure, namely the major and the minor paths described earlier. The expressions describing the pressure along these two paths have been highly simplified by the assumed idealized structure of the tree, in particular the assumption that the bifurcation index α and the power law index γ do not change from one bifurcation to the next throughout the tree structure.

It is important to emphasize, again, that these idealized conditions do not prevail in the cardiovascular system and they are being used here only to illustrate the process of determining the pressure distribution within the tree. The same process can be used to determine the pressure distribution without these assumptions, given the actual values of α and γ at individual bifurcations which can be determined from measurements of the three vessel radii at each bifurcation.

More generally, any other tube segment, within any other tree structure, will be reached by a unique path which is more easily described by moving *upstream* along the tree structure, from the location of that segment to the root segment of the tree. The j, k notation described in Sect. 7.5 makes the task fairly simple. Thus, the path from a segment j, k is to the root segment of the tree is constructed by moving upstream, from branches to parents as in Eqs. 7.56 and 7.57. As an example, from segment (4, 5) to the root segment of the tree the path is

$$\begin{aligned} \textbf{branch}(4,5) &\rightarrow \textbf{parent}(3,3) \\ &\rightarrow \textbf{parent}(2,2) \\ &\rightarrow \textbf{parent}(1,1) \\ &\rightarrow \textbf{Root}(0,1) \end{aligned}$$

and from segment (4, 14) to the root segment of the tree the path is

$$\begin{aligned} \textbf{branch}(4,14) &\rightarrow \textbf{parent}(3,7) \\ &\rightarrow \textbf{parent}(2,4) \\ &\rightarrow \textbf{parent}(1,2) \\ &\rightarrow \textbf{Root}(0,1) \end{aligned}$$

The pressure distribution along these paths are constructed by moving *upstream* from the root segment of the tree to the designated branch segment as in Eq. 7.71 but with the appropriate sequence of segments and appropriate assumptions about the progression of flow rates, tube lengths, and tube radii. The process is clearly more tedious than in the idealized cases of the major or minor paths considered earlier, but the principles are the same.

The pressure distributions along the two bounding paths and along all other paths within the 5-level tree structure are shown in Figs. 7.15, 7.16 and 7.17 where the singular nature of the two bounding paths is seen again in terms of the pressure distributions within the entire tree structure.

Figures 7.15, 7.16 and 7.17 also show the critical dependence of the pressure distribution on the value of the power law index γ in the relation between flow rate and vessel radius (Eq. 3.98). Again, the cube law (γ = 3) appears to present the ideal compromise as concluded in the previous chapter. However, vessel radii actually measured in the cardiovascular system have shown that the cube law is not met *exactly* but with considerable scatter. ^{12,13}

7.7 What Is an "Artery"?

The tree structure considered in the previous section was highly idealized in the sense that all the bifurcations within the tree were assumed to have the same properties, and the lengths of all tube segments were assumed to be related to the corresponding tube radii in the same way. These idealized conditions do not exist in the arterial tree. Data from the cardiovascular systems of humans and animals, based on direct measurements of vessel segment diameters and lengths, have shown consistently that bifurcation properties vary widely within the vascular tree, and vessel segment lengths do not relate to vessel segment radii in any simple or consistent way.

¹²Kassab GS, Rider CA, Tang NJ, Fung YC, Bloor CM, 1993. Morphometry of pig coronary arterial trees. American Journal of Physiology 265:H350–H365.

¹³Zamir M. Vascular system of the human heart: Some branching and scaling issues. In: Brown JH, West GB (eds.). Scaling in Biology. Oxford University Press, 2000.

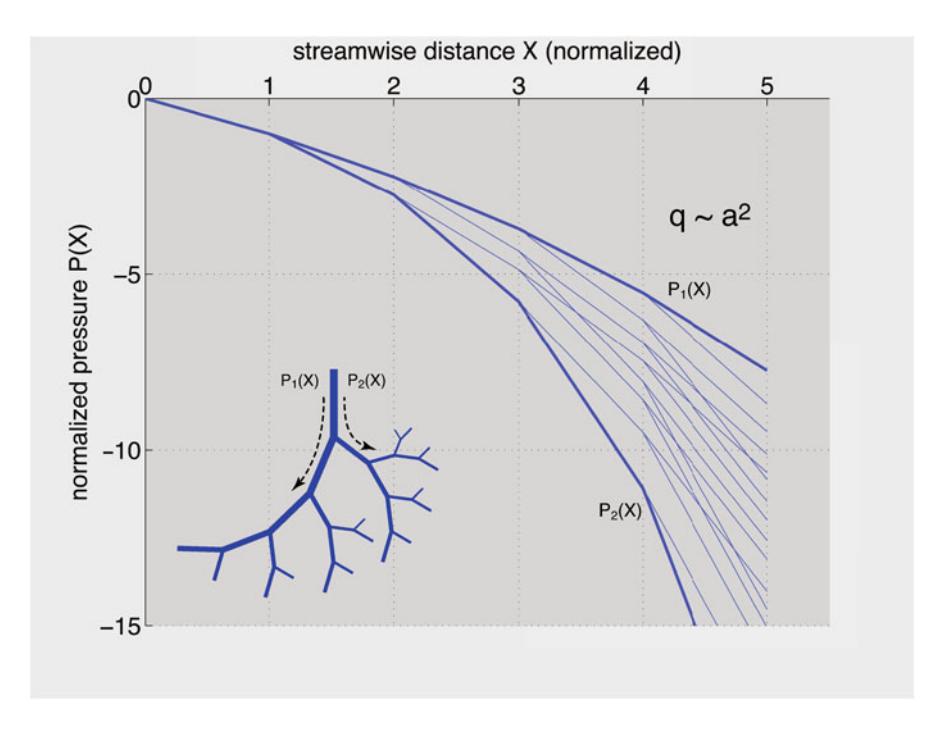


Fig. 7.15 Pressure distributions along paths from the root segment to all terminal segments of the 5-level tree structure shown in the *inset*. The *two bold curves* represent the pressure distributions along the two "bounding paths", the pressure distributions along all other paths fall in between those two. The pressure falls linearly in each segment in accordance with the pressure drop in Poiseuille flow, but the magnitude of the drop depends on the radius of each vessel segment and on the amount of flow. Results in this figure are based on the assumption that the flow rate in a vessel segment is proportional to the square of its radius (square law).

Interestingly, however, the *laws* governing the branching structure of arterial trees seem to hold despite a background of considerable scatter in vessel segment and bifurcation properties. Specifically, despite very high variability in measured values of the bifurcation index α (Eq. 7.1) and vessel segment lengths, the power laws on which the ratios of parent-to-branch radii or cross sectional areas (Eqs. 7.50 and 7.13) are found to hold remarkably well.^{14,15}

Thus the "major" and "minor" paths considered in the previous section were only possible because of the idealized tree structure on which they were based. In reality, as discussed at the end of the previous section, in order to determine the pressure distribution along a certain path within an arterial tree structure, the path must be

¹⁴Kassab GS, Rider CA, Tang NJ, Fung YC, Bloor CM, 1993. Morphometry of pig coronary arterial trees. American Journal of Physiology 265:H350–H365.

¹⁵Zamir M. Vascular system of the human heart: Some branching and scaling issues. In: Brown JH, West GB (eds.). Scaling in Biology. Oxford University Press, 2000.

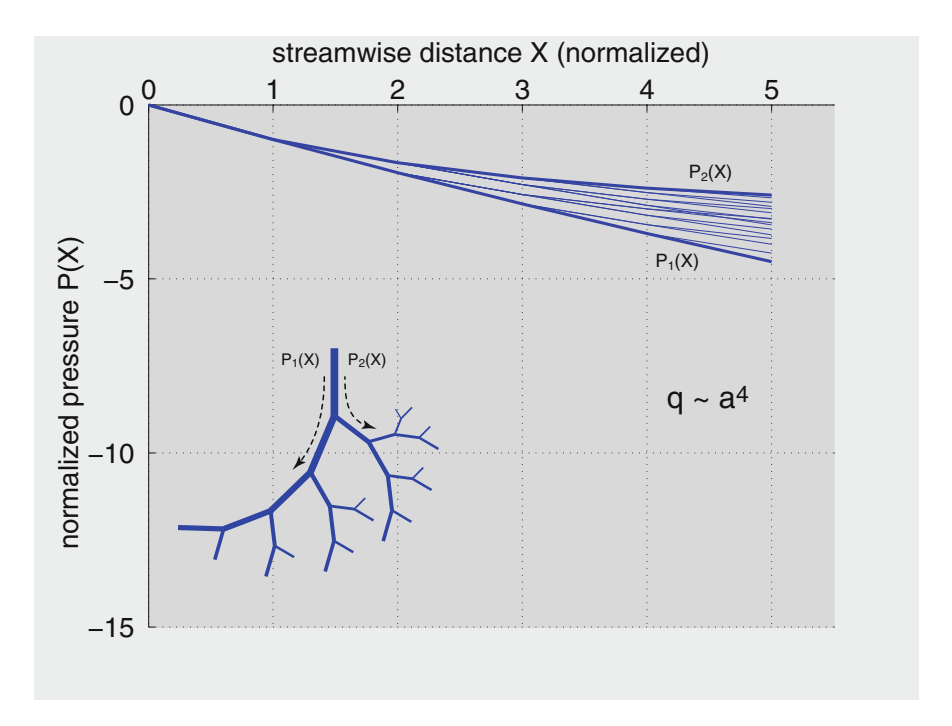


Fig. 7.16 Pressure distributions in the 5-level tree structure as in Fig. 7.15, but here the results are based on the assumption that the flow rate in a vessel segment is proportional to the fourth power of its radius (quartic law). It is seen that under this assumption the pressure drops more steeply along the path of branches with the larger radii than it does along the path of branches with the smaller radii, which is somewhat unlikely on physiological or fluid dynamic grounds.

constructed by piecing together, sequentially, all the vessel segments comprising that path. The task may seem intractable or impractical, but if measurements of segment lengths and diameters are available, along with the corresponding j,k coordinates of these segments, then the task of computing the pressure distribution along that path is in fact fairly trivial.

Variability in the branching structure of arterial trees therefore calls into question the meaning of the terms "artery" or "vessel" which are widely used in hemodynamics and, more importantly, in the clinical setting. What is an artery? (Fig. 7.18).

In a typical arterial tree or sub-tree consisting of 20 or more generations there would potentially be 2^{20} vessel segments at the terminal end of the tree. The path from the root segment of the tree to each of these terminal segments may strictly be identified as an "artery", because it is a unique path in the sense that the vessel segments comprising the path to each of the terminal segments will be different. There will be many *shared* segments with other paths along the tree structure, but in total the sequence of segments leading to each terminal segment will be different.

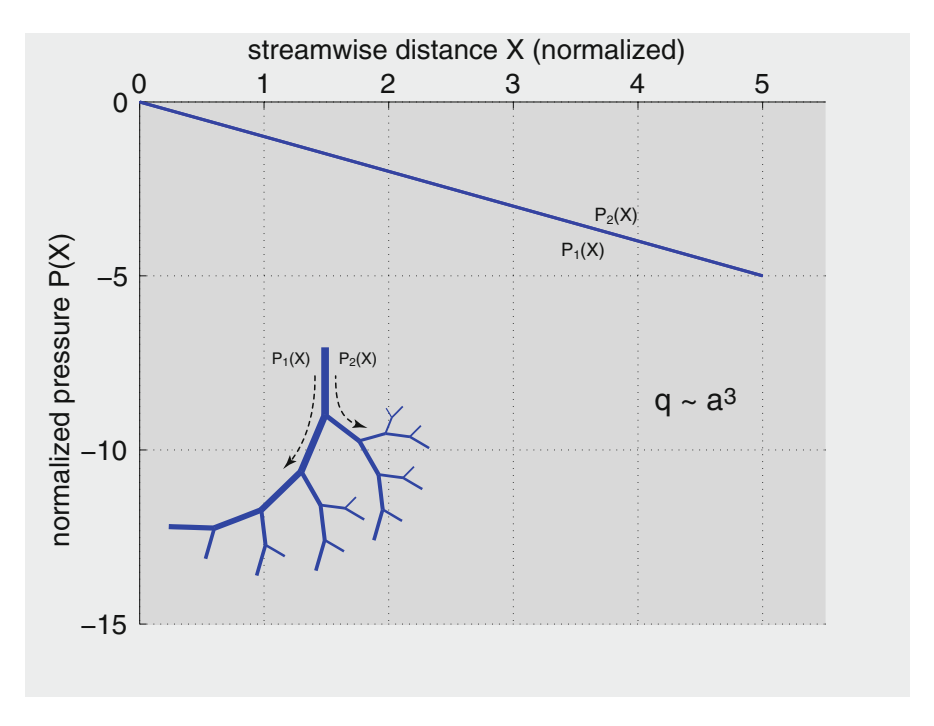


Fig. 7.17 Pressure distributions in the 5-level tree structure as in Fig. 7.15, but here the results are based on the assumption that the flow rate in a vessel segment is proportional to the third power of its radius, which is widely known as the "cube law". Under this assumption the pressure distributions are identical along all paths from the root segment of the tree to the terminal branches, which lends strong theoretical support to the validity of the cube law.

Indeed, the sequence of vessel segments leading from the root segment of the tree to *any segment* within the tree structure is unique.

If an "artery" is defined as a sequence of consecutive arterial segments within an arterial tree structure, therefore, the number of such "arteries" within the tree structure will be so large as to render the term "artery" of little use. Yet, in the heart and in the brain, indeed in the entire cardiovascular system, arteries are routinely *named*: the "left coronary", the "middle cerebral" and, most famously, the "aorta". Is the aorta an "artery" in the sense that it can be defined in terms of a consecutive sequence of vessel segments? We know well where this sequence starts, but where does it end?

To the surgeon or anatomist this discussion may seem somewhat "esoteric" because in the clinical setting one "knows" where the left and right coronary arteries begin and where they end. They and other arteries are generally defined in anatomical terms, but there is wide variability in the way the paths of these arteries unfold in different subjects [pathology (flow strategy) paper]. From the standpoint of hemodynamics, therefore, that is from the standpoint of the mathematics and physics of the flow, an anatomically based definition of an artery does not provide



Fig. 7.18 An "arterial segment" can be accurately defined as the vascular interval between two consecutive vascular junctions. By contrast: What is an 'artery'? The calculation of pressure and flow along a certain path within a vascular tree requires a prescribed sequence of consecutive arterial segments and, as illustrated here, there are typically many such sequences within a tree structure. The term "artery" does not usually identify one of these uniquely but is rather used within an anatomical context.

the required basis for an analysis of the flow. Only a well defined path in terms of a sequence of consecutive vessel segments through the vascular tree structure can provide that basis, and even then it can only do so on an individual basis in different subjects. Indeed, the recognition of this reality has led in recent years to the rise of the important notion and practice of "patient-specific" hemodynamics. ^{16,17}

The wide variability (heterogeneity) in the value of the bifurcation index α (Eq. 7.1) in an arterial tree and hence the wide variability in the hierarchical structure of the tree is not to be interpreted as the result of a *random* process. Rather, it highlights the fact that the hierarchical structure of the tree is determined largely

¹⁶Antiga L, Piccinelli M, Botti L, Ene-Iordache B, Remuzzi A, Steinman DA. An image-based modeling framework for patient-specific computational hemodynamics. Medical and Biological Engineering and Computing 11:1097–112.

¹⁷Kim HJ, Vignon-Clementel IE, Coogan JS, Figueroa CA, Jansen KE, Taylor CA. Patient-specific modeling of blood flow and pressure in human coronary arteries. Annals of Biomedical Engineering 10:3195–209.

by *functional* considerations. A good demonstration of this is found in the coronary circulation where the notion of "distributing" and "delivering" vessels has been used to describe two categories of arteries. Briefly, the first describes a vessel that undergoes a sequence of highly *asymmetrical* bifurcations, giving rise to so called "side branches", and thereby keeping its own diameter very little changed in the process. The second describes a vessel that undergoes a sequence of *symmetrical* bifurcations and its diameter is thereby diminishing rapidly in the process. The change in diameter is obtained by following a "major path" as in the previous section, whereby the larger of the two branches is selected at each successive bifurcations. Using the cube law for this purpose, the diameter of the vessel after successive bifurcations is determined from Eq. 7.5, writing

$$\begin{cases} \frac{d_1}{d_0} = (1 + \alpha^3)^{-1/3} \\ \frac{d_2}{d_0} = \frac{d_2}{d_1} \times \frac{d_1}{d_0} = (1 + \alpha^3)^{-2/3} \\ \frac{d_3}{d_0} = \frac{d_3}{d_2} \times \frac{d_2}{d_1} \times \frac{d_1}{d_0} = (1 + \alpha^3)^{-3/3} \\ \vdots \\ \frac{d_n}{d_0} = \frac{d_n}{d_{n-1}} \times \frac{d_{n-1}}{d_{n-2}} \times \dots \times \frac{d_1}{d_0} = (1 + \alpha^3)^{-n/3} \end{cases}$$
(7.81)

Using this progression, for a vessel that undergoes 20 successive *symmetrical* bifurcations, for which $\alpha = 1.0$, the ratio of its final to original diameters is

$$(1+1)^{(-20/3)} \approx 0.00984 \tag{7.82}$$

while for a vessel that undergoes 20 successive highly asymmetrical bifurcations, giving rise to so called "side branches" for which say $\alpha = 0.01$, the ratio of final to original diameters of the vessel is

$$(1+0.01)^{(-20/3)} \approx 0.99999 \tag{7.83}$$

In the first case the diameter of the vessel diminishes to only one percent of it original diameter, while in the case the diameter of the vessel remains practically unchanged. These two extremes and others in between are illustrated graphically in Fig. 7.19

On that basis two types of vessels were identified in the coronary circulation: "delivering" vessel that branch profusely and reach the capillary bed rapidly in

¹⁸Zamir M, 1988. Distributing and delivering vessels of the human heart. Journal of General Physiology 91:725–735.

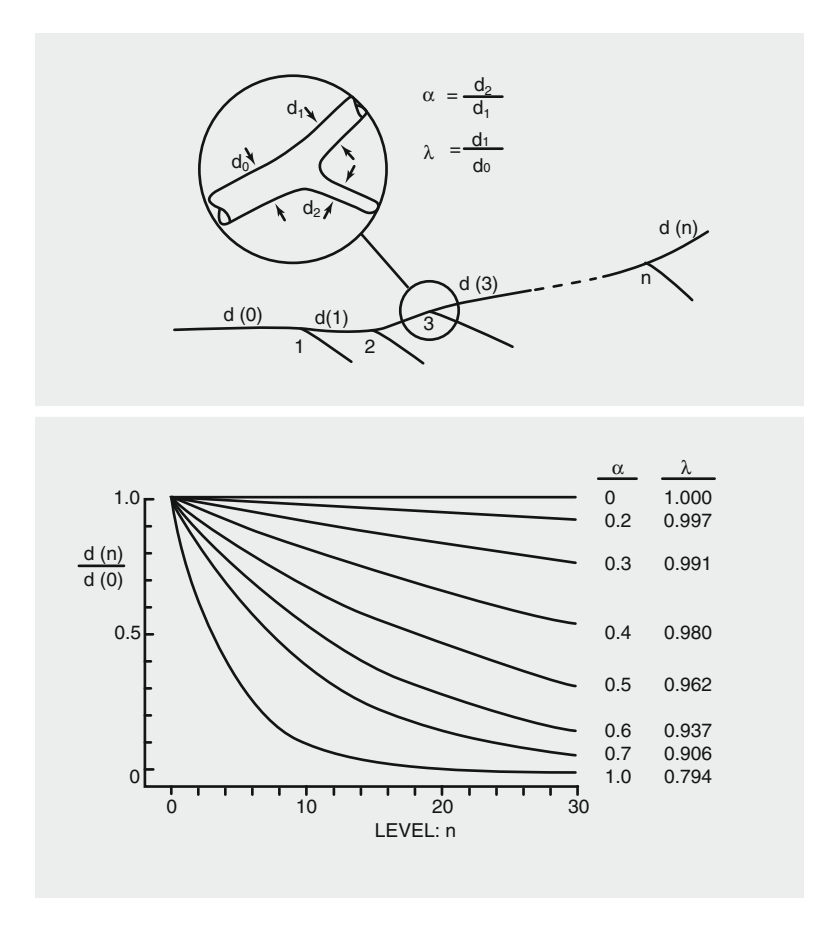


Fig. 7.19 The rate at which the diameter of a vessel decreases as it progresses along its course is an indicator of its function. At each bifurcation which the vessel undergoes along its course, the amount by which the parent diameter diminishes depends on the bifurcation index α as defined in the figure. Each curve in the lower panel represents the course of a vessel for a particular value of α . The diameter, d(n), of the vessel following n bifurcation sites is expressed as a fraction of its initial diameter, d(0). Along the uppermost curves, the diameter of the vessel decreases slowly, while along the lowest curves the reverse is true. Adapted from Zamir (1988; see Footnote 18).

terms of the number of generations, and "distributing" vessel that give rise to mostly side branches and thereby maintain their diameter in the process. An example of these two types of vessels is shown in Fig. 7.20. Delivering vessels were thus identified with vessels that penetrate the myocardium, while distributing vessels were identified with vessels that circle the myocardium and distribute blood to different regions. Thus, the notion of delivering and distribution arteries in some way provides a basis for "naming" the main arteries in the coronary circulation, although the problem of identifying these arteries with quantifiable paths for blood flow remain as discussed earlier.



Fig. 7.20 A cast of the left anterior descending artery of a human heart and its branches. The branches, being delivering vessels, typically divide more profusely and terminate more rapidly than the main distributing vessel. The difference between the two types of behavior may provide the basis for referring to the distributing vessel anatomically as an "artery" but the difficulties of identifying it as a quantifiable path for blood flow remain. Adapted from Zamir (1988; see Footnote 18).

The ultimate conclusion of this section is that the notion of an "artery" or a "vessel" is of very little use from the perspective of mathematics and physics of hemodynamics within the highly variable structure the arterial tree. Only a prescribed sequence of *vessel segments* can be used to determine the pressure or flow distribution along a given path within that structure. Unlike the difficulties associated with the definition of an "artery" or a "vessel", an "arterial segment" or a "vessel segment" is accurately defined as the vascular interval between two consecutive bifurcations.

7.8 Pulsatile Flow in Branching Rigid Tubes

There are two complications in progressing from the problem of *steady flow* in a hierarchical tree structure of branching tubes considered in Sect. 7.6 to *pulsatile flow* in a hierarchical tree structure of branching *elastic tubes*. The first complication arises, as seen in Chap. 4, because the properties of pulsatile flow depend on a

combination of frequency and *tube diameter*, therefore these properties will be affected by the change in vessel diameters as the flow encounters each bifurcation within the tree structure. The second complication arises, as seen in Sect. 5.1 and Chap. 6, because pulsatile flow in elastic tubes gives rise to *wave propagation* and, in a tree structure, this in turn gives rise to *wave reflections* as the propagating wave encounters each bifurcation within the tree structure.

In the cardiovascular system both of these complications are present because of the branching structure of the vascular tree and because the blood vessels comprising that tree are not rigid. Pulsatile flow through elastic branching tubes is therefore the ultimate target for a model of flow in the vascular tree, but it is more instructive to approach that target in two steps rather than one. Accordingly, in this section we consider pulsatile flow in rigid branching tubes and in the next section we progress to branching elastic tubes.

From Chap. 4 we have seen that a key parameter that determines the properties of pulsatile flow in a rigid tube is the frequency parameter, also known as the Womersley number,

$$\Omega = \sqrt{\frac{\rho\omega}{\mu}} a \tag{7.84}$$

If the flow in a tree structure, made up of many rigid tube segments, is driven by an oscillatory input pressure of the form

$$k_{\phi}(t) = k_0 e^{i\omega t} \tag{7.85}$$

then the frequency of oscillation ω in Eq. 7.84 for tube segments throughout the tree will be the same as the frequency of that input pressure. If it is assumed further that the fluid density ρ and viscosity μ in that equation remain constant throughout the tree, then the value of the frequency parameter Ω will change only with the radius a of tube segments within the tree.

To illustrate the variation of Ω along the 5-level tree structure considered in Sect. 7.6, taking the following property values

$$\begin{cases} \rho = 1.0 \quad \text{g/cm}^3 \\ \mu = 0.04 \quad \text{g/(cm s)} \\ \omega = 1.0 \quad \text{cycles/s} \\ = 2\pi \quad \text{radians/s} \end{cases}$$
 (7.86)

the value of the frequency parameter in Eq. 7.84 is then given by

$$\Omega = \sqrt{12.5 \times \pi} \times d \tag{7.87}$$

where d is the diameter of the tube in cm. This expression can be used to map out the values of Ω along the 5-level tree structure used in Sect. 7.6 for steady flow, using a power law relation between flow and tube diameter to determine the progression of segment diameters along the tree structure.

As an example, we consider a tree with root segment diameter $d=0.4\,\mathrm{cm}$, which is representative of the radius of a main human coronary artery. The diameters of subsequent branch segments are then given by Eq. 7.77 where the values of the bifurcation index α and the power law index γ can be prescribed to determine the sequence of diameters along any path downstream from the root segment. With the diameters of all tube segments within the tree structure now known, the corresponding values of the frequency parameter Ω can be calculated from Eq. 7.87 and mapped out throughout the tree structure as shown in Figs.7.21 and 7.22. In general the value of Ω decreases along any path from the root segment of the tree to the periphery. It decreases most rapidly along the "minor" bounding path which, as we recall, consists of branch segments with the smaller diameter at each bifurcation,

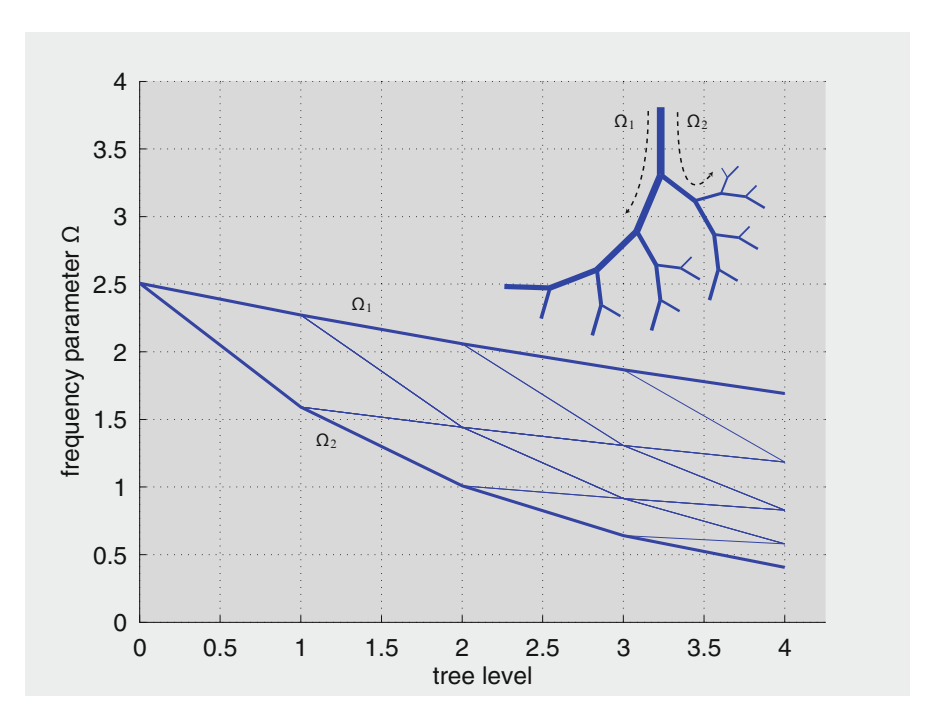


Fig. 7.21 Values of the frequency parameter Ω at different segments of the 5-level tree shown in the *inset*. The tree is based on a power law relation between flow rate and vessel radius, with power law index $\gamma = 3.0$ and bifurcation index $\alpha = 0.7$. The values of Ω decrease most rapidly along the bounding path marked Ω_2 consisting of branch segments with the smaller radii at each bifurcation, and most slowly along the other bounding path, marked Ω_1 . Values of Ω at other branch segments fall in between these two extremes.

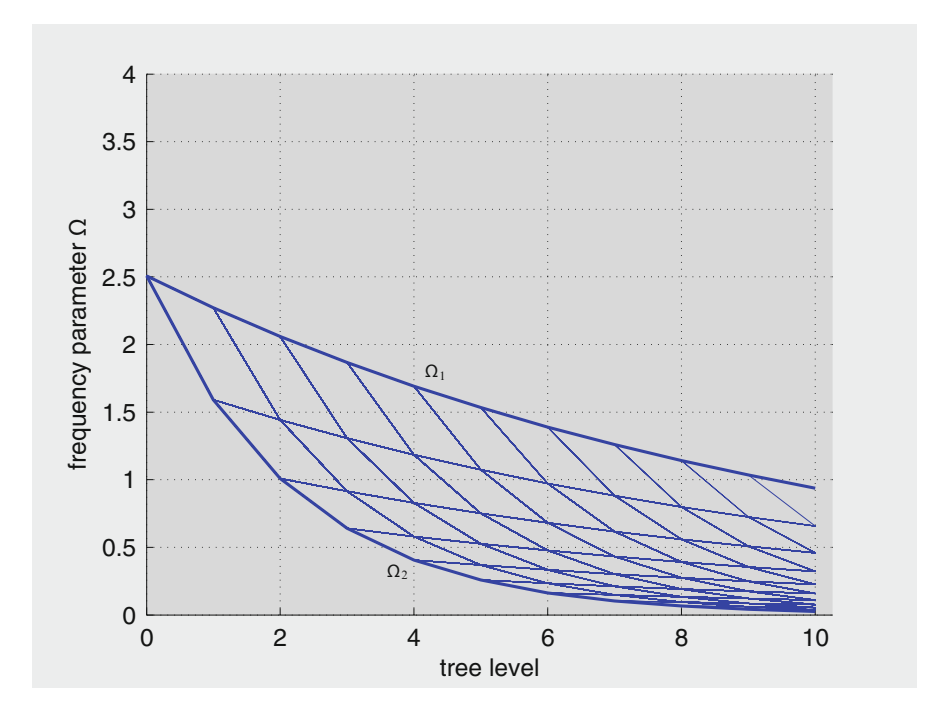


Fig. 7.22 Values of the frequency parameter Ω in a tree with the same parameters as that in Fig. 7.21 but here the tree has 11 levels (marked 0 to 10). Values of Ω continue to decrease, ultimately reaching towards zero.

and more slowly along the "major" path. This is to be expected in view of Eq. 7.87 where the value of Ω is seen to be directly related to tube diameter.

The distribution of the frequency parameter Ω within the tree structure determines the corresponding distribution of other properties of the flow. Of particular interest is the peak flow rate, and the peak shear stress, reached in each pulsating cycle. The values of both of these properties and the distribution of these values within the tree structure will depend on the distribution of the frequency parameter.

The peak flow rate reached within the oscillatory cycle in each tube segment within the tree, which we shall refer to simply as "peak flow" and denote it by \hat{q}_{ϕ} . Using Eq. 4.43 for the oscillatory flow rate $q_{\phi}(t)$, the peak flow rate \hat{q}_{ϕ} in normalized form and in the notation of Sect. 4.7 is given by

$$\frac{\hat{q}_{\phi}(t)}{q_s} = \left| \frac{8}{i\Omega^2} \left(1 - \frac{2J_1(\Lambda)}{\Lambda J_0(\Lambda)} \right) \right| \tag{7.88}$$

The distribution of peak flow within the 5-level vascular tree is shown in Fig. 7.23. Because it is normalized in terms of the steady flow rate q_s in Poiseuille flow, the value of this peak flow is a measure of how close the oscillatory flow at different levels of the tree comes to a fully developed Poiseuille flow driven by

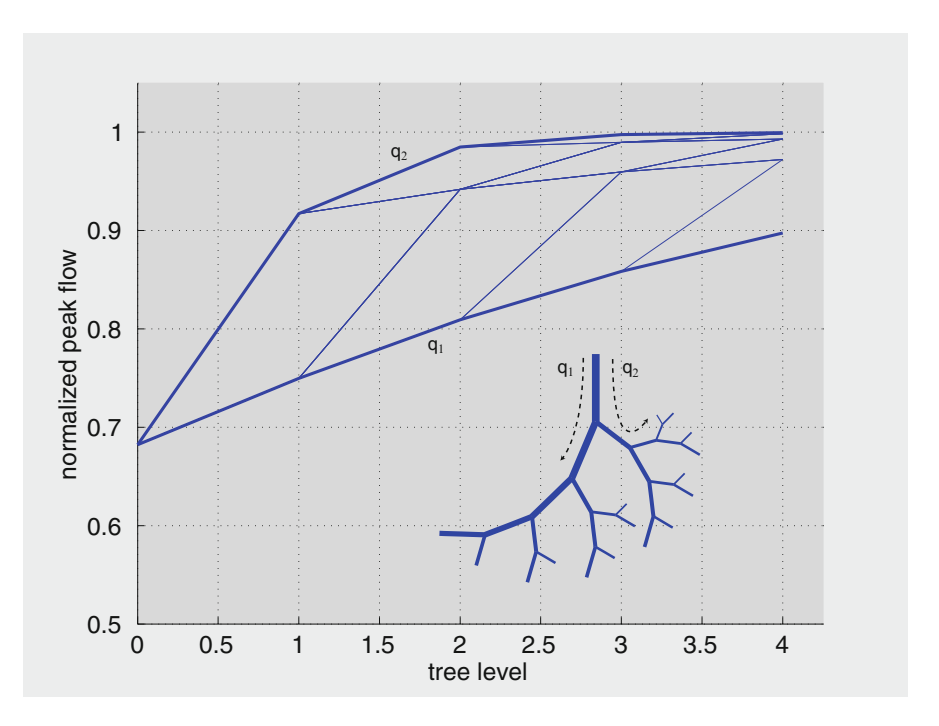


Fig. 7.23 Normalized peak flow rates reached at different branch segments of the 5-level tree shown in the *inset*. A value of 1.0 represents a peak flow equal to that in steady flow. This value is reached more rapidly along the bounding path marked q_2 consisting of branch segments with the smaller radii, and more slowly along the other path, marked q_1 . Other lines represent values of the peak flow along other paths within the tree structure.

the same pressure gradient as oscillatory pressure gradient at that point in time. Thus, a normalized peak flow of 1.0 represents an oscillatory flow in which the velocity profile at each point in time is a Poiseuille flow profile, while values less than 1.0 represent oscillatory flows in which peak flow does not quite reach the corresponding Poiseuille flow value. The results in Fig. 7.23 indicate that peak flows reach the Poiseuille flow values more rapidly along the *major* bounding path they do along the *minor* path. The reason for this is that the oscillatory flow profile is closer to a Poiseuille profile at smaller values of the frequency parameter Ω (Eq. 7.88), which occur along the minor path.

The peak shear stress reached within the oscillatory cycle in each tube segment within the tree, which we shall refer to simply as "peak shear" and denote it by $\hat{\tau}_{\phi}$. Using Eq. 4.47 for the oscillatory flow shear stress $\tau_{\phi}(t)$, the peak shear $\hat{\tau}_{\phi}$ in normalized form and in the notation of Sect. 4.8 is given by

$$\frac{\hat{\tau}_{\phi}(t)}{\tau_{s}} = \left| \frac{2}{\Lambda} \left(\frac{J_{1}(\Lambda)}{J_{0}(\Lambda)} \right) \right| \tag{7.89}$$

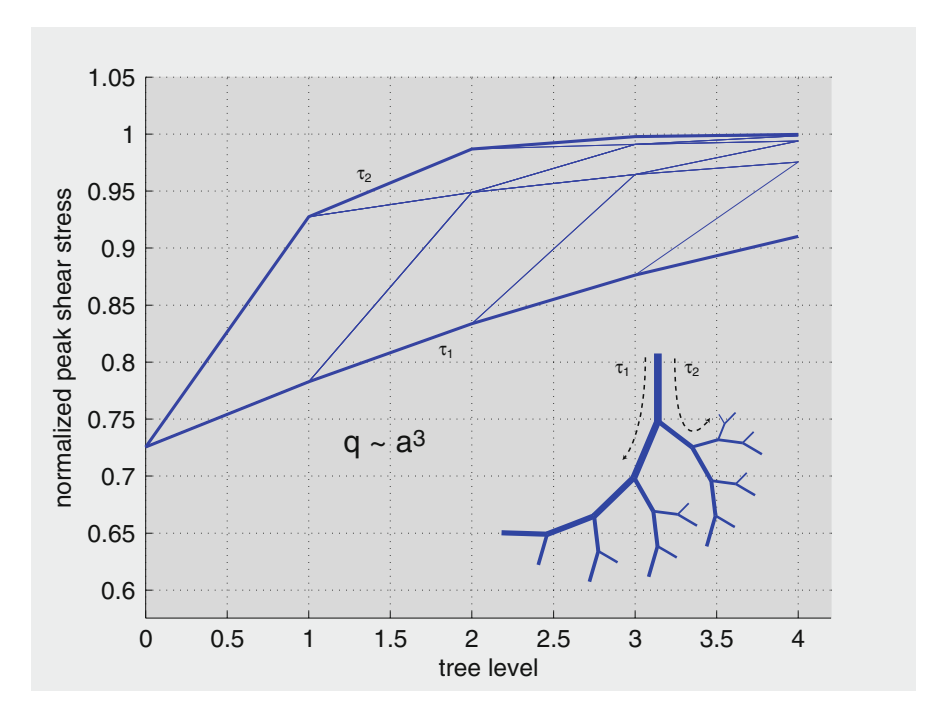


Fig. 7.24 Normalized peak shear stress reached at different branch segments of the 5-level tree shown in the *inset*. A value of 1.0 represents a peak shear stress equal to that in steady flow. This value is reached more rapidly along the bounding path marked τ_2 consisting of branch segments with the smaller radii, and more slowly along the other path, marked τ_1 . Other lines represent values of the peak flow along other paths within the tree structure. The results are based on the cube law relation between flow rate and vessel radius, $q \sim a^{\gamma}$, $\gamma = 3.0$, as indicated in the *inset*.

Again, because of the way it is normalized, the value of the peak shear stress is here expressed as a fraction of the constant shear stress in steady Poiseuille flow. Thus, a normalized value of 1.0 represents peak oscillatory shear stress equal to that in Poiseuille flow. The distribution of peak shear stress within the 5-level tree is shown in Fig. 7.24. It is similar to that of peak flow rate, as would be expected, because shear stress is high at high flow rates and low at low flow rates.

We recall that in *steady* flow, a cube law relation between vessel radius and flow rate, namely $q \sim a^3$, ensures a constant shear stress throughout the tree structure, as was demonstrated in Sect. 7.6. This is not the case in *pulsatile* flow, as we see in Fig. 7.24 where the results are based on the cube law. Other values of the power law index, namely $\gamma = 2.0$ and $\gamma = 4.0$, produce similar results as shown in Figs. 7.25 and 7.26. The reason for this is that in steady flow the shear stress depends on the ratio of flow rate over the third power of the radius (Eq. 3.50), while in pulsatile flow the corresponding relation (Eq. 4.45) is not as simple.

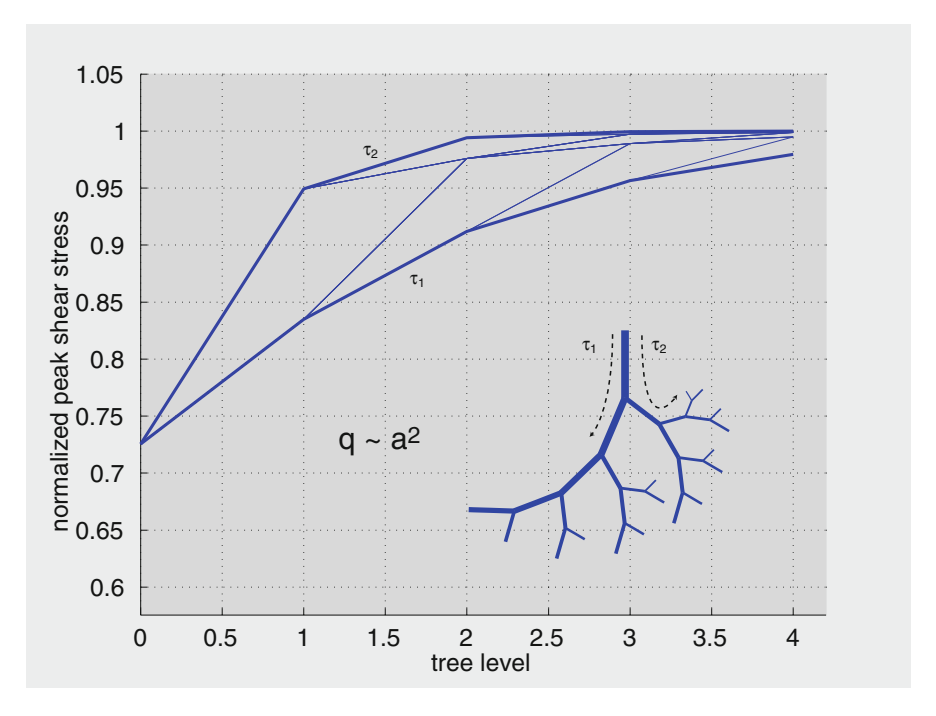


Fig. 7.25 Normalized peak shear stress reached at different branch segments of the 5-level tree shown in the *inset*, as in Fig. 7.23, but here the results are based on a power law index $\gamma = 2.0$.

7.9 Wave Speed in Branching Elastic Tubes

In Sect. 5.9 we saw that the wave speed c in pulsatile flow in an elastic tube depends on the frequency parameter Ω such that when $\Omega > 3$ the wave speed approaches the Moens-Korteweg wave speed c_0 (Eq. 5.1), but when $\Omega < 3$ the value of c departs significantly from the value of c_0 . In fact, the value of c becomes complex, with both its real and imaginary parts depending strongly on the value of Ω .

An estimate of the range of values of Ω in the cardiovascular system can be derived in general from Eq. 7.84 and, at a fundamental frequency of 1 Hz from Eq. 7.87. In the latter case, with the prescribed values of the fluid density and viscosity, Ω depends only on the diameter of the tube. Thus, using Eq. 7.87 we find that in a human aorta of 2.5 cm in diameter the value of Ω is approximately 15.67, while in a pre-capillary arteriole of 0.025 mm in diameter the value of Ω is approximately 0.016. Therefore, in much of the arterial tree the value of Ω will be less than 3.0 and hence the wave speed c will depart significantly from the Moens-Korteweg wave speed c_0 . Indeed, in the example of a 5-level tree structure used in the previous section, where the root diameter of the tree is 4 mm, the value of Ω was found to be less than 3.0 throughout the entire tree (Figs. 7.21 and 7.22). We continue to use this tree structure as an example in the present section.

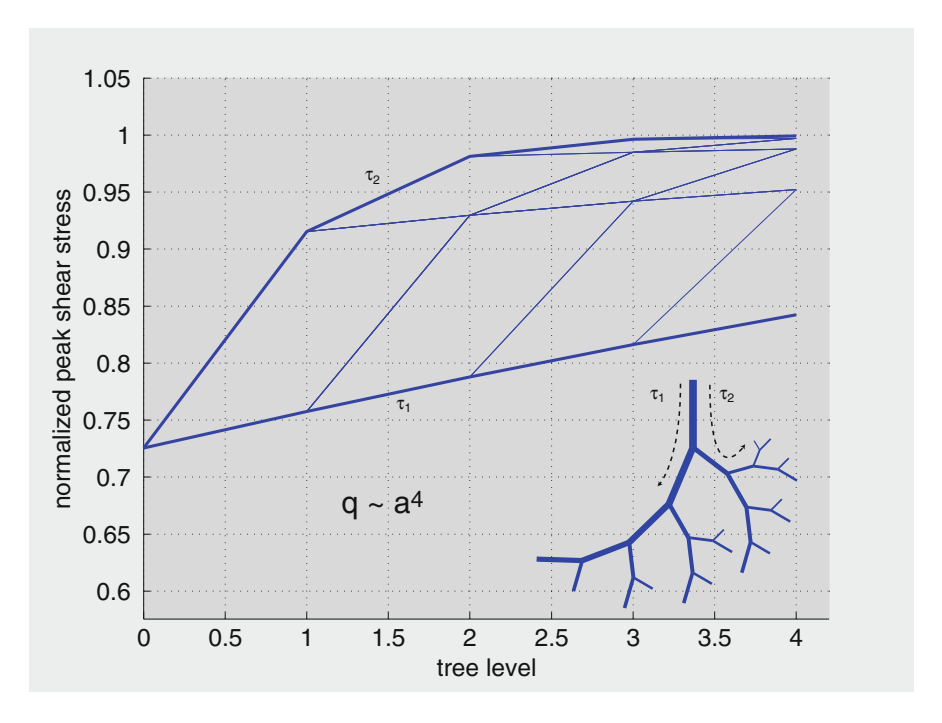


Fig. 7.26 Normalized peak shear stress reached at different branch segments of the 5-level tree shown in the *inset*, as in Fig. 7.23, but here the results are based on a power law index $\gamma = 4.0$.

Given the values of Ω for each vessel segment in that tree structure, the corresponding values of the wave speed c can then be calculated, using the solution for pulsatile flow in an elastic tube described in Sect. 5.9. Results are shown in Figs.7.27 and 7.28 where the hierarchy of the tree has been extended to 10 generations, and where the real and the imaginary parts of the wave speed are shown normalized in terms of the Moens-Korteweg wave speed c_0 . The figures indicate that at the root segment of this tree the real part of the wave speed is below the normalized value of 1.0, which means that it is below the Moens-Korteweg value. Thereafter, at smaller and smaller branch segments, the wave speed continues to decrease in value, more rapidly along the *minor* bounding path. Both the real and imaginary parts of c ultimately vanish at the peripheral levels of the tree, consistent with the dependence of c on the frequency parameter Ω .

Based on these values of c, the wave-length-to-tube-length ratio can also be calculated for each vessel segment using the diameters and lengths of vessel segments prescribed for this tree. The length λ of a propagating wave is related to the wave speed c and the angular frequency ω by

$$\lambda = \frac{2\pi c}{\omega} \tag{7.90}$$

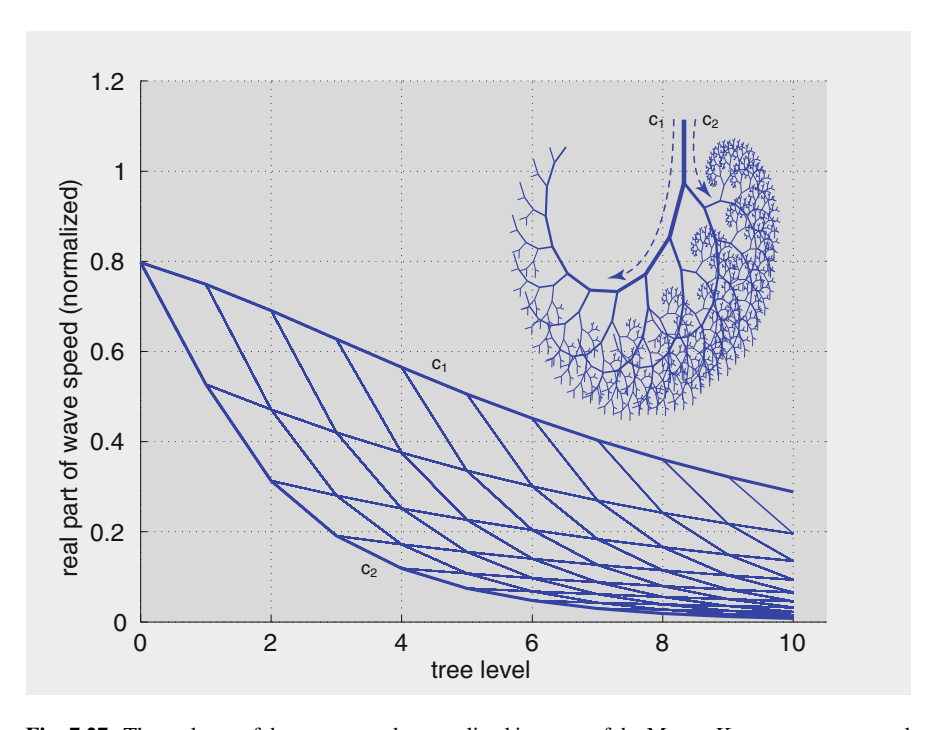


Fig. 7.27 The real part of the wave speed, normalized in terms of the Moens-Korteweg wave speed c_0 , in a vascular tree model in which the root segment has approximately the same diameter (4 mm) as a main coronary artery in the human heart and in which subsequent branching follows the cube law with power law index $\gamma=3.0$ as described in Sect. 8.4 and bifurcation index $\alpha=0.7$. The two bounding paths marked c_1,c_2 in the tree model are singular paths along which the branch with the larger diameter is followed at each junction in one case (c_1) , and the branch with the smaller diameter is followed in the second (c_2) . They represent two paths along which the real part of the wave speed decreases most slowly (c_1) , or most rapidly (c_2) , as indicated on the graph. Everywhere else within the tree structure the value of the real part of the wave speed is bound by these two curves. Thus, since the normalized values are everywhere less than 1.0, the figure indicates that the wave speed is everywhere lower than the Moens-Korteweg wave speed.

and the wave-length-to-tube-length ratio is then

$$\overline{\lambda} = \frac{\lambda}{L} = \frac{2\pi c}{\omega L} \tag{7.91}$$

where L is the tube length. If it is assumed further that the length of tube segments throughout this tree structure are a simple multiple of the corresponding diameters of these segments (usually taken as \sim 10), then at a fundamental frequency of 1 Hz, i.e. $\omega = 2\pi$, we finally have

$$\overline{\lambda} = \frac{c}{10 \times d} \tag{7.92}$$

Thus the distribution of wave-length-to-tube-length ratio within the tree structure can now be determined from the prescribed hierarchy of diameters at different

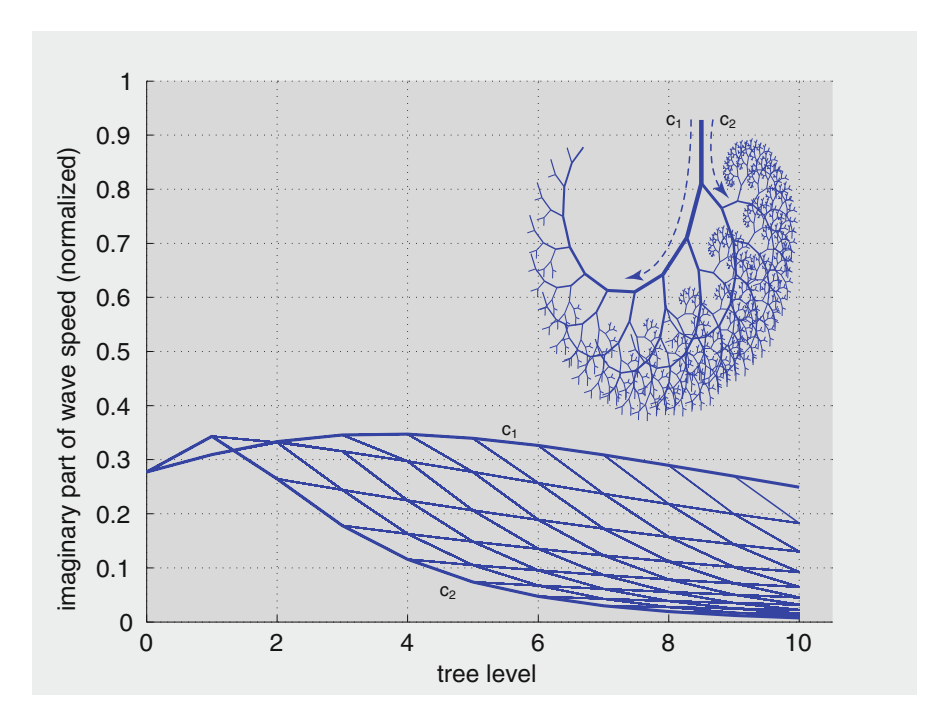


Fig. 7.28 The imaginary part of the wave speed associated with the real part shown in Fig. 7.27. Since the Moens-Korteweg wave speed is purely real, it follows that the wave speed here is different from the Moens-Korteweg wave speed everywhere along the tree structure, consistent with the results in Fig. 7.27. Remaining caption is the same as in that figure.

levels of the tree, which in this case was based on the cube law as described earlier (Sect. 3.11). Results are shown in Fig. 7.29 where it is seen that in a tree structure such as this, with 4 mm root diameter, as in the coronary arterial tree for example, values of $\bar{\lambda}$ are well above 100 throughout the tree structure.

As was shown in Sect. 5.11, at high wave-length-to-tube-length ratio pulsatile flow in a single isolated *elastic* tube approaches the corresponding flow in a single isolated *rigid* tube. Therefore, pulsatile flow in a rigid tube, which is much simpler analytically, can be used as a good approximation for the corresponding flow in an elastic tube. As discussed further in that Section, however, this approximation is valid *only in the absence of wave reflections*, and this condition clearly cannot be met in the arterial tree because of the inherent branching structure of the tree.

In summary, tube segments within the arterial tree cannot be treated as isolated tubes that are free from wave reflections and, consequently, pulsatile flow in an arterial tree consisting of elastic branching tube segments cannot be approximated by pulsatile flow in a tree consisting of rigid branching tube segments. As a consequence, and as discussed in Sect. 6.6, pulsatile flow in elastic branching tubes must be based not on the characteristic impedance of these tubes but on their effective impedance.

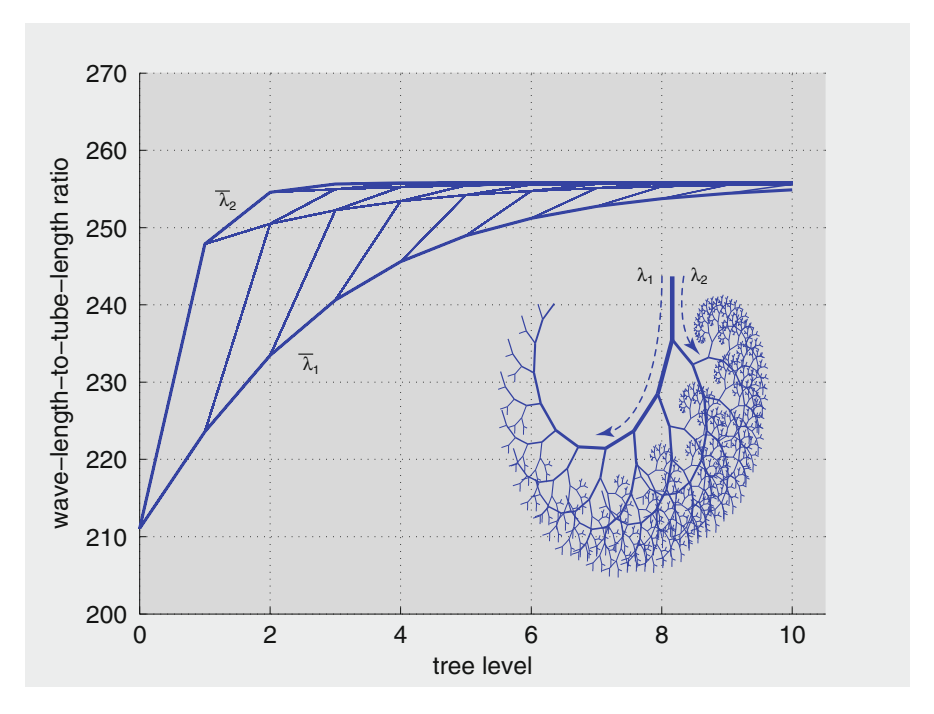


Fig. 7.29 The ratio of wave length to tube length $(\overline{\lambda} = \lambda/L)$ for vessel segments along the same 11-level tree model used in Fig. 7.27 and using values of the wave speed shown in that figure. The two bounding paths marked $\overline{\lambda}_1$ and $\overline{\lambda}_2$ correspond to those marked c_1, c_2 in Fig. 7.27 and have the same interpretation. The figure indicates that the value of $\overline{\lambda}$ is significantly above 100 everywhere along the tree structure, which means that the effects of wave propagation on flow within individual vessel segments is minimal *if wave reflections are absent*. Because of the large number of vessel junctions, however, wave reflections are ubiquitous and their effects on pressure and flow within the tree structure must be calculated.

7.10 Effective Impedance, Admittance

From a functional standpoint, the effects of wave reflections in a tube or vascular tree can be thought of in terms of the way they affect the opposition to flow. The term "opposition" is used here deliberately because the opposition to pulsatile flow in the presence of wave reflections is neither pure "resistance" as it is in steady flow, nor pure "impedance" as it is in oscillatory flow in an elastic tube in the absence of wave reflections.

The opposition to pulsatile flow in the presence of wave reflections is described by a modified impedance usually referred to as "effective" impedance. The pure impedance in oscillatory flow in the absence of wave reflections is then renamed "characteristic impedance" to differentiate between the two. Thus, the difference between the characteristic impedance and the effective impedance in a tube or vascular tree is a direct and functionally meaningful measure of the effects of wave reflections.

In general, opposition to flow is defined in terms of the amount of flow produced by a given amount of driving pressure. Thus in *steady* Poiseuille flow the ratio of pressure difference driving the flow to flow rate is termed the "resistance" to flow, as discussed in Sect. 3.8. In oscillatory flow, if the driving pressure and the flow rate are simple harmonic (sine or cosine) functions, the ratio of the *amplitudes* of pressure over flow is termed the "impedance" as discussed in Sect. 6.5.

The *resistance* in steady Poiseuille flow in a tube depends on only *static* properties of the tube and of the fluid (Eq. 3.58). The *characteristic impedance* in oscillatory flow through an elastic tube (Eq. 6.67), in the absence of wave reflections, depends on static properties of the tube wall and of the fluid as well as on the wave speed (which may in turn depend on frequency if the viscosity of the fluid is not neglected). In the presence of wave reflections, the *effective impedance* depends further on the extent of wave reflections.

Similar discussion and terminology apply to *admittance* which is the reciprocal of impedance, thus the terms "characteristic admittance" and "effective admittance" are interpreted in the same way as in the case of impedance.

From the results in Sect. 6.5, an input oscillatory pressure of the form

$$p_{in}(t) = p_0 e^{i\omega t} (7.93)$$

in an elastic tube, in the absence of wave reflections, leads to pressure and flow waves within the tube, respectively, of the form

$$\begin{cases}
P(x,t) = p_0 e^{i\omega(t-x/c)} \\
Q(x,t) = q_0 e^{i\omega(t-x/c)}
\end{cases}$$
(7.94)

where

$$\begin{cases} q_0 = Y_0 p_0 \\ Y_0 = \frac{\pi a^2}{\rho c} \end{cases}$$
 (7.95)

a is tube radius, ρ is fluid density and c is wave speed which is assumed constant within the tube. It is seen that

$$\frac{Q(0,t)}{P(0,t)} = \frac{q_0}{p_0}
= Y_0$$
(7.96)

The name "admittance" for Y_0 is thus appropriate as it represents a measure of the amount of oscillatory flow which the tube "admits" for a given oscillatory

pressure. Similarly, the reciprocal of Y_0 , which represents the extent to which the tube "impedes" the flow, is then given the name "impedance" and is defined by

$$Z_{0} = \frac{1}{Y_{0}}$$

$$= \frac{q_{0}}{p_{0}}$$

$$= \frac{P(0, t)}{Q(0, t)}$$

$$= \frac{\rho c}{\pi a^{2}}$$
(7.97)

In the way they are defined here, Y_0 and Z_0 are referred to as "input" admittance and "input" impedance, respectively, because they are based on pressure and flow at the input end of the tube.

It is important to note that Y_0 , Z_0 represent the admittance and impedance in a given tube not only in the absence of wave reflections but also on the assumption of constant wave speed within the tube. As we saw in Sect. 5.9, this constant wave speed is typically not equal to the Moens-Korteweg wave speed but must be determined from the solution for pulsatile flow in an elastic tube *for each vessel segment*. It depends on the frequency ω and therefore Y_0 , Z_0 will also depend on ω .

In the presence of wave reflections, the pressure and flow waves are no longer given by Eq. 7.94 because they then consist of both forward and backward moving waves as discussed in Sect. 6.4. As determined for the pressure in detail in that section, and using similar analysis for the flow wave, the two waves are now given by

$$\begin{cases}
P(x,t) = p_0 e^{i\omega(t-x/c)} + Rp_0 e^{i\omega(t-(2l-x)/c)} \\
Q(x,t) = q_0 e^{i\omega(t-x/c)} - Rq_0 e^{i\omega(t-(2l-x)/c)}
\end{cases}$$
(7.99)

from which it is clear that admittance or impedance are no longer determined by p_0, q_0 only. For this reason they are now denoted by Y_e, Z_e and referred to as the "effective" admittance and "effective" impedance, respectively, to distinguish these from the characteristic admittance and impedance. They are defined to have the same meaning as before, however, in terms of the pressure and flow at input to the tube, namely, as in Eq. 7.96

$$\frac{Q(0,t)}{P(0,t)} = \frac{q_0 - Rq_0 e^{-i\omega(2l/c)}}{p_0 + Rp_0 e^{-i\omega(2l/c)}}$$

$$= Y_0 \left(\frac{1 - Re^{-i\omega(2l/c)}}{1 + Re^{-i\omega(2l/c)}}\right)$$

$$= Y_e \tag{7.100}$$

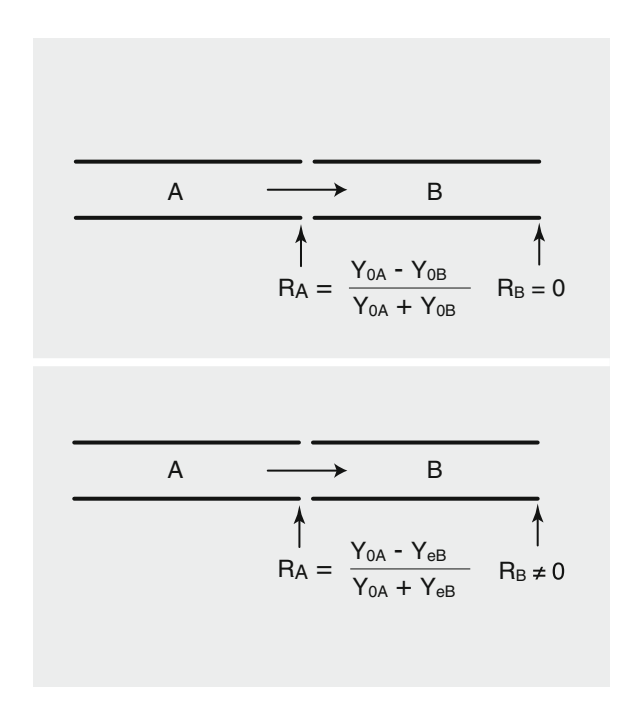


Fig. 7.30 The reflection coefficient R_A at the junction between two tubes depends on the difference between the characteristic admittances Y_{0A} of the first tube and Y_{0B} of the second if wave reflections are absent (top), or the difference between the characteristic admittance Y_{0A} of the first tube and the effective admittance Y_{eB} of the second if wave reflections are present (bottom).

If wave reflections arise at a junction between two tubes denoted by A and B whose characteristic admittances are Y_{0A} and Y_{0B} , and if there are no further reflections at the downstream end of the second tube, as shown schematically in Fig. 7.30, then the reflection coefficient R at the junction can be expressed in terms of the two characteristic admittances

$$R = \frac{Y_{0A} - Y_{0B}}{Y_{0A} + Y_{0B}} \tag{7.101}$$

But if there *are* wave reflections at the downstream end of the second tube then its admittance is now its effective admittance Y_{eA} , and the expression for the reflection coefficient becomes

$$R = \frac{Y_{0A} - Y_{eB}}{Y_{0A} + Y_{eB}} \tag{7.102}$$

Similarly, at a bifurcation, if the two branches are denoted by subscripts *B* and *C* as illustrated schematically in Fig. 7.31, since the combined admittance of the two

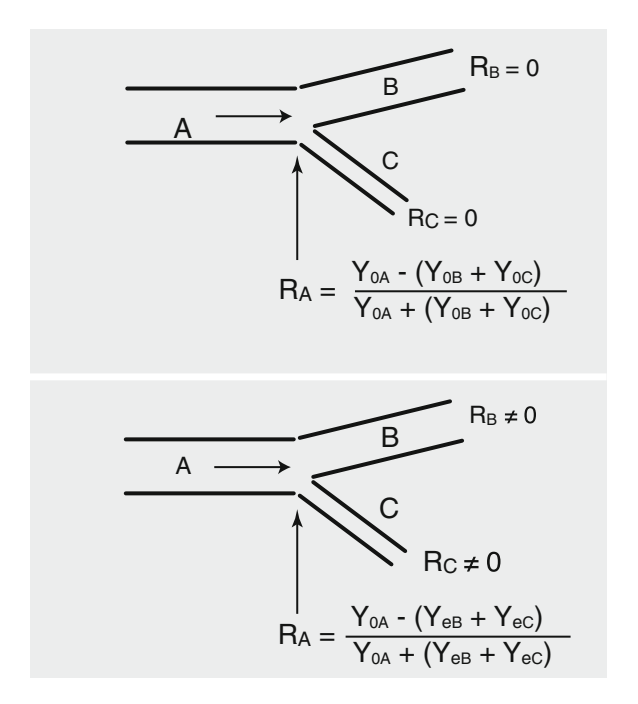


Fig. 7.31 The reflection coefficient R_A at an arterial bifurcation depends on the difference between the characteristic admittance Y_{0A} of the parent vessel segment and the sum of the characteristic admittances Y_{0B} , Y_{0C} of the two branch segments if wave reflections are absent (top), or the difference between the characteristic admittance Y_{0A} of the parent vessel segment and the sum of the effective admittance Y_{eB} , Y_{eC} of the two branch segments if wave reflections are present (bottom).

branches is simply the sum of the two (hence it is convenient to use admittance rather than impedance in the analysis of branching trees), then in the absence of wave reflections at the downstream ends of the two branches the reflection coefficient is given by

$$R = \frac{Y_{0A} - (Y_{0B} + Y_{0C})}{Y_{0A} + (Y_{0B} + Y_{0C})}$$
(7.103)

while in the presence of wave reflections it is given by

$$R = \frac{Y_{0A} - (Y_{eB} + Y_{eC})}{Y_{0A} + (Y_{eB} + Y_{eC})}$$
(7.104)

In an arterial tree the effective admittance of each vessel segment depends on wave reflections from all junction sites downstream of that segment. To calculate these, we may use Eq. 7.100 for the effective admittance of the parent vessel segment, with the reflection coefficient as given by Eq. 7.104, that is,

$$Y_{eA} = Y_{0A} \left\{ \frac{1 - Re^{-i\omega(2l_A/c_A)}}{1 + Re^{-i\omega(2l_A/c_A)}} \right\}$$
(7.105)

It is then convenient to eliminate the reflection coefficient R from this expression by using Eq. 7.104 to substitute for R. The result, after some algebra (as in Sect. 6.7, Eq. 6.91), is

$$\begin{cases} Y_{eA} = Y_{0A} \left(\frac{(Y_{eB} + Y_{eC}) + iY_{0A} \tan \theta}{Y_{0A} + i(Y_{eB} + Y_{eC}) \tan \theta} \right) \\ R = \frac{Y_{0A} - (Y_{eB} + Y_{eC})}{Y_{0A} + (Y_{eB} + Y_{eC})} \\ \theta = \frac{\omega l_A}{c_A} \end{cases}$$
(7.106)

In this form we see that the effective admittance of the parent vessel segment in a bifurcation is determined by its characteristic admittance and the effective admittance of the two branches. If there are no wave reflections at the downstream ends of the two branches, then their effective admittances are the same as their characteristic admittances.

Chapter 8 Dynamics of Pulsatile Blood Flow I

8.1 Introduction

Solutions of fluid flow problems, to fully determine the dynamics of the fluid, including a mapping of the velocity field and of the relation between the prevailing pressure and flow fields, are possible only in the most simply constructed cases and mostly in the physical sciences. Fluid flow problems in biology, by contrast, are rarely simply constructed and can rarely be solved directly. The problem of flow in a tube, for example, has a simple so called "Poiseuille flow" solution when the tube is rigid, its cross section is perfectly circular, the tube is long enough for the flow to be fully developed, and the fluid is a smooth "continuum" that has the simple rheological properties of a "Newtonian" fluid in which the shear stress is related linearly to the velocity gradients. Barely any of these ideal conditions is met in biological problems involving flow in tubes, most notably the problem of blood flow in arteries which is the subject of this book. Here the fluid is not a smooth continuum but a suspension in plasma of discrete red and other blood cells and, as we saw in the previous chapter, the system does not consist of a single tube but of many millions of tube segments that are joined together in a hierarchical tree structure. The segments are rarely long enough or perfectly circular to support fully developed Poiseuille flow, and the details of flow at their junctions are highly complicated and depend strongly on the exact geometry of each junction. Furthermore, the precise branching structure of the arterial tree or sub-trees within the cardiovascular system can rarely be mapped to the last detail so as to allow a mathematical solution of the flow problem based on a given tree structure as was done in the previous chapter.

In the previous chapter many of these difficulties were overcome by idealizing the problem to the point that it could be solved analytically. Is there another way?

A key feature of the approach used in the previous chapter, indeed in all the previous chapters so far, starting with the Navier-Stokes equations in Chap. 2,

is that the analysis there is based on the application of Newton's law of motion at every "point" within the flow field as discussed at great length in that chapter. The result is a point-by-point description of the flow.

This amount of detail may be necessary in some problems where the required information is localized, as in the flow within an aneurysm or around a plaque in a single artery, but in other problems where the required information is more global in nature, as in the dynamics of the coronary or cerebral circulations as a whole, or indeed the dynamics of the entire systemic circulation, the point-by-point approach is not only unnecessary but is inappropriate in that it does not provide the required information.

In an arterial tree this situation occurs on two scales. First, on the scale of the flow within each individual vessel segment, the steady part of the flow is being described point-by-point in terms of Poiseuille velocity profiles and the oscillatory part of the flow is being described in terms of wave propagation properties at each point *x* along that segment. Second, on the scale of the tree as a whole, the flow is being described in each one of possibly millions of individual vessel segments. Again, this amount of detail may be useful in some problems involving the relationship between the branching structure of a vascular tree and its function. But in other problems, as in the diagnosis of the health state of an entire vascular bed in relation to disease or aging, for example, this amount of detail is not only unnecessary but unattainable because it requires prior knowledge of the branching geometry of tree structure which is rarely available.

The notion that the vascular tree is not merely a passive system of tubes but a living organ, as discussed in the previous chapter, reinforces the need to study the properties of that organ as a whole in terms of its overall performance rather than in terms of point-by-point events within its structure. In the clinical setting, what matters in the end is how this organ is performing its function as the life line of its host tissue, be that in the heart, in the brain, or in any other part of the body.

In Chaps. 4 and 5 we saw the stark difference between pulsatile flow in a rigid tube compared with that in an elastic tube, due entirely to the difference in compliance of the two tubes, the compliance of the rigid tube being zero. Thus, as a vascular bed stiffens with age or disease, for example, what effect does this have on the function of that bed, and how do we assess the nature and magnitude of that effect? While this question was actually answered in the previous chapter, the answer was based on a theoretically prescribed vascular branching structure.

In the present chapter we consider a way of looking at the dynamics of arterial trees not point-by-point within each vessel segment, or segment-by-segment within each tree structure, but by "lumping" the properties of these individual components all together under what is generally known as the "lumped parameter concept".

8.2 The Lumped Parameter Concept

The relation between pressure and flow in a tube depends on such properties of the tube as its diameter, length, and elasticity. It also depends on the form of the driving pressure, in particular on whether the pressure is steady or pulsatile. The relation between pressure and flow in an *arterial tree* consisting of a large number of tube segments depends not only on all such factors in each tube segment but also on events at the junctions between tube segments and on how the properties of individual segments are distributed within the tree structure. The overwhelming complexity of this problem is the background rationale for the "lumped parameter" concept.

Briefly, the lumped parameter concept proposes that the complex structure of a vascular bed can be ignored and the bed can be replaced by a single tube that has the combined or "lumped" properties of the vascular bed as a whole. This is clearly a variant of the more familiar "black box" concept, in which a complex system is enclosed by an imaginary box and only the relationship between the input and output from the box is examined to learn something about the characteristics of the system within the box.

In a well defined circulation such as that of heart or the brain, for example, where access to the complex vasculature that serves these two organs is extremely limited, the information that can be gleaned from input and output to the system provides a valuable insight into the state of the vascular beds within. As in the case of a black box, here the input in each case is the pressure driving the flow into the vascular bed and the output is the flow which this driving pressure produces. For a given driving pressure, it is clear that the resulting flow will be different at different states of the vascular system, particularly so under conditions of pulsatile flow where more properties of the system become involved, most prominently the compliance of the blood vessels.

Much the same can be said about the systemic circulation as a whole. In fact, in this case it is common practice to examine features of the pressure and flow waveforms that emerge from the left ventricle to gain some insight into the state of the systemic vasculature as a whole. Any change in that state produces changes in the pressure and flow waveforms and in the relationship between them. It is common practice, for example, to measure the wave speed (pulse wave velocity) in the systemic circulation to assess the compliance of the systemic vasculature. This is an application of the lumped parameter concept because in the calculation of the wave speed the very complex structure of the systemic vasculature and the complex distribution of parameters that goes with it are all ignored in the process, being replaced by one set of lumped parameters.

Above all, the lumped parameter concept provides the required tool to examine the <u>dynamics</u> of pulsatile flow in an arterial tree or a vascular bed as a whole. This tool is not available in a point-by-point description of the flow.

In the remainder of this chapter we shall see in detail how the relationship between the driving pressure and the flow which it produces in a vascular bed depends critically on the "lumped" properties of that bed, and how an understanding of this relationship provides a valuable insight into the state of that bed.

8.3 Flow in a Tube Revisited

The lumped parameter concept discussed in the previous section is based on the assumption that flow through a complex vascular bed can be replaced by the flow in a single tube with "equivalent" properties. It is important therefore that flow in a tube as discussed in previous chapters be revisited in order to examine the assumptions on which this concept is based and to identify the equivalent properties of the flow in a tube to be used in the process.

Consistent with the lumped parameter concept, in what follows the flow in a tube will be considered as a bulk of fluid moving *en masse* rather than as individual fluid elements as has been done in earlier chapters. This bulk of fluid will be subject to the laws of motion but not point-by-point as in the Navier-Stokes equations or in the description of Poiseuille flow. Instead, we consider the forces that affect the bulk of fluid as a whole, starting with the resistance to flow.

The most important form of resistance to flow in a tube is that due to viscous friction at the interface between the fluid and the tube wall. It is important because it is present when flow is steady or oscillatory and it always dissipates energy. Because of this, it is usually referred to simply as "the resistance", and we shall follow this practice in this book. As described in Sect. 3.7, this resistance to flow in a tube arises because of a combination of the no-slip boundary condition at the tube wall and the viscous property of the fluid.

From the results in Sect. 3.8, the relation between the flow rate q and the driving pressure Δp , is given by (Eq. 3.56)

$$\Delta p_s = \left(\frac{8\mu l}{\pi a^4}\right) q_s$$

with the term inside the brackets being identified as the resistance to flow. It is important to note, as indicated by the subscript s, that this result is based on the assumption of steady flow. In the context of the lumped parameter concept we shall dispense with this subscript and associate this resistance to flow always with the viscous resistance to flow in steady flow and denote it by R, thus writing

$$q = \frac{\Delta p}{R} \tag{8.1}$$

where

$$R = \left(\frac{8\mu l}{\pi a^4}\right) \tag{8.2}$$

We recall that the pressure drop Δp was defined as the difference between pressure upstream minus pressure downstream (Eq. 3.28), therefore it is positive in the direction of the flow, as is the flow rate q.

Equation 8.3 is a simple example of the application of the lumped parameter concept in that the flow in a tube is reduced to a simple relation between the flow rate q and the driving pressure difference Δp . The relation between q and Δp is the cornerstone of the lumped parameter concept. In Eq. 8.3 the relation involves only one parameter, namely R, but we shall see that as other factors affect the flow, other parameters will be required. Equation 8.3 is therefore singular in the sense that it is valid only when the viscous shear force at the tube wall is the single force resisting the flow in a tube, which, as we saw in Sect. 3.7, occurs only in steady Poiseuille flow.

The significance of the above statement is that it applies equally to the flow in a *branching tree structure* so long as viscous shear at the tube walls is the only force resisting the flow or, equivalently, so long as the flow in all tube segments is fully developed Poiseuille flow. Of course, these ideal conditions are rarely met in the vascular tree because vascular segments at least in part of the tree would be too short for flow to reach the fully developed state (Sect. 3.4).

In the lumped parameter concept this difficulty is dealt with by identifying the pressure drop Δp in Eq. 8.3 specifically as the pressure drop required to overcome the viscous resistance forces in all tube segments within a vascular tree. Regardless of whether these forces arise in fully developed flow or not, they are all "lumped" together into a single resistance force R, and it is in this sense that R becomes a "lumped" parameter. The pressure force required to overcome this lumped resistance is then appropriately denoted by ΔP_r , writing

$$q = \frac{\Delta P_r}{R} \tag{8.3}$$

The subscript r is added to indicate clearly that ΔP_r is the amount of driving pressure related to overcoming only the viscous resistance force.

The fact that this resistance force may not be occurring in fully developed regions of the flow is dealt with by recalling, as described in Sect. 3.4, that in the entry region of flow in a tube the flow is being accelerated towards the fully developed state, and this acceleration requires an added amount of driving pressure.

Thus, in lumped parameter analysis it is recognized that in general ΔP_r is only part of the total pressure required to drive the flow in a tube. Other parts will be required to overcome other forms of resistance to flow, such as acceleration or deceleration of the flow, compliance of the tube wall, and possibly wave reflections within a tree structure. The ultimate step in lumped parameter analysis is to compare simultaneous measurements of the flow rate q and driving pressure Δp in a vascular system, whether in steady or pulsatile flow. If the relation between the measured q and Δp is the same as that in Eq. 8.3, then the only forces opposing the flow in that system are due to viscous resistance to flow. If the relation between the measured q and Δp is not the same as that in Eq. 8.3, then there are other forces opposing the flow and these must be accounted for as will be described in the coming sections.

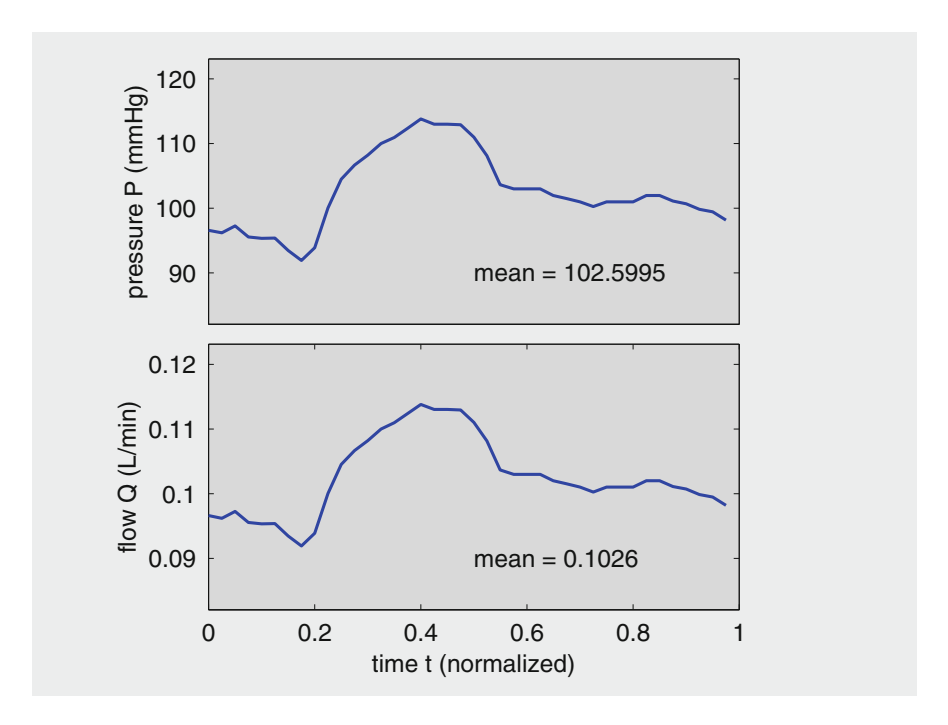


Fig. 8.1 Pressure wave (*top*) and corresponding flow wave (*bottom*) when opposition to flow is only resistance *R*. The two waves have identical form but cannot be put together because of their different scales and physical units.

Thus the pressure drop ΔP_r emerges as an important *baseline* reference pressure drop, and Eq. 8.3 emerges as an important reference relation between pressure and flow. According to that relation, the measured pressure and flow will have the same form when the only force resisting the flow is that of viscous resistance. In fact, if a scaled form of the flow rate, namely the product $q \times R$, is used instead of q, then Eq. 8.3 can be put in the form

$$q \times R = \Delta P_r \tag{8.4}$$

and the scaled flow rate then actually becomes *equal to* the pressure drop Δp . The measured time course of $q \times R$ and Δp , whether under steady or pulsatile flow conditions, can then be plotted in the same figure using the same scale (Figs. 8.1 and 8.2).

The cornerstone of the lumped parameter method of analysis is the fact that if viscous resistance to flow is the only force opposing the flow in a given vascular system, then the curves representing $q \times R$ and Δp in this figure will be identical. On the other hand, and more importantly, if other opposing forces are at play, the two curves will be different and, as stated earlier, these forces must be accounted for.

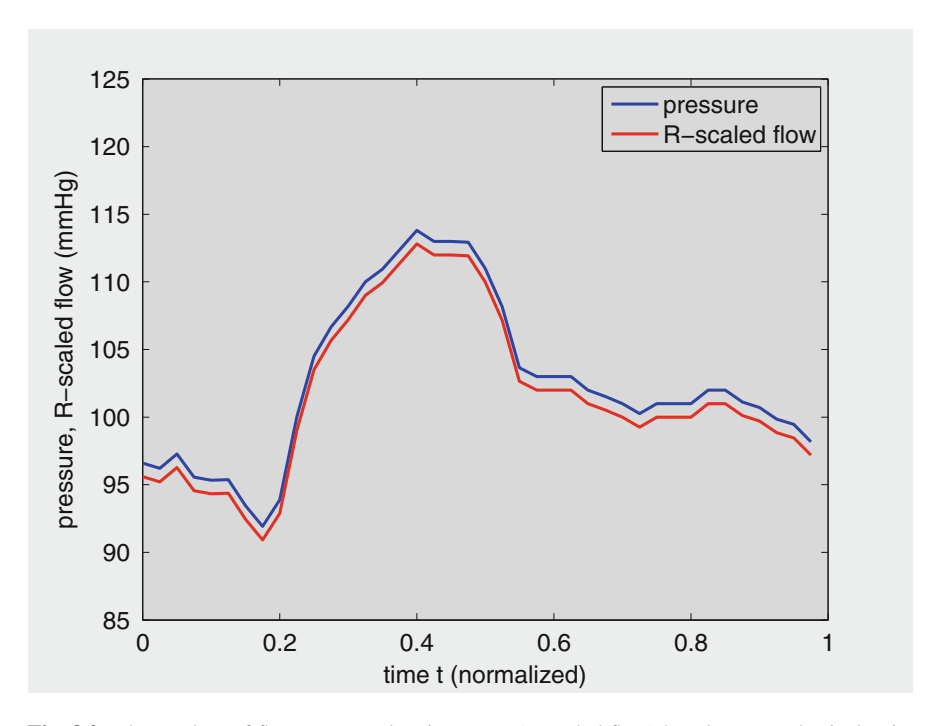


Fig. 8.2 The product of flow rate q and resistance R (R-scaled flow) has the same physical units as pressure p. In the example of Fig. 8.1, the pressure is in mmHg, the flow is in L/min while the resistance R is in mmHg/(L/min), thus the product $R \times q$ has the units of mmHg and can be put on the same scale as p as shown in the figure (the two curves are slightly shifted to make them visibly distinct). The use of R-scaled flow is useful because the pressure and R-scaled curves coincide *only when the opposition to flow consists of pure resistance*. Therefore, any discrepancy between the two curves indicates that other forms of opposition to flow are present as will be discussed in the present chapter.

8.4 Transient and Steady States

If the pressure driving the flow in a tube is constant, the corresponding flow rate will also be constant, assuming that the fluid and tube properties on which the resistance to flow is based are also constant. Thus, if in the lumped parameter relation between the flow rate and pressure in Eq. 8.3 we set $\Delta p = \Delta p_0$ and $R = R_0$ where the subscript '0' is being used to denote constant quantities, then the flow rate q will be given by

$$q = \frac{\Delta p_0}{R_0} \tag{8.5}$$

and will therefore also be constant, and the flow is then said to be in "steady state". A pertinent example here, of course, is fully developed Poiseuille flow, as described in Sect. 3.8, because Eq. 8.3 was actually derived from fully developed Poiseuille flow.

However, flow in a tube need not be fully developed to be steady, and Eq. 8.5 is not limited to fully developed Poiseuille flow although it was based on that flow in the previous section. Flow in the entry region of a tube, as described in Sect. 3.4, is not fully developed but is steady in the sense that if the pressure driving the flow is constant, flow in the entry region of the tube does not change with time. Equation 8.5 will remain valid because the relation between the flow rate q and the pressure Δp_0 will continue to hold, albeit with a different value of the resistance, say R_1 , because resistance to flow in the entry region of the tube is different from that in the fully developed region.

Thus the lumped parameter concept captures the flow in both the developing and the fully developed region of the flow in a tube and combines the resistances in the two regions of the flow into one lumped resistance R_1 . This is a simple, though important, example of the application of this concept and of Eq. 8.5. It is important because in many vessel segments within an arterial tree the flow is not fully developed. Thus, if the pressure driving the flow into an arterial tree is constant, Eq. 8.5 will continue to hold, first by lumping the resistances in each vessel segment into one, and then by lumping the resistances of all vessel segments into one. The relation between the flow rate and the driving pressure will continue to hold, though now with a new lumped resistance R_{lumped}

$$q = \frac{\Delta p_0}{R_{lumped}} \tag{8.6}$$

Now, if the pressure driving the flow in a tube or a branching tree structure changes to another constant value, say from Δp_0 to Δp_1 , the flow rate will adjust to this new value of the driving pressure until it reaches a new value, say q_1 , appropriate for the new value of the driving pressure, and the flow is then said to have reached a new steady state. But the change from the first steady state to the second *will not occur instantaneously* because of (a) the inertia of the fluid and (b) any elastic or viscoelastic effects within the vessel wall. These factors will be discussed in detail in the coming sections. Here we point out only that during the period of adjustment from the first steady state to the second steady state the flow is said to be in "transient state".

It is important not to confuse "transient" and "steady state" being discussed here, with "developing" and "fully developed" flow discussed in Sect. 3.4.

Broadly speaking, developing and fully developed flow have to do with flow development in space, as in the entrance region of a tube, while transient and steady states have to do with flow development in time, as when the pressure driving the flow is changed.

There is one exception to the above rule, namely the case of *oscillatory flow*. Oscillatory flow is in fact considered as steady flow, both by definition and by the fact that while the pressure and flow in oscillatory flow change in time *within each cycle*, they do not change from one cycle to the next. This extends the scope of the lumped parameter concept to pulsatile flow where, as we shall see, remarkably,

Eq. 8.6 will continue to hold but with the resistance R being replaced by the impedance Z, that is

$$q = \frac{\Delta p_0}{Z_{lumped}} \tag{8.7}$$

This simple equation is truly remarkable in its scope because as long as the driving pressure Δp is either constant or a periodic function of time, the flow rate will be related to the driving pressure via a lumped resistance or impedance which represents the lumped resistances or impedances of the vascular system at hand. It is indeed the principal tool in the lumped parameter concept and, as we shall see in the next chapter, combined with the method of Fourier decomposition of composite pressure waveforms, it provides a powerful method of analyzing the relation between the pressure and flow waveforms at the input to a vascular bed to determine the impedance that would give rise to that relation, and thereby determine in turn the lumped properties of the bed that would give rise to that impedance.

It is important to note that Eq. 8.7 is valid only in steady state. But as stated above this includes steady state oscillation, which is the quintessential problem in the cardiovascular system because this is the pattern of driving pressure produced by the heart. There are transient states, however, that take the system from one steady state to another. The dynamics of these transient states are discussed in the remainder of this chapter.

8.5 Fluid Inertia: Inductance

Acceleration in fluid flow may occur in one of two ways: in space or in time. Acceleration in space occurs when the space available to a stream of fluid is decreasing, so the fluid must increase its velocity to go through a reduced amount of space. Flow in a tube with a narrowing, as in a bottle neck, is an example (Fig. 8.3). Velocity at the narrowing must be higher than it is elsewhere, since the flow rate through the tube must be everywhere the same by conservation of mass, and since it is assumed here that the flow is *incompressible*, that is fluid density is not changing. Thus the fluid is in a state of acceleration as it goes through the narrowing. The acceleration is *in space*, that is, in the sense that fluid elements are being accelerated as they progress along the tube.

Another, less obvious, example of acceleration in space occurs at the entrance to a tube. If fluid enters with uniform velocity, elements of the fluid along the tube axis must accelerate to reach the maximum velocity in Poiseuille flow, while fluid elements near the tube wall are slowed down by the viscous resistance to meet the condition of no-slip at the tube wall (Fig. 8.4). Thus in the entrance region of the tube some fluid is in a state of acceleration and some is in a state of deceleration, in both cases the change is occurring *in space*, that is as the fluid progresses along the tube.

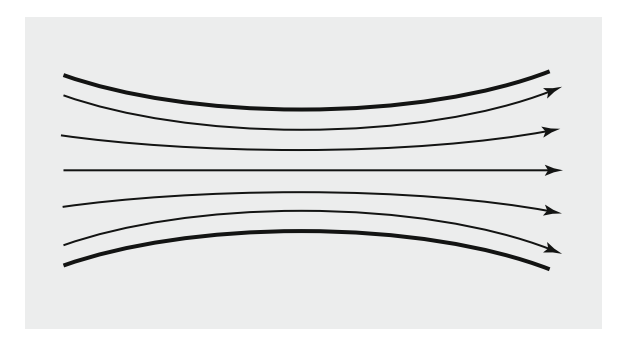


Fig. 8.3 Flow in a tube with a narrowing causes fluid elements to accelerate as they approach the narrowing and decelerate as they leave, assuming that the fluid is incompressible. Flow velocity is highest at the neck of the narrowing as indicated by the closeness of the streamlines there. Both the acceleration and deceleration are occurring in space, in the sense that the change in velocity is occurring as fluid elements progress along the tube.

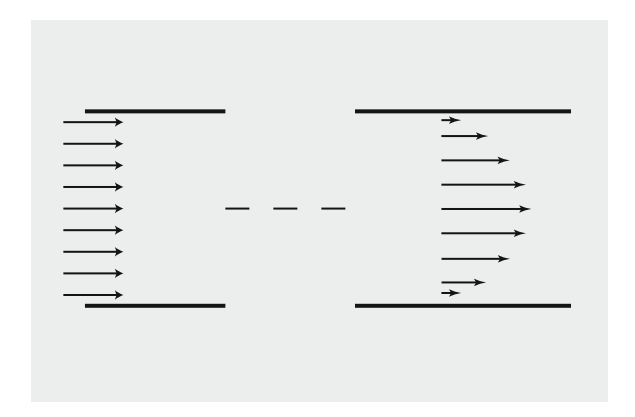


Fig. 8.4 Flow in the entrance region of a tube provides another example of acceleration and deceleration *in space*. If fluid enters with uniform velocity, elements of the fluid along the tube axis must accelerate to meet the maximum velocity in Poiseuille flow, while fluid elements near the tube wall are slowed down by the viscous resistance and condition of no-slip at the tube wall.

One of the most important features of acceleration or deceleration in space is that it occurs in *steady* flow, that is in a state of flow which does not change in time. In steady flow the velocity field does not change with time, that is the velocities at fixed positions within the flow field are fixed and acceleration and deceleration occur as fluid elements move from one position to the next. It is in this sense that acceleration and deceleration in steady flow are seen as occurring *in space*.

Acceleration or deceleration *in time*, by contrast, is associated with *unsteady* flow, a state of flow in which the velocity distribution within the flow field changes with time. This situation occurs when the pressure driving the flow is not constant in time, as is the case in pulsatile blood flow where the driving pressure changes in an oscillatory manner. In this case acceleration and deceleration are occurring *in time*, in the sense that the velocity at fixed positions within the flow field is changing in time (Fig. 8.5).

	+ + + + + + + + + + + + + + + + + + +
+ + + + + + + + + + + +	

Fig. 8.5 Changing flow field in oscillatory flow. *Different panels* represent different points in time within the oscillatory cycle. Velocity is changing in time at fixed positions in space within the flow field. Acceleration and deceleration is occurring *in time*.

When a mass of fluid is accelerated or decelerated *in time*, the fluid does not respond immediately, because of its inertia. Thus if the pressure difference Δp driving the flow in a tube changes suddenly to a higher level, it takes the flow rate q some time before it adjusts to a new value appropriate for the new driving pressure difference. This "reluctance" of the fluid to respond immediately is a form of resistance which would appropriately be referred to as "inertance" but is commonly known as *inductance* because of an electrical analogy to be discussed later.

Unlike the *viscous* resistance to flow which is present at constant flow rate, inductance is only present when flow is being accelerated or decelerated, that is only when there is change in the flow rate. In fact it is the *rate of change* of flow rate that is being resisted by the fluid, which means that a force is required to bring about such change. In the case of flow in a tube this means that a pressure difference ΔP_l would be required specifically for this purpose, the subscript L is there to distinguish this pressure difference from that required to maintain the flow against the viscous resistance. More precisely, the required force is proportional to the rate of change of flow rate, that is

$$\Delta P_l = L \frac{dq}{dt} \tag{8.8}$$

Again, the symbol L is commonly used for the inertial constant because of analogy with inductance in electric systems.

The basis of this relation can be found in the mechanics of an isolated mass m, governed by Newton's law of motion, as was previously applied to a fluid element but is now being applied to a bulk of fluid as whole within a tube. The law required that the product of mass and acceleration be equal to the net force acting on that mass. If the force is denoted by F and the position of the mass is denoted by x, the law can be written as

$$m\frac{d^2x}{dt^2} = F (8.9)$$

where t is time. In general this equation is a vector equation because both F and x are vectors, but for the present purpose it is sufficient to work in only one dimension. In fluid flow the corresponding situation would be that of flow in a tube being accelerated, or decelerated, in one direction, namely along the axis of the tube. If the viscous effect at the tube wall is neglected for now (as it is accounted for separately below), then the body of fluid may be considered to move freely along the tube, as a bolus, in accordance with Newton's law. If the diameter of the tube is d, then the mass of such bolus of length l, being a cylindrical volume of fluid of diameter d and length l, is $\rho l \pi d^2 / 4$, where ρ is the density of the fluid. If the velocity of the bolus is u and the pressure difference driving it is ΔP_l then Eq. 8.9 applied to this mass gives

$$\frac{\rho l \pi d^2}{4} \frac{du}{dt} = \Delta P_l \frac{\pi d^2}{4} \tag{8.10}$$

Since q is the volumetric flow rate, then $q = u\pi d^2/4$ and the above can be put in the form

$$\Delta P_l = \left(\frac{4\rho l}{\pi d^2}\right) \frac{dq}{dt} \tag{8.11}$$

Comparison of this with Eq. 8.8 indicates that the constant L in that equation corresponds to the bracketed term above, that is

$$L = \left(\frac{4\rho l}{\pi d^2}\right) \tag{8.12}$$

Thus Eq. 8.8 and the concept of inductance on which it is based have a basis in simple mechanics.

The total pressure difference Δp required to drive the flow in a tube in the presence of change in flow rate is the sum of the pressure difference needed to overcome the force of resistance due to inductance, namely ΔP_l , plus the pressure difference needed to overcome the force of resistance due to viscosity, namely ΔP_r as discussed in the previous section, that is

$$\Delta p = \Delta P_r + \Delta P_l \tag{8.13}$$

Substituting for ΔP_r from Eq. 8.4 and for ΔP_l from Eq. 8.8, we then have

$$\Delta p = Rq + L\frac{dq}{dt} \tag{8.14}$$

This is a first order ordinary differential equation which has the general solution¹

$$q(t) = \frac{e^{-t/(L/R)}}{L} \int \Delta p \ e^{t/(L/R)} dt \tag{8.15}$$

If the driving pressure difference is constant, say

$$\Delta p = \Delta p_0 \tag{8.16}$$

Then Eq. 8.15 gives upon integration

$$q(t) = \frac{\Delta p_0}{R} + Ae^{-t/(L/R)}$$
 (8.17)

where A is a constant of integration. If the flow rate is zero at t=0, we find $A=-\Delta p_0/R$ and the solution finally becomes

$$q(t) = \frac{\Delta p_0}{R} \left(1 - e^{-t/(L/R)} \right)$$
 (8.18)

As time goes on, the exponential term vanishes, leaving the flow rate at a constant value of $\Delta p_0/R$, which is what it would be against a resistance R and with a constant driving pressure difference Δp_0 (Eq. 8.5). At that value the flow is in *steady state*, while prior to that it is in a *transient state*.

The effect of inertia of the fluid is thus seen to cause the flow to take a certain amount of time to reach steady state. As the driving pressure difference is applied, the flow rate increases from zero to its ultimate value but because of inertia it takes a certain amount of time to reach that value. The higher the inertial effect the longer time it takes the flow to reach steady state (Fig. 8.6).

The ratio L/R has the dimensions of time and is a measure of the time delay caused by the inertial effect. It is usually referred to as the "inertial time constant" and we shall denote it here by t_l , that is

$$t_l = \frac{L}{R} \tag{8.19}$$

¹Kreyszig E, 1983. Advanced Engineering Mathematics. Wiley, New York.

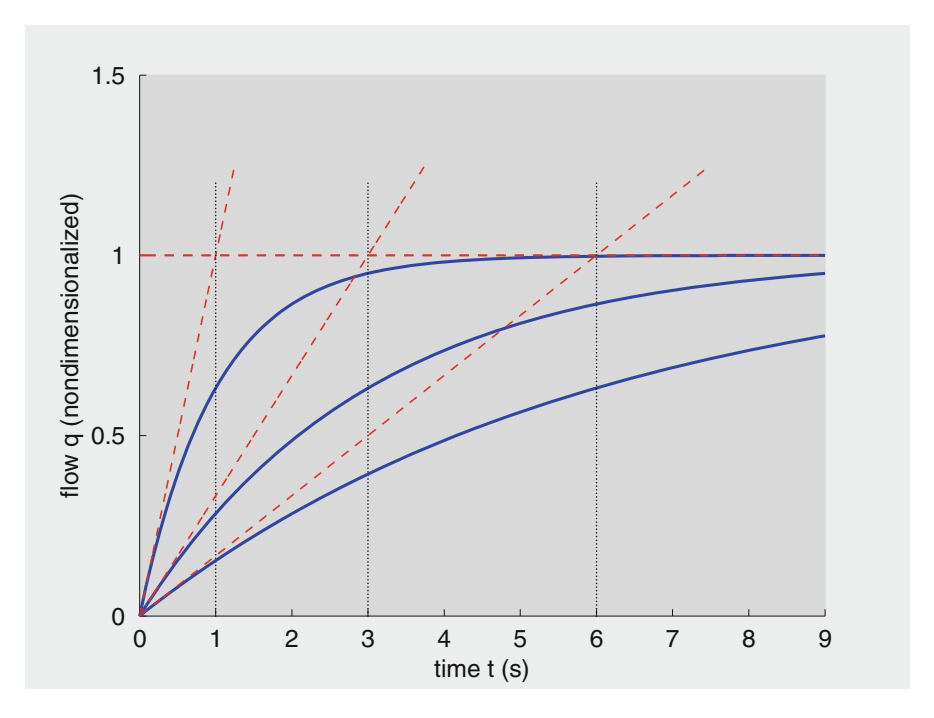


Fig. 8.6 If the pressure difference driving the flow in a tube is suddenly increased from 0 to some fixed value Δp_0 , the flow increases gradually (*solid curves*) until it reaches the value $\Delta p_0/R$ (*dashed lines*). At that value the flow is said to be in *steady state*, while prior to that it is in a *transient state*. In steady state the flow rate has the value which it would have against a resistance R and with a driving pressure difference Δp_0 (Eq. 8.3), but because of fluid inertia the flow rate takes time to reach this value, the higher the inertia the longer the time. A measure of this effect is the so called "inertial time constant" $t_l = L/R$, which has the dimension of time when L and R are as defined in Eqs. 8.12 and 8.2. The *three solid curves* above, from left to right, correspond to $t_l = 1.0, 3.0, 6.0$ s. The time it takes the flow curve to reach its ultimate value is directly related to the value of t_l , and the reciprocal of t_l represents the initial slope with which the flow curve moves towards its asymptotic value. In the absence of the inertial effect ($L/R = t_l = 0$), the flow curve would "jump" to the asymptotic value at time t = 0 and remain on it thereafter.

The higher the value of t_l the higher the prevailing inertial effect and the longer is the time required for the flow to reach steady state. It is important to note, however, that the approach to steady flow is *asymptotic*, as seen in Fig. 8.6, which means that, strictly, the flow takes an infinite amount of time to reach steady state. For practical purposes, however, the flow is sufficiently close to steady state in a finite and usually very short amount of time. The inertial time constant t_l is a measure of that time.

More precisely, if we introduce a nondimensional (normalized) flow rate

$$\overline{q}(t) = \frac{q(t)}{\Delta p_0/R} \tag{8.20}$$

then Eq. 8.18 becomes

$$\bar{q}(t) = 1 - e^{-t/t_l} \tag{8.21}$$

and upon differentiation we find

$$\frac{d\,\overline{q}}{dt}(t) = \frac{1}{t_l}e^{-t/t_l}$$

$$\frac{d\,\overline{q}}{dt}(0) = \frac{1}{t_l} \tag{8.22}$$

Thus the reciprocal of t_l represents the initial slope with which the flow curve moves towards its asymptotic value. The higher the inertial effect the higher the value of t_l and hence the lower the initial slope of the flow curve and the longer it takes the flow to reach its asymptotic value. Also, because the asymptotic value of the flow is here set at a normalized value of 1.0, then t_l also represents the time it takes the flow to reach this asymptotic value if, hypothetically, it continued with its initial slope, as illustrated in Fig. 8.6.

If the driving pressure gradient Δp increases linearly with time, say

$$\Delta p = \frac{\Delta p_0}{T} t \tag{8.23}$$

where Δp_0 is a constant and T is a fixed time interval, Eq. 8.15 gives upon integration (by parts) and simplification

$$q(t) = \frac{\Delta p_0}{TR} \left(t - \frac{L}{R} \right) + Ae^{-t/(L/R)}$$
(8.24)

where A is a constant of integration. If the flow rate is zero at t = 0, we find

$$A = \frac{\Delta p_0 L}{TR^2}$$

and the solution becomes

$$q(t) = \frac{\Delta p_0}{TR} \left(t - \frac{L}{R} + \frac{L}{R} e^{-t/(L/R)} \right)$$
 (8.25)

or in nondimensional form

$$\overline{q}(t) = \frac{q(t)}{\Delta p_0 / R} = \frac{t}{T} - \frac{t_l}{T} \left(1 - e^{-(t/T)/(t_l/T)} \right)$$
(8.26)

The form of the solution suggests that the appropriate time variable in this case is the fractional time t/T, where T may, for example, be taken as the total interval over which the flow takes place, hence t/T has the range 0–1.0. As in the previous case, the effect of inertia is embodied in the value of inertial time constant t_l . Again, since t_l has the dimension of time, it is appropriate in this case to consider values of the inertial time constant t_l/T , as this indeed is the parameter required in the above equation.

Results for $t_l/T = 0.1, 0.3, 0.5$ are shown in Fig. 8.7. As the driving pressure difference Δp increases, both the flow rate and its derivative begin to increase,

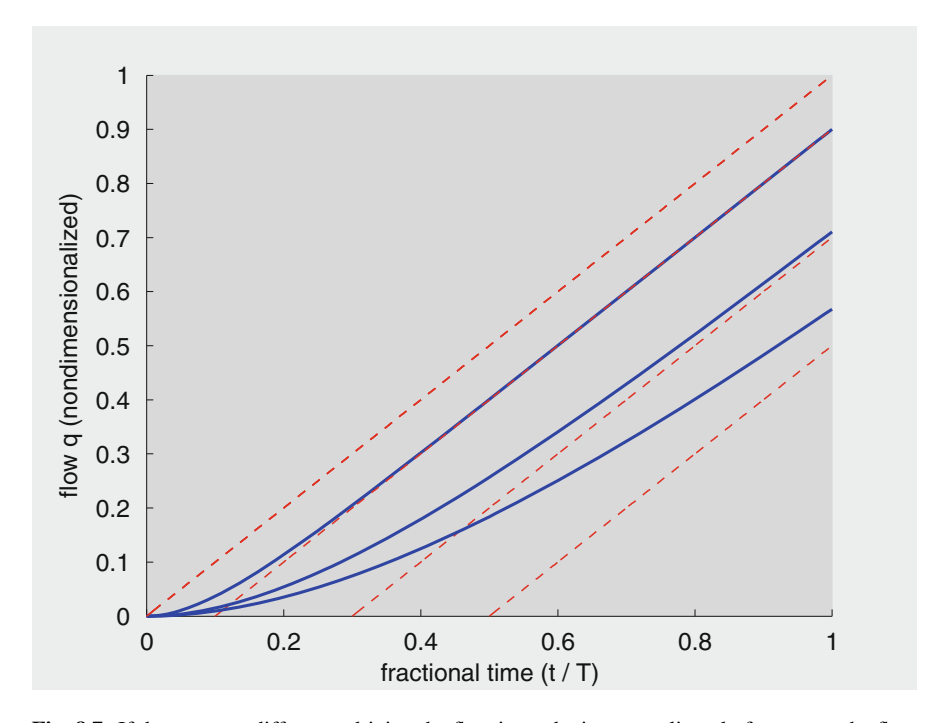


Fig. 8.7 If the pressure difference driving the flow in a tube increases linearly from zero, the flow rate begins to increase, but because of inertia it requires a certain amount of time to reach a value appropriate for the prevailing value of the pressure difference. But since in this case the pressure difference is continually increasing, the flow rate is never able to reach that appropriate value. What the flow rate is able to achieve as time goes on is a *quasi-steady state* in which its value is a fixed amount below what it should be. Thus, asymptotically, the flow acquires the same form as the driving pressure, namely that of a linearly increasing function with a unit slope (Eq. 8.27), but, because of the inertial effect the flow curve is shifted along the time axis by an amount equal to the value of t_l/T as shown. The *three solid curves* above, from left to right respectively, correspond to $t_l/T = L/RT = 0.1, 0.3, 0.5$, where T is total time interval over which flow is taking place, here taken as 1.0. The *dashed curve* through the origin represents the normalized pressure as well as what the flow rate would be in the absence of inertial effects, that is when t_l/T is zero. The *other three dashed curves* represent the asymptotes of the flow curves for $t_l/T = L/RT = 0.1, 0.3, 0.5$. The higher the value of t_l/T the larger the ultimate gap between pressure and flow and hence the higher the inertial effect.

but as in the previous case, because of inertia, it takes a certain amount of time for the flow to reach a value appropriate for the prevailing value of the pressure difference. But since in this case the pressure difference is continually increasing, the flow rate is never able to reach that appropriate value. What the flow rate is able to achieve as time goes on is a state in which its value is a *fixed amount* below what it should be. We may refer to this state as a *quasi-steady state* since, strictly, steady state is usually defined as one in which the flow rate is either constant or periodic. In the present case it is continually increasing. Nevertheless, it is possible here to distinguish (Fig. 8.7) between an initial period where the flow rate is adjusting to the new pressure difference, which may be referred to as a transient state, and a final period in which the flow rate is still changing but now at a fixed rate, the same rate at which the driving pressure difference is changing. It is in this sense that the latter may be referred to as a quasi-steady state.

From Eq. 8.26 we see that the quasi-steady state is reached asymptotically as the exponential term vanishes and the flow rate reduces to

$$\overline{q}(t) \sim \frac{t}{T} - \frac{t_l}{T} \tag{8.27}$$

Thus, asymptotically, the flow acquires the same form as the driving pressure (Eq. 8.23), but because of the inertial effect the flow curve is shifted along the time axis by an amount equal to the value of t_l/T as shown in Fig. 8.7. This shift represents the time interval by which the flow rate lags behind the prevailing pressure difference. The higher the inertial effect, the higher the value of t_l and the larger this ultimate gap between pressure and flow. Also, this gap between the flow and driving pressure never closes in this case because the driving pressure is continuously changing. Only in the case of constant driving pressure does the flow ultimately "catch up" with the prevailing pressure and in a sense "overcome" the inertial effect as it reaches steady state. In the case of continuously changing pressure, as in the present case, the inertial effect is present in the transient as well as in the quasi-steady state.

If, finally, the driving pressure difference Δp varies as a *periodic* function of time, say

$$\Delta p = \Delta p_0 \sin \omega t \tag{8.28}$$

where ω is the angular frequency of the oscillation, then Eq. 8.15 gives upon integration (by parts again)

$$q(t) = \frac{\Delta p_0(R\sin\omega t - \omega L\cos\omega t)}{R^2 + \omega^2 L^2} + Ae^{-(R/L)t}$$
(8.29)

where A is a constant of integration. If the flow rate is zero at time t = 0, we find

$$A = \Delta p_0 \omega L / (R^2 + \omega^2 L^2)$$
 (8.30)

and the solution becomes

$$q(t) = \frac{\Delta p_0}{R^2 + \omega^2 L^2} \left(R \sin \omega t - \omega L \cos \omega t + \omega L e^{-(R/L)t} \right)$$
(8.31)

A more useful form of the solution is obtained by combining the two trigonometric terms to give

$$\begin{cases} q(t) = \frac{\Delta p_0}{\sqrt{R^2 + \omega^2 L^2}} \left(\sin(\omega t - \theta) - \frac{\omega L}{\sqrt{R^2 + \omega^2 L^2}} e^{-(R/L)t} \right) \\ \theta = \tan^{-1} \left(\frac{\omega L}{R} \right) \end{cases}$$
(8.32)

or in nondimensional form

$$\begin{cases} \overline{q}(t) = \frac{q(t)}{\Delta p_0/R} = \frac{1}{\sqrt{1 + \omega^2 t_l^2}} \left(\sin(\omega t - \theta) - \frac{\omega t_l}{\sqrt{1 + \omega^2 t_l^2}} e^{-t/t_l} \right) \\ \theta = \tan^{-1}(\omega t_l) \end{cases}$$
(8.33)

In this form we see that as the exponential term vanishes, the flow rate becomes the same function of time as the oscillatory pressure difference, but with a phase angle shift θ . The size of the shift is higher the higher the inertia of the fluid, that is the higher the value of the inertial time constant $t_l (= L/R)$. Thus here we see essentially the same behavior of the fluid as in the previous case. The flow begins with a transient period in which it attempts to satisfy the prevailing pressure difference, but it never does. Instead, a steady state is reached in which the flow rate oscillates with the same frequency as the pressure difference driving the flow. It is a true "steady state" in this case, by common definition of that term.² In this state the flow rate oscillates in tandem with but lags behind the pressure difference by a fixed angle θ . The higher the inertial effect the larger is θ , and in the absence of inertial effects $\theta = 0$, as can be seen from Eq. 8.33. The *amplitude* of flow oscillation, which represents the highest flow rate reached at the peak of each cycle, from Eq. 8.33, is given by

$$|\overline{q}(t)| = \frac{1}{\sqrt{1 + \omega^2 t_l^2}} \tag{8.34}$$

²Kreyszig E, 1983. Advanced Engineering Mathematics. Wiley, New York.

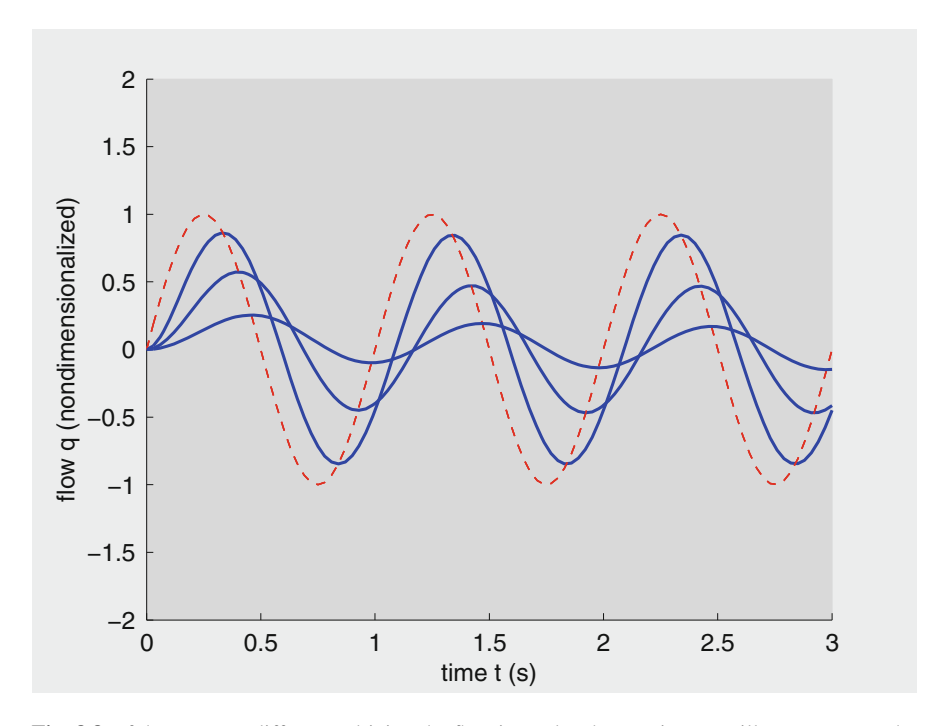


Fig. 8.8 If the pressure difference driving the flow in a tube changes in an oscillatory manner, the flow rate attempts to follow the same oscillatory pattern, but because of inertia it requires a certain amount of time to reach that pattern. When it does, however, the flow rate lags behind the pressure difference by a fixed phase angle θ and its amplitude is lower than what it would be in the absence of inertial effects, which here has the normalized value of 1.0. The *three solid curves* above, from the highest peak to the lowest, respectively, correspond to $t_l = L/R = 0.1, 0.3, 1.0 s$. It is seen that the higher the value of the inertial time constant t_l the larger the phase angle θ and the lower the amplitude of the flow oscillations. The *dashed curve* represents the normalized pressure as well as what the flow rate would be in the absence of inertial effects, that is when t_l is zero.

thus the higher the inertial effect, hence the higher the value of t_l , the lower the amplitude of flow oscillation, as shown in Fig. 8.8. In the absence of inertial effects the amplitude of flow oscillation would be 1.0 (Fig. 8.8).

In summary, when fluid is accelerated or decelerated, fluid *inertia* gives rise to another form of opposition to flow, commonly referred to as inductance. The immediate effect of inductance is to delay the response of the fluid to a change in the driving pressure difference. The flow rate does not "match" the prevailing pressure difference immediately but with a time delay. In that "transient state" the flow rate is attempting to reach a value appropriate for the prevailing pressure difference, and it ultimately does so if the prevailing pressure difference does not change any further. But if the driving pressure difference continues to change, as in oscillatory flow, the flow rate never reaches that appropriate value. It falls short and lags behind, more so at higher values of the inertial constant.

8.6 Elasticity of the Tube Wall: Compliance

A tube in which the walls are rigid offers a fixed amount of space within it, hence the volume of fluid filling it must also be fixed, assuming, here and throughout this discussion, that the fluid is incompressible. By the law of conservation of mass, flow rate q_1 entering the tube must equal flow rate q_2 at exit. There is thus only one flow rate q through the tube, which may vary at different points in time depending on the applied pressure gradient, but at any point in time it must be the same at all points along the tube.

When flow is occurring in a *nonrigid* tube, by contrast, two new effects come into play:

- First, the volume of fluid contained within the tube may change, like the volume of air in a balloon as it is inflated. This effect known as the tube's *compliance* or, in the context of electrical analogy, it is known as *capacitance* in relation to a change in the charge within a capacitor. We shall use the two terms interchangeably.
- Second, a *local* change of pressure within the tube causes a *local* change in the volume of fluid which then propagates as a wave crest (or valley) down the tube at a finite speed known as the wave speed as discussed more fully in Sect. 5.2.

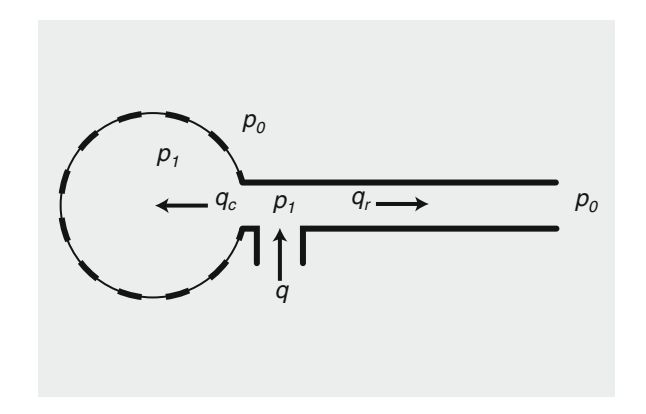
While both the effects result from elasticity of the tube wall, there is a fundamental difference between them which provides a basis for dealing with them separately. Under the effect of compliance there is a change in the *total volume* of fluid contained within the tube, again, as in the case of a balloon that is being inflated or deflated. Under the effect of wave propagation, by contrast, there is no change in the total volume of fluid within the tube- the change of volume occurs only locally. It is important to emphasize, however, that while this difference makes it possible to separate the two effects on theoretical grounds, it does not imply that the two effects actually occur separately in practice.

An instructive way of looking at the difference between the two effects of elasticity of the vessel wall is by noting that total changes in volume occur largely in the transient state, while local changes in volume occur in the steady state of wave propagation.

The dynamics of wave propagation have been described extensively in previous chapters. In this section we focus on the transient effects of compliance.

Since compliance of the tube wall affects the *total volume* of fluid within the tube, flow rate at entrance to the tube may no longer be the same as that at exit. This is because some of the flow at the entrance may go towards inflating the tube while some of the flow at exit may have come from a deflation of the tube. A convenient way of modeling this situation is to imagine flow going into a rigid tube to which a balloon is attached such that fluid has the option of flowing through the tube as well as inflating the balloon as depicted schematically in Fig. 8.9. The choice of a rigid tube is essential in order to eliminate the possibility of local changes in volume

Fig. 8.9 Compliance effect of flow in an elastic tube can be modeled by flow into a rigid tube with a balloon attached at one end. Flow rate q entering the system may go into the balloon or into the tube or both. Pressure p_1 at entry into the system is equal to pressure prevailing inside the balloon. Pressure at exit from the rigid tube is p_0 , the same as that outside the balloon.



that would occur in wave propagation. Thus, the combination of a rigid tube and a balloon captures the transient changes in total volume in isolation from those of wave propagation.

Schematically, we consider the entrance to the balloon to be the same as the entrance to the rigid tube, and the pressure p_1 at entry into the system is equal to pressure prevailing within the balloon. Pressure outside the balloon and at exit from the tube is p_0 . Flow through the tube and flow into the balloon are thus *in parallel*, in the sense that they can occur *independently* of each other. Flow into the system has the option of inflating the balloon or flowing down the tube, not unlike flow from the left ventricle into the aorta, which has the option of going downstream or inflating the aorta, or do some of each.

Consider the general scenario in which some of the flow rate will go towards inflating the balloon and some will go through the rigid tube. We shall refer to these as "capacitive" and "resistive" flow rates and denote them by q_c and q_r respectively.

Flow down the rigid tube will driven by the pressure difference $p_1 - p_0$ against the viscous resistance R such that, as in Eq. 8.3, we have

$$\begin{cases} q_r = \frac{\Delta p_r}{R} \\ \Delta p_r = p_1 - p_0 \end{cases}$$
(8.35)

For flow into the balloon we note first that the balloon is in an inflated state when pressure inside the balloon is higher than pressure outside it, that is when $p_1 > p_0$ or p > 0. If the volume of fluid contained within the balloon in this state is v, then the compliance C of the balloon is usually defined by the amount of *change* in the pressure difference δp required to produce a change δv in the volume of the balloon, that is

$$C = \frac{\delta v}{\delta(\Delta p)} \tag{8.36}$$

The awkward notation in the denominator emphasizes the fact that it is not the pressure difference Δp that produces the change in volume but a change in that pressure difference. Also, in this form it is seen that a higher value of C represents a balloon that requires less change in Δp to produce a given change in volume, that is a balloon that is more elastic, or more compliant.

Thus, unlike resistive flow q_r , which is driven by the pressure difference Δp , capacitive flow q_c requires a change in Δp . This is because flow in the rigid tube is resisted by the viscous shear stress at the tube wall, while flow into the balloon is resisted by the stretching of the balloon wall.

The change in volume δv in Eq. 8.36 is not a useful entity to work with in blood flow because it is not easily accessible. A more useful entity is the capacitive flow rate q_c representing the amount of flow going into or out of the balloon, which of course can be related to δv in the following way. As before, we assume that fluid is incompressible, hence the only way in which a change in the volume of fluid within the balloon can occur is by having a nonzero capacitive flow q_c going into or out of the balloon. If a constant capacitive flow rate q_c occurs over a time interval δt , the corresponding change in volume of fluid within the balloon will be

$$\delta v = q_c \delta t \tag{8.37}$$

which upon substitution into Eq. 8.36 gives

$$C = \frac{q_c \delta t}{\delta(\Delta p)} \tag{8.38}$$

or

$$q_c = C \frac{\delta(\Delta p)}{\delta t} \tag{8.39}$$

In the limit, if Δp is a continuous function of time, then q_c correspondingly becomes a continuous function of time, given by

$$q_c = C \frac{d(\Delta p)}{dt} \tag{8.40}$$

This result shows clearly, again, that flow rate into the balloon depends not on the pressure difference Δp but on the time rate of change of that difference. Also, by noting that total flow rate q into the system must equal the sum of the two partial flow rates, that is

$$q = q_c + q_r \tag{8.41}$$

we see clearly that the input flow rate q will not in general be equal to the output flow q_r .

We thus note that in the presence of compliance, flow rate q into a vascular system will not in general be equal to flow rate q_r out of the system.

The outcome depends on the form of the pressure difference Δp . We explore the following three scenarios.

(i) If the pressure difference $p_1 - p_0$ is constant, that is

$$\Delta p = \Delta p_{10} \tag{8.42}$$

where Δp_{10} is a constant, then Eqs. 8.40 and 8.35 give

$$\begin{cases} q_r = \frac{\Delta p_{10}}{R} \\ q_c = 0 \end{cases} \tag{8.43}$$

Under this scenario the flow is entirely through the tube. Flow into the balloon is zero because the rate of change of Δp is zero (although Δp itself is not zero). The volume of the balloon remains unchanged in this case.

(ii) If $p_1 - p_0$ increases linearly with time, from zero at time t = 0 to Δp_{10} at t = T, where Δp_{10} is a constant as before, then

$$\Delta p = \Delta p_{10} \times \frac{t}{T} \tag{8.44}$$

and from Eqs. 8.40 and 8.35 we find

$$\begin{cases} q_r = \frac{\Delta p_{10}}{R} \frac{t}{T} \\ q_c = C \frac{\Delta p_{10}}{T} \end{cases}$$
(8.45)

Under this scenario there is constant flow into the balloon because the rate of change of Δp with time is constant. Flow through the tube is increasing linearly with time as Δp increases with time. To compare the two graphically it is easier to put them in nondimensional forms, writing

$$\begin{cases} \overline{q}_r = \frac{q_r}{\Delta p_{10}R} = \frac{t}{T} \\ \overline{q}_c = \frac{q_c}{\Delta p_{10}R} = \frac{RC}{T} \end{cases}$$
(8.46)

The product RC is seen to have the physical dimensions of time and is referred to as the "capacitive time constant". We shall denote it by t_c , in analogy with the inertial time constant (t_l) , writing

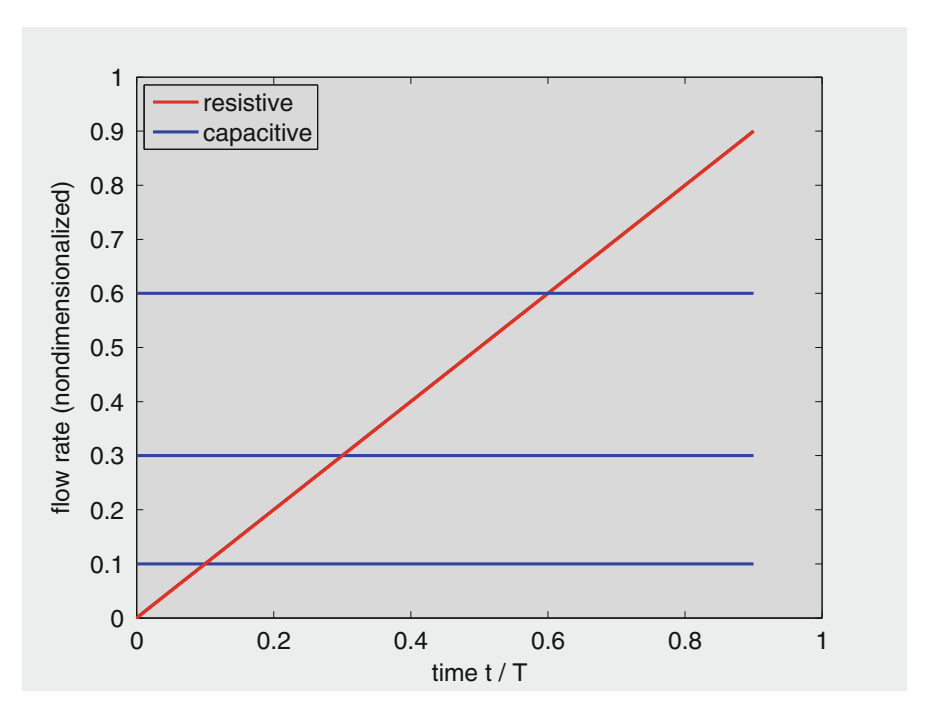


Fig. 8.10 Comparison of resistive and capacitive flow rates when the driving pressure Δp is increasing linearly with time over a time interval T and at three different values of the capacitive time constant: $t_c = 0.6, 0.3, 0.1$. In all cases, capacitive flow is constant since it depends on the rate of change of Δp , while resistive flow increases linearly with time since it depends on Δp itself and the resistance R is constant. Higher values of the capacitive constant t_c correspond to higher compliance, thus allowing more flow into the balloon.

$$t_c = RC \tag{8.47}$$

and the two flow rates in nondimensional form become

$$\begin{cases} \overline{q}_r = \frac{t}{T} \\ \overline{q}_c = \frac{t_c}{T} \end{cases}$$
(8.48)

Figure 8.10 compares these flow rates at different values of t_c . We recall that higher values of t_c (= RC) are associated with higher compliance, allowing more flow to go into the balloon. Thus, as seen in the figure, capacitive flow is constant at a value in fact equal to t_c/T , while resistive flow (flow through the tube) increases linearly as t/T.

(iii) Finally, if the pressure differences $p_1 - p_0$ is oscillatory, such that

$$\Delta p = \Delta p_{10} \sin \omega t \tag{8.49}$$

where ω is the angular frequency of oscillation, then from Eqs. 8.40 and 8.35 we find

$$\begin{cases} q_r = \frac{\Delta p_{10}}{R} \sin \omega t \\ q_c = \Delta p_{10} \ \omega \ C \cos \omega t \end{cases}$$
 (8.50)

As expected, both q_c and q_r are oscillatory functions of time, with the same frequency as the driving pressure, namely ω . In nondimensional form

$$\begin{cases} \overline{q}_r = \sin \omega t \\ \overline{q}_c = \omega t_c \cos \omega t \end{cases}$$
 (8.51)

The two flows are compared graphically in Fig. 8.11, where it is seen that the proportion of the flow rate that goes into the balloon in each cycle depends on the value of the capacitive time constant t_c . As in the previous case, higher values of t_c correspond to higher compliance, thus allowing more flow into the balloon. The resistive flow, on the other hand, is unaffected by the value of t_c and has the same form as the driving pressure, noting that inertial effects are not included here. The combination of compliance and resistance depicted in Fig. 8.11 forms the basis of the classical "windkessel" concept that dates back to the seventeenth century³ whereby pulsatile flow is seen to consist of an initial phase in which fluid is driven mostly into an expanding chamber, followed by a second phase in which the chamber contracts, driving fluid out of the chamber and thereby creating forward flow. Precisely how forward flow is created, will be discussed in the next chapter.

8.7 Mechanical Analogy

The mechanics of flow in a tube or a system of tubes can be identified, by analogy, with the basic mechanics of a solid object in motion under the influence of certain forces and conditions. Both situations are governed by the same laws of physics, and it should not be surprising that the analytical descriptions of their mechanics are analogous. What is different between the two situations, and what makes the analogy useful, stems from a difference not in the governing laws but in the type of forces and conditions involved and in the variables used in the two cases.

³See: Milnor WR. Hemodynamics. Williams & Wilkins, Baltimore, 1989.

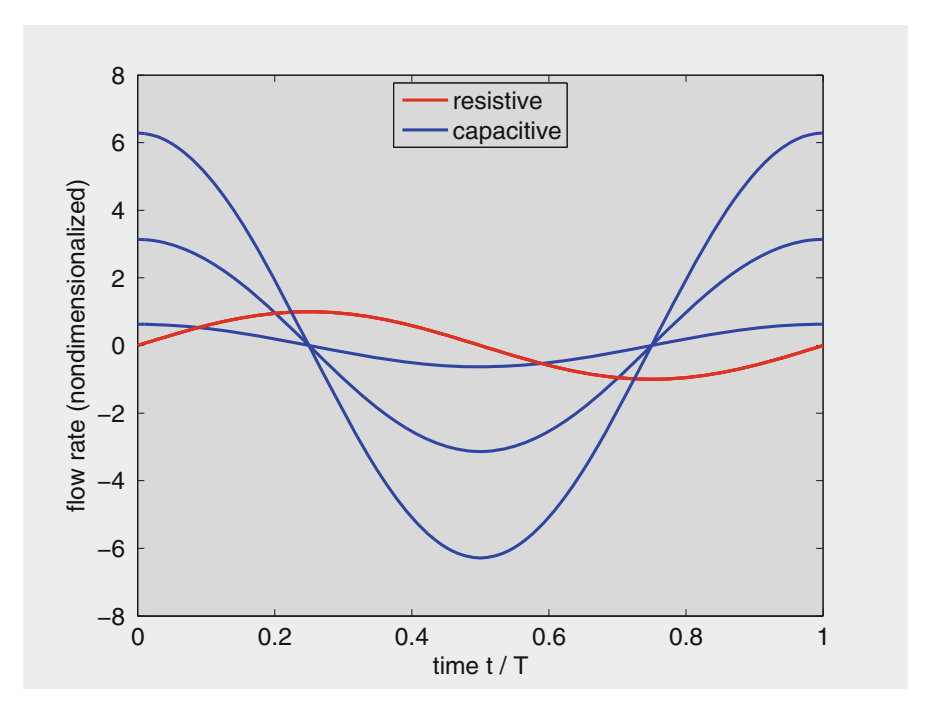


Fig. 8.11 Comparison of resistive and capacitive flow rates when the driving pressure Δp is an oscillatory function of time of period T. The resistive flow has the same form as the driving pressure since inertial effects are not included here and since it is unaffected by the value of the capacitive time constant t_c . The capacitive flow in each cycle, on the other hand, is higher with higher values of t_c because of higher compliance of the balloon. The three capacitive flow curves shown corresponds to $t_c/T=0.1,0.6,1.0$.

In the classical mass-damper-spring system, the motion of a solid object may be opposed by a spring resistance proportional to the displacement of the object, a damper resistance proportional to the rate of change of displacement (or velocity) of the object, and to an inertial resistance proportional to the second rate of displacement (or acceleration) of the object. While in fluid flow these forces and conditions are not present in the same form, they are present in equivalent forms which obey the same governing laws, hence the basis for the analogy.

For example, in fluid flow the compliance (or capacitance) of a tube or a system of tubes is analogous to the spring in the mechanical system, the viscous resistance between the fluid and the tube wall is analogous to the damper resistance, and the inertia of the fluid is analogous to the inertia of a solid object in motion.

⁴Meriam JL, 1980. Engineering Mechanics, Statics and Dynamics. John Wiley and Sons, New York.

⁵Ginsberg JH, Genin J, 1984. Statics and Dynamics. John Wiley and Sons, New York.

These properties have already been discussed in earlier sections, what is required in this section is only to show how they translate into the corresponding properties of the mechanical system. The translation is not a direct one because the basic variables used in the mechanical system, namely mass, displacement and rates of displacement, are not readily available or convenient to work with in the fluid flow system.

Despite these difficulties, the mechanical analogy is a useful tool in modeling a blood flow system because the analogy itself as it applies to each individual element is clearly valid. Thus, the relation between the flow rate q and pressure drop Δp in a tube, derived in Sect. 8.5, namely

$$\Delta p = L \frac{dq}{dt} \tag{8.52}$$

where *L* is the inertance, or inertial constant, of a bolus of fluid within the tube was shown in that section to be equivalent to the basic law of motion

$$F = m\frac{du}{dt} \tag{8.53}$$

where m is the mass of a solid object in motion, u is its velocity, and F is the force acting on it. The analogy between the two equations is apparent and the correspondence between the two situations is illustrated in Fig. 8.12. The driving pressure difference Δp in the fluid flow system corresponds to the acting force F in the mechanical system, while the inertance E corresponds to the mass E0, and the flow rate E1 corresponds to the velocity E2. In both cases the underlying law is the same, namely "force equals mass times acceleration", but as stated earlier, the variables used in the two situations are not the same. In particular, Eq. 8.52 avoids the use of mass or acceleration because these must be related to a specific object. Flow rate E3 and an inertial parameter E4 are used instead which relate to the entire body of fluid rather than to a specific element of that body.

Similarly, the viscous resistance to flow in a tube, discussed in Sect. 8.3, and the resulting relation between the pressure difference Δp and the flow rate q, namely

$$\Delta p = Rq \tag{8.54}$$

where *R* is the resistance to flow due to viscosity of the fluid and the condition of no-slip at the tube wall, is analogous to the classical law of friction at a solid-solid interface

$$F = fu \tag{8.55}$$

where f is the coefficient of friction at the interface, u is the relative velocity between the two surfaces, and F is the driving force. Again, the analogy between the two equations is apparent, and the two situations are illustrated in Fig. 8.13.

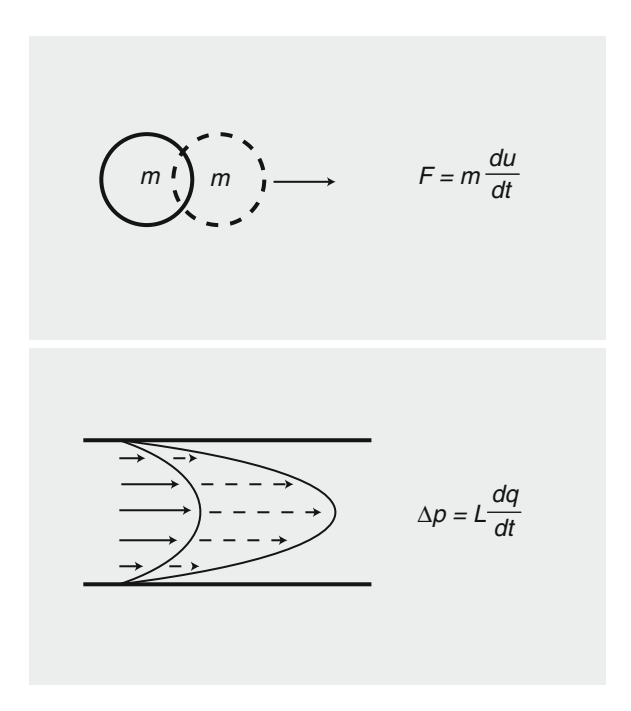


Fig. 8.12 Mechanical analogy between flow in a tube and the motion of a solid object in classical mechanics. The driving pressure difference Δp in the fluid flow system corresponds to the acting force F in the classical mechanics system, while the inertance L corresponds to the mass m, and the flow rate q corresponds to the velocity u. In both cases the underlying law is "force equals mass times acceleration".

Here the pressure difference Δp corresponds to the driving force F and the flow rate q corresponds the velocity u, as before, and the viscous resistance R corresponds to the friction coefficient f. Finally, the compliance of an elastic tube, discussed in Sect. 8.6, and the resulting relation between the pressure difference Δp and the change in volume Δv , namely

$$\delta(\Delta p) = \frac{1}{C} \delta v$$

$$= \frac{1}{C} \int q dt$$
(8.56)

$$\delta v = \int q dt \tag{8.57}$$

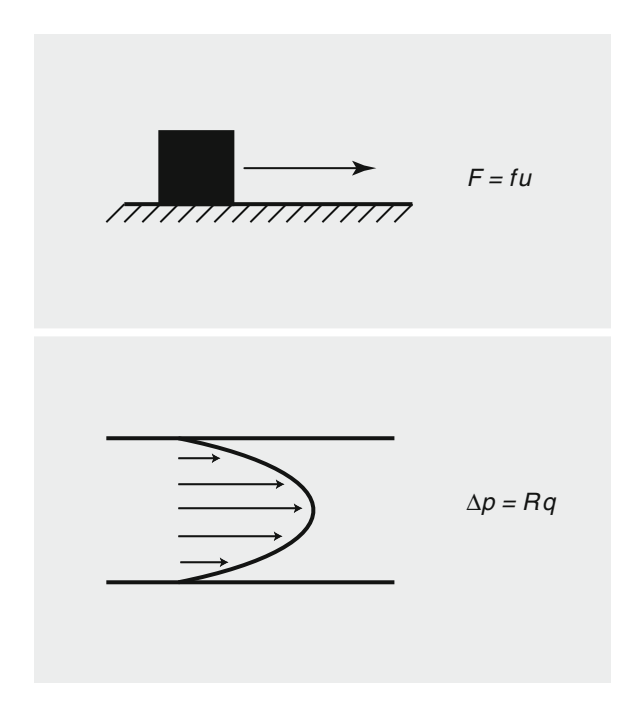


Fig. 8.13 Mechanical analogy between the viscous friction at the interface between fluid and tube wall, represented by velocity gradient at the tube wall, and the friction law in classical mechanics at the interface between two solid objects. Here the pressure difference Δp in the tube corresponds to the driving force F in the classical mechanics system, the flow rate q corresponds to the friction velocity u, and the viscous resistance R corresponds to the friction coefficient f.

where C is the compliance of the tube, is analogous to the classical Hook's law for an elastic spring, namely

$$F = k\delta x$$

$$= k \int u dt \tag{8.58}$$

$$\delta x = \int u dt \tag{8.59}$$

where k is the spring constant, δx is the spring extension and F is the applied force. In the integral terms above, the spring extension is expressed in terms of the velocity u with which the spring is being extended, and the change in volume δv of the elastic tube/balloon is expressed in terms of the flow rate q. The analogy between the two equations is apparent, with $\delta(\Delta p)$ corresponding to the applied force F, the awkward notation is there to emphasize again that capacitive flow is driven not by Δp but by a *change* in Δp . The analogy between the two situations is illustrated in Fig. 8.14.

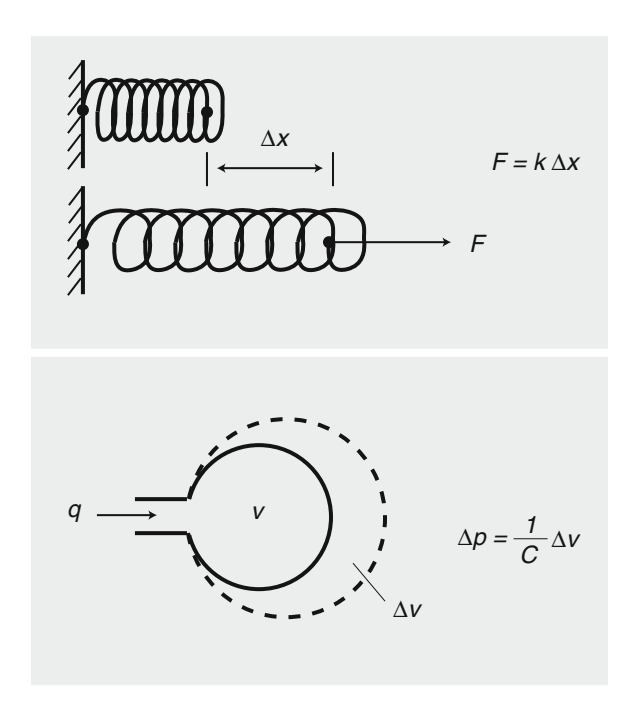


Fig. 8.14 Mechanical analogy: between the compliance effect of flow in an elastic tube, here represented by a balloon, and the stretch of an elastic spring according to Hook's law. The pressure difference Δp in the flow system corresponds to the applied force F in the spring system, the change in volume Δv of the tube/balloon corresponds to the change in length Δx of the spring, and 1/C in the flow system corresponds to the spring constant k, where C is a measure of the compliance of the tube/balloon, as defined by Eq. 8.38.

In summary, flow in an elastic tube is governed by the same physical laws and the same equations as the motion in a mechanical mass-damper-spring system. By this so called "mechanical analogy", fluid inertia in the fluid flow system is equivalent to the inertia of the mass in the mechanical system, viscous resistance in the fluid flow system is equivalent to damper resistance in the mechanical system, and compliance of the tube in the fluid flow system is equivalent to the stretch of the spring in the mechanical system. The analogy is useful because the elements of the mechanical system are more familiar and their functions can be visualized more clearly than those in the fluid flow system.

8.8 Electrical Analogy

The dynamics of a pulsatile blood flow system can also be modelled, by analogy, in terms of an electric circuit with the basic elements of resistance, capacitance, and inductance. The analogy is subject to the same limitations as the mechanical analogy

discussed in the previous section, namely the assumption that these elements can be identified with lumped properties of the blood flow system that is being modeled. Electrical analogies have been used extensively in the study of pulsatile blood flow because electric circuits are much easier to manipulate, both analytically and experimentally, and are thus a convenient modeling tool. An electrical model of a blood flow system can actually be built and tested experimentally, which makes the electrical analogy particularly useful in the study of pulsatile blood flow.

In the electrical analogy the potential difference or voltage, V, corresponds to the pressure difference Δp in the blood flow system, and the electric current I along a conductor corresponds to the flow rate q along a tube. The basis of the analogy is that the relation between the voltage V and current I across an inductor L, namely⁶

$$V = L \frac{dI}{dt} \tag{8.60}$$

is analogous to the corresponding relation between the pressure difference and flow rate in a tube, as in Eq. 8.52, namely

$$\Delta p = L \frac{dq}{dt}$$

where the inertia of the fluid is seen to produce an effect analogous to that of an inductor, in the electrical system. The analogy is illustrated in Fig. 8.15.

Similarly, the relation between the voltage and current across a resistor R, namely

$$V = I \times R \tag{8.61}$$

is analogous to the relation between the pressure difference and flow rate in a tube, as in Eq. 8.4,

$$\Delta p = q \times R \tag{8.62}$$

where viscous friction between fluid and the tube wall is seen to produce an effect analogous to that of a resistor in the electrical system. The analogy is illustrated in Fig. 8.16.

Finally, the relation between the voltage across and current into a capacitor namely

$$V = \frac{1}{C} \Delta Q$$

⁶Cogdell JR, 1999. Foundations of Electric Circuits. Prentice Hall, Upper Saddle River, NJ.

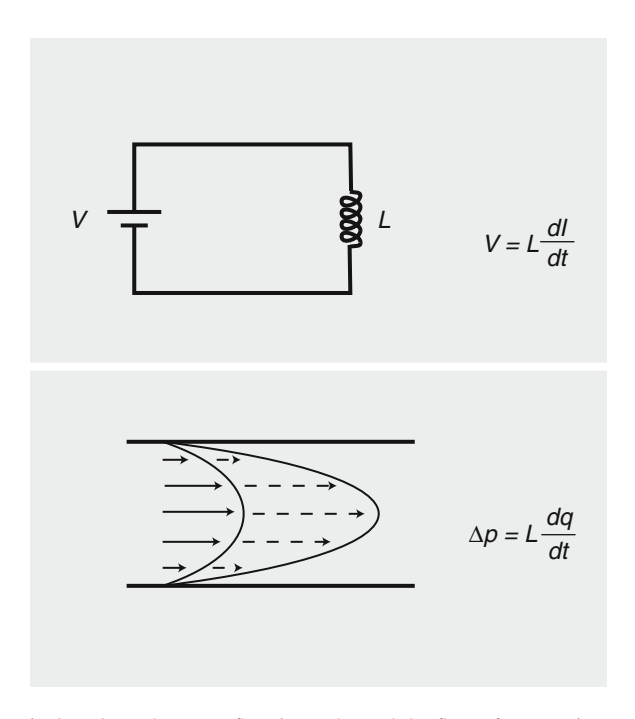


Fig. 8.15 Electrical analogy: between flow in a tube and the flow of current in an electric circuit, in the presence of inductance L in both systems. The driving pressure difference Δp in the fluid flow system corresponds to the voltage V in the electrical system, and the flow rate q corresponds to the electric current I. Inductance in the fluid flow system is due to a change in the flow rate, which is associated with acceleration or deceleration of a mass of fluid, while inductance in the electrical system is due to change in the current, which is associated with acceleration or deceleration of a mass of electrons.

$$=\frac{1}{C}\int Idt \tag{8.63}$$

$$\Delta Q = \int I dt \tag{8.64}$$

where C is the capacitance and ΔQ is the accumulated electric charge on the capacitor, is analogous to the relation between the pressure difference and flow rate into an elastic tube (Eq. 8.56).

$$\delta(\Delta p) = \frac{1}{C} \delta v$$
$$= \frac{1}{C} \int q dt$$
$$\delta v = \int q dt$$

8.9 Summary 279

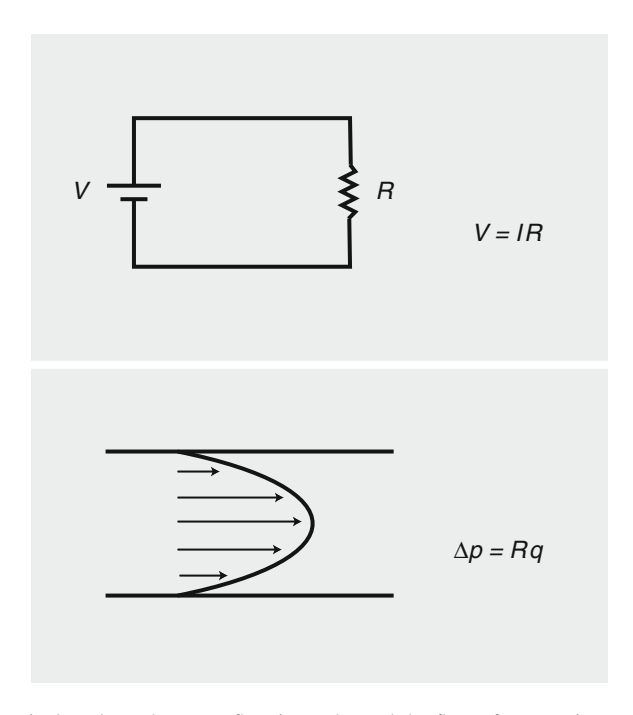


Fig. 8.16 Electrical analogy: between flow in a tube and the flow of current in an electric circuit, in the presence of resistance R in both systems. The driving pressure difference Δp in the fluid flow system corresponds to the voltage V in the electrical system, and the flow rate q corresponds to the electric current I. Resistance in the fluid flow system is due to loss of kinetic energy because of viscous friction between fluid and the tube wall, while in the electrical system it is due to loss of electric energy within the resistor. Interestingly, in both cases the lost energy is converted to heat.

Here, because of the elasticity of the tube wall, the accumulated volume of fluid within the tube can change in analogy with a change in the electric charge accumulated on the capacitor. The analogy is illustrated in Fig. 8.17.

8.9 Summary

Flow in a tube viewed as the motion of fluid *in bulk* rather than point-by-point as was done in earlier chapters provides a different method of analysis than was done earlier. The most important advantage of this method is that it makes it possible to use mechanical and electrical analogies which are well known and the dynamics of which are well understood.

Under these analogies, the electrical, mechanical, and fluid flow systems are all characterized by a driving force which may be referred to as the "input", a consequent motion or flow which may be referred to as the "output", and three types of opposition to that output which are known as "inductive", "resistive",

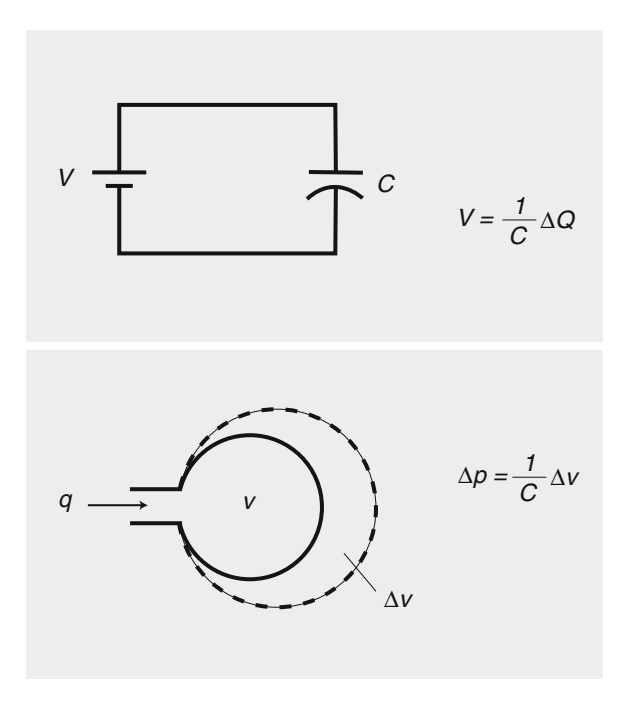


Fig. 8.17 Electrical analogy: between flow in a tube and the flow of current in an electric circuit, in the presence of capacitance C in both systems. The driving pressure difference Δp in the fluid flow system corresponds to the voltage V in the electrical system, and the flow rate q corresponds to the electric current I. Capacitance in the fluid flow system is due to a change in the volume v of fluid within an elastic tube, here represented by an expandable balloon, while in the electrical system it is due to a change in the total electric charge Q on a capacitor. The change in volume Δv in the fluid flow system is attained by a sustained flow rate into or out of the balloon, while the change in electric charge ΔQ on the capacitor is attained by a sustained current into or out of the capacitor.

and "capacitive" elements or forces. Different terminologies are sometimes used in each of the three systems, but the relation between input and output against the opposition forces is the same in all three systems.

In the electrical system the input is potential difference or voltage V, the output is current I, and the three elements of opposition are an inductor, a resistor, and a capacitor, represented respectively by their parameters L, R, C. The relations between input and output via these elements are given by

$$\begin{cases} V = L \frac{dI}{dt} & inductive \\ V = R \times I & resistive \\ V = \frac{1}{C} \int I dt & capacitive \end{cases}$$
 (8.65)

8.9 Summary 281

In the mechanical system the input is an external force F, the output is velocity u, and the three elements of opposition are mass, friction, and a spring, represented respectively by their parameters m, f, k. The relations between input and output via these elements are given by

$$\begin{cases} F = m\frac{du}{dt} & inductive \\ F = f \times u & resistive \\ F = k \int udt & capacitive \end{cases}$$
 (8.66)

In the fluid flow system, finally, the input is a pressure difference Δp , the output is flow rate q, and the three elements of opposition are fluid inertia, fluid viscosity, and tube compliance, represented respectively by their parameters L, R, C. The relations between input and output via these elements are given by

$$\begin{cases} \Delta p = L \frac{dq}{dt} & inductive \\ \Delta p = R \times q & resistive \\ \Delta p = \frac{1}{C} \int q dt & capacitive \end{cases}$$
(8.67)

For flow in a tube of length l and radius a, assuming Poiseuille flow throughout, the resistance and inductance parameters are respectively given by (Eqs. 8.2 and 8.12)

$$\begin{cases}
R = \left(\frac{8\mu l}{\pi a^4}\right) \\
L = \left(\frac{\rho l}{\pi a^2}\right)
\end{cases}$$
(8.68)

while the compliance parameter C is determined by the elasticity of the tube wall.

The lumped parameter concept makes it possible to extend the parameters R, L, C characterizing the flow in a single tube to parameters of the same type characterizing the flow in a vascular tree consisting of a large number of tube segments.

While the values of these parameters will be different for the tree as a whole than they are for a single tube, the functional relation between the driving pressure difference and the resulting flow rate will be the same as it is for a single tube and therefore as outlined in this chapter.

The most important application of the lumped parameter concept, therefore, is in using it in combination with the electrical and mechanical analogies to actually find the values of the parameters R, L, C characterizing a given vascular bed where the driving pressure difference and the resulting flow rate can be measured. Since the relations between the driving pressure difference and the resulting flow rate must be in accordance with those in Eq. 8.67, then the values of R, L, C must be such that the measured pressure and flow are the same as those dictated by Eq. 8.67.

The lumped parameter concept in combination with the mechanical and electrical analogies thus provides a powerful and non-invasive diagnostic tool for determining the properties of a vascular bed to assess the functional "health" of that bed.

Chapter 9 Dynamics of Pulsatile Blood Flow II

9.1 Introduction

The way in which each of the three basic effects of *resistance R*, *inductance L*, and *compliance C*, influence the dynamics of the flow in tubes were considered separately in the previous chapter. In the present chapter we examine how they work together to determine fully the dynamics of flow in tubes.

We recall that in the way they were defined, the parameters R, L, C apply equally to the dynamics of flow in a single tube as they do to the dynamics of flow in an entire vascular bed, providing that the bed is in the form of a hierarchical branching tree structure, or in fact any form of branching structure that emanates from a single root vascular segment. In the case of a vascular bed the three parameters represent the *collective* effects of resistance, inductance, and compliance within the entire bed and are therefore aptly referred to as "lumped" parameters. This is indeed where the lumped parameter concept outlined in the previous chapter finds its most important application, because the relation between driving pressure and resulting flow for the entire bed can then be determined in terms of these lumped parameters.

More specifically, if the driving pressure and resulting flow rate in a vascular bed can actually be measured at the point of entry to that bed, then the established relation between pressure and flow can be used in reverse to determine the values of the lumped parameters R, L, C that characterize that bed

An example where this can be done relatively easily is that of obtaining measurements of pressure and flow at a brachial artery to determine values of the lumped parameters R, L, C that characterize the downstream vasculature emanating from that artery and hence much of the arterial side of the vascular bed of the arm. Similarly, measurements of pressure and flow at an iliac, coronary, carotid, or indeed at the ascending aorta, would provide values of the lumped parameters characterizing vascular beds in the leg, the heart, the brain, or the systemic

circulation as a whole. This makes the lumped parameter method a very powerful diagnostic tool for determining the dynamic "fitness" of a vascular bed, in normal or pathological states. At the basis of this method is an established relation between the driving pressure and the corresponding flow in a given vascular bed. The way in which this relation is established is considered in the present chapter.

9.2 Pulsatile Blood Flow Revisited

In pulsatile blood flow, both the pressure and the flow are *periodic* functions of time and, as such, each can be divided into a steady part and an oscillatory part as discussed in Sect. 4.3. The steady part of the pressure drives the steady part of the forward flow while the oscillatory part of the pressure drives the oscillatory part of the flow, back and forth and with zero net forward flow (Sect. 4.3).

While this is an accurate picture of pulsatile blood flow, it raises some questions for the uninitiated. How does pulsatile blood flow produce a reasonably continuous forward flow? Not necessarily constant but continuous forward flow. In essence, how do the steady and the oscillatory parts of pulsatile blood flow work (together?) to optimize forward flow?

To the physiologist the answer to this question is embedded in the classical Windkessel concept mentioned briefly at the end of Sect. 8.6, namely: "fluid is stored within the Windkessel chamber when pressure is high in systole and released when pressure is low in diastole". Thus the Windkessel effect is proposed as a mechanism for absorbing the force of the high pressure peak in systole, thereby producing a more continuous and somewhat less "jerky" forward flow.

To the mathematician the question at hand is more acute because, as stated earlier, the steady and the oscillatory parts of pulsatile blood flow are completely separable. This would suggest that forward flow is produced entirely by the steady part of the driving pressure, *independently of the oscillatory part*. In other words, here the Windkessel effect of absorbing the pressure peak is not clear because here it seems as if forward flow is not being affected by the oscillatory part of the flow. Why then is mathematical work on pulsatile blood flow, including the classical solutions described in Chaps. 4 and 5, is focused specifically and almost exclusively on the oscillatory part of the system? In this section we address these questions.

One mechanism by which the oscillatory part of pulsatile blood flow may affect the steady part is that of wave reflections. The subject was discussed in Chap. 6 where, briefly, it was shown that wave reflections (which are generated by the oscillatory part of the flow) can modify the pressure distribution within the vascular system and thereby change the steady part of the flow. Since this effect has already been fully examined in Chap. 6, in this section and in the context of the questions at hand we focus specifically on how *in the absence of wave reflections* the steady and the oscillatory parts of pulsatile blood flow affect each other.

We shall find that the oscillatory part of pulsatile blood flow plays a critical role in the efficiency and dynamics of the flow, although when considered *in isolation*

it appears to produce a net forward flow of zero. Paradoxically, however, focus on the oscillatory part of the flow in isolation is both legitimate and useful because it provides an understanding of this critical part of pulsatile blood flow.

9.3 Resistive-Capacitive Interplay I

The main conclusion from the previous section is that the oscillatory part of pulsatile blood flow is at the very core of the dynamics of that flow and, in turn, the interplay between the *resistive* and the *capacitive* parts of the oscillatory flow is at the very core of the dynamics of that flow. Indeed, the dynamics of the resistive-capacitive interplay will be pursued in several forthcoming sections of the book. In the present section we illustrate this interplay in its most basic form.

For this purpose we consider a simple combination of resistance R and compliance C in parallel to represent the resistive and the capacitive parts of the pulsatile flow system, respectively. While this model is highly simplified, it is perfectly adequate for illustrating the phenomenon at hand. The essence of the phenomenon, as depicted schematically in Fig. 8.9, is that the flow entering the system has the option of going against the resistance in the rigid tube or against the compliance of the elastic balloon. This option is only available when the resistive and capacitive elements of the system are in parallel, not in series. The parallel option is at the core of the Windkessel concept because it represents the physiological conditions which the concept was designed to address, namely the conditions facing blood flow as it leaves the left ventricle. The flow has the option of going against the resistance to flow within the arterial tree or against the compliance of the arterial tree.

It is important that resistive flow and capacitive flow not be confused with the steady and the oscillatory parts of pulsatile blood flow. In a rigid tube, for example, the steady part and the oscillatory part of the flow are both entirely resistive because they are both unfolding against the resistance to flow at the tube wall. In an elastic tube this situation is mitigated somewhat by turning some of the oscillatory flow into capacitive flow. Thus in this case some of the resistive flow is steady and some is oscillatory, while the capacitive flow is entirely oscillatory.

It is also important to note that the option provided by the parallel arrangement of compliance and resistance is not an "either/or" option. In general the flow will divide itself according to the relative opposition provided by the compliance and resistance at hand. There are two different ways of viewing this division, one in which flow into the parallel system is seen as being driven by a common source of *pressure* (not *constant* but common) and another in which it is seen as being driven by a common source of *flow rate*. We examine both scenarios below to illustrate the different pictures which they provide.

In the first scenario, consider a parallel arrangement of compliance C and resistance R driven by a *common source of pressure*, say

$$P(t) = P_s + P_{\phi}(t)$$

$$= P_s + P_0 e^{i\omega t}$$
(9.1)

Here the notation of Sect. 4.3 is being used, where P_s, P_ϕ are the steady and the oscillatory parts of the driving pressure, respectively, P_0 is amplitude of the oscillatory pressure, ω is angular frequency and t is time. The pressure in this form is pulsatile in the sense that it consists of a steady part and an oscillatory part to simulate somewhat that aspect of pulsatile blood pressure. This simulation is very crude, of course, but it serves the purpose of the present section. More accurate pulsatile pressure wave forms will be considered in the next two chapters.

From the results in Sects. 8.3 and 8.6, the resistive and capacitive flow rates, to be denoted by q_r , q_c , respectively, are given by

$$\begin{cases} q_r = \frac{P}{R} \\ q_c = C\frac{dP}{dt} \end{cases}$$
 (9.2)

where, for simplicity, P is being used here to represent the pressure difference ΔP used in Sects. 8.3 and 8.6.

Substituting for the pressure, we find

$$\begin{cases} q_r = \frac{1}{R} (P_s + P_0 e^{i\omega t}) \\ q_c = C P_0 i\omega e^{i\omega t} \end{cases}$$
(9.3)

Using the capacitive time constant introduced in Sect. 8.6

$$t_0 = R \times C$$

and noting that

$$\omega = \frac{2\pi}{T} \tag{9.4}$$

where T is the period of oscillation, the resistive and capacitive flow rates can be put in the following nondimensional (normalized) form

$$\begin{cases} \overline{q}_r = \frac{q_r}{P_s/R} = 1 + \lambda_p e^{i2\pi(t/T)} \\ \overline{q}_c = \frac{q_c}{P_s/R} = i2\pi(t_c/T)\lambda_p e^{i2\pi(t/T)} \end{cases}$$
(9.5)

where

$$\lambda_p = \frac{P_0}{P_s} \tag{9.6}$$

It may seem from these results that the resistive and the capacitive flows and capacitive flow are in this case independent of each other and a change in the properties of one does not change the other. This is not the case, however, since a change in the value of the compliance C will in fact change the amplitude of the oscillatory part of both the resistive and the capacitive flows (Eq. 9.3). This is seen more clearly as we consider the second scenario below.

In the second scenario, consider a parallel arrangement of compliance C and resistance R driven by a *common source of flow*, say

$$Q(t) = Q_s + Q_{\phi}(t) \tag{9.7}$$

$$=Q_s + Q_0 e^{i\omega t} (9.8)$$

with obvious notation, as in the first scenario. The resistive and capacitive flow rates and capacitive flow are again given by Eq. 9.2 but here we also use the fact that the two flows are coupled such that

$$q_r + q_c = Q (9.9)$$

Substituting for q_r and q_c from Eq. 9.2 and for Q from Eq. 9.7, we find

$$C\frac{dP}{dt} + \frac{P}{R} = Q_s + Q_0 e^{i\omega t}$$
(9.10)

Solving this equation for the pressure P, and omitting the details, we find

$$P = RQ_s + \left(\frac{RQ_0}{1 + CRi\omega}\right)e^{i\omega t} \tag{9.11}$$

Substituting this pressure into the expressions for q_r and q_c in Eq. 9.2, and using the same notation as in the first scenario, we find, after some algebra

$$\begin{cases} q_r = Q_s + \left(\frac{Q_0 e^{i\omega t}}{1 + i\omega CR}\right) \\ q_c = \left(\frac{i\omega CRQ_0 e^{i\omega t}}{1 + i\omega CR}\right) \end{cases}$$
(9.12)

or in non-dimensional form

$$\begin{cases} \overline{q}_r = \frac{q_r}{Q_s} = 1 + \left(\frac{\lambda_q}{1 + i2\pi(t_c/T)}\right) e^{i2\pi(t/T)} \\ \overline{q}_c = \frac{q_c}{Q_s} = \left(\frac{i2\pi(t_c/T)\lambda_q}{1 + i2\pi(t_c/T)}\right) e^{i2\pi(t/T)} \end{cases}$$

$$(9.13)$$

where

$$\lambda_q = \frac{Q_0}{Q_s} \tag{9.14}$$

Here it is seen more clearly how the resistive and the capacitive flows and capacitive flow are coupled such that a change in one (via a change in t_c) affects the other. This is illustrated graphically in Fig. 9.1. The two different views of pulsatile blood flow which the above two scenarios provide are implicit in much of our understanding of the subject, the first in mathematical analysis and the second in the Windkessel concept.

To the uninitiated they provide the grounds for considerable confusion because when discussion of the Windkessel concept in pulsatile blood flow is limited to only the effect of absorbing the shock of the pressure peak in systole, then the resistive-capacitive interplay enabled by the Windkessel effect, which is the key biological aspect of pulsatile blood flow, is entirely missed.

In pulsatile blood flow biology has produced a system in which part of the oscillatory resistive flow is exchanged for oscillatory capacitive flow, with a considerable energy saving in the process. The saving is obtained because resistive flow dissipates energy while capacitive flow stores that energy and later releases it.

It was shown in Sect. 4.10 that in the extreme case of a strictly rigid tube, the energy expenditure by the oscillatory part of the flow, which is purely resistive in this case, amounts to 50% of the energy expenditure for the steady part of the flow. In an elastic tube all of this *wasted* energy expenditure on the oscillatory part of the flow can be saved if (a) the tube wall is purely elastic and (b) the resistive flow oscillations are completely eliminated.

In pulsatile blood flow these two requirements are not fully met, although under normal circumstances they are met sufficiently to provide considerable energy saving and hence efficient dynamics of the oscillatory part of the flow. In aging or under pathological conditions, however, when vessel wall properties depart considerably from being purely elastic, both the efficiency and dynamics of the flow are disrupted. The heart ultimately bears the brunt of these disruptions since it must provide the energy required for driving the flow.

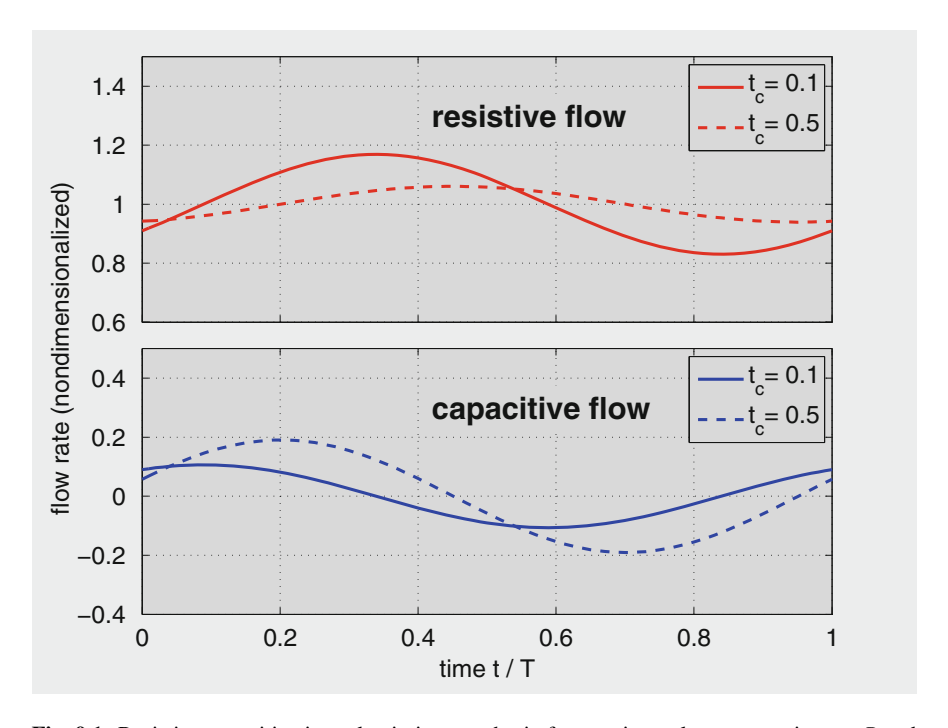


Fig. 9.1 Resistive-capacitive interplay in its most basic form, using only a pure resistance R and a purely elastic compliance C. A decrease in the value of $t_c \ (= R \times C)$ causes a shift of oscillatory flow from the capacitive chamber to the resistive path, thereby increasing energy dissipation as discussed in the text. The change may come about because of vascular stiffening, which reduces the value of C, or because of vasodilation, which reduces the value of R. While this model is highly simplified, it illustrates the very essence of the resistive-capacitive interplay in pulsatile blood flow. It also illustrates the important role which the dynamics of the oscillatory part of the flow play and the clinical implications of this role. The loss of vascular compliance, with age or disease, then leads to a shift of oscillatory flow from the capacitive chamber to the resistive path, thus increasing energy dissipation (loss) which must be supplied by the heart. The common use of vasodilators to provide relief to an ailing heart is based of course on lowering the resistance R and thereby reducing the energy required to drive the steady part of the flow. Oddly, however, this will also increase energy dissipation incurred by the oscillatory part of the flow which must be provided by the heart.

9.4 The Capacitive Chamber

In the previous section it was established that pulsatile blood flow, because of its periodicity, can always be divided into a steady part which represents the equivalent of steady Poiseuille flow, and an oscillatory part which represents the oscillatory dynamics of the flow. It was shown in the previous section that a key characteristic of the oscillatory part of the flow, namely that of having the option of resistive vs capacitive flow, can be captured by a resistance R and compliance C in parallel.

In principle, the parallel *R*, *C* system captures the key characteristic of the oscillatory part of pulsatile blood flow, namely that of consisting of one path along which flow is being allowed to go through at a steady pace, and another path along which fluid is being accumulated and then released in an oscillatory manner and with no net flow through. This picture of the oscillatory part of pulsatile blood flow does not change *in principle*, but in reality the capacitive path along which fluid is being accumulated and then released consists of more than purely elastic compliance *C*. For the purpose of discussion we shall use the term "capacitive chamber" to refer to the full form of this path which we consider in this section.

In the previous section the capacitive chamber was taken to consist of only compliance C and this compliance was considered to be purely elastic as discussed in Sect. 8.6. In reality blood vessel tissue is not purely elastic, it is "viscoelastic" in the sense that it has an element of viscosity. A purely elastic material resists stretch. A viscoelastic material resists stretch plus rate of stretch. In terms of the volume q of a balloon, following Sect. 8.6, for a purely elastic material the pressure gradient required to drive flow into the balloon is proportional to the flow rate q, that is

$$\frac{d(\Delta p_c)}{dt} = \frac{1}{C}q\tag{9.15}$$

where Δp_c is the pressure difference across the balloon which, upon integration, is then given by

$$\Delta p_c = \frac{1}{C} \int q \, dt \tag{9.16}$$

For a viscoelastic material the pressure gradient required to drive flow into the balloon is proportional to the flow rate q as well as the rate at which the flow rate is changing, that is

$$\frac{d(\Delta p_{ve})}{dt} = \frac{1}{C}q + K\frac{dq}{dt} \tag{9.17}$$

where Δp_{ve} is the pressure difference across the balloon which, upon integration, is then given by

$$\Delta p_{ve} = \frac{1}{C} \int q \, dt + Kq \tag{9.18}$$

Thus the pressure difference across a viscoelastic balloon (capacitor) is the sum of the pressure difference across a purely elastic balloon plus a resistance-like term proportional to the flow rate, that is

$$\Delta p_{ve} = \Delta p_c + \Delta p_k \tag{9.19}$$

where

$$\Delta p_k = Kq \tag{9.20}$$

This additional pressure difference is required to overcome the viscous resistance to stretch within the viscoelastic material of the balloon wall. Thus, mathematically, the parameter K is analogous to the parameter R representing the resistance to flow against the viscous resistance between the fluid and the tube wall. It is important that the two not be confused.

The effects of repeated acceleration and deceleration along the capacitance chamber were considered in Sect. 8.5 where it was shown that these effects are represented by an inductance parameter L such that

$$\Delta p_l = L \frac{dq}{dt} \tag{9.21}$$

The elements of elasticity, viscoelasticity, and inductance along the capacitive chamber represented by C, K, L are in series in the sense that the flow has no option but to go through all three of them. Thus, if the total pressure to drive flow through the chamber is denoted by Δp , then

$$\Delta p_l + \Delta p_k + \Delta p_c = \Delta p \tag{9.22}$$

Substituting for the individual pressure drops from Eqs. 9.16, 9.20, 9.21, this becomes an equation for the oscillatory flow rate q along the capacitive chamber

$$L\frac{dq}{dt} + Kq + \frac{1}{C} \int qdt = \Delta p \tag{9.23}$$

Equation 9.23 governs the dynamics of the capacitive chamber and, in effect, much of the dynamics of pulsatile blood flow. It consists of the pressure difference Δp required to drive the flow on one side, and the three forms of "opposition to flow" on the other. The flow rate q governed by this equation, it will be recalled, is purely oscillatory with no net forward flow because the dynamics of this part of pulsatile blood flow is purely oscillatory. In subsequent sections we examine the solutions of this equation under different conditions.

The solution of Eq. 9.23 is facilitated by differentiating once to get

$$L\frac{d^2q}{dt^2} + K\frac{dq}{dt} + \frac{1}{C}q = \frac{d(\Delta p)}{dt}$$
(9.24)

The general solution of this equation can be put in the form

$$q(t) = q_h(t) + q_p(t) (9.25)$$

where q_h is the *homogeneous* part of the solution of Eq. 9.24 and the *general* solution of

$$L\frac{d^2q_h}{dt^2} + K\frac{dq_h}{dt} + \frac{1}{C}q_h = 0 (9.26)$$

while q_p is the particular part of the solution of Eq. 9.24 and a particular solution of

$$L\frac{d^2q_p}{dt^2} + K\frac{dq_p}{dt} + \frac{1}{C}q_p = \frac{d(\Delta p)}{dt}$$
(9.27)

These two parts of the solution of Eq. 9.24 represent two different aspects of the dynamics of the capacitive chamber which are pursued separately in the next two sections.

9.5 Transient States

In this section we examine the solution of Eq. 9.26 and the interpretation of that solution for the homogeneous part of the oscillatory flow rate within the capacitive chamber, namely

$$L\frac{d^2q_h}{dt^2} + K\frac{dq_h}{dt} + \frac{1}{C}q_h = 0$$

The interpretation of this equation in the context of the full dynamics of the capacitive chamber is that it represents the three elements of opposition to flow but in the absence of any driving pressure difference, that is when Δp in Eq. 9.24 is zero. The dynamics of the capacitive chamber under these conditions are appropriately referred to as "free dynamics" while those under a nonzero Δp are referred to as "forced dynamics". Dynamics of the capacitive chamber in pulsatile blood flow are forced dynamics because of the driving pressure provided by the heart. However, we shall find that the free dynamics of that system provide important clues about the dynamic characteristics of the system.

It is convenient to reduce the number of parameters by introducing time constants

$$\begin{cases} t_{lk} = L/K \\ t_{ck} = CK \end{cases} \tag{9.28}$$

thus the equation becomes

$$t_{lk}\frac{d^2q_h}{dt^2} + \frac{dq_h}{dt} + \frac{1}{t_{ck}}q_h = 0 (9.29)$$

9.5 Transient States 293

This equation is a standard second order linear differential equation with constant coefficients. Its solution depends on the nature of the roots of the associated so called "indicial" equation

$$t_{lk}\alpha^2 + \alpha + \frac{1}{t_{ck}} = 0 {(9.30)}$$

The roots are in general given by

$$\alpha = \frac{-1 \pm \sqrt{1 - (4t_{lk}/t_{ck})}}{2t_{lk}} \tag{9.31}$$

but the solution of the governing equation (Eq. 9.29) and hence the dynamics of the system depend critically on whether these roots are real or complex, which in turn depends on the relative values of the time constants t_{lk} , t_{ck} .

If $4t_{lk} < t_{ck}$, then Eq. 9.30 has two distinct real roots, given by

$$\begin{cases}
\alpha_1 = \frac{-1 + \sqrt{1 - (4t_{lk}/t_{ck})}}{2t_{lk}} \\
\alpha_2 = \frac{-1 - \sqrt{1 - (4t_{lk}/t_{ck})}}{2t_{lk}}
\end{cases} (9.32)$$

and the solution of the governing equation is given by

$$q_h(t) = Ae^{\alpha_1 t} + Be^{\alpha_2 t} \tag{9.33}$$

where A, B are arbitrary constants. Given the values of the flow rate at time t = 0, namely q(0), and the rate of change of the flow rate at the same time, namely q'(0), we find

$$\begin{cases}
A = \frac{-\alpha_2 q_h(0) + q'_h(0)}{\alpha_1 - \alpha_2} \\
B = \frac{\alpha_1 q_h(0) - q'_h(0)}{\alpha_1 - \alpha_2}
\end{cases} (9.34)$$

If $4t_{lk} > t_{ck}$, then Eq. 9.30 has two complex (conjugate) roots, given by

$$\begin{cases} \alpha_1 = a + ib \\ \alpha_2 = a - ib \end{cases} \tag{9.35}$$

¹Kreyszig E, 1983. Advanced Engineering Mathematics. Wiley, New York.

where

$$\begin{cases} a = \frac{-1}{2t_{lk}} \\ b = \frac{\sqrt{(4t_{lk}/t_{ck}) - 1}}{2t_{lk}} \\ i = \sqrt{-1} \end{cases}$$
 (9.36)

and the solution of the governing equation is given by

$$q_h(t) = \{A\cos(bt) + B\sin(bt)\}e^{at}$$
 (9.37)

where A, B are arbitrary constants. Given the values of q(0) and q'(0), again, we find

$$\begin{cases} A = q_h(0) \\ B = \frac{-aq_h(0) + q'_h(0)}{b} \end{cases}$$
(9.38)

Finally if $4t_{lk} = t_{ck}$, then Eq. 9.30 has two identical real roots, given by

$$\alpha_1 = \alpha_2 = a = \frac{-1}{2t_{lk}} \tag{9.39}$$

and the solution of the governing equation is given by

$$q_h(t) = (A + Bt) e^{at} (9.40)$$

where A, B are arbitrary constants. Given the values of q(0) and q'(0), we find

$$\begin{cases} A = q_h(0) \\ B = -aq_h(0) + q'_h(0) \end{cases}$$
(9.41)

It must be remembered that the flow under these scenarios is free from any external driving force, but it is unfolding under the effects of inertance L, viscoelastic resistance K, and compliance C. The dynamics of the system are "free" in the sense that the system is under *only* internal forces.

At time t = 0 the dynamics are triggered with a pre-existing flow rate q(0) through the system, and for the purpose of illustration we take q(0) = 1 and q'(0) = 0. This flow will diminish because it has no external driving force and it is opposed by the tube resistance R and by the elasticity of the balloon wall as flow stretches it. The only driving force which keeps some flow going at this phase is an *internal* force due to the inertial effect, namely the momentum which the fluid has by virtue of the pre-existing velocity with which it was started. Since this momentum

9.5 Transient States 295

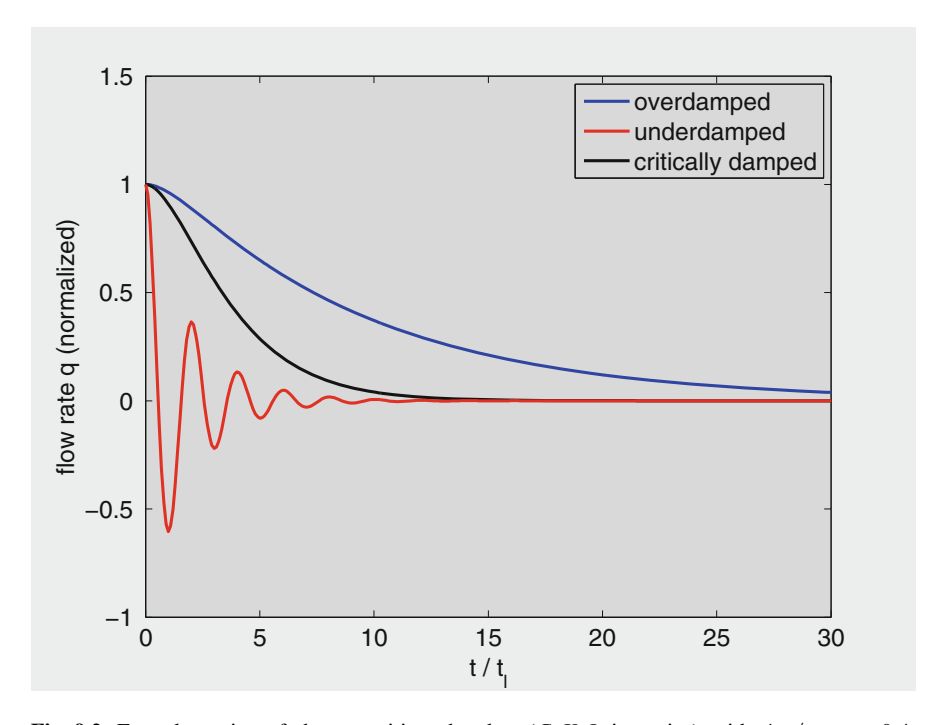


Fig. 9.2 Free dynamics of the capacitive chamber (C, K, L) in series) with $4t_{lk}/t_{ck} = 0.4$, $4t_{lk}/t_{ck} = 1.0$, and $4t_{lk}/t_{ck} = 40$. The three values produce what is usually referred to as "overdamped", "critically damped", and "underdamped" dynamics, respectively.

is finite and is not being renewed by any external force, it is ultimately exhausted and the fluid comes to rest. The flow rate ultimately becomes zero.

At this point one of two possible scenarios may unfold: the balloon may recoil and send fluid back, thus reversing the flow direction, or the balloon may simply absorb the increased volume of fluid and come to equilibrium at a new volume. In the mechanical system analogy this is equivalent to the compression (or expansion) of a spring and then letting go. The spring may then simply return to its neutral position or overshoot and undergo some diminishing oscillations about that position.

Which of the two scenarios occurs depends on the rate at which the flow rate diminishes, which in turn depends on the relative values of the inertial and capacitance effects. Recalling that $t_{lk} = L/K$, $t_{ck} = CK$, if the value of the ratio $4t_{lk}/t_{ck}$ is below 1.0, the balloon does not recoil, as seen in the top curve in Fig. 9.2. If the value of the ratio is higher than 1.0, the balloon recoils, leading to the oscillations seen in the bottom curve. These two scenarios are referred to as being "overdamped" and "underdamped" respectively. One singular scenario, namely that corresponding to $4t_{lk}/t_{ck} = 1.0$, is referred to as being "critically damped" in the sense that it acts as the dividing line between the underdamped and the overdamped cases, as shown by the middle curve in Fig. 9.2.

The free dynamics of a dynamical system do not represent its dynamics under the action of external forces but they do represent the intrinsic dynamics of the system. An understanding of these dynamics is important because they ultimately determine how the system responds to a change in its properties such as a change in the relative values of C, K, L. This change, which may be the result of disease or intervention, may cause the system to cross over from one type of dynamic behavior to another.

9.6 Steady State Oscillations

Free dynamics of the capacitive chamber considered in the previous section represents only the homogeneous part of the general solution of Eq. 9.24 for the oscillatory flow rate q(t) within the capacitive chamber. The remainder of the solution, as explained in Sect. 9.4, is a particular solution of Eq. 9.27 which we consider in this section.

For this purpose we consider a driving pressure Δp in the form of a complex function as in Sect. 4.4, writing

$$\Delta p = \Delta p_0 e^{i\omega t} \tag{9.42}$$

where Δp_0 is a constant as before, representing the amplitude of the input oscillatory pressure. Upon substitution in Eq. 9.27, we have

$$L\frac{d^2q_p}{dt^2} + K\frac{dq_p}{dt} + \frac{1}{C}q_p = i\omega\Delta p_0 e^{i\omega t}$$
(9.43)

or in terms of the time constants introduced in the previous section

$$t_{lk}\frac{d^2q}{dt^2} + \frac{dq}{dt} + \frac{q}{t_{ck}} = \frac{i\omega\Delta p_0 e^{i\omega t}}{K}$$
(9.44)

A particular solution of this equation, because of the exponential term on the right, has the form²

$$q_p(t) = Me^{i\omega t} (9.45)$$

where M is a constant to be determined below and is not to be confused with the *arbitrary* constants A, B in the homogeneous part of the solution obtained in the previous section. The constant M is determined simply by substituting the assumed form of q_p from Eq. 9.45 into Eq. 9.43 to find, after some algebra

²Kreyszig E, 1983. Advanced Engineering Mathematics. Wiley, New York.

$$M = \frac{\Delta p_0}{K + i\left(\omega L - \frac{1}{\omega C}\right)} \tag{9.46}$$

or in terms of the time constants

$$M = \frac{\Delta p_0 / K}{1 + i \left(\omega t_{lk} - \frac{1}{\omega t_{ck}}\right)} \tag{9.47}$$

Substituting this value of M into Eq. 9.45, the particular part of the flow rate is now completely determined, namely

$$q_p(t) = \frac{\Delta p_0}{K + i\left(\omega L - \frac{1}{\omega C}\right)} e^{i\omega t}$$
(9.48)

or in nondimensional form

$$\overline{q}_p(t) = \frac{q_p(t)}{\Delta p_0/K} = \frac{1}{1 + i\left(\omega t_{lk} - \frac{1}{\omega t_{ck}}\right)} e^{i\omega t}$$
(9.49)

It is clear from this form of $q_p(t)$ that it is an *oscillatory* function of time. For given values of the lumped parameters C, K, L, both the frequency and amplitude of the oscillations are fixed, thus the dynamics of the flow rate under these conditions are appropriately referred to as "steady state oscillations".

9.7 Full Dynamics of the Capacitive Chamber

It is clear now that the capacitive chamber is indeed the chamber of the pulsatile blood flow system and its dynamics are at the core of the dynamics of pulsatile blood flow. We recall that the main function of this part of the system is the exchange of dissipative viscous resistance energy for recoverable viscoelastic energy as described in Sect. 9.2. An apt mechanical analogy is that in which the energy dissipated by friction is eliminated or considerably reduced by the use of a lubricant. To say that the capacitive chamber acts as a "lubricant" in pulsatile blood flow is indeed not only an apt analogy but a useful one because it places the dynamics of the chamber correctly within the dynamics of pulsatile blood flow. A disruption in the dynamics of the capacitive chamber is indeed not unlike that of a disruption in the function of a lubricant in a mechanical system. In both cases the result is energy loss due to dissipation by friction.

The full dynamics of oscillatory flow q(t) within the capacitive chamber consists of the sum of the homogeneous part $q_h(t)$ and the particular part $q_p(t)$ as determined in the previous two sections, namely, using Eqs. 9.33 and 9.52

$$q(t) = q_h(t) + q_p(t)$$

$$= Ae^{\alpha_1 t} + Be^{\alpha_2 t} + \frac{\Delta p_0}{K + i\left(\omega L - \frac{1}{\omega C}\right)}e^{i\omega t}$$
(9.50)

$$= Ae^{\alpha_1 t} + Be^{\alpha_2 t} + \frac{\Delta p_0 / K}{1 + i\left(\omega t_{lk} - \frac{1}{\omega t_{ck}}\right)}e^{i\omega t}$$

$$(9.51)$$

where A, B and α_1, α_2 are as determined in Sect. 9.5, depending on the particular damping scenario at hand.

Equation 9.51 indicates that the dynamics of the oscillatory flow rate within the capacitive chamber unfold by a transient phase at first (represented by the first two terms in the equation), followed by a phase of steady state oscillations (represented by the last term). The transient phase merges with the steady state phase as the first two terms die out in time. The time it takes for this to occur is strictly infinite because the two phases merge asymptotically, but in reality the state of steady-state oscillations is reached within a few oscillatory cycles depending on the damping scenario at hand. Examples of the three scenarios are shown in Figs. 9.3, 9.4 and 9.5.

It is important that the time t=0 in Figs. 9.3, 9.4, and 9.5 not be viewed as the "beginning of time" and, correspondingly, that the transient state not be considered as relevant only at the beginning of time. Because, strictly, there is no beginning of time in pulsatile blood flow, other than at the embryonic stage which is only a singular event and which is not the subject of present discussion. The more important "beginning of time" in the present context is the onset of any event that moves the dynamics of the capacitive chamber away from a state of steady state oscillations, not unlike that of disrupting the swings of a pendulum. At the onset of each such event the system must go through a transient state before returning to a state of steady state oscillations. This is the context in which the time t=0 in Figs. 9.3, 9.4, and 9.5 is to be interpreted.

The above discussion reiterates the principal theme that blood flow may be disrupted not only by blocked or narrowed passages but by disorderly dynamics. Each time the orderly dynamics of the capacitive chamber is disturbed, its function as a "lubricant" is disturbed until the system is able to return to its steady state oscillations. If the dynamics of the capacitive chamber is chronically disturbed, its function is chronically compromised. Pulsatile blood flow is then less efficient, more energy is required to drive it, and the heart must supply the extra energy. Heart "disease" must not be thought of as a consequence of only vascular pathologies but also of dynamic pathologies. Dynamic pathologies may result from any conditions that alter the lumped parameters of the system and hence alter its dynamical state.

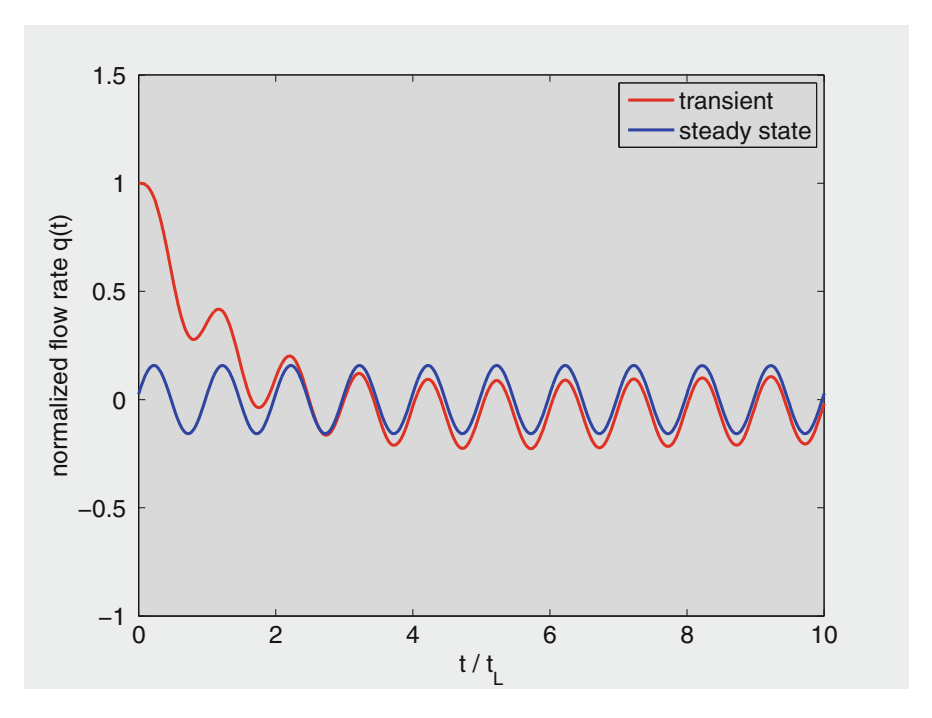


Fig. 9.3 Overdamped dynamics of the capacitive chamber (C, K, L in series) under oscillatory driving pressure.

9.8 The Concept of Reactance

The concepts of reactance and impedance arise in the dynamics of pulsatile blood flow and form the focus of much of the analytical as well as experimental work on the subject. It must be emphasized from the outset that these concepts relate to the phase of steady state oscillations only. The reason for this emphasis is that these concepts are so widely used that it is usually only implied, but rarely explicitly stated, that their use is limited to steady state dynamics only, not to the transient state. Thus, in introducing these concepts here, and using them in subsequent sections, it must be clear from the outset that we are now dealing with only the *particular* solution of the governing equation obtained in Sect. 9.6, namely

$$q_p(t) = \frac{\Delta p_0}{K + i\left(\omega L - \frac{1}{\omega C}\right)} e^{i\omega t}$$
(9.52)

where the driving pressure is given by

$$\Delta p = \Delta p_0 e^{i\omega t} \tag{9.53}$$

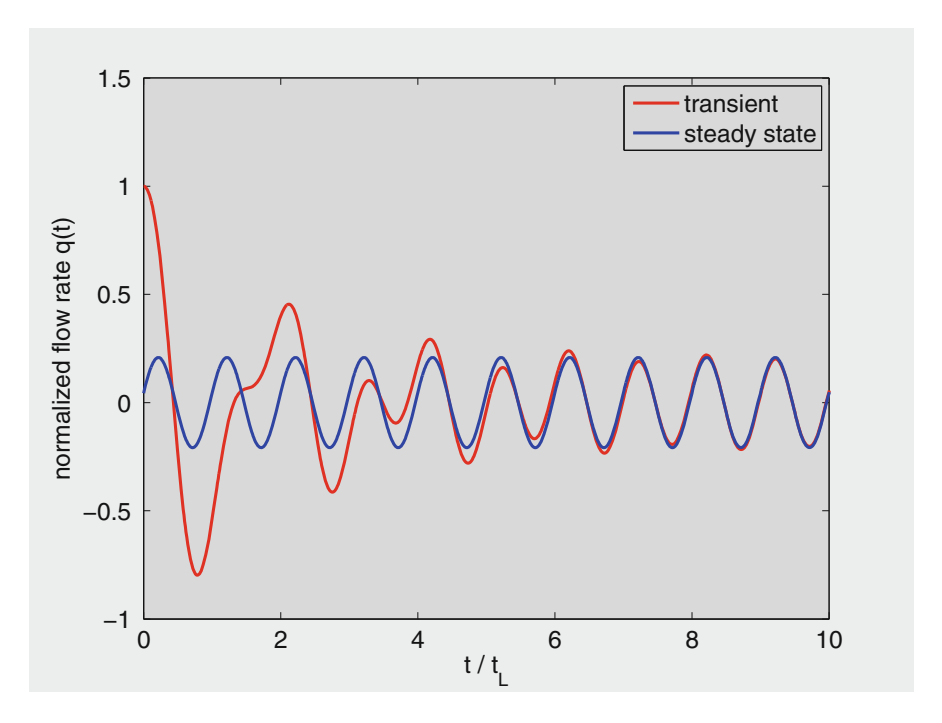


Fig. 9.4 Underdamped dynamics of the capacitive chamber (C, K, L in series) under oscillatory driving pressure.

For the purpose of the present section we shall use only the real part of this driving pressure, namely

$$\Delta p(t) = \Delta p_0 \cos \omega t \tag{9.54}$$

The corresponding part of the solution for the flow rate q(t) is the real part of $q_p(t)$ in Eq. 9.52 which, omitting the algebra, is given by

$$q(t) = \Re(q_p(t))$$

$$= \Re\left(\frac{\Delta p_0}{K + i\left(\omega L - \frac{1}{\omega C}\right)}e^{i\omega t}\right)$$

$$= \Delta p_0\left(\frac{K\cos\omega t + S\sin\omega t}{K^2 + S^2}\right) \tag{9.55}$$

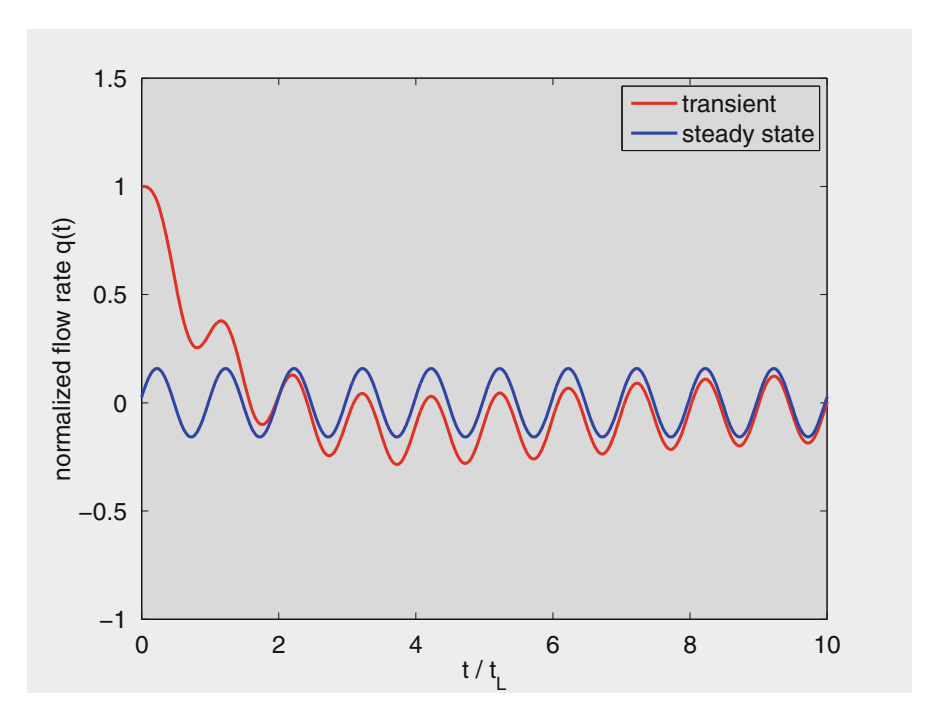


Fig. 9.5 Critically damped dynamics of the capacitive chamber (C, K, L in series) under oscillatory driving pressure.

where

$$S = \omega L - \frac{1}{\omega C} \tag{9.56}$$

The subscript p for the particular parts of the solution discussed in the previous section has been dropped.

It is thus implied here, and whenever the concepts of reactance and impedance are used, that q(t) represents only the particular part of the solution, which, as discussed in the previous section, corresponds to the steady state dynamics of the C, K, L system. Indeed, a meaningful definition of reactance or impedance is only possible when the driving pressure $\Delta p(t)$ and consequently the flow rate q(t) are simple harmonic functions as in Eqs. 9.54 and 9.55 above.

Using standard trigonometric identities, Eq. 9.55 can be simplified further to

$$q(t) = \frac{\Delta p_0}{\sqrt{K^2 + S^2}} \cos(\omega t - \theta)$$
 (9.57)

where

$$an \theta = \frac{S}{K} \tag{9.58}$$

To discuss the nature and effect of the quantity S, we begin by noting that when S = 0, Eqs. 9.55 and 9.57 give

$$q(t) = \frac{\Delta p_0}{K} \cos \omega t$$

$$= \frac{\Delta p}{K} \tag{9.59}$$

which we recognize as the simple expression for the flow rate through a resistance K when the driving pressure drop across it is Δp .

Thus, in the dynamics of the C, K, L system the quantity S as defined in Eq. 9.56 embodies the combined effects of inductance L and capacitance C such that when S=0 the system behaves as a simple resistance. When $S\neq 0$, it is clear from a comparison of Eq. 9.57 and 9.59 that S acts as an added form of opposition to flow, resulting from the presence of inductance and capacitance. It is also noted from the presence of ω in the expression for S that this added form of opposition occurs only in oscillatory flow. By analogy with the same phenomenon in the flow of alternating current in an electric circuit, S is generally referred to as the "reactance". It is a form of opposition to flow, but it differs from K in that it occurs only in oscillatory flow. Also, unlike the viscous resistance R in Poiseuille flow, the reactance S does not actually dissipate flow energy, it merely stores it and releases it within each oscillatory cycle.

From Eq. 9.56 we note that there are two ways in which the reactance S can be zero. First, when the capacitance and inductance effects are simply absent, that is when

$$\begin{cases} L = 0 \\ \frac{1}{C} = 0 \end{cases} \tag{9.60}$$

which together lead to S = 0. Second, when the values of ω , L, C are such that

$$C = \frac{1}{\omega^2 L} \tag{9.61}$$

which again leads to S = 0.

While the first of the above circumstances is trivial, the second has a clear physiological significance because it deals with the critical balance between the effects of compliance and inductance in pulsatile blood flow. If the values of the frequency ω and inductance L in Eq. 9.56 are considered fixed, then the value of S

now depends on the compliance C only. Starting at the limit where a blood vessel is rigid, the compliance C is zero and its reciprocal is infinite. The value of S from Eq. 9.56 is then infinite and negative, and the corresponding value of the phase angle θ from Eq. 9.58 is $-\pi/2$. Equation 9.57 then indicates that the flow is *leading* the pressure drop by $\pi/2$. As the compliance gradually increases from this extreme value, the values of S and θ remain negative at first but continue to increase until at some point they both become zero. The value of C at which this occurs is that given in Eq. 9.61.

At this critical value of C the reactance is zero, the phase angle between the flow and pressure drop is also zero, and the *amplitude* of the flow rate has its highest value. That is, altogether, and using Eq. 9.57, we have

$$\begin{cases} S = 0 \\ \theta = 0 \\ |q(t)| = \frac{\Delta p_0}{K} \end{cases}$$
 (9.62)

As compliance continues to increase beyond this point, the value of S becomes positive, the phase angle θ also becomes positive, which means that flow is now *lagging* the pressure drop, and the amplitude of the flow rate begins to decrease again from its maximum value.

To illustrate these results graphically, it is convenient to use a normalized form of the flow rate, namely

$$\overline{q}(t) = \frac{q(t)}{\Delta p_0 / K} \tag{9.63}$$

$$=\frac{1}{\sqrt{1+(S/K)^2}}\cos(\omega t - \theta) \tag{9.64}$$

Also, instead of using the actual compliance C, it is more convenient to use the capacitive time constant

$$t_{ck} = CK (9.65)$$

If K is assumed to be constant, t_{ck} is a direct measure of C and, using the inertial time constant

$$t_{lk} = L/K \tag{9.66}$$

the reactance S can be expressed in terms of these two time constants as

$$\frac{S}{K} = \omega t_{lk} - \frac{1}{\omega t_{ck}} \tag{9.67}$$

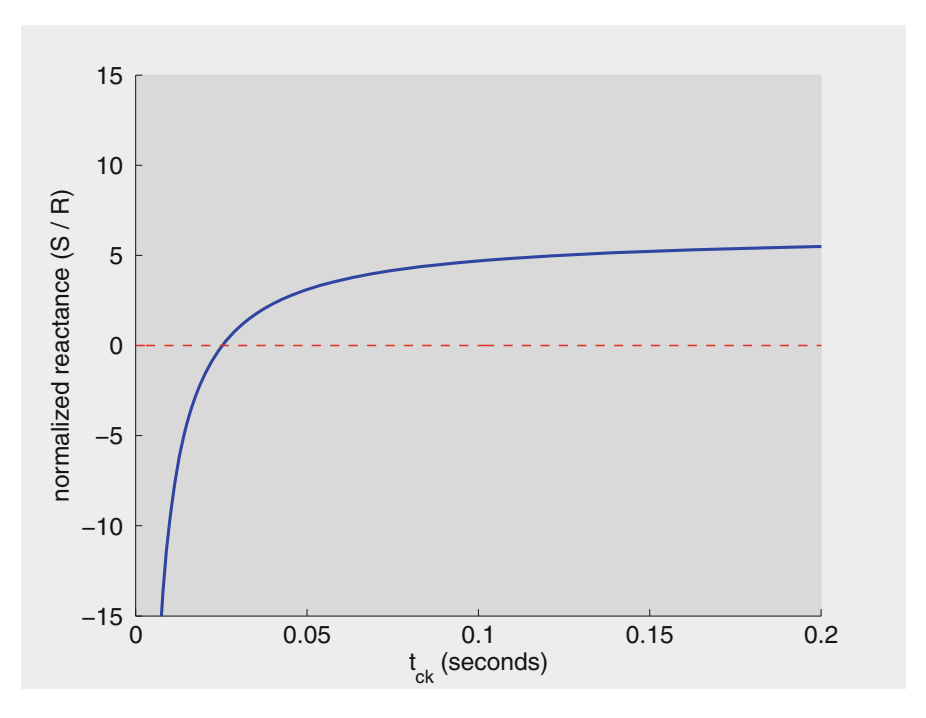


Fig. 9.6 Normalized value of the reactance (S/R), as a function of the capacitive time constant t_{ck} . Of particular significance is the point at which reactance becomes zero, which occurs at $t_{ck} = 1/4\pi^2 \approx 0.0253$.

Figure 9.6 shows the variation of the reactance as the capacitive time constant t_{ck} increases from zero to large values. In that sequence the value of S changes from large negative to positive, thus passing zero at one particular value of t_{ck} which we shall denote by $t_{ck,0}$, and which from Eq. 9.61 is given by

$$t_{ck,0} = \frac{1}{\omega^2 t_{lk}} \tag{9.68}$$

If the frequency of oscillation is taken as 1.0 cycles/s (Hz) so that the *angular* frequency ω is 2π radians/s, and if the inertial time constant t_{lk} is used as the normalizing unit of time, which is equivalent to taking $t_{lk}=1.0\,\mathrm{s}$, then Eq. 9.68 gives

$$t_{ck,0} = \frac{1}{(2\pi)^2} \approx 0.0253 s \tag{9.69}$$

as seen in Fig. 9.6. At higher values of t_{ck} , as capacitance effects become more significant, the normalized reactance S/K approaches the constant value, from Eq. 9.67, $2\pi \approx 6.283$, again as seen in that figure. Corresponding values of the

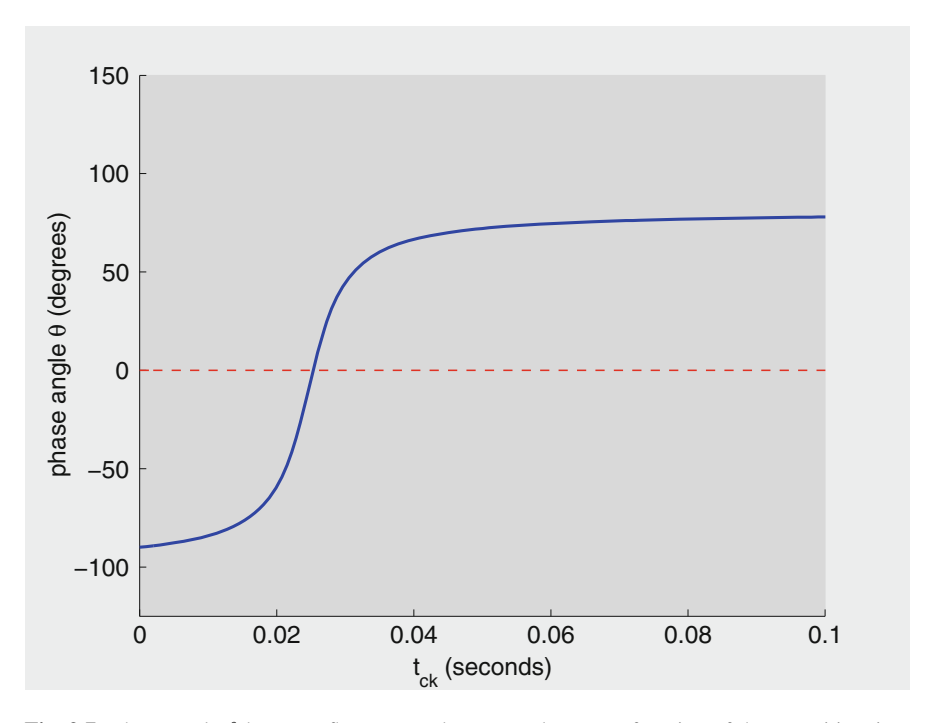


Fig. 9.7 Phase angle θ between flow rate and pressure drop, as a function of the capacitive time constant t_{ck} . The angle becomes zero and changes sign at the same critical value of t_C where reactance is zero (Fig. 9.6), namely $t_{ck} = 1/4\pi^2 \approx 0.0253$.

phase angle θ are shown in Fig. 9.7, where it is seen that the phase angle is zero at the same critical value of t_{ck} where the reactance is zero, namely at $t_{ck} \approx 0.0253$. At higher values of t_{ck} the angle is positive, which means that flow is lagging behind the pressure drop, while at lower values of t_{ck} the reverse is true. This change in phase shift is illustrated in Figs. 9.8, 9.9, and 9.10 where values of t_{ck} near the critical value are taken. It is remarkable that only a small departure from the critical value of t_{ck} is needed to produce a significant change in phase angle. A similar change occurs in the *amplitude* of the flow wave, which can be put in the normalized form

$$|\overline{q}(t)| = \frac{1}{\sqrt{1 + (S/K)^2}}$$
 (9.70)

In this form the amplitude has the normalized value of 1.0 when S = 0, which occurs at the critical value of t_{ck} . Figures 9.8, 9.9, and 9.10 show clearly that this is the *maximum* value of the flow amplitude. At all other values of t_{ck} the flow wave is affected both in phase and amplitude.

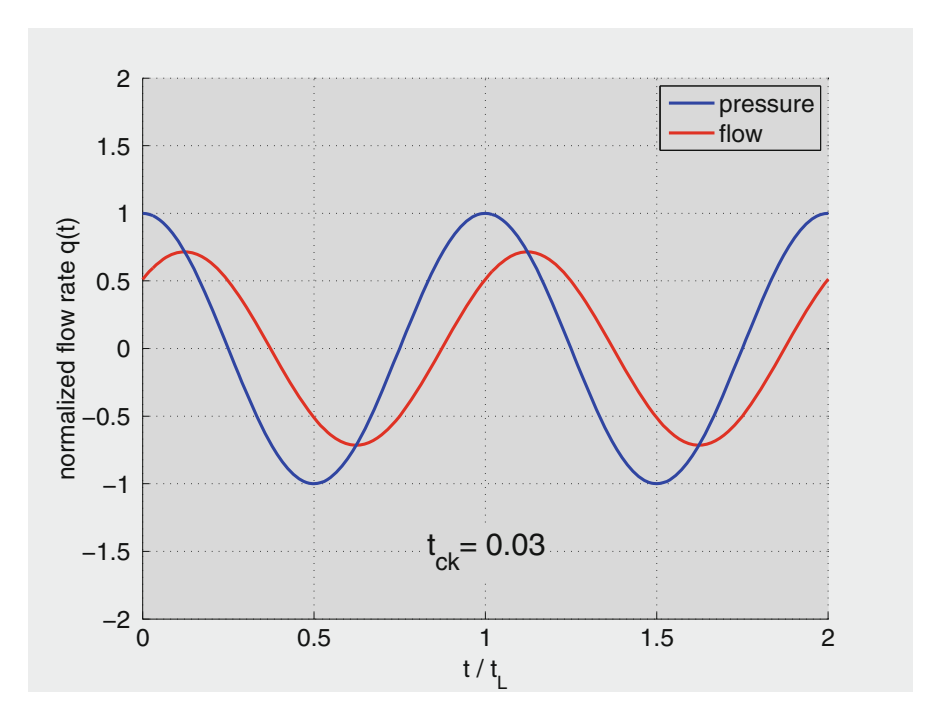


Fig. 9.8 Normalized flow rate compared with pressure drop (*dashed curve*) within the oscillatory cycle, and with $t_{ck} = 0.03$ s, which is just above critical value of $t_{ck} = 0.0253$ at which the two curves would be identical. Flow rate lags behind pressure drop and flow amplitude is below maximum.

The results in Figs. 9.8, 9.9, and 9.10 have significant implications regarding the dynamics of the capacitive chamber. They point to conditions under which the capacitive chamber as represented by the C, K, L system in series will operate most optimally with specific values of the parameters C, K (L being held constant), and any small departure from these values moves the dynamics of the chamber away from these optimum conditions. Under these conditions the reactance is zero, that is the effects of inductance and compliance are eliminated, and the only remaining opposition to the oscillatory flow is the viscoelasticity K.

The mere existence of these optimal conditions, and their critical dependence on the values of C, K, L, have obvious clinical implications. They point to how any change in the properties of the system, whether they are caused by disease or clinical intervention, may move the system away from its optimal dynamics.

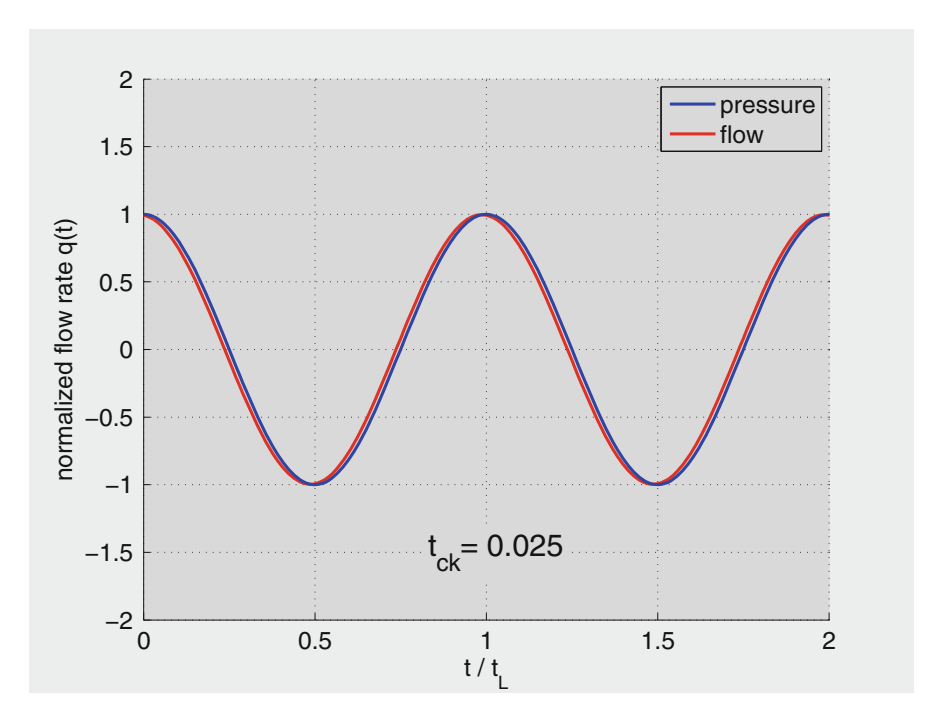


Fig. 9.9 Normalized flow rate compared with pressure drop (*dashed curve*) within the oscillatory cycle, and with $t_{ck} = 0.025$ s, which is very close to critical value of $t_{ck} = 0.0253$ at which the two curves would be indistinguishable. Flow rate is in phase with pressure drop and flow amplitude is maximum.

9.9 Impedance, Complex Impedance

The concept of "impedance", like that of reactance, arises in the *steady state oscillations* of the capacitive chamber as represented by the C, K, L system in series under a simple oscillatory driving pressure drop and, as emphasized in the previous section, it is only valid, indeed only meaningful, in the context of that steady state oscillations. As in the case of reactance, the concept of impedance is borrowed from the flow of alternating current in electric circuits, but it has wide applications in the dynamics of pulsatile blood flow.

Broadly speaking, impedance plays the same role in the relationship between pressure and flow in steady state oscillations as the resistance R does in steady Poiseuille flow. Thus, if the impedance is denoted by Z, then the concept of impedance allows us to write

$$q(t) = \frac{\Delta p(t)}{Z} \quad in \ steady \ state \ oscillations \tag{9.71}$$

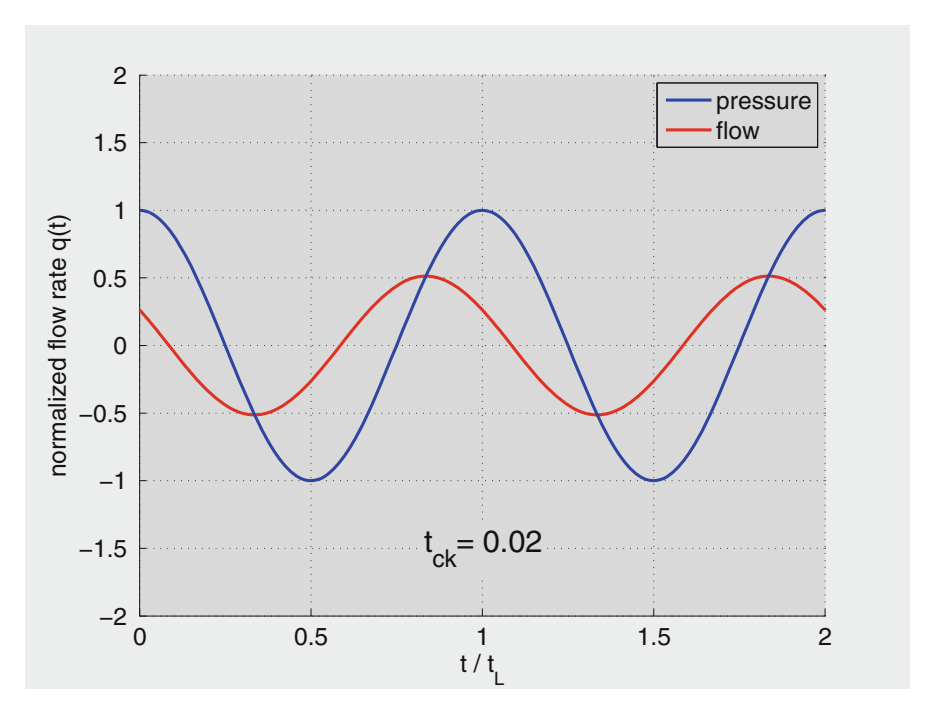


Fig. 9.10 Normalized flow rate compared with pressure drop (*dashed curve*) within the oscillatory cycle, and with $t_{ck} = 0.02$ s, which is just below critical value of $t_C = 0.0253$ at which the two curves would be identical. Flow rate leads pressure drop and flow amplitude is below maximum.

in analogy with

$$q = \frac{\Delta p}{R} \quad in \ steady \ Poiseuille \ flow \tag{9.72}$$

Thus, impedance represents "impediment" or "opposition" to steady state flow oscillations in the same way that resistance represents impediment to steady flow.

By its definition, impedance depends on the frequency of oscillations and, from what we have seen in previous sections it is then best treated in terms of the complex exponential function. Thus, in Sect. 9.6 we found

$$q(t) = \frac{\Delta p_0}{K + i\left(\omega L - \frac{1}{\omega C}\right)} e^{i\omega t} \tag{9.73}$$

where the subscript p used in that section for the "particular solution" has been dropped because, as stated earlier, by the very definition of impedance it is implied that we are only dealing with steady state oscillations as determined by the particular solution of the governing equation.

As Eq. 9.75 represents the relation between pressure and flow under the three elements of the capacitive chamber C, K, L in steady state oscillations, we can put it in the form of Eq. 9.71

$$q(t) = \frac{\Delta p(t)}{Z} \tag{9.74}$$

where

$$\begin{cases} \Delta p(t) = \Delta p_0 e^{i\omega t} \\ Z = K + i \left(\omega L - \frac{1}{\omega C}\right) \end{cases}$$
(9.75)

Furthermore, we may break the impedance Z into partial impedances Z_k , Z_l , Z_c representing the effects of viscoelasticity, inductance, and compliance, respectively, and then by considering each of these effects in isolation (with the other two being absent) we find

$$\begin{cases} Z_k = K & viscoelasticity \\ Z_l = i\omega L & inductance \\ Z_c = \frac{1}{i\omega C} & capacitance \end{cases}$$
(9.76)

It is clear from this and Eq. 9.75 that the partial impedances of the capacitive chamber, representing the three components of the capacitive chamber *in series*, add up, such that

$$Z = Z_k + Z_l + Z_c \tag{9.77}$$

Thus in steady state oscillations partial impedances in series add up in the same way that in steady flow partial resistances in series add up. The reason in both cases is that when the components of impedance (or resistance) are in series, the total pressure drop required to overcome the total opposition to oscillatory (or steady) flow is the sum of the partial pressure drops, that is

$$\Delta p = \Delta p_k + \Delta p_l + \Delta p_c \tag{9.78}$$

and since the three components are in series, the flow rate q is the same, hence

$$\begin{cases} \Delta p_k = qZ_k \\ \Delta p_l = qZ_l \\ \Delta p_c = qZ_c \\ \Delta p = qZ \end{cases}$$

$$(9.79)$$

To complete the basic elements of the pulsatile blood flow system requires that a resistive element R now be added in parallel with the capacitive chamber. For this purpose we now denote the total impedance of the capacitive chamber by Z_b and that of the resistive path by Z_r , and the corresponding flow rates by q_b and q_r respectively.

The flow rates q_b and q_r along the two paths are of course different but they are driven by a common source of pressure since the two paths are parallel. Therefore, if the common pressure difference is denoted by Δp , then

$$\begin{cases}
q_b = \frac{\Delta p}{Z_b} \\
q_r = \frac{\Delta p}{Z_r}
\end{cases}$$
(9.80)

If the total flow rate is now denoted by q and the total impedance by Z, then since

$$q = q_b + q_r \tag{9.81}$$

we finally have

$$\frac{\Delta p}{Z} = \frac{\Delta p}{Z_b} + \frac{\Delta p}{Z_c} \tag{9.82}$$

or

$$\frac{1}{Z} = \frac{1}{Z_b} + \frac{1}{Z_r} \tag{9.83}$$

Equations 9.77 and 9.83 are of course well known rules for adding impedances in series and in parallel, respectively, as in the analogy of electric circuits.

In summary, the two basic paths characterizing pulsatile blood flow can be represented by two impedances in parallel: Z_b along the capacitive chamber and Z_r along the resistive path, where

$$\begin{cases} Z_b = K + i \left(\omega L - \frac{1}{\omega C} \right) & capacitive chamber \\ Z_r = R & resistive path \end{cases}$$
 (9.84)

The total impedance of pulsatile blood flow, from Eq. 9.83, is then

$$Z = \frac{Z_r Z_b}{Z_r + Z_b} \tag{9.85}$$

and substituting for the individual impedances we finally have

$$Z = \frac{R\left(\omega KC + i(\omega^2 LC - 1)\right)}{\omega C(R + K) + i(\omega^2 LC - 1)}$$
(9.86)

Equation 9.86 represents the total impedance of the two principal components of pulsatile blood flow, namely the resistive component and the capacitive component, in terms of the four lumped parameters characterizing the system, namely R, C, K, L. The two components and the four parameters together constitute the fundamental ingredients for the dynamics of pulsatile blood flow. The impedance may therefore be applied to the entire systemic circulation or to any sub-system thereof because it contains the required ingredients. While the resistive path or the capacitive chamber may contain a more complicated combination of these ingredients, the two options available to the flow, namely resistive and capacitive in parallel, must remain unchanged. Similarly while the values of the lumped parameters R, C, K, L will be different in different systems, the fundamental characteristics which they represent remain unchanged in providing the basic ingredients required for the dynamics of pulsatile blood flow. The only element missing from this discussion is the effect of wave reflections discussed in Chap. 6. The way this effect may be integrated into the dynamics of pulsatile blood flow is discussed in the next section.

9.10 Pressure-Flow Relations

The ultimate utility of the impedance Z introduced in the previous section is to provide the relation between pressure and flow under steady state oscillations and in the presence of inertial, elastic or viscoelastic effects, in the same way that the resistance R provides that relation in the absence of these effects. The relation between pressure and flow then in turn provides a measure of the "opposition" to oscillatory flow in the same way that the relation between pressure and flow in Poiseuille flow provides a measure of the resistance to flow in that case.

In all cases the general relation between the flow rate q(t) and the driving pressure difference $\Delta p(t)$ is of the form of Eq. 9.71 of the previous section, namely

$$q(t) = \frac{\Delta p(t)}{Z} \tag{9.87}$$

where Z is the impedance. To illustrate the utility of this relation, we take an oscillatory driving pressure wave in the form of a single harmonic (sine or cosine) and use the complex exponential function for that purpose as before

$$\Delta p(t) = \Delta p_0 e^{i\omega t} \tag{9.88}$$

More complex pressure waveforms, such as those delivered by the heart, will be considered in the next two chapters. In the present section the focus is on the basic forms of pressure-flow relations under the effects of the basic elements of the pulsatile flow system.

The most basic form of pressure-flow relation, of course, occurs under simple resistance R, as in Poiseuille flow, only now both the pressure and flow are oscillatory. In this case (Eq. 9.84)

$$\begin{cases} Z_r = R \\ q(t) = \frac{\Delta p}{Z_r} \\ = \frac{\Delta p_0}{R} e^{i\omega t} \end{cases}$$
(9.89)

The flow is precisely the same oscillatory function of time as the driving pressure (Eq. 9.88), which provides a good reference case for pressure-flow relations under different conditions.

In the case of viscoelasticity, using Eq. 9.76 of the previous section, we

$$\begin{cases} Z_k = K \\ q(t) = \frac{\Delta p}{Z_k} \\ = \frac{\Delta p_0}{K} e^{i\omega t} \end{cases}$$
(9.90)

which indicates that here too the flow is precisely the same oscillatory function of time as the driving pressure. Thus, as noted previously, the effect of viscoelasticity, which represents viscous resistance to stretch within the vessel wall, is the same as the effect of viscous resistance to flow at the interface between the wall and the moving fluid.

In the case of inductance, using Eq. 9.76 of the previous section, we

$$\begin{cases} Z_{l} = i\omega L \\ q(t) = \frac{\Delta p}{Z_{l}} \\ = \frac{\Delta p_{0}}{i\omega L} e^{i\omega t} \\ = \frac{\Delta p_{0}}{\omega L} (\sin \omega t - i\cos \omega t) \end{cases}$$

$$(9.91)$$

which indicates that here

$$\begin{cases} \Re(q(t)) = \frac{\Delta p_0}{\omega L} \sin \omega t \\ \Im(q(t)) = -\frac{\Delta p_0}{\omega L} \cos \omega t \end{cases}$$
(9.92)

while the real and imaginary parts of the driving pressure (Eq. 9.88) are $\Delta p_0 \cos \omega t$ and $\Delta p_0 \sin \omega t$ respectively. Thus, the imaginary part of the pressure, $\Delta p_0 \sin \omega t$, reaches its first peak at $\omega t = \pi/2$ while the imaginary part of the flow, $-\frac{\Delta p_0}{\omega L} \cos \omega t$ reaches its first peak at $\omega t = \pi$. Inductance has the effect of shifting the flow wave 90° behind the pressure.

In the case of compliance, using Eq. 9.76 of the previous section, we

$$\begin{cases} Z_c &= \frac{1}{i\omega C} \\ q(t) &= \frac{\Delta p}{Z_c} \\ &= \Delta p_0 i\omega C e^{i\omega t} \\ &= \Delta p_0 \omega C (-\sin \omega t + i\cos \omega t) \end{cases}$$
(9.93)

thus, here

$$\begin{cases}
\Re(q(t)) = \Delta p_0 \omega C(-\sin \omega t) \\
\Im(q(t)) = \Delta p_0 \omega C(\cos \omega t)
\end{cases}$$
(9.94)

while, as before, the real and imaginary parts of the driving pressure (Eq. 9.88) are $\Delta p_0 \cos \omega t$ and $\Delta p_0 \sin \omega t$ respectively. Thus, the imaginary part of the pressure, $\Delta p_0 \sin \omega t$, reaches its first peak at $\omega t = \pi/2$ while the imaginary part of the flow, $\Delta p_0 \omega C(\cos \omega t)$ reaches its first peak at $\omega t = 2\pi$. Peak capacitive flow (into a capacitive chamber) occurs 270° behind the peak in pressure. The reason for this, of course, is that flow into a capacitive chamber is driven not by pressure but by pressure *gradient*. Thus peak flow into a capacitive chamber occurs at the first peak in pressure *gradient* following the first peak in pressure, which occurs at $\omega t = 2\pi$.

While it is instructive to consider these effects on pressure-flow relations, as was done above, in general these effects rarely occur in isolation. Thus, for the capacitive chamber as a whole the effects of capacitance, viscoelasticity, and inductance are combined such that

$$\begin{cases} Z_b = K + i(\omega L - \frac{1}{\omega C}) \\ q(t) = \frac{\Delta p}{Z_b} \\ = \frac{\omega C \Delta p_0 e^{i\omega t}}{\omega KC + i(\omega^2 LC - 1)} \end{cases}$$
(9.95)

The real and imaginary parts of the flow rate correspond to the real and imaginary parts of the driving pressure, respectively, that is

$$\begin{cases} \Delta p = \Delta p_0 \cos \omega t \\ q(t) = \omega C \Delta p_0 \times \Re \left\{ \frac{e^{i\omega t}}{\omega KC + i(\omega^2 LC - 1)} \right\} \end{cases}$$
(9.96)

$$\begin{cases} \Delta p = \Delta p_0 \sin \omega t \\ q(t) = \omega C \Delta p_0 \times \Im \left\{ \frac{e^{i\omega t}}{\omega KC + i(\omega^2 LC - 1)} \right\} \end{cases}$$
(9.97)

It is clear that the pressure-flow relation is no longer simple in this case, both the amplitude and phase of the flow being dependent on the lumped parameters of the capacitive chamber as well as on the frequency.

Finally, if the capacitive chamber is now combined with the resistive path, using the total impedance in Eq. 9.86 of the previous section, we then have

$$\begin{cases}
Z = \frac{R(\omega KC + i(\omega^2 LC - 1))}{\omega C(R + K) + i(\omega^2 LC - 1)} \\
q(t) = \frac{\Delta p}{Z} \\
= \left\{ \frac{\omega C(R + K) + i(\omega^2 LC - 1)}{R(\omega KC + i(\omega^2 LC - 1))} \right\} \Delta p_0 e^{i\omega t}
\end{cases}$$
(9.98)

Again, the real and imaginary parts of the flow rate correspond to the real and imaginary parts of the driving pressure, respectively, that is

$$\begin{cases}
\Delta p = \Delta p_0 \cos \omega t \\
q(t) = \Delta p_0 \times \Re \left\{ \frac{\omega C(R+K) + i(\omega^2 LC - 1)}{R(\omega KC + i(\omega^2 LC - 1))} e^{i\omega t} \right\}
\end{cases} (9.99)$$

$$\begin{cases}
\Delta p = \Delta p_0 \sin \omega t \\
q(t) = \Delta p_0 \times \Im \left\{ \frac{\omega C(R+K) + i(\omega^2 LC - 1)}{R(\omega KC + i(\omega^2 LC - 1))} e^{i\omega t} \right\}
\end{cases} (9.100)$$

In practice there is no need to evaluate the expressions for the real and imaginary parts of the flow explicitly since it involves rather tedious algebra. Computations can be made using any software such as Matlab where the real and the imaginary parts are extracted in the process.

To sum up this section, it is important to clarify the concept of "impedance" and its role in the dynamics of pulsatile blood flow, particularly in comparison with the more clearly understood concept of "resistance". Some confusion arises because both terms are sometimes used rather loosely to mean simply any form of "opposition" to flow.

As noted in earlier sections, pulsatile blood flow consists of a steady flow part and an oscillatory flow part. A distinction between the concepts of resistance and impedance can be made by saying that resistance has to do with opposition to the steady part of pulsatile flow while impedance has to do with opposition to the oscillatory part of the flow.

Another useful though not strict distinction between the two concepts is that resistance is usually associated with energy dissipation due to viscous shear between the moving fluid and the tube wall, while impedance is usually associated with the repeated inflation and deflation of the capacitive chamber where much of the energy spent in one part of the oscillatory cycle is recovered in another part of the cycle. This distinction is not strict because the latter involves some energy dissipation due to viscous resistance to stretch within the vessel wall as represented by the parameter K and described in Sect. 9.4. Also, the oscillatory part of pulsatile blood flow, representing the repeated inflation and deflation of the capacitive chamber, involves some energy dissipation due to viscous shear at the tube wall because of oscillatory flow within the resistive path as represented by the parameter K in the impedance of the full oscillatory flow system which includes both the resistive path and the capacitive chamber (Eq. 9.86).

Chapter 10 Analysis of Composite Waveforms

10.1 Introduction

The oscillatory pressure drops used in all previous chapters have been of a particularly simple form, namely that of a trigonometric sine or cosine function. These simple waveforms have specific properties that make them particularly useful for the study of oscillatory systems, but the ultimate aim in pulsatile blood flow is to examine the dynamics of such systems under oscillatory pressure drops of more general forms, in particular the forms of pressure waves generated by the heart. In what follows, and for reasons to become clear shortly, we shall refer to these generically as "composite" wave forms.

An example of a composite waveform is shown in Fig. 10.1, compared with a simple sine wave. The first difference to be observed, of course, is the strictly *regular* form of the sine wave compared with the highly irregular form of the composite wave. It is this simple regular form of the sine wave that makes it possible to describe it by a simple analytical function. How to describe the irregular form of the composite wave is the subject of the present chapter.

Of course, a composite wave can be described numerically, by tabulating the position of discrete points along the wave, as shown in Fig. 10.2 and in Table 10.1, but this is a rather awkward method of description. It is certainly not as elegant or efficient as the description of a sine or cosine wave, which can be accomplished by the use of a simple analytical function. More important, the steady state solutions obtained in the previous chapter were possible only because the pressure drop Δp driving the flow was assumed to have the simple *analytical* form of trigonometric sine or cosine, or both as in the complex exponential function. If Δp can only be described in numerical form, the analytical solutions of the previous chapter would not be possible.

In one of mathematics' most beautiful triumphs this difficulty is completely resolved, using a technique known as Fourier analysis, named after its

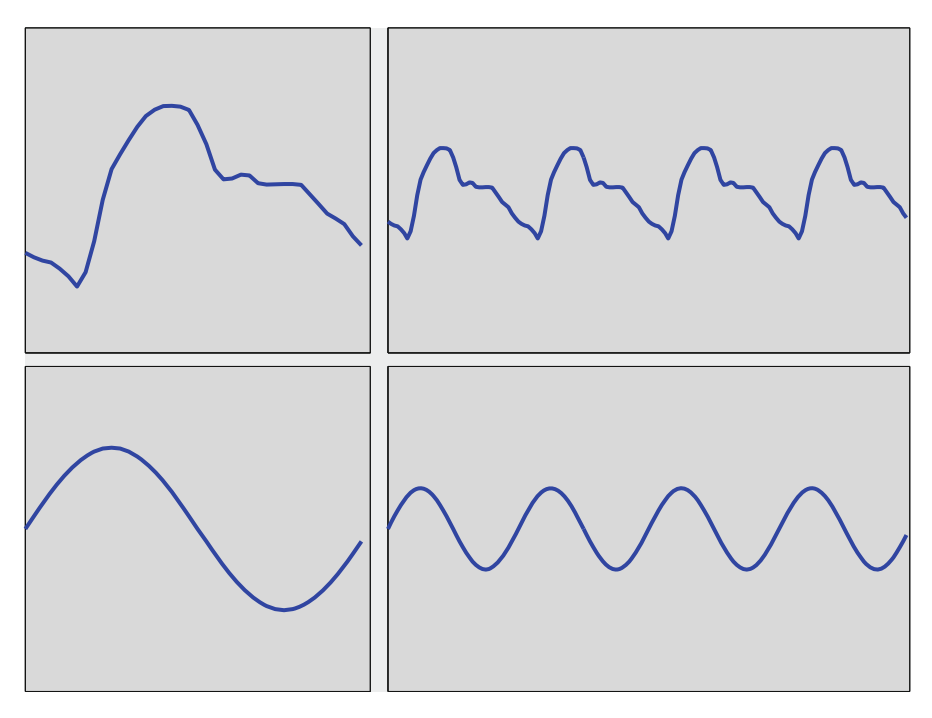


Fig. 10.1 Comparison of a composite waveform (*top*) with the very simple form of the sine wave (*bottom*). While they are both *periodic*, as seen on the right, the composite wave is highly irregular and is therefore not easy to describe analytically.

original author. The theory of Fourier analysis shows that a composite wave such as that shown at the top of Fig. 10.1 can actually be decomposed into a series of sine and cosine waves like the one shown at the bottom of that figure. The composite wave is simply the sum of these so called "harmonics", each of which is a simple sine or cosine wave. This makes it possible to express the composite waveform of the pressure drop Δp driving the flow in an oscillatory system simply as the sum of the sine and cosine functions which constitute that particular composite waveform. The steady state oscillation solution of the governing equation can then be obtained for each of these sine and cosine functions separately, and then these solutions are collected into a whole. Thus, the steady state oscillation solutions obtained in the previous chapter, which were limited to pressure drops of simple sine or cosine waveforms, are not irrelevant to the case of pressure drops of composite waveforms. In fact, they are highly relevant in that they provide the "building blocks" from which a solution with a pressure drop of a composite waveform is constructed.

The theory of Fourier analysis is well established and fairly straightforward, but its application to the analysis of specific composite waveforms involves some tedious calculations and some algebraic intricacies which can only be illustrated by considering specific examples. While mathematical software packages such as

10.1 Introduction 319

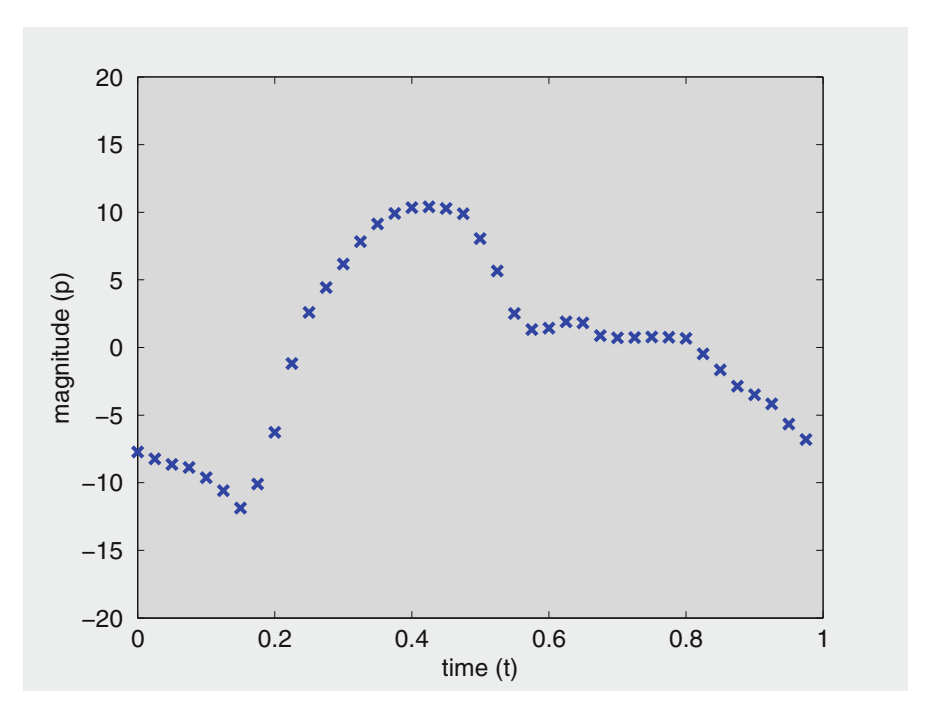


Fig. 10.2 A composite wave can be described numerically by tabulating the positions of discrete points along the wave, as shown in Table 10.1. The axes are marked generically as t for time and p for pressure. This numerical description is not adequate for obtaining the steady state dynamics associated with this wave, but Fourier analysis shows that the wave can be decomposed into a series of constituent sine and cosine waves for which the dynamics can be obtained, as was done in previous chapters.

MATLAB and MATHEMATICA now have specific tools under the heading of Fast Fourier Transforms (FFT) that can handle much of the tedious calculations, these tools cannot be used reliably, or indeed meaningfully, without a basic understanding of the analytical intricacies involved. For this reason, and since "understanding" is one of the main missions of this book, in subsequent sections we consider a series of examples that are intended mainly to illustrate the analytical process involved. In each case, the purpose of the analysis is to find the Fourier series representation of the given waveform, that is to find the series of sine and cosine waves that make up the given waveform. The focus in all cases is on using the *analytical formulation* of Fourier analysis, the use of FFT is best described by the documentation of the particular software package being used.

¹Brigham EO, 1988. The Fast Fourier Transform and its Applications. Prentice Hall, Englewood Cliffs, NJ.

²Walker JS, 1988. Fourier Analysis. Oxford University Press, New York.

Table 10.1 A numerical description of the composite wave shown in Fig. 10.2, giving the position (t, p) of each of the discrete points shown along the curve.

t	p	t	p
0.000	-7.7183	0.500	8.0597
0.025	-8.2383	0.525	5.6717
0.050	-8.6444	0.550	2.5232
0.075	-8.8797	0.575	1.3301
0.100	-9.6337	0.600	1.4405
0.125	-10.5957	0.625	1.9094
0.150	-11.8705	0.650	1.8145
0.175	-10.0942	0.675	0.8738
0.200	-6.2839	0.700	0.7055
0.225	-1.1857	0.725	0.7343
0.250	2.6043	0.750	0.7788
0.275	4.4323	0.775	0.7495
0.300	6.1785	0.800	0.6711
0.325	7.8211	0.825	-0.4796
0.350	9.1311	0.850	-1.6541
0.375	9.9138	0.875	-2.8643
0.400	10.3447	0.900	-3.4902
0.425	10.4011	0.925	-4.1714
0.450	10.2807	0.950	-5.6581
0.475	9.8951	0.975	-6.8024

10.2 Basic Theory

In mathematical language, the pressure and flow waveforms occurring in pulsatile blood flow are said to be "periodic functions". A function f(x) is said to be periodic in the variable x if

$$f(x+T) = f(x) \tag{10.1}$$

where T is then said to be the *period* of that function. An obvious example is the trigonometric function $f(\omega t) = \sin \omega t$ for which

$$\begin{cases} f(x+2\pi) = \sin(x+2\pi) \\ = \sin x \cos 2\pi + \cos x \sin 2\pi \\ = \sin x \times 1 + 0 \\ = \sin x \\ = f(x) \end{cases}$$
 (10.2)

therefore, $f(x) = \sin x$ is a periodic function with a period $T = 2\pi$. The function is seen graphically in Fig. 10.1 (bottom) where the meaning of the period T is quite

10.2 Basic Theory 321

clear, namely the time interval over which the function assumes a complete cycle of its values. The composite wave seen in Fig. 10.1 (top) also represents a periodic function, although the function in this case does not have a simple mathematical representation. Nevertheless, the composite wave in Fig. 10.1 represents a periodic function because we can see graphically that the function has a well defined period over which it assumes a complete cycle of its values.

Another example of a periodic function which we used in previous sections and which again has a period $T = 2\pi$ is $f(x) = e^{ix}$, because

$$\begin{cases} f(x+2\pi) = e^{i(x+2\pi)} \\ = e^{i2\pi}e^{ix} \\ = (\cos 2\pi + i\sin 2\pi)e^{ix} \\ = (1+0)e^{ix} \\ = e^{ix} \\ = f(x) \end{cases}$$
(10.3)

The theory of Fourier analysis has shown that a periodic function of period T can be expressed as a sum of sine and cosine functions, such that

$$f(t) = \sum_{n=0}^{\infty} A_n \cos\left(\frac{2\pi nt}{T}\right) + \sum_{n=1}^{\infty} B_n \sin\left(\frac{2\pi nt}{T}\right)$$
 (10.4)

or in expanded form

$$f(t) = A_0 + A_1 \cos\left(\frac{2\pi t}{T}\right) + A_2 \cos\left(\frac{4\pi t}{T}\right) + \dots$$

$$+ B_1 \sin\left(\frac{2\pi t}{T}\right) + B_2 \sin\left(\frac{4\pi t}{T}\right) + \dots$$
(10.5)

where the A's and B's are constants known as "Fourier coefficients" and are given by

$$\begin{cases} A_0 = \frac{1}{T} \int_0^T f(t)dt \\ A_n = \frac{2}{T} \int_0^T f(t) \cos\left(\frac{2\pi nt}{T}\right) dt \\ B_n = \frac{2}{T} \int_0^T f(t) \sin\left(\frac{2\pi nt}{T}\right) dt \end{cases}$$
(10.6)

The infinite series in Eq. 10.4 are called Fourier series, and this representation of the function f(t) is then referred to as the Fourier series representation of that function.

We note from the definition of A_0 that it represents the *average value* of the periodic function f(t) over one period. We note further that there are actually *two* series in Eq. 10.4 and that, except for A_0 , the remaining terms in the two series are *paired*, meaning that the terms in A_1 and B_1 have the same argument, namely $2\pi t/T$, and the next two terms again have the same argument, namely $4\pi t/T$, etc. This makes it possible to combine each pair, using standard trigonometric identities, whereby we can write

$$A_1 \cos\left(\frac{2\pi nt}{T}\right) + B_1 \sin\left(\frac{2\pi nt}{T}\right) = M_1 \cos\left(\frac{2n\pi t}{T} - \phi_1\right)$$
 (10.7)

where M_1 , ϕ_1 are two new constants, related to A_1 , B_1 by

$$\begin{cases}
A_1 = M_1 \cos \phi_1 \\
B_1 = M_1 \sin \phi_1
\end{cases}$$
(10.8)

This pairing process can now be repeated for each pair of terms in Eq. 10.5, with the result that the two Fourier series can be combined into one, namely

$$f(t) = A_0 + M_1 \cos\left(\frac{2\pi t}{T} - \phi_1\right) + M_2 \cos\left(\frac{4\pi t}{T} - \phi_2\right)$$
$$+ M_3 \cos\left(\frac{6\pi t}{T} - \phi_3\right) + \dots$$
(10.9)

or in more compact form

$$f(t) = A_0 + \sum_{n=1}^{\infty} M_n \cos\left(\frac{2n\pi t}{T} - \phi_n\right)$$
 (10.10)

where

$$\begin{cases} A_n = M_n \cos \phi_n \\ B_n = M_n \sin \phi_n \end{cases}$$
 (10.11)

therefore

$$\begin{cases} M_n = \sqrt{A_n^2 + B_n^2} \\ \phi_n = \tan^{-1} \left(\frac{B_n}{A_n} \right) \end{cases}$$
 (10.12)

10.2 Basic Theory 323

Eq. 10.10 provides a more compact Fourier series representation of the function f(t) in that it contains only one series instead of two. In this representation each term except the first is a simple cosine wave with M as its amplitude and ϕ as its phase. Because these waves add up to constitute the function f(t), they are referred to as the "harmonics" of this periodic function.

We note in Eq. 10.10 that in the first harmonic the cosine function has the same value at t = 0 and at t = T, therefore this harmonic has a period T, which is the same as the period of the original function f(t). For this reason it is referred to as the "fundamental harmonic". In the second harmonic, by comparison, the cosine function has the same value at t = 0 and at t = T/2. Therefore, this harmonic has a period T/2 which is half the period of f(t). This pattern continues to higher harmonics.

Because of the reciprocal relation between the period and the frequency of a periodic function, the above pattern can be expressed in terms of the frequencies of the different harmonics. Thus, if f_r is the frequency of the periodic function f(t) in cycles/s (Hz), then

$$f_r = \frac{1}{T} \tag{10.13}$$

and the corresponding angular frequency ω is given by

$$\begin{cases} \omega = 2\pi f_r \\ = \frac{2\pi}{T} \quad \text{radians/s} \end{cases}$$
 (10.14)

Thus the Fourier series representation in Eq. 10.10 can now be put in the form

$$f(t) = A_0 + M_1 \cos(\omega t - \phi_1) + M_2 \cos(2\omega t - \phi_2) + M_3 \cos(3\omega t - \phi_3) + \dots$$
(10.15)

in which it is seen clearly that the frequency of the first harmonic is ω , the same as the frequency of the original function f(t) and is therefore referred to as the "fundamental frequency". The frequency of the second harmonic is 2ω , and of the third is 3ω , etc. These are important properties of the harmonics of a periodic function which we shall see more clearly later as we consider specific functions. In particular, we shall see that the *amplitudes* of successive harmonics usually diminish fairly rapidly and in most cases it is found that the first ten harmonics are sufficient for producing a good representation of a given periodic function such as the composite pressure wave produced by the heart. In that case, the fundamental frequency is the beating frequency of the heart which, under resting conditions, is approximately 1 Hz, thus the frequency of the tenth harmonic would be 10 Hz. It is for this reason that frequencies as high as $10 \, \text{Hz}$ are sometimes considered in the analysis of pulsatile blood flow as we did in some previous sections.

10.3 Example: Single-Step Waveform

Thus, in this spirit consider the simple waveform consisting of a single step shown in Fig. 10.3, which has a period T = 1 as seen graphically, and which is defined by

$$\begin{cases} f(t) = 1, & 0 \le t < \frac{1}{2} \\ = 0, & \frac{1}{2} \le t < 1 \end{cases}$$
 (10.16)

Following the theory presented in the previous section, the Fourier series representation of this periodic function is given by (Eq. 10.4)

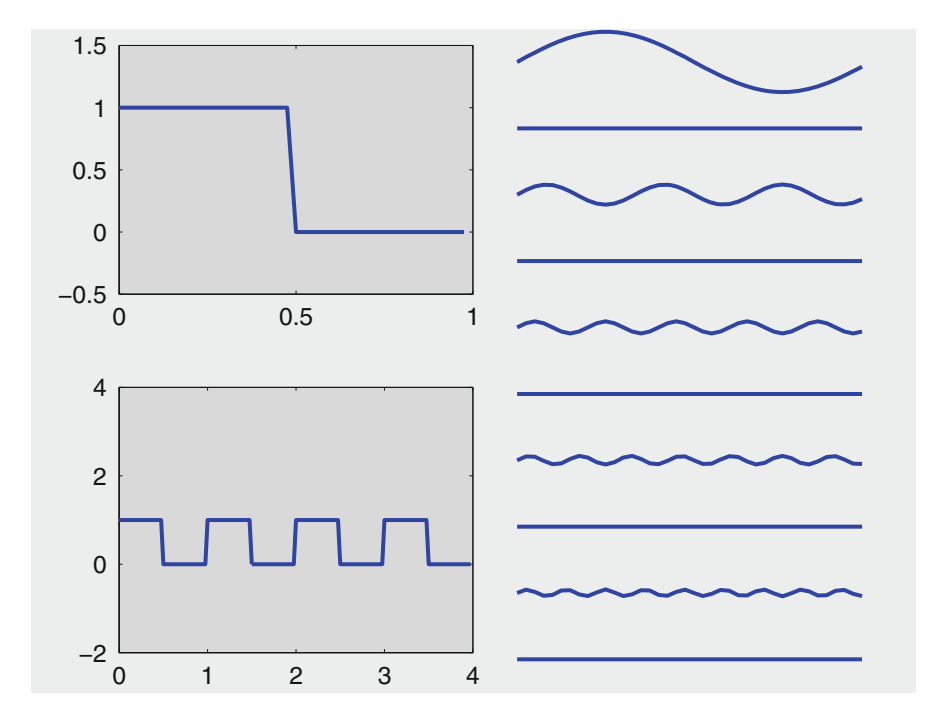


Fig. 10.3 A simple waveform consisting of a single step and having a period T=1 as seen in the *left two panels*. The first ten harmonics of this waveform are shown on the *right*. The *even* harmonics, namely harmonics 2, 4, 6, 8, 10 are zero in this case and make no contribution to the Fourier composition of this waveform, as seen on the *right*. The series is led by the fundamental harmonic which has the same period and hence the same frequency as the original wave, namely the fundamental period and fundamental frequency. The period of the third harmonic is one third of the fundamental period and hence its frequency is three times the fundamental frequency, etc.

$$f(t) = \sum_{n=0}^{\infty} A_n \cos\left(\frac{2\pi nt}{T}\right) + \sum_{n=1}^{\infty} B_n \sin\left(\frac{2\pi nt}{T}\right)$$

$$= A_0 + A_1 \cos\left(\frac{2\pi t}{T}\right) + A_2 \cos\left(\frac{4\pi t}{T}\right) + \dots$$

$$+ B_1 \sin\left(\frac{2\pi t}{T}\right) + B_2 \sin\left(\frac{4\pi t}{T}\right) + \dots$$
(10.17)

and, using Eq. 10.6 to find the Fourier coefficients, recalling that T=1 in this case, we have

$$A_{0} = \frac{1}{T} \int_{0}^{T} f(t)dt$$

$$= \int_{0}^{1} f(t)dt$$

$$= \int_{0}^{1/2} 1 \times dt + \int_{1/2}^{1} 0 \times dt$$

$$= \frac{1}{2}$$
(10.18)

Note that by its definition (Eq. 10.6), A_0 represents the *average value* of the periodic function over one period, which in Fig. 10.3 is seen graphically to be 1/2, in agreement with the above result.

For the other coefficients, we find

$$A_n = \frac{2}{T} \int_0^T p(t) \cos\left(\frac{2n\pi t}{T}\right) dt$$

$$= 2 \int_0^1 f(t) \cos(2n\pi t) dt$$

$$= 2 \int_0^{1/2} 1 \times \cos(2n\pi t) dt + 2 \int_{1/2}^1 0 \times \cos(2n\pi t) dt$$

$$= 2 \int_0^{1/2} \cos(2n\pi t) dt$$

$$= \frac{\sin(2n\pi t)}{n\pi} \Big|_0^{1/2}$$

$$= 0 \quad \text{for all } n$$

$$(10.19)$$

and similarly

$$B_{n} = \frac{2}{T} \int_{0}^{T} p(t) \sin\left(\frac{2n\pi t}{T}\right) dt$$

$$= 2 \int_{0}^{1} p(t) \sin(2n\pi t) dt$$

$$= 2 \int_{0}^{1/2} 1 \times \sin(2n\pi t) dt + 2 \int_{1/2}^{1} 0 \times \sin(2n\pi t) dt$$

$$= 2 \int_{0}^{1/2} \sin(2n\pi t) dt$$

$$= \frac{-\cos(2n\pi t)}{n\pi} \Big|_{0}^{1/2}$$

$$= \frac{1 - \cos n\pi}{n\pi}$$
(10.21)

Substituting these values of the Fourier coefficients in Eq. 10.17, we obtain the required Fourier series representation of this waveform, namely

$$f(t) = \frac{1}{2} + \sum_{n=1}^{\infty} \left\{ \frac{1 - \cos n\pi}{n\pi} \right\} \sin(2n\pi)$$

$$= \frac{1}{2} + \frac{2}{\pi} \sin(2n\pi) + 0 + \frac{2}{3\pi} \sin(6n\pi) + 0 \dots$$

$$+ \frac{2}{5\pi} \sin(10n\pi) + 0 \dots$$

$$= \frac{1}{2} + \frac{2}{\pi} \sin(2n\pi) + \frac{2}{3\pi} \sin(6n\pi) + \frac{2}{5\pi} \sin(10n\pi) \dots$$
 (10.22)

To put the series in the more compact form of Eq. 10.12, that is, in terms of the amplitudes M_n and phase angles ϕ_n of the individual harmonics that make up the waveform, we use Eq. 10.12 to find

$$M_n = \sqrt{A_n^2 + B_n^2}$$

$$= B_n \quad \text{since } A_n = 0 \text{ for all } n$$

$$= \left(\frac{1 - \cos n\pi}{n\pi}\right)$$
(10.23)

and

$$\phi_n = \tan^{-1} \left(\frac{B_n}{A_n} \right)$$

$$= \pm \frac{\pi}{2} \quad \text{since } A_n = 0 \text{ for all } n$$
(10.24)

Which of the two values of ϕ is appropriate is determined by satisfying Eq. 10.12, namely

$$B_n = M_n \sin \phi_n \tag{10.25}$$

Since $M_n = B_n$ in this case (Eq. 10.12), this gives $\sin \phi_n = 1$, and therefore

$$\phi_n = \frac{\pi}{2} \quad \text{for all } n \tag{10.26}$$

Substituting these values of M_n and ϕ_n into Eq. 10.15 gives

$$p(t) = A_0 + \sum_{n=0}^{\infty} M_n \cos(2n\pi t - \phi_n)$$

$$= \frac{1}{2} + \sum_{n=0}^{\infty} \left\{ \frac{1 - \cos n\pi}{n\pi} \right\} \cos(2n\pi t - \frac{\pi}{2})$$

$$= \frac{1}{2} + \sum_{n=0}^{\infty} \left\{ \frac{1 - \cos n\pi}{n\pi} \right\} \sin(2n\pi t)$$

$$= \frac{1}{2} + \frac{2}{\pi} \sin(2\pi t) + \frac{2}{3\pi} \sin(6\pi t) + \frac{2}{5\pi} \sin(10\pi t) \dots$$
 (10.27)

which is identical with the result in Eq. 10.22.

Thus, in the present example, because of the very simple form of the wave, the two different forms of Fourier series representation in Eqs. 10.22 and 10.27 are identical. More precisely, the Fourier series representation of this simple waveform consists of only one series (not two as in Eq. 10.17), hence the compact and the noncompact forms of the Fourier representation are the same. Furthermore, we shall find that the determination of the phase angle ϕ is in general more troublesome than it is in the present simple case. The reason for this is that the range of the inverse tangent function used in Eq. 10.12 is limited to the interval $-\pi/2$ to $+\pi/2$ and therefore does not yield all possible angles.

If the harmonics of this waveform are denoted by $f_1(t), f_2(t), f_3(t) \dots$, then the result in Eq. 10.27 can be written as

$$f(t) = \frac{1}{2} + f_1(t) + f_2(t) + f_3(t) \dots$$
 (10.28)

where the individual harmonics are given by

$$\begin{cases} f_1(t) &= \frac{2}{\pi} \sin(2\pi t) \\ f_2(t) &= 0 \\ f_3(t) &= \frac{2}{3\pi} \sin(6\pi t) \\ f_4(t) &= 0 \\ &\vdots \end{cases}$$
 (10.29)

It is seen that the first harmonic has the same period and hence the same frequency as the original wave, namely the fundamental period and fundamental frequency. The second and other even-numbered harmonics are zero in this case. The period of the third harmonic is one third of the fundamental period and hence its frequency is three times the fundamental frequency, etc. The first ten harmonics are shown graphically in Fig. 10.3.

One of the most important pillars of the theory of Fourier analysis is that the *amplitudes* of successive harmonics become successively smaller and hence they make successively smaller contribution to the Fourier representation of the periodic function in hand. This is highly important for practical purposes because the infinite series representing the periodic function can then be truncated at some point without committing large error. This is illustrated graphically in Fig. 10.4, where different Fourier series representations are shown, based on the first one, four, seven, and ten harmonics.

A Fourier series representation based on the first 50 harmonics is shown in Fig. 10.5 where these properties can be observed. We shall see later that a larger number of harmonics does not always produce a more accurate Fourier series representation. Specifically, when the description of a given periodic function is available in only *numerical* form, as in Table 10.1 for the cardiac wave, new complications arise which make the optimum number of harmonics dependent on the number of data points available in the numerical description of the waveform.

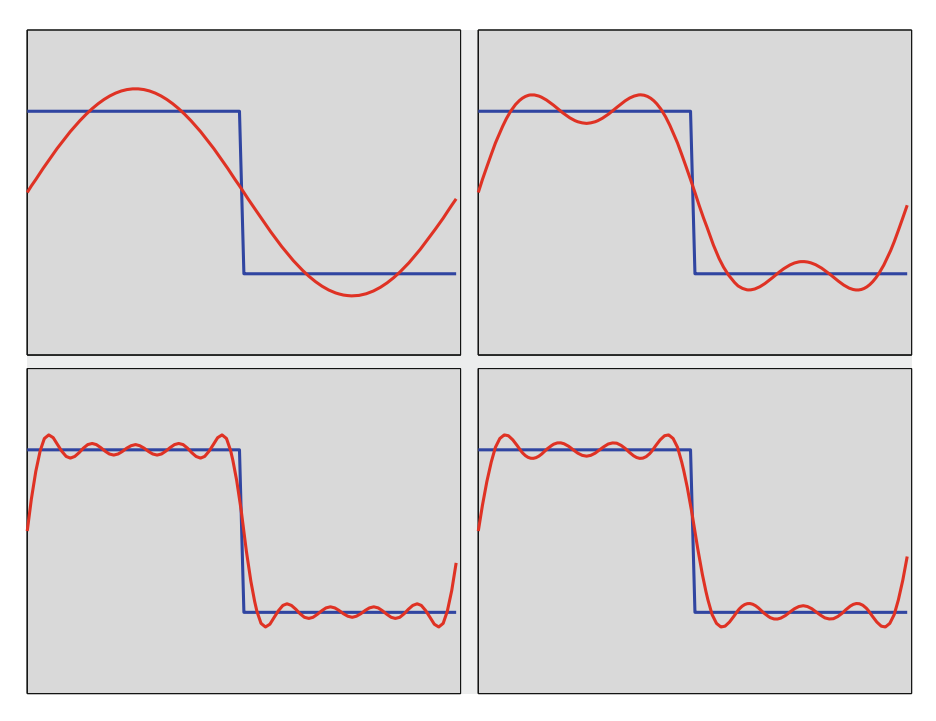


Fig. 10.4 Fourier series representations of the single-step waveform, based on the first one, four, seven, and ten harmonics, clockwise from top left corner.

10.4 Example: Piecewise Waveform

Consider next a "piecewise" waveform consisting of several steps, as shown in Fig. 10.6, and defined by

$$\begin{cases} f(t) &= 4t, \quad 0 \le t < \frac{1}{4} \\ &= 1, \quad \frac{1}{4} \le t < \frac{1}{2} \\ &= \frac{1}{2}, \quad \frac{1}{2} \le t < \frac{3}{4} \\ &= 0, \quad \frac{3}{4} \le t < 1 \end{cases}$$
(10.30)

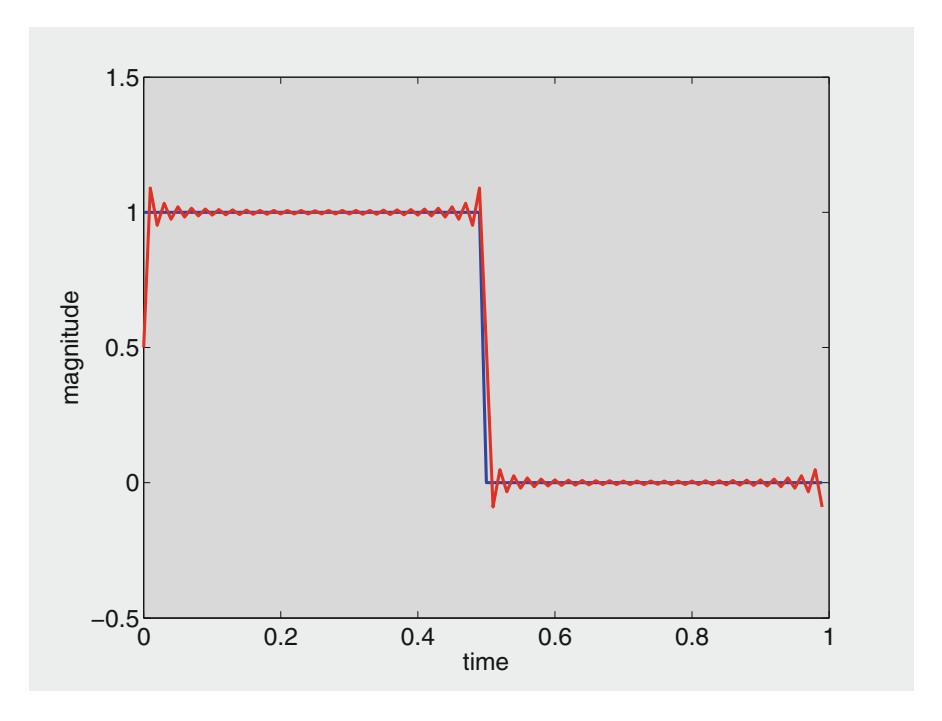


Fig. 10.5 Fourier series representation of the single-step waveform based on the first 50 harmonics.

As in the previous section, the Fourier series representation of this periodic function is given by

$$f(t) = \sum_{n=0}^{\infty} A_n \cos\left(\frac{2n\pi t}{T}\right) + \sum_{n=1}^{\infty} B_n \sin\left(\frac{2n\pi t}{T}\right)$$

$$= A_0 + A_1 \cos\left(\frac{2\pi t}{T}\right) + A_2 \cos\left(\frac{4\pi t}{T}\right) + \dots$$

$$+ B_1 \sin\left(\frac{2\pi t}{T}\right) + B_2 \sin\left(\frac{4\pi t}{T}\right) + \dots$$
(10.31)

and the Fourier coefficients, recalling that T = 1, are given by

$$A_0 = \frac{1}{T} \int_0^T f(t)dt$$
$$= \int_0^1 f(t)dt$$

$$= \int_{0}^{1/4} 4t \times dt + \int_{1/4}^{1/2} 1 \times dt + \int_{1/2}^{3/4} \frac{1}{2} \times dt + \int_{3/4}^{1} 0 \times dt$$

$$= 2t^{2} \Big|_{0}^{1/4} + t \Big|_{1/4}^{1/2} + \frac{1}{2}t \Big|_{1/2}^{3/4} + 0$$

$$= \frac{1}{8} + \frac{1}{4} + \frac{1}{8}$$

$$= \frac{1}{2}$$
(10.32)

Again, we note that by its definition (Eq. 10.6), the coefficient A_0 represents the average value of the periodic function over one period. The result is seen to be correct from the graphical representation of the waveform in Fig. 10.6. For the other Fourier coefficients we have

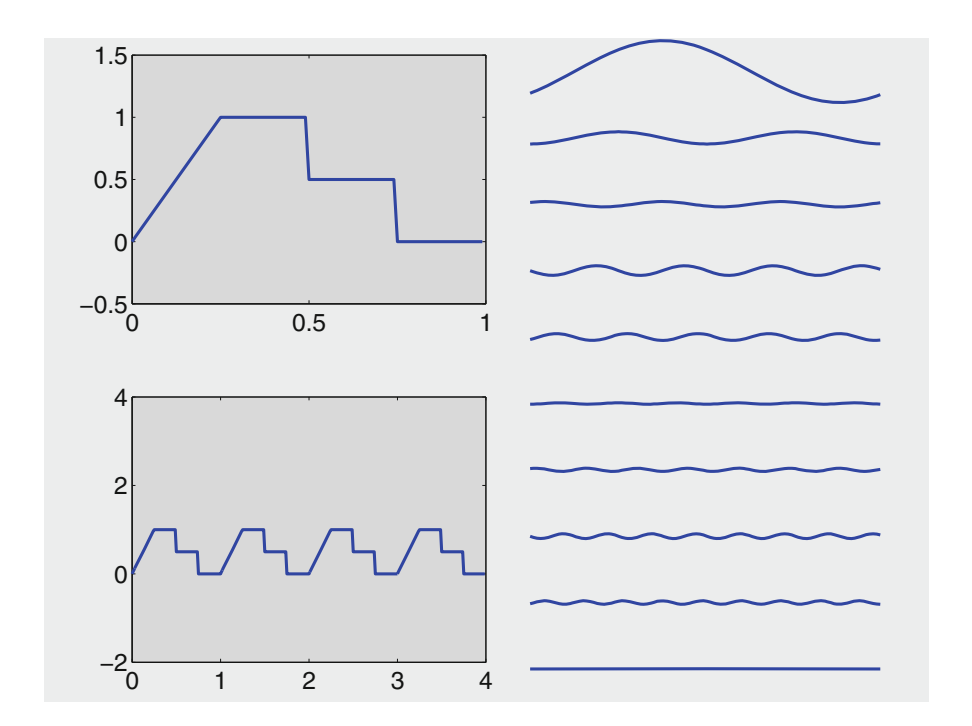


Fig. 10.6 A composite "piecewise" waveform consisting of several steps and having a period T=1 as seen in the *left two panels*. The first ten harmonics of this waveform are shown on the *right*. The series is led by the fundamental harmonic which has the same period and hence the same frequency as the original wave, namely the fundamental period and fundamental frequency. The periods of the second and third harmonics are one half and one third of the fundamental period, respectively, and hence their frequencies are two and three times the fundamental frequency, etc.

$$A_{n} = \frac{2}{T} \int_{0}^{T} p(t) \cos\left(\frac{2n\pi t}{T}\right) dt$$

$$= 2 \int_{0}^{1} p(t) \cos(2n\pi t) dt$$

$$= 2 \int_{0}^{1/4} 4t \cos(2n\pi t) dt + 2 \int_{1/4}^{1/2} \cos(2n\pi t) dt$$

$$+ 2 \int_{1/2}^{3/4} \frac{1}{2} \cos(2n\pi t) dt + \int_{3/4}^{1} 0 \times dt$$

$$= 4 \left\{ \frac{\cos(2n\pi t)}{2(n\pi)^{2}} + \frac{t \sin(2n\pi t)}{n\pi} \right\} \Big|_{0}^{1/4}$$

$$+ \frac{\sin(2n\pi t)}{n\pi} \Big|_{1/4}^{1/2} + \frac{\sin(2n\pi t)}{2n\pi} \Big|_{1/2}^{3/4} + 0$$

$$= \frac{2}{(n\pi)^{2}} \left[\cos\left(\frac{n\pi}{2}\right) - 1 \right] + \frac{1}{2n\pi} \sin\left(\frac{3n\pi}{2}\right)$$
(10.33)

where the first integral above was evaluated using integration by parts and applying the indefinite integral identity^{3,4,5}

$$\int x \cos kx dx = \frac{\cos kx}{k^2} + \frac{x \sin kx}{k}$$
 (10.34)

Similarly

$$B_n = \frac{2}{T} \int_0^T p(t) \sin\left(\frac{2n\pi t}{T}\right) dt$$

$$= 2 \int_0^1 p(t) \sin(2n\pi t) dt$$

$$= 2 \int_0^{1/4} 4t \sin(2n\pi t) dt + 2 \int_{1/4}^{1/2} \sin(2n\pi t) dt$$

³Gradshteyn IS, Ryzhik IM, 1965. Table of Integrals, Series, and Products. Academic Press, New York.

⁴Spiegel MR, 1968. Mathematical Handbook of Formulas and Tables. McGraw-Hill, New York.

⁵Beyer WH, 1978. CRC Handbook of Mathematical Sciences, CRC Press, West Palm Beach, FL.

$$+2\int_{1/2}^{3/4} \frac{1}{2} \sin(2n\pi t) dt + \int_{3/4}^{1} 0 \times dt$$

$$= 4 \left\{ \frac{\sin(2n\pi t)}{2(n\pi)^{2}} - \frac{t \cos(2n\pi t)}{n\pi} \right\} \Big|_{0}^{1/4}$$

$$- \frac{\cos(2n\pi t)}{n\pi} \Big|_{1/4}^{1/2} - \frac{\cos(2n\pi t)}{2n\pi} \Big|_{1/2}^{3/4} + 0$$

$$= \frac{2}{(n\pi)^{2}} \sin\left(\frac{n\pi}{2}\right) - \frac{1}{2n\pi} \cos(n\pi) - \frac{1}{2n\pi} \cos\left(\frac{3n\pi}{2}\right)$$
(10.35)

Here again the first integral was evaluated using integration by parts and applying the indefinite integral identity^{6,7,8}

$$\int x \sin kx dx = \frac{\sin kx}{k^2} - \frac{x \cos kx}{k}$$
 (10.36)

Substitution of these expressions for the Fourier coefficients in Eq. 10.31 makes the resulting expression for the Fourier series rather cumbersome. Instead, numerical values of A_n , B_n , M_n , ϕ_n can be simply tabulated for the required number of harmonics, as shown in Table 10.2.

Values of M_n in Table 10.2 are determined from Eq. 10.12

$$M_n = \sqrt{A_n^2 + B_n^2}$$

However, as mentioned in the previous section, the phase angles ϕ_n must satisfy *both* conditions in Eq. 10.11, namely

$$A_n = M_n \cos \phi_n \tag{10.37}$$

$$B_n = M_n \sin \phi_n \tag{10.38}$$

These two conditions cannot be replaced by the single condition

$$\phi_n = \tan^{-1} \left(\frac{B_n}{A_n} \right) \tag{10.39}$$

⁶Gradshteyn IS, Ryzhik IM, 1965. Table of Integrals, Series, and Products. Academic Press, New York.

⁷Spiegel MR, 1968. Mathematical Handbook of Formulas and Tables. McGraw-Hill, New York.

⁸Beyer WH, 1978. CRC Handbook of Mathematical Sciences, CRC Press, West Palm Beach, FL.

Table 10.2 Numerical					
values of Fourier coefficients					
for the first ten harmonics of					
the piecewise waveform					
shown in Fig. 10.6.					
for the first ten harmonics of the piecewise waveform					

n	A_n	B_n	M_n	ϕ_n (°)
1	-0.36180	0.36180	0.51166	135
2	-0.10132	0.00000	0.10132	180
3	0.03054	0.03054	0.04318	45
4	0.00000	-0.07958	0.07958	-90
5	-0.03994	0.03994	0.05648	135
6	-0.01126	0.00000	0.01126	180
7	0.01860	0.01860	0.02631	45
8	0.00000	-0.03979	0.03979	-90
9	-0.02019	0.02019	0.02855	135
10	-0.004053	0.00000	0.00405	180

because the range of values of the inverse tangent function is limited to the interval $-\pi/2$ to $\pi/2$. For example, using the values of A_1, B_1 from the table, Eq. 10.39 gives

$$\phi_1 = \tan^{-1} \left(\frac{B_1}{A_1} \right) \tag{10.40}$$

$$= \tan^{-1} \left(\frac{0.3618}{-0.3618} \right) \tag{10.41}$$

$$= \tan^{-1}(-1) \tag{10.42}$$

$$=-\frac{\pi}{4}\tag{10.43}$$

This value of ϕ_1 is incorrect because it does not satisfy Eqs. 10.37 and 10.38. Substituting $\phi_1 = -\pi/4$ in these equations gives

$$A_1 = M_1 \cos\left(-\pi/4\right) \tag{10.44}$$

$$= 0.51166 \times 0.7071 \tag{10.45}$$

$$= 0.3618$$
 (10.46)

and

$$B_1 = M_1 \sin\left(-\pi/4\right) \tag{10.47}$$

$$= 0.51166 \times (-0.7071) \tag{10.48}$$

$$=-0.3618$$
 (10.49)

These values of A_1 , B_1 are incorrect, the actual values are $A_1 = -0.3618$, $B_1 = 0.3618$ as indicated in the table. The correct value of ϕ_1 , that is, a value of ϕ_1 which satisfies both of Eqs. 10.37 and 10.38, is actually $3\pi/4$ or 135° as indicated in the

table. This value is obtained by writing A_1, B_1 as the real and imaginary parts of a complex number

$$z_1 = A_1 + iB_1 \tag{10.50}$$

then the correct value of ϕ_1 is obtained as the argument ("arg") of z_1 , that is

$$\phi_1 = \arg(z_1) \tag{10.51}$$

where the function "arg" is the angle of a complex number in the complex plane or Argand diagram, measured in an anticlockwise direction from the real axis and having the range of values $-\pi$ to π , as illustrated in Fig. 10.7. Numerical values of the coefficients A_1, B_1 can now be extracted from Table 10.2 to construct the Fourier series representation of the piecewise waveform in its full form, as in Eq. 10.31, giving

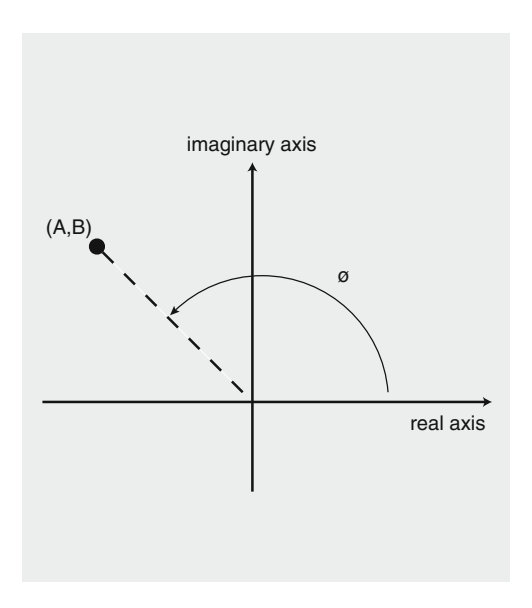


Fig. 10.7 The phase angle ϕ of a harmonic with coefficients A,B is correctly obtained as the argument of the complex number z=A+iB. This angle, $\phi=\arg(z)$, is measured in an anticlockwise direction from the real axis, as shown, and has the range of values $-\pi$ to π . The example shown here is that of the first harmonic of the piecewise waveform for which the values of the coefficients (from Table 10.2) are $A_1=-0.3618$ and $B_1=0.3618$, which are shown in the complex plane above as the coordinates of the complex number z, and which give $\phi=\arg(-0.3618+i\times0.3618)=3\pi/4=135^\circ$ as given in Table 10.2. The inverse tangent function in this case would give an incorrect value, namely $\phi=\tan^{-1}(B/A)=\tan^{-1}(-1)=\pi/4=45^\circ$.

$$f(t) = \sum_{n=0}^{\infty} A_n \cos\left(\frac{2n\pi t}{T}\right) + \sum_{n=1}^{\infty} B_n \sin\left(\frac{2n\pi t}{T}\right)$$

$$= A_0 + A_1 \cos\left(\frac{2\pi t}{T}\right) + A_2 \cos\left(\frac{4\pi t}{T}\right) + \dots$$

$$+ B_1 \sin\left(\frac{2\pi t}{T}\right) + B_2 \sin\left(\frac{4\pi t}{T}\right) + \dots$$

$$= 0.5 - 0.3618 \times \cos(2\pi t) - 0.10132 \times \cos(4\pi t)$$

$$+ 0.030536 \times \cos(6\pi t) + 0.3618 \times \sin(2\pi t)$$

$$+ 0.030536 \times \sin(6\pi t) + \dots$$
(10.52)

Or, numerical values of M_n , ϕ_n can be used from Table 10.2 to put the series in its compact form, as in Eq. 10.10

$$f(t) = A_0 + \sum_{n=0}^{\infty} M_n \cos\left(\frac{2n\pi t}{T} - \phi_n\right)$$

$$= A_0 + M_1 \cos\left(\frac{2\pi t}{T} - \phi_1\right) + M_2 \cos\left(\frac{4\pi t}{T} - \phi_2\right)$$

$$+ M_3 \cos\left(\frac{6\pi t}{T} - \phi_3\right) + \dots$$

$$= 0.5 + 0.51166 \times \cos\left(2\pi t - 135 \times \pi/180\right)$$

$$+ 0.10132 \times \cos\left(4\pi t - 180 \times \pi/180\right)$$

$$+ 0.043184 \times \cos\left(6\pi t - 45 \times \pi/180\right) + \dots$$
(10.53)

As in the previous example, if the harmonics of this waveform are denoted by $f_1(t), f_2(t), f_3(t)$ etc., then the individual harmonics are given by

$$\begin{cases} f_1(t) &= 0.51166 \times \cos(2\pi t - 135 \times \pi/180) \\ f_2(t) &= 0.10132 \times \cos(4\pi t - 180 \times \pi/180) \\ f_3(t) &= 0.043184 \times \cos(6\pi t - 45 \times \pi/180) \\ &\vdots \\ f_{10}(t) &= 0.0040528 \times \cos(20\pi t - 180 \times \pi/180) \end{cases}$$
(10.54)

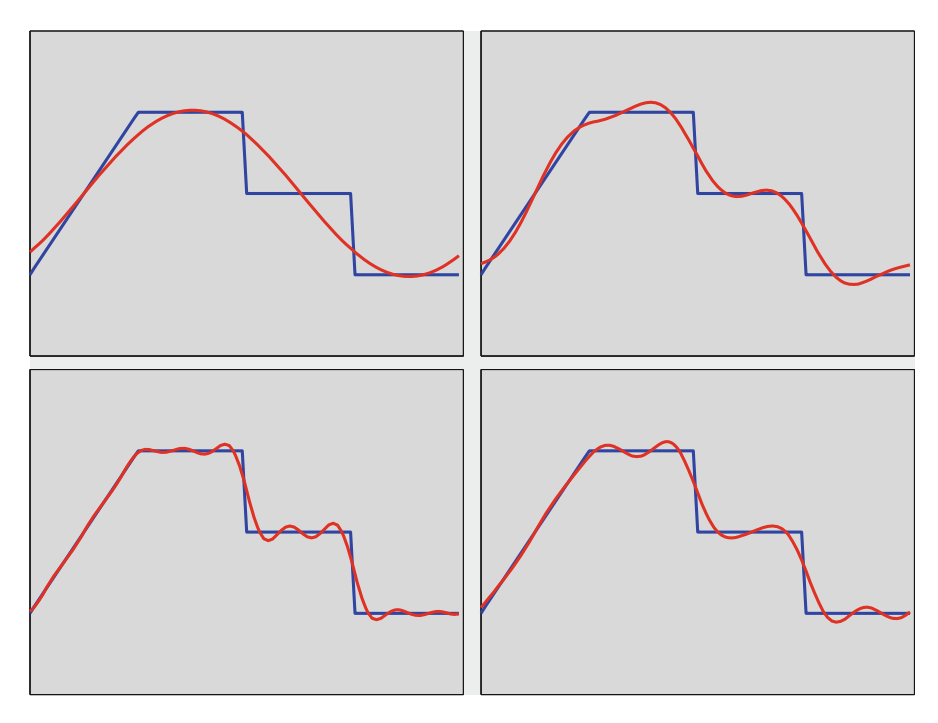


Fig. 10.8 Fourier series representations of the piecewise waveform in Fig. 10.6, based on the first one, four, seven, and ten harmonics, clockwise from top left corner.

Again, it is seen that the first harmonic has the same period and hence the same frequency as the original wave, namely the fundamental period and fundamental frequency. The period of the second harmonic is one half of the fundamental period and hence its frequency is twice the fundamental frequency, etc. The first ten harmonics are shown graphically in Fig. 10.6.

Figure 10.8 shows the accuracy of this Fourier representation of the piecewise waveform when only the first one, four, seven, and ten harmonics are used.

A Fourier representation with the first 50 harmonics is shown in Fig. 10.9.

10.5 Numerical Formulation

The waveforms considered in the previous two sections were rather artificially constructed in order to illustrate the basic concepts of Fourier analysis and the basic steps involved in its application to specific waveforms. In the context of pulsatile blood flow, however, the specific waveforms of interest are those of the pressure and flow waveforms generated by the pumping action of the left ventricle, as in the example shown in Fig. 10.2. One important feature of this waveform which is

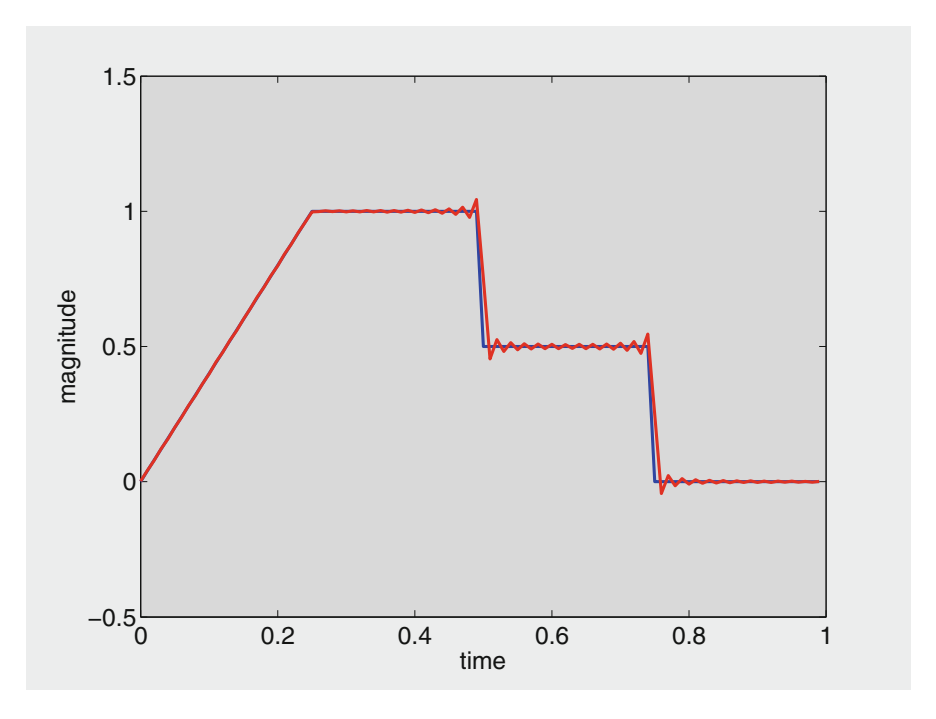


Fig. 10.9 Fourier series representation of the piecewise waveform in Fig. 10.9, based on the first 50 harmonics.

not shared by the examples of the previous two sections is that it cannot be presented in *analytical* form.

As stated in the introduction to this chapter, a composite pressure waveform of the type shown in Fig. 10.2 is generally available only in *numerical* form, that is as a set of points, tabulated as in Table 10.1 or presented graphically as in Fig. 10.2. This is the most natural way in which the waveform would present itself in practice where the set of points would come from pressure or flow measurements at some accessible point within the system and at small time intervals during the oscillatory cycle as shown in Table 10.1.

The aim of the present section is to present a numerical formulation of Fourier analysis, that is to show how a set of points such as this would be used in the process of Fourier analysis to produce the Fourier series representation of the waveform. Once this representation has been achieved, the waveform becomes like any other waveform, expressed in terms of a series of sine and cosine functions, or in terms of its harmonics as in the examples of the previous sections. Indeed, the data in Table 10.1 may be regarded as a *periodic function* like any other we have considered so far, the only difference here is that the function is presented in numerical form rather than analytically. Each pair of values (f, t) in the table represents one point in Fig. 10.2, and the entire set of values in the table produce the waveform shown in the figure.

Let the number of points available be denoted by N, which is not to be confused with n which we shall continue to use for the number of harmonics. The Fourier analysis process is considerably easier, of course, when the points are spaced at regular intervals of time within the oscillatory cycle, and we shall proceed on that basis. In fact, if the original set points are not equally spaced in time, it would be best first to place them on a "best-fit" curve and then extract a new set of points from that curve at regular time intervals.

If the period of the waveform at hand is denoted by T, and the time interval between successive data points is denoted by Δt , then

$$\Delta t = \frac{T}{N} \tag{10.55}$$

In Table 10.1 the period has been normalized to T = 1.0 and the number of points N = 40, therefore $\Delta t = 1/40 = 0.025$ as noted from successive points in the table. If the time at the beginning of the oscillatory cycle is set at t = 0, and if this and subsequent points in time are denoted by t_0 , t_1 , t_3 etc., then these points are given by

$$\begin{cases} t_0 = 0 \\ t_1 = 1 \times \Delta t \\ t_2 = 2 \times \Delta t \\ t_3 = 3 \times \Delta t \end{cases}$$

$$\vdots$$

$$t_{N-1} = (N-1) \times \Delta t$$

$$\vdots$$

Note that there are a total of N points in time within one oscillatory cycle. If the corresponding values of f(t) are denoted similarly by f_0, f_1, f_2 etc., then

$$\begin{cases}
f_0 = f(t_0) \\
f_1 = f(t_1) \\
f_2 = f(t_2) \\
f_3 = f(t_3) \\
\vdots \\
f_{N-1} = f(t_{N-1})
\end{cases} (10.57)$$

The general form of the Fourier series representation of the composite waveform in Fig. 10.2 is the same as that in the previous two sections (Eq. 10.17), namely

$$f(t) = \sum_{n=0}^{\infty} A_n \cos\left(\frac{2n\pi t}{T}\right) + \sum_{n=1}^{\infty} B_n \sin\left(\frac{2n\pi t}{T}\right)$$
$$= A_0 + A_1 \cos\left(\frac{2\pi t}{T}\right) + A_2 \cos\left(\frac{4\pi t}{T}\right) + \dots$$
$$+ B_1 \sin\left(\frac{2\pi t}{T}\right) + B_2 \sin\left(\frac{4\pi t}{T}\right) + \dots$$

but the Fourier coefficients A_n , B_n in the present case cannot be evaluated by means of integrals as before, because the periodic function f(t) is not available in *analytical* form. But the function is available in *numerical* form, as in Table 10.1, therefore the required integrals can be formulated and evaluated numerically in a fairly straightforward manner as described below.

If each of the N points describing the periodic function f(t) is associated with one time interval Δt , then the N points together cover the entire period T. In the simplest numerical formulation, the value of the function f(t) at t_0 , namely f_0 , is taken to remain constant over the small time interval Δt associated with t_0 , then the value of f(t) at t_1 , namely f_1 , is taken to remain constant over the next time interval, etc., with the result that the periodic function f(t) is presented graphically as shown in Fig. 10.10. This graphical presentation provides the basis for the numerical formulation and evaluation of the Fourier coefficients A_n , B_n .

Briefly, each of the integrals required in the evaluation of the coefficients is reformulated as a *sum*, using standard methods of numerical integration⁹. Thus, for A_0 we have (Eq. 10.6)

$$A_0 = \frac{1}{T} \int_0^T p(t)dt$$
 (10.58)

The integral on the right represents the area under the curve of f(t) in Fig. 10.10 over one period. A standard approximation of this area is the sum of the areas of the N long thin rectangles of width Δt rising from the t axis to the curve. This makes it possible to write

$$A_{0} \approx \frac{1}{T} \{ f_{0} \Delta t + f_{1} \Delta t + f_{2} \Delta t \dots f_{N-1} \Delta t \}$$

$$\approx \frac{1}{N} \{ f_{0} + f_{1} + f_{2} + \dots + f_{N-1} \}$$

$$\approx \frac{1}{N} \sum_{k=0}^{N-1} f_{k}$$
(10.59)

⁹Kreyszig E, 1983. Advanced Engineering Mathematics. Wiley, New York.

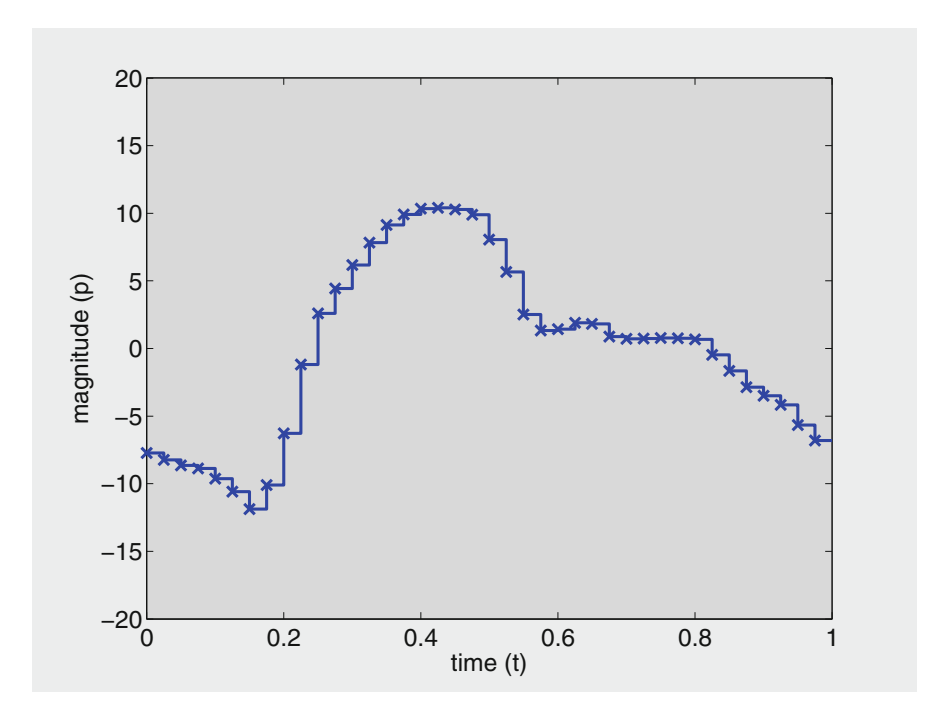


Fig. 10.10 Graphical presentation of the periodic function p(t), when the description of the function is available only *numerically*. The data points shown are based on the data in Table 10.1 for the composite waveform in Fig. 10.1. In a numerical formulation of Fourier analysis, each data point is associated with the small time interval Δt between it and the next data point, and over each such Δt the value of p is taken to remain constant as shown in the figure. This allows the numerical formulation and evaluation of the Fourier coefficients A_n , B_n as described in the text.

having used Eq. 10.55 in the process. The degree of approximation clearly depends on the number of data points available for representing the function f(t) or, equivalently, on the size of the time interval Δt relative to the period T.

Numerical expressions for A_n and B_n are obtained in the same way, although the integrals in this case involve the product of f(t) and a sine or cosine function and therefore do not represent simply the area under the f(t) curve. Nevertheless, using the integral expressions for these coefficients from Eq. 10.6 and converting the integrals involved into sums as for A_0 , we find

$$A_n = \frac{2}{T} \int_0^T f(t) \cos\left(\frac{2n\pi t}{T}\right) dt$$

$$\approx \frac{2}{T} \left\{ f_0 \cos\left(\frac{2n\pi t_0}{T}\right) \Delta t + f_1 \cos\left(\frac{2n\pi t_1}{T}\right) \Delta t + \dots + f_{N-1} \cos\left(\frac{2n\pi t_{N-1}}{T}\right) \Delta t \right\}$$

$$\approx \frac{2}{N} \left\{ f_0 \cos\left(\frac{2n\pi t_0}{T}\right) + f_1 \cos\left(\frac{2n\pi t_1}{T}\right) + \dots + f_{N-1} \cos\left(\frac{2n\pi t_{N-1}}{T}\right) \right\}$$

$$\approx \frac{2}{N} \sum_{k=0}^{N-1} f_k \cos\left(\frac{2n\pi t_k}{T}\right)$$
(10.60)

and similarly

$$B_{n} = \frac{2}{T} \int_{0}^{T} f(t) \sin\left(\frac{2n\pi t}{T}\right) dt$$

$$\approx \frac{2}{T} \left\{ f_{0} \sin\left(\frac{2n\pi t_{0}}{T}\right) \Delta t + f_{1} \sin\left(\frac{2n\pi t_{1}}{T}\right) \Delta t + \dots + f_{N-1} \sin\left(\frac{2n\pi t_{N-1}}{T}\right) \Delta t \right\}$$

$$\approx \frac{2}{N} \left\{ f_{0} \sin\left(\frac{2n\pi t_{0}}{T}\right) + f_{1} \sin\left(\frac{2n\pi t_{1}}{T}\right) + \dots + f_{N-1} \sin\left(\frac{2n\pi t_{N-1}}{T}\right) \right\}$$

$$\approx \frac{2}{N} \sum_{k=0}^{N-1} f_{k} \sin\left(\frac{2n\pi t_{k}}{T}\right)$$

$$(10.61)$$

These expressions are valid generally for any periodic function f(t) for which a numerical description is available in terms of N data points as in Table 10.1. The expressions are used specifically for that case in the next section.

10.6 Example: "Cardiac" Waveform

It is important to emphasize at the outset that the term "Cardiac" is being used here in an entirely generic manner. It should not be taken to imply that there is a *unique* pressure or flow waveform generated by the heart. The pressure or flow waveform generated by the heart is not only different from one heart to the next, but is highly variable from beat to beat within the same heart. It is also highly dependent on the prevailing physiological conditions both in health and in disease. Thus, the cardiac

waveform to be considered in the present section and based on the data in Table 10.1 is only an example that has the general characteristics of a cardiac waveform and that is being used here merely to illustrate how a composite pressure or flow wave of this form is dealt with by the method of Fourier analysis. In this respect, the discussion to follow can be applied in the same way to any other composite pressure or flow waveform. All is required is a set of data that define the particular waveform at hand, as the data in Table 10.1.

Using the numerical formulation of the previous section and the numerical data in Table 10.1 for the cardiac waveform shown in Fig. 10.1, we are now in a position to apply the numerical formulation of Fourier analysis to this wave and to find its harmonics. Essentially, the analysis is the same as for other waves except for the evaluation of the Fourier coefficients A_n , B_n , which in this case must be done numerically.

For A_0 , using Eq. 10.59 and values from Table 10.1, we find

$$A_0 \approx \frac{1}{N} \{ f_0 + f_1 + f_2 + \dots + f_{N-1} \}$$

$$\approx \frac{1}{40} \{ -7.7183 - 8.2383 - 8.6444 + \dots - 6.8024 \}$$

$$\approx 0.00000475$$

$$\approx 0$$
(10.62)

We recall from previous examples that A_0 represents the average value of the periodic function f(t) over one complete period. Thus, the fact that this average value is zero in this case indicates that the waveform in Fig. 10.2 represents only the *oscillatory* part of the cardiac wave, any constant part has been removed. It is always possible, and in fact desirable, to remove any constant average from a waveform before applying Fourier analysis to it because the analysis is concerned with only the oscillatory part. This principle is illustrated graphically in Fig. 10.11.

For the other Fourier coefficients, using Eq. 10.60 and the data in Table 10.1, and noting that the number of data points N = 40 and the period T = 1.0, we find

$$A_{n} \approx \frac{2}{N} \left\{ f_{0} \cos \left(\frac{2n\pi t_{0}}{T} \right) + f_{1} \cos \left(\frac{2n\pi t_{1}}{T} \right) + \dots + f_{N-1} \cos \left(\frac{2n\pi t_{N-1}}{T} \right) \right\}$$

$$\approx \frac{1}{20} \left\{ -7.7183 \times \cos \left(2n\pi \times 0 \right) -8.2383 \times \cos \left(2n\pi \times 0.025 \right) + \dots -6.8024 \times \cos \left(2n\pi \times 0.975 \right) \right\}$$
(10.63)

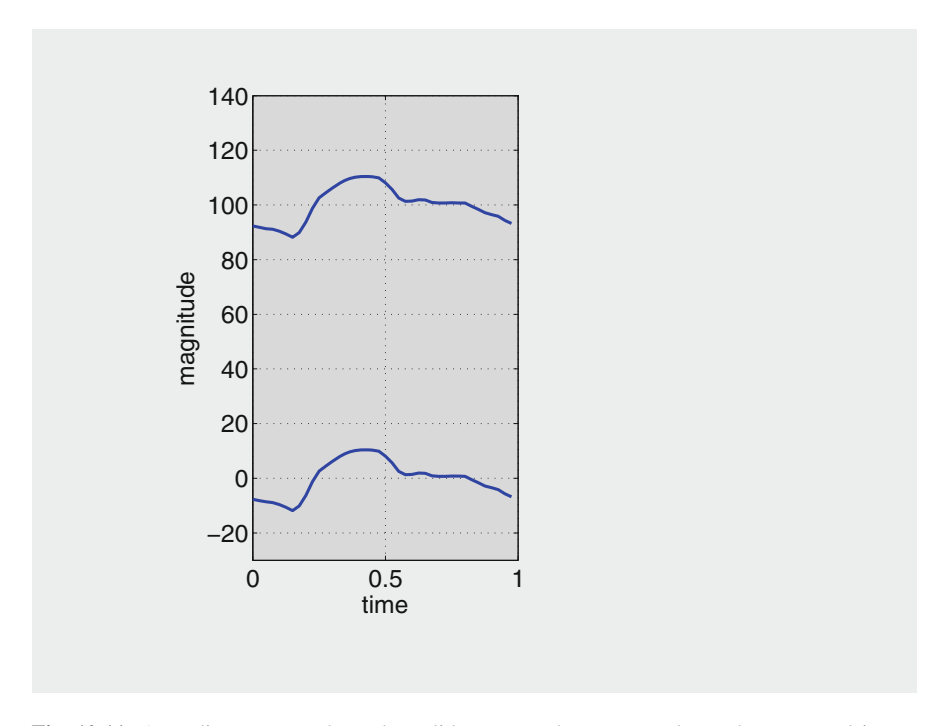


Fig. 10.11 A cardiac wave such as the solid curve at the top can always be separated into a constant part and a purely oscillatory part. The purely oscillatory part is shown at the bottom and it has the property that its average over one period is zero. In Fourier analysis the constant part of the wave is represented by A_0 , thus the result $A_0 = 0$ in Eq. 10.62 indicates that the data on which the result is based represents only the oscillatory part of the waveform, any constant part has been removed.

Similarly, using Eq. 10.61 and the data in Table 10.1, and noting that the number of data points N = 40 and the period T = 1.0, we find

$$B_{n} \approx \frac{2}{N} \left\{ f_{0} \sin\left(\frac{2n\pi t_{0}}{T}\right) + f_{1} \sin\left(\frac{2n\pi t_{1}}{T}\right) + \dots + f_{N-1} \sin\left(\frac{2n\pi t_{N-1}}{T}\right) \right\}$$

$$\approx \frac{1}{20} \left\{ -7.7183 \times \sin(2n\pi \times 0) - 8.2383 \times \sin(2n\pi \times 0.025) + \dots - 6.8024 \times \sin(2n\pi \times 0.975) \right\}$$
(10.64)

Table 10.3 Values of the Fourier coefficients for the cardiac wave shown in Fig. 10.11, using Eqs. 10.60 and 10.61 with n = 1, 2...10.

n	A_n	B_n	M_n	ϕ_n (°)
1	-7.98840	0.15707	7.99000	178.8736
2	-0.42846	-4.41890	4.43960	-95.5381
3	0.88370	0.46246	0.99740	27.6238
4	0.68508	0.28468	0.74187	22.5649
5	-0.35969	0.87460	0.94567	112.3553
6	-0.30961	-0.28316	0.41956	-137.5548
7	-0.53143	-0.20924	0.57114	-158.5089
8	0.26366	-0.15171	0.30419	-29.9153
9	0.02955	0.06432	0.07078	65.3256
10	0.04842	0.16564	0.17258	73.7050

We recall that values of n in these expressions refer to different harmonics. Thus, evaluating these for the first ten harmonics (n = 1, 2, ..., 10), the results are shown numerically in Table 10.3.

With the values of M_n and ϕ_n in Table 10.3, the Fourier representation of this waveform can be put in the more compact form of Eqs. 10.10 and 10.15, namely

$$f(t) = A_0 + \sum_{n=0}^{\infty} M_n \cos\left(\frac{2n\pi t}{T} - \phi_n\right)$$

$$= A_0 + M_1 \cos\left(\frac{2\pi t}{T} - \phi_1\right) + M_2 \cos\left(\frac{4\pi t}{T} - \phi_2\right)$$

$$+ M_3 \cos\left(\frac{6\pi t}{T} - \phi_3\right) + \dots$$
(10.65)

with the individual harmonics given by

$$f_{1}(t) = M_{1} \cos\left(\frac{2\pi t}{T} - \phi_{1}\right)$$

$$\approx 7.99 \times \cos\left(2\pi t - \frac{178.8736 \times \pi}{180}\right)$$

$$f_{2}(t) = M_{2} \cos\left(\frac{4\pi t}{T} - \phi_{2}\right)$$

$$\approx 4.4396 \times \cos\left(4\pi t - \frac{-95.5381 \times \pi}{180}\right)$$
(10.67)

:

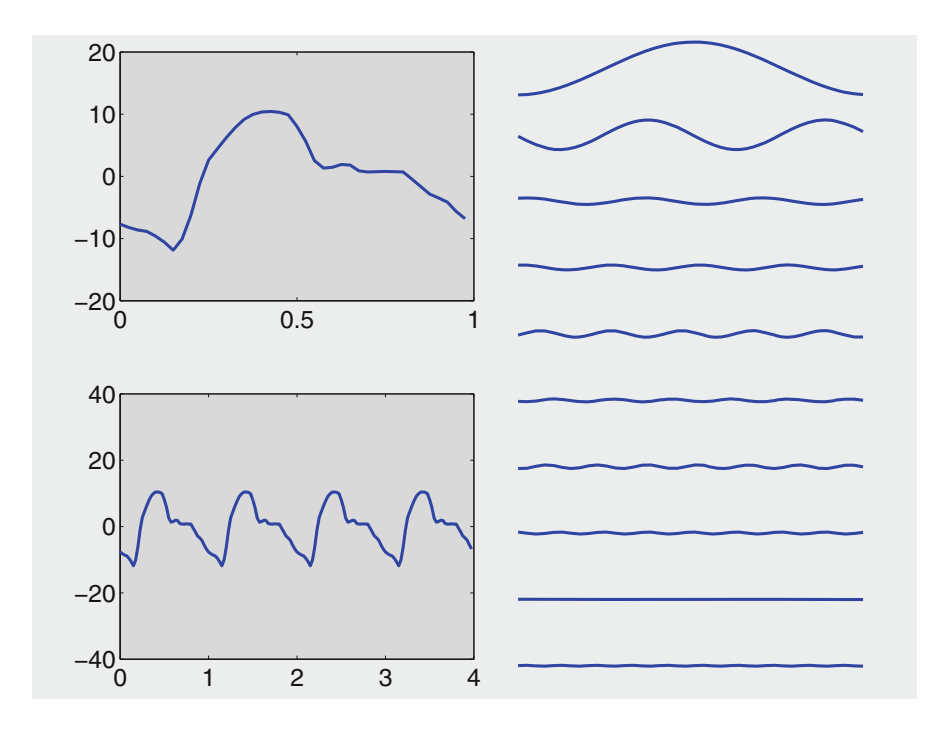


Fig. 10.12 The cardiac waveform of Fig. 10.1 with its first ten harmonics, using the results in Eqs. 10.65-10.68.

$$f_{10}(t) = M_{10} \cos\left(\frac{20\pi t}{T} - \phi_{10}\right)$$

$$\approx 0.17258 \times \cos\left(20\pi t - \frac{73.705 \times \pi}{180}\right)$$
(10.68)

These results are illustrated in Fig. 10.12 where the cardiac waveform and its first ten harmonics are shown.

Figure 10.13 shows the accuracy of this Fourier representation of the cardiac waveform when only the first one, four, seven, and ten harmonics are used. It is seen that the representation is fairly accurate with only the first seven harmonics. By contrast, Fourier representations of the single-step and the piecewise waveforms considered in the previous sections were less accurate with as many as fifty harmonics. The reason for this can be seen clearly in Fig. 10.5. The presence of *step changes* in those cases, and the behaviour of the Fourier curves in the vicinity of these steps, shows that Fourier series have difficulty replicating step changes. The

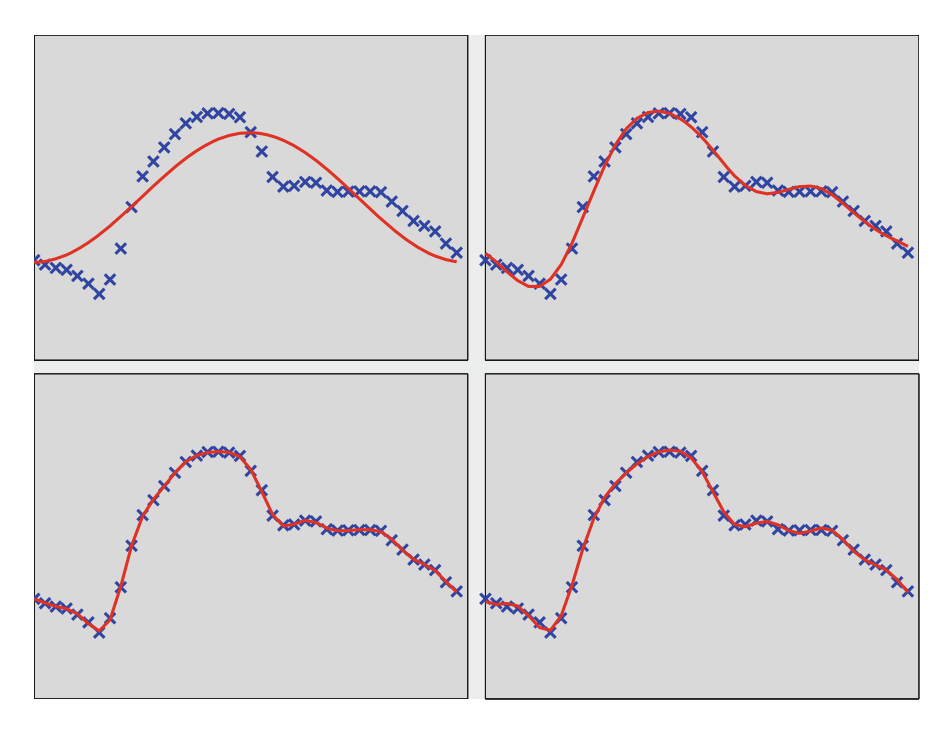


Fig. 10.13 Fourier series representations of the cardiac waveform, based on the first one, four, seven, and ten harmonics, clockwise from top left corner.

cardiac waveform does not contain such changes, thus higher accuracy is achieved with a relatively small number of harmonics.

In fact, as mentioned earlier, when the waveform to be represented by a Fourier series is available only in numerical form, the number of harmonics that produces the most accurate representation becomes dependent on the number of data points available in the numerical description of the waveform. Broadly speaking, the theory of Fourier analysis has shown that if the number of data points available is N, then the number of harmonics that produces the most accurate representation (Nyquist rule) is N/2. A smaller or a larger number of harmonics produce a less accurate representation, for different reasons. This is an oversimplification of the underlying theory, but it provides a useful guide, indeed a necessary guide, for practical application of Fourier analysis to specific waveforms.

¹⁰Brigham EO, 1988. The Fast Fourier Transform and its Applications. Prentice Hall, Englewood Cliffs, NJ.

¹¹Walker JS, 1988. Fourier Analysis. Oxford University Press, New York.

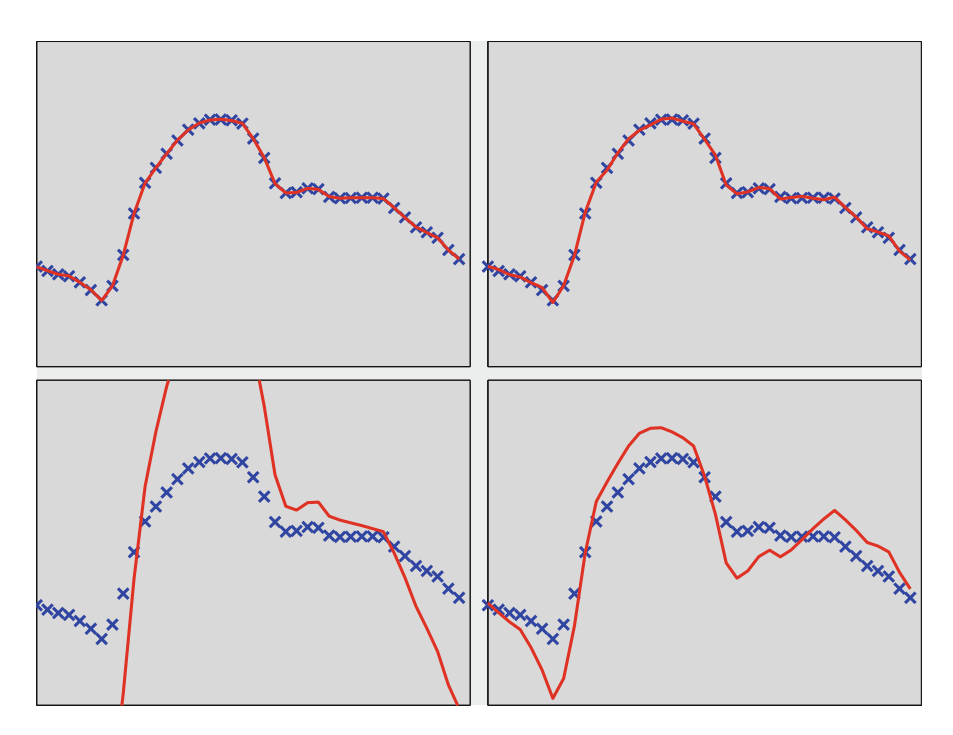


Fig. 10.14 Fourier series representation of the cardiac waveform, based on the first 20, 30, 38, and 45 harmonics, clockwise from top left corner.

For the cardiac waveform being considered in this section, the number of data points in the numerical description of the wave (Table 10.1) is 40, thus the number of harmonics required to produce the most accurate representation is 20. However, it turns out that this maximum accuracy is reached along a fairly shallow (not sharp) peak, thus the optimum number of harmonics need not be treated precisely. In other words, 19 or 21 harmonics will not produce significant differences. In fact, as seen in Fig. 10.13, both seven and ten harmonics produce fairly accurate representations, and the difference between them is barely detectable. A Fourier representation with precisely 20 harmonics is shown in Fig. 10.14, compared with representations using 30, 38, and 45 harmonics. It is seen that only in the latter two cases the representation breaks down.

Chapter 11 Dynamics of Pulsatile Blood Flow III

11.1 Introduction

In this chapter we use the tools developed in previous chapters to put together a model of pulsatile blood flow that includes the key elements of the blood flow system. Specifically, in what follows we consider a system consisting of a "resistive path" and a "capacitive chamber" in parallel, these terms being used in the way that they were defined and used in Chap. 9. Flow through the system shall be considered to be driven by a "cardiac" waveform, again, this term being used in a generic manner as in Sect. 10.6.

We recall that the principal difference between the two elements of the pulsatile blood flow system is that flow through the resistive path has a net throughput while flow through the capacitive chamber has zero throughput. Another important difference between the two is that the energy spent on driving the flow through the resistive path is totally dissipated (lost) while the energy spent on driving the flow through the capacitive chamber is largely recovered.

We recall further that the flows through the resistive path and the capacitive chamber are not to be confused with "steady" and "oscillatory flow", as explained in Sect. 9.3. There is in fact some oscillatory flow through the resistive path as explained in that section. The ultimate utility of the capacitive chamber is to reduce this oscillatory flow through the resistive path to a minimum and thereby reduce energy dissipation to a minimum.

Opposition to flow through the resistive path is caused by the shear force between the fluid and the vessel wall and is represented by what is commonly referred to as the "resistance" *R*. Opposition to flow within the capacitive chamber is caused by fluid inertia, elastic compliance of the vessel wall, and viscous resistance to stretch within the wall material, represented by what is commonly referred to as the

"inertance" L, the "compliance" (or "capacitance") C, and the "viscoelasticity" K. These three components are in series with each other, and together they constitute the "impedance" Z_b to oscillatory flow within the capacitive chamber, using the notation of Sect. 9.9. The combination of this impedance and the resistance to flow along the resistive path, in parallel, constitute the total impedance Z of the entire system. These basic elements and their arrangement provide the most elementary model of pulsatile blood flow in that it includes all the necessary ingredients that characterize the flow not only in the systemic circulation but any sub-circulation thereof.

The effects of wave reflections, which as discussed in Chap. 6 are an inseparable feature of pulsatile blood flow, may seem to be missing from the above picture. However, they are actually embedded within the concept of "effective impedance" discussed in Sect. 6.6. Briefly, the primary effect of wave reflections in a vascular system is a change in the pressure distribution within the system which in turn leads to a change in the impedance of the system. The change is both in terms of the distribution of local impedance within the system and in terms of the global impedance of the system as a whole.

In what follows the above model is used to illustrate some of the salient features of pulsatile blood flow. The emphasis shall be on using the analytical methods and basic understanding developed in previous chapters. This is not only to provide continuity with previous chapters but, more importantly, to provide a self-contained analytical basis of the results to follow. As mentioned previously, while these results can now be obtained by ready made FFT routines in standard mathematical software packages, the focus in this book is on the analytical basis of these routines.

11.2 Composite Pressure-Flow Relations

The relation between pressure and flow is at the very core of hemodynamics. Indeed, it is the central issue in the dynamics of pulsatile blood flow and has been the subject of much of this book so far. However, in previous sections the relation between pressure and flow was examined under restricted conditions in which the driving pressure was of a particularly simple form, namely that of a single harmonic (sine or cosine), or the opposition to flow was of a particularly simple form, consisting of only some elements of the resistive path and the capacitive chamber. In the present chapter the aim is to examine the relation between pressure and flow when the driving pressure has a composite waveform and the opposition to flow includes all the elements of the resistive path and the capacitive chamber.

In previous sections we have seen that when the driving pressure P(t) is in the form of a single harmonic (sine, cosine, or complex exponential), the corresponding flow Q(t) is of the same form, so that we can write as we did in previous sections

$$\begin{cases} P(t) = P_0 e^{i\omega t} \\ Q(t) = Q_0 e^{i\omega t} \end{cases}$$
 (11.1)

Again, for simpler notation in this and subsequent sections we continue to denote the driving pressure as P(t) instead of $\Delta p(t)$ which was done in earlier sections.

When the form of the driving pressure is *not* a single harmonic, however, the relation between pressure and flow in Eq. 11.1 no longer applies. In particular, if the driving pressure is in the form of a composite cardiac wave, the corresponding flow wave will also be in the form of a composite wave but in general not the same composite wave as the pressure. What then is the relation between P(t) and Q(t) in this case? In other words, if P(t) is in the form of a general function of time f(t), then

$$\begin{cases} P(t) = f(t) \\ Q(t) = ? \end{cases}$$
 (11.2)

Of course, the particular case of interest here is that in which f(t) is a periodic function of time as discussed in Chap. 10. In that case, since the function can be decomposed into the sum of individual harmonics, each of which can be expressed as a complex exponential function, then Eq. 11.1 dictates that for each harmonic of the pressure waveform there will be a corresponding harmonic of the flow waveform. Thus, if the harmonics of the pressure are denoted by $p_1(t)$, $p_2(t)$, etc., and the corresponding harmonics of the flow waveform are denoted by $q_1(t)$, $q_2(t)$, etc., then using Eq. 11.1 we have

$$\begin{cases} p_{1}(t) = p_{10}e^{i\omega t} \\ q_{1}(t) = q_{10}e^{i\omega t} \end{cases}$$

$$\begin{cases} p_{2}(t) = p_{20}e^{i\omega t} \\ q_{2}(t) = q_{20}e^{i\omega t} \end{cases}$$
(11.4)

$$\begin{cases} p_2(t) = p_{20}e^{i\omega t} \\ q_2(t) = q_{20}e^{i\omega t} \end{cases}$$
 (11.4)

etc., where the subscript '0' is being used to denote amplitude as in Eq. 11.1. Based on these relations, the answer to the question posed in Eq. 11.2 is then

$$\begin{cases}
P(t) = p_1(t) + p_2(t) + \cdots \\
Q(t) = q_1(t) + q_2(t) + \cdots
\end{cases}$$
(11.5)

This is the basis of the relation between pressure and flow in pulsatile blood flow. We shall see that of particular interest is the *shape* of the flow waveform compared with that of the pressure waveform. The reason for this is that the relation between each pair of harmonics p, q depends on the prevailing impedance which in turn depends on the properties of the resistive path and capacitive chamber as well as on the frequency of that particular pair of harmonics as we saw in previous sections and as we shall see in more detail in the remainder of this chapter.

Thus the relation between pressure and flow in pulsatile blood flow is a powerful diagnostic tool not unlike that of the relation between the input and output associated with a black box. Indeed, a vascular bed consisting of many millions of vessel segments is not unlike a black box because its properties are practically inaccessible. The relation between pressure and flow within that bed provides a window onto these properties.

11.3 Baseline Example: Pure Resistance

In the hypothetical case where the opposition to flow in pulsatile blood flow consists of only pure resistance *R*, there is a singular relation between the pressure and flow waveforms which provides an important "baseline" case with which all other cases can be compared. In this section we illustrate this important case, using the cardiac pressure waveform in Table 11.1 and shown in Fig. 11.1.

To obtain the corresponding flow waveform, using the scheme outlined in the previous section, the pressure waveform is decomposed into its harmonics as outlined in Chap. 10, noting in this case that the pressure wave contains the mean as well as the oscillatory part. The results for the first ten harmonics are shown numerically in Table 11.2.

Since the only opposition to flow in this case is the resistance R, then the relation between pressure and flow harmonics is a particularly simple one (Eq. 9.89), namely

$$q_n(t) = \frac{p_n(t)}{R}$$
 $n = 1, 2, ..., 10$ (11.6)

Table 11.1 A numerical description of the cardiac wave shown in Fig. 11.1, giving the pressure (*P*) at different times *t* within the oscillatory cycle. The oscillatory period has been normalized to 1.0. The pressure data include both the mean and the oscillatory part of the pressure.

t	P	t	P
0.000	96.60	0.500	111.00
0.025	96.21	0.525	108.15
0.050	97.27	0.550	103.65
0.075	95.56	0.575	103.00
0.100	95.34	0.600	103.00
0.125	95.38	0.625	103.00
0.150	93.46	0.650	102.00
0.175	91.92	0.675	101.53
0.200	93.88	0.700	101.00
0.225	100.04	0.725	100.26
0.250	104.50	0.750	101.00
0.275	106.68	0.775	101.00
0.300	108.20	0.800	101.00
0.325	110.00	0.825	102.00
0.350	110.95	0.850	102.00
0.375	112.38	0.875	101.13
0.400	113.80	0.900	100.70
0.425	113.00	0.925	99.86
0.450	113.00	0.950	99.47
0.475	112.93	0.975	98.18

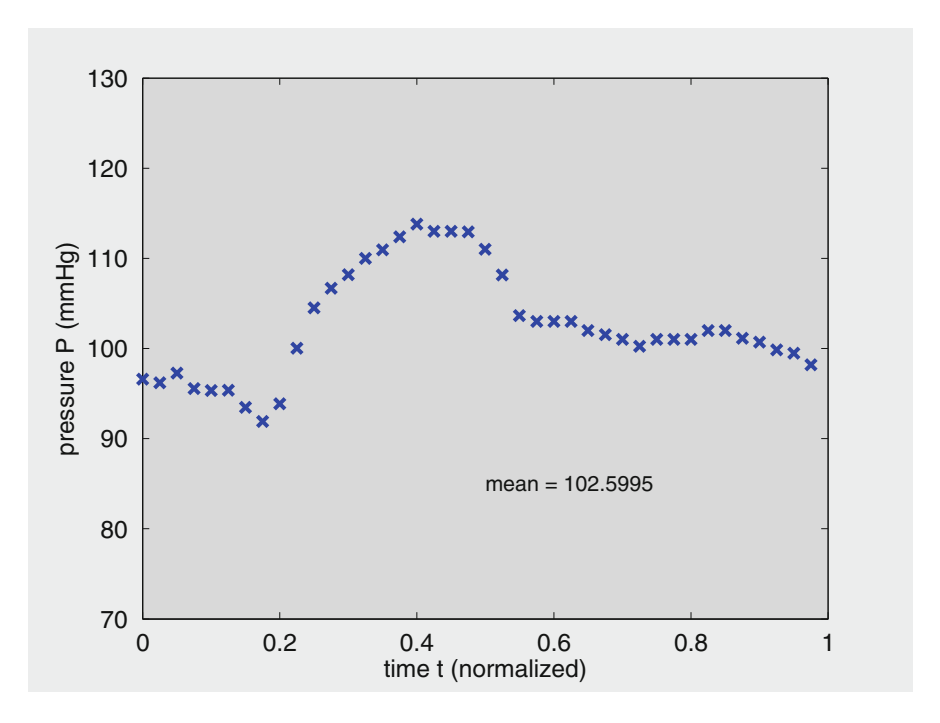


Fig. 11.1 A "cardiac" pressure wave used as an example to illustrate how the corresponding flow wave is obtained from the given pressure waveform.

Table 11.2 Fourier coefficients of the first ten harmonics of the pressure wave in Fig. 11.1.

n	A_n	B_n	M_n	φ _n (°)
1	-6.5901	0.94298	6.65720	171.8568
2	1.08200	-4.66400	4.78780	-76.9394
3	0.74761	0.62007	0.97129	39.6723
4	0.15931	0.39243	0.42353	67.9050
5	-0.77719	0.93475	1.21560	129.7415
6	-0.28180	-0.56377	0.63028	-116.5580
7	-0.19808	-0.38691	0.43467	-117.1109
8	0.55090	-0.07722	0.55628	-7.9796
9	-0.23510	0.22975	0.32872	135.6601
10	-0.13825	0.18000	0.22696	127.5263

For the purpose of the present section, to illustrate the numerical analysis involved, we now pursue this example with an estimate of the resistance R in the human systemic circulation in order to produce typical values of pressure and flow as they occur in this system, with the emphasis being on the numerical relations involved rather than on the numerical values.

In the human systemic circulation, taking a cardiac output of 5 L/min and a mean arterial pressure of 100 mmHg, an estimate of total resistance would be

$$R = \frac{100 \text{ mmHg}}{5 \text{ L/min}}$$

$$= 20 \left\lceil \frac{\text{mmHg}}{\text{L/min}} \right\rceil$$
(11.7)

Using this value of R in Eq. 11.6, and using the compact form (Eq. 10.10) of the first ten harmonics of the pressure wave, namely

$$p_n(t) = M_n \cos\left(\frac{2\pi nt}{T} - \phi_n\right) \quad n = 1, 2, \dots, 10$$
 (11.8)

then with values for M_n and ϕ_n taken from Table 11.2 we find

$$\begin{cases} q_1(t) = p_1(t)/R \\ = \frac{6.6572}{20} \times \cos(2\pi t - 171.8568 \times \pi/180) \quad [\text{L/min}] \\ q_2(t) = p_2(t)/R \\ = \frac{4.7878}{20} \times \cos(4\pi t + 76.9394 \times \pi/180) \quad [\text{L/min}] \end{cases}$$

$$\vdots$$

$$q_{10}(t) = p_{10}(t)/R$$

$$= \frac{0.22696}{20} \times \cos(20\pi t - 127.5263 \times \pi/180) \quad [\text{L/min}]$$
for the standy part of the flav

and for the steady part of the flow

$$\begin{cases}
\overline{q} = \overline{p}/R \\
= \frac{102.5995}{20} \quad \text{[L/min]}
\end{cases}$$
(11.10)

where $\overline{p}(t)$ is the mean value of the pressure as determined from Table 11.1

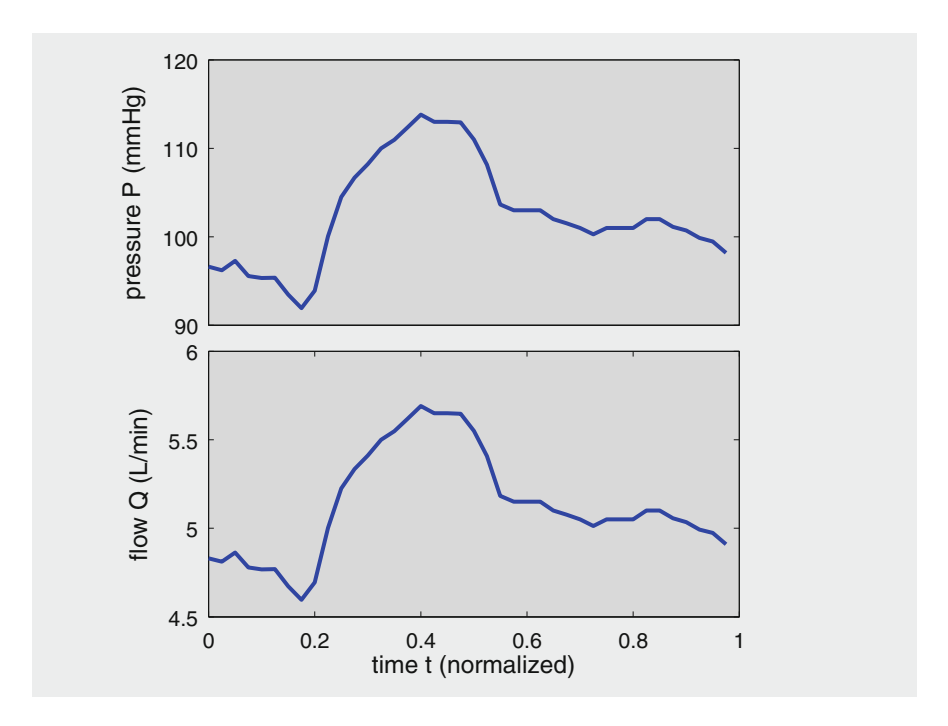


Fig. 11.2 Cardiac pressure wave (top) and corresponding flow wave (bottom) when opposition to flow consists of only resistance R which has been estimated at 20 mmHg/L/min. We see that in this baseline case of pure resistance the pressure and flow waves have precisely the same form, the flow wave being only scaled by the value of the resistance R.

These components of Q(t) can now be added to give the composite flow waveform Q(t) produced by the composite pressure wave P(t), that is

$$Q(t) = \overline{q} + q_1(t) + q_2(t) + \dots + q_{10}(t)$$
(11.11)

which is shown graphically together with the pressure wave in Fig. 11.2.

It is seen that the pressure and flow waveforms have the same shape in this case, which is what makes the case of flow under pure resistance a "baseline" case. In all other cases the shape of the flow waveform would be different from that of the pressure waveform. To further facilitate the comparison, the pressure and flow waves can be put on the same scale by using what we shall refer to as "R-scaled flow" and denote by \tilde{Q} where

$$\tilde{Q} = R \times Q \tag{11.12}$$

Thus Eq. 11.11 can now be put in the form

$$\tilde{Q}(t) = \tilde{q} + \tilde{q}_1(t) + \tilde{q}_2(t) + \ldots + \tilde{q}_{10}(t)$$
 (11.13)

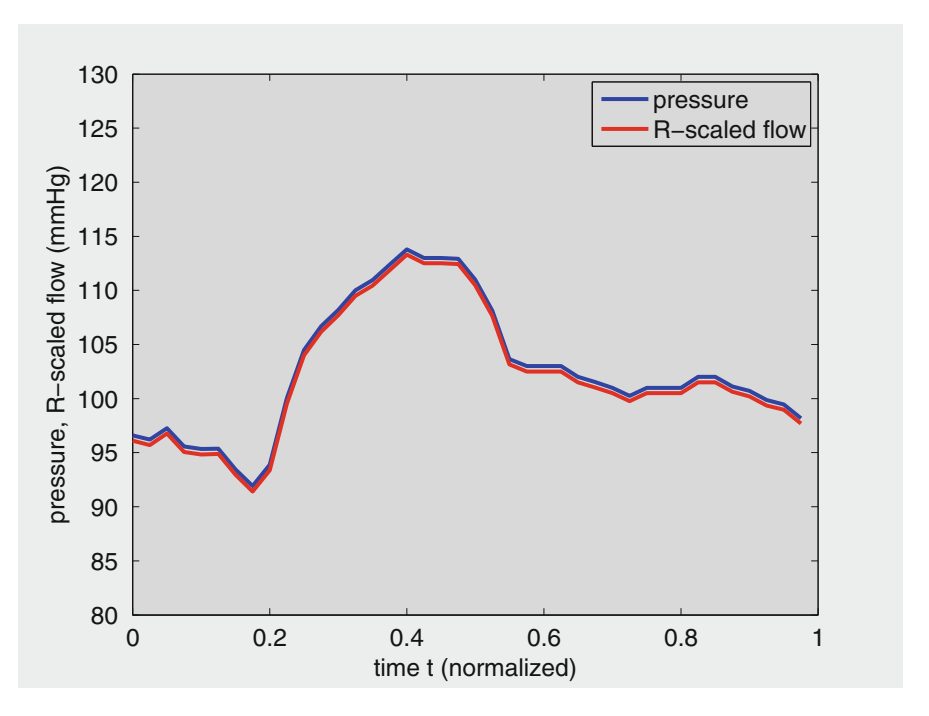


Fig. 11.3 When studying pressure-flow relations it is convenient to plot the pressure and flow waves to the same scale so as to compare their waveforms. This can be achieved as seen here by plotting P(t) (solid curve) and the "R-scaled" flow $R \times Q(t)$ (dashed) instead of q(t). When the opposition to flow consists of only resistance R as it is in this case, the two curves become graphically identical. In this figure they are slightly shifted to make them visibly distinct. The use of R-scaled flow is particularly useful when other elements of the RLC system are present. In such cases any small change in the form of the flow wave can be detected more easily and can be attributed directly to inertial (L) or capacitive (C) effects only, because the effects of resistance (R) have been scaled out.

with the result that the pressure and (*R*-scaled) flow waves can now put on the same scale as shown in Fig. 11.3 where it is seen more clearly that in this singular baseline case they are identical.

The use of *R*-scaled flow is useful not only when the opposition to flow consists of pure resistance but also, and particularly so, when other elements of the resistive path and capacitive chamber are present. In such cases, as we shall see, any departure in the shape of the flow wave from that of the pressure wave can be detected more easily and can be attributed directly to the presence of inertial, capacitive, or viscoelastic effects.

11.4 Resistive-Capacitive Interplay II

The interplay between oscillatory flow along the resistive path and oscillatory flow within the capacitive chamber was discussed at great length in Sect. 9.3. As discussed in that section, this interplay, or interchange, between these two oscillatory flows is at the very core of pulsatile blood flow, and for this reason we revisit this subject again in the present chapter.

As discussed in Sect. 9.3, it is important to recall that flow along the resistive path and flow within the capacitive chamber are not to be confused with "steady flow" and "oscillatory flow" because flow along the resistive path is not entirely steady. Indeed, the ultimate efficiency of pulsatile blood flow is attained when the oscillatory part of the flow occurs largely within the capacitive chamber where energy expenditure is much lower than it is along the resistive path. This is the essence of the resistive-capacitive interplay in pulsatile blood flow as was illustrated in Sect. 9.3, using single harmonic pressure and flow waves and only resistance *R* and compliance *C*. In the present chapter we explore the resistive capacitive interplay further by using composite pressure and flow waves in the present section, and including all elements of the resistive path and capacitive chamber in the next section.

We consider resistance R and compliance C in parallel and, as in Sect. 9.3, with flow rate into the system denoted by Q(t) and is such that

$$Q(t) = q_r(t) + q_c(t) (11.14)$$

where $q_r(t)$ and $q_c(t)$ are flow rates through the resistance R and within the capacitor C, respectively.

When Q(t) is a single harmonic function, that is, as in Sect. 9.3, if we take

$$Q(t) = Q_0 e^{i\omega t} \tag{11.15}$$

it was shown in that section that the resistive and capacitive flow rates are given by (Eq. 9.12)

$$\begin{cases} q_r = \left(\frac{Q_0 e^{i\omega t}}{1 + i\omega CR}\right) \\ q_c = \left(\frac{i\omega CR Q_0 e^{i\omega t}}{1 + i\omega CR}\right) \end{cases}$$

where the steady part of the flow, Q_s in Eq. 9.12, is being omitted here so that the focus is on only the oscillatory part of the flow. The resistive-capacitive interplay involves the oscillatory part of the flow only.

Another way of obtaining these results is by noting that Eq. 11.14 can be put in the form

$$\frac{P(t)}{Z} = \frac{P(t)}{Z_r} + \frac{P(t)}{Z_c}$$
 (11.16)

where P(t) is the (common) pressure driving the flow into the parallel system, Z is the total impedance of the parallel system, Z_r is the impedance of the resistive path and Z_c is the impedance of the capacitive chamber which in the present case consists of only purely elastic compliance.

The impedances in Eq. 11.18, as determined in Sect. 9.9 are given by

$$\begin{cases} Z_r = R \\ Z_c = \frac{1}{i\omega C} \end{cases}$$
 (11.17)

and since

$$\frac{1}{Z} = \frac{1}{Z_r} + \frac{1}{Z_c} \tag{11.18}$$

then

$$\begin{cases}
Z = \frac{Z_r Z_c}{Z_r + Z_c} \\
= \frac{R}{1 + i\omega C}
\end{cases}$$
(11.19)

It then follows that

$$P(t) = ZQ(t) = ZQ_0e^{i\omega t} (11.20)$$

$$\begin{cases} q_r(t) = \frac{P(t)}{Z_r} \\ = \frac{Z}{Z_r} Q_0 e^{i\omega t} \\ = \frac{Q_0 e^{i\omega t}}{1 + i\omega RC} \end{cases}$$
(11.21)

and

$$\begin{cases} q_c(t) = \frac{P(t)}{Z_c} \\ = \frac{Z}{Z_c} Q_0 e^{i\omega t} \\ = \frac{i\omega RC Q_0 e^{i\omega t}}{1 + i\omega RC} \end{cases}$$
(11.22)

While the above results apply to the simple case where (a) the pressure and flow waves consist of only a single harmonic each, and (b) the resistive path and capacitive chamber are represented by only a resistance R and purely elastic compliance C, respectively, the results nevertheless serve well the purpose of illustrating the basic interplay between the resistive path and capacitive chamber.

Since the only opposition to flow here is a resistance R and compliance C, in parallel, it is clear on physical grounds that higher values of R or higher values of C will lead to a larger proportion of the oscillatory flow to be diverted to the capacitive side of the system, while lower values of R or C will lead to oscillatory flow to be diverted to the resistive side. This can also be seen clearly in Eq. 11.44 where

$$\begin{cases} as \quad C, R \to \infty : & q_r(t) \to 0 \\ & q_c(t) \to Q_n(t) \end{cases}$$
 (11.23)

and

$$\begin{cases} as & C, R \to 0: \quad q_r(t) \to Q_n(t) \\ q_c(t) \to 0 \end{cases}$$
 (11.24)

The resistive-capacitive interplay is an interplay between the two extremes in Eqs. 11.23 and 11.24. In the first case, oscillatory flow within the system occurs entirely on the capacitive side, in the second case it occurs entirely on the resistive side. These two extreme scenarios are illustrated in Fig. 11.4.

The important difference between the two, as discussed in Sect. 9.3, is that in the first scenario, in which the compliance *C* is purely elastic in this case, the energy used to drive the oscillatory part of the flow is completely "recycled". In the second scenario it is completely dissipated (lost). As discussed in Sect. 9.3, this is indeed the primary benefit of the Windkessel effect. Absorbing the shock of the pressure rise in systole is only secondary.

The clinical implications of these results lie in their relevance to the pumping "load" of the heart. The extra energy dissipated when more of the oscillatory flow is diverted to the resistive side of the parallel R, C system must ultimately be supplied by the heart. Thus, the loss of elasticity of blood vessels in aging or disease, which is usually seen in terms of its effect on blood pressure, must also be seen in terms of its effect on the pumping load of the heart. The resulting

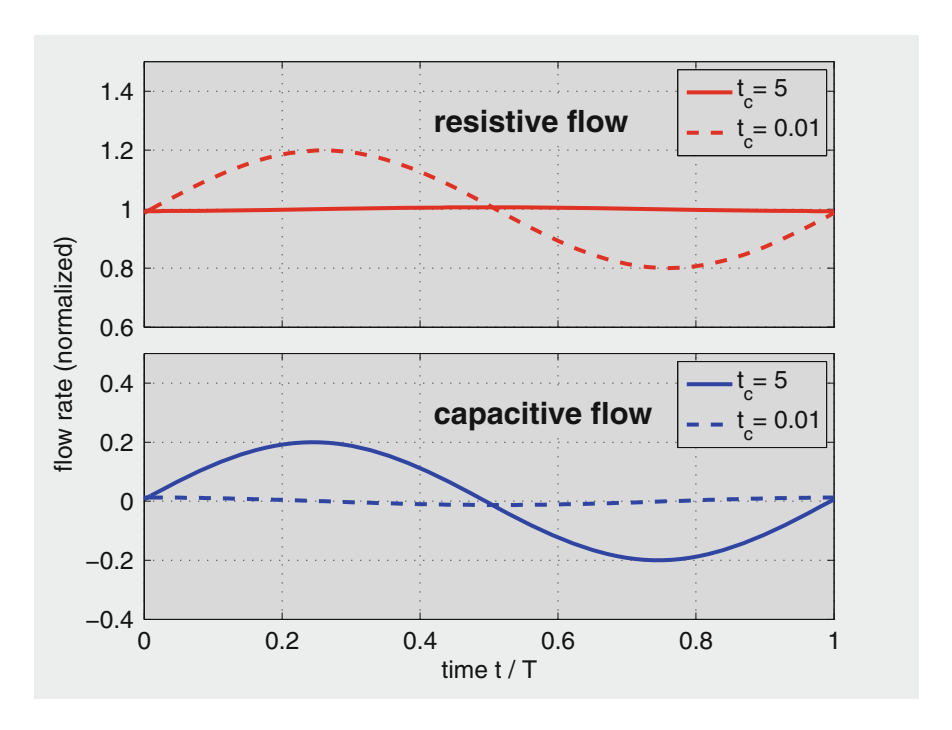


Fig. 11.4 Two extremes in the interplay between the resistive and the capacitive flow, as depicted in Eqs. 11.23 and 11.24. At high value of the capacitive time constant t_c (= $R \times C$) oscillatory flow is almost entirely within the capacitive chamber, while at low values of t_c oscillatory flow is almost entirely within the resistive path. The first of these scenarios is of course the "optimum" for the pulsatile blood flow system because it incurs the least energy dissipation for the oscillatory part of the flow.

risk factor lies not only in "the heart having to pump against higher blood pressure" but also in that it has to dissipate more energy in the process.

11.5 Resistive-Capacitive Interplay III

In the previous section, the interplay between the resistive path and the capacitive chamber was illustrated in terms of a resistance R in parallel with only a purely elastic compliance C. In the present section we examine this interplay when the capacitive chamber is represented by all its elements, namely the compliance C, inertance L, and viscoelasticity K, in series with each other and in parallel with a resistance R along the resistive path. The process involved is much the same as in the previous two sections, therefore some of the details are omitted.

We proceed as in the previous section with an oscillatory flow rate Q(t) as input into the parallel system, with its harmonics given by

$$Q(t) = Q_0 e^{i\omega_n t} ag{11.25}$$

with some of this flow rate (q_r) going into the resistive path and the rest (q_b) going into the capacitive chamber, such that

$$Q(t) = q_r(t) + q_b(t) (11.26)$$

where the subscript 'b' is now used to refer to the capacitive chamber because it consists of more than the compliance C.

The corresponding oscillatory pressure P(t) required to drive the flow is then of the form

$$P(t) = P_0 e^{i\omega t} \tag{11.27}$$

which is related to the flow rate by

$$P(t) = ZO(t) \tag{11.28}$$

where Z is the total impedance of the parallel system.

The total impedance Z is related to the impedance of the resistive path (Z_r) and that of the capacitive chamber (Z_h) by

$$\frac{1}{Z} = \frac{1}{Z_r} + \frac{1}{Z_b} \tag{11.29}$$

or

$$Z = \frac{Z_r Z_b}{Z_r + Z_b}$$
 (11.30)

The individual impedances of the resistive path and of the capacitive chamber have been obtained previously (Eq. 9.84), namely

$$\begin{cases} Z_r = R \\ Z_b = K + i \left(\omega L - \frac{1}{\omega C}\right) \end{cases}$$
 (11.31)

thus the total impedance is given by

$$Z = \frac{R\left(\omega KC + i(\omega^2 LC - 1)\right)}{\omega C(R + K) + i(\omega^2 LC - 1)}$$
(11.32)

It then follows that

$$P(t) = ZQ(t) = ZQ_0e^{i\omega t}$$
(11.33)

$$\begin{cases} q_r(t) = \frac{P(t)}{Z_r} \\ = \frac{Z}{Z_r} Q_0 e^{i\omega t} \\ = \frac{(\omega KC + i(\omega^2 LC - 1)) Q_0 e^{i\omega t}}{\omega C(R + K) + i(\omega^2 LC - 1)} \\ = \frac{(\omega KC + i(\omega^2 LC - 1)) Q(t)}{\omega C(R + K) + i(\omega^2 LC - 1)} \end{cases}$$
(11.34)

and

$$\begin{cases} q_b(t) = \frac{P(t)}{Z_b} \\ = \frac{Z}{Z_b} Q_0 e^{i\omega t} \\ = \frac{\omega RCQ_0 e^{i\omega t}}{\omega C(R+K) + i(\omega^2 LC - 1)} \\ = \frac{\omega RCQ(t)}{\omega C(R+K) + i(\omega^2 LC - 1)} \end{cases}$$
(11.35)

While the resistive-capacitive interplay here seems more complex, the main principle is the same as that seen in the previous section, namely, if flow into the capacitive chamber is prevented for any reason then oscillatory flow is diverted to the resistive path. Thus, here again we find, as in the previous section, that

$$\begin{cases} as & C, R \to \infty : \quad q_r(t) \to 0 \\ & q_b(t) \to Q(t) \end{cases}$$
 (11.36)

and

$$\begin{cases} as & C, R \to 0: \quad q_r(t) \to Q(t) \\ & q_b(t) \to 0 \end{cases}$$
 (11.37)

However, the added effects of viscoelasticity and inertance here, as represented by K, L respectively, provide other scenarios for the resistive-capacitive interplay. On physical grounds, it is clear that if viscous effects within the capacitive chamber become so large as to prevent the chamber from expanding, then oscillatory flow will be diverted into the resistive path. In the limit, Eqs. 11.57 and 11.58 give

$$\begin{cases} as \quad K \to \infty : \quad q_r(t) \to Q(t) \\ q_b(t) \to 0 \end{cases} \tag{11.38}$$

The effects of inertance are perhaps less obvious. These effects come into play as a result of acceleration and deceleration of the fluid. Thus, on physical grounds, it is intuitively clear that inertial effects present higher resistance to fluid acceleration into the capacitive chamber than they do to fluid acceleration along the resistive path. This is seen more clearly from Eqs. 11.57 and 11.58 where we readily find

$$\begin{cases} as \quad L \to \infty : \quad q_r(t) \to Q(t) \\ q_b(t) \to 0 \end{cases}$$
 (11.39)

Finally, in the absence of inertance and viscoelastic effects, the capacitive chamber becomes a purely elastic chamber, as in the previous section. Thus, as a test, in this limit we find that the resistive and capacitive flow rates in Eqs. 11.57 and 11.58 reduce to

$$\begin{cases} as \quad K, L \to 0: \quad q_r \to \left(\frac{Q(t)}{1 + i\omega CR}\right) \\ q_c \to \left(\frac{i\omega CRQ(t)}{1 + i\omega CR}\right) \end{cases}$$
(11.40)

which are identical with the results obtained in Eq. 11.44 of the previous section. Some of the above scenarios are illustrated in Figs. 11.5, 11.6, and 11.7.

11.6 Resistive-Capacitive Interplay IV

The results of the previous two section can be extended in a straightforward manner to the case where the pressure P(t) and flow Q(t) are composite waves (periodic functions). In this section we illustrate the results with the composite wave shown in Fig. 11.8.

When Q(t) is a periodic function, we have seen that it can be decomposed such that

$$\begin{cases}
Q(t) = Q_1(t) + Q_2(t) + \cdots \\
= \sum_{n=1}^{n=N} Q_n
\end{cases}$$
(11.41)

where each of $Q_1(t)$, $Q_2(t)$, etc. is a single harmonic function, n is a running index and N is the number of harmonics which Q(t) has been decomposed into.

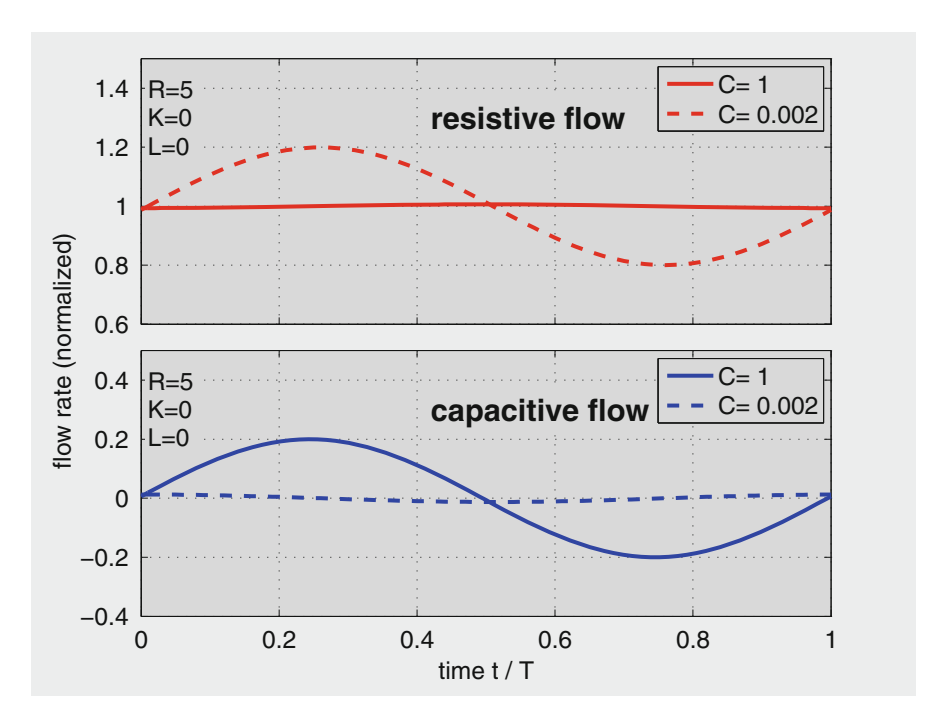


Fig. 11.5 In the absence of inertial and viscoelastic effects, the capacitive chamber becomes purely elastic and the resistive-capacitive interplay becomes the same as that considered in the previous section (Eq. 11.40, Fig. 11.4).

The results of the previous section, which were derived for single harmonics, can therefore be applied to the harmonics of Q(t) individually, writing as in Eqs. 11.15 and 11.14

$$\begin{cases}
Q_n(t) = Q_{n,0}e^{i\omega_n t} \\
= q_{n,r}(t) + q_{n,c}(t)
\end{cases}$$
(11.42)

and then, as in Eqs. 11.21 and 11.22

$$\begin{cases} q_{n,r} = \left(\frac{Q_{n,0}e^{i\omega_n t}}{1 + i\omega_n CR}\right) \\ q_{n,c} = \left(\frac{i\omega_n CRQ_{n,0}e^{i\omega_n t}}{1 + i\omega_n CR}\right) \end{cases}$$
(11.43)

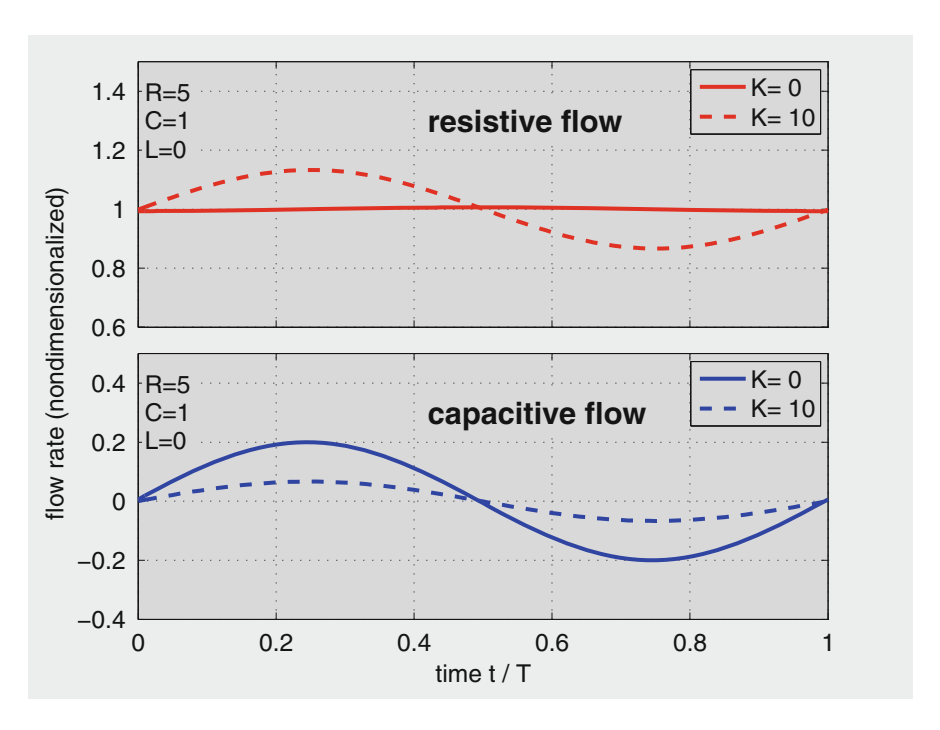


Fig. 11.6 Effect of viscoelasticity (*K*) on the resistive-capacitive interplay.

or, using Eq. 11.42

$$\begin{cases} q_{n,r} = \left(\frac{Q_n(t)}{1 + i\omega_n CR}\right) \\ q_{n,c} = \left(\frac{i\omega_n CRQ_n(t)}{1 + i\omega_n CR}\right) \end{cases}$$
(11.44)

The total flow rate into the parallel R, C system is then given by

$$\begin{cases} Q(t) = Q_1(t) + Q_2(t) + \dots + Q_N(t) \\ = \sum_{n=0}^{N} Q_n(t) \end{cases}$$
(11.45)

The resistive and capacitive flow rates are then correspondingly given by

$$\begin{cases} q_r(t) &= q_{1,r}(t) + q_{2,r}(t) + \dots + q_{N,r}(t) \\ &= \sum_{n=0}^{N} q_{n,r}(t) \end{cases}$$
(11.46)

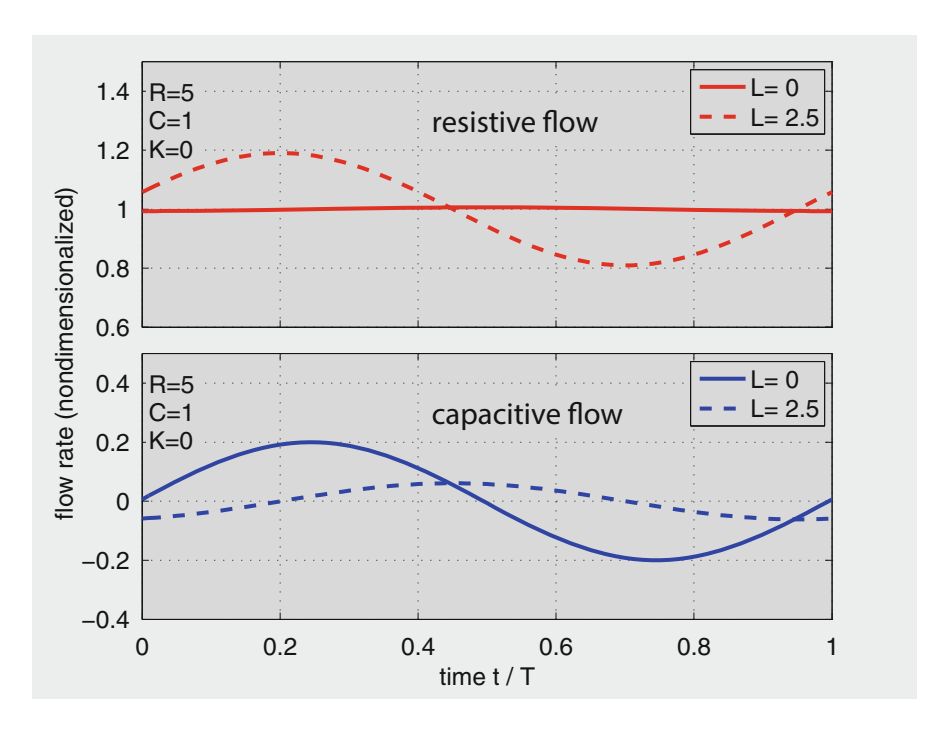


Fig. 11.7 Effect of inductance (*L*) on the resistive-capacitive interplay.

$$\begin{cases} q_c(t) &= q_{1,c}(t) + q_{2,c}(t) + \dots + q_{N,c}(t) \\ &= \sum_{n=0}^{N} q_{n,c}(t) \end{cases}$$
(11.47)

Results based on the composite wave in Fig. 11.8 are shown in Fig. 11.9.

11.7 Resistive-Capacitive Interplay V

In the previous section, the interplay between the resistive path and the capacitive chamber was illustrated in terms of a resistance R in parallel with only a purely elastic compliance C. In the present section, finally, we examine this interplay when the capacitive chamber is represented by all its elements, namely the compliance C, inertance L, and viscoelasticity K, in series with each other and in parallel with a resistance R along the resistive path. The process involved is much the same as in the previous two sections, therefore some of the details are omitted.

We proceed as in the previous section with an oscillatory flow rate Q(t) as input into the parallel system, with its harmonics given by

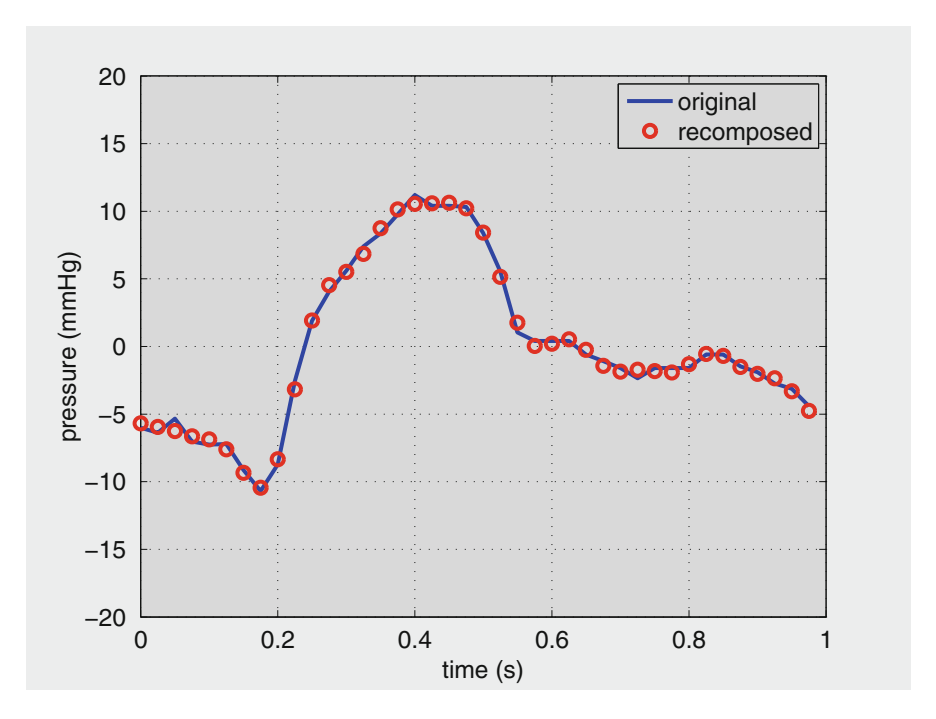


Fig. 11.8 A composite wave being used to illustrate the resistive-capacitive interplay in this and the next section. The wave is decomposed into its harmonic components and the analysis then proceeds separately for each harmonic as in the previous two sections and the results are put together as described in the text. The figure shows the wave in its original form and as it is recomposed based on the first ten harmonics.

$$Q_n(t) = Q_{n,0}e^{i\omega_n t}$$
 $n = 1, 2, \dots N$ (11.48)

For each harmonic n the fraction of oscillatory flow rate going into the resistive path and that going into the capacitive chamber are denoted by $q_{n,r}$ and $q_{n,b}$ respectively and are such that

$$Q_n(t) = q_{n,r}(t) + q_{n,b}(t)$$
(11.49)

where subscript *b* is now used to refer to the capacitive chamber.

Similarly, the oscillatory pressure P(t) required to drive the flow is represented by its harmonics

$$P_n(t) = P_{n,0}e^{i\omega_n t}$$
 $n = 1, 2, \dots N$ (11.50)

and the relation between the pressure and flow harmonics is given by

$$P_n(t) = Z_n Q_n(t) \tag{11.51}$$

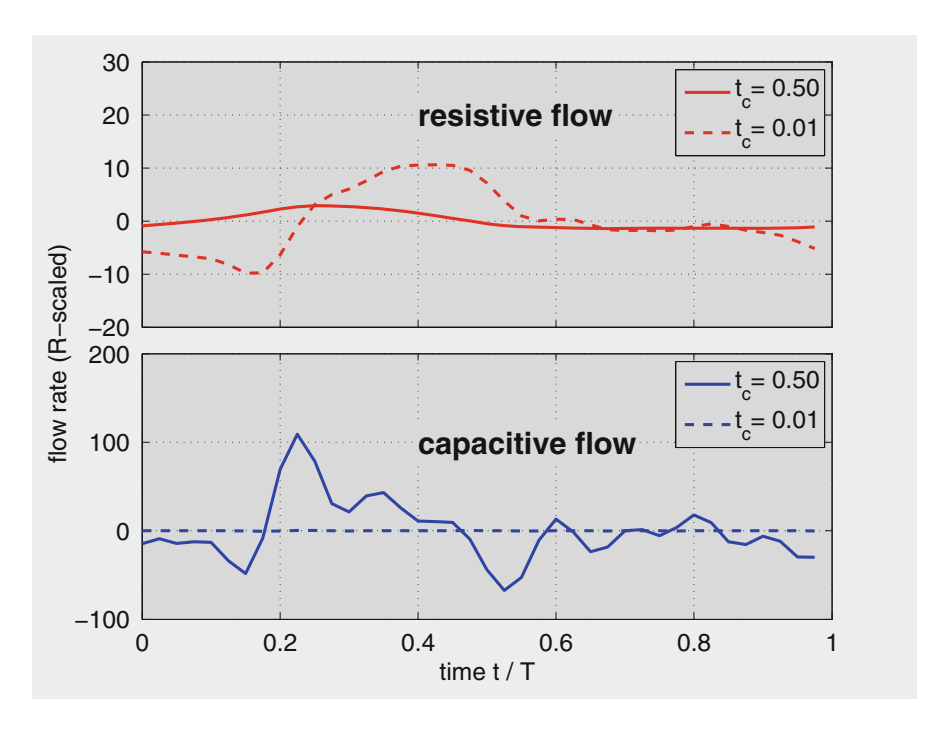


Fig. 11.9 Resistive capacitive-interplay under the composite pressure wave shown in Fig. 11.8. While the interplay is here only between resistance R and purely elastic compliance C, the results are more complicated because the interplay is frequency-dependent and therefore applies differently to each harmonic of the composite wave. Nevertheless, the main principle of the resistive-capacitive interaction remains. At low values of t_c (= $R \times C$) the oscillatory flow is almost entirely resistive while at higher values of t_c it is almost entirely capacitive. The figure also illustrates rather dramatically that capacitive flow is determined not by the pressure but by the rate of change of pressure with time, hence it is determined by the derivative of the waveform in Fig. 11.8.

where Z_n is the total impedance of the parallel system, which is different for each harmonic because of its dependence on the frequency ω_n of that harmonic, hence the subscript n.

The total impedance Z_n is related to the impedances of the resistive path and capacitive chamber, $Z_{n,r}$, $Z_{n,b}$ respectively, by

$$\frac{1}{Z_n} = \frac{1}{Z_{n,r}} + \frac{1}{Z_{n,b}} \tag{11.52}$$

or

$$Z_n = \frac{Z_{n,r} Z_{n,b}}{Z_{n,r} + Z_{n,b}} \tag{11.53}$$

The individual impedances of the resistive path and of the capacitive chamber have been obtained previously (Eq. 9.84), namely

$$\begin{cases}
Z_{n,r} = R \\
Z_{n,b} = K + i \left(\omega_n L - \frac{1}{\omega_n C} \right)
\end{cases}$$
(11.54)

thus the total impedance is given by

$$Z_n = \frac{R\left(\omega_n KC + i(\omega_n^2 LC - 1)\right)}{\omega_n C(R + K) + i(\omega_n^2 LC - 1)}$$
(11.55)

It then follows that

$$P_{n}(t) = Z_{n}Q_{n}(t) = Z_{n}Q_{0n}e^{i\omega t}$$

$$\begin{cases} q_{n,r}(t) = \frac{P_{n}(t)}{Z_{n,r}} \\ = \frac{Z_{n}}{Z_{n,r}}Q_{0n}e^{i\omega_{n}t} \\ = \frac{(\omega_{n}KC + i(\omega_{n}^{2}LC - 1))Q_{0n}e^{i\omega_{n}t}}{\omega_{n}C(R + K) + i(\omega_{n}^{2}LC - 1)} \\ = \frac{(\omega_{n}KC + i(\omega_{n}^{2}LC - 1))Q_{n}(t)}{\omega_{n}C(R + K) + i(\omega_{n}^{2}LC - 1)} \end{cases}$$
(11.57)

and

$$\begin{cases} q_{n,b}(t) = \frac{P_n(t)}{Z_{n,b}} \\ = \frac{Z_n}{Z_{n,b}} Q_{0n} e^{i\omega_n t} \\ = \frac{\omega_n RCQ_{0n} e^{i\omega_n t}}{\omega_n C(R+K) + i(\omega_n^2 LC - 1)} \\ = \frac{\omega_n RCQ_n(t)}{\omega_n C(R+K) + i(\omega_n^2 LC - 1)} \end{cases}$$
(11.58)

While the resistive-capacitive interplay here seems more complex, the main principle is the same as that seen in the previous section, namely, if flow into the

capacitive chamber is prevented for any reason then oscillatory flow is diverted to the resistive path. Thus, here again we find, as in the previous section, that

$$\begin{cases} as \quad C, R \to \infty : \quad q_{n,r}(t) \to 0 \\ q_{n,b}(t) \to Q_n(t) \end{cases}$$
 (11.59)

and

$$\begin{cases} as \quad C, R \to 0: \quad q_{n,r}(t) \to Q_n(t) \\ q_{n,b}(t) \to 0 \end{cases}$$
 (11.60)

However, the added effects of viscoelasticity and inertance here, as represented by K, L respectively, provide other scenarios for the resistive-capacitive interplay. On physical grounds, it is clear that if viscous effects within the capacitive chamber become so large as to prevent the chamber from expanding, then oscillatory flow will be diverted into the resistive path. In the limit, Eqs. 11.57 and 11.58 give

$$\begin{cases} as \quad K \to \infty : \quad q_{n,r}(t) \to Q_n(t) \\ q_{n,b}(t) \to 0 \end{cases}$$
 (11.61)

The effects of inertance are perhaps less obvious. These effects come into play as a result of acceleration and deceleration of the fluid. Thus, on physical grounds, it is intuitively clear that inertial effects present higher resistance to fluid acceleration into the capacitive chamber than they do to fluid acceleration along the resistive path. This is seen more clearly from Eqs. 11.57 and 11.58 where we readily find

$$\begin{cases} as \quad L \to \infty : \quad q_{n,r}(t) \to Q_n(t) \\ q_{n,b}(t) \to 0 \end{cases}$$
 (11.62)

Finally, in the absence of inertial and viscoelastic effects, the capacitive chamber becomes a purely elastic chamber, as in the previous section. Thus, as a test, in this limit we find that the resistive and capacitive flow rates in Eqs. 11.57 and 11.58 reduce to

$$\begin{cases} as \quad K, L \to 0: \quad q_{n,r} \to \left(\frac{Q_n(t)}{1 + i\omega_n CR}\right) \\ q_{n,c} \to \left(\frac{i\omega_n CRQ_n(t)}{1 + i\omega_n CR}\right) \end{cases}$$
(11.63)

which are identical with the results obtained in Eq. 11.44 of the previous section as illustrated in Fig. 11.10. Other scenarios are shown in Figs. 11.11 and 11.12.

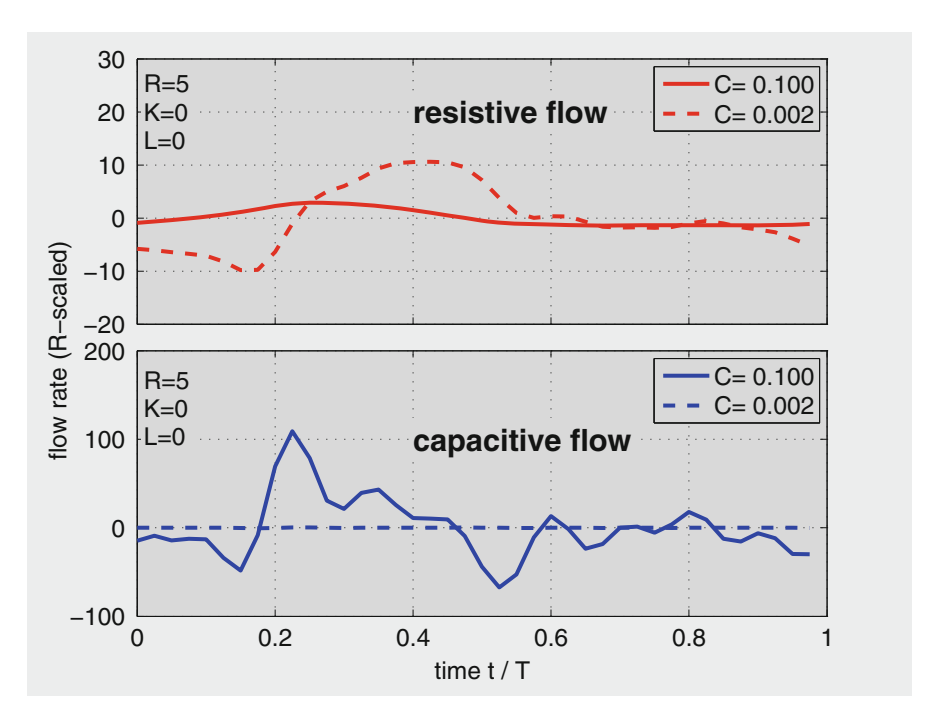


Fig. 11.10 In the absence of viscoelasticity and inertial effects, the capacitive chamber becomes purely elastic and the resistive-capacitive interplay becomes the same as that considered in the previous section (Eq. 11.63, Fig. 11.9).

The clinical implications of these results, as discussed in Sect. 11.4, lie in their relevance to the pumping "load" of the heart as oscillatory flow is shifted from the capacitive chamber to the resistive path, or vice versa, because of changes in the conditions controlling the dynamics of the system as represented by changes in the values of the parameters R, C, K, L. Physiological conditions that may lead to changes in the values of R and C are fairly obvious, as in vasoconstriction and vascular stiffening, respectively. However, conditions that may lead to changes in K and L are less obvious.

While much is known about the elasticity of blood vessels and about the cellular matrix that produces this property within the vessel wall, very little is known about the viscoelastic property. While this property of the vessel wall is well known to exist, and while changes in this property as represented by changes in the value of K may have a significant effect on the dynamics of pulsatile flow in general and on the resistive-capacitive interplay in particular as shown in this section, very little is know about the origin of this property within the vessel wall.

Similar remarks apply to changes in the inertial effects within a vascular bed, as represented by the parameter L. While changes in the inertia of blood may

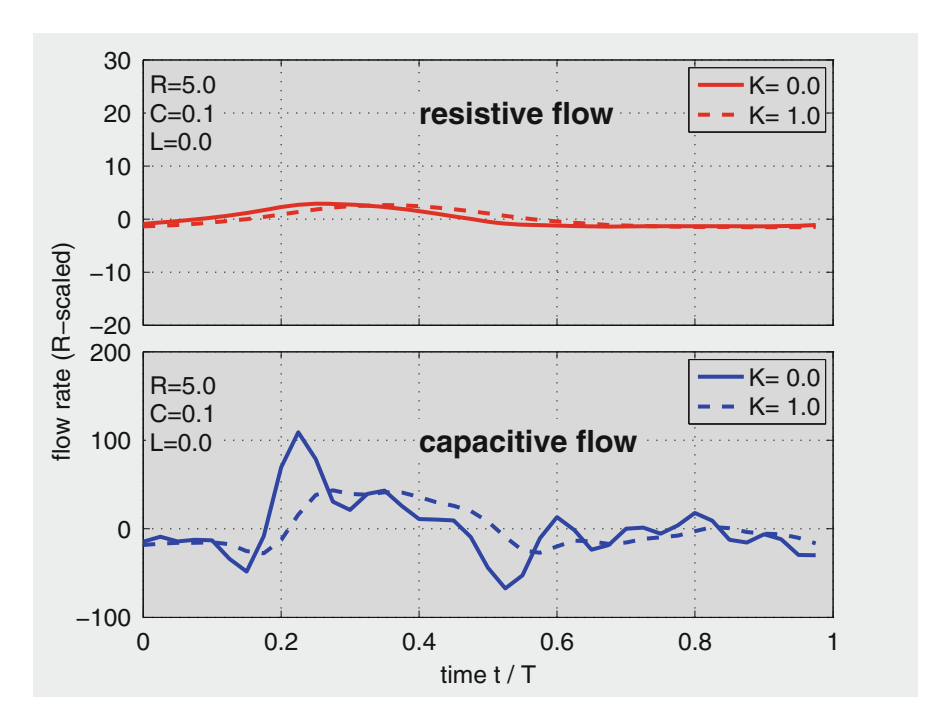


Fig. 11.11 Viscoelasticity (K) acts as a *resistance to stretch* within the vessel wall and thus has the effect of modulating (or "smoothing out") the capacitive flow as seen in the figure. At very high values of K this resistance overrides the elasticity of the wall and the capacitive chamber becomes effectively "rigid" as shown in Eq. 11.61.

be an obvious source of such changes, the more likely source is a change in the geometrical structure of the vascular bed including vasoconstriction or vasodilation, acute or chronic. Such changes will alter the acceleration and deceleration environment within the vascular bed and, as seen in the above scenarios, will affect the dynamics of the flow.

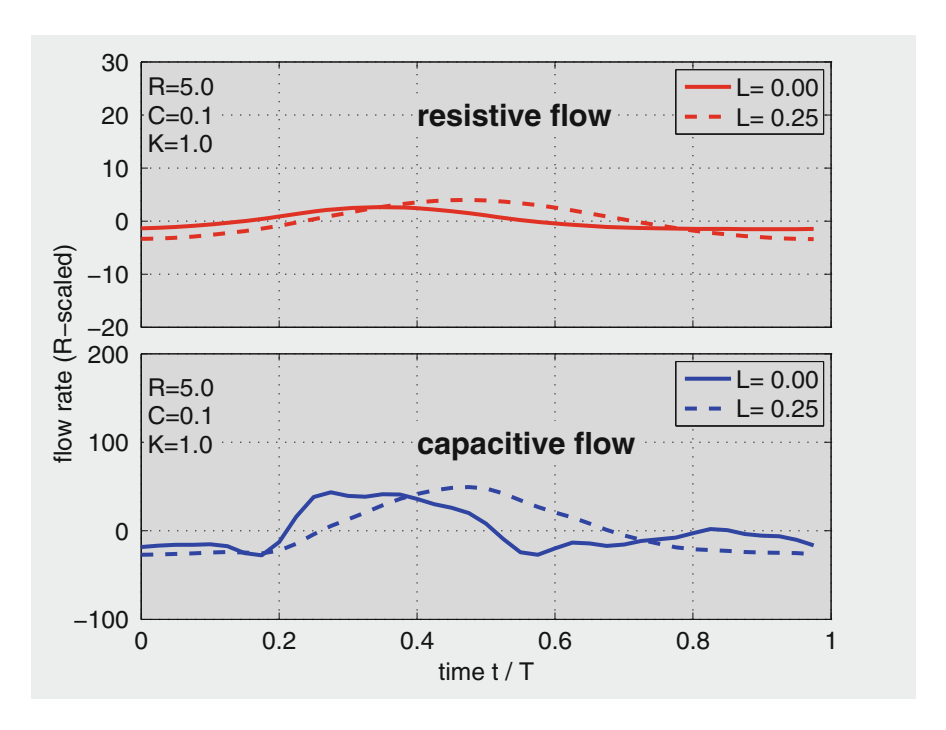


Fig. 11.12 Inertial effects as represented by the parameter *L*. The main effect of this property is to produce a *phase shift* in the dynamics of the flow and thus disrupt the harmony between the driving pressure and oscillatory momentum of the flow, not unlike that of disrupting the oscillatory momentum of a pendulum. While elastic and viscoelastic effects may be related somewhat to measurable properties of the vessel wall, inertial effects are extremely difficult to assess because they depend on acceleration and deceleration of the flow which in turn depend on *space and time* as seen in Sect. 2.5. Thus, any change in the topology of the integrated lumen of a vascular bed, whether by disease or intervention, such as vasodilation or vasoconstriction, may cause a disruption in the dynamics of the flow.

Chapter 12 Dynamic Pathologies

12.1 Introduction

The main task of the cardiovascular system is to bring blood flow to within reach of billions of cells within the body, *individually*. There is a capillary with continuously moving blood within reach of every living cell within the body. The vascular system required to achieve this task is of an immense proportion. There are likely more "tube segments" within a single human body than there are in any man-made fluid flow system on the planet (Figs. 12.1 and 12.2).

Along with this immense *structural* aspect of the cardiovascular system there is the *dynamical* aspect, namely that of orchestrating the *flow* within the system. Flow from a single source, the heart, must reach the billions of capillaries throughout the body, individually, and then return to the heart, repeatedly. The pressure required to drive this flow is not *steady* as it would be from an elevated water tank, but *pulsatile*. It is provided by repeated ejection of fluid from the heart in a rhythmic manner, approximately once every second. It is from this rhythmic action of the heart that all the dynamical aspects of the cardiovascular system originate.

It is remarkable that while the dynamical aspects of pulsatile blood flow have been studied by mathematicians as much as its structural and functional aspects have been studied by physiologists, the focus of clinical concern with the working of the system in health or in disease has been largely, indeed almost exclusively, with the structural aspects of the system, that is with the working of the system under steady flow conditions where a vessel free from pathology is seen as a guarantee of flow within that vessel. Yet, as we have seen in the previous chapter, when the dynamics of the system are considered, this guarantee is no longer valid.

That is not to say that the structural aspects of the cardiovascular system and its working under steady flow conditions are not important. The effects of a blocked or narrowed artery are as clearly visible as they are incontrovertible. It is to say only

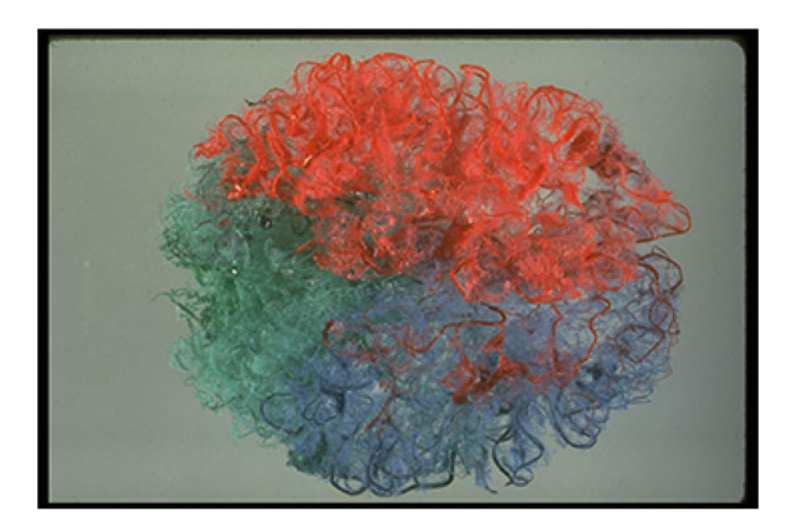


Fig. 12.1 Cast of vasculature of the human brain. *Red and blue colors* indicate vasculature from the left and right carotid arteries, respectively, *green* represents vasculature from the vertebral arteries. Venous vasculature and capillaries are absent.



Fig. 12.2 Cast of vasculature of the human kidney. As in Fig. 12.1, venous vasculature and capillaries are absent. There are likely more "tube segments" within a single human body than there are in any man-made fluid flow system on the planet.

that an anomaly in the *dynamics* of the system, though not as visible as a structural anomaly, may be equally important because it may disrupt the continuous flow of blood just as a structural anomaly does. It is not unreasonable therefore to use the term "pathology" here in the same way that the term is used in general, but we now distinguish between a static or "structural pathology" and a "dynamic pathology".

A dynamic pathology may arise as a result of any acute or chronic change in the characteristic parameters of the system, namely R, C, K, L. Whether the change is caused by disease, aging, pharmaceutical or surgical intervention, the result is a change in the dynamics of the system as seen in previous chapters. In the present chapter we examine this notion with some specific examples.

12.2 Swing in the Park

The dynamics of a freely hanging pendulum depend on several static or structural parameters such as the length of the suspending rod or string, the weight of the suspended mass, and any friction at the pivoting joint that allows the pendulum to swing. It is a fairly common experience that the orderly swings of the pendulum can be very easily disrupted with an external force *without any change in the static parameters of the system*. In other words, the working of the pendulum can be disrupted by a *dynamic pathology* in the same way that it can be by a *static pathology* such as a broken string or a rusty pivoting joint.

Anyone who has pushed a child on a swing in the park, or remembers his or her own experience as a child on the swing, will know the exquisite harmony that must exist between the timing of the applied force and the oscillatory momentum of the swing. Any discord between the two will cause the swing to lose rather than gain momentum, thus producing a dynamic pathology. The structure of the swing is fully intact, but its dynamics are deranged.

The dynamics of a freely hanging pendulum is an example of a system of *free oscillation* characterized by the absence of an external driving force. Pulsatile blood flow is a system of *forced oscillations* characterized by the presence of an external driving force, namely the pumping pressure produced by the heart. In Chap. 9 it was shown that the dynamics of pulsatile blood flow can in fact be separated (mathematically) into a set of free oscillations that depend only on the properties of the system, plus a set of forced oscillations that depend heavily on the nature of the external force.

The dynamics of a swing in the park provide a useful example of a system which may operate as a system of free oscillations or one of forced oscillations. If the oscillations of the swing, with a child on the seat, are allowed to continue without any attempt by the seated child or by an attending adult to *force* these oscillations, the dynamics of the system will ultimately unfold freely and in a fairly predictable manner. But if either the child or the adult attempt to force the oscillations of the swing, the outcome becomes highly complex and not as readily predictable because it is now heavily dependent on the form of the applied force.

This example, which may seem trivial at first, provides a very useful and fairly accurate analogy for the dynamics of pulsatile blood flow. Any discord between the pumping pressure wave produced by the heart and the prevailing oscillatory flow within the vascular system will cause a dynamic pathology. The pathology may be chronic, due to slow and permanent changes in the characteristic properties (R, C, K, L) of the system caused by disease or aging,

for example. Or it may be acute, caused by a momentary disruption in the dynamics of the system caused by vasoconstriction, for example, or by a sudden change in the form or rhythm of the pressure wave produced by the heart.

In the remainder of this chapter we discuss different scenarios in which dynamic pathologies may arise. Because much of the dynamics of pulsatile blood flow occurs within the *oscillatory* part of the flow, we shall find that the discussion is primarily about the dynamics of this part of the flow.

12.3 Dynamic Markers I

The resistive-capacitive interplay examined extensively in the previous two chapters provides the most important ground for dynamic pathologies. Briefly, it was seen that the *oscillatory* part of pulsatile blood flow is divided into a *resistive* part and a *capacitive* part. The first occurs within the resistive path and the energy required to drive it is therefore completely dissipated (lost), while the second occurs within the capacitive chamber and the energy required to drive it is largely recovered. Both produce zero net flow over each oscillatory cycle, but the interplay between them has a significant effect on the dynamics of the flow.

It is not unreasonable to assume that the cardiovascular system is designed such that under normal circumstances much of the oscillatory flow is diverted to the capacitive chamber. The extent to which these optimal conditions prevail in the cardiovascular system as a whole or in any part thereof provides important markers of the dynamic "health" or "pathology" of the system.

This can in fact be examined by direct measurements of pressure and flow waves within an intact vascular bed. The pressure wave can be used to generate a flow wave using the relation established in Sect. 11.6, namely

$$Q_n(t) = \frac{P_n(t)}{Z_n}, \quad n = 1, 2, \dots N$$
 (12.1)

where $Q_n(t)$ and $P_n(t)$ are the harmonics of the measured flow and pressure waves, respectively, and Z_n are the corresponding harmonics of the impedance

$$Z_n = \frac{R\left(\omega_n KC + i(\omega_n^2 LC - 1)\right)}{\omega_n C(R + K) + i(\omega_n^2 LC - 1)}, \quad n = 1, 2, \dots N$$
(12.2)

where ω_n are the harmonic frequencies and R, C, K, L are properties of the vascular bed.

In Eq. 12.1 the harmonics of the pressure wave $P_n(t)$ can be determined by decomposing the measured wave as described in Chap. 10 but the lumped properties

R, C, K, L of the bed in which the pressure was measured, which are required for determining Z_n , are unknown. However, since the pressure wave was measured simultaneously with the corresponding flow wave, the values of R, C, K, L can be determined in an iterative manner by matching the predicted flow wave in Eq. 12.1 with the measured flow wave. The values of R, C, K, L at which the two flow waves match can then be declared as the values of these properties for the bed in which the pressure and flow waves were measured.

The above method provides a power noninvasive tool for determining the lumped properties of a vascular bed. Indeed, because of access and other practical reasons, it is clearly the only possible tool for determining the collective properties of the millions of blood vessels in a vascular bed. An example of this process applied to the vascular bed of the arm is shown in Figs. 12.3 and 12.4 where simultaneous measurements of pulsatile pressure and flow waves were made at the brachial artery.¹

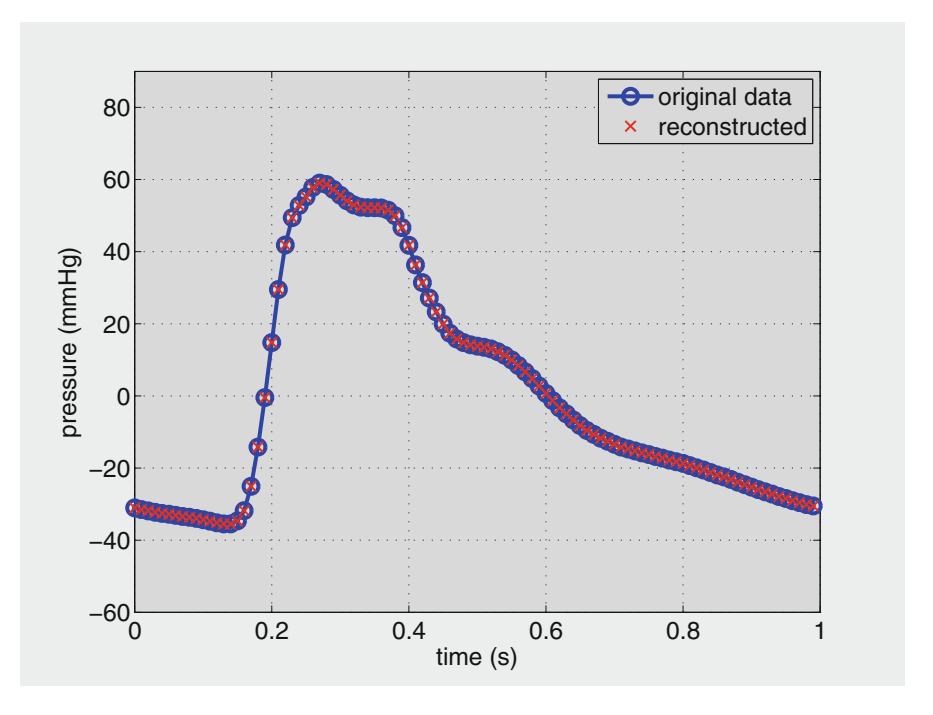


Fig. 12.3 Pressure wave measured at the brachial artery of a human subject (see Footnote 1). The figure shows the wave based on 100 original data points and a Fourier reconstruction of the wave based on the first 50 harmonics as described in Chap. 10.

¹Zamir M, Norton K, Fleischhauer A, Frances MF, Goswami R, Usselman CW, Nolan RP, Shoemaker JK, 2009. Dynamic responsiveness of the vascular bed as a regulatory mechanism in vasomotor control. The Journal of General Physiology. DOI: 10.1085/jgp.200910218.

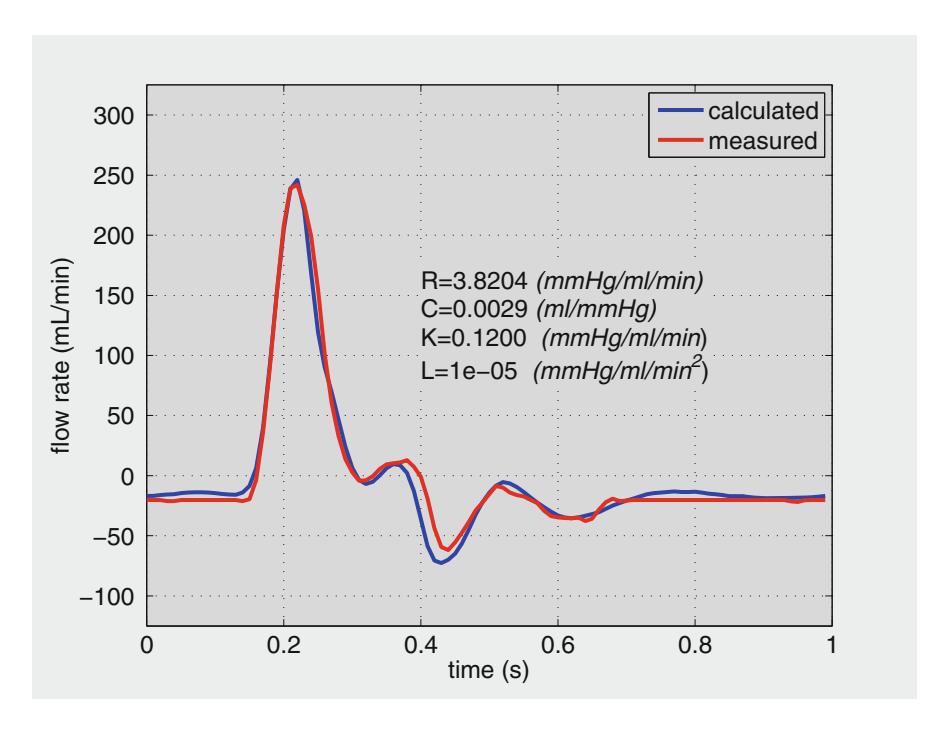


Fig. 12.4 Flow wave calculated as described in the text and based on the first 50 harmonics of the pressure wave in Fig. 12.3, compared with the flow wave measured simultaneously with that pressure wave (see Footnote 1). In the calculation of the flow wave the values of the parameters R, C, K, L are adjusted iteratively to achieve the smallest error between the measured and the calculated waves.

For the purpose of the present section, the flow wave $Q_n(t)$ in Fig. 12.4 can now be divided into its resistive $q_{n,r}$ and capacitive $q_{n,b}$ components as determined in Sect. 11.7, namely

$$\begin{cases} q_{n,r}(t) = \frac{(\omega_n KC + i(\omega_n^2 LC - 1))Q_n(t)}{\omega_n C(R + K) + i(\omega_n^2 LC - 1)} \\ q_{n,b}(t) = \frac{\omega_n RCQ_n(t)}{\omega_n C(R + K) + i(\omega_n^2 LC - 1)} \end{cases}$$
(12.3)

where we note, of course, that

$$q_{n,r} + q_{n,b} = Q_n(t) (12.4)$$

The corresponding flow waveforms are finally obtained by adding the harmonic components

$$\begin{cases} Q(t) = \sum_{n=1}^{N} Q_n(t) \\ q_r(t) = \sum_{n=1}^{N} q_{n,r}(t) \\ q_b(t) = \sum_{n=1}^{N} q_{n,b}(t) \end{cases}$$
(12.5)

It will be recalled that the division of oscillatory flow into a resistive and a capacitive component is a critical marker of the dynamic "health" or "pathology" of the vascular bed in which this division is observed. The result for the flow wave in the vascular bed of the arm is shown in Fig. 12.5.

The result is an example of "healthy dynamics" in which the oscillatory flow occurs almost entirely within the capacitive chamber, therefore the pumping energy of the heart expended on the oscillatory part of the flow is almost completely

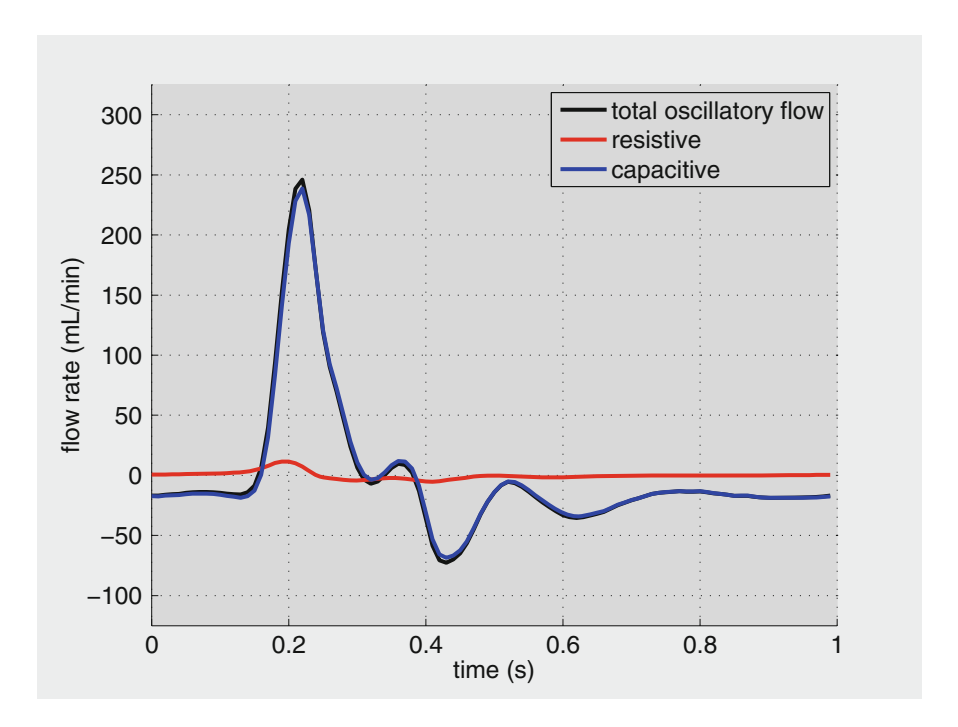


Fig. 12.5 Division of the oscillatory flow rate seen in Fig. 12.4 into "resistive" and "capacitive" components. The observed division is remarkable in that the overwhelming proportion of the flow goes through the capacitive chamber with very little through the resistive path, which indicates a state of "healthy dynamics" in this vascular bed.

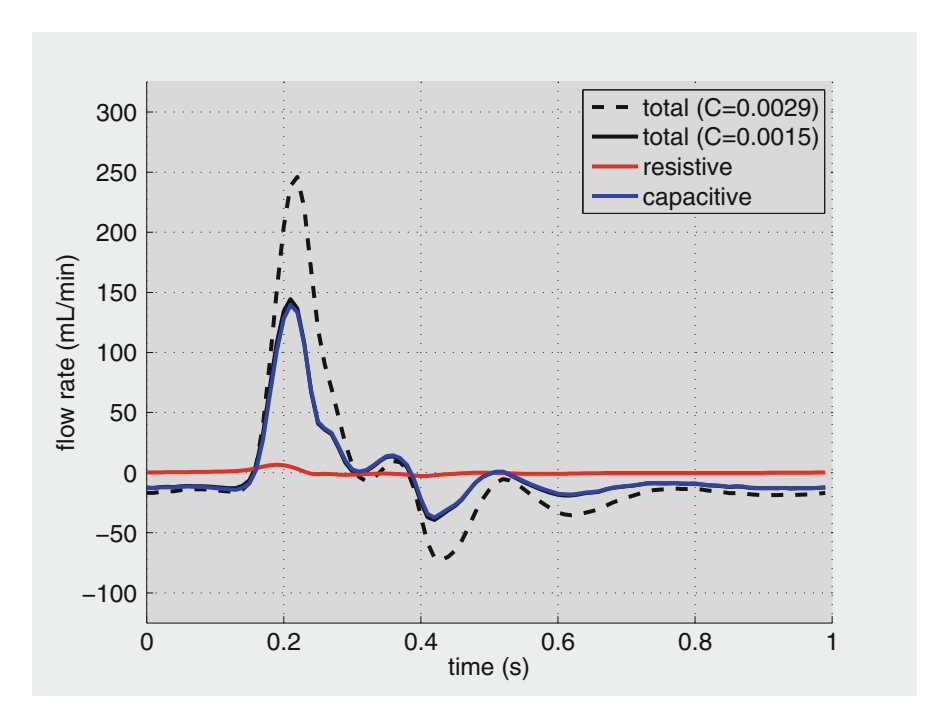


Fig. 12.6 The effect of reduced compliance *C* from its value under the healthy dynamic conditions seen in Fig. 12.4. While the division of oscillatory flow into resistive and capacitive components remains favorable, *the peak of both components and hence the peak of total oscillatory flow in systole are all considerably reduced.*

recovered. If the properties of the vascular bed change from their values under these optimal dynamics, the result is a "dynamic pathology" in which more of the oscillatory flow occurs along the resistive path where much of the pumping energy of the heart is *dissipated* (*lost*). Scenarios where the values of *C*, *K*, *L* are changed to simulate different dynamic pathologies are shown in Figs. 12.6, 12.7, and 12.8.

The common conclusion from these results is that any change in properties of the capacitive chamber, as represented by C, K, L will affect the dynamics of the oscillatory part of pulsatile blood flow. The most dramatic of these effects is seen to be that of a change in the value of the inertial parameter L. This change may come about by any alteration in the acceleration and deceleration environment available to the oscillatory flow within a given vascular bed, such as vasodilation or vasoconstriction.

Thus, while vasodilation is a well established clinical strategy for reducing the resistance to the steady part of pulsatile blood flow and thereby providing relief to an ailing heart, its effect on the oscillatory part of the flow cannot be ignored because, paradoxically, it may present the heart with a dynamic pathology.

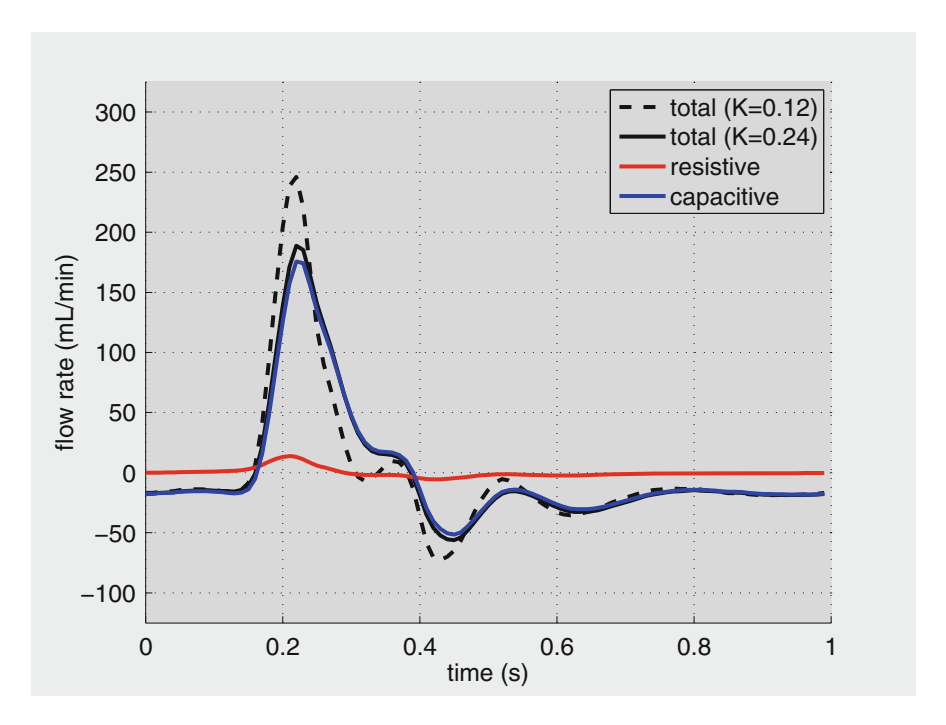


Fig. 12.7 Viscoelasticity as represented by the parameter K acts as resistance to stretch within the vessel wall. A higher value of K, as seen here, leads to lower peak flow in systole, lower capacitive flow, but somewhat higher resistive flow. The latter is caused by higher opposition to flow into the capacitive chamber, hence some of the oscillatory flow is diverted into the resistive path.

Changes in the "elasticity" of the vessel wall, which affect values of the parameters C and K, have the overall effect of reducing the systolic peak of the oscillatory flow. While both of these properties represent "opposition" to stretch within the vessel wall, it is important to recall from Sect. 9.4 that the first (C) represents opposition to the *amount of stretch* while the second represents opposition to the *rate of stretch*, that is the rate at which the stretch is occurring in time. While "pure" elasticity as represented by the parameter C is generally associated with elastin within vessel wall, less is known about the source of viscoelasticity within the cellular matrix of the wall material. In the clinical setting the two effects are usually combined under the general headings of "vascular stiffening" or "hardening of the arteries".

Vascular stiffening, in disease or aging, is generally seen as a risk factor for hypertension because of higher pulse wave velocity and wave reflections (Sect. 5.9, Chap. 6) which in turn is seen as a risk factor for heart disease because of the increased "load" of the heart as it pumps against higher blood pressure. The results in Figs. 12.6 and 12.7 indicate that a more menacing,

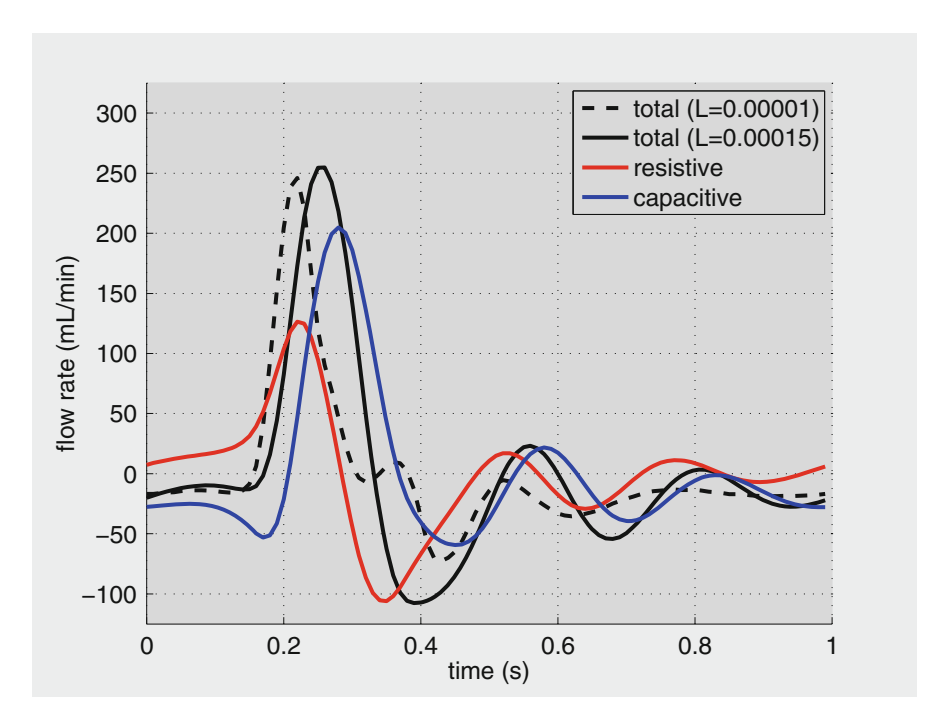


Fig. 12.8 Increased inertial effects, as represented by a higher value of L, produce a considerable derangement of the oscillatory flow and provide the quintessential example of a "dynamic pathology". Peak flow is actually increased but a considerable proportion of it is diverted to the resistive path. Furthermore, compared with the "healthy dynamics" in Fig. 12.5, there is a clear phase discord between different components of the flow not unlike an untimely push of a swing in the park.

or at least an equally menacing, effect of this dynamic pathology is that in reducing the systolic peak of the oscillatory part of the flow, the heart is less able to use the capacitive chamber for recycling much of its pumping energy.

12.4 Dynamic Markers II

The branching architecture within a vascular bed provides another important ground for dynamic pathologies, that is another way in which the dynamics of pulsatile blood flow can be disrupted. This is because the branching architecture determines the pattern of wave reflection and hence the pattern of admittance or impedance within the bed. That is, it determines the extent to which the bed "admits" or "impedes" the oscillatory part of pulsatile blood flow. Any change in this architecture may thus lead to dynamic pathology. The markers for such pathology are clearly not as readily available as those discussed in the previous section,

because they involve the detailed architecture of the vascular bed in question. Nevertheless, in this section we illustrate the consequences of changes in vascular branching architecture, using the 11-level vascular tree of Fig. 7.12.

There are a number of ways in which the admittance environment within a vascular bed can become acutely or chronically pathological. A key factor in all cases is the wave speed or "pulse wave velocity". Anything that affects the propagation of the pressure pulse through the vascular bed will affect the admittance environment within the bed. In the previous section the focus was on changes in the lumped properties of the vascular bed, in the present section we focus on changes in the detailed architecture of the bed. The two are not unrelated, of course, because a change in the branching architecture of the bed, for example, will also affect the acceleration and deceleration environment of the bed and hence the lumped inertance parameter *L*. Similarly, a change in the elasticity or viscoelasticity of the vessels which changes the lumped compliance properties *C*, *K* of the bed as a whole will also affect the pulse wave velocity and hence the admittance environment within the bed.

A measure of the effects of wave reflections in a vascular tree is the difference between the characteristic and the effective admittances of all vessel segments within that tree. The characteristic admittances can be calculated from the prescribed properties of these segments, using Eq. 7.95. The calculation of effective admittances, since it involves the effects of wave reflections from all junctions up to and including the upstream ends of the peripheral terminal segments, must therefore begin at this end of the tree. From known or prescribed reflection coefficients at these ends, the effective admittances of the terminal vessel segments are determined, using Eq. 7.106. If there are no wave reflections at these ends, then the reflection coefficients are zero and the effective admittances of the terminal branches are the same as their characteristic admittances. In either case, the calculation can then progress to the next upstream level of the tree in which each vessel segment is a parent segment in a bifurcation in which the two branches are two of the peripheral segments, thus the effective admittance of the parent segment is determined using Eq. 7.106. This process then continues to the next upstream level of the tree, and so on, until the root segment is reached.

More specifically, the reflection coefficient at the downstream end of a tube segment in a tree structure is determined by the characteristic admittance of that segment and by the *effective* admittances of the two branch segments forming the bifurcation at that end, as determined in Sect. 6.7. If the position of the vessel segment under consideration is j, k, then the positions of the two branch segments at its downstream end $(x_{j,k} = l_{j,k})$ are j + 1, 2k - 1 and j + 1, 2k, as illustrated in Fig. 7.12. Using the results of Sect. 7.10, therefore, Eq. 7.106 expressed in the notation of the present section gives for the reflection coefficient

$$R_{j,k} = \frac{Y_{0,j,k} - (Y_{e,j+1,2k-1} + Y_{e,j+1,2k})}{Y_{0,j,k} + (Y_{e,j+1,2k-1} + Y_{e,j+1,2k})}$$
(12.6)

The characteristic admittance Y_0 is defined by Eq. 6.66 and is determined by the radius of the tube segment and by the wave speed which again may be taken as c or c_0 as discussed above, depending on the desired accuracy. The effective admittance Y_e , using Eq. 7.106 in present notation, is given by

$$\begin{cases} Y_{e,j,k} = Y_{0,j,k} \times \left(\frac{(Y_{e,j+1,2k-1} + Y_{e,j+1,2k}) + iY_{0,j,k} \tan \theta_{j,k}}{Y_{0,j,k} + i(Y_{e,j+1,2k-1} + Y_{e,j+1,2k}) \tan \theta_{j,k}} \right) \\ \theta_{j,k} = \frac{\omega l_{j,k}}{c_{j,k}} \end{cases}$$
(12.7)

The results of such calculations are illustrated for the 11-level tree model in Fig. 12.9.

The difference between the distribution of characteristic admittances and that of effective admittances, which is due entirely to the effects of wave reflections, is seen to be fairly large. Furthermore, because these effects are *cumulative*, they reach their highest value at the root of the tree as observed in the figure. The most important aspect of these results, however, is that the effects of wave reflections in this tree model are seen to produce *higher* admittance, and hence lower impedance, within the tree.

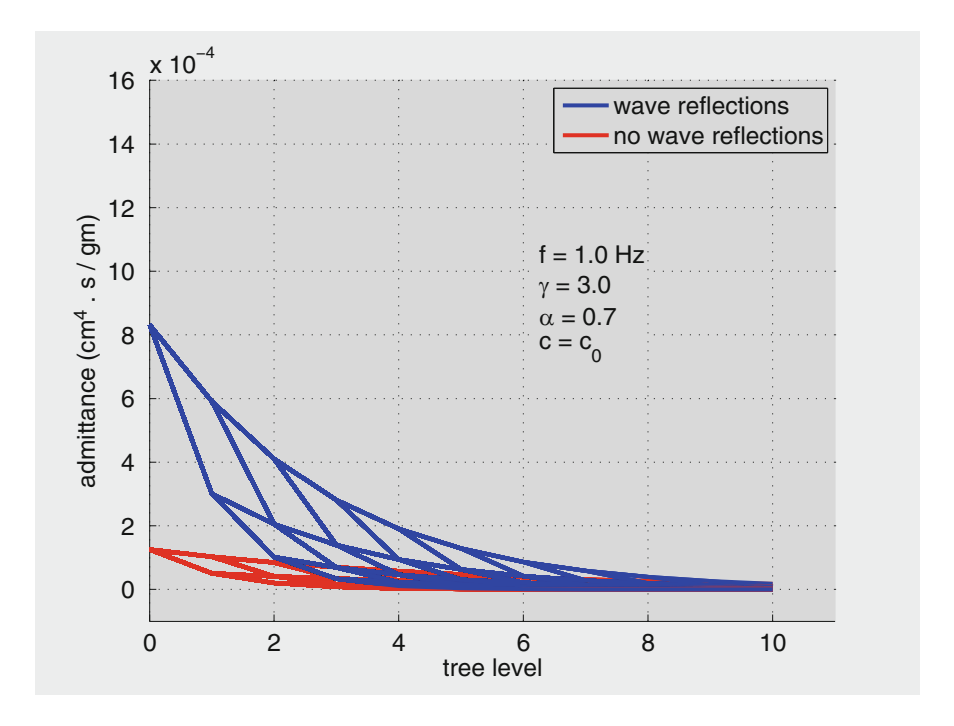


Fig. 12.9 Absolute values of the effective and the characteristic admittances at different levels of the 11-level tree model, with parameter values as shown in the figure. The difference between the two distributions is due entirely to wave reflections.

Furthermore, as seen in Fig. 7.29, the wave-length-to-tube-length ratios in this tree model are everywhere well above 100. In Sect. 5.11 it was shown that under these circumstances, and in the absence of wave reflections, the velocity profiles of pulsatile flow in an elastic tube are much the same as those in rigid tube. The results of the present section show that in the presence of wave reflections this is not the case, particularly as these reflections compound within a tree structure.

The situation is somewhat more complicated, however, because the wave speed c involved in the wave-length-to-tube-length ratio $\overline{\lambda}$ is also a function of frequency as in Eq. 7.91

$$\overline{\lambda} = \frac{\lambda}{L} = \frac{2\pi c}{\omega L}$$

In Fig. 12.9 this was simplified by taking $c=c_0$ where c_0 is the constant Moen-Korteweg wave speed. In order to account for this effect, the calculations of characteristic admittances in these figures must be repeated by using a value of c obtained from the solution for pulsatile flow in an elastic tube for each vessel segment (Sect. 5.9). The results are shown in Fig.12.10. This "refinement" produces essentially the same results, though with even *higher* effects of wave reflections.

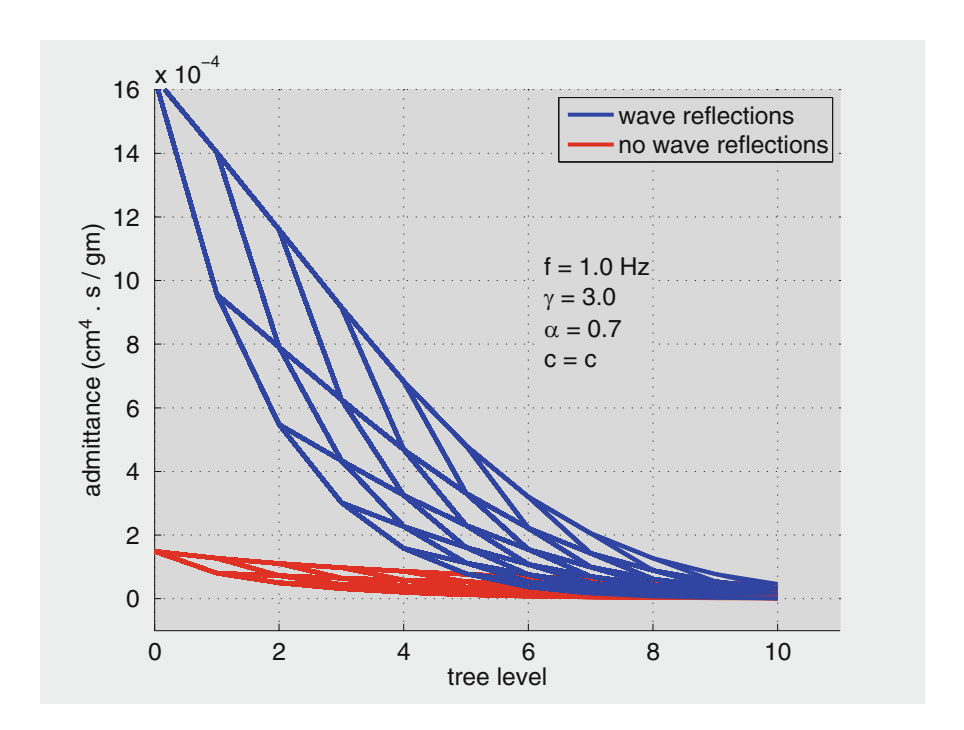


Fig. 12.10 Absolute values of the effective and characteristic admittances at different levels of the 11-level tree model at a frequency of 1 Hz, as in Fig. 12.9, but here using a value of the wave speed c obtained from a solution of the pulsatile flow in an elastic tube for each vessel segment.

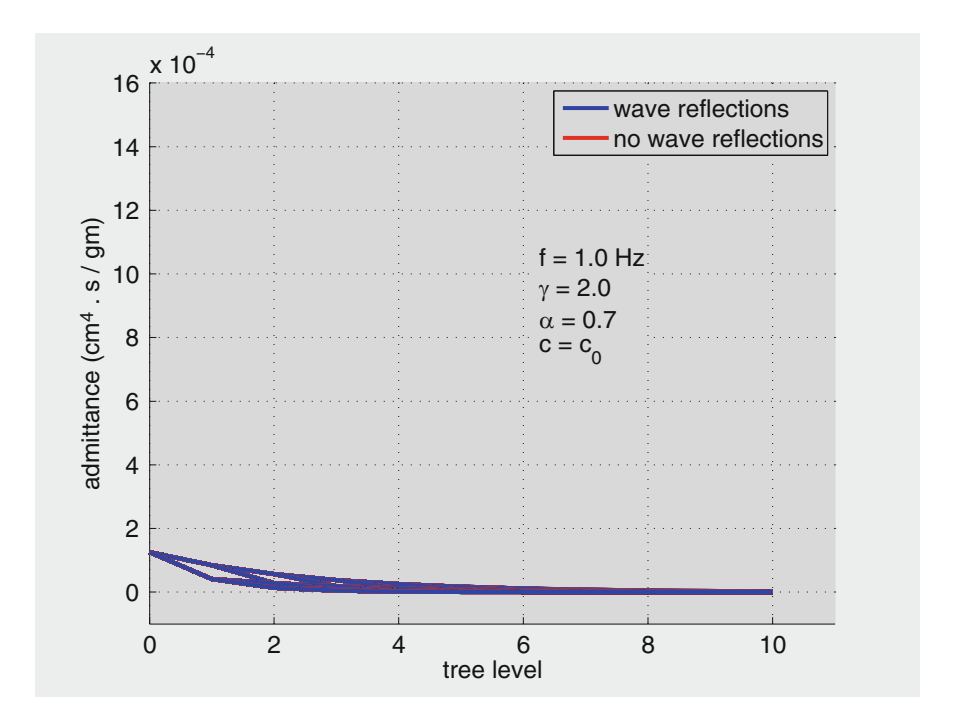


Fig. 12.11 Absolute values of the effective and characteristic admittances (which in this case coincide) at different levels of the 11-level tree model at a frequency of 1 Hz and $c=c_0$, as in Fig. 12.9, but here using a square law ($\gamma=2$) for the hierarchy of radii at different levels of the tree. The law produces what is generally referred to as "impedance matching" at arterial bifurcations because under the square law the impedance of the parent vessel is equal to the combined impedance of the two branches. Under these conditions the effective admittances are everywhere the same as the corresponding characteristic admittances, which means that the effects of wave reflections are entirely eliminated. It is important to note that impedance matching requires not only $\gamma=2$ but also $c=c_0$.

Finally, the results in Figs.12.9 and 12.10 are based on a tree model in which the hierarchy of vessel radii follows the cube law, namely $\gamma=3.0$ as discussed in Sect. 3.11. An instructive case to consider is a model based on the square law, namely $\gamma=2.0$, and $c=c_0$. The results are shown in Fig. 12.11, where the effects of wave reflections are seen to be totally absent and the distributions of characteristic and of effective admittances are identical. The result shown is for a frequency f=1 Hz, but the same results are obtained for other frequencies. The reason for this rather singular result is that under a power law index $\gamma=2.0$, the sum of cross-sectional areas of the two branches at a bifurcation is equal to the cross-sectional area of the parent, that is (Eq. 7.48)

$$a_p^2 = a_a^2 + a_b^2 (12.8)$$

where a is vessel radius and subscripts p, 1, 2 are being used here to identify the parent tube segment and two branches, respectively. The characteristic admittances of the three tube segments forming the bifurcations, using Eq. 7.95, are given by

$$\begin{cases} Y_{0p} = \frac{\pi a_p^2}{\rho c_p} \\ Y_{0a} = \frac{\pi a_a^2}{\rho c_a} \\ Y_{0b} = \frac{\pi a_b^2}{\rho c_b} \end{cases}$$
(12.9)

and the corresponding characteristic impedances are given by

$$\begin{cases}
Z_{0p} = \frac{\rho c_p}{\pi a_p^2} \\
Z_{0a} = \frac{\rho c_a}{\pi a_a^2} \\
Z_{0b} = \frac{\rho c_b}{\pi a_b^2}
\end{cases}$$
(12.10)

If now we set

$$c_p = c_a = c_b = c_0 (12.11)$$

which is actually implied in the solution of the wave equations (Sect. 6.2) on which the definition of admittance in Eq. 12.9 are based, it then follows from Eqs. 12.8 and 12.9 that

$$Y_{0p} = Y_{0a} + Y_{0b} (12.12)$$

and

$$\frac{1}{Z_{0p}} = \frac{1}{Z_{0a}} + \frac{1}{Z_{0b}} \tag{12.13}$$

which constitute what is generally referred to as "impedance matching" at the bifurcation, meaning that the propagating wave does not encounter any change of impedance (or admittance) as it crosses the bifurcation and hence there are no wave reflections at the junction. Since this is true at all bifurcations of the 11-level tree model, with $\gamma=2$, it follows that no wave reflections arise throughout the tree and hence the effective admittances are everywhere the same as the corresponding characteristic admittances as observed in Fig. 12.11.

It has been suggested that "square law" conditions ($\gamma=2.0$) prevail in the first few generations of the aorta,² and that this is a deliberate design feature of the vascular system which has the advantage of avoiding wave reflection effects at these upstream generations of the vascular tree. This may indeed be the case in the larger vessels of the vascular tree where values of the frequency parameter Ω are sufficiently high that the wave speed is close to the constant Moen-Korteweg wave speed c_0 , as seen in Fig. 5.14, which the conditions for impedance matching require.

However, in a smaller sub-tree structure such as that of the coronary circulation where values of Ω are typically much lower as seen in Fig. 7.22, the wave speed is significantly different from c_0 as seen in Fig. 5.14. Thus, strictly, for application to the coronary circulation the calculations on which the results of impedance matching in Fig. 12.11 are based must be repeated using the actual value of c obtained from a solution for pulsatile flow in an elastic tube, as in Sect. 5.9 for each vessel segment. The results are shown in Fig. 12.12 where it is seen clearly

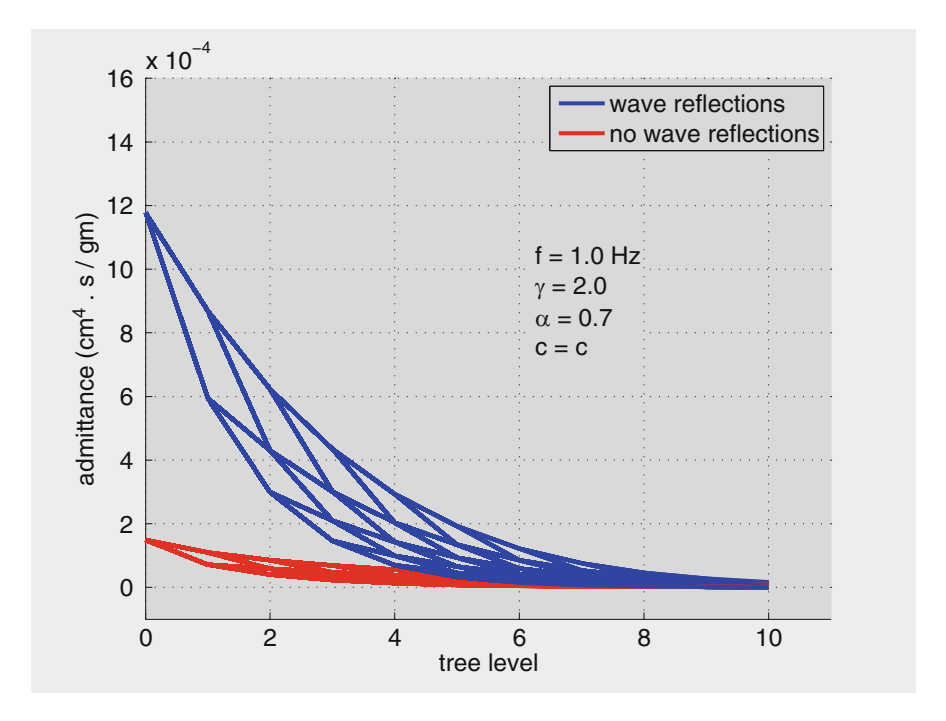


Fig. 12.12 Absolute values of the effective and characteristic admittances at different levels of the 11-level tree model, as in Fig. 12.11, but here using a value of the wave speed c obtained from a solution of the pulsatile flow in an elastic tube for each vessel segment, instead of $c = c_0$ on which the results in Fig. 12.11 are based. The results show that impedance matching does not occur in this case because it requires $\gamma = 2$ and $c = c_0$.

²West GB, Brown JH, Enquist BJ, 1997. A general model for the origin of allometric scaling laws in biology. Science 276:122–126.

that impedance matching does not occur at the junctions, and effective admittances are significantly different from the corresponding characteristic admittances in most of the tree structure.

In summary, the effects of wave reflections in the cardiovascular system are not to be seen as necessarily negative or obstructive to the flow. Indeed, wave reflection sites are so pervasive within the vascular tree that it would be highly surprising to find that biology has neglected this aspect of hemodynamics within the arterial tree. Under normal circumstances, wave reflections produce effective impedances that are more favorable to the dynamics of the oscillatory part of pulsatile blood flow as seen in this section. Any change in these optimal circumstances, whether it is caused by disease or intervention, will lead to a dynamic pathology.

12.5 Coronary Blood Flow

Coronary blood flow is blood flow to the heart for its own metabolic needs, and because the heart is itself the driver of this flow, there is a measure of "symbiotic" relationship between the dynamics of the heart as a pump and the dynamics of its own blood supply. There are three distinct aspects of coronary blood flow that make the dynamics of the flow more complex and more susceptible to dynamic pathologies.

First, coronary vasculature, that is vessels that supply blood to the heart itself for its own metabolic needs, are embedded within the heart muscle as shown in Fig. 12.13. When the heart muscle contracts to eject blood to the rest of the body, the vessels are squeezed shut and blood supply to the heart is momentarily stopped. Only when the heart muscle relaxes the supply is restored. Thus the oscillatory character of coronary blood flow is dictated largely by contractions of the heart muscle rather than by the pressure pulse generated by the heart itself. As a result, while blood flow to the rest of the body peaks in systole, coronary blood flow peaks in diastole.

Second, because of the central role of the heart as a pump for blood supply to the entire body, and because the demand for blood flow from the rest of the body is highly variable, from a low in a resting state to a high in an aerobic activity, coronary blood flow has the capacity to increase "on demand" by as much as five or six fold, a feature generally referred to as "coronary flow reserve".^{3,4,5,6,7} Thus the

³Gregg DE, 1950. Coronary Circulation in Health and Disease. Lea & Febiger, Philadelphia, PA.

⁴Marcus ML, 1983. The Coronary Circulation in Health and Disease. McGraw-Hill, New York.

⁵Kajiya F, Klassen GA, Spaan JAE, Hoffman JIE (eds), 1990. Coronary Circulation: Basic Mechanism and Clinical Relevance. Springer-Verlag, Tokyo.

⁶Spaan JAE 1991. Coronary Blood Flow. Kluwer Academic Publishers, Dordrecht, The Netherlands.

⁷Zamir M. The Physics of Coronary Blood Flow. Springer, New York, 2005.

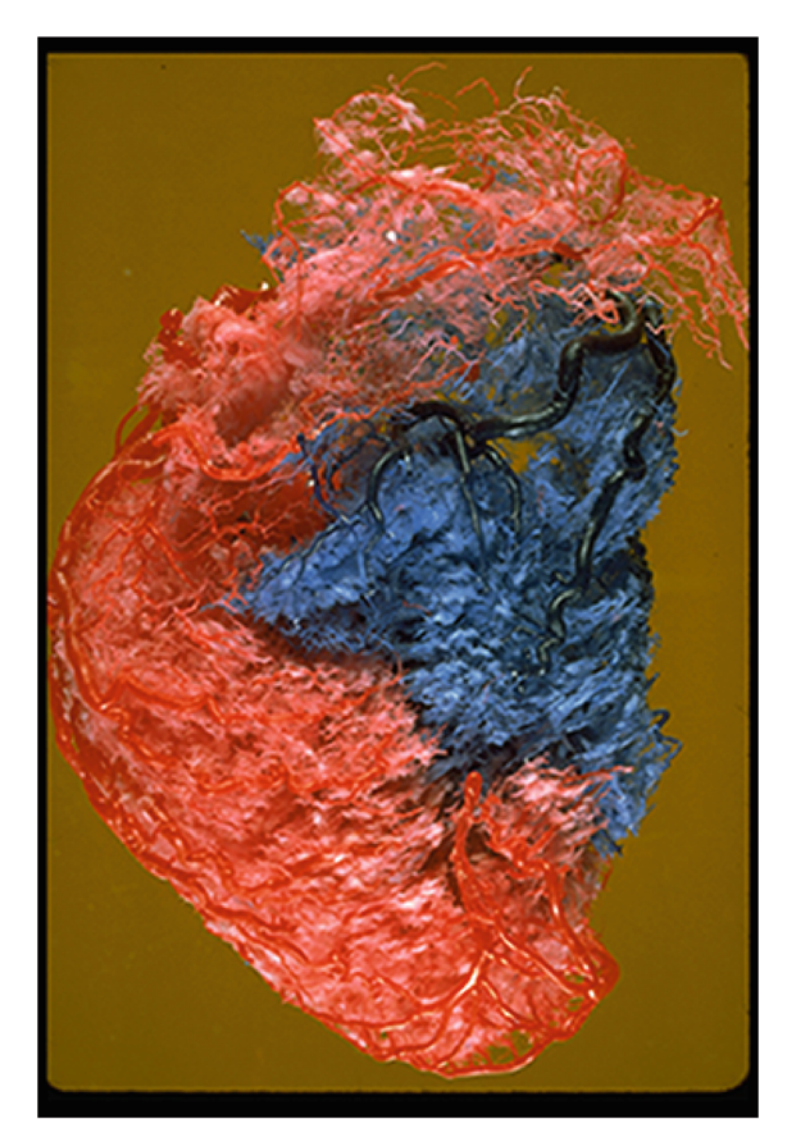


Fig. 12.13 Cast of coronary arterial vasculature of the human heart. *Red and blue colors* represent vasculature from the left and right coronary arteries, respectively. Venous vasculature is not included. Only some capillaries can be seen as clumps of white fluff, the vast majority have been excluded from forming in the cast so as not to obscure other vasculature. *This entire vasculature is embedded within the heart tissue, much of it within the myocardium and is therefore subject to contractions of the heart muscle*.

dynamics of coronary blood flow can be far more "volatile" than the dynamics of pulsatile blood flow in other parts of the cardiovascular system. Not only is the flow pulsatile but it can frequently be in a state (Sect. 9.7) in which it is more susceptible to dynamic pathologies.

Third, because of the repeated opening and closing of coronary vasculature embedded within the cardiac muscle, the branching architecture of the coronary vasculature is in a state of *constantly varying geometry*. This has enormous impact on wave reflections within the coronary vasculature because wave reflections depend critically on the geometry of branching architecture within the vascular bed. Furthermore, because the source of the varying architecture is the repeated contraction of the heart muscle, this presents the heart with the opportunity of controlling the pattern of wave reflections within its own vasculature. Wave reflections, as seen in the previous section, tend to enhance the admittance of oscillatory flow within the vascular bed. This has indeed been shown to occur in the vasculature of the human heart as shown in Fig. 12.14, suggesting that "Reflection effects endow the peripheral regions of the [coronary arterial] tree with a mechanism of 'sucking' flow towards them, somewhat like a sponge, although the sucking action in a sponge is

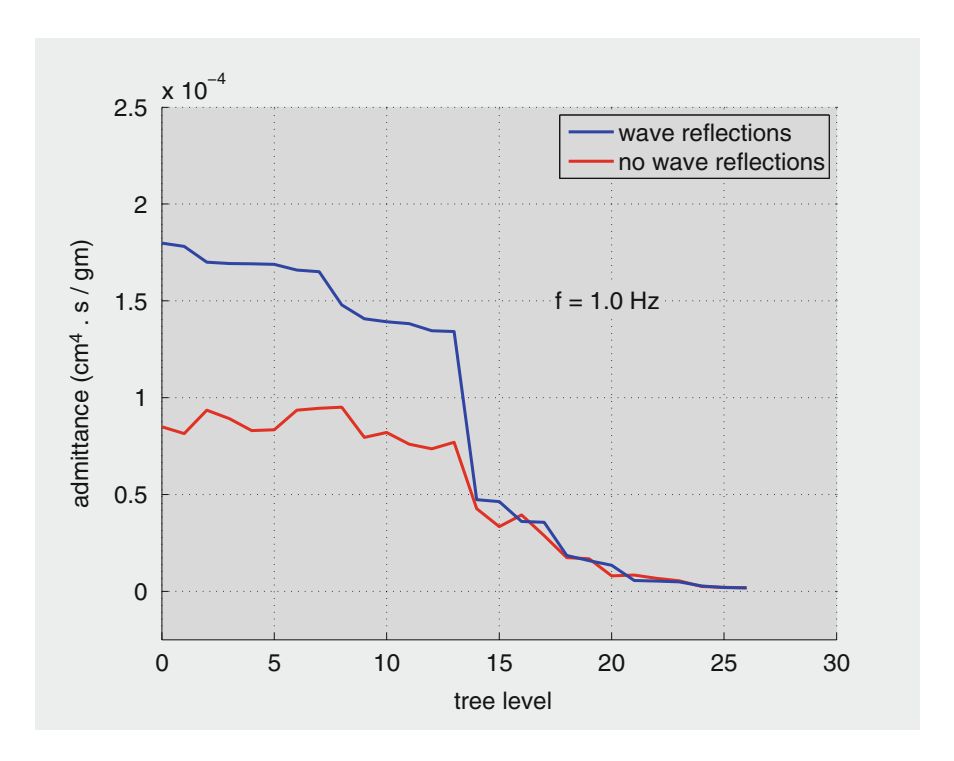


Fig. 12.14 Characteristic and effective admittances of 27 segments of the right coronary artery of a human heart, based on measurements of vessel lengths and diameters of the right coronary arterial tree. Compare with Fig. 12.10 where the results are based on a theoretical 11-level tree structure. Adapted from Zamir (1998; see Footnote 8).

caused by an entirely different mechanism." and that "In coronary blood flow, wave reflection effects ... may play a significant 'silent' role in coronary heart disease ..."

Each of these unique features of coronary blood flow presents a clear potential for dynamic pathologies, acute or chronic, yet, for obvious reasons, the focus in the clinical setting is usually on structural pathologies: blood cholesterol level, coronary artery disease. While the presence of these and other structural pathologies have a clear and direct impact on coronary blood flow, the above results suggest that the absence of structural pathologies does not guarantee the integrity of blood supply to the heart. Coronary blood flow can be equally disrupted by **dynamic** pathologies.

Arrhythmia, in all its forms, is a familiar example of a dynamic pathology. It is a direct insult on the oscillatory character of the pressure wave generated by the heart and specifically on the harmony between this pressure wave and the resistive and capacitive characteristics of the vascular system. In short, it is a direct insult on the *dynamics* of the flow. It is indeed not unlike an insult on the dynamics of a swing in the park by an untimely pull or push. The subsequent course of the deranged dynamics is not predictable and the consequences are not easy to assess. A footprint of the cause of derangement is absent, which is the hallmark of dynamic pathologies.

Another phenomenon that has the attributes of a dynamic pathology is "sudden cardiac death" in which, essentially, the timing of the event cannot be explained in terms of a structural pathology alone. The cause of death in all cases is a "...precipitous fall in cardiac output to levels that can no longer sustain cerebral or cardiac function...". The fall in cardiac output is usually associated with a disruption in heart rhythm in one form or another: ventricular fibrillation, tachycardia, bradycardia, and the like, all of which have to do with a disruption in the oscillatory dynamics of the flow.

Yet another example of a dynamic pathology is that of the "Broken Heart Syndrome" in which "Emotional stress can precipitate severe, reversible left ventricular dysfunction in patients without coronary disease. Exaggerated sympathetic stimulation is probably central to the cause of this syndrome." The syndrome was found to be marked by highly elevated plasma levels of catecholamines and "stress-related neuropeptides". These agents are known to control parameters that affect the dynamics of the coronary circulation as they produce changes in vascular calibers

⁸Zamir M, 1998. Mechanics of blood supply to the heart: Wave reflection effects in a right coronary artery. Proceedings of the Royal Society of London B 265:439–444.

⁹Osborn MJ, 1996. Sudden cardiac death: A. Mechanisms, incidence, and prevention of sudden cardiac death. In: Mayo Clinic Practice of Cardiology, pp. 862–894. Giuliani ER, Gersh BJ, McGoon, MD, Hayes DL, Schaff HV (eds). Mosby, St. Louis, MO.

¹⁰Wittstein IS, Thiemann DR, Lima JAC, Baughman KL, Schulman SP, Gerstenblith G, Wu KC, Rade JJ, Bivalacqua TJ, Champion HC, 2005. Neurohumoral features of myocardial stunning due to sudden emotional stress. New England Journal of Medicine 352:539–548.

and vascular resistance. The broken heart syndrome may therefore be considered as another example of a disruption in, indeed a direct insult on, the dynamics of coronary blood flow.

Unlike structural pathologies, dynamic pathologies do not leave a "footprint" after they have been resolved or after they have produced their damage. Following sudden cardiac death, indeed following any death attributed to heart disease, only structural pathologies can usually be found. Any **dynamic** pathologies that may have been involved are not in evidence because they are no longer at play.

Appendix A Viscosity: A Story

How does the viscosity of fluids come about? What in the structure of fluids gives rise to this property? More specifically, what in the structure of fluids allows a fluid body to deform freely without resistance or force, yet puts out resistance to the <u>rate</u> at which the deformation is taking place?

Imagine two long trains running side by side on parallel tracks, carrying a large flock of children to a ball game. Children being what they are, unable to wait for their destination, they start the game on the trains. Balls fly in both trains and in all directions, and with the windows open, some balls fly from one train to the other.

As long as the trains run at exactly the same speed, this exchange of balls occurs as if the two trains were one, and when a ball arrives it makes no difference whether it came from the same train or from the other.

If one train begins to move faster than the other, however, balls being exchanged between the two trains will now be affected by the difference in speed between the two trains. Balls entering the fast train from the slower one, as they collide with the first object in the fast train, will be speeded up by that collision to acquire the speed of the fast train. Similarly, balls entering the slow train from the fast one, as they collide, will be slowed down to the speed of the slow train.

When a slow moving ball is hit by a faster moving train and is speeded up by it, the train suffers a small loss of momentum which, of course, may not be noticeable if there is only one ball. But if a large number of slow balls are hit by a faster moving train, the loss of momentum by the train can be sufficiently large to affect the train's engine and be noticed by the driver. The same is true, of course, if a large number of fast moving balls are hit by a slower moving train, in this case the train can gain sufficient momentum to be noticed.

Thus, if the train drivers after moving at the same speed for some time and having exhausted all the small talk that they can muster decide to have a little race with each other, they will be in for a surprise.

As one driver attempts to pull his train a little faster, he notices some unusual sluggishness: more power than usual is needed to accelerate. He communicates the puzzle to the driver of the other train who then attempts to speed up his own train and meets with the same mysterious added resistance.

The drivers conclude, without knowing why, that the trains resist any attempt to move them at different speeds. The only thing we know more than they do is the underlying reason for that resistance. The trains resist any *rate of shear* between them because of the wild game going on inside, which the drivers are totally unaware of.

The mechanics of this resistance to rate of shear are precisely the mechanics of fluid viscosity.

The flying balls in the case of fluids are the molecules. They are in a state of constant wobble, chaotic dance in all directions which causes them to have occasional collisions with each other. Any attempt to produce rate of shear between two neighboring layers of fluid causes collisions of faster moving molecules with the slower moving layer, and between slower moving molecules with the faster moving layer. The result is a resistance of precisely the same type as that between the two trains.

The train story is re-enacted every time an attempt is made to shear two neighboring layers of fluid at any significant (non-zero) rate or, more accurately, an attempt to create a "velocity gradient", an attempt to move two neighboring layers of fluid at different speeds. The viscous property of fluids resists velocity gradients.

A small amount of viscous fluid such as thick liquid honey rubbed back and forth between the thumb and index finger will clearly demonstrate this effect. But shear rate between neighboring layers of fluid exists whenever there is flow, because flow is essentially a shearing motion. Thus, fluid viscosity and viscous resistance to rate of shear is an ever present factor in the behavior of fluids.

Appendix B Poiseuille Flow: A Story

A somewhat animated picture of the flow in a tube is that of a chain of swimmers attempting to save each other from a swift current. The two swimmers closest to the river banks manage to grab onto the banks, each with one hand, stretching the other hand out to help one of their friends. Two swimmers closest to these hands grab on to them each with one hand, stretching the other hand out to help another friend. This goes on and on as swimmers further and further away from the banks connect to this human chain, until two hands clinch at the center of the river and close the chain.

If we permit ourselves to believe this story, and if we continue to use it as an analogy, we gain a helpful visual image of what fluid elements actually do when fluid flows through a tube.

Under the force of the swift current the two swimmers closest to the banks are fully anchored on one side but are drifting a little on the other side, the side of their free hands. The next two swimmers are drifting by the same amount on one side, since they are holding hands with the first two swimmers on that side, but are drifting a little more on the other side, the side of their free hands, and so on. The amount of drifting is higher and higher for swimmers further and further away from the banks, being highest for swimmers at the center of the river.

Thus the chain of swimmers under the force of the current takes on the shape of a belly-curve, somewhat like the shape of a blown sail, in cross section. Better still, like the shape of the floating edge of a fishing net stretched out from one bank of a river to the other. In all cases the highest dip in the curve occurs at the center, furthest away from the points of anchor.

Fluid elements in a tube are much smaller than swimmers in a river, of course, and there are other differences in the two situations, but the analogy is useful.

In the case of the swimmers the driving force is the force of the swift current which acts to push each swimmer forward along the river. In the case of fluid flow

through a tube the driving force is higher pressure at the one end of the tube, created by a pump or some other means. This pressure acts to push each element of the fluid forward along the tube, as the swift current does to each swimmer.

An important difference between the plight of the swimmers and that of fluid elements is that the swimmers do not want to go on drifting while fluid elements do. More accurately, the swimmers *cannot* go on drifting, but fluid elements *can*. The chain of swimmers, like a fully blown sail, cannot drift any further once their arms become fully stretched. The chain of fluid elements never become fully stretched since fluid elements can stretch indefinitely. They are in fact deforming rather than just stretching. A fluid element is typically being sheared by a faster moving neighbor on one side and a slower moving neighbor on the other. It continues to hold hands with both neighbors, never letting go, never needing to let go, because it can deform indefinitely. Elements of fluid thus drift continuously down the tube as they deform, producing what we call flow.

A picture of the flow in a tube thus emerges in which cylindrical layers of the fluid move forward, one inside the other in a concentric fashion. The layers do not slide over each other as they move but rather shear each other as the inner ones move faster than the outer ones and as they remain forever stuck to each other. The layer in contact with the wall of the tube does not move at all on that side but its other side is able to move slowly. This slow movement is matched by the movement on one side of the next layer of fluid, but the other side of this layer moves a little faster, and so on.

It is as if each layer of the fluid is acting to shield the next layer from the dragging effect of the inner wall of the tube, as if each layer is acting to enable the next layer to move a little faster than itself. Fluid elements always act in this way, they are a heroic bunch. This is what makes flow possible, and what gives flow its unique qualities. Flow in a tube is not at all like a bullet. It is a fully orchestrated act, a well calculated scheme.

A bend in the tube or a change in its caliber, an obstacle, or a detour into a branch, present no problems. The scheme unfolds just the same. The carpet is laid over the wall of the tube wherever that wall is and wherever that wall leads to. One layer after another then move over this carpet and over each other in a well calculated, well ordered manner. Any obstacle along the way is carpeted just the same and layers move over or around it as the case may be. As long as the driving pressure is still behind it, and as long as there is still an opening for fluid to get through, however small that opening is, flow along the tube continues. It is nothing like a bullet. A bullet cannot do that.

A	cube law, 195
acceleration, 21	effective admittance, 246
components, 21–23	generations, 195
acceleration in space, 255, 256	living organ?, 191, 215
in steady flow, 256	major, minor paths, 225
acceleration in time, 256, 257	power law, 221
in unsteady flow, 256	power law index, 224
acceleration, deceleration	pressure distribution, 216
in space, 255	reflection coefficient, 246
in time, 255	wave reflections, 245
admittance, 242	arterial tree:bounding paths, 224
characteristic, 178, 180, 181, 242, 243	arterial tree:major, minor paths, 221
effective, 180, 181, 242, 243	arterial trees
input, 181, 243	bifurcation, 211
amplitude, 264, 265	generation, 213
angular frequency, 129, 263, 271, 323	hierarchical tree structure, 213
arbitrary constants, 296	level, 213
arterial bifurcation, 192, 205	sequential position, 213
area ratio, 193	artery?, 226, 228, 231
bifurcation index, 193	asymptotic value, 263
branching angles, 196	
branching angles, 198	
cube law, 193, 194	В
efficiency, optimality, 196, 198	Bessel equations, 88
geometrical structure, 193, 194	Bessel functions, 88, 132
optimal design, 209	at high frequency, 111, 113
power law index, 209–212	at low frequency, 103
pressure distribution, 210–212	properties, 89, 90
pressure drop, 210	bifurcation, 205, 244
shear stress, 209, 210	power law, 208
steady flow, 205, 206	pressure distribution, 206, 207
arterial segment, 228, 231	steady flow, 205, 206
arterial tree, 247	bifurcation index, 208, 212, 213, 217, 239
bounding paths, 225	blood
branches, 213	essence of life?, 1

blood flow	characteristic impedance, 178, 241–243
dynamics, 130	characteristic impedance, admittance, 244,
essence of life, 1	245, 389
body forces, 24, 25	classical solution
boundary forces, 24, 25	for oscillatory flow in a rigid tube, 91
bounding path, 224	complex conjugate roots, 293
bounding paths, 233, 236, 241	complex exponential function, 87, 131
branching elastic tubes	compliance, 266–268, 270, 271, 303
wave speed, 237–239	composite wave, waveform, 318, 355
branching rigid tubes	composite waveforms, 317
frequency parameter, 233	"cardiac", 342
peak flow rate, 234, 235	Fourier analysis, 317, 318
peak shear stress, 235–238	fundamental frequency, 323, 337
pulsatile flow in, 232	fundamental harmonics, 323
branching tree, 213–215	fundamental period, 337
structure, 213	harmonics, 318, 323
branching tree structure, 216	numerical description, 317, 319
branching trees	numerical form, 338
bounding paths, 217	Nyquist rule, 347
j,k notation, 213, 214, 216, 217	periodic functions, 320
major, minor paths, 217	piecewise, 329, 331, 334, 337, 338
missing branches, 214	single-step, 324
navigation through, 215	conservation of mass, 17, 18
position coordinates, 213, 214, 216	at a point, 17, 18
branching tubes, 192	equation, 19, 20
bifurcation, 192	constitutive equations, 36, 37
hierarchical tree structure, 192	continuum, 247
	continuum concept, 9
	coronary arteries, 233
C	distributing, delivering vessels, 229-231
capacitive chamber, 289–292, 295, 310, 311,	coronary blood flow, 391
378	arrhythmia, 394
compliance, 294	broken heart syndrome, 394
critically damped dynamics, 301	coronary flow reserve, 391
dynamics, 306	coronary vasculature, 391-393
free dynamics, 296	dynamic pathology, 391, 394, 395
full dynamics, 298	effective admittance, 393
inertance, 294	oscillatory character, 391
optimal dynamics, 306	structural pathology, 394, 395
orderly dynamics, 298	sudden cardiac death, 394
overdamped dynamics, 299	transient oscillatory state, 393
resistance, 294	wave reflections, 393
steady state oscillations, 297, 298, 307	coronary circulation, 390
underdamped dynamics, 300	dynamics, 394
capacitive effects, 356	cube law, 74, 224, 227, 236, 239
capacitive flow, 267, 268, 270, 285, 287, 288	
capacitive time constant, 269–271, 305	
cardiac pressure wave, 353	D
cardiac pressure wave, numerical description,	deceleration, see acceleration
352	deformation
cardiac pressure wave, waveform, 328,	continuous, 32
345–348	rate of, 32
characteristic admittance, 178, 180, 181, 242,	density at a point, 11
243	displacement, 273

dynamic of pulsatile blood flow dynamic fitness, 284	underdamped, 295 viscoelasticity, 290
dynamic pathologies, 298	wave reflections, 284, 350
dynamic pathology, 376, 377, 382, 391 acute, 378	Windkessel concept, 284, 285, 288
arrhythmia, 394	
broken heart syndrome, 394	E
chronic, 377	effective admittance, 180, 181, 242, 243
compliance effects, 382	in an arterial tree, 246
coronary blood flow, 391, 394	effective impedance, 181, 241–243
cube law, 388	effective impedance, admittance, 244, 245,
effective admittance, 385, 386	386, 389
footprint, 394, 395	elastic branching tubes
hanging pendulum, 377	pulsatile flow in, 232
0 01	elastic tube, 267, 387
impedance matching, 388–391	
in forced oscillations, 377	elasticity, 5, 266
in free oscillations, 377	equations, 133
inertial effects, 384	modulus of, 127
markers, 378, 381	Young's modulus, 127
pulse wave velocity, 385	electric circuit, 280
reflection coefficients, 385	electric current, 277
resistive-capacitive interplay, 378	electrical analogy, 257, 266, 276–280, 302
square law, 388	acceleration, deceleration, 278
static pathology, 377	capacitance, 276, 280
sudden cardiac death, 394	capacitor, 277–279
swing in the park, 377	delectric current, 278
vascular branching architecture, 384	elastic tube, 278
vascular stiffening, 383	elasticity, 279
vasodilation, 382	electric charge, 278, 280
viscoelastic effects, 383	electric circuit, 278, 279
vs structural pathology, 376	electric current, 277, 279, 280
wave reflection effects, 385	flow in a tube, 279, 280
wave reflections, 384, 386, 387	flow in tube, 278
wave speed, 385, 387	flow rate, 277–280
dynamics of arterial trees, 248	inductance, 276, 278
lumped parameter concept, 248	inductor, 277
dynamics of pulsatile blood flow	inertia, 277
capacitive chamber, 289–292, 295, 349	lumped properties, 277
capacitive flow, 285, 287, 288	potential difference, voltage, 277
composite waveforms, 351	pressure difference, 277–280
critically damped, 295	resistance, 276, 279
effective impedance, 350	resistor, 277
forced dynamics, 292	voltage, 277–280
free dynamics, 292, 294, 295	elliptic cross sections, 68
lumped parameters, 283	coordinate system, 119
oscillatory flow, 349	Mathieu functions, 116
overdamped, 295	oscillatory flow, 116, 120, 121
pressure-flow relations, 350	steady flow, 68
resistive flow, 285, 287, 288	entry flow, 50
resistive path, 289, 349	entry length, 50, 51
resistive-capacitive interplay, 285, 289,	entry region, 50
357, 359, 360, 362, 364–366	equation of continuity, 21, 38
single harmonics, 350	Eulerian method, 16
steady flow, 349	Eulerian velocities, 16, 17

F	fluids
fast Fourier transform, 319	on molecular scale, 7
flow, 6, 30, 32	force dynamics, 292
laminar, 47	Fourier analysis, 319, 328
turbulent, 47	analytical formulation, 319
flow in a tube, 198, 265, 281	Fourier coefficients, 321
developing, 254	Fourier series, 322
entrance region, 255, 256	fundamental frequency, 323
fully developed, 254	fundamental harmonics, 323
revisited, 250	harmonics, 323
flow in branching tubes, 191	numerical formulation, 338, 340, 341, 343
flow in tubes, 43–45, 191, 247	periodic functions, 321
arterial tree, 191	theory, 321
average velocity, 61	Fourier coefficients, 321, 325, 326, 330, 333,
balance of forces, 56	341, 345, 353
clinical relevance, 64	numerical formulation, 343
electrical analogy, 63	Fourier series, 322
energy expenditure, 62, 64, 65	compact representation, 323
entry flow, 50	Fourier series, representation, 322, 324,
entry length, 50, 51	326–330, 340, 346–348
entry region, 50	free dynamics, 292, 294, 295
flow rate, 61	frequency, 129, 263
fully developed, 53, 55, 60	angular, 129
fully developed flow, 50	fundamental, 129
governing equations, 54, 55, 57	frequency equation, 147
in series, 198, 199, 204	frequency parameter, 232, 233, 237
maximum velocity, 61	fully developed flow, 50, 53, 55
no-slip, 59, 60	fully developed state, 254
of elliptic cross sections, 68, 69, 71	fundamental frequency, 129, 323, 324, 328,
partially developed, 51	331
peak velocity, 60	fundamental harmonic, 324, 331
pressure distribution, 204	fundamental period, 324, 328, 331
pressure drop, 58	1 , , ,
pressure gradient, 58	
pumping power, 63, 64, 66	G
shear stress, 61	geometrical point, 11
steady, 53, 55	
tube lengths, 202	
two tubes or one?, 75, 80	Н
velocity profile, 45, 50, 61	harmonics, 318, 323, 328, 346–348, 353
fluid	hierarchical tree structure, 247
as a continuum, 8, 9	
as a rock?, 2	
fluid element, 8, 10	I
fluid state, 2	impedance, 130, 241-243, 255, 299, 301, 307,
life without?, 2, 3	308
fluidity	characteristic, 178, 241–243
bordering on magic, 4	complex exponential function, 308
defined, 5	effective, 181, 241–243
life without?, 2	input, 181, 243
of blood, 1	incompressible fluid, 255, 266, 268
on molecular scale, 7	indicial equation, 293
what is-?, 4	inductance, 255, 257, 258, 265

inductor, 277	Moens-Korteweg wave speed, 127, 237–239,
inertance, 257	243
inertance, inertial constant, 273	momentum equations, 39
inertia, 255, 257, 259, 260, 262, 263, 265	motion field, 13, 14
inertial constant, 258, 265	murmur, 49
inertial effect, 259, 262	Murray's law, 74
inertial effects, 263, 265, 356	and shear stress, 74
inertial time constant, 259, 260, 262, 264, 265,	generalized, 74, 75
304	Murray, Cecil D, 72
input admittance, 181, 243	
input impedance, 181, 243	
	N
	Navier-Stokes equations, 39, 53
L	in cylindrical polar Cartesian coordinates,
Lagrangian method, 15, 16	40
laminar flow, 47	in rectangular Cartesian coordinates, 40
long wave approximation, 130, 133, 142	simplified, 53
lumped parameter analysis, 251, 252	Newton
lumped parameter concept, 249–251, 254,	law of motion, 13, 14, 24, 30, 31
255	Newtonian fluid, 33, 34, 36, 37, 247
dynamics of arterial trees, 248	Is blood a -?, 34
lumped parameters, 249, 283	no-slip, 45, 46, 59, 60, 250
lumped properties, 249, 250, 255	no-slip condition, 255, 256
	nonrigid tube, 266
	numerical form, formulation, 338, 340, 341,
M	347
macroscopic scale, 8	
major, minor paths, 221	
mass, 273	0
material coordinates, 11, 14	opposition to flow, 241, 242
material point, 11	oscillatory flow, 84, 254
mechanical analogy, 271, 273–276	oscillatory flow in a rigid tube, 123
compliance, 272, 275, 276	at high frequency, 111, 113, 115–118
damper friction, 276	at low frequency, 103, 106, 107, 109, 110,
damper resistance, 272	116
elastic spring, 275, 276	classical solution, 91
friction coefficient, 273, 275	compared with Poiseuille flow, 92
	energy and power expenditure, 98, 101, 102
Hook's law, 275, 276	flow rate, 93, 96
inertance, 274 inertia, 276	of elliptic cross sections, 116, 120, 121
•	purposeless, 94
inertial resistance, 272	shear stress, 96, 98
law of friction, 273, 275	
mass, 274, 276	velocity profiles, 94 wave propagation?, 129, 130
mass-damper-spring system, 276	1 1 0
resistance, 272, 273, 276	oscillatory flow in an elastic tube, 123, 124,
spring, 276	153
spring constant, 275, 276	governing equations, 130
spring resistance, 272	long wave approximation, 130, 133
mechanical properties, 31	wave motion, 123, 126, 127
microscopic scale, 8	wave propagation, 125, 126, 128
modulus of elasticity, 129, 138	wave reflections, 126, 129
Moen Korteweg wave speed equation, 146	wave speed, 126, 127
Moen-Korteweg wave speed, 128, 163, 387,	oscillatory part, 343, 344
390	oscillatory pressure, flow, 271

P	primary wave reflection, 185
parabolic velocity profile, 60	pulsatile blood flow, 310, 311
partially developed flow, 51	as a swing in the park, 377
patient-specific, 228	beginning of time?, 298
peak flow, 234, 235	capacitive chamber, 310, 311
peak flow rate	capacitive component, 311
in branching rigid tubes, 234, 235	dynamic pathology, 377
peak shear, 235	dynamics, 311
peak shear stress, 236	impedance, 299, 301
in branching rigid tubes, 235–238	reactance, 299, 301–305
period, 320, 323	resistive component, 311
periodic function, 263, 321	resistive path, 310, 311
phase angle, 265, 333, 335	steady state, 299
phase shift, 264	transient state, 299
plasticity, 5	wave reflections, 311
point	pulsatile flow, 256
equations, 10	= steady + oscillatory, 84
geometrical, 11	frequency parameter, 232, 233
has mass?, 10	in branching rigid tubes, 232
material, 11	in elastic branching tubes, 232
within a fluid body, 10	oscillatory part, 84, 285, 286
point equations, 13	pressure gradient, 86
point-by-point description, 248, 249	steady part, 285, 286
vs global description, 248	using complex exponential function, 87
Poiseuille flow, 60, 200, 255, 256, 281	Why?, 82
fully developed, 206	Womersley number, 232
properties, 60	pulsatile flow in an elastic tube
pulsatile, 83	axial velocity, 150, 151
Poisson's ratio, 138	classical solution, 150, 156
position coordinates, 11, 14	flow rate, 156
power law, 221, 233	properties, 151
power law index, 224, 239, 388	radial velocity, 152
cube law, 227	wave reflections, 155
quartic law, 226	pulsatile Poiseuille flow, 83
square law, 225	pulsatile pressure gradient, 86
pressure, 36, 37	pulse wave velocity, 128, 145
mechanical definition, 37	
thermodynamic, 37	
pressure difference, 273	Q
pressure distribution, 204	quartic law, 226
pressure gradient	quasi-steady state, 262, 263
pulsatile, 86	
pressure wave, 353	
pressure-flow relations, 311	R
as a diagnostic tool, 351	reactance, 130, 299, 301–305
baseline case, 352, 355	reflection coefficient, 170, 178, 181, 182, 385
compliance, 313	at a bifurcation, 245
flow waveform, 352	between two tubes, 244
harmonics, 352	reflection coefficients
impedance, 311	successive, 183
inductance, 312	resistance, 130, 241, 242, 250, 256, 259, 267,
R-scaled, 356	352, 353
resistance, 312	resistive flow, 267, 268, 270, 271, 285, 287,
viscoelasticity, 312	288

resistive path, 289, 310, 311, 378 resistive-capacitive interplay, 285, 364–366, 369, 371 "healthy" dynamics, 381 capacitive chamber, 366, 370 clinical implications, 359, 371 composite waves, 363, 367, 368 inertance effects, 370 inertial effects, 373 viscoelastic effects, 370 viscoelasticity, 372 resistive-capasitive interplay dynamic pathology, 378 Reynolds number, 48 Reynolds, Osborne, 47 rigid tube, 129 rigidity, 5	turbulence and murmur, 49 high-Reynolds-number-, 49 turbulent flow, 47 V velocity gradient, 32, 33 and viscosity, 398 velocity profile, 50 parabolic, 60 vessel segment, 231 viscoelasticity, 290 viscosity, 32, 34, 35, 128, 250 a story, 397 and velocity gradient, 398 coefficient of, 33, 36
	W
S	wall thickness, 128
sand	wave crest, 127
does not flow, 8	wave equations, 164
is not a continuum, 8	one dimensional, 162, 164
is not a fluid, 7	solution, 167
secondary wave reflection, 185	wave length, 128, 129, 238–241
single-step waveform, 324	estimate, 129
solidity, 5	wave propagation, 128, 130
square law, 225, 390	at infinite speed, 159
steady flow, 53, 55, 250	transmission line theory, 163
steady state, 253, 254, 259, 260, 263, 264	wave length, 128 wave reflection
steady state oscillations, 297	primary, 185
stress tensor, 26, 27, 38, 62	secondary, 185
components, 28, 29	wave reflections, 129, 159, 160, 241, 243–245
in cylindrical polar coordinates, 41	284, 388
symmetry, 38	one dimensional, 163
sudden cardiac death, 395	primary, 169
	secondary, 169
m	transmission line, 160
T	wave speed, 126-129, 145, 238, 243, 387
thin wall approximation, 138	attenuation, 147
thin wall assumption, 146	dispersion, 147
time delay, 265 transient state, 254, 255, 259, 260, 263,	estimate, 128
265	imaginary part, 238, 240
transmission line, 160	in branching elastic tubes, 237–239
transmission line theory, 160, 163	infinite, 128
tube wall, 134	Moen-Korteweg, 163
balance of forces, 135	Moens-Korteweg, 127, 128, 237, 239
modulus of elasticity, 138	real part, 238, 239
Poisson's ratio, 138	wave speed equation, 146 windkessel, 271
thick, 134	Windkessel concept, 284, 285
thin, 134	Womersley number, 232
Young's modulus, 138	Trometaley number, 232
tube wall motion	V
governing equations, 137	Y
stress-strain relations, 137	Young's modulus, 129, 138